Ground compaction due to vibrodriving of piles

Bement, R.A.P.

Ground Compaction due to Vibrodriving of Piles

by

R.A.P Bement BSc., MSc.

A thesis submitted for the degree of

Doctor of Philosophy

School of Engineering

University of Durham

March 1996

Abstract

Civil engineering construction frequently requires the use of piles to carry structural loads to stronger ground strata or to control lateral ground movements. A variety of techniques are available to install piles into the ground. Of central interest to this research is the vibratory hammer, or vibrodriver, which is the preferred method used to drive piles into granular soils.

The installation of sheet and bearing piles by vibrodriver causes periodic vibration in the adjacent ground which is severe very close to the piles, but attenuates with distance. A potential consequential effect of the vibrations that are caused by vibrodriving is ground compaction, which may be observed as differential surface settlement. It is desirable that vibration induced ground compaction settlement should be estimated for contracts where loose to medium-dense granular soils occur, especially when buildings on shallow foundations or poorly bedded service pipes are adjacent. It is unlikely that a simple *in-situ* soils test will allow accurate, specific estimates, but rather that a range of vibratory tests should be performed which can then be used as a knowledge base. Settlement trends and associated parameters can then be identified which will allow the prediction of settlement with reference to the *in-situ* soil and the ground vibration data. This argument forms the basis of the laboratory test programme.

A range of granular soils were studied using an adapted 150mm Rowe cell (a hydraulic oedometer). Use of the Rowe cell enabled samples to experience compaction under effective stress conditions that are appropriate for equivalent soils in the field. The complete cell was mounted on an electromagnetic shaker and after static consolidation, the samples were vibrated under maintained hydraulic load, at frequencies and accelerations that are appropriate for soils adjacent to vibrodrivers. Change in sample height was recorded for controlled vertical (and horizontal) vibrations, typically in the range of 0.1*g* to 5.0*g* at 25Hz and 40Hz. Soils were tested under a range of effective stresses and moisture content.

The results of the laboratory programme and subsequent data analysis are presented in tables and diagrams. Expressions that describe a good relationship between acceleration, soil type, relative density and static load allow upperbound estimates of vibratory settlements to be made for accelerations of up to 6.0*g*. An additional expression is presented that accounts for the influence of moisture content, ground vibration frequency and vibration duration. Summary tables are presented that define categories of vibration induced ground compaction settlement based on settlement potential, risk and severity. The use of the settlement equations and the influence of various parameters are demonstrated for a range of example applications. In addition, data is abstracted from case studies found in the literature and sites that were visited during the research. The abstracted data are then used to perform settlement estimates which are compared to the reported examples. Good correlation between observed and calculated settlement is demonstrated in many cases. However, in some instances, it appears that ground settlements were exacerbated by at least one additional mechanism, such as cumulative pore water pressure increase, or lateral movement of sheet piles. In addition, extraction of piles by vibrodriver appears to contribute significantly to the reported cases of ground settlement.

Acknowledgements

I would like to express my grateful thanks to my supervisor Dr A.R. Selby for his continuous help and interest during this research programme. I found his advice and constructive discussion very beneficial.

I would also like to thank the sponsors of the research programme, British Steel Piling Technical Division, and in particular, Mr C. Tuck and Mr R. Dinnis for their support, discussion and efforts on my behalf.

In addition, I must thank the technical staff of the School of Engineering, particularly Mr B. McEleavey, Mr S. Richardson and Mr B. Scurr for their assistance and company during the long hours spent in the laboratory.

Also, I would like to thank Graham McKelvey, Katharine Stocks, Darren McCauley, Martin Ryan, Richard Towns, Monica Calado, Haluk Bayrakdar, Suzanne Elliot and Lisa Parkin, who I met whilst at Durham, for being friends.

Big thanks to Orla Ryan (who I met at a Grad Soc disco!) for putting up with me during the long hours that were spent on writing this thesis, putting me up when I ran out of money and agreeing to marry me.

Finally I would like to thank my old school geography teacher, Mr. Harvey Luke. He was a good teacher; strict, encouraging and friendly, and inspired me to take an interest in the earth sciences and to think for myself.

Statement of Copyright

Declaration

No material from this thesis has been previously submitted for a degree at this or any other university.

Table of Contents

Chapter 5: Results and Applications

List of Tables

List of Figures

List of Plates

Notation

A	amplitude of vibration
A	sample area
a	acceleration
c	shear strength
c	wave velocity
C_c	coefficient of curvature
C_r	relative compaction
D_c	coefficient of distribution
D_{max}	maximum particle size
D_r	relative density
D_x	non-dimensional distribution coefficient

E	Young's modulus of elasticity
E	vibrodriver energy input per blow
e	void ratio
f	frequency
f'	ratio of vibrodriver frequency to test frequency
f_c	centrifugal force
f_h	horizontal component of centrifugal force
f_v	vertical component of centrifugal force
G	shear modulus
G_s	specific gravity
g	gravity of the earth
h	sample height
K_m	coefficient of shear strain
K_o	coefficient of earth pressure at rest
M_w	mass of water
M_s	mass of solids
m	mass
P	compression wave
Q	Love wave
R	Rayleigh wave
r	distance
r_d	stress reduction coefficient
S	Shear wave
S_f	soil factor
S_v	vibratory settlement
$\mathrm{S_v}$	vertically polarised shear wave
$\mathrm{S_h}$	horizontally polarised shear wave
S_r	saturation
T	period of vibration
t	time
U_c	coefficient of uniformity
u	pore water pressure
u_a	atmospheric pressure
$-u_w$	negative pore water pressure
V_p	compression wave velocity
V_s	shear wave velocity
V_w	volume of water
V_v	volume of void spaces
v	particle velocity

W	hammer energy input per blow
w	moisture content
z	depth of soil unit
BP	back pressure
CLB	coarse Leighton Buzzard sand
CMC	consolidated moisture content
CSS	coarse sharp sand
CSS>63	coarse sharp sand sieved to remove <63μ fraction
DP	Diaphragm pressure
FUS	fine uniform sand
GMS	Garside medium sand
LDS	Ling Dynamics Systems
LVDT	linear variable displacement transducer
MLB	medium Leighton Buzzard sand
MSS	medium sharp sand
MUS	medium uniform sand
NC	normally consolidated soil
OC	overconsolidated soil
PDR	portable digital recorder
ppa	peak particle acceleration
ppd	peak particle displacement
ppv	peak particle velocity
SFG	sandy fine gravel
SFMG	sandy fine to medium gravel
SCB	sample confining bag
SFS	silty fine sand
SPT-N	standard penetration resistance blow-count value
χ	a factor related to saturation
Φ	friction angle
γ	unit weight
γ_d	dry density
γ_{dmax}	maximum dry density
ε	normal strain
θ	angular distance
λ	wavelength of vibration
ν	Poisson's ratio
π	3.142
ρ_b	soil bulk density

σ	total stress
σ'	effective stress
σ_d	vertical dynamic stress
σ_{dp}	axial stress
σ_h	horizontal stress
σ_v	vertical stress, overburden stress
σ_z	vertically acting (air) pressure
τ_{av}	average shear stress
τ_{max}	maximum shear stress
ω	angular velocity

" And every one that heareth these sayings of mine,
and doeth them not, shall be likened unto a foolish
man, which built his house upon the sand "

ST. MATHEW 8. 26

CHAPTER 1
INTRODUCTION

1.1 Introduction

Civil engineering construction activity frequently requires the use of bearing piles to carry structural loads to deeper, stronger ground strata; and sheet piles which are used as temporary or permanent works to control lateral ground movements or to prevent water from entering excavations. A variety of techniques are used to install piles into the ground, such as driving, jacking and boring. Pile driving is performed using two main types of hammer; impact hammer and vibratory hammer (or vibrodriver). The choice of hammer depends on a number of factors such as soil conditions and the size of the pile. In general, vibrodrivers achieve rapid driving in granular soil, and are a popular choice among contractors because of the low noise and vibration levels that are produced. In addition, vibrodrivers are used to extract piles, which impact hammers are unable to do. The installation of sheet and bearing piles by vibrodriver causes periodic vibrations in the adjacent ground, which are severe very close to the pile but attenuate with stand-off distance. Use of the vibrodriving technique is the central focus of this research, because a potential consequential effect of the vibrations that are caused by vibrodriving or extraction is ground compaction, which may be observed as surface settlement. The potential magnitude of such ground compaction is influenced by site conditions; trafficking for example, can reduce the potential considerably.

Ground vibrations that are generated by vibrodriving of piles into granular soils have been reported by a number of authors, e.g. Selby (1989), Uromeihy (1990), Oliver and Selby (1991). Statistical treatment by Attewell *et al.* (1992) allows the confident prediction of typical vibration magnitudes in terms of hammer energy and stand-off distance from the pile. Well-documented and detailed case histories of vibratory compaction settlements are less common. However, examples may be found in the literature, the majority of which have been published by the geotechnical press of the USA, e.g. Dowding (1994) and Lacy and Gould (1985). The differential settlements that are caused by vibration induced ground compaction settlement may cause damage to structures, roads and buried services.

Other factors that can directly cause or contribute to damage of structures include: ground displacements caused by driven piles; loss of ground in pile boring; lateral movement in excavations; settlement caused by the lowering of ground water level (CIRIA Technical Note 142, 1992); differential settlement of foundations upon loading; thermal expansion or contraction of structural elements; shrinkage or swelling of clay soils; frost heave and the deterioration of construction materials. Much work has been carried out that investigated building damage resulting from differential ground settlements and lateral ground movements, e.g. Skempton and MacDonald (1956), Terzaghi and Peck (1948), Burland and Wroth (1975), Boscardin and Cording (1987) and Symons *et al.* (1988).

It is desirable that vibration induced ground settlements should be estimated for those contracts where loose to medium-dense granular soils occur, especially when buildings on shallow foundations or poorly bedded service pipes are adjacent. It is unlikely that a simple *in-situ* soils test will allow accurate, specific estimate, but rather that a range of vibratory tests should be undertaken which can then be used as a knowledge base. Settlement trends and parameters can then be identified from this that will allow the prediction of settlement with reference to *in-situ* soil and the ground vibration data. This argument forms the basis for the laboratory test programme.

1.2 The General Subject Area and Related Processes

The installation or extraction of sheet and bearing piles using vibratory piling equipment has three consequential effects. The first is whether vibrations transmitted into adjacent building cause cosmetic or structural damage; the risk from estimated vibration levels may be assessed in the context of various national standards and the Eurocode7. The second issue is the degree of disturbance to the occupants of adjacent buildings in terms of vibration dose values. The third aspect is the settlement which may be caused by the action of vibrations upon soil fabric; it is this subject that is considered in this research.

The action of vibration upon loose to medium-dense sandy or silty soil (conditions ideal for vibrodriving), is to cause compaction by rearranging the soil particles into a denser configuration. In the field, the magnitude of compaction will be influenced by a range of factors, such as: the soil density; particle size distribution characteristics; moisture content; overburden pressure and by the severity and duration of the piling vibrations. Whilst there has been extensive research into the use of vibratory rollers and vibrating plate compactors, e.g. d'Appolonia (1967) and Parsons (1992), such work has concentrated on the top half metre of soil. In addition, much work has also been carried out concerning seismic effects on soils, and in particular, liquefaction, e.g. Seed and Silver (1972). However, the frequencies, durations and strain magnitudes that are associated with earthquakes are of a different order to those associated with pile driving. Consequently, there is a need for research into the fundamental behaviour of granular soils subjected to vibrations that are typical of those associated with vibrodriving, which when combined with current knowledge of vibration magnitudes, can lead to estimates of induced ground compaction settlement.

The susceptibility of granular soils to densification induced by vibration is exploited by a number of ground improving construction techniques. Such techniques increase soil density to improve bearing capacity and reduce settlements, and include: dynamic compaction, deep blasting, vibrocompaction (flotation) and vibrodisplacement. Case studies concerned with these techniques may be found in Solymar (1984) and La Fosse and Gelormino (1991).

1.3 Civil Engineering Related Vibration

Civil engineering work will always generate construction related noise and vibration of varying intensity and duration. The size and location of the project will determine the degree to which the work causes an environmental disturbance. Construction related environmental disturbance, specifically that which is generated by pile driving activities may be divided broadly into the annoyance caused to humans, and damage to adjacent buildings from ground vibrations. The Control of Pollution Act (1974) defines noise, including vibration, as nuisance (whilst not defining any limit) and gives local authorities wide ranging powers to restrict its cause and minimise its effects. If restrictions are imposed, then construction operations may be modified, suspended or even terminated.

The effect that ground vibrations have on building response is dependent on a number of factors including: the magnitude of vibration; the stiffness and damping characteristics of the building and its construction materials; the dimensions of the building and the relationship between the natural frequencies of the building and the ground. Ground vibrations that are transmitted to a building may cause structural, serviceability and aesthetic damage. However, there are no universally applied rules that enable the prediction, limitation and categorisation of damage that is attributed to piling vibrations. Different parameters and categories are used to define levels of risk and damage in different countries.

In Britain, BRE Digest 353 (1990) gives guidance concerning building response to vibrations and provides examples of the differences between some of the national standards. For example, the German standard (DIN 4150: Part 3: 1986) uses the maximum values of vibration velocity recorded for the x, y and z axes (i.e. 2 horizontal and 1 vertical). The Swiss standard (SN 640 312:1978) uses the true peak resultant velocity. In Sweden; the vertical component of particle velocity is used. The British standard (BS 5228: Part 4: 1986) was specifically formulated to describe ground vibration from piling construction operations (Whyley and Sarsby, 1992) and their effect on buildings.

Typical values of limiting of peak particle velocities are presented in Table 1.1 (where structural damage already exists, such limits may be lowered by up to 50%). Sensitive equipment, such as computers, can be adversely affected by building vibrations that are below the safe limits that were set for the building structure (Boyle, 1990).

Type of Structure	Peak Particle Velocity (mm/sec)	
	Continuous Vibration	Transient Vibration
Ruins, buildings of architectural merit	2	4
Residential	5	10
Light commercial	10	20
Heavy commercial	15	30

Table 1.1 Typical values of vibration limits (British Steel, 1994).

Vibration magnitudes can be accurately measured, and work has been carried out that allows reasonable estimates of vibration levels with stand-off distance, e.g. Attewell *et al.* (1992). However, predicting the effects of vibration has intrinsic uncertainties because each piling operation is a unique combination of processes and ground conditions. Each site and its surroundings is unique and each adjacent structure has its own special characteristics. Broadly based guidelines, essentially in terms of risk, are the current approach. However, expert judgement is still required for specific assessment.

The effect of vibrations on humans depends on a range of variables. The human body can detect very low levels of vibration; 0.15-0.3 mm/s (peak particle velocity) in the frequency range of 1-80 Hz (BS 6472, 1984). As vibration intensity increases, vibrations become irritating, annoying and frightening. The degree of annoyance felt by an individual is based on a number of factors, including: the physical and mental condition and attitude of the person concerned; the proximity of the vibration source; the duration and time of day, and the quality of the pre-existing environment. For example, in an urban environment, serious complaints are probable when peak velocity is greater than 0.4mm/sec. It is not possible to define a level of intensity that will be acceptable in any particular circumstances because of the impossibility of giving objective definitions of such terms as 'annoying' and 'public nuisance'. Good public relations between workers and local residents, that are likely to be affected by, or perceive vibrations and noise will tend to reduce the level of annoyance. Table 1.2 presents data that is based on available information and past experience (British Steel, 1994). Vertical peak particle values are given; below which, the probability of complaint is low.

Area	Peak Particle Velocity (mm/sec)	
	Continuous Vibration	Transient Vibration
Sensitive locations, e.g. hospitals	0.15	0.15
Residential	0.3	1.0
Offices, shops	0.6	2.0
Workshop, factory	1.2	4.0

Table 1.2. Typical values of human tolerance limits (British Steel, 1994).

Where piling vibrations are considered to be unacceptably annoying or risk of damage is considered to be too high, several options may be considered, such as: alternative foundation design; alternative pile types and/or process; reduction of driving energy; isolation of vibration; continuous monitoring and good public relations (CIRIA Technical Note 142, 1992).

1.4 Particular Concerns of the Research

Construction related damage to neighbouring buildings is often attributed to the direct transmission of vibration. Apparently, less regard is given to the effect that vibrations have on the soils that are transmitting them. However, an important indirect cause of damage to structures results from vibration-induced ground settlements in granular soils (CIRIA Technical Note 142, 1992), where settlements tend to be differential in nature. Consequential structural damage will be more significant where shallow foundations overlie loose to medium dense deposits. Settlements can be expected for stand-off distances of approximately 10 pile diameters and sometimes as much as 10-15m from driven piles. In addition, in exceptional circumstances, movements can be induced at greater distances, e.g. where loose sand overlies dense gravel (or rock) and ground vibrations are transmitted along the dense layer. Ground settlements of up to 300mm are also possible for driving pile groups into granular soil (CIRIA Technical Note 142, 1992).

The central concern of this research is the investigation of the effects of vibratory pile driving on adjacent granular soils, with possible damage to buildings. It is assumed that ground vibration has no immediate compactive or consolidation effect on cohesive material, and the possible long term effects of pore water pressure equilibration that occur subsequently to a vibropiling operation are ignored.

Due to the contractually sensitive nature of the problem, examples of damaging settlements are rarely publicised. This implies that: vibration induced ground settlement that damages buildings does not occur; it occurs in a small number of cases and/or the damage is (primarily) attributed to some other mechanism or combinations of mechanisms; it does occur but is not publicised due to contractual concerns or even arbitration and litigation, or companies with experience of the problem keep any information private, for commercial advantage (Jonker, 1995).

Within the limited publications, soils susceptible to densification by vibration are reported to be narrowly graded, single sized clean sands and silty sands with a relative density of less than about 50-55%. In these materials, damage to structures attributed to soil movements resulting from pile driving can be more significant than structural damage due to transmitted vibration (Dowding, 1994).

1.5 Aims and Objectives

The central objective of the present investigation is the construction of a database of information on the vibratory compaction of granular soils. Information will then be abstracted from the database to identify settlement trends and parameters. The ultimate research product, equations and summary tables, will enable the potential vibratory ground compaction settlement to be estimated before the start of piling operations, i.e. during the planning and design stage. Altering the construction method prior to the start of operations is considered to be preferable to the time and financial costs that could be incurred if remedial work to repair or rebuild damaged structures is required, or litigation as claims are pursued through the courts. In addition to preventing the potential costs associated with the effects of ground settlement; it will be beneficial to the construction industry if this research is of use during public relation exercises.

Much consideration has been given to the damaging effects that ground vibrations have when transmitted directly into buildings (e.g. Uromeihy, 1990). However, it appears that much less regard is given to the indirect effects of ground vibrations that cause loose to medium dense sands to settle, and then induce angular distortion in the buildings founded in such soils. The cause of damage has the potential to be misdiagnosed if only direct transmission of ground vibrations is considered, due to a lack of the appreciation of other mechanisms, such as ground compaction settlement and forward movement of sheet-pile walls. Vibration induced ground compaction settlement causing damage to buildings has been reported at vibration levels below the threshold values that some National Standards set to prevent direct vibration damage. At the Deep Foundations Institute Conference on Piling and Deep Foundations (1994) the delegates were asked to cite examples of building damage caused by direct transmission of vibration; none of the delegates reported experience of this phenomenon. However, when asked to report any cases where vibration induced ground compaction settlements caused building damage, three positive responses were made. On face value, this could imply that direct vibration limits are set too severely, and less control is applied to avoid damage caused by soil settlements.

1.6 The Research Programme

It is recognised that spatial variations in ground vibrations that are generated by vibrodriving are slow and smooth (Selby, 1989), although the variation within a cycle is rapid. Thus, a test facility was required in which granular samples could be prepared and statically equilibrated, following which the entire assembly could be vibrated. In the test programme, the vibratory compaction of a range of granular soils was studied using a modified 150mm diameter Rowe cell (a hydraulic oedometer) which enabled samples to experience compaction under effective static stress conditions that were appropriate to equivalent soils in the field. A novel sample preparation technique was developed to overcome the difficulties that were experienced during preliminary testing.

The complete cell was mounted on an electromagnetic shaker and after static consolidation, the samples were vibrated under maintained hydraulic load, at frequencies and accelerations that are appropriate to soils adjacent to vibrodrivers. The change in sample height was recorded for controlled vertical (and horizontal) vibrations, typically in the range of $0.1g$ to $5.0g$ at 25 and 40Hz. Soils were tested under a range of effective stresses (10, 20, 50 and 100kPa) and moisture contents. A number of miscellaneous tests were performed to check some assumptions concerning test method and vibratory settlement behaviour.

In addition to the laboratory programme, four construction sites were visited on a number of occasions to obtain ground vibration and settlement data. Ground vibration was measured using an array of triaxial geophones, and recorded on a portable digital recorder (PDR), for subsequent data processing. The detailed description and operation of the PDR unit may be found elsewhere (Uromeihy, 1990). Ground settlements were monitored using a surveyor's level and survey pins.

1.7 Thesis Structure

Pile driving operations transmit energy into the ground which propagates as body waves and surface waves. Chapter two provides an overview of the types of vibrations that are generated by vibrodriving, their propagation and attenuation characteristics. In addition, vibration generated during pile driving and types of pile and hammer are briefly described. More attention is given to the development and mechanism of vibrodrivers.

The nature of granular soils and the influence of post-depositional processes is described in Chapter three. Also reviewed is the subject of soil dynamics, with the applications and laboratory tests that can be performed to assess the contribution of various factors on the dynamic response of granular material. Examples of vibratory tests that have been performed by various authors to examine the compaction characteristics of sands caused by vibrations are presented. In addition, case studies concerning the ground settlements induced by pile driving that have been reported by a number of authors are summarised and additional observations are included.

The standard Rowe cell was developed in the 1960's to test the consolidation properties of cohesive soils. Hydraulically loaded samples are tested under effective stress conditions, and pore water pressure is measured. In the current laboratory test programme, 201 vibratory tests (not including preliminary and repeat tests) were performed between January 1992 and October 1995, using an adapted Rowe cell. The soils that were used, the development and modifications of the equipment and the test procedure are detailed in Chapter four.

The laboratory results, subsequent analysis and observation of settlement trends are presented in Chapter five. Equations that describe the significance of soil type, density, overburden pressure, vibration acceleration magnitude, moisture state, frequency and duration of vibration upon compaction are presented. A range of example applications are developed and discussed. Finally a risk assessment procedure is proposed using summary tables that relate soil settlement potential, risk and severity.

The reliability of various elements of the laboratory test programme, subsequent data processing, evaluation and details of improvement to equipment is discussed in Chapter six. In addition, a number of piling related ground settlement case studies are presented which are taken from site work and the literature. Ground profile and vibration data are abstracted and used in the settlement equations, in order to compare reported and recorded settlement with the settlements generated using the vibration settlement equations. The agreements and differences between actual and estimated settlements are discussed.

Finally, conclusions are drawn from the results, and broad suggestions for further work are given in Chapter seven.

CHAPTER 2
GROUND VIBRATIONS

2.1 Introduction

Vibration may be represented as the displacement of a point (amplitude), the rate of change of displacement (particle velocity), or the rate of change of particle velocity (particle acceleration) (Sections 2.2-2.4). In engineering practice, particle velocity (v) is used frequently to describe ground vibration magnitude. Less consideration is given to wave velocity (c), which may be used in the calculation of ground strain. The measurement of vibration at the ground surface is usually expressed in terms of (peak) particle velocity, which is accepted as being the appropriate measure for the determination of the potential for direct damage to structures.

As a pile is driven into the ground, spherically expanding compression (P waves) and shear (S) waves are generated (Section 2.5). As these body waves expand outward from the pile, they are reflected and/or refracted at the soil-surface and other acoustic interfaces. The characteristics of such ground vibrations are influenced by a number of variables, including: type of pile and piling method; the nature of the *in-situ* deposits; stand-off distance and the condition of the building and its foundations. As the zone of interest focuses on piling operations, ground response to the vibrations becomes less well understood. However, criteria are available to assess the risk to structures that are subjected to piling induced vibrations. These criteria should not be regarded as rigid rules and should be expertly interpreted with regard to specific site conditions (Whyley and Sarsby, 1992). Figure 2.1 summarises the many variables that are associated with pile driving induced ground vibration.

The chapter provides basic background information on vibration, propagation, attenuation (Section 2.6), examples of types of waves, piles and (vibratory) piling methods (Section 2.7) and ground condition (Section 2.8). The contents are covered in more detail in established soil dynamics texts such as Prakash (1981), Das (1983) and in the CIRIA Technical Note 142 (1992). Note that the Technical Note 142 does not provide guidance within stand-off distances 'of the order of metres'.

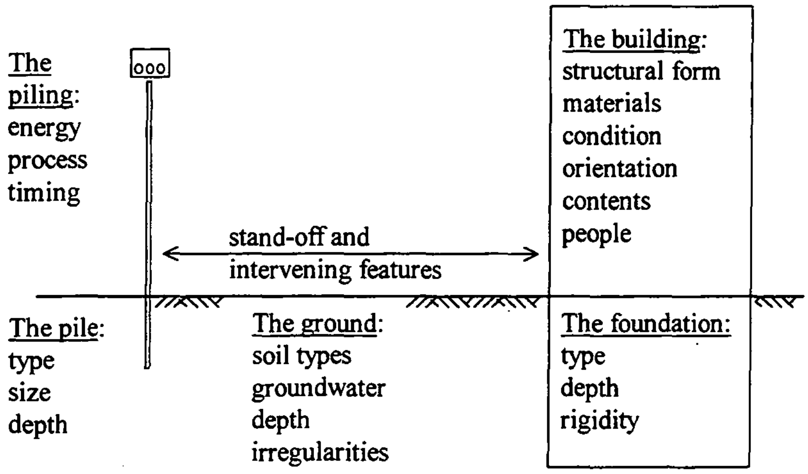

Figure 2.1 Summary of the variables associated with ground-borne vibration and piling (from the CIRIA Technical Note 142, 1992).

2.2 Vibration Terms and Definitions

The definitions given below describe aspects of simple harmonic (sinusoidal) vibration:

Amplitude (A) - This is the maximum displacement of a body from its equilibrium position (i.e. single amplitude). Peak-to-peak amplitude is described as the double amplitude. Amplitude is also used to loosely describe the magnitude of particle velocity and acceleration.

Period (T) - The duration of one complete vibration cycle.

Wavelength (λ) - This is the distance between any two identical parts of adjacent vibration cycles. Wavelength is proportional to wave velocity and inversely proportional to frequency (i.e. $\lambda = c/f$)

Frequency (f) - The number of vibrations occurring in a given period of time, in cycles per second..

Wave Velocity (c) - The ratio of the change in distance position (Δx) to the time change (Δt) i.e. $c = (\Delta x / \Delta t)$

Angular Velocity (ω) - This the ratio of the change in angular position ($\Delta\theta$) to the change in time (Δt), i.e. $\omega = (\Delta\theta / \Delta t)$ (radians/sec)

Particle Velocity (v) - This is the rate of change in vibration displacement with time.

Free Vibration - The vibration of a system under the action of its internal forces (i.e. natural frequency).

Forced Vibration - The vibration of a system due to excitation of external forces, occurring at the frequency of the exciting force.

Resonance - This state occurs when an exciting frequency coincides with a system's natural frequency. At resonance, a system's amplitude may be dramatically enhanced.

Degrees of Freedom - The number of independent co-ordinates necessary to describe the motion of a system. A free particle may have three degrees of freedom in three orthogonal positions (longitudinal, transverse and vertical). A rigid block may have six degrees of freedom; three describing its displacements along x, y and z axes which are known as lateral, longitudinal, and vertical, and three describing the rotations of the block about x, y and z axes i.e. pitching, rocking/rolling and yawing.

Damping - When the motion of a particle is affected by friction, the amplitude of vibration decreases with time. The friction force is directly proportional to the velocity of a medium having lower wave velocity, such as granular soil, and proportional to the square of the velocity of a medium with higher wave velocity such as dense soil and rock.

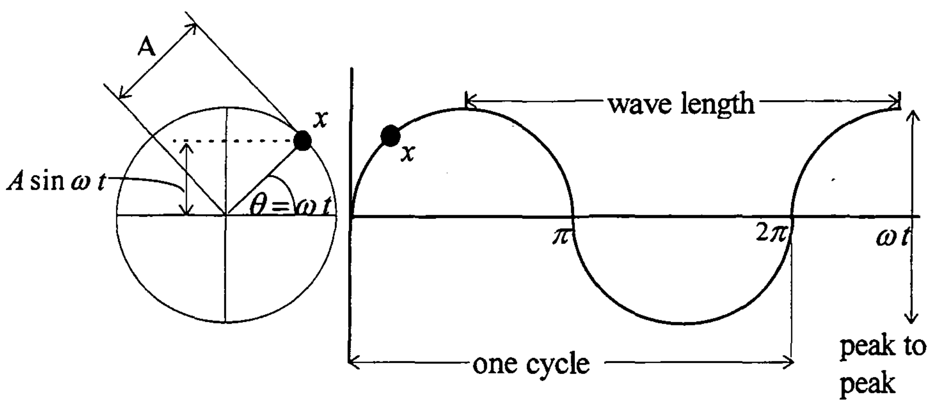

Figure 2.2. The character of sinusoidal vibration.

2.3 Vibratory Motion

Types of vibratory motion can be classified depending on the vibration source, the medium transmitting the vibrations and their time dependence:

Transient Vibration - This is characterised by the occurrence of an impulsive force, causing a maximum motion of relatively short duration. Earthquakes, blasting and dynamic compaction create transient vibrations.

Periodic Vibration - The same form of vibration motion occurs repeatedly. Sinusoidal vibration is the basic form of periodic motion generated for example, by vibratory hammers.

Random Vibration - The occurrence of dynamic events are not predictable and no instantaneous value can be expected over time. Seismic activity and movement of heavy compaction plant generate random vibrations.

2.4 Measure of Vibration.

The amplitude of a vibration may be expressed in terms of particle displacement, velocity and acceleration. For a sinusoidal vibration, these quantities are related. Referring to Figure 2.2, in which the motion of a point around a circle is projected on to a straight line, the vertical position of the point represents the particle displacement and the amplitude:

$$x = A \sin \omega t = \text{harmonic motion} \qquad \text{(eqtn 2.1)}$$

where: x = position of a point

A = amplitude

ω = angular velocity

t = time

Particle velocity can be obtained by differentiating eqtn 2.1 with respect to time:

$$v = \omega A \cos \omega t$$

or,

$$v = \omega A \sin(\omega t + \pi / 2) \qquad \text{(eqtn 2.2)}$$

Additionally, differentiation of eqtn 2.2 with respect to time gives the particle acceleration:

$$a = -\omega^2 A \sin \omega t$$

or,

$$a = \omega^2 A \sin(\omega t + \pi) \qquad \text{(eqtn 2.3)}$$

Equations 2.2 and 2.3 show that acceleration and velocity are harmonic and can be represented by the vectors ωx and $\omega^2 x$, rotating at the same speed as x. These lead the displacement vector by $\pi/2$ and π respectively, i.e. the acceleration vector leads the velocity vector by 90° and the displacement vector by 180°. The phase relationships between displacement, velocity and acceleration are illustrated in Figure 2.3. For a harmonic (sinusoidal) vibration, if the amplitude of one of the above quantities together with its relevant frequency is known, all other quantities are easily obtained.

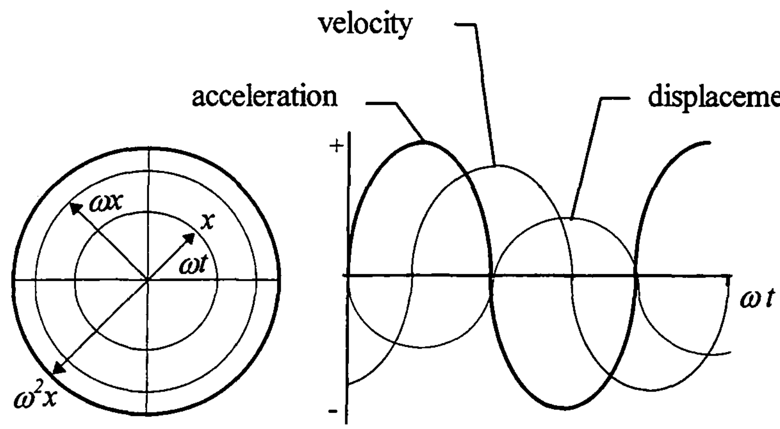

Figure 2.3. The relationship between acceleration, velocity and displacement.

2.5 Wave Propagation

Propagation of vibrations depends primarily on the type of wave, ground condition (e.g. its stiffness, density and degree of saturation), and the boundaries between different layers (which cause reflection and refraction) especially at the ground surface. Reflections occurring at the ground surface may produce a complex array of particle motions, especially if interaction occurs with other wave forms. The free propagation of ground vibration is seen to occur at a characteristic frequency particular to the soil type and density range, examples of which are given in Table 2.1.

Ground vibrations may be categorised into two forms, i.e. body waves (which propagate through soil and rock) and surface waves. Body waves are classified according to the propagation direction as compressional waves or shear waves.

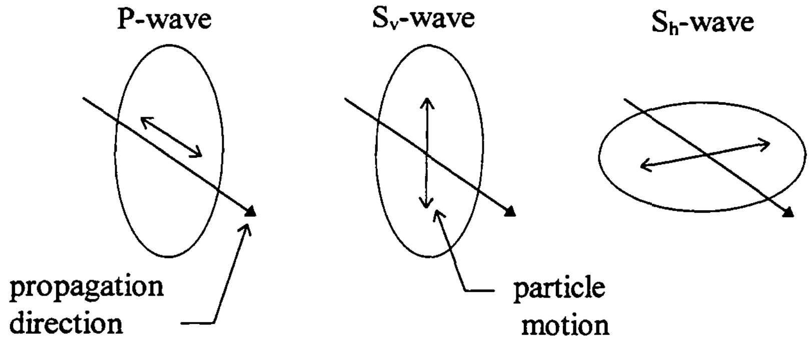

Figure 2.4. Particle motion due to different body waves.

Soil/rock type	Characteristic Frequency (Hz)
Very soft silts and clays	5 - 20
Soft clays and loose sands	10 - 25
Dense sands and gravels, stiff clays	15 - 40
Weak rocks	30 - 80
Strong rocks	> 50

Table 2.1. Characteristic propagation frequency of selected soil and rock. (from the CIRIA Technical Note 142, 1992).

2.5.1 Compressional Waves (P-waves)

These waves (also known as dilational, longitudinal and primary waves), cause particles to vibrate parallel to the direction of the wave propagation (see Figure 2.4). Volume change occurs in the propagation medium as the particles vibrate back and forth causing compression and expansion. The degree of soil saturation directly affects P-wave propagation velocity. Because water is relatively incompressible compared to the soil skeleton, the measurement of P-wave velocity in a saturated soil does not represent the velocity in the soil alone. Das (1983), suggested that a P-wave propagates in a saturated soil via the pore water and the soil skeleton, i.e. two components; a 'fluid' wave and a 'frame' wave.

2.5.2 Shear Waves (S-waves)

These waves (also known as transverse, distortional, equivoluminal and secondary waves), cause particles to vibrate perpendicularly to the direction of the wave propagation. S-waves may be polarised into a single plane, e.g. a vertical plane (S_v-

wave) or a horizontal plane (S_h-wave) (Figure 2.4). A propagating S-wave causes a change of shape (distortion) of an element in the medium, but no volume change. Figure 2.5 illustrates the wave forms generating by pile driving.

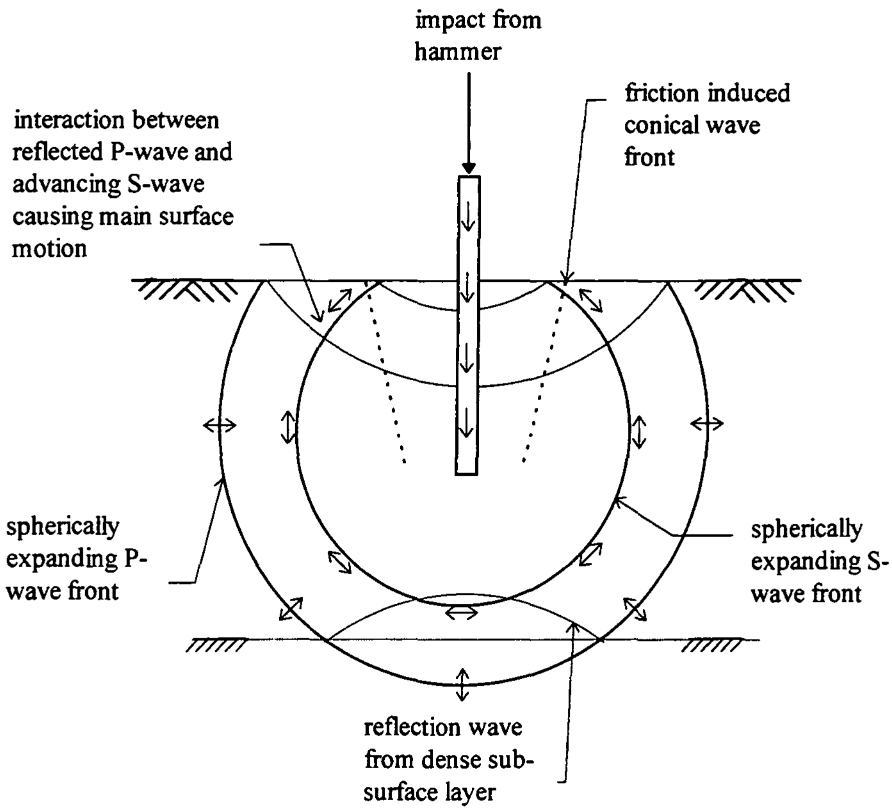

Figure 2.5 Propagation of ground vibrations from a pile driving operation (after Attewell and Farmer, 1973).

Propagation of a shear wave depends on the degree of saturation of the medium. Because pore water has no shear strength, the S-wave velocity in a saturated soil represents the wave velocity in the soil only if the particles remain in direct contact. The propagation velocity (usually given in m/s) of body waves is related to the elastic properties of the material through which they pass (typical values are presented in Table 2.2):

P-wave velocity = $V_P = \sqrt{\dfrac{\lambda + 2G}{\rho}}$ S-wave velocity = $V_s = \sqrt{\dfrac{G}{\rho}}$

where: G = shear modulus

ρ = density

$\lambda = \dfrac{2\nu G}{(1-2\nu)}$, where ν = Poisson's ratio

Material	Velocities (m/s) V_P	V_s	Poissons Ratio (ν)	Unit Weight (MN/m^3)	Young's Modulus (E) (MN/m^2)	Shear * modulus (G) (MN/m^2)
loose sand	1450-1550 (185-450)	100-250	0.48-0.50 (0.30-0.35)	1.5-1.8	44-330	15-110
medium sand	1500-1750 (325-650)	200-350	0.47-0.49 (0.2-0.3)	1.7-2.1	200-750	70-250
dense sand	1700-2000 (550-1300)	350-700	0.45-0.48 (0.15-0.3)	1.9-2.2	670-3000	230-1000
firm clay	1500-1700	180-300	0.47-0.50	1.7-2.1	160-570	55-190

Table 2.2. Typical physical properties of soil (from the CIRIA Technical Note 142, 1992) (values in brackets are for non-saturated material).

2.5.3 Surface Waves

These waves exist at the surface or in the vicinity of bounded media that have different acoustic impedances (i.e. different densities, for example). Surfaces waves include Rayleigh Waves (R-waves) which are a combination of multiply refracted and reflected P and S_v waves, with no horizontal shear component and Love Waves (Q-waves) which are horizontally polarised shear (S_h) waves transmitted through a surface layer. R and Q waves may be observed within the large scale that is associated with seismic wavetrains. These waves do not become distinct until body waves have suffered a large degree of attenuation. On the smaller scale associated with construction related vibration, it is unlikely that such waves will have separated sufficiently to allow their discrete identification. Bhandri (1981), considered that Rayleigh waves were the 'most important' wave; vertical components compact the soil in depth close to the vibration source, the horizontal component becomes more significant as distance increases.

* Where: $E = 2G(1+\nu)$ and $G = \dfrac{E}{2(1+\nu)}$

In addition to the above surface waves, low amplitude shear waves are produced by skin-friction along the soil/pile interface and a surface wave is created when this shear wave intercepts the surface. Similar to pure body waves, these waves are significant only in a zone close to the pile (approximately 3-4 times the pile penetration depth). Table 2.3 summarises the characteristics of body and surface waves.

Compressive wave	Shear wave	Rayleigh wave
Highest propagation velocity	Intermediate propagation velocity	Lowest propagation velocity
Longitudinal oscillation	Transverse oscillation	Vertical oscillation, but develops horizontal component with distance
Propagation velocity increased below water table	Propagation velocity decreased below water table	Propagation velocity unaffected by groundwater but generally lower in partially saturated soil
Propagation velocity increases with material stiffness	Propagation velocity increases with material stiffness	Propagation velocity increases with material stiffness and is independent of frequency in homogeneous material
Energy proportion propagated is low	Energy proportion propagated is intermediate	Energy proportion propagated is high
Displacement amplitude is proportional to $\frac{1}{\text{distance}}$	Displacement amplitude is proportional to $\frac{1}{\text{distance}}$ except along the ground surface when amplitude is proportional to $\frac{1}{(\text{distance})^2}$	Displacement amplitude is proportional to $\frac{1}{(\text{distance})^{0.5}}$

Table 2.3. Summary of the characteristics of propagation waves (generated by loading half-space) (from the CIRIA Technical Note 142, 1992).

2.6 Attenuation of Ground Vibrations

A soil particle experiencing vibration responds to the combined effects of different levels of wave energy, which induce a particle motion that reaches a peak value before reducing as the wave passes. The techniques of wave propagation mechanics enable the superposition of vibrations to be filtered, separated and analysed, for applications such as geophysical and archaeological mapping, in addition to construction related concerns.

Wave propagation attenuation is affected by the properties of the soil or rock and by the amplitude of motions (the cyclic strain magnitude). The magnitude of ground motion, at a given distance from a vibration source, principally depends on the magnitude of the source and the attenuation characteristics of the ground.

Attenuation of ground vibration (surface and body waves) occurs due to geometric enlargement with distance from the source. This damping can be attributed to the decrease in the energy density of the wave as it expands outwards and encompasses a greater volume of soil. As a result of the decrease in energy density, there is a corresponding decrease in the amplitude of particle vibration. In addition to geometrical damping, there also exists a material damping as the wave propagates through the soil. This damping is associated with the expenditure of energy that is necessary to overcome the internal frictional resistance that exists between particles as wave fronts pass through soil. Material damping has been found to be a function of the void ratio, shear strain and confining pressure of a soil unit. The contribution of the frictional characteristics of a soil on attenuation is small compared to the effects of geometrical damping (Ming *et al.*, 1989). Thus, for most practical purposes this effect can be neglected and only geometrical attenuation factors need to be considered.

Empirical relations have been developed that express attenuation in terms of the reduction of peak particle velocity (*ppv*) with distance. Theoretically, P and S waves attenuate at a rate that is inversely proportional to the stand-off distance. Whereas, surface waves attenuate at a rate that is inversely proportional to the square root of the surface distance. Closer to the source, P and S waves attenuate through complex processes which are frequency dependant; the higher frequencies are attenuated more rapidly than lower frequencies. Buried objects, such as adjacent foundations, service pipes and layers of discrete acoustic impedance (density and soil type), will modify the form of the vibration.

Because of the many variables involved, no explicit relations exist that allow the accurate predictions of magnitude for specific source energy and ground conditions. Approximate empirical relations have been developed based on case studies (Uromeihy, 1990), and these concentrated on deriving simulated resultant peak particle velocities at the ground surface. The dominant wave component being measured is the surface wave. For example, Attewell and Farmer (1973) suggested the following conservative relation:

$$v = 1.5\sqrt{E}/r$$

where: E = pile energy input per blow (kJ)

r = surface distance (m)

v = peak particle velocity (mm/s)

Work reported by Attewell *et al.* (1990), Attewell *et al.* (1992) and Oliver and Selby (1991) developed a knowledge-based system which can be used to make broad predictions of vibration levels for a given site with particular types of pile and hammer. This work confirms the general relationship:

$$v = b\left(\frac{\sqrt{E}}{r}\right)^x$$

Note that the above expression should only be used for stand-off distances that are greater than approximately 10m. For impact hammers, the suggested vibration velocity estimation can be based on the following parameters: $b = 1.33$ and $x = 0.73$. For vibrodrivers, the parameters for estimation purposes are: $b = 1.18$ and $x = 0.98$.

More recent work has derived the following relationship, for granular soils and stand-off distances greater than 2m:

$$ppv = \frac{1 \times w^{0.5}}{r} \quad (r > 2\text{m})$$

where: w = input energy per cycle (kJ) (after Attewell, Selby and O'Donnel, 1992).

2.7 Vibration From Pile Driving

The use of piled foundations is a construction method that is used to transmit structural loads to lower ground levels which are capable of sustaining the applied loads. Piles are usually driven into the ground by means of driving hammers such as hydraulic, diesel and vibrodrivers. Hammers are designed to maximise driving performance and minimise ground vibrations generated during driving activity.

The technique of pile driving uses a hammer falling through a particular drop height, to transfer energy to the pile-head and advance the pile into the ground. The transferred energy travels down the pile and a proportion is transmitted into the surrounding soil through the pile-toe and pile-shaft. The energy transmitted into the soil propagates as spherically expanding body waves. The major source of energy that causes ground vibration is produced by toe penetration, while shaft friction contributes lower energy levels. Ground waves resulting from toe penetration have significant components of P waves and shear (S_v) waves (Selby, 1989). The magnitude of the vibration generated by pile driving is primarily controlled by three factors i.e. pile type, hammer type and ground conditions. Records of ground vibrations show that within 10m of piling activities, levels of vibration varied between 5-25mm/s at frequencies of 15-60Hz (approximately 0.05-1.0*g*) for a range of drivers, pile types and ground conditions (Uromeihy, 1990).

When ground vibrations and soil disturbance are restricted to negligible levels, other methods such as augered cast *in-situ* piles may be necessary. In addition, static load-type hydraulic piling machines are available (e.g. the Yosa 'Still Walker') that presses-in piles without vibrations. Such equipment is popular in Japan and is now spreading to Europe, North America and Asian countries.

2.7.1 Types of Pile and Hammer

Piles are structural members which can be made of materials such as steel, concrete or timber. Bearing piles are used in the construction of foundations, which carry superstructure loads to deeper and stronger strata, increasing bearing capacity and reducing the potential settlements of foundations in weak compressible soils. Thin walled sheet piles are used in engineering construction projects such as land reclamation projects and sea defence works.

Generally, piles are classified with respect to the method by which load is transferred to the soil, for example:

<u>Friction piles</u> - The applied load is transmitted to the surrounding soil primarily through friction at the soil-pile shaft interface, although some of the load is carried by the pile toe.

<u>End bearing piles</u> - The pile is driven into a layer having a high bearing capacity and the applied load is transferred from the pile to the surrounding soil mainly through the pile toe, although some of the load is carried by skin friction.

The British Standard BS 5228: Part 4 (1986), classifies piles according to their functions, either as:

Load bearing piles - These include jacked, driven and bored piles

Retaining piles - Which include sheet-piles and diaphragm walls.

In addition, piles may be classified as displacement piles, small-displacement piles or non-displacement piles. The soil around a displacement pile is disturbed and laterally displaced during pile driving. The properties of the surrounding soil are changed, and demonstrate local compaction in cohesionless soils and a reduction of the shear strength in cohesive soils. Small displacements piles, such as H-section and steel sheet piles, cause small changes in the strength and properties of the surrounding soil provided that such piling activity does not induce plugging. In the case of non-displacement piles (augered, bored piles and drilled casings), the volume of excavated soils corresponds to the volume of the pile.

Driven piles are installed into the ground by means of a hammer. A hammer is a device that inputs sufficient energy to drive a pile into the ground. There are many types of hammers available to suit driving different types of piles in varied ground conditions. The selection of the most effective type of hammer for a given task involves the consideration of the length and weight of the pile, and the ground conditions. Redhead (1986), suggested that the selection of a successful driving hammer depends on the dimensions of the pile, soil and site conditions, the working load and factor of safety, whether the piles are vertical or raking and any other special requirements.

Hammers may be classified into two main types, (a) impact hammers, which include drop hammers, steam and air hammers, diesel hammers and hydraulic hammers and (b), vibratory hammers. For information concerning such hammers, reference should be made to manufacturer's handbooks, and available texts, including Harris (1983) and Tomlinson (1977).

A pile driving assembly using a drop hammer, consists of a Leader which has the function of holding and guiding the pile and hammer at its correct alignment from the stage of first pitching in position to the final penetration. A cap which is made of cast steel, is attached to the top of the pile to protect the pile-head from damage that may be potentially caused by the hammer during driving. A cushion (or dolly) may be used between the pile-head and the cap to reduce damage from the hammer impulses. Both cushion and dolly are made of wood or plastic. The ram is the rising and falling part of the hammer which delivers the blows. The notional input energy of most impact hammers can be obtained by multiplying the ram weight by the drop height, i.e. ram mass x g x drop height (Kg x 9.81m.s^{-2} x m = Nm = J).

With good construction practice including a carefully aligned vibrodriver, and piles that are well-supported by a gate, vibrations can drop very quickly to acceptable levels. At other sites, with somewhat more relaxed vibrodriving controls, much larger peak particle velocities have been recorded at considerable stand-off distance. For example, if a hammer is set such that an eccentric strike is delivered to the pile, greater surface vibration (additional P waves) can occur in the direction of eccentricity. Work carried out by Selby (1989) reported that for given conditions that produce ground vibrations of approximately 1.5g at a 0.25m stand-off, an eccentric hammer strike caused approximately 2.5g for the same stand-off distance

2.7.2 Vibratory Hammers

The vibratory hammer, or vibrodriver, is a type of hammer that introduces continuous sinusoidal vibration into the soil and the adjacent ground during its operation. The soil particles are forced to vibrate at the operating frequency of the vibrodriver, irrespective of the preferred frequency of the ground. The forced vibration may be made up of a number of component frequencies, but the dominant frequency will be that of the vibrodriver. This method is used to reduce the pile-soil interface friction and toe resistance during driving, and hence driving time (O'Neil *et al.*, 1990), allowing pile penetration under a relatively small surcharge. The vibrodriver is suitable for driving most types of pile in granular soil deposits.

Vibrodrivers may be classified into two main groups, i.e. sub-sonic vibrodrivers which operate between 6-50Hz, and sonic vibrodrivers operating up to 140-150Hz. According to PTC Vibrofonceur (1986), vibrodrivers are also classified with respect to their driving frequencies, i.e. standard, or high frequency "City" vibrodrivers (above approximately 35Hz).

Research into the vibratory driving of piles and practical applications began in Germany in the 1930's. The concept of vibrodriving was discovered at approximately the same time in Russia, as a by-product of soil dynamics research. In 1953 definitive theoretical treatments of vibrodriving and hammering were developed by Neimark (1953), and Blekhman (1954). Tatarnikov designed the VP low frequency range of machines (7-16Hz) in 1955, to extend the method to piles of larger point resistance, assisting penetration. In 1959, Barkan used the concept of pile-soil resonance to increase the capacity of vibrodrivers. At the same time, in the USA, Bodine developed a high frequency resonant driver, exploiting the resonance of the pile (rather than the soil-pile system). By 1962 vibrodrivers were being produced commercially in West Germany, France, USA, USSR and Japan (Rodger and Littlejohn, 1980). By 1980 it was reported that in the USSR, about 400,000Mg of sheet piling and more than 100 million metres of exploration boreholes were installed by vibrodrivers.

From the range of available published information it would appear that the choice of frequency of vibrations should be related to soil type: coarse grained soils, 4-10Hz; fine-medium sands, 10-40Hz; cohesive soils 40-100Hz. In addition, a high displacement amplitude (10-20mm) should be selected for piles with a high point resistance, and a small displacement amplitude (1-10mm) for piles with a small point resistance (Rodger and Littlejohn, 1980).

Currently, a wide range of models are available with a range of input energy and frequency. Recently, the vibrodriver has become a popular choice among pile driving contractors, especially when piling is undertaken in residential areas where low noise and vibration levels are demanded by the local authorities.

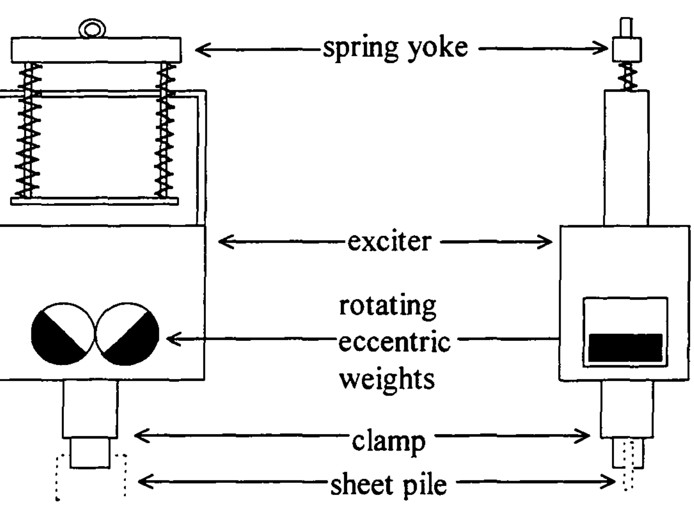

Figure 2.6. The basic components of a vibrodriver.

As an example comparison between vibrodrivers and drop hammers, a steam hammer was reported to drive a pile some 20m in 90 minutes. A vibrodriver working approximately 9m away, sank a similar pile 21m in 42 seconds. The soil at the site was very-fine to coarse sand with some gravel and trace silt. In another case, a vibrodriver installed and extracted a 22.5m pile seven times, while the stream hammer drove a pile 3.6m (Prakash, 1981).

The advantages of the vibrodriver over other forms of hammer (i.e. drop hammers) are: that vibrodrivers can be used for both driving and extraction; they produce low piling vibrations; driving noise is low; it achieves rapid driving in granular conditions; there is a low risk of damage to the pile head; and they are lightweight compared to impact hammers. The disadvantages are: that vibrodrivers are generally not suitable for driving in cohesive soils; not very efficient in medium dense to dense granular materials; their use causes a substantial increase in ground vibration when the operating frequency matches the resonant frequency of the adjacent soil and during driving operations and the load-carrying capacity of a pile cannot be estimated.

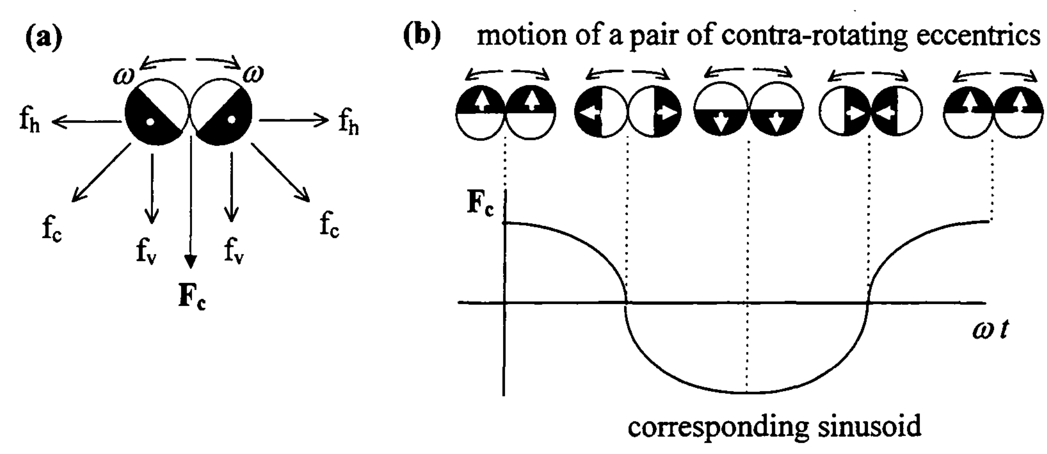

Figure 2.7. The principle of vibrodriver operation.

2.7.3 The Standard Vibrodriver

Standard vibrodrivers are comprised of three units: a vibro-hammer, a power pack and pressure cables. A vibrodriver consists of several pairs of eccentric masses rotating at the same angular velocity, in opposite directions. The rotating masses are driven by either electric motor, or more commonly by hydraulic action. Each eccentric mass produces a centrifugal force (f_c), in which the horizontal components (f_h) cancel each other out while the vertical components (f_v) are additive, giving a vertical resultant (F_c), and cause a reciprocating force of the hammer (see Figure 2.7a). The vertical forces are greatest when the eccentrics reach the top or bottom positions. The mechanism of the hammer operation and the components of a vibrodriver are illustrated in Figures 2.6 and 2.7b, respectively. If each eccentric mass is expressed as $m/2$ and their position from the centre of the mounting shaft is r, then f_v at the top and bottom position is:

$$f_v = 0.5\, mr\omega^2$$

and,

$$F_c = f_v + f_v = mr\omega^2$$

where ω is the angular velocity (rads/s) of the eccentric masses.

When the eccentrics are at some angle described as ωt from the vertical, then f_v is given by :

$$f_v = mr\omega^2 \sin(\omega t) = f_c \sin(\omega t)$$

Figure 2.7 also shows the relationship between the applied force and the amplitude of the wave generated during the operations of the hammer.

A pair of hydraulically adjustable clamping jaws allows the hammer to be fitted on to different sizes and profiles of pile head. Spring or shock absorbers are used to prevent transmission of the vibration from the hammer to the crane carrier. The whole unit is housed in a steel case and suspended from the crane by a lifting rope. The operation of the hammer, control of the running frequency and the action of the clamping device can be performed using a hand-held remote control device.

The basic principal behind this type of hammer is to reduce the friction forces between the two moving elements of the pile and soil by applying vibration to the pile through the hammer. The applied vibration causes a temporary state of instability or liquefaction in the surrounding soil which causes a reduction of friction at the pile-soil interface. The pile is then driven down under the combined weights of the pile and hammer assembly. The energy per cycle of a vibrodriver is approximately equal to the power divided by the frequency. Table 2.4 provides specification data for a selection of vibrodrivers.

Note that some diesel and air hammers operate at a stroke rate of approximately 1Hz or higher, which is approaching the response of vibrodrivers and hence the character of the vibrations in the surrounding soil. For example, the DE 50-C (diesel hammer) operates at just less than 1Hz and the MKT Air Hammer #6 operates at 6Hz.

	Manufacturer and Vibro-Driver Model				
Specifications	ICE 428B*	PTC 13HF1	MKT V-17	ICE 815	ICE 1412
Eccentric moment (kgm)	4	13	(~ 25)	46	115
Maximum centrifugal force (kN)	340	755	802	1250	2300
Frequency (Hz)	47	38	28	13 - 26	13 - 23
Maximum amplitude (mm)	10	22	19	20.4	27
Power pack (kW)	84	120	196	300	442
Energy/cycle (kJ/cycle)	2	3	7	11	19

Table 2.4. A range of typical vibrodrivers and specifications.

2.8 Ground Condition

In cohesionless soils, a driven H-pile will displace soil radially outwards and possibly downwards. Local compaction may occur due to the introduction of the pile volume into the soil. The magnitude of compaction depends of the initial soil density, degree of saturation, type of driven pile and the input energy from the hammer. Induced vibration in the soil may compact loose soil, and loosen a dense soil. Plugging may occur when an open ended tubular pile is driven, introducing high lateral stresses acting on the internal surface of the tube.

In cohesive soil, depending on its density and pore pressure, the driven pile may cause the soil to be displaced, remoulded, sheared or distorted and a high pore water pressure may develop around the driven pile. In stiff clay, because the soil cannot be compacted (the volume tends to remain constant), the soil may respond to the intruding

*where: ICE = International Construction Equipment BV, Holland. PTC = Procedes Techneques de Construction, France. MKT = McKiernan-Terry Manufacturing Inc., USA.

pile volume by demonstrating some upward ground movement. The upward movement may produce an extensive radial cracking system in the soil around the driven pile.

The instantaneous increase in pore pressure in loose and saturated cohesionless soil causes a reduction in the shear strength of the soil which leads to liquefaction. The loss of strength occurs due to a transfer of intergranular stress from the grains to pore water. The application of sudden stresses during pile driving from the driving equipment to the soil may increase the pore water pressure of the soil which consequently increases the possibility of local liquefaction around the driven pile. Risk of liquefaction is higher when a vibrodriver is used than any other type of impact hammer because the vibrodriver introduces a continuous vibration into the ground which lasts for a longer period of time. Since the pressure wave introduced by an impact hammer is discrete, its effect is less. The occurrence of liquefaction develops the process of consolidation and settlement of the soil.

When a pile is driven into strong stratum, e.g. towards bedrock, the pile may shatter, disrupt and break the weathered and weak rock. The resistance will be at its maximum at the pile base and the driving should stop as soon as the pile reaches bedrock, otherwise some damage may occur at the pile toe, reducing its bearing capacity.

2.9 Other Sources of Ground Vibration

In addition to vibrations generated by pile driving, ground vibrations are generated by a number of natural or artificial processes. Natural vibrations, such as earthquakes, release a large magnitude of energy in a very short time period, and severe damage may be caused to buildings and structural foundations. Artificial vibrations, generated by civil projects, occur frequently; their effects are less damaging than natural vibrations, and are potentially controllable.

The maximum energy released from an artificial source, excluding nuclear blasts, is up to 10^9 joules. A medium sized earthquake can release energy of 10^{12} joules (Skip, 1984). Energy released by an earthquake may cause two types of displacement on the ground surface: permanent and transient (Ambraseys and Jackson, 1984). Faults are typical examples of permanent displacement which are caused by the lateral movements of the crustal surface.

Frequencies of vibration generated by natural sources are usually much lower than those caused by artificial vibration. The dominant frequencies of earthquakes, for example, are in the order of 1-10Hz, and those of wind are typically between 0.005-0.5Hz. Recent studies of the vibrations recorded from artificial sources showed a frequency range of 10-50Hz for rail traffic, 15-50Hz from quarry blasting and 15-85Hz from pile driving operations.

CHAPTER 3
GRANULAR SOIL

3.1 Introduction

Soil is a natural material that is formed by the complex interrelationship between the agents of erosion, transportation and deposition (Section 3.2). 'Granular soils' are those which contain a majority of particles of large size (see BS 5930:1981, for the classification of soils in terms of particle size distribution characteristics), such that the soil behaviour is dominated by the interparticle friction which is proportional to effective intergranular stress. Geological materials are inherently variable, inelastic, heterogeneous, often anisotropic and complexity is the rule (Section 3.5). Because of this complexity, motions generated by such processes as pile driving are complicated and not easily amenable to theoretical treatment (Ming *et al.*, 1989).

The study of soil mechanics (and the related disciplines of geotechnical engineering and engineering geology) describes the mechanical properties and strain behaviour of soil (and rock) when subjected to changing stress. Because many soil mechanics texts are available (e.g. Craig, 1989, Atkinson, 1993, Attewell and Farmer, 1976, and BS 1377, 1990), the physical description, mechanical properties and the standard tests performed to quantify soils are not described here in detail.

More germane to this research is an introduction to the study of soil dynamics (Section 3.6). The characteristics of soils that are relevant to engineering applications and the tests that are performed to study them are outlined. Dynamic tests allow the study of soils under dynamic loads. Tests may be performed at small strain, or until a criterion of sample failure is achieved, such as liquefaction. The parameters that influence liquefaction potential include: the grain size distribution of granular soil; the density of the material; the vibration characteristics; location of drainage and dimensions of the deposit; the magnitude and nature of the superimposed loads; the method of soil formation and soil fabric; period under sustained load; previous strain history and degree of saturation (Section 3.10). The method by which such parameters are studied is determined by appropriate strain magnitudes: small strains (around 10^{-5}) are investigated using the resonant column test; larger strains may be investigated using cyclic shear test, cyclic triaxial test and shaking table test (Section 3.6.1-3.6.5). Soil dynamics texts by Das (1983) and Prakash (1981) are recommended for further reading.

It is well known, in the study of granular mechanics, that noncohesive soils may be compacted by vibration. Compaction of granular soil by surface vibration was introduced in Germany in the 1930's (d'Appolonia *et al.*, 1969), and the subject of dynamic sand compaction has seen much interest in the last four decades (Section 3.8). Much experimental work and theoretical data are available on the subject (Sawicki, 1987). It is recognised that a paper by Seed and Lee (1966) began the interest in the cyclic response of saturated granular materials. Early work involved the development of new experimental techniques and qualitative descriptions of sand behaviour under cyclic loading (Silver and Seed, 1971a,b). Sawicki (1987) reported that extensive reviews on the subject of cyclic loading are available by Zienkiewicz *et al.* (1978), Finn (1982), Ishihara and Towhata (1982) and Martin and Seed (1982).

Ground settlement *per se* does not damage structures; differential ground settlement causes angular distortion and ground strains that cause damage. In the study of ground settlements, it has been assumed that a given set of circumstances produce unique settlement values. However, field measurements show that settlements can vary appreciably over quite short distances in apparently uniform deposits. Data show that more variation occurs in sands than in clays, further emphasising the difficulties of settlement prediction in these materials (New and O'Reilly, 1991). Note that Seed and Silver (1972) emphasize that even under static load conditions, the evaluation of settlements in sand deposits are subject to considerable error, in the order of ± 25 - 50%. For the complex conditions associated with dynamic events, it is unreasonable to expect that settlement estimations could be made with even this degree of accuracy. However, even approximate evaluations of potential settlement are adequate for many purposes.

3.2. A Note on Soil Formation

Much of the geomorphology of the British Isles shows evidence of direct or indirect glacial activity. Direct activity is related to the action of the glaciers that formed features such as 'U'-shaped valleys, tarns (mountain lakes) and moraines (formed by material deposited during glacial retreat). Indirect activity may be found in areas that were not glaciated, but did experience glacial outwash that deposited gravels, sands and fines, in the area of Britain south of a line drawn from the Bristol Channel to the mouth of the Thames. There are relatively few places in Britain where there are deep uniform deposits.

The maritime temperate climate of the British Isles implies relatively high rainfall and a dominance of fluvial processes that affect soil deposit morphology (spatial distribution and composition). In addition, the physical processes of 'freeze-thaw' act initially to split rock fragments from a parent material, and contribute material to upland water courses.

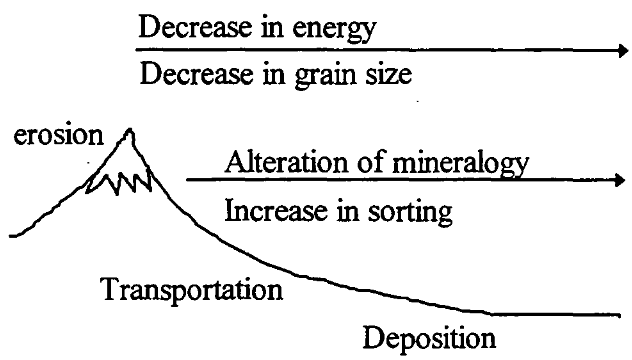

Figure 3.1. Summary of the surface processes.

Water moves from a high energy level to a low energy level: a mountain stream will eventually meet the sea as an estuary. A high energy mountain stream is characterised by narrow channels and carries a bedload of relatively large, angular material which may be scree brought down from the sides of a 'U'-shaped valley. Progressing downstream, tributaries will join to form larger channels, relief is reduced and flow energy decreases. Particle size is reduced also by attrition and maximum size of the transported material decreases.

If a sediment trap is encountered, i.e. an upland lake, the relatively still water causes a particle size differentiation. As the energy of the transportation agent is reduced, heavier particles will be deposited first, then progressively finer material. Thus, a river that flows from the lake to the sea may not transport material that reflects the geology of upland areas above the lake.

As relief becomes less steep, energy levels and erosion decrease and deposition tends to dominate. In addition, the mineralogy of the river material becomes less diverse as minerals that are less resistant to physical and chemical alteration are broken down and deposited. For example, mica is weathered to form clay minerals. By the mouth of a river (and at other sediment traps) sand deposits will dominate, because quartz is the most physically and chemically resistant of the common rock forming minerals. Such sand deposits may be further sorted into size ranges by the action of tides, for example. Natural harbours (low energy environment) and other energy shadows will tend to demonstrate accumulations of mud (clays and silts).

	Water	Air	Ice	Gravity
Size	Reduction due to solution	Considerable reduction	Considerable grinding & impact	Considerable impact
Shape and roundness	Rounding of sand & gravel	High degree of rounding	Angular, soled particles	Angular, non-spherical
Surface texture	Sand: smooth, polished Silt: little effect	Impact produces frosted surfaces	Striated surfaces	Striated surfaces
Sorting	Considerable sorting	Very considerable sorting	Very little sorting	No sorting

Table 3.1. The effects of transportation on soil particles.

Thus, the action of fluvial transportation tends to reduce the size, angularity and diversity of mineralogy at different rates, depending on the resistance of the rock and its constituent mineralogies (see Figure 3.1). The action of aeolian transport (by air, over the land surface) will cause a similar breakdown of material, but may lead to strongly uniform particle sizing. Table 3.1 summarises the effects of various transportation agents on soil particles.

3.3 The Nature of Granular Soil

For engineering purposes, a soil may be described as any natural uncemented or weakly cemented accumulation of mineral particles, generated by the weathering of rock (or pre-existing soil) and includes the void spaces between the particles and the presence of air and water within the voids. Soils may also be weakly cemented by the precipitation of (ferruginous, calcareous, siliceous) minerals, oxides and organic matter. A deposit of 'mineral particles' placed by artificial means (i.e. by man), is known as 'fill'.

The process of soil formation involves the physical and/or chemical breakdown of a parent material. Physical weathering produces particles that have the same chemical composition as that of the parent material (a sandstone may be weathered to produce sand). The particles produced are described as equidimensional or 'bulky', and can be angular to rounded (end members of a continuous series), flat to spherical and all intermediate forms (see Figure 3.2). In addition, minor features independent of size, shape or degree of roundness are known as the 'surface texture' of the particle. Terms used to describe surface texture are: smooth or rough, dull or polished, striated, frosted, etched or pitted, and reflect the abrasive effects of the transportation agent(s) (see Table 3.1). Size ranges produced are wide, i.e. from boulders to rock flour (which is formed by the grinding action of glaciers). Structural arrangement may be described 'as single' grain, where each particle is in direct physical contact with adjacent particles forming the soil 'skeleton', there being no other bond or cohesion acting between individual grains. The strength of the soil skeleton is a function of the number of particle surface-surface contacts and the load which generates interparticle friction. Interparticle (electro-chemical) forces are negligible compared with those generated by gravity and external load.

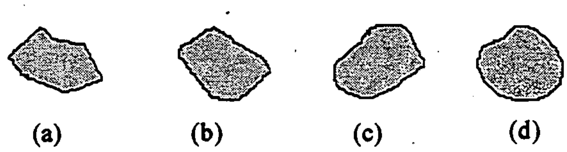

Figure 3.2. Form of soil particles; (a) angular, (b) subangular, (c) subrounded and (d) rounded.

Chemical processes of weathering alters the mineral form of the parent material by the interactions of agents such as water, oxygen and carbon dioxide. Chemical weathering ultimately forms groups of crystalline particles of colloidal size (< 0.002mm), and are known as the clay minerals. Most clay minerals are plate-like, have a high specific surface (high surface area to volume ratio) and the mechanical properties are therefore highly influenced by surface processes. Such soils are not included in the present investigation.

The engineering behaviour of a granular deposit depends on the existing structure of the soil mass, i.e. the shape, orientation and size distribution of particles within the soil mass (also known as the 'fabric' and 'architecture'), the forces acting between adjacent soil particles and pore water pressure. When describing cohesive material, soil structure also implies the mineral composition of the soil, the electrical properties of the surface of the particles, the physical characteristics and ionic composition of the pore water.

3.4 Terms and Definitions

Soils may be described as two or three phased systems, i.e. a fully saturated (or dry) soil consists of solid particles and (air or) water (two phase); a partially saturated soil has solid particles, with water and air filling the void spaces (three phase). The physical description of a soil can be made through observation of the colour, size and shape of the grains and additional *in-situ* structure (see BS 5930:1981, the British Standard for site investigation for detail). More useful to the engineer than the physical appearance of soils is the mechanical behaviour, i.e. strength and stiffness characteristics. A range of standard laboratory tests may be performed to quantify soil behaviour, which are detailed for example, in BS 1377: 1990 and Head (1984). The terms and definitions that are particularly relevant to this research are listed below:

<u>Particle size distribution:</u> Particle size distribution shows the percentage by weight of particles within various size ranges. For granular soils this may be carried out by sieving. The particle size distribution curve is plotted on semi-log paper allows the determination of the coefficient of uniformity.

<u>Coefficient of uniformity</u> (U_c): This is a parameter that characterises the range of particle sizes that form a soil. Soils that (effectively) consist of a single particle size are described as highly uniform, and have a uniformity coefficient that approaches unity. A soil with a wide range of particles (termed 'well graded' by engineers and 'poorly sorted' by geologists) will have a high value of U_c, which is defined as:

$$U_c = \frac{D_{60}}{D_{10}}$$

Where D_{60} = the size such that 60% of the particles are smaller than that denoted.

D_{10} = the size such that 10% of the particles are smaller than that denoted.

Moisture Content (w): This is the ratio of the mass of water (M_w) to the mass of solids (M_s) (usually presented as a percentage), and may be determined gravimetrically, using the oven drying technique:

$$w = \frac{M_w}{M_s}$$

Degree of saturation (S_r): This is the ratio of the volume of water (V_w) to the total volume of void spaces (V_v), where for a fully saturated soil, $S_r = 1$:

$$S_r = \frac{V_v}{V_s}$$

The void ratio (e): The ratio of the volume of voids (V_v) to the total volume of solids (V_s) is described as the void ratio:

$$e = \frac{V_v}{V_s}$$

Soil bulk density (ρ_b) : This the ratio of the total mass (M) of a soil to the total volume (V):

$$\rho_b = \frac{M}{V}$$

The units for density are kg/m^3 or Mg/m^3. The density of water (1000kg/m^3) is denoted by ρ_w.

Specific gravity of solid particles (G_s): Specific gravity is a ratio of the mass of solids (M_s) in a soil sample to the product of the volume of solids (V_s) and the density of water (ρ_w), i.e.:

$$G_s = \frac{M_s}{V_s\,\rho_w}$$

Unit weight (γ): The unit weight of a soil is the ratio of the total weight (W) (a force, i.e. Mg, mass multiplied by the acceleration due to gravity) to the total volume (V):

$$\gamma = \frac{W}{V} = \frac{Mg}{V}$$

in kN/m^3.

Relative Density (D_r): Because of the difficulty of obtaining undisturbed granular samples, it is necessary to obtain values of relative density, *in-situ*. Relative density is the relationship between the actual (field or laboratory) value of void ratio (e), and the limiting values of e_{max} and e_{min}, which are determined in the laboratory (see Head, 1984), where:

$$Dr = \frac{e_{max} - e}{e_{max} - e_{min}}$$

It has been demonstrated (e.g. Skempton, 1986) that standard penetration resistance SPT-N is primarily affected by overburden pressure. Soils with the same relative density will have different SPT-N values at different depths. Secondary influences on standard penetration resistance include soil grading and shape, degree of overconsolidation and time. Standard penetration resistance is seen to increase with increasing particle size, increasing overconsolidation ratio and ageing. Bazara (1967), using the data from 1,300 penetration values suggested the following empirical relationship between relative density, SPT-N values (N) and overburden pressure (σ_v).

$$N = 20D_r^2(1 + 2\sigma_v) \qquad \text{for } \sigma_v \leq 72\text{kPa}$$

and,

$$N = 20D_r^2(3.25 + 0.5\sigma_v) \qquad \text{for } \sigma_v \geq 72\text{kPa}$$

It has been suggested that relative compaction (Cr) is a more appropriate parameter than relative density to describe cohesionless soil *in-situ* density and settlement potential (New, 1978b). Relative compaction is given by:

$$Cr = \frac{\gamma_d}{\gamma_{d\,max}}$$

where: γ_d = *in-situ* dry density

γ_{dmax} = maximum dry density (determined using a standard laboratory technique, as described in BS 1377, 1990)

Relative compaction may be related to relative density using $Cr = 0.8 + 0.2Dr$.

Dr	Classification	N-value	$(N_1)_{60}$
0 - 15	Very loose	0 - 4	0 - 3
15 - 35	Loose	4 - 10	3 - 8
35 - 65	Medium Dense	10 - 30	8 - 25
65 - 85	Dense	30 - 50	25 - 42
85 - 100	Very Dense	> 50	42 - 58

Table 3.2. Relative density of sands. Where $(N_1)_{60}$ is the normalised blow count at σ_v = 100kPa (after Terzaghi and Peck, 1948; and Gibbs and Holtz, 1957; and Skempton, 1986).

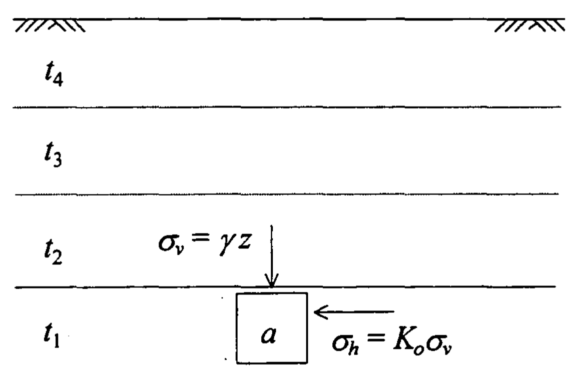

Figure 3.3. Normal stress acting upon an evolving unit of soil.

3.5. Post Depositional Influence

A number of factors will influence the mechanical properties of a soil after initial deposition. The factors that affect soil behaviour are stress, water content, time/ageing and fabric (see Table 3.3).

3.5.1 Stress

During the formation of soil, the stress at any given elevation continues to build up as the surcharge of soil over the point increases (see Figure 3.3). The diagram shows a unit of soil (a) deposited in time (t_1), experiencing an increase in overburden stress through time (t_1 to t_4), as deposition proceeds. With time, and an increase in stress, the soil unit experiences consolidation (known as 'compaction' by geologists), i.e. a reduction in volume as pore water is expelled, which allows the re-ordering of particles to a more dense configuration. Thus, the physical properties at any given elevation in a sedimentary soil are continuously changing (in geological time) as the deposit evolves.

A soil element that is at equilibrium under the maximum stress that it has ever experienced is described as 'normally consolidated' (NC), whereas a soil under a stress less than that to which it was once consolidated is 'over consolidated' (OC). More relevant to cohesive soils than to granular soil, increasing the stress on a soil unit causes an increase in density and shear strength, and a decrease in compressibility and permeability. Changes that occur due to a reduction in stress are usually less than those caused by a stress increase of equal magnitude. Of more significance to the densification of granular material are the effects of dynamic loading (see later) such as earthquakes and construction related activities.

Under static conditions, the vertical stress (σ_v) that acts upon a unit of soil is the product of the unit weight of the soil (γ) and the depth (z), i.e. γz. The horizontal stress on a unit of soil (σ_h) is equal to $K_o\sigma_v$, where K_o, the coefficient of earth pressure at-rest (when lateral strain is zero) is reasonably approximated by:

$$K_o = 1 - \sin\Phi' \qquad \text{for NC soils}$$

and,

$$K_o = (1 - \sin\Phi')(OCR)^{\sin\Phi'} \qquad \text{for OC soils}$$

where: Φ' = internal angle of friction determined from triaxial tests. Typical values of K_o are: 0.8 for compacted layered sand; 0.4 for dense sand; 0.6 for loose sand and 0.6 for normally consolidated clay.

Granular soil consists of individual particles that are in contact with each other, maintaining a state of equilibrium under a given stress condition that is induced by the external forces and self weight acting on the soil mass. Distribution of the magnitude and direction of the forces at grain-grain contact points equilibrates with the external forces. When external forces change, the contact forces change in both magnitude and direction to maintain equilibrium. Deformation of a soil mass will occur in response to changing external forces.

Because the moduli of deformation of individual soil grains is very high compared with the overall modulus of the soil mass, the deformation of the soil mass is due to the movement of grains (sliding and/or rotating) and not to a change in particle shape, i.e. a change in fabric occurs due to a change in the stress regime (Ueng & Lee, 1990). Horne (1965) considered that in a soil mass, relative movement between grains is due to sliding rather than rotation. No movement will occur between grains if the change in magnitude and direction of an external stress is less than the angle of friction resistance. Oda (1978), observed that slip and non-slip contacts exist in granular material under shear loading and that the properties of slip and non-slip contacts depend on the soil fabric and stress conditions, but only slip contacts cause the soil mass to deform. Coop and Lee (1993) testing (carbonate, silica and decomposed granitic) sands under a wide range of static stress (50kPa-58MPa) stated; that under *static* conditions, the principal means of volumetric compression is by particle crushing. Mitchell (1976), presented data that demonstrated that negligible grain crushing occurs below a major principal stress of 100kPa.

Factors Influencing Behaviour of a Deposit	Factors Contributing to Changes in Soil Behaviour
Sedimentary Soil Nature of sediments Methods of transportation and deposition Nature of depostional environment Compacted Soil Nature of soil Amount of water Amount and type of compaction	Stress Time Water Environment Disturbance

Table 3.3. The factors influencing soil behaviour.

3.5.2 Water

In a fully saturated soil unit, assuming that soil particles are able to move, a reduction in volume due to external loading occurs due to expulsion of water. In dry or partially saturated soil, volume reduction tends to occur as the air that fills the void spaces is initially compressed, and then expelled.

Water has volumetric strength and stiffness, but no shear resistance. Consequently, a saturated soil unit that experiences shear stress resists deformation only by the friction forces generated within the soil 'skeleton'. However, under saturated conditions, a normal stress is resisted by the soil skeleton and the water, which increases in pressure (Craig, 1987).

Pore water pressure (a hydrostatic stress) acts equally in all directions, and on the entire surface of a particle. The increase in pore water pressure due to an imposed load, will reduce the magnitude of the increase in the intergranular stress of the soil skeleton. The reduction of the stress at particle-particle contacts reduces the ability of a soil unit to resist deformation (shear and volumetric strain). That is; a change in pore water pressure alters the strength and stiffness properties of a saturated soil unit. The total stress (σ) that acts on a soil unit is the sum of stress carried by the soil skeleton and the stress transferred to the pore water (u), which is described as the effective normal stress (σ'), given by:

$$\sigma = \sigma' + u$$

The behaviour of partially saturated soils differs from that of saturated or completely dry soils (Meissner and Becker, 1995). This is due to the surface tension (or suction) forces that are generated at air-water interfaces, within the void spaces of a soil unit. Suction provides a granular soil with an apparent cohesion (an increase in 'strength'), and an ability to sustain tension forces and resist deformation. The effective stress equation for partially saturated soils is:

$$\sigma = \sigma' + u_a - \chi \left(u_a - u_w\right)$$

(from Craig, 1989)

where: χ = a factor related to saturation (Sr) (where, $Sr = 1 = \chi$, and $Sr = 0 = \chi$)

u_a = atmospheric pressure

$-u_w$= negative pore water pressure

Suction has two components: matrix suction, which is due to surface tension forces at the interfaces between water and gas (air), and solute suction which is due to the presence of dissolved salts in the pore water. The magnitude of suction depends on a number of factors, such as pore water chemistry, particle size distribution characteristics, size of void spaces, degree of saturation, fabric and temperature. In general, partially saturated clays and silts will demonstrate greater suction than partially saturated sands (see Figure 3.4). Thus, the change in the strength properties of a desaturating silty soil will be more significant than that of a sandy material.

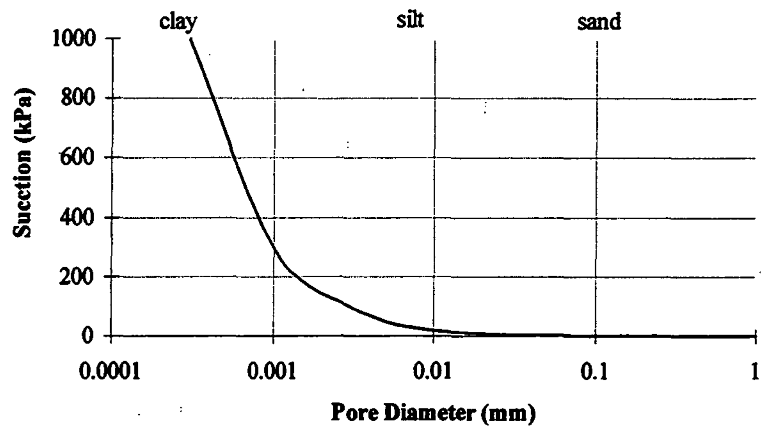

Figure 3.4. The influence of pore size diameter on limiting values of suction for a soil with uniformly shaped pores (from Toll *et al.*, 1987).

3.5.3 Time and Ageing

Time is the dependant variable for the other factors (stress, water and environment) that contribute to change in soil properties. It has been observed that freshly deposited or densified (clean) sands exhibit stiffening and strength increase up to periods of several months, i.e. "ageing" (Mitchell and Solymar, 1984) after all the density changes are complete. Dowding and Hryciw (1986) reported a significant increase in cone-penetration resistance over a period of 1-15 days after the dissipation of blasting generated pore pressures.

According to Seed (1979), ageing increase in resistance to loading is due to cementation/welding at grain-grain contacts, which is associated with secondary compression (i.e. volume change after dissipation of excess pore water pressure). However, Daramola (1980), reported that a mechanism less brittle than that of cementation is responsible for increased resistance to deformation.

Mitchell and Solymar (1984) considered that the most probable cause of this time-dependant strength gain (ageing) in quartz soils involves the formation of a silica acid gell on particle surfaces and precipitation of silica or other materials from solution as cement at grain-grain contacts. Dowding and Hryciw (1986) argued that the cement bonding mechanism required that sand grains remain stationary after deposition or densification, so that connections by a cementing agent is possible. Mesri *et al.* (1990) believed that improved resistance to deformation through time was more reasonably attributed to the continual particle rearrangement after deposition. A gradual increase in sliding resistance through micro interlocking of surface roughness and increased geometrical grain interference through time was proposed.

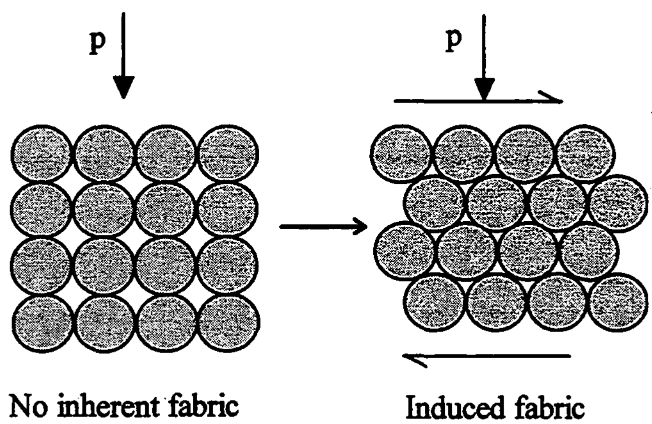

Figure 3.5. Generation of induced fabric due to shear forces.

3.5.4 Fabric

It is recognised that the spatial arrangement of soil particles, associated voids and particle shape, i.e. soil *fabric* (Oda, 1978) contributes significantly to the behaviour of granular soils that are subjected to stress changes.

Volume change and shear deformation depend significantly on the pre-existing static stress before additional loading begins. During increasing load, the work done on a soil sample is dissipated by rearranging the particles which induces irrecoverable strain (Timmerman and Wu,1969).

Two types of fabric may be recognised when describing the response of a non-cohesive soil to changes in applied external forces:

<u>Inherent fabric</u> - This type of fabric is established by sample preparation in the laboratory and in natural soils as a result of the depositional process. Inherent fabric associated with sample preparation technique affects both the densification and the

liquefaction potential of samples. For example, a sample formed from slightly elongated grains by air pluviation, normally shows that the grains tend to lie with their long axis in the horizontal plane, whereas when the same sand is partially saturated and the sample is formed by tamping, the distribution of the orientations of the long axes is essentially random.

Induced fabric - This fabric is produced during deformation caused by applied loading of a sample (Nemat-Nasser and Takahashi, 1983). A sample with no inherent fabric, such as one formed from identical spherical grains will form an induced fabric when subjected to shear forces. The particles rearrange themselves and grain-grain contacts are redistributed, essentially characterising the fabric (see Figure 3.5).

With time and post-depositional changes in stress and environment, a soil may have a higher strength in the undisturbed state than it does in the remoulded state (which applies primarily to cohesive deposits). The term 'sensitivity' may be used to describe this difference in strength and is determined by the ratio of the strength in the undisturbed state to that in the remoulded state. An important factor to consider when performing laboratory tests is whether the (inherent) fabric produced by a particular method of sample preparation is similar to that found in the equivalent natural deposit. Soil behaviour is highly dependant on laboratory sample preparation technique (Mulilis *et al.*, 1977, Muira and Toki, 1982), examples of which include:

Moist tamping - This is the oldest sample preparation method, that uses tamping in layers (Lambe, 1951) of moist or dry soil. The method models a soil fabric generated by rolled construction of fills. Fine grained soils prepared by moist tamping are seen to undergo large strains during saturation which is attributed to the break-down of suction forces (Marcusson and Gilbert, 1972, Chang *et al.* 1982, Sladen *et al.* 1985).

Air pluviation - This technique models deposits formed by aeolian (wind) process and generally consist of well-sorted sand and/or silt (i.e. loess). Air pluviation of well-graded sand or silty sand is not as successful as air pluviation of uniform sand. This is due to the tendency of well-graded sands to experience particle segregation, and as the fines content increases the sample heterogeneity is seen to increase. Subsequent saturation of a sample can disrupt an initial inherent fabric by washing out of the fines. Studies conducted to examine the effects of sample preparation on soil strength have shown large differences in the triaxial behaviour of clean sands prepared by air pluviation and moist tamping (Muira and Toki 1982, Tatsuoka *et al.* 1986).

Water pluviation - This procedure is similar to air pluviation, but sand is pluviated through (boiled, de-aired) water, ensuring sample saturation. The technique is described by a number of workers, such as Lee and Seed (1967), Finn *et al.* (1971), and Vaid and Negussey (1984). Water pluviation mimics the deposition of sand through water (e.g. river, glacial outwash, tidal). Oda (1978) stated that natural alluvial soils and water pluviated soils exhibit similar fabric and behaviour. Because the terminal velocity of particles falling through water is lower than that of particles falling through air, the relative density of water pluviated soils tends to be lower than air pluviated samples. Water pluviated soils are generally more compressible during consolidation than moist tamped sands. Water pluviation should only be performed on uniform sands (Vaid and Negussey, 1984), because well graded or silty sands generally segregate and form non-uniform samples.

Slurry technique - This method of sample preparation is performed to overcome the problems associated with the water pluviation of well graded or silty sands. Samples are formed that are essentially homogenous with respect to void ratio and particle size gradation (regardless of gradation and fines content). The slurry method is reported to mimic soil fabric of natural fluvial or hydraulic fill deposits (Keurbis and Vaid 1988).

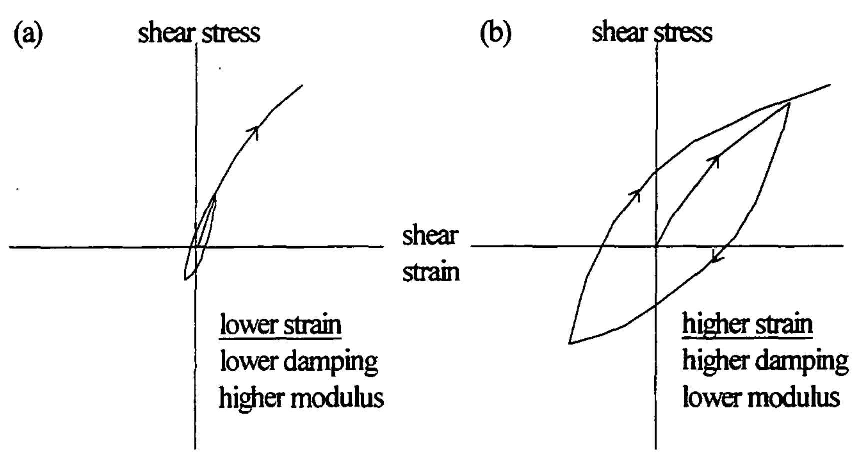

Figure 3.6. Effect of shear magnitude on dynamic soil properties (after Silver and Seed, 1971a).

3.6 Applications of Soil Dynamics

Most soils demonstrate non-linear stress strain properties (see Figure 3.6). Thus, the form of the hysteresis loop that indicates the stress-strain behaviour of soils under cyclic loading conditions for large and small strains is different (Silver and Seed, 1971a). At higher strains, the non-linearity of soil behaviour is more pronounced (Figure 3.6b).

The difference between dynamic loading and static loading is the effect of every subsequent cycle of loading as it is superimposed on an already existing material stress field (Alyoshin, 1994). A stress that is smaller than a static failure stress can cause very large strains if the load is applied repeatedly. During dynamic loading of cohesionless soils, a part of the energy is accumulated in the form of kinetic energy of the particles and is spent on their relative displacement, causing the soil density to alter (Voznesensky, 1994). The dynamic response of granular materials can result in: the compaction of loose sand, with any degree of liquefaction; liquefaction of saturated loose-medium dense sand; dilatancy in comparatively dense sands of low saturation, resulting in density decrease and consequent loss of strength and some softening of dense saturated sands, resulting from strain accumulation, without liquefaction (see Figure 3.7).

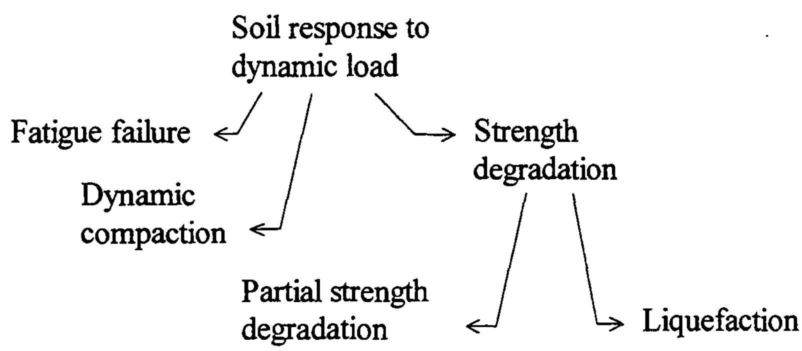

Figure 3.7. Typical soil response to dynamic loading (after Voznesensky, 1994).

Soil dynamics is the branch of soil mechanics that is concerned with the study of phenomena such as: the liquefaction of soils; vibratory compaction; dynamic earth pressures on retaining structures; analysis of soil-structure interaction and bearing capacity of shallow foundations caused by natural and man-made phenomena such as earthquakes, wind and wave action, quarry blasting, traffic, operation of reciprocating and rotating machines and construction operations such as pile driving.

Machine vibrations have often caused differential settlements of foundations that have required remedial action or limitations on machine operations. Vibrations that are caused by pile driving have caused damaging building settlements. Settlements due to traffic vibrations have caused building distortion and cracks (Silver and Seed, 1971b).

When the loads that are transmitted to a structure or soil change rapidly enough to cause the inertia forces to be relatively significant when compared to the existing static forces, calculations are required that enable the estimation and limitation of the resulting strains. The rate of loading at which a problem may be defined as 'dynamic' is determined by the mass of soil involved. For example, a typical laboratory sample will experience significant inertial forces when the frequency of loading is greater than 25Hz. However, a large dam may experience significant dynamic forces at frequencies as low as 0.5Hz. Using experimental and analytical data, design criteria for foundations subject to dynamic loads are available to the engineer. Satisfactory design involves the consideration of the cyclic displacements that result due to the elastic response of a soil-foundation system to dynamic loads and the permanent displacements that occur due to compaction of soil below a structure.

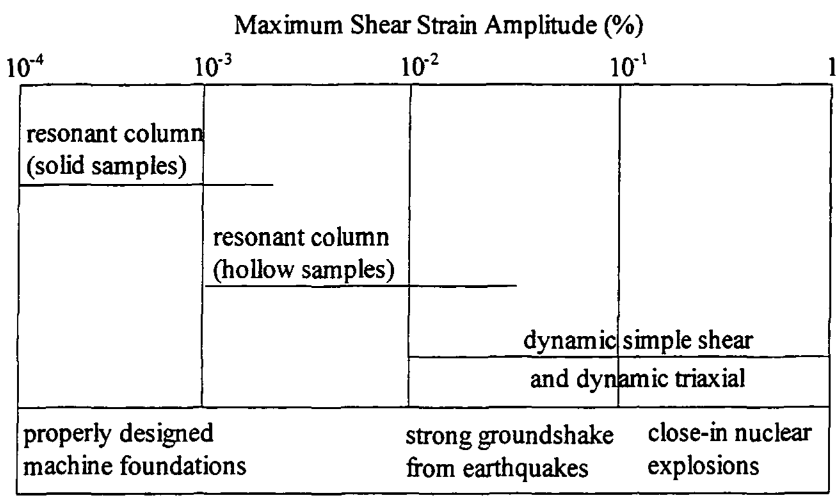

Figure 3.8. Laboratory methods for determining shear stress-strain properties of cohesionless soil (After Silver and Seed, 1971a).

The discipline of soil dynamics may be divided into two areas that reflect the geotechnical application:

a) Soil-supported structures may be affected by forces that originate outside the soil, e.g. rotating machines, dropping of weights, wind and wave action. Estimating the response of a soil to such external loads and estimating transitory and permanent displacements of a soil supported foundation is necessary.

b) The other form of the problem originates from the soil, not from the external forces acting on the structure. Such forces are transmitted to the structure which will react with its own characteristics, as well as those from the soil. For example, the motion of soil caused by the operation of compressors, pile drivers or earthquakes.

There are a number of soil dynamics tests such as the resonant column, cyclic triaxial, cyclic shear and shaking table test that are commonly used in practice (see Figure 3.8). Behaviour of soils is strain dependant; use of a particular test reflects the magnitude of strain and rate of stress reversal (frequency) imposed on to a sample until some failure criterion is achieved. Such tests are overviewed in the following sections.

3.6.1 Resonant Column Test

The resonant column test is based on the theory of wave propagation in prismatic rods (Richart *et al.*, 1970). Tests are performed to investigate the elastic and damping properties of soil (Young's modulus, shear modulus and damping ratio) under low stress levels. By varying the frequency of oscillation, a hollow or solid cylinder of soil (in the order of 35mm diameter by 72mm, Amini *et al.*, 1988) is vibrated at its lowest damped natural (resonant) frequency, either longitudinally or torsionally. Typical values of strain amplitude generated vary from approximately 0.001-1.0% or less for longitudinal vibrations and approximately 10^{-4} rads for torsional vibrations.

Values of compression wave velocity (V_p) and shear wave velocity (V_s) are produced that allow Young's Modulus (E) and shear modulus (G) to be derived (see Section 2.5.2). Damping ratio may be determined from the record of the free-vibration decay curve (Amini *et al.*, 1988). Methods and apparatus description of the resonant column tests can be found in Drnevich *et al.* (1967). Typical values of V_p, V_s, Poisson's Ratio, shear modulus and Young's Modulus are given in Table 2.2. It has been observed that values of V_p and V_s increase with increase in average confining stress. Additionally, the values of V_p and V_s are seen to decrease slightly in saturated samples, because an increase in unit weight occurs as void spaces are filled with water. V_s is also seen to be independent of gradation, and relative density, but dependant on void ratio and effective confining pressure (Hardin and Richart, 1963).

Shimming and Grey (1984) used the resonant column apparatus to examine the influence of soil suction on values of low amplitude shear modulus. The influence was observed to be greatest for soils having the smallest effective grain diameter (D_{10}), and the lowest confining pressure.

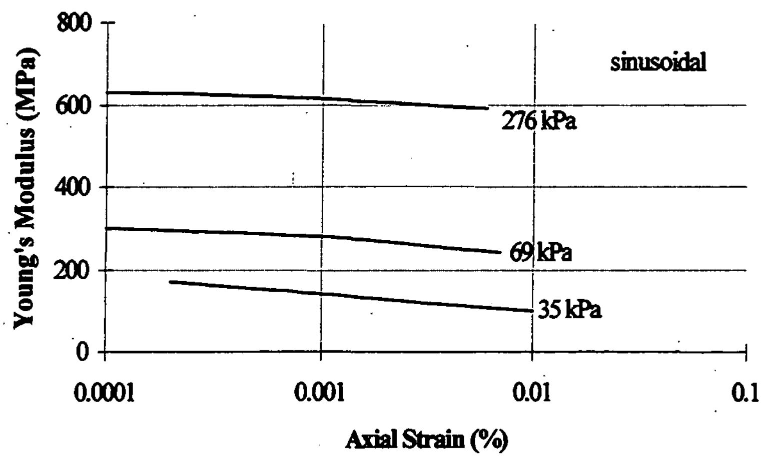

Figure 3.9 Effect of axial strain on Young's Modulus for three confining pressures (after Zhang and Aggour, 1995).

Amini *et al.* (1988) performed tests using random torsional excitation of dry sand to model the effects of earthquake loading. The results indicated that damping values are higher, and shear moduli lower than the data obtained for equivalent sinusoidal loading tests under the same rms strain. This was attributed to the fact that; for the same displacement rms, random excitations will have higher peaks than the sinusoidal signal. Zhang and Aggour (1995), conducted resonant column tests that examined the effects of three types of longitudinal excitation: sinusoidal, random and impulse on Ottawa 20-30 sand. They observed that the Young's modulus decreased with increasing axial strain (see Figure 3.9) and was not significantly affected by loading type.

3.6.2 Cyclic Triaxial Test

Earthquakes cause stress reversals to occur within the soil, which produce soil deformations (shear displacements) and a corresponding decrease in soil strength. Cyclic triaxial (drained and undrained) tests are performed to examine the dynamic soil strength response of saturated, partially saturated and dry soils. The dynamic properties of soil are also influenced by the stress condition, void ratio, ambient stress and vibration history, strain amplitude, frequency of vibration, soil structure, temperature and grain characteristics (Meissner and Becker, 1995).

Samples (with a 1:2 diameter to height ratio) are subjected to an increase in axial stress (σ_{dp}), or alternatively an increase in the axial stress of ($\sigma_{dp}/2$) and a decrease in the lateral stress of ($\sigma_{dp}/2$). The normal stress on a 45° plane is unchanged and the shear stress on the 45° plane is ($\sigma_{dp}/2$). Cyclic shear stresses of one half the peak deviator stress are applied at a wide range of frequencies, for example of 0.1Hz (Vaid *et al.*, 1990), 0.02Hz (Erten and Maher, 1995) and up to 50Hz (Meissner and Becker, 1995). Cyclic shear strength may be defined as that value of ($\sigma_{dp}/2$) that is required to cause failure in a specified number of cycles. Sample failure is commonly defined in two ways: as being a particular level of excessive strain, e.g. Prakash (1981) defines failure as 20% of maximum axial strain, whereas Erten and Maher (1995) use 5% and 10% of peak to peak axial strain, or when initial liquefaction occurs. The use of one failure criterion over another has been based on the amount of permissible strain, which is related to the importance of the project (Haldar and Miller, 1984).

Undrained laboratory tests that model liquefaction are shear related, and performed using transient loads to estimate the likelihood of the liquefaction of a granular soil unit. Lee and Seed (1967) reported that increase in cyclic shear stress or strain; decrease in confining pressure and decrease in relative density reduces the number of cycles to initial liquefaction (see Figure 3.10). Dynamic triaxial tests may be used to model 'rapid' loading rates (cycling loads between approximately 0.1-10Hz), appropriate for earthquakes. Slower, stress controlled load rates may also be used, and such tests are very similar to standard triaxial tests.

Drained cyclic load triaxial tests may be performed to study occurrences where liquefaction does not take place. Lee and Albaisa (1974) reported that compared to the dramatic effects that are associated with destructive earthquakes, ground settlement of less than 1%, or even 2-3%, is not very spectacular. It is not surprising that large quantities of field or other laboratory data do not seem to be available. During drained tests under low static stress, permanent volume change was found to be much larger than permanent shear strain. The reverse occurred when the static shear stresses were relatively high (Chang, 1988).

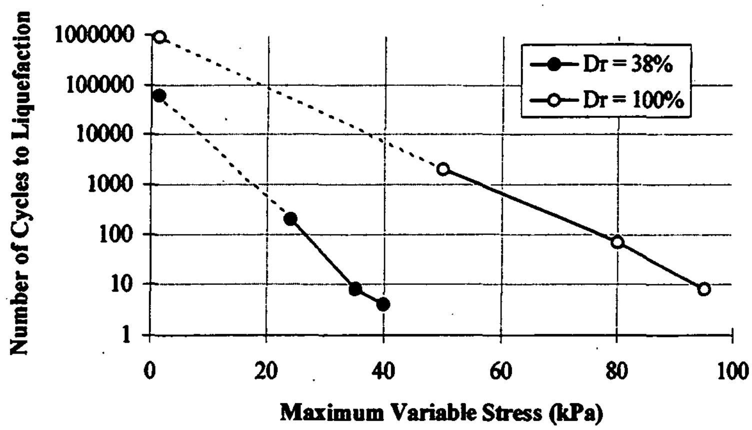

Figure 3.10. Number of cycles to initial liquefaction of a fine river sand, for a range of variable stress with a confining pressure of 100kPa (after Lee and Seed, 1967).

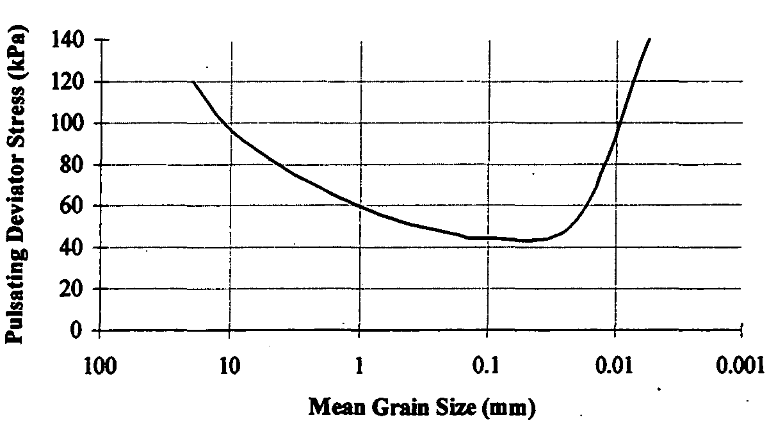

Figure 3.11. Comparison of (0.1Hz) pulsating loading strengths of soils with different grain size after 30 cycles (D_r = 50%, for 20% strain and σ_c = 105kPa, after Lee and Fitton, 1969).

It has been observed that the effects of particle-size distribution and grain shape are less significant than the grain size, i.e. coarser grained soils experience larger volumetric strains (see Figure 3.11) (Lee and Fitton, 1969; Lee and Albaisa, 1974; Vaid *et al.*, 1990). However, grain shape may be a more fundamental parameter than grain size because larger particles in a given soil unit tend to be more rounded. Lee and Albaisa (1974) suggested that soils with the same mean grain size (D_{50}) and relative density will demonstrate similar volume changes, regardless of the value of the coefficient of uniformity.

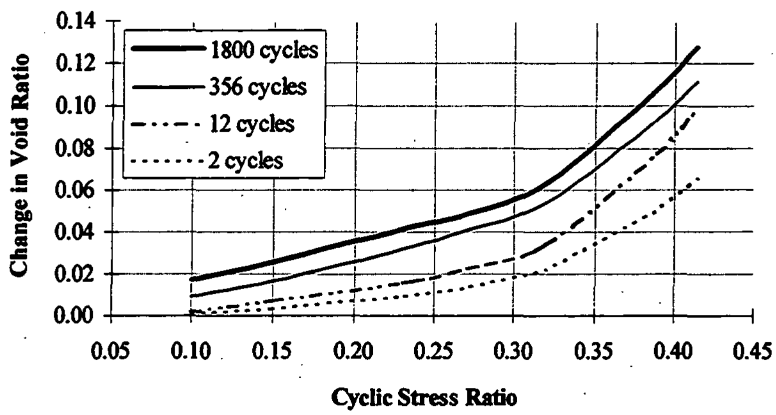

Figure 3.12 The relationship between applied stress ratio and the change in void ratio (after Tokue, 1979).

3.6.3 Cyclic Shear Test

Peacock and Seed (1968) demonstrated that simple cyclic shear tests provide better simulations of earthquake induced stresses on soil elements below level surfaces than triaxial tests (Lee and Fitton, 1969). Comparative studies suggested that; for design purposes, strength determined by pulsating triaxial tests should be reduced by 50%. Laboratory tests are performed using cycles that are typically in the frequency range of approximately 0.1-1Hz. Tokue (1979) found that shear and volumetric deformations converged rapidly in approximately 10 cycles, regardless of the ratio of shear stress to overburden pressure. In addition, rotation of the shear direction has little effect on volumetric change. Figure 3.12 shows the relationship between stress ratio and volume change. It has been observed for cohesive soils, that as frequency increases, the angle of internal friction (Φ) remains constant, but the strength parameter (c) is seen to decrease. More compressible soils show a greater decrease in strength.

Silver and Seed (1971a) studied the controlling parameters of cyclic shear strains (applied at 1Hz) using dry sand in simple shear equipment (developed by the Norwegian Geotechnical Institute). Constant initial relative density, static load and shear strain amplitude were varied to obtain resulting vertical strains. It was observed that for a given normal stress and shear strain amplitude, vertical strain increased with the number of cycles (note: a large proportion of vertical strains was observed in the first few cycles) (see Figure 3.13a,b). Additionally, a small amount of compaction (an increase in the initial relative density) significantly reduced the final cyclic shear strains (see Figure 3.14). In addition, simple cyclic shear tests performed in the range 300-2000kPa on dry sands, led to the conclusion that vertical strains are not significantly affected by vertical stress and depend only on shear strains that exceed 0.05%. However, it was considered that vertical stress may affect strains at stresses below the range used.

Sawicki (1987), who carried out a review of research into compaction due to cyclic shearing, summarised the data (which relates to dry or free draining sand) as follows: compaction depends on the amplitude of cyclic strain; the rate of compaction decreases as the number of cycles increases; compaction does not depend on the frequency of cyclic loading; compaction does not depend on the value of confining pressure; compaction depends on the initial value of relative density.

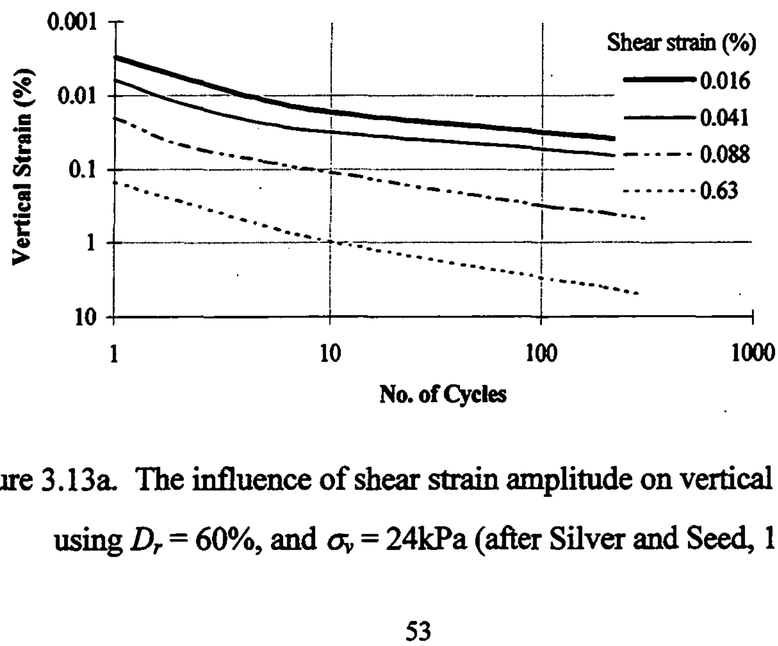

Figure 3.13a. The influence of shear strain amplitude on vertical strain, using $D_r = 60\%$, and $\sigma_v = 24$kPa (after Silver and Seed, 1971b).

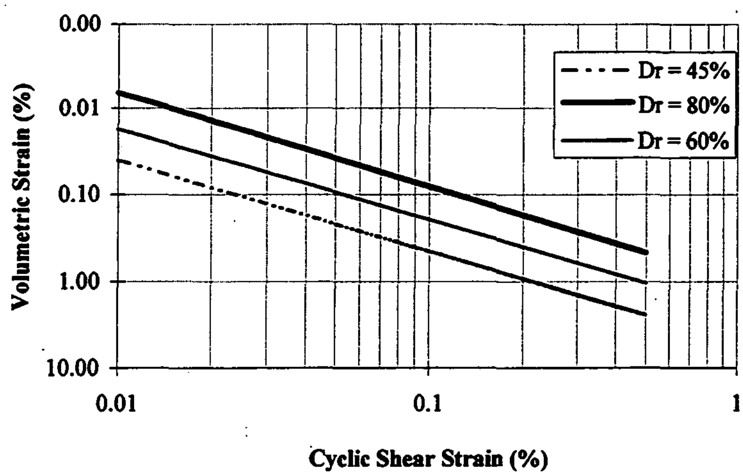

Figure 3.13b. The relationship between volumetric and shear strain for dry sands (after 15 cycles)(after Silver and Seed, 1971a).

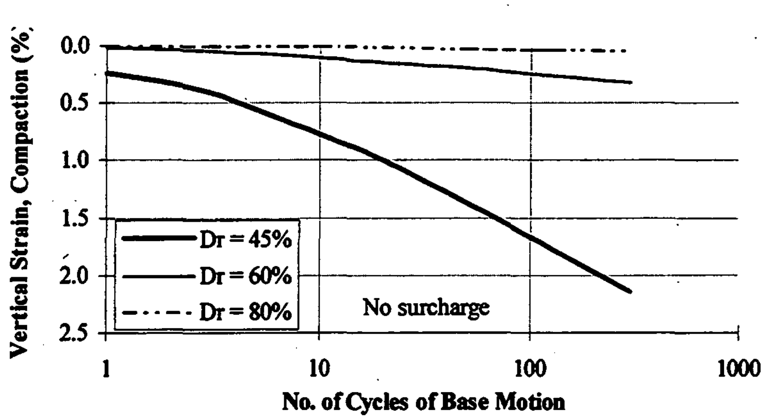

Figure 3.14. The effect of relative density on settlement of a sand layer, using acceleration of 0.3g (after Seed and Silver, 1972).

3.6.4 Shaking Table Test

Shaking table tests allow the simulation of field conditions of K_o and are considered to have certain advantages over cyclic triaxial and simple shear (Finn, 1982), by more closely reproducing *in-situ* conditions (Haldar and Miller, 1984). However, Cascone and Maugeri (1995) state that shaking table test are usually not able to reproduce the stresses that occur in the field, especially when modelling soil-structure interactions, because of the reduced dimensions of the test. Shaking tables have

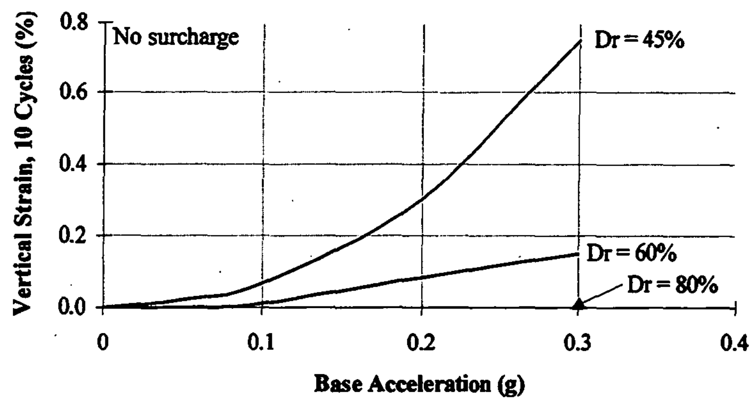

Table 3.15. The influence of relative density and acceleration on vertical strain (after Seed and Silver, 1972).

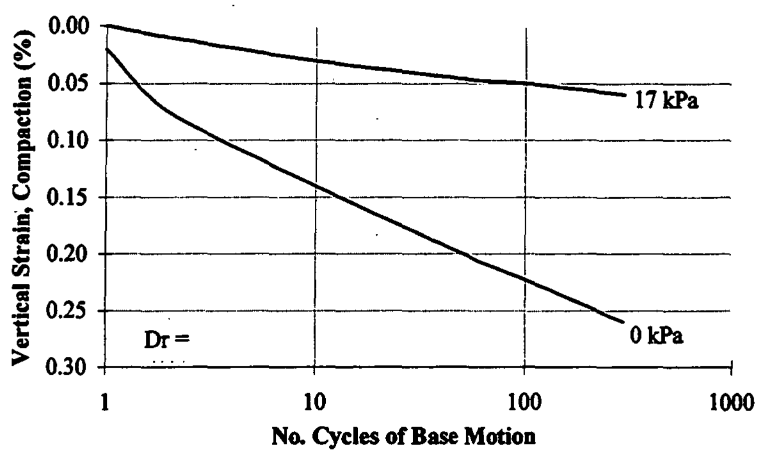

Figure 3.16. The effect of surcharge on vertical strain at 4Hz and 0.3g (after Seed and Silver, 1972).

Parameters of concern include: sample preparation technique; soil fabric; particle size distribution, mean grain size (D_{50}) and particle shape; frequency and acceleration (typically up to about 0.3g) of the uniform cyclic load and nonsymmetrical stress cycles (see Figure 3.15). Uniform accelerations are developed in the samples at low frequencies under plane-strain conditions that correspond to the propagation of shear waves *in-situ*. In addition, the pore water pressures generated in the soil mass during liquefaction may be monitored.

Seed and Lee (1972) related that overburden pressure has no significant effect on shear induced settlements. Overburden pressure affects the compaction characteristics of a sand and the shear strains that are induced by a given base motion (see Figure 3.16), with the result that it has no significant influence on the two. Thus, under given test conditions, vertical settlement of sand due to a series of horizontal shear strain cycles appears to depend only on the number and magnitude of the strain cycles involved.

3.6.5 Additional Tests

A range of other tests have been performed to examine the dynamic properties of soils. Centrifuge tests (e.g. Arulanandan and Sybico, 1993) are used to investigate scale model soil-structure interaction, such as bridge design. In order to develop the same stresses in a $1/n$ scale model, as in the field, it is necessary to increase the gravitational acceleration by the linear scale factor n. For example, a scale model of 1:60, will require acceleration to $60g$.

Earthquake	Date	Soil type	Relative density (%)	Maximum accel. (g)	Duration (*sec*)	Liquefaction
Niigata	1802	sand	53	0.12	20	no
Mino Owari	1891	sand & gravel	75	0.35	75	no
Tohnankai	1944	silt & sand	30	0.08	70	yes
Alaska	1964	sandy gravel	100	0.12	180	no
Alaska	1964	sand & gravel	68	0.25	180	yes
Tokachioki	1968	sand	55	0.18	45	yes

Table 3.4. Examples of ground condition and earthquake data (After Seed and Idriss, 1971).

3.7. Seismic Effects on Granular Soil.

Field observations of earthquake induced settlements in saturated sands range from less than a centimetre to approximately 50cms (Tokimatsu and Seed, 1987). Saturated soils appear to be the most susceptible to loss of strength due to earthquakes, because; within the relatively short vibration duration, very little drainage can occur in large soil masses to relieve the increase in pore water pressure. In addition, it is seen that increase in pore water pressures, and the associated problems, occur in level deposits. The significance of this is that there are no static shear stresses acting on horizontal planes of soil elements below level surfaces. During earthquakes both compression and shear waves propagate upwards through the soil. However, the compression waves (probably) have minimal effect on the strength of the soil because changes in the normal pressure will be transferred entirely by the pore water (Lee and Fitton, 1969). Thus, earthquakes are considered to be represented by upward propagating horizontal cyclic shear stresses (see Table 3.4 for examples of earthquake data).

To demonstrate the serious consequences of ground settlements that are associated with earthquakes, consider the Erzincan earthquake of north east Turkey, that occurred on the 13th March, 1992. This was a shallow earthquake (approximately 15-30km deep), of magnitude 6.8, which caused extensive property damage and the death of over 500 people. Peak measured accelerations were 0.5g (east-west), 0.4g (north-south), and 0.25g vertically (Hencher and Acar, 1995).

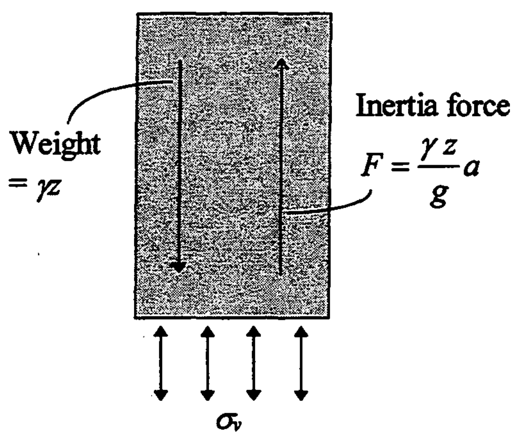

Figure 3.17. Forces acting upon a soil unit during vertical vibration, without vertical confining stress. Where: γ = soil unit weight; z = height of soil unit; g = acceleration due to gravity; a = applied acceleration; σ_v = vertical vibration.

3.8 Vibrations in Granular Soil

After initial deposition and equilibration of the external and internal stresses, additional settlement may occur due to the vibrational effects of occurrences such as pile driving, earthquakes and machine vibrations.

The magnitude of the frictional resistance that is generated at particle-particle contacts depends on the normal contact pressure, which remains unaltered as long as static conditions prevail. Vibration or dynamic effects may bring granular particles into a pulsating movement causing them to move alternately closer to, and farther from, each other. Thus, the total area of the momentary contact surfaces may be radically decreased, and the influence of friction substantially reduced. This behaviour allows granular soils to be readily compacted by vibration and applies to dry, or saturated, sands and gravels. If the material is partially saturated, the influence of suction causes the granular material to behave with a degree of apparent cohesion (where the sand acquires compressive and tensile strength as a result of interparticle adhesion due to capillary attraction).

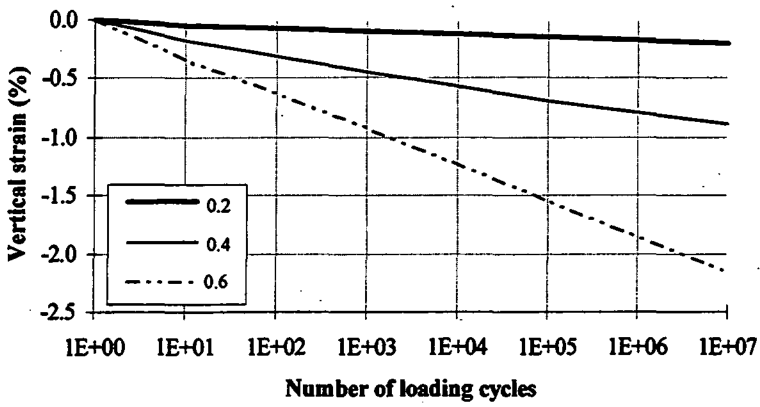

Figure 3.18. Compression of sands under controlled cyclic vertical stress. $D_r = 60\%$, $\sigma_v = 138$kPa, frequency = 1.8-6Hz ($\sigma_d/\sigma_v = 0.2$, 0.4 and 0.6) (After d'Appolonia, 1970).

3.8.1 Vertical Stress and Vertical Acceleration.

A sand receiving cyclic (e.g. sinusoidal) acceleration experiences an inertia force that acts in the opposite direction to the acceleration force (see Figure 3.17). This increases the stress experienced by the sample, to a value above the level of the static stress, before the application of the acceleration. For example, a sand sample that is accelerated sinusoidally to 0.6g will experience a vertical stress fluctuation between 1.6 and 0.4 times the initial static stress. When the acceleration increases to 1g the downwards vertical stress acting within the sample drops to zero. Because saturated and dry sands are not able to sustain tension the particles experience a 'free fall' condition. When the container begins to accelerate upwards, the particles impact on to the container and move with the container until the downwards phase begins. The 'free fall' behaviour accounts for the marked increase in, for example, sample densification for vibration tests that are performed above $1g$ (see Figure 3.19).

Many studies in the 1960's were performed to determine the maximum density of dry or moist sands under vibratory loading (Silver and Seed, 1971b). Almost all the methods involved using high amplitude vertical vibration with some magnitude of surcharge pressure.

The effect of cycling controlled vertical stress at low frequencies, i.e. low acceleration on confined noncohesive soils, has been described by d'Appolonia *et al* (1969). Sand was confined in a mould by vertically acting air pressure (σ_z). Vertical dynamic stress of amplitude (σ_d) was repeatedly applied. The settlement was recorded after a given number of cycles. This form of test is described as imparting 'repeated stress at negligible acceleration' to a sample and models phenomena such as the settlement observed under a machine foundation subject to vertical vibration (see Figure 3.18). Additional tests were performed on sand using controlled vertical acceleration, which produced relatively small dynamic strains. The confined sand was attached to a vibrating table, and vibrated for a given length of time. This form of test contrasts with the repeated stress tests in that the specimen experiences 'repeated acceleration with small dynamic stress'.

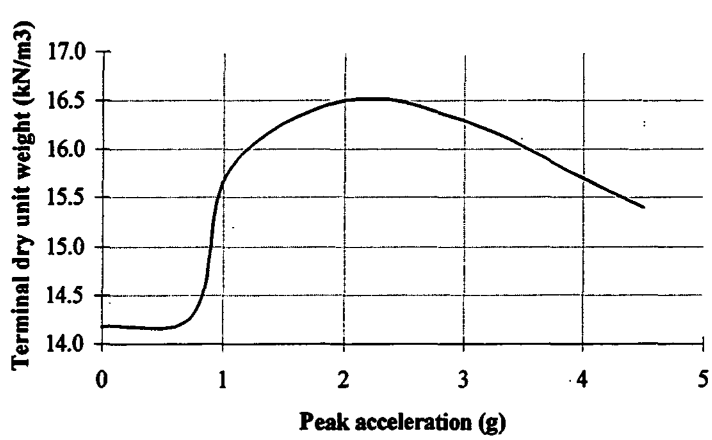

Figure 3.19. Density increase of sands under controlled vertical acceleration, with zero confining pressure (after d'Appolonia *et al.*, 1969).

Whitman and Ortigosa (1969) conducted similar tests and concluded that: when dynamic stresses are small, no noticeable densification occurs below approximately 1.0*g*; when dynamic stresses are small compared to static load, there is still no noticeable densification and vertical accelerations during earthquakes can cause very little densification.

Controlled vertical acceleration tests (up to 6*g*) on partially saturated clayey sands by Krizek and Fernandez (1971) indicated that significant vibratory densification rarely occurs below 1*g*. It was suggested that any slight densification that occurs below 1*g* was due to locally unstable intergranular arrangements. Under zero confining stress, density was seen to slightly decreases after 2*g*. For similar test conditions, increasing the percentage of fines tended to decrease the ultimate density. Similarly, increasing the moisture content was seen to significantly reduce ultimate density. The settlements obtained for soils having greater than 10-30% fines was in the order of 75% of the values obtained for equivalent 'clean' sands. In addition, the acceleration that was required to cause significant densification increased with increase in surcharge pressure.

Timmerman and Wu (1969) reported that the effect of acceleration on a granular soil was pronounced when of the order of 0.5*g* or higher. In addition, for accelerations of up to 0.1*g*, stress rather than frequency controlled sample strains. Frequencies between 2.5Hz and 25Hz affected the rate of strain, not the magnitude of strain. This was attributed to the fact that a longer pulse duration for the same applied stress allows grains more time to move past each other during each cycle before vibration reverses, and the grains are moved in the opposite direction (Norman-Gregory and Selig, 1989).

It is widely understood that peak acceleration is the main parameter that controls foundation settlement (Krizek and Fernandez, 1971). Depending on additional variables, including relative density, solid particles attain an equilibrium condition under a given peak acceleration. For additional settlement to occur, acceleration must be increased above this threshold level.

Brumund and Leonards (1972) studied the settlement of circular foundations on sand that was subjected to vertical vibrations. It was observed that settlement increased with the mass of the foundation (for given acceleration and frequency). In addition, settlement was seen to increase linearly with increase in acceleration (for a given foundation mass) (see Figure 3.20).

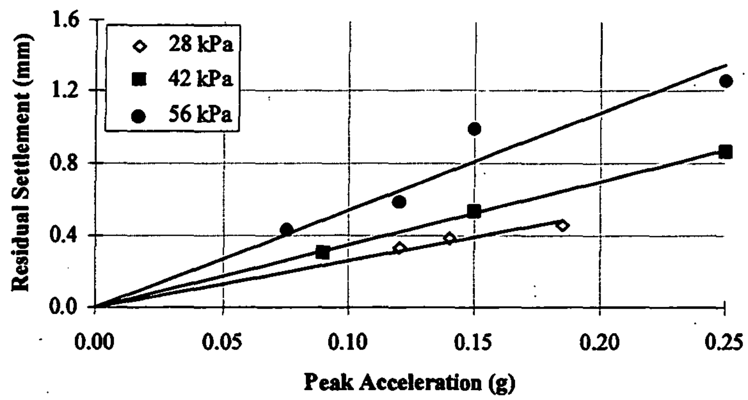

Figure 3.20 The effects of stress of foundation on settlement (after Brumund and Leonards, 1972).

A laboratory study by New (1978a) was performed on samples in the order of 150mm diameter and 125mm high, to obtain an estimate of the vibration level (up to 2-3*g* at 100Hz) at which settlement is initiated in partially saturated (on the order of 10% moisture content) fine to medium sands. A number of observations were made: the higher the initial relative density, the lower the final settlement; samples were less affected by vertical vibrations than by horizontal vibrations; initial vibratory settlements tended to occur between 0.1g-0.2*g*; under accelerations of 2-3*g*, settlements evolved were in the order of 4-8%; the majority of settlement (for a given vibration) occurred within a few seconds. However, this study did not closely simulate field conditions which would have a significant influence on vibration induced settlements. Effective stress in the soil, due to overburden, will increase the soil strength and increase the energy level that is required to re-order the particle structure. In addition, multidirectional shaking present in the field will tend to reduce the vibration threshold levels that were observed for unidirectional vibrations. New (1978) reported that the results were consistent with those obtained by other workers, such as d'Appolonia *et al.*, (1969), Silver and Seed (1971a, 1972), Brumund and Leonards (1972), Lee and Albaisa (1974) and Pyke *et al.* (1975).

The dynamic compaction of submerged granular fills was studied by Oteo (1983), and Salas and Oteo (1978). Three soils, a quartz sand and two pyroclastic (red and black picon) sands (U_c~2.5, Dr~45%) were consolidated under a range of static loads in a 25cm Rowe cell. After equilibration under a given stress, the samples were then subjected to horizontal vibrations of 25Hz for ten minutes. The induced vibratory settlements were measured (approximately 2-7%), and the static load was increased and the test procedure repeated (see Figure 3.21). The sands demonstrated different sensitivities under maintained static load, and under pressures above 150kPa all the vibration induced settlements were negligible. The data show that the compressibility of material that is subjected to constant vertical pressure between 20-80kPa can be considerably reduced by vibration, and that at depths below 16-18m vibration produces virtually no compaction. Figure 3.22 presents an analogy between the liquefaction of a granular material and the optimum depth range for soil improvement using dynamic compaction techniques such as vibrofloatation and the terraprobe.

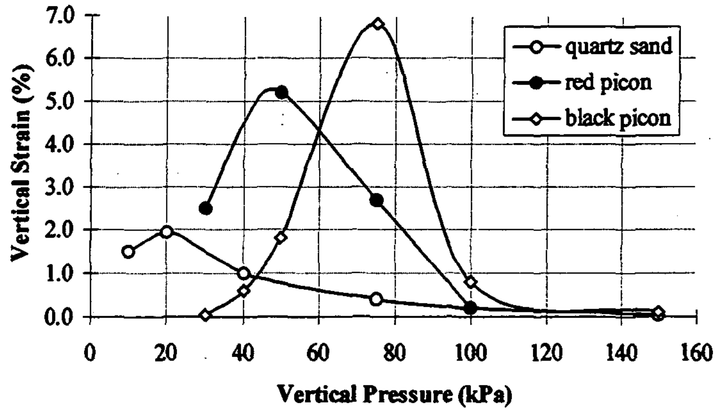

Figure 3.21. Vertical strain due to vibration under a range of maintained pressures (after Oteo, 1983).

Richards *et al.* (1990) report that under earthquake conditions, horizontal vibration effects are dominant over the vertical acceleration components. However, vertical acceleration is of paramount importance to the behaviour of soil that is experiencing vibrations resulting from activities such as vibratory piling, machinery vibrations and vibratory compactors (Barkan, 1960; Jumikis (1969); Richart *et al.* 1970; Das, 1983), and workers such as Kim *et al.* (1994) and Kattis *et al.* (1995) have used vertical sinusoidal vibrations when modelling the effects of ground vibrations.

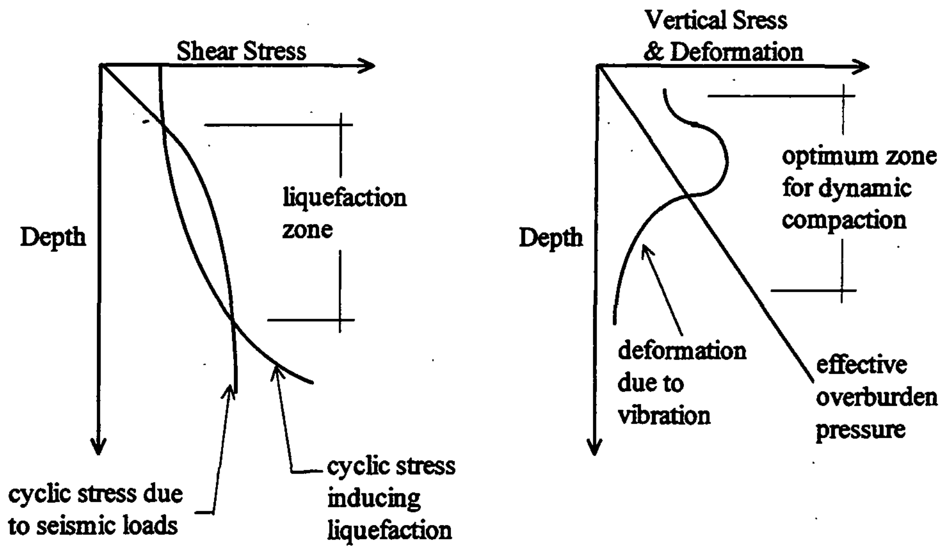

Figure 3.22. An analogy between liquefaction (after Seed and Idriss, 1971) and the optimum zone for dynamic compaction (after Oteo, 1983).

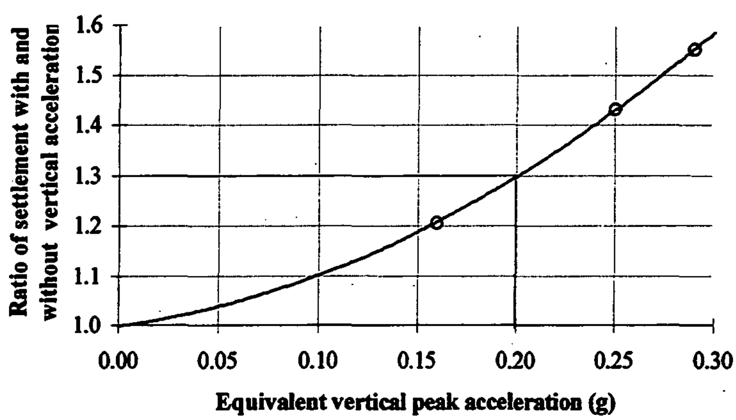

Figure 3.23. Effect of vertical motion superimposed on horizontal motion (after Pyke *et al.*, 1975) - a vertical acceleration of 0.2g modifies the settlement obtained by horizontal base acceleration by a factor of 1.3.

3.8.2 Multidirectional Vibration.

Studies observing the effect of a dry sand layer subject to multidirectional shaking, i.e. accelerations in the x, y and z directions have been carried out (Pyke *et al.*, 1975). It was presumed that induced vibratory settlements due to combined horizontal motions, are approximately equal to the sum of settlements caused by the vibration components acting separately. The imposition of vertical acceleration was seen to significantly increase settlement (see Figure 3.23), which shows the effect of vertical acceleration on Monterey No. 0 sand, with an initial relative density of 60%.

3.9 Ground Settlements Induced by Pile Driving.

Pile driving causes compaction in loose granular soil creating a high vibration amplitude, especially in the vertical direction (Uromeihy, 1990). Laboratory studies have demonstrated that volume decrease can occur at very low cyclic strain amplitudes after many repetitions (pile driving), as well as under relatively few cycles at large strains (earthquakes) (Silver and Seed, 1971). The material properties of concern appear to be those that are traditionally associated with liquefaction potential (Lacy and Gould, 1985), such as vibration amplitude, number of cycles, soil properties and the position of the water table. However, it is not clear that excess pore water pressures, which presumably decrease the natural frequency of sand, positively increase the final magnitude of vibratory settlements (Dowding, 1994). Table 3.6 presents summary data from one of the most complete summaries of cases involving piling induced ground settlements. The data are taken from the New York City area, and the soils are late glacial outwash sands and silts. Dowding (1994) reported that the soils that are most susceptible to vibration induced settlement are narrowly-graded, clean (<10% fines) uniform sands with relative densities below approximately 50%. Settlement may also be possible if the silt fraction is of a uniform size or non-plastic. Note that many glacial outwash deposits contain gravel and cobbles that raise SPT-N values by blocking penetration. Thus, high N values may not accurately reflect the true lower density of the sand matrix within which gravel lies (Dowding, 1994).

Case	Pile Depth (m)	Distance of effect (m)
Lacy and Gould	30	45
	40	37
Clough and Chameau	12	11-15
Linehan *et al.*	>23	18

Table 3.5. Distance of measurable settlements (from Dowding, 1994).

Case	Pile type	Hammer type	Distance •(m)	PPV (mm/s)	Uc	Dr (%)	Comments
1	14HP73	Impact	6.1	5	4	♣50	Buildings settled 76mms
2	45cm pipe	Vulcan 010	-	-	3	♣50	38mm settlement of street
3	14HP73	Vulcan 08	1.5 - 9	2.5	4	♣45	Structure settled 76mm
4	27cm pipe	Vulcan 08	3 - 25	23-2.5	2	40	Structure settled 76mm
5	12HP53	MKT 10B3	1.1 c-c	-	4	40	Ground between piles settled 840mms
6	Hoesch 134	ICE 812	0.9	-	4	♣50	Building settled 60mm
7	PZ-27	ICE 416	3 - 7.6	-	-	25	Ramp settled 76mm as sheeting removed
8	PZ-27	ICE 812	1.2 from sewer	-	-	30	Sewer settled 150mm
9	Hoesch 134	ICE 812	1.2 from sewer	-	4	45	Sewer settled 76mm as sheeting removed
10	Steel H	Impact	edge of pier	-	!10 - 4	13 - 40	pier foundation settled 250mm
11	Sheet pile	Foster 4000	5 - 18	15 - 0.5	!4	15 - 85	monolithic structure settled 35mm
12	Steel H, sheet	diesel, vibratory	above pipe	100 - 2	!3 - 7	♣20	gas main settled 50mm
13	sheet piles	ICE 812	1.5 - 45	50 - 0.5	-	35 - 65	Ground settled up to 150mm
14	12HP74	Hammer	3m	0.5g	♣3	♣40	Building settled 64mm and displaced by 51mm

Table 3.6.Case studies summary (from Lacy and Gould (1985)(1-9), Picornell and del Monte (1982)(10), Linehan *et al.* (1988)(12), Clough and Chameau (1980)(13), Lukas and Gill (1992) (14)).

Other authors, such as Holloway *et al.* (1980), Clough and Chameau, (1980) (see Figure 3.24), Picornell and del Monte (1984), Lukas and Gill (1992) and Linehan *et al.* (1988) have also reported significant ground surface settlements as large as 25-30mm (at 4m stand-off) that were attributed to the vibrations generated during piling activities.

These authors have noted that vibratory densification can occur metres away from the source i.e. the pile, and have suggested that settlement may occur at distances

• Distance from pile to measurement

♣ Mean value

! Estimated based on (1-9) *Uc* of glacial sands and relative density terms after Terzarghi and Peck (1948) as far as the penetration depth of the pile (see Table 3.5). However, Bhandri (1981) reported that negligible structural damage occurs when SPT-N values are greater than 25, at a distance of 15-20m from the vibration source.

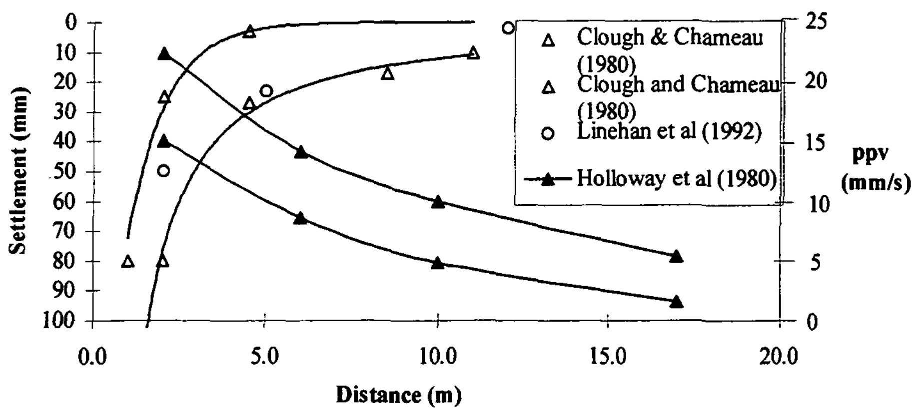

Figure 3.24. Comparison of settlement and particle velocities produced by pile driving (from Dowding, 1994) (closed symbols are peak particle velocity data).

Because the settlements that are induced by pile-driving are the result of the repetition of very small individual disturbances, the factors that increase the total vibration energy input, or the duration, will increase settlements. These include factors such as depth of overburden, intensity of final driving resistance, number of piles and the overall size of the site. This implies that the size of a construction operation can change a situation from insignificant vibration effects to damaging settlements. In 1994, Dowding related that the prediction of settlement produced in cohesionless sands was not susceptible to a simple mathematical evaluation based on vibration magnitudes. An informed judgement requires knowledge of gradation, relative density, site geometry, groundwater levels and hammer energy. The vulnerability of adjacent structures to settlements, as opposed to vibrations directly transmitted to the structure, must be judged.

However, Lukas and Gill (1992) have applied the procedures developed by Silver and Seed (1971b) and Lee and Albaisa (1974) to estimate the settlements produced by earthquakes to produce a theoretical estimate of ground settlements induced from vibration acceleration during pile driving. Using an average acceleration of $0.15g$ (at 9.1m from the piling operation), 12.2m of loose sands was calculated to settle 99mm (for 300 cycles) and 125mm (for 2000 cycles). The procedure used is summarised as follows:

a) Divide the soil profile into thin layers of equal relative density.

b) Compute the overburden pressure at the mid-point of each layer.

c) Determine the shear modulus (G) for each layer, using the relationship:

$$G = 1000 K_m \sigma_v^m$$

where: σ_v = vertical confining pressure

m = an exponent varying between 0.6 and 0.7

K_m = a coefficient that varies with shear strain.

For the likely range of shear strain occurring during pile driving (0.1-1%), K_m is in the range 0.3-0.9kPa.

d) Find the shear stress in each layer, using:

$$\tau_{max} = \gamma \, h \, a_{max} \, r_d$$

where: a_{max} = acceleration

γh = overburden pressure

r_d = stress reduction coefficient, which varies from 1.0 at the surface to 0.9 at 9.6m and reduces parabolically to 6.5 at 20m depth.

e) Determine the average shear stress* from $\tau_{av} = 0.65\,\tau_{max}$

f) Calculate shear strain = τ_{av} /G

g) Obtain vertical or volumetric strain for each layer, using the relationship given in Figure 3.13b.

h) Compute the settlement for each layer from the volumetric strain. The settlement for the actual number of cycles (blows) during pile driving can be extrapolated from charts given by Silver and Seed (1971).

* Note that the actual time-history of shear stress at any point in a soil deposit during an earthquake will have an irregular form. Thus, it is necessary to determine the equivalent uniform average shear stress. It has been found ("with a reasonable degree of accuracy") that, based on laboratory data, the average equivalent uniform shear stress τ_{av} is approximately 65% of the maximum shear stress (Silver and Seed, 1971b).

Note that Lukas and Gill (1992) used extrapolation for the actual number of blows during pile driving from charts that were given by Seed and Silver (1972), which tend to overestimate the strain values for greater than 10 cycles, by a factor of approximately 1.4.

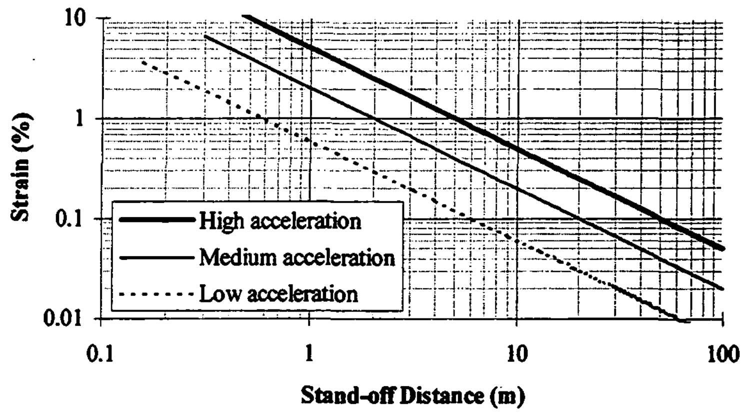

Figure 3.25. Vertical strain induced in loose to medium sand by vibratory sheetpile driving (Clough and O'Rourke, 1990).

Clough and O'Rourke (1990) monitored the ground settlements that were induced for a number of vibratory driving projects that installed sheet piles into loose to medium-dense sands. The data obtained are presented in Figure 3.25 and provide a plot of vertical strain in the ground caused by pile driving vibrations. The data take into account that the sheet piles were driven in a long line on either side of the point of interest. Surface settlements are obtained by selecting the strain at an appropriate distance, and multiplying the value by the depth of sand through which the piles are to be driven.

3.10 Liquefaction

Liquefaction of soils is a complex problem on which a great deal of experimental and numerical research has been carried out (Erten and Maher, 1995). Liquefaction occurs under certain field conditions, where pore water pressure increases due to change in the stress state. Monotonic, cyclic and transient stress increases describe the forms of loading that occur due to activities such as dead loading, traffic, wind, machine loads, earthquakes and pile driving activities. Unlike normal (or 'static') conditions where pore water pressure can dissipate, a cyclic stress regime may not allow significant dissipation of pore water pressure between load cycles. A cumulative increase in pore water pressure is then possible (see Figure 3.26). Under such conditions, where drainage is effectively prevented or restricted, pore water pressure may increase until it becomes equal to the overburden pressure causing the effective stress to be zero. In this state, a granular material will have no strength, is unable to support applied shear stress and will behave as a viscous fluid. Loss of strength occurs because the intergranular stress of the particles is transferred to the pore water. Partial transfer of intergranular stress causes partial loss of strength, and even if liquefaction is not seen to occur, may contribute to foundation bearing capacity failure and resulting differential settlement of structures. Bolton and Williams (1990) relates that if strain amplitudes are limited to below the threshold strain (10^{-4} (0.01%) for sands and 4×10^{-4} for clays), or if unrestricted consolidation is provided, no liquefaction will occur.

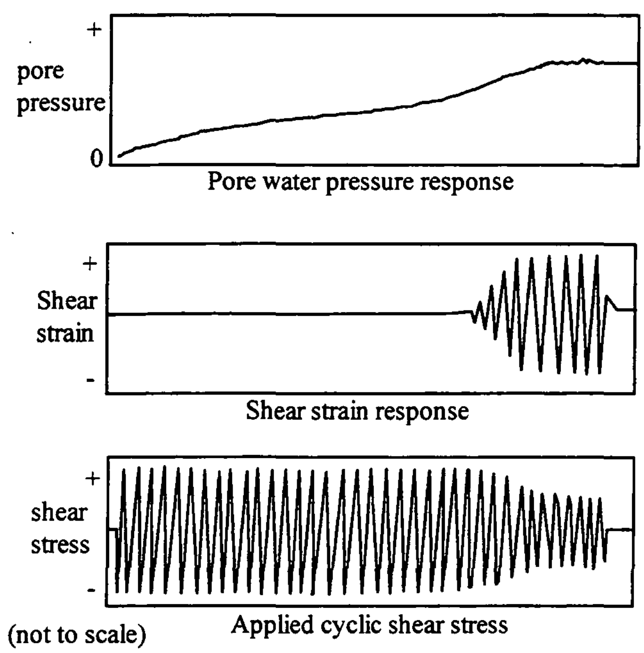

Figure 3.26. Record of a typical pulsating load test on loose sand in simple shear conditions (after Peacock and Seed, 1969).

The vibratory piling method exploits the phenomenon of (localised) liquefaction around the pile-toe to allow the penetration of piles into granular soils under relatively light surcharge. In general, piling causes liquefaction in the soil adjacent to the pile, because of the high accelerations produced within stand-off distances of about 0.5m. In addition, authors such as Lacy and Gould (1985) and Dowding (1994) report the occurrence of liquefaction at greater distances, i.e. in the order of metres.

Work carried out by Rodger and Littlejohn (1980) identifies a phenomenon described as 'seismic shear fluidization', which occurs at pore water pressures below which liquefaction may take place. Three distinct states are identified that control the occurrence of fluidization: a 'sub-threshold' (elastic response) state that occurs below 0.6*g*, where interparticle friction occurs although overburden pressure is periodic; a 'trans-threshold' state exists between 0.7-1.5*g*, where shear strength decreases and is governed by the exponential function of acceleration, which is characterised by soil-type variables and magnitude of the overburden pressure; in the third state (fluidized response) the shear strength reduction reaches a maximum (in theory this should occur when acceleration reaches 1*g*), which in practice occurs at about 1.5*g* due to interparticle friction. Initial fluidization can lead to an increase in pore water pressure which may ultimately lead to complete liquefaction. The two phenomena are thus related, and liquefaction may be considered to be a limiting case of shear fluidization.

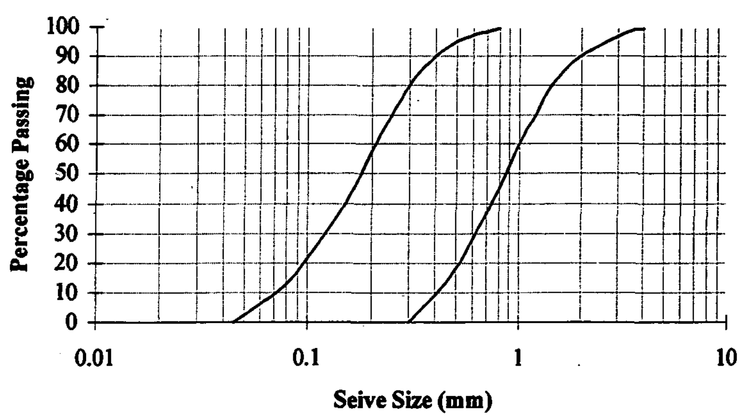

Figure 3.27. The envelope of particle sizes that are susceptible to liquefaction (after Bhandri, 1981).

Liquefaction may also occur due to seepage of water, where the overburden stress is relatively small compared to the hydraulic gradient. This is a different mechanism to cyclic stress induced liquefaction, but the reduction of (confining) stress to zero is a common factor.

Because liquefaction can be induced by construction related activities, there is a need to investigate the factors that control a soils potential to experience liquefaction. The factors that are associated with liquefaction potential are:

Grain size distribution - For given conditions, fine uniform sands are more susceptible to liquefaction than coarser (and well-graded) material (see Figure 3.27). For the same relative density and confining pressure, grain size distribution and shape was considerably less significant than the maximum grain size (Lee and Fitton, 1969). The permeability, and hence pore water pressure dissipation in coarse materials is greater than that of fine grained soil (Das, 1983). The presence of (low plasticity) fines i.e. silt, especially exceeding 10% of the particle size range, was observed to have a pronounced effect on the liquefaction resistance of undrained sands (Erten and Maher, 1995).

Initial relative density - Increase in the relative density of a granular material tends to decease the magnitude of strains and therefore, settlement (see Figure 3.28).

Vibration characteristics - The nature, magnitude and type of dynamic loading control the onset of initial liquefaction. For example, shock loading may induce liquefaction of an entire soil layer. However, steady-state vibrations after a number of cycles can cause liquefaction to begin at the top of a layer and propagate downwards. Initial vibrations liquefy the top layer(s), which carry relatively light load and reduce the overburden pressure on the lower layers, which then experience an increasing tendency to liquefy. Research suggests that under earthquake conditions, which generate multidirectional shaking at depth, propagating upwards, pore water pressure increases more rapidly than that generated by unidirectional vibrations. Resistance to liquefaction is seen to decrease with increase of acceleration amplitude (because induced shear stresses within the sample are a function of the acceleration amplitude).

Location of drainage and dimensions of the deposit - A large granular deposit, with a relatively large drainage path, may liquefy under rapid loading conditions (e.g. earthquakes) because the rate of pore water pressure dissipation is reduced. Similarly, a granular layer that has drainage pathway(s) restricted by the presence of a cohesive layer will similarly experience an increased tendency to liquefy because of drainage restrictions.

Magnitude and nature of the superimposed loads - Under isotropic stress conditions (generated during laboratory testing, for example), as effective (confining) stress increases, the intensity and/or duration of vibrations necessary to induce initial liquefaction must be increased. Under field conditions, where isotropic stress does not occur, the coefficient of earth pressure at rest (K_o) is an important parameter influencing liquefaction. For a value of K_o greater than 0.5, initial liquefaction was caused when the stress condition was increased by approximately 50 percent (Seed, 1976). This implies that isotropic triaxial testing does not simulate field conditions, and generates conservative estimates. Note that stress path testing can simulate anisitropic conditions.

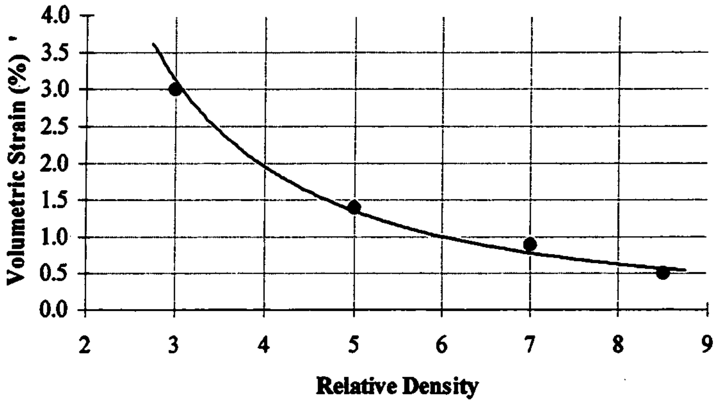

Figure 3.28 The effect of initial relative density on volumetric strain post-liquefaction (after Lee and Albaisa, 1974).Using the mean data of 33 tests in the range 100-430kPa, D_{50} = 0.6mm.

Method of soil formation - The fabric of an *in-situ* granular material, such as the orientation of soil particles, is a significant parameter. Similarly, laboratory sample preparation technique (which is performed to model *in-situ* fabric) greatly influences liquefaction behaviour.

Soil behaving (flowing) like a liquid is not confined to the saturated condition. For example, loess (a wind deposited weakly cemented silty material, that tends to have very high void ratios) was seen to 'dry flow' during the 1920 earthquake in China.

Period under sustained load - The characteristics associated with the ageing of a deposit influence liquefaction potential. For a given soil type, a strength increase is observed over time, due to the combined effects of processes such as cold welding and cementation of individual particles. Hence, for given stress conditions, older deposits are less susceptible to liquefaction. Florin and Ivanov (1961), observed that surcharge reduces liquefaction.

Previous strain history - It has been demonstrated that a laboratory sample with a strain history (with no increase in density) required greater stress to induce liquefaction than a fresh sample (Das, 1983). However, Nemat-Nasser and Takahashi (1990) noted that once a sample is liquefied, its resistance (after reconsolidation) to further liquefaction may be considerably diminished, even though the density of the material may have increased.

Degree of saturation - Because air is compressible, the liquefaction of a soil containing air bubbles (i.e. partially saturated) is reduced. The increase in pore water pressure is reduced as such entrapped air is compressed.

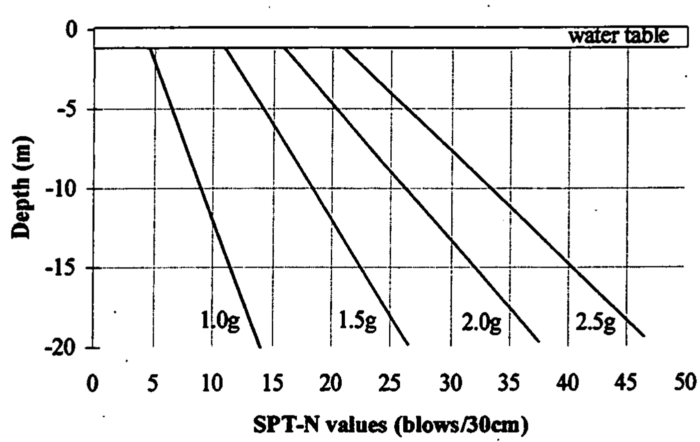

Figure 3.29. Values of SPT-N for which liquefaction is not likely to occur under any given earthquake condition (after Seed and Idriss, 1971).

When liquefaction is considered likely, the soil may be treated by such processes as vibrocompaction, deep blasting and dynamic consolidation. These soil treatment processes cause the collapse of the loose soil structure, increase the density and, hence, increase the soil's strength, which decreases liquefaction potential. Studies by a number of authors e.g. Casagrande (1936), Seed and Lee (1966), Lee and Seed (1967), Prakash and Gupta (1970), Finn *et al.* (1976), have demonstrated that a soil's potential to liquefy is directly proportional to a number of parameters (see above). However, Das (1983) considered that using SPT-N values may allow the determination of liquefaction potential using one parameter (Christian and Swiger, 1975). Ohasaki (1970) recommended that, as a rough guide, liquefaction will not tend to occur if the SPT-N values exceed twice the depth of the soil unit (in metres). If liquefaction does not occur, resulting volumetric strains are always likely to be less than about 1%, and values in the order of 2 - 3%, or greater may occur for liquefaction (ignoring shear deformations) (Lee and Albaisa, 1974). In general terms, conditions when liquefaction is not likely to occur are presented in Figure 3.24.

3.11 Summary

Soil is a natural material and is inherently variable in terms of its physical characteristics. Laboratory tests must be performed to assess a given soil's stress-strain behaviour. Data are then used to allow the safe and economic design of, for example, soil-structure systems.

A number of factors contribute to a material's mechanical properties, such as particle size characteristics and density. Laboratory testing requires the removal of a sample from an *in-situ* deposit. Because cohesive soils have strength, when normal stress is zero, obtaining undisturbed samples is relatively straightforward. However, because the strength of granular material is frictional and requires normal stress, it is susceptible to severe disturbance during sampling. Thus, disturbed granular material is prepared in the laboratory such that its physical character, in terms of soil fabric, models the *in-situ* equivalent as closely as possible. However, even if relative density and fabric are representative, the reconstituted sample will have lost the strain-history and age characteristics of the *in-situ* soil. This can, for example, generate errors when studying liquefaction. For the same conditions, an *in-situ* soil tends to demonstrate greater resistance to liquefaction than laboratory samples.

Dynamic soils testing is concerned with evolving design criteria that account for the effects of phenomena such as earthquakes, wind and wave action and construction related activities. There are a number of tests that may be performed, including the resonant column, cyclic triaxial, cyclic shear and the shaking table. Simulations are performed that use values of frequency, acceleration, strains and failure criteria that reflect *in-situ* conditions and the amount of permissible strain.

Tests are broadly divided into those which impart repeated stress at small acceleration and those which use repeated acceleration with small dynamic stress. The former are more typically applied to model the effects of natural phenomena such as earthquakes and wind loads. The latter more frequently model the consequences of man-made vibrations, including those resulting from construction activities. Examples of ground settlements that were induced during pile driving are included.

CHAPTER 4
LABORATORY TECHNIQUE

4.1 Introduction

The primary requirement of the laboratory test programme was equipment that could be used to measure height and volume change under controlled conditions that closely model the response of an *in-situ* granular soil when subject to ground vibrations generated during vibropiling operations.

The Rowe cell, developed in the 1960's, was designed to overcome the limitations of the basic consolidation apparatus, the mechanical oedometer. The Rowe cell uses hydrostatic pressure acting on a rubber diaphragm to load and consolidate a soil sample. The ability to measure pore water pressure and control drainage and drainage conditions of large samples produces more reliable data for settlement analysis than the standard oedometer. Rowe cell components, ancillary equipment and basic standard test procedure are outlined in Section 4.3. More detail concerning the versatility and applications of the Rowe cell is described in a number of texts, notably Head (1984) and BS 1377: Part 6 (1990).

The Rowe cell is able to apply and maintain stresses appropriate to those generated within soil due to overburden and additional surcharge loads. In addition, this capability can be maintained during vibration of the whole system. The reasons why the Rowe cell was selected as the central apparatus of the research are given in Section 4.4. The adaptations of the hardware, modification to the standard test procedure and the shift in the emphasis of use from the standard application are also described.

Preparation of representative soil samples within the cell is critical to the success of the programme. The several methods available are listed in Section 4.6.1, and the phases of the development of the sample preparation technique from simple at-moisture-state placement within the cell to the preferred method are outlined. Initial consolidation is intended to mimic the stress and moisture history of an equivalent *in-situ* soil. In general terms, British soils tend to be transported by, and deposited in, water (e.g. glacial outwash, river and estuarine environments), i.e. as saturated material. As the basic geological cycle proceeds with time, continued deposition loads the material beneath. Hence, a given unit of soil will experience consolidation with time. During this process, the soil may experience cycles of erosion and transportation, and also fluctuations in moisture state.

Due to the granular nature of the material being studied, the term 'consolidation' as applied to the standard Rowe cell test performed on cohesive material loses much of its importance. Because the granular material is highly permeable, dissipation of pore water pressure generated at the start of static loading is rapid (taking seconds to minutes). Hence, the increase in interparticle stresses generated to balance the applied static vertical stress is similarly rapid. Volume changes due to an applied uniform stress are small, because the modulus of deformation of sand grains is very high. The volume will only decrease significantly, at much higher loads (MPa) than applicable to this research, through grain crushing. This behaviour is modified by the grading characteristics of the materials being tested, i.e. the presence of a small percentage of fines (passing 63μm) will increase consolidation time, and density may reflect the imposed stress.

The full test procedure is detailed in Section 4.6.2 and 4.6.3, in terms of both static loading, and subsequent vibratory testing. The description relates to the vibratory testing of saturated samples. Modifications to this test are presented in terms of testing with sample moisture content being the variable of particular interest. Also included is the test procedure to impose horizontal vibration on to saturated samples.

4.2 Historical Development of the Rowe Cell.

The Rowe cell was developed in Manchester by Professor Rowe to overcome the disadvantages of the mechanical oedometer test* (Rowe and Barden, 1966). Unlike the oedometer that uses a weights and lever system to load samples, a Rowe cell uses water pressure acting on a flexible diaphragm to load the test sample hydraulically. The Rowe cell allows the control of drainage and measurement of pore water pressure during a consolidation test. A range of drainage conditions are possible, and back pressure can be applied to the sample.

Apparatus using a diaphragm to load confined sand samples was originally described by Rowe (1954). Air pressure was applied to a flat flexible membrane in

*Consolidation testing using the standard oedometer is detailed in BS 1377: Part 5, 1990 contact with a 250 mm diameter sample. A bellows-type diaphragm was developed for the present design of Rowe cells allowing large sample settlement (Rowe and Barden, 1966). Cells of 3, 6, 10 and 20 inch diameter (76, 152, 254, and 508mm, respectively) were manufactured at Manchester University. The 3 inch diameter cell was commercially available in 1966, and the 6 and 10 inch sizes followed in 1967. The 500 mm cell was intended for research purposes only.

Oedometers using hydraulic loading were independently designed by Bishop, Green and Skinner at Imperial College, London (Simons and Beng, 1969). Provisions were made for pore water pressure measurement and the application of back pressure.

The effect of wall friction in a conventional oedometer was studied by Leonards and Girault (1961). They found that a Teflon coating on a cell wall virtually eliminated friction for loads above a certain critical value in that type of cell. Silicone grease has been found to be equally effective, and is now used in the standard Rowe cell.

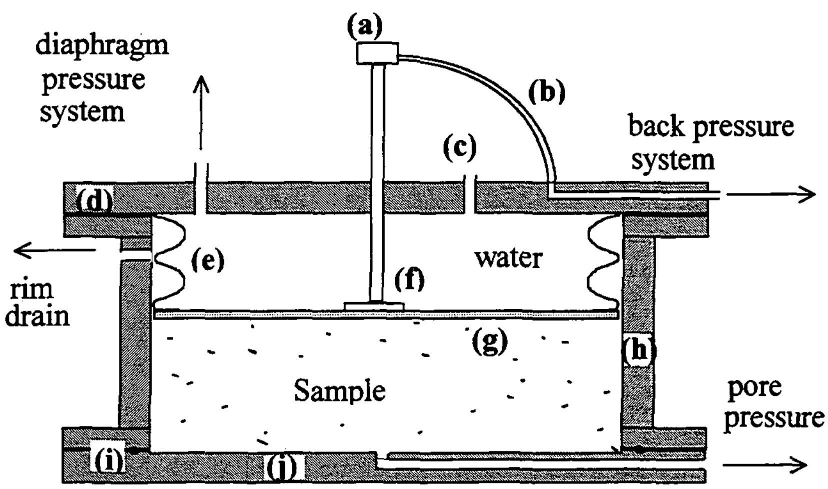

(a) Dial gauge/LVDT base rest	(b) Flexible drainage lead
(c) Diaphragm Air bleed	(d) Cell top
(e) Diaphragm	(f) Drainage spindle
(g) Rigid load/drainage disc	(h) Cell body
(i) Rubber 'o'-ring seal	(j) Cell base

Figure 4.1. Diagram of a standard Rowe cell.

4.3 Advantages of the Standard Rowe Cell

As a one-dimensional consolidation apparatus, the Rowe cell has many advantages over the standard mechanical oedometer. The main features responsible for these improvements are the hydraulic loading system, control facilities, ability to measure pore water pressure and the capability of testing samples of large diameter.

A typical hydraulic loading system allows pressures of up to 1000kPa to be applied, which is less susceptible to extraneous vibrations that the oedometers lever loading system can magnify. Drainage of the sample can be controlled and several different drainage conditions can be imposed on the sample. Control of drainage and drainage conditions enable samples to be loaded in the undrained condition, allowing the full development of pore water pressure. Consequently, the initial immediate settlement can be measured separately from the consolidation settlement which starts when the drainage line is opened. Pore water pressure can be measured accurately at any time, enabling the beginning and the end of primary consolidation to be positively established. Volume of water draining from the sample can be measured, as well as surface settlement.

The sample can be saturated by applying increments of back pressure in upward flow (until a satisfactory B value[♣] is achieved), or by controlling the applied effective stress before starting consolidation. Tests can be performed under elevated back pressure, (ensuring fully saturated conditions), which allows rapid pore water pressure response and ensures reliable time relationships (Lowe *et al.* 1964). The sample can be loaded either by applying a uniform pressure over the surface ('free strain') or through a rigid plate, which maintains the loaded surface plane ('uniform strain'). Fine control of loading, including initial loads at low pressures can be accomplished easily.

Tests on large samples provide more reliable data for settlement analysis (in reality a three-dimensional problem), than conventional oedometer tests on small samples. Large samples (i.e. a least 150mm in diameter and 50mm thick) have been found to give higher and more reliable values of the coefficient of consolidation especially under low stress, than conventional oedometer test samples (McGowen *et al.*

[♣] 'B value' is an expression indicating degree of sample saturation and is defined as the ratio of pore pressure increase to total stress increase. A fully saturated sample will have a B value of 100 %. In practice, this value is usually not possible to obtain, and B values of 95% and above are usually considered to be acceptable.

1974). Better agreement has been reported between predicted and observed rates and magnitudes of settlement (Lo *et al.* 1976). This is attributed to the relatively small effect of structural viscosity in larger samples. In layered deposits, use of large sample size enables the effect of soil fabric to be taken into account in the consolidation process, thereby enabling a realistic estimate of the rate of consolidation to be made (Rowe, 1968 and 1972). Large samples generally suffer appreciably less disturbance to the microfabric than do small samples. Excessive disturbance may obscure the effects of stress history; may give a low value of preconsolidation pressure and overconsolidation ratio and may give a high value of the coefficient of volume compressibility at low stress. Large samples permit reliable measurements of permeability, both vertically and horizontally, under known stress conditions and with account taken of the effect of soil fabric.

4.3.1 Central Components

A Rowe cell comprises three main components: the base plate, cell body and top plate. Large diameter cell bodies (250mm and above) are flanged at each end, with bolt holes for securing the base and cover. Standard smaller cells use long tie bolts that secure the cell body between the base and top plates.

The cell is fitted with a bellows-type rubber diaphragm, the outer edge of which acts as the seal between the cell top and body. The diaphragm transmits a uniform load to the soil sample using hydrostatic pressure. A hollow spindle passes through low-friction rubber 'o'-ring seals in the centre of the cover. The lower end of the spindle passes through the centre of the diaphragm, allowing sample drainage. The upper end of the spindle is connected by flexible tubing to the drainage valve fitted to the edge of the cell top. The blanked-off upper end of the spindle provides a bearing for a settlement dial gauge, which is rigidly supported by a bracket assembly fitted to the cell top. The top cover has an inlet for connection to the constant pressure water system for applying the vertical load onto the sample, via the diaphragm, and an air bleed (Figure 4.1 shows the diagram of a standard Rowe cell). The cell base is fitted with a recess for an 'o'-ring to seal against the lower body flange. At the centre of the base a small circular recess provides the main pore water pressure measuring point connecting to a pressure transducer.

Accessory items include a rigid loading plate, sintered bronze drainage discs, pressure transducers, a dial gauge and LVDTs (linear variable displacement transducers).

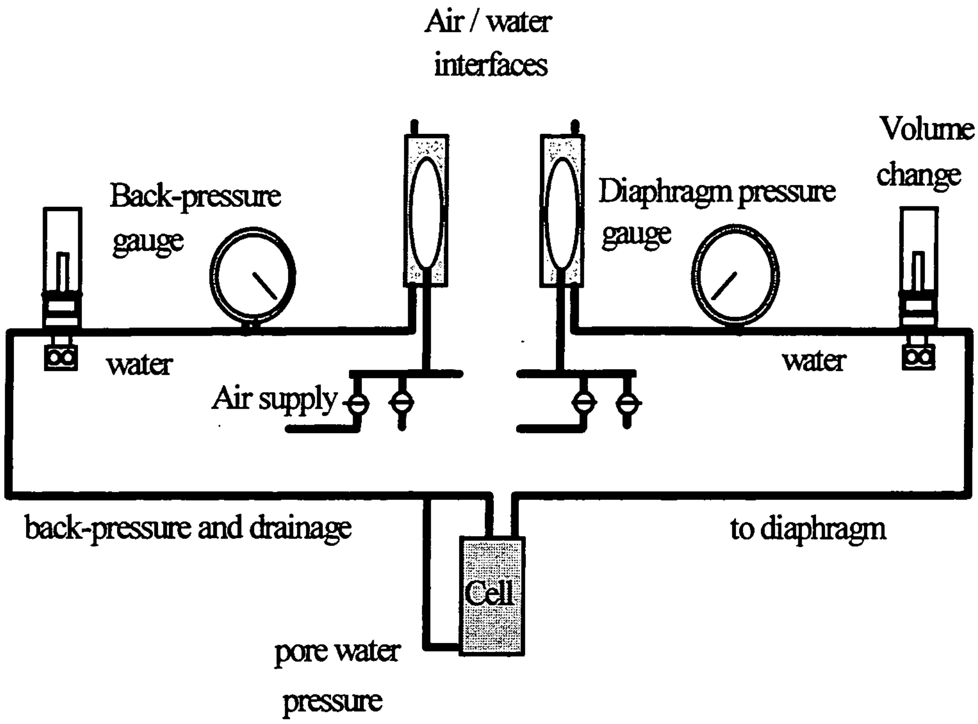

Figure 4.2. Pressure systems supplying the Rowe cell.

4.3.2 Ancillary Equipment.

Necessary for a standard Rowe cell test are two independently controlled hydraulic pressure systems, each capable of supplying a maximum pressure of up to 1000kPa. One supplies the hydraulic pressure that loads the diaphragm, the other supplies the back pressure and drainage line. An air/water interface system generates the required hydraulic pressure. Each pressure system has a pressure gauge of test grade on the water line close to the cell (see Figure 4.2). Also required: a volume-change gauge with digital voltage readout on the back pressure line; power supply for pressure transducers; system for de-airing water under a vacuum; vacuum pump and pipework; elevated water reservoir and an immersion tank to contain the cell when being assembled.

4.3.3 The Standard Test Procedure.

The basic consolidation test (see BS 1377: Part 6: 1990) is described as the single vertical drainage test allowing pore water pressure to be measured at the bottom face of the sample. Several applications are possible due to the versatility of the Rowe cell. Briefly, the usual applications are: consolidation with vertical or horizontal drainage; measurement of vertical or horizontal permeability; choice of loading condition, i.e. 'fixed' or 'free' strain; simulation of drainage wells for the establishment of the optimum spacing of vertical drains; consolidation of soil initially deposited as a slurry, to investigate properties of fresh sediments whether natural or man-made; cyclic load testing and response; observation of instantaneous peak pore pressure readings in liquefaction tests and consolidation under controlled conditions using various loads.

4.3.4 A Note on Cyclic Tests.

In many applications of repeated loading, measurement of transient pore pressures and effective shear strength are the most important factors and require specially adapted triaxial compression test equipment. Cyclic tests in a consolidation cell are not relevant to stability, but indicate the degree of settlement to be expected.

Frequency, f (Hz)	Acceleration,* (g)	Velocity, v (mm/s)	Displacement, A (mm)
25	3.0	187	1.2
25	1.0	63	0.4
25	0.5	31	0.2
25	0.1	6.3	0.04
40	1.0	39	0.16
120	1.0	13	0.02

Table 4.1. Properties of vibrations used for tests

4.4 Test Requirements

In the first instance, apparatus was required to impose on to a sample the static stresses that an *in-situ* equivalent soil would experience (10, 20, 50 and 100kPa) down to approximately 10m depth. Loose samples were required to be consolidated under

* where: $v = \dfrac{a}{2\pi f}$, $a = v.2\pi f$, $A = \dfrac{v}{2\pi f}$

appropriate static load. The clear choice lay with the Rowe cell that could maintain a given pressure during vibration, whilst the sample skeleton was reducing in volume.

Secondly, the vibrations generated by vibropiling are well defined as sinusoidal, at the same frequency as the vibrodriver and are comprised of vertical and horizontal components. While particle acceleration varies rapidly with time during a single cycle of vibration, the spatial variation is slow and smooth (Selby, 1989), so that a laboratory sized sample of soil *in-situ* would experience negligible differences in dynamic stress. For example, a saturated loose sand experiencing a vibration of 1g, at 25Hz will demonstrate a maximum amplitude of 0.4mm (see Table 4.1. for examples of accelerations and corresponding amplitudes). If the propagation velocity of a compression wave (V_p) is taken to be 1500m/s, then the wavelength (λ) is some 60m. Across the diameter of a Rowe cell (i.e. 0.15m) this corresponds to approximately 1×10^{-6}mm. Under the same conditions, a dense sand (V_p = 1800m/s) has a wavelength of 72m (data taken from Table 2.4). An unsaturated loose sand will demonstrate a compression wavelength of some 8m (which corresponds to approximately 7×10^{-6}mm for a Rowe cell size sample). This displacement of 0.4mm in 60m is adequately modelled by the Rowe cell mounted on an electromagnetic shaker that vibrates the Rowe cell vertically (or horizontally) in its entirety at frequencies and accelerations that are representative of those generated during vibro-piling operations (see Figure 3.4).

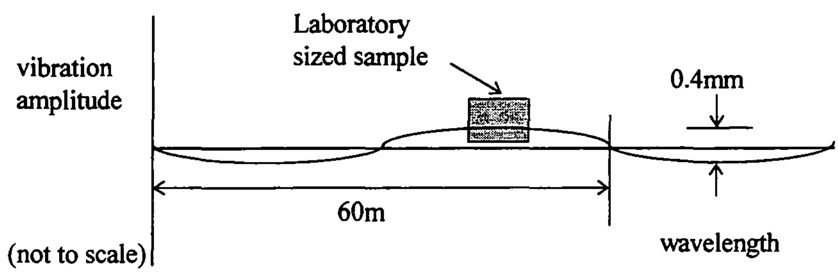

Figure 4.3. *In-situ* amplitude and wavelength (25Hz and 1g).

In addition, the direct strains that a laboratory sample experiences during vibration should be representative of *in-situ* conditions. For example, consider the following case where a loose sand sample weighing 2.5kg is experiencing an acceleration of 1.0*g* under maintained static stress (see Figure 4.4). The maximum variable force is:

$$\max \mathrm{F}(t) = m.a$$

where: max F(t) = maximum force due to sample mass and vibration = 24.5N

m = mass of sample = 2.5kg

a = acceleration = 9.81m/s^2

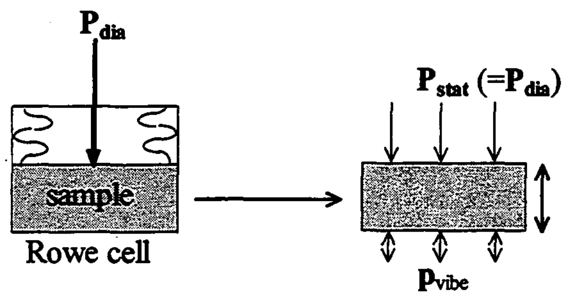

Figure 4.4. Variation in sample stress due to vibration.

The variable sample stress is given by:

$$p_{vibe} = \frac{\max \mathrm{F}(t)}{\mathrm{A}}$$

where:

p_{vibe} = maximum variable stress = 1.35kPa

A = sample area = 0.0182m^2

The direct maximum strain is then:

$$\gamma \max = \frac{p_{vibe}}{\mathrm{E}}$$

where:

E = Young's Modulus (for a loose sand use 44MPa)

γmax = maximum strain = 30.6 x 10^{-6}

Compare this value of maximum variable sample strain (30$_{\mu}\varepsilon$) with a representative *in-situ* value of 41$_{\mu}\varepsilon$:

$$\gamma \max = \frac{v}{c}$$

where:

v = peak particle velocity (for 1g at 25Hz = 62mm/s)

c = wave velocity (for a loose sand = 1500m/s)

The above shows that a reasonable correlation exists between direct maximum sample strain (approximately 30$_{\mu}\varepsilon$) and a representative loose saturated *in-situ* equivalent sand (in the order of 40$_{\mu}\varepsilon$).

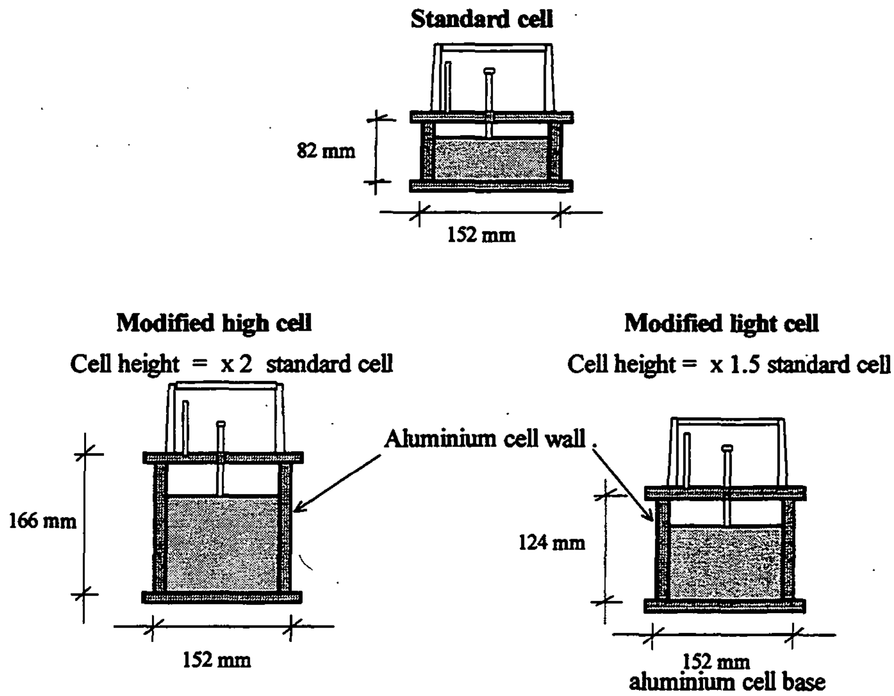

Figure 4.5. The dimensions of the available Rowe cells (see Plate 4.13).

4.5 Adaptations and Modifications.

The standard 150mm Rowe cell test is used to bring samples to a state of density that equivalent *in-situ* soil units experience, and to investigate the consolidation properties of cohesive materials when subjected to change in static load(s). The main purpose of the Rowe cell in this application was not one of (static) consolidation, rather it was used to facilitate vibratory settlement, whilst maintaining the applied static sample stress. This required a number of adaptations to the standard cell design to allow efficient sample testing. Adaptations and modifications to the test apparatus and procedure included the use of non-cohesive, high permeability soils, the effective saturation of which was considered to be achieved upon introduction to the flooded cell during test assembly. Additionally, the tests were vibratory rather then cyclic, i.e. instead of cycling the diaphragm load (producing a high cyclic stress with negligible acceleration), the entire Rowe cell assembly was vibrated using a powerful electrodynamic shaker, producing negligible cyclic stress with high acceleration.

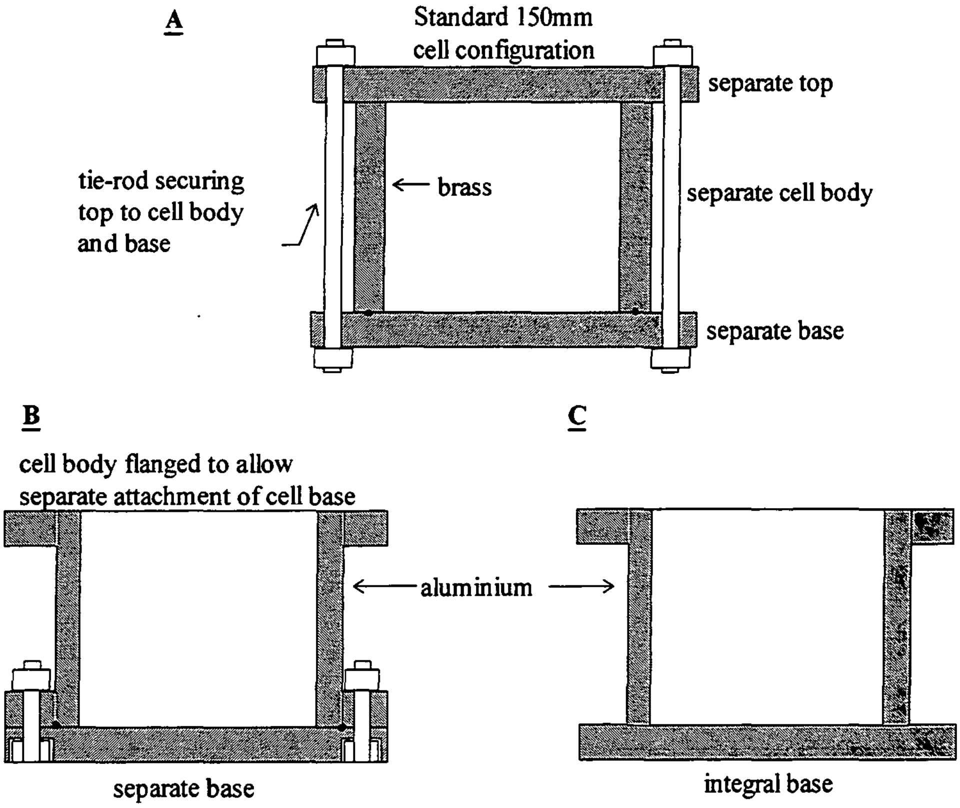

Figure 4.6. Modification of the standard 150mm Rowe Cell. Cell types B and C were used during the laboratory test programme.

Initially, a standard 150mm Rowe cell was used for preliminary testing during development of the test facility. The standard 150mm Rowe cell is comprised of a steel base plate, a separate brass cell body and an aluminium alloy top cover. The cell was assembled and secured by tie-bolts between the top and bottom plates. Unfortunately, it was difficult to prevent sand particles becoming trapped between the cell body and base plate during assembly, which compromised the cell integrity and caused water leakage, even with the rubber 'o'-ring and application of silicone grease. This problem was exacerbated by the design of the cell which only allowed intimate contact between the cell parts when the tie-rods were tightened. This was not convenient for sample preparation and general cell manipulation.

The design of the standard 150mm Rowe cell required uprating to allow good sample preparation. The larger Rowe cells have a cell body that is flanged at both ends, which allows the top and bottom covers to be bolted to the cell body individually. Consequently, a cell was fabricated that copied the bolting method of the larger cells. This prevented sand particles being trapped between the cell body and cell base, and was convenient for flooding of the cell, prior to sample placement (see Figure 4.6).

Because a portion of testing was carried out on dry and partially saturated samples, the back pressure system was not used in these cases. Thus, as required, expansion of the diaphragm was used to obtain volume change during such tests, using a volume change device in the diaphragm pressure system.

Some of the granular soils under test exhibited very small settlement upon vibrating. To increase the reliability of the results, a new cell body was manufactured of twice the standard height, giving a sample height some three times that possible in the standard 150mm cell (see Figure 4.5). Because the sample height was increased by a factor of three, settlements were increased, which allowed greater differentiation of the effects of the test conditions upon a given soil type. However, some soils showed large vibratory settlements and numerous volume change valve reversals and dial gauge extensions during testing were required. Such operations served to complicate the test procedure and data analysis. In addition, turning the valves on a volume change device caused a change in the hydrostatic pressure of approximately 1.5kPa. During testing, and especially during vibration, this was seen to produce either: an increase in the settlement rate when the valves were pulled out, or a decrease in the settlement rate when the valves were pushed in. Such effects were clearly undesirable because the vibratory settlement response of soils were influenced by change(s) in the maintained static load, which could increase inherrent error during later data analysis. Because high acceleration tests (to 6*g*) produced large reduction in sample volume, such tests required more volume changes than low vibration acceleration tests. Also an initially larger sample, prepared in the tall modified cell, tended to experience more volume reduction and hence more volume changes. To reduce the frequency of the problem, the volume change device on the diaphragm pressure system was disconnected. In addition, a cell body that was 1.5 times the standard cell height was fabricated which allowed a sample height of twice that of the standard cell (see Figure 4.4); this also reduced the number of volume changes required during testing. Thus, when low acceleration tests were performed, volume change valve turns were required only during the first minute of the static consolidation test.

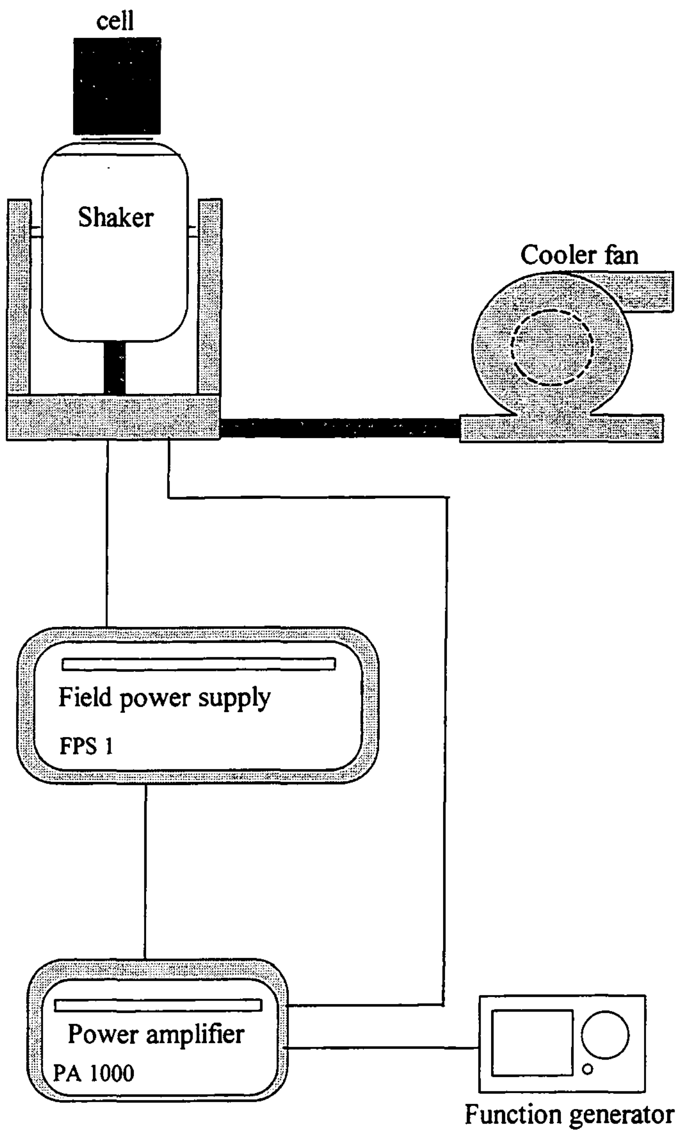

Figure 4.7. The shaker system.

4.6 The Shaker System

During the vibration phase of the tests, the entire Rowe cell assembly was mounted on a powerful electro-magnetic shaker. The shaker system was comprised of an electrodynamic unit, driven by a power amplifier acting on an analogue signal from a signal generator, and a field power supply control unit (see Figure 4.8).

The Ling Dynamic Systems 550 series Vibration Generator is a wide frequency band electrodynamic transducer capable of producing a peak sine vector force of 665N. The Vibration Generator nominally operates in the frequency range of 5-6300Hz (operation below 5Hz is possible with a suitable amplifier), from either a sine wave or random signal input and is driven by power amplifiers of up to 1kVA.

The 550 series Vibration Generator consists of a magnetic structure which houses and supports the armature and field coils. Field and armature coils are suction air cooled by means of a remotely located fan. The Vibration Generator is trunnion mounted and can be locked in the vertical or horizontal position by means of clamp bolts. A built-in air load support (up to 550kPa) allows a maximum payload capacity of 25kg with full relative displacement (see Figure 4.7).

The Amplifier is a nominal 1000VA air cooled linear amplifier that has been designed to drive reactive loads such as vibration generators. Fast acting security circuits are used to protect the amplifier under all known overload conditions including direct short circuits, thermal overload, cooling fan failure and external vibration generator faults. The control and interlock circuits are arranged so that the amplifier cannot provide output current if there is an internal or external fault. The exact fault condition is indicated by an L.E.D. lamp mounted on the front panel.

The control circuits include true R.M.S. current metering that indicates the r.m.s. output current on an L.E.D. bar graph. The over-current protection circuit can be adjusted to switch off the amplifier when the output current reaches a pre-set level anywhere between 0-100% of the maximum current.

The Field Power Supply is the control centre of the vibrator system. The unit supplies the vibrator field coils, the vibrator cooling blower, the power amplifier and houses the degauss coil adjustment potentiometer. Simple interlock circuits ensure the vibration system is powered in the correct sequence and, in the event of failure, prevents possible damage occurring to the system.

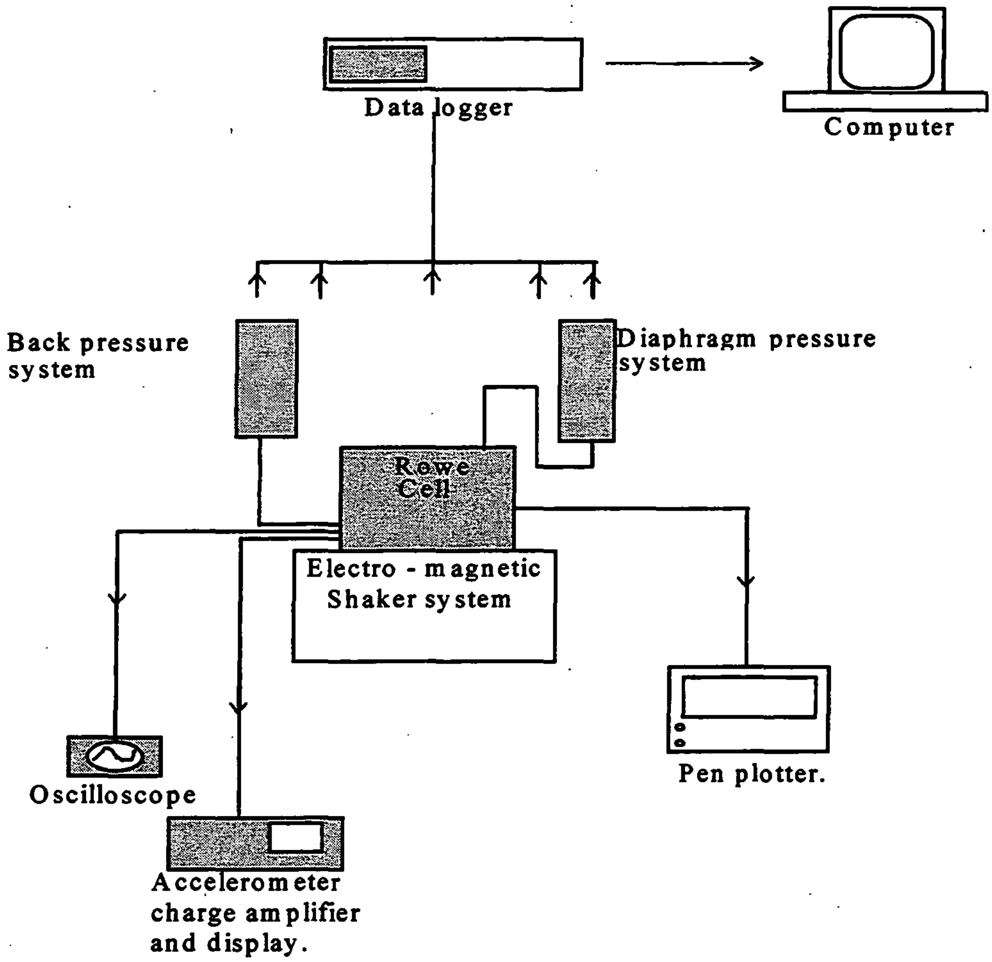

Figure 4.8 The complete laboratory system (see Plate 4.2).

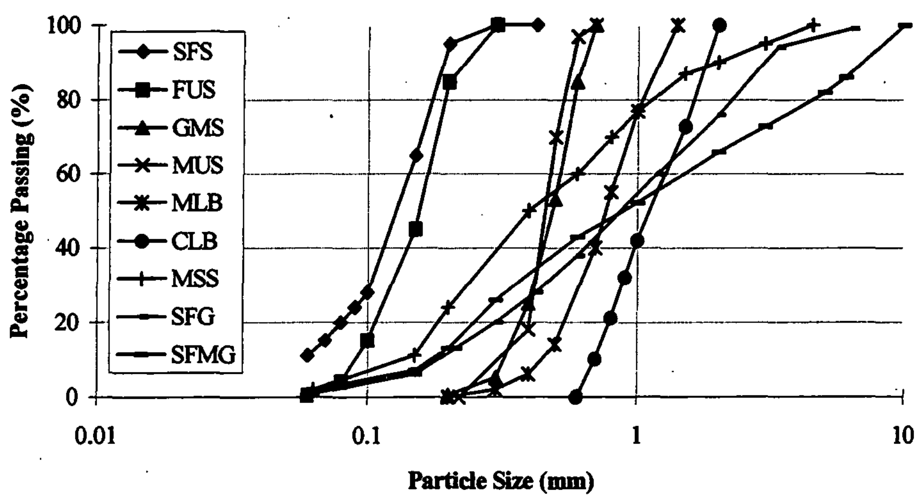

Figure 4.9. Particle size distribution of the soils (see Table 4.2).

Soil type	D_{10} (mm)	D_{30} (mm)	D_{60} (mm)	D_{90} (mm)	D_{max} (mm)	U_c	C_c	Sphericity	Angularity
SFS	0.06	0.13	0.15	0.17	0.30	2.42	1.94	d	3
FUS	0.09	0.14	0.17	0.26	0.43	1.89	1.28	b-d	2-3
GMS	0.31	0.43	0.53	0.68	0.90	1.71	1.10	b-d	2-3
MUS	0.38	0.45	0.56	0.64	0.70	1.47	0.95	d	3
MLB	0.45	0.61	0.84	1.10	1.20	1.87	0.98	d	2
CLB	0.70	0.87	1.25	1.95	2.00	1.79	0.87	d	3
MSS	0.15	0.24	0.60	1.60	4.30	4.14	0.63	b-d	1-4
SFG	0.17	0.45	1.20	3.30	6.30	7.06	0.99	b-d	1-4
SFMG	0.18	0.24	1.55	8.00	10.00	8.61	0.52	a-d	1-4

1 rounded, 2 subrounded, 3 subangular, 4 angular, a flat, b oblate, c subspherical, d spherical

Table 4.2. Summary of soil-type grading characteristics (see Figure 4.9).

	Friction Angle (ϕ)	Specific Gravity (G_s)	e_{min}	e_{max}
SFS	33	2.66	0.645	1.08
FUS	29	2.67	0.640	0.994
GMS	30	2.64	0.558	0.784
MUS	32	2.61	0.623	0.748
MLB	37	2.64	0.613	0.835
CLB	32	2.63	0.601	0.771
MSS	32	2.65	0.432	0.848
SFG	34	2.63	0.595	0.892
SFMG	35	2.63	0.247	0.616

Table 4.3. Summary of the soil-type physical characteristics.

4.7 Soil Types

The nine soils selected for this work covered a wide range of particle sizes, from uniform sands to well graded (poorly sorted) sandy gravel (see Figure 4.9 and Table 4.2). The majority of the soils occurred naturally, and were obtained by direct excavation or from a quarried supply (sometimes screened). Standard laboratory tests were conducted on all the soils (see Appendix 1), including grading, friction angle from shear box tests, maximum and minimum void ratios, and the production of thin sections* to demonstrate particle shape. Minimum void ratios were taken to be the void ratio after completion of the highest acceleration increment during vibratory testing.

Note that a coarse sharp sand was initially used during the high acceleration tests. However, the grading of the source material changed so that the material that was supplied became a medium sharp sand. The only difference between the two materials

* The thin sections were prepared by placing loose specimens in expoxy resin (under vacuum to remove trapped air). When the resin had hardened, the samples were cut to 30μ slices and mounted on microscope slides. Photographs were taken and are shown as Plates 4.6 to 4.15. The use of thin-sections is a common technique used by geologists to aid in the identification of mineral species and hence, rock type.

was assumed to be a change in the particle size distribution, so the physical properties (ϕ, G_s, e_{min}, e_{max}) of the coarse sharp sand (see Plate 4.13) were taken to be the same as those of the medium sharp sand. The soil types were:

Silty Fine Sand (SFS): A subrounded to subangular, pale brown, silty fine quartz sand from a construction site on the southern perimeter of Durham; U_c = 2.3, C_c = 1.9, e_{max} = 1.08 and e_{min} = 0.645 (see Plate 4.6).

Fine Uniform Sand (FUS): A subrounded to subangular, beige, fine uniform quartz sand from Leighton Buzzard; U_c = 1.9. C_c = 1.3, e_{max} = 0.994 and e_{min} = 0.640 (see Plate 4.7).

Garside Medium Sand (GMS): A subrounded to subangular, yellow, medium uniform quartz sand from Lancashire; U_c = 1.7, C_c = 1.1, e_{max} = 0.784 and e_{min} = 0.558 (Plate 4.8).

Medium Uniform Sand (MUS): A subrounded to subangular, beige, medium uniform quartz sand from Cheshire; U_c = 1.5, C_c = 1.0, e_{max} = 0.748 and e_{min} = 0.623 (see Plate 4.9).

Medium Leighton Buzzard Sand (MLB): A rounded to angular, orange, medium uniform quartz sand; U_c = 1.9, C_c = 1.0, e_{max} = 0.835 and e_{min} = 0.613 (see Plate 4.10).

Coarse Leighton Buzzard Sand (CLB): A subrounded to angular, beige, coarse uniform quartz sand; U_c = 1.8, C_c = 0.9, e_{max} = 0.771 and e_{min} = 0.601 (see Plate 4.11).

Medium Sharp Sand (MSS): A round to angular, brown, medium to coarse well-graded river-dredged sand of mixed mineralogy (particles of sedimentary and igneous rock) from Scorton, N. Yorks; U_c = 4.2, C_c = 0.6, e_{max} = 0.848 and e_{min} = 0.432 (see Plate 4.12).

Sandy Fine Gravel (SFG) : A round to angular, grey-brown, well-graded sand to fine gravel of mixed mineralogy (particles of sedimentary and igneous rock) from a quarry near Penrith; U_c = 7.1, C_c = 1.0, e_{max} = 0.892 and e_{min} = 0.595 (see Plate 4.14).

Sandy Fine to Medium Gravel (SFMG): A round to angular, orange-brown, well-graded sand to medium gravel of mixed mineralogy (particles of sedimentary and igneous rock) excavated from the A19 Improvement at Aisenby; U_c = 8.6, C_c = 0.5, e_{max} = 0.616 and e_{min} = 0.247 (see Plate 4.15).

4.8 Vibratory Rowe Cell Test Procedure.

The vibratory Rowe cell test, as developed for this work, may be divided into four parts: the pre-test preparation and system checks; application of static load; vibratory settlement response and post-test sample evaluation. A saturated soil test is described below (dry and partially saturated tests are detailed in Section 4.8.5).

4.8.1 Sample Preparation.

Prior to testing, bulk samples were placed into containers of suitable size and manually mixed with distilled water to effect pre-test saturation. Several methods of sample preparation were attempted prior to the development of the accepted method, including :

a) Simple at-moisture-state placement - An oven dried sample was mixed with water to produce a partially saturated material that was air pluviated into the cell and lightly skimmed to form a horizontal surface. The sample was saturated by slowly flooding from the cell base upwards . The load/drainage disc was then set on the sample surface.

This method, although straightforward, produced a number of problems associated with sample particle migration. Due to the granular nature of the material, the initial application of static load caused some particles to migrate from the sample through the gap between the load/drainage disc and the cell wall. Subsequent vibratory testing tended to increase migration along preferred sections around the disc (probably reflecting initial movement during static loading). The final effects of sample migration were: the removal of material from the sample; partial or serious blocking of the back pressure drainage line in the centre of the diaphragm; jamming of the disc (due to particles caught between the disc and cell wall) and due to the mode of sample loss, a degree of disc rotation about the horizontal axis. Such occurrences adversely affected the confidence of the settlement results because the data obtained did not only reflect the tendency of the material to reduce in volume due to a reduction in void space, but also the effects of sample loss and preferred disc mobility.

b) Confined slurry - The confined slurry technique was developed to prevent the problems described above, whilst allowing sample manipulation and maintaining a loose sample structure prior to the application of static load.

A sample was placed into a fine-meshed nylon bag* to ensure that during application of static load and subsequent vibration, the material behaved as a coherent unit of soil, i.e. the sample confining bag (SCB) stopped particle migration between the disc and the cell wall, so avoiding jamming of the disc. Thus, observed settlements

* The foot section taken from standard nylon tights. Different types of material were evaluated for use: 10 denier allowed particles to move through the mesh; 20 denier was too elastic and constricted the sample immediately below the load/drainage disc. It was found that 15 denier was a good workable compromise material, preventing sample migration without constraining the distortion of the whole sample upon loading.

could be attributed to a reduction in the volume of the soil mass as a whole, and not due to loss of material from the initial mass from beneath the disc.

The slurry technique was used throughout because it allowed good sample control and behaviour during testing, although it produced a range of relative densities. Two forms of confined slurry were used before the final modification:

i) A previously submerged sample was placed into a damp SCB and the open end was then knotted to prevent sample loss. The sample was shaped into a rough cylinder, narrower than the internal diameter of the cell, prior to placement into the cell. After flooding, a load/drainage disc was placed on to the sample. This method prevented particle migration (although some fines were lost as 'cloudy water' on application of static load, and again when experiencing vibrations at or above 3.0*g*). However, completed tests, on removal of the disc, showed a tendency to be 'necked' by the SCB below the disc, i.e. the knotted bag formed a confining volume that restricted the ability of the sample to achieve full static compaction potential. This suggested that the vibratory settlements observed were probably exaggerated with respect to an equivalent sample in the field under the same conditions. This method was then modified:

ii) Samples were placed into the SCB as described above. However, the modification required that instead of tying the bag, it was allowed to rest loosely upon the top surface of the sample and partially cover it. Because the top of the sample was not laterally confined by the SCB, 'necking' did not occur. To minimise potential particle migration, a disc of geofabric♣ was placed on the sample, beneath the fold of the SCB resting on the sample surface. However, whilst 'necking' was prevented, some particle migration did occur. Hence, further modification was required.

c) Disc in-place confined slurry technique - The sample was placed into the SCB (see Figure 4.10) and the disc was placed within the SCB, onto the sample in the SCB; the SCB was then drawn up and over the disc. The SCB was then 'over loosened', producing a free-standing sample wider than the internal diameter of the Rowe cell. This ensured that the nylon mesh did not act in tension to constrain the movement of the material. The wider sample required additional distortion (i.e. loosening) during placement into the cell.

♣ Spunbonded polypropylene.

Any grains adhering to the material of the SCB above the disc were washed down below the disc level. This ensured that particles were not trapped between the disc and the SCB, which could have caused eventual jamming and/or tearing of the nylon mesh. The clean SCB material was doubled-back over the sample to form a double-layer (see Figure 4.11), and partially cover the upper surface of the disc. This placed more nylon mesh into the potential migration path of particles, and reduced the space between the disc and cell wall which further protected against movement of particles.

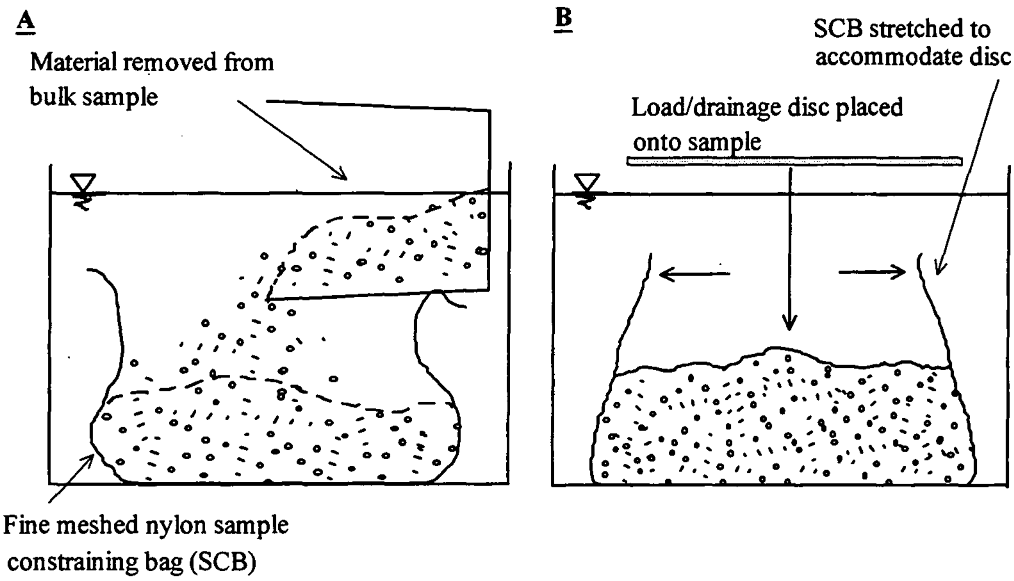

Figure 4.10. (A)The test-sample being placed into the sample confining bag (SCB), and (B) placing the load/drainage disc.

Two loops of nylon mesh material were used to lift the sample to the cell, (see Figure 4.11) and allowed placement and manipulation of the sample in the cell. The sample was slowly lowered into the distilled and de-aired water filling the cell (see Figure 4.12). During the travel down to the cell base, the sample was gently rocked from side to side to encourage the extrusion of any trapped air. When the sample reached the cell base, one of the loops was cut and removed. The remaining loop was used to adjust the sample (if required), so that it was horizontal and central in the cell. The sample was now prepared for cell assembly and application of static load.

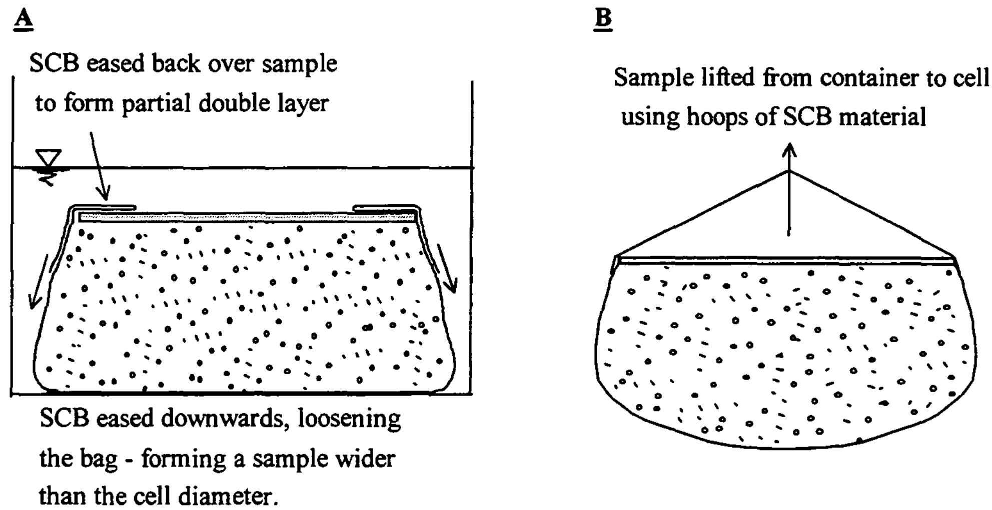

Figure 4.11. (A) Positioning the SCB onto the disc, and (B) removing to the Rowe cell.

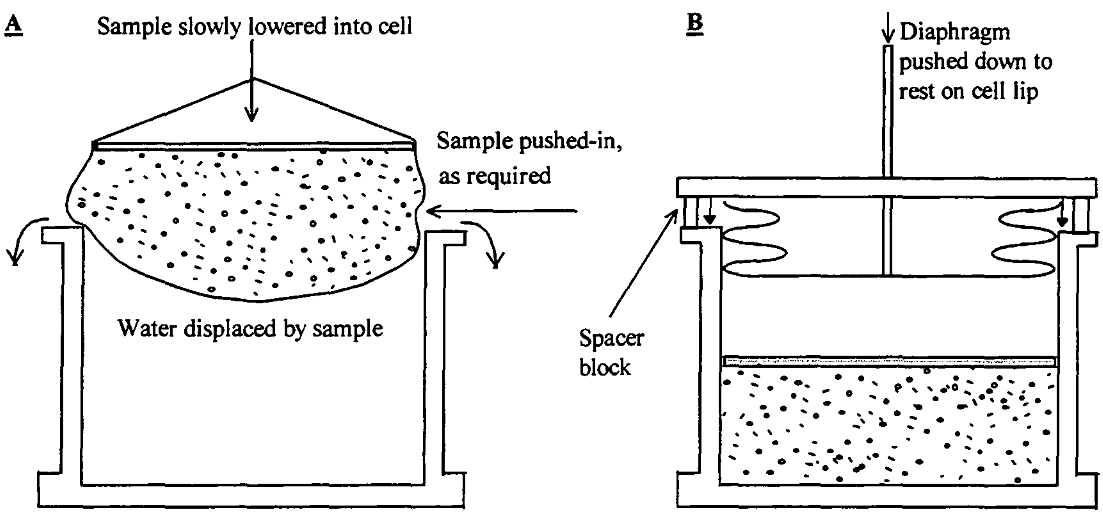

Figure 4.12. (A) Placement of the sample into the cell, and (B) lowering the diaphragm.

4.8.2 Static Loading and Consolidation

The diaphragm pressure (DP), back pressure (BP) and pore water pressure lines were connected into the cell at the appropriate points. Three spacer blocks were placed onto the cell-body lip. The cell top/diaphragm assembly was placed onto the spacer blocks and centralised over the cell base. A drop of lubricating oil was placed on the spindle next to the cell top, to encourage free movement of the spindle to changes of sample height. The BP line was opened and de-aired water trickled out from the diaphragm drainage hole, removing any trapped air from the BP line. The diaphragm was then lowered partly into the cell by pushing down on the drainage spindle (displacing water over the side of the cell). The water flowing out from the BP line ensured that no air was trapped during the lowering of the diaphragm. The DP line was opened, and the diaphragm filled.

The cell top was held in position after the removal of the spacer blocks, and then moved downwards, relative to the spindle position (and not pressed down as a unit onto the sample which could cause unwanted pre-compaction), until the lip of the diaphragm rested on the cell top. After bolting down, the DP line was briefly opened which extruded air trapped in the diaphragm via the air-bleed valve in the cell top. All valves were then shut prior to the application of the required static pressures.

Static loads required for testing were chosen to represent pressures generated by overburden to depths of about 10m. Static loads of 10, 20, 50 and 100kPa were selected. Because the force exerted by the diaphragm on to the load/drainage was reduced due to diaphragm stiffness and side friction, a diaphragm calibration was required. It was found that the following relationship was necessary to modify diaphragm pressure to generate the static loads required (see Appendix 4.2 for details). Pressure applied to sample = 0.85 x (Diaphragm pressure)-2.46. A constant value of back pressure (i.e. 50kPa) was used for all tests. Thus, to produce the effective stresses required (i.e. 10, 20, 50, 100kPa), diaphragm pressures required were 74, 85, 120 and 179kPa (see Table 4.3).

The required diaphragm pressure and back pressure was set using the output of the 3.5bar pressure transducers displayed on a digital voltmeter. All transducer outputs were checked and recorded. The DP and BP lines were opened together, and primary static consolidation occurred rapidly (a duration of seconds to minutes). For convenience of testing, the sample was left under static load overnight.

4.8.3 Vibratory Settlement

After selecting the required frequency on the function generator (i.e. 25, 40 or 120Hz) the vibratory system was powered-up. Pressurised air was supplied to the shaker body which raised the shaking platform to the central position for that payload (i.e. the

Rowe cell plus sample), to prevent over-travel, allow full peak-to-peak displacement and protect the vibrator from damage.

Diaphragm Pressure (kPa)	Back Pressure (kPa)	Effective Stress (kPa)
74	50	10
85	50	20
120	50	50
179	50	100

Table 4.4. The hydrostatic (diaphragm and back) pressures used during testing.

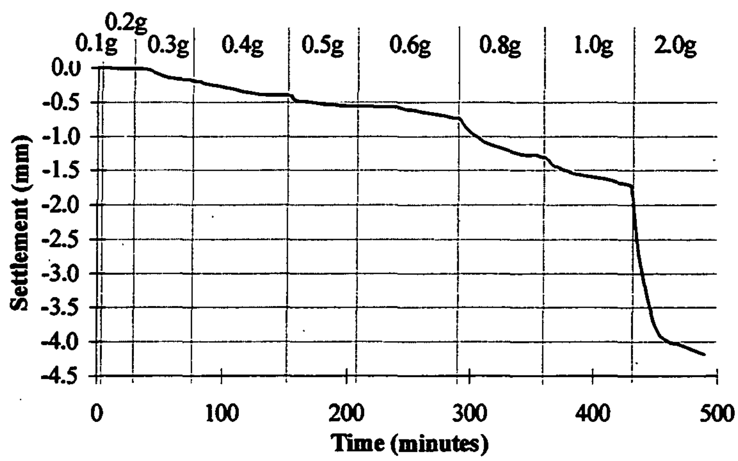

Figure 4.13 Typical form of a vibratory test result.

One minute prior to the application of vibration, the data logger was set to scan at ten second intervals. Data logger recorded test information was used as data back-up. Then the signal generator voltage was increased from zero so that the shaker vibrated at 0.1g (detected by an accelerometer), which was displayed on the accelerometer's calibration unit. Manual readings of height and volume change were taken after the first 30 seconds, 1 minute, 2 minutes, 5 minutes and subsequently, every 10 minutes until no further settlement was observed*. The recording interval of the data logger was similarly

* Tests performed at 25Hz were taken to be complete, under a particular increment of acceleration when the settlement rate approached zero, as indicated by the pen plotter. Later tests, performed at 40Hz took about 2 to 3 times as long to complete an increment of acceleration then the 25Hz tests. To enable completion of the 40Hz data, and to complete a vibration test in one day, a time limit of 1 hour per vibration increment was imposed on testing. Settlement data obtained were then extrapolated to 2 hrs.

increased during testing. The vibration was reduced to zero, and volume change and settlement LVDT readings were recorded prior to continuation of vibration at the next increment of acceleration. The sequence of incrementing the acceleration by 0.1g up to 0.6g, then onto 0.8g, 1.0g and 2.0g was applied for the majority of tests. However, in addition, a series of tests were performed starting at 1g which proceeded in increments of 1g up to 5-6g to examine the settlement response of soil to higher magnitude vibrations.

The shaker system was powered down and all power to the system shaker, peripheral devices and transducers switched off. Figure 4.13 shows a typical test result.

4.8.4 Post Test Vibratory Settlement Determination.

After the Rowe cell was removed from the shaker, the height of the drainage spindle above the cell top was recorded to back-up subsequent sample height determination. Back pressure and diaphragm pressure lines were disconnected. After removal of the cell top, a depth gauge (accurate to 0.02mm) was used to record the depth to the sample from the top of the cell at four places around the edge of the sample. Depth to sample was taken as the mean of these four values (which showed a maximum variation in the order of ± 0.5mm) . Post-test sample height (h1) was calculated as the mean depth to sample taken from the internal cell height. The cumulative settlement obtained during vibration (Δh), added to the post-test sample height, produced the pre-test sample height (h0). Vibratory settlement (%h) was then expressed as the vibratory settlement divided by the pre-test sample height.

After the measurements required to determine settlement were taken, the sample was removed from the cell for moisture content determination by the oven drying method. Plate 4.1 shows an oven dried sample in a sample confining bag.

4.8.5 Partially Saturated and Dried Tests

In the laboratory, all samples were statically loaded in the saturated state. Depending on the moisture content required for subsequent testing, samples either remained in the cell (for saturated vibratory tests) or the cell was dismantled for samples requiring partially saturated or dried vibratory testing. The procedures for dried and partially saturated samples were as follows:

a) Dried Sample Treatment - After dismantling the cell, water submerging the sample was drained from the cell. The sample and cell were then weighed (for later determination of the consolidated moisture content (CMC)), and placed into an oven (at $50^{o}C$). Periodic checks of the drying-back mass were performed until achieving constant dry mass (usually after about two days). The sample was left to cool and air-equilibrate.

The original static stress was applied after replacing the cell top for subsequent vibration testing.

b) Partially Saturated Sample Treatment - The CMC of all test data fell within the range of values, (typically) between 22% and 28% (see Appendix 3). Because of the variation in moisture contents, a mean value of CMC (i.e. 25%) was taken as a reasonable 'global' value. Partially saturated soils were dried back to a value of 0.5CMC.

Samples being prepared for partially saturated testing were placed onto electronic scales, and a 100W lamp was lowered over the sample. The mass of the sample was monitored as the heat from the lamp dried the sample back, until the mass that gives a moisture content of about 12.5% was attained. The sample was then sealed and allowed to cool and equilibrate, prior to cell re-assembly.

A number of tests were performed that examined the effect of degree of saturation on vibratory settlement, using the medium uniform sand.

4.8.6 Additional Vibration Tests

Compression waves propagating out from the pile have vertical and horizontal components. Close to the pile, the vertical component is dominant, and as stand-off distance increases, the horizontal component tends to dominate. However, because magnitudes of vibration are greatest near to the pile, and attenuation is rapid, the use of vertical vibration is considered to adequately model *in-situ* conditions. To check this assumption, a limited number of tests were performed using horizontal vibration, and indicated broadly similar settlement response compared with equivalent tests performed using vertical vibration.

<u>Horizontal Vibration</u> - In addition to vertical vibration tests, horizontally orientated vibration tests were performed. To protect the shaker from damage, the Rowe cell was suspended by wire from the ceiling attached to a frame that was bolted to the cell top. The Rowe cell was bolted to the shaker which had been turned through ninety degrees,

allowing the application of horizontal (compression) vibration (see Plate 4.4). Because of contrasting physical characteristics, a medium sharp sand and a medium Leighton Buzzard sand were selected for testing. The soils were tested over the usual range of static stresses, in the saturated state. In addition to the compression waves that are produced by vibropiling, shear waves are also generated. Thus, laboratory test were performed to investigate the effects of shear waves on granular material.

<u>Shear Vibration</u> - Torsional shear vibration was applied to a sample by exploiting the design of the Rowe cell. Because the drainage spindle was free to rotate at the centre of the cell top, a strip of metal (flexible in the vertical plane, but stiff in the horizontal plane) was attached to the spindle. The metal strip was then attached to two horizontally mounted small vibrator units (LDS PA 100) that were set to act out of phase. The vibrators then agitated the metal strip at 40Hz up to accelerations of 0.75g, in increments of 0.1g. The spindle was then caused to rotate back and forth through a small arc, which turned the diaphragm and subjected the sample to shear vibrations (see Plate 4.5).

This method required that the load/drainage disc was integral with the spindle, to ensure that the vibrations generated were transmitted to the sample. The sample preparation technique required modification: the sample, in a SCB, was placed into the cell without a load/drainage disc. Assembly of the cell brought the load drainage disc to rest on the sample. Good contact between the sample and disc was achieved; an imprint of the load disc was observed on the sample surface.

4.9 Summary

The Rowe cell was selected as the central element of the laboratory test facility. Satisfying the test requirements, it allowed static consolidation of loose granular samples; maintained effective static stress during vibration and permitted sample volume reduction. Mounted on an electromagnetic shaker, the cell was vibrated at frequencies and accelerations that were representative of the *in-situ* vibrations generated during pile driving operations.

The standard 150mm Rowe cell was uprated to better suit the application of this research. A novel sample technique was developed, allowing good sample preparation control and reliable behaviour during subsequent static loading and vibration.

Nine granular soils were tested under a range of maintained static loads (10, 20, 50 and 100kPa), over a range of accelerations (0.1g up to 6.0g), at 25 and 40Hz using vertical, horizontal and shear vibrations in a saturated, partially saturated and dried state (Table 4.5. summarises the laboratory test programme). The results from the laboratory test programme and the analysis are presented in the following chapter.

Range of granular soils
Frequencies of 25, 40, 120Hz
Accelerations of 0.1 - 0.6, 0.8, 1.0, 2.0g
Acceleration of 1.0 - 6.0g
Static loads of 10, 20, 50, 100kPa
Saturated, dried-back, partially saturated
Time length of vibration
Vertical, horizontal, shear vibration
Miscellaneous tests

Table 4.5. Summary of the laboratory programme.

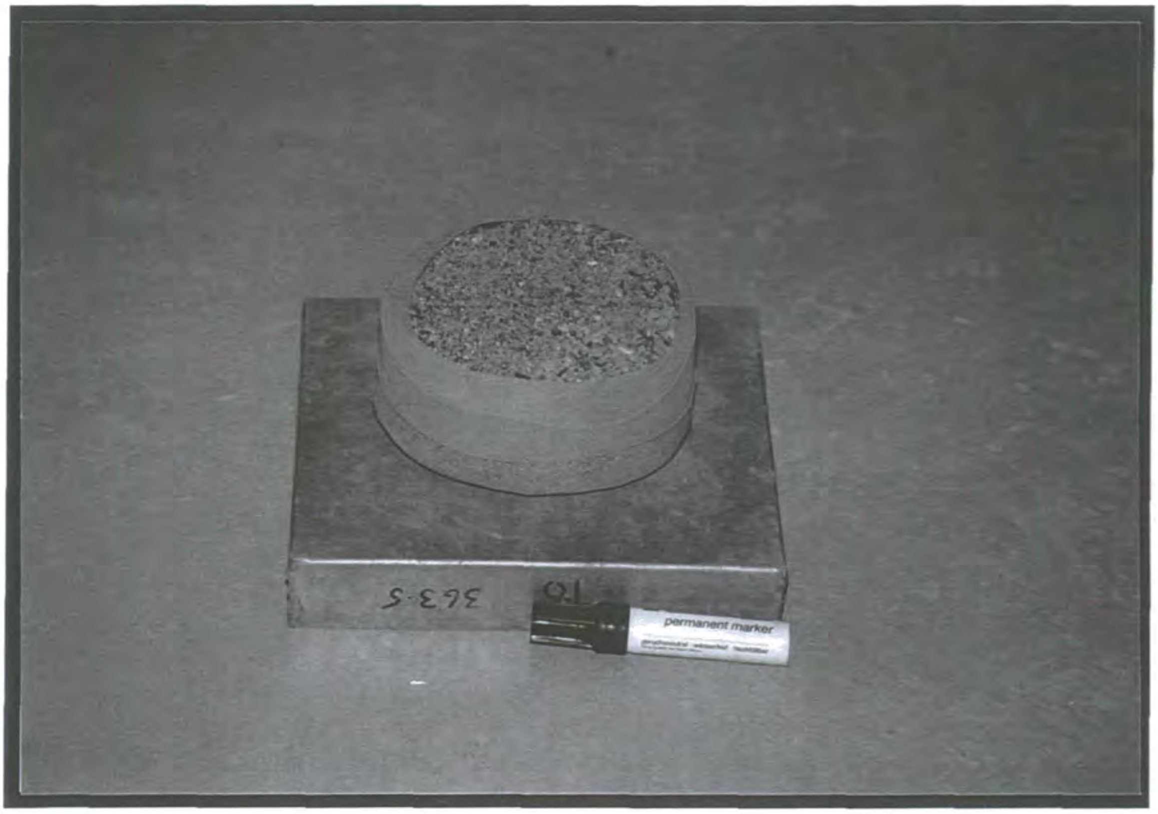

Plate 4.1. Post-test sandy fine to medium gravel in the sample confining bag after oven drying for moisture content determination.

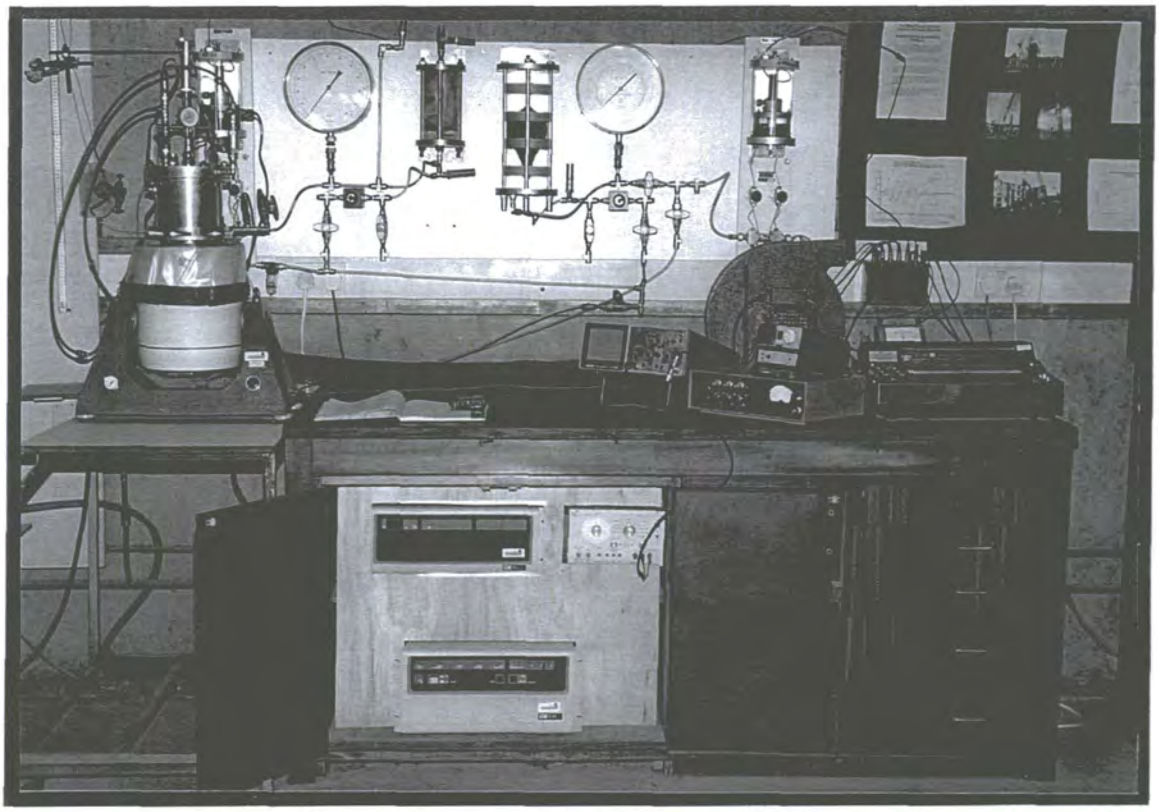

Plate 4.2. The laboratory test facility, with cell in the vertical vibration orientation.

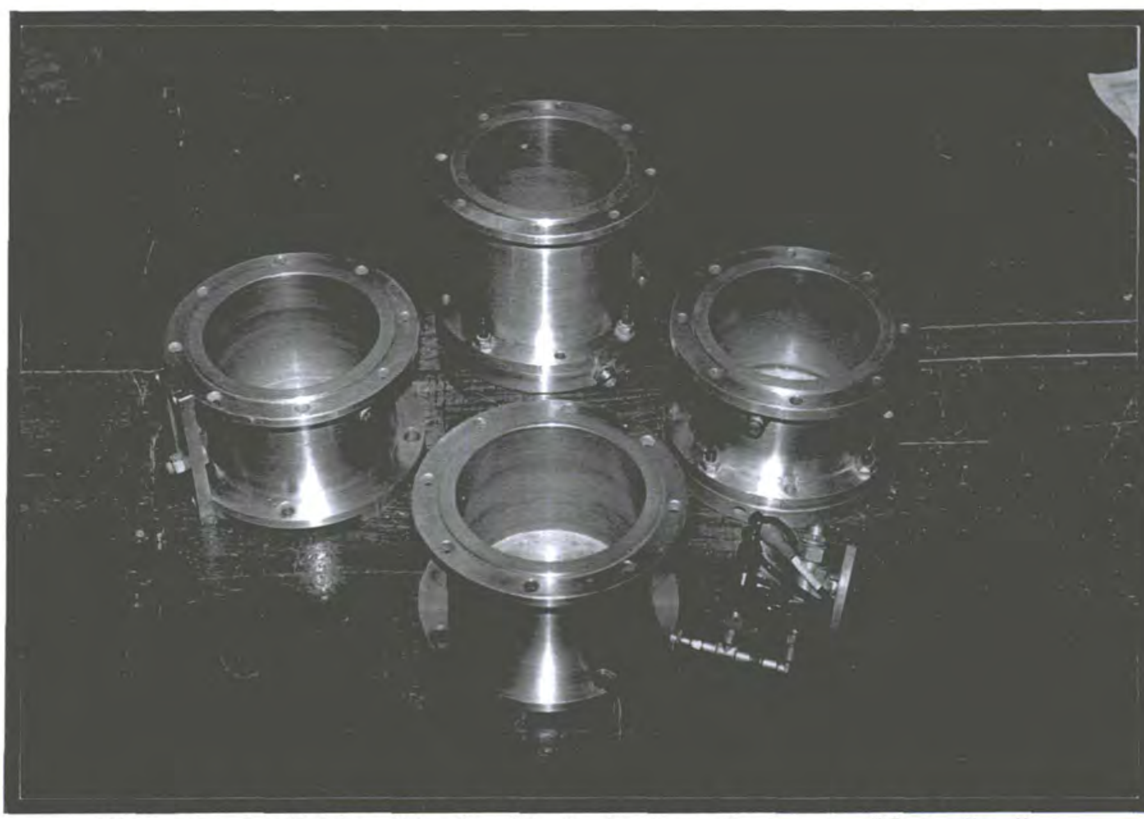

Plate 4.3. Available cell bodies (clockwise from the top: modified tall cell; modified cell; modified cell with integral base; cell adapted for horizontal vibration).

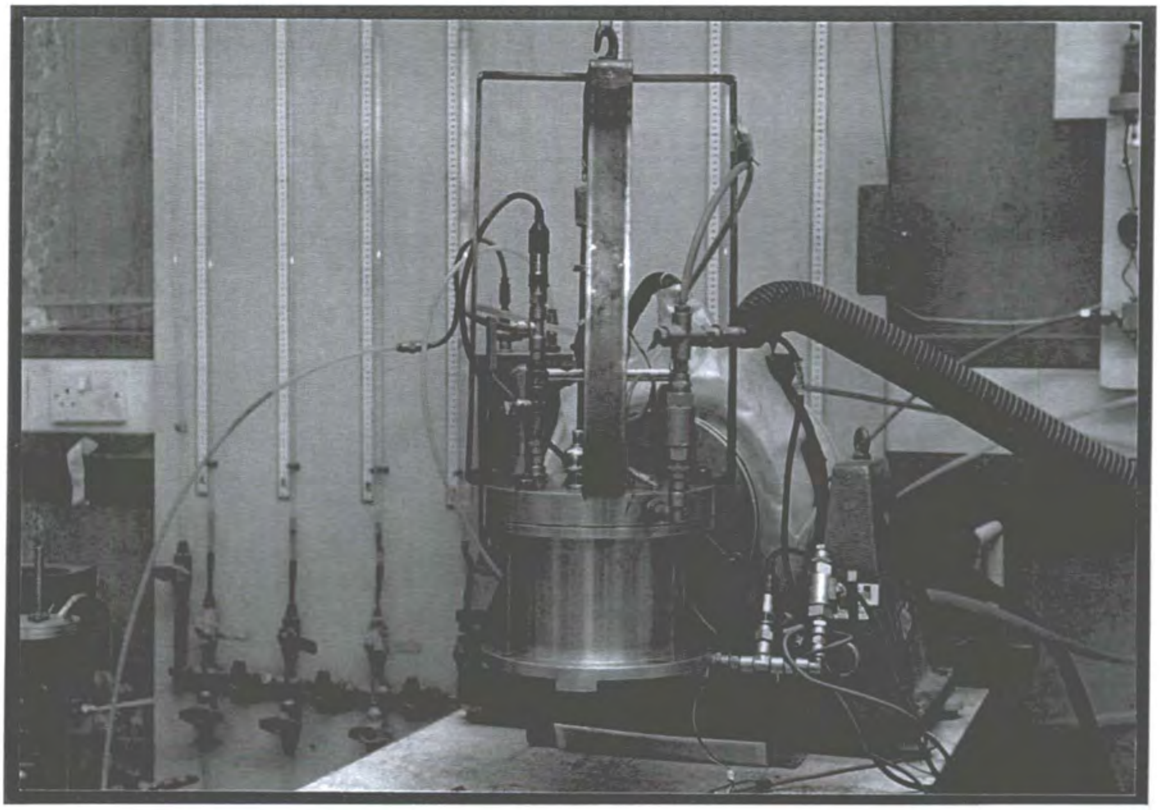

Plate 4.4. Rowe cell and shaker configured for horizontal vibration.

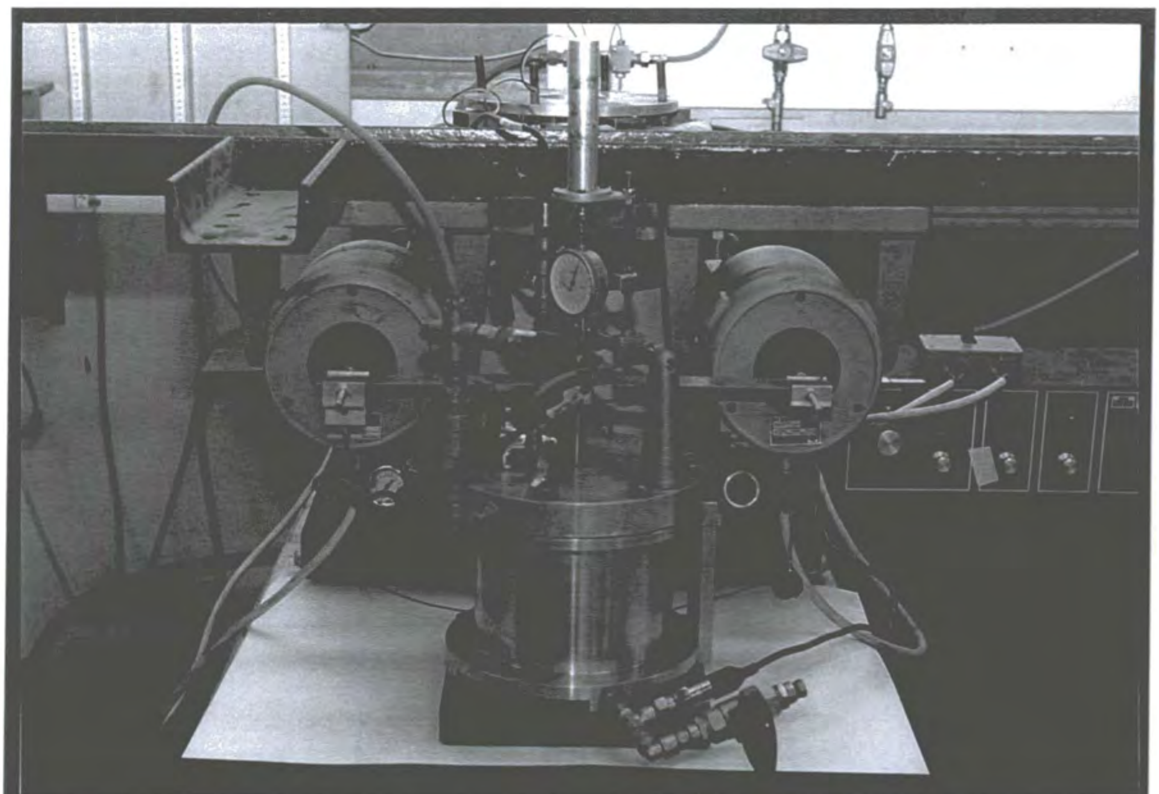

Plate 4.5. Rowe cell and shakers configured for torsional shear vibration.

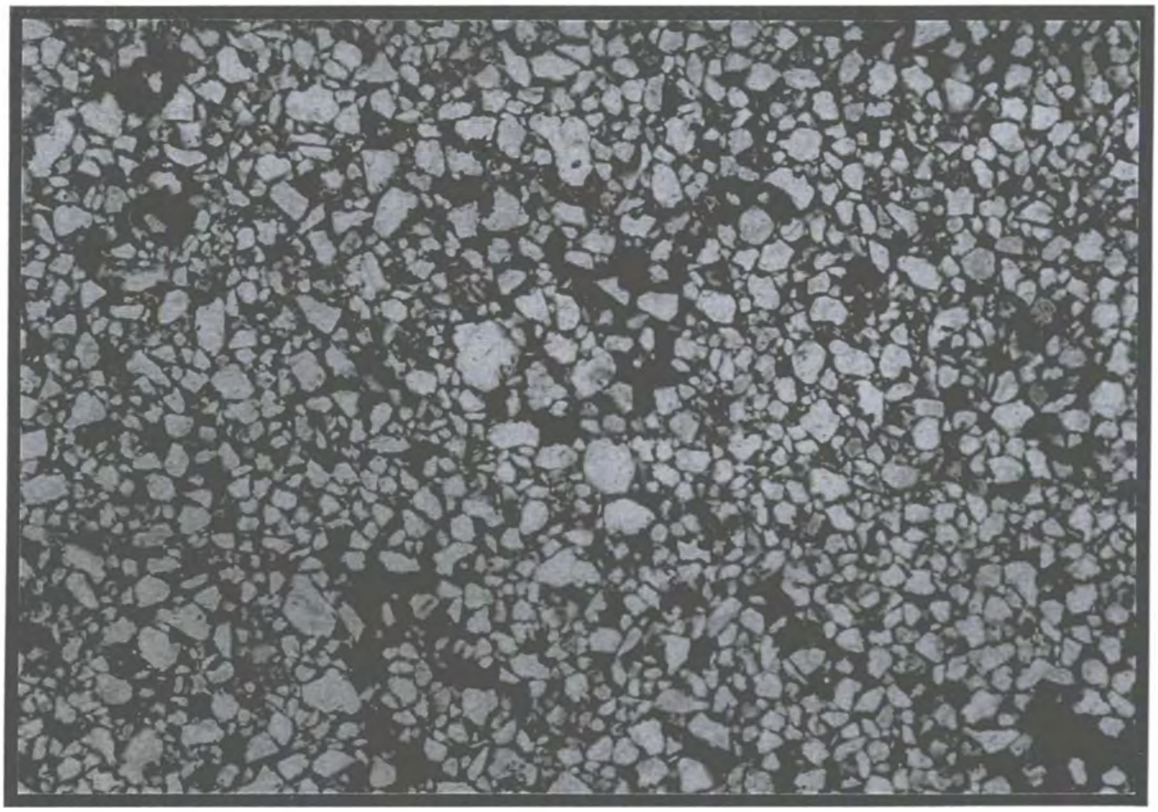

Plate 4.6. Thin-section of silty fine sand (x 25 magnification).

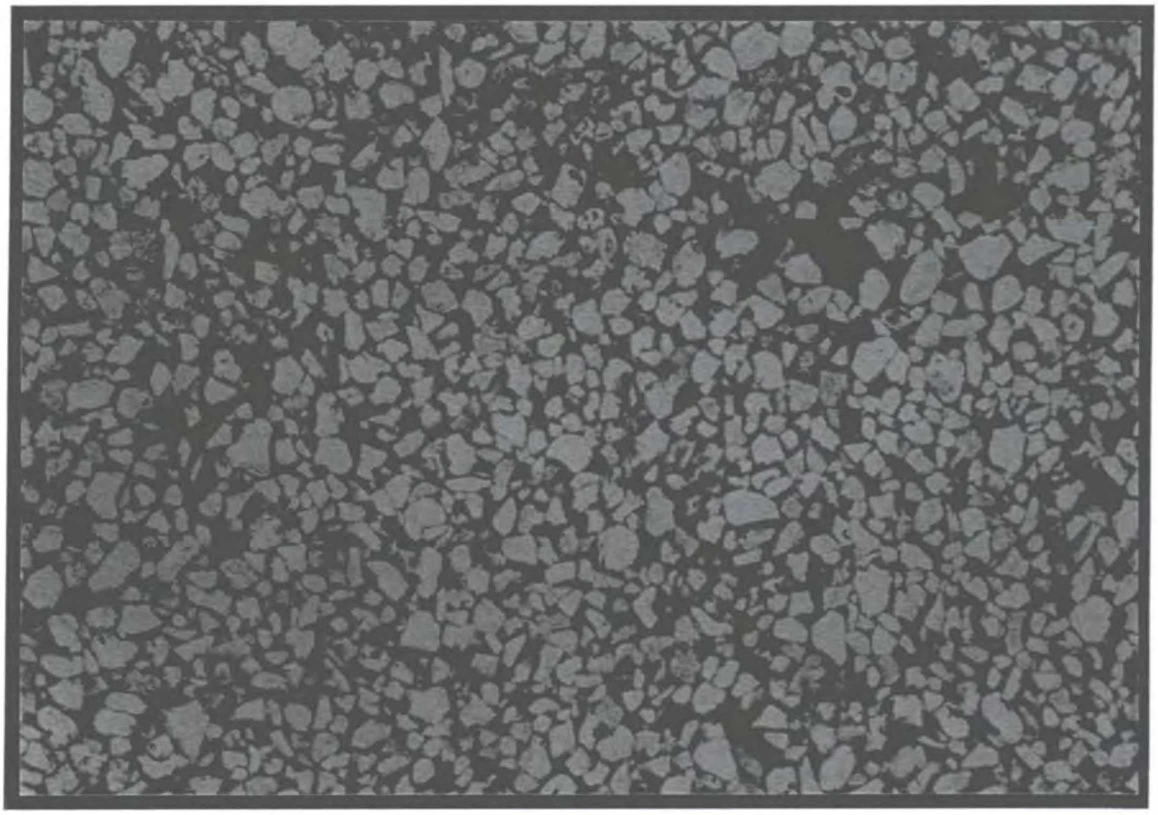

Plate 4.7. Thin-section of fine uniform sand (x 25 magnification).

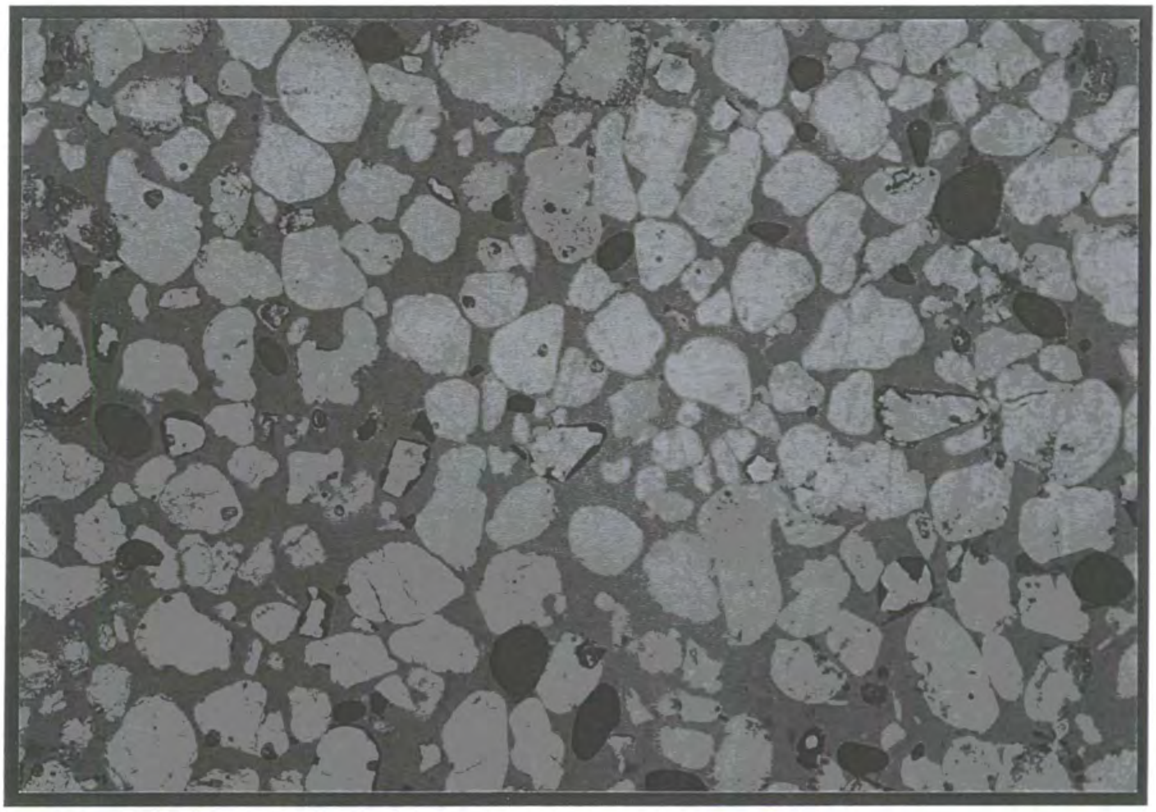

Plate 4.8. Thin-section of Garside medium sand (x 25 magnification).

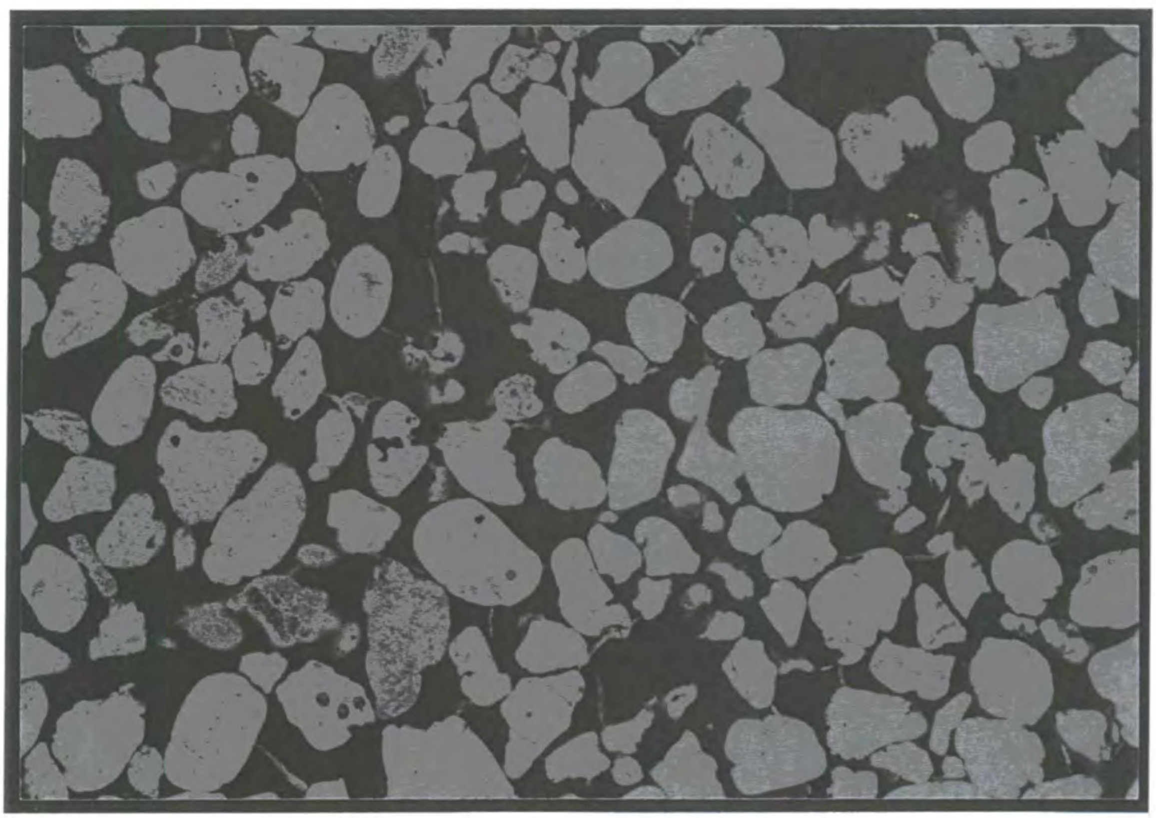

Plate 4.9. Thin-section of medium uniform sand (x 25 magnification).

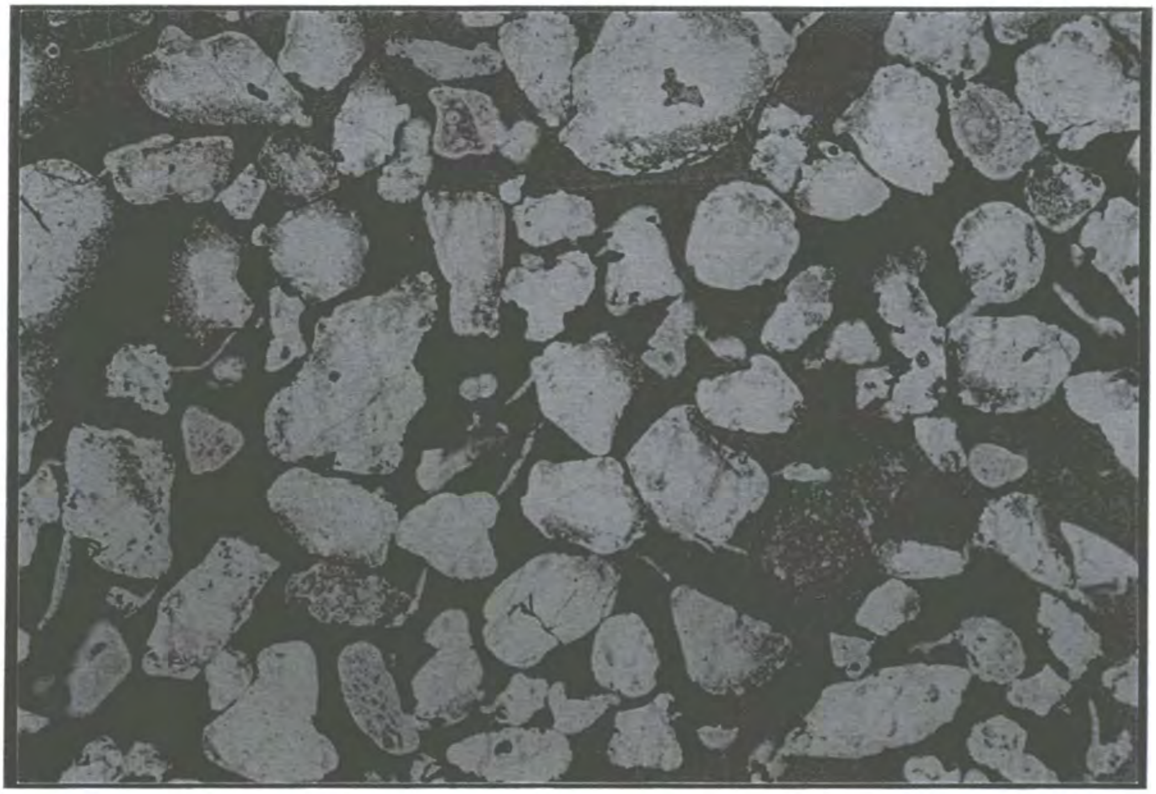

Plate 4.10. Thin-section of medium Leighton Buzzard sand (x 25 magnification).

Plate 4.11. Thin-section of coarse Leighton Buzzard sand (x 25 magnification).

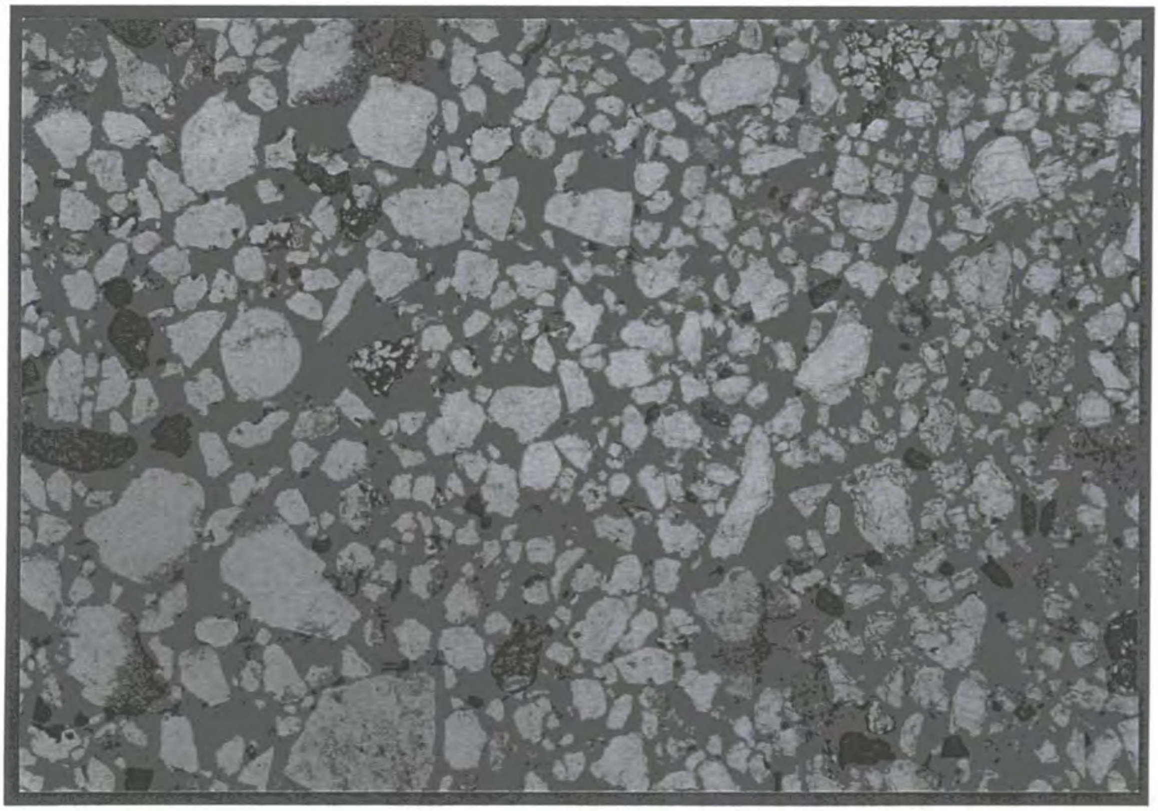

Plate 4.12. Thin-section of medium sharp sand (x 25 magnification).

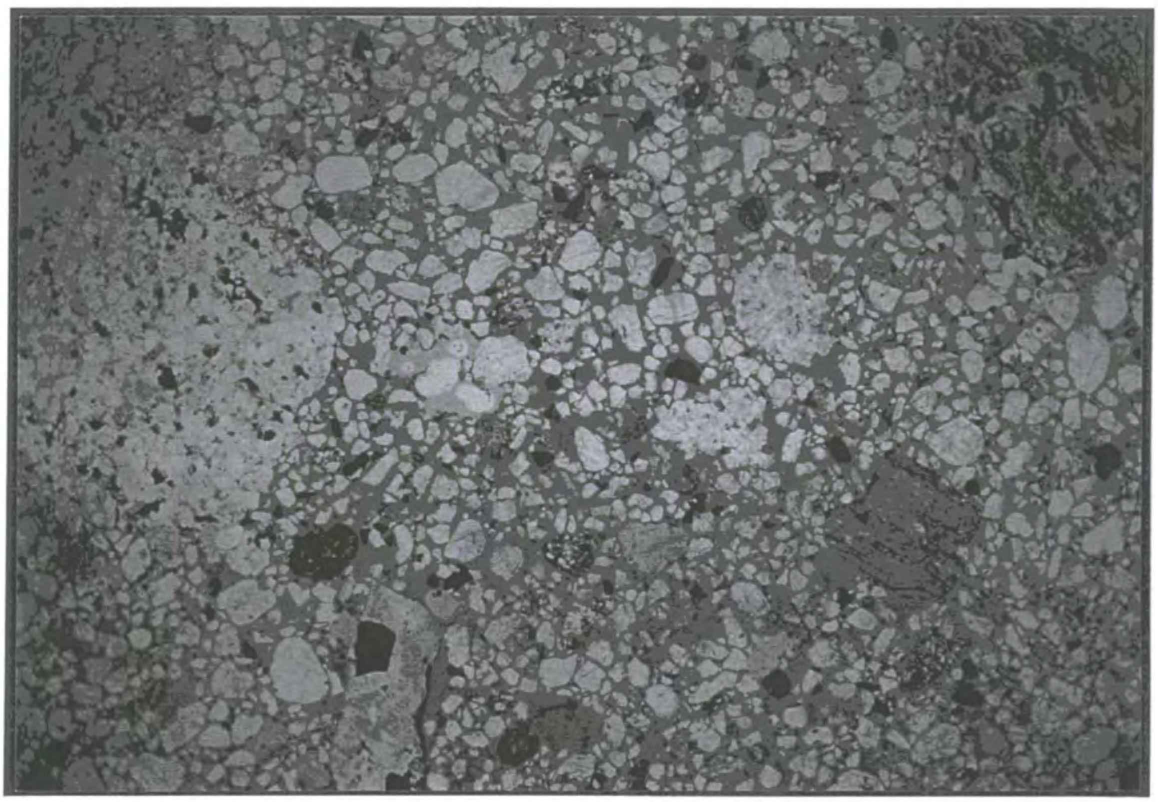

Plate 4.13. Thin-section of coarse sharp sand (x 25 magnification).

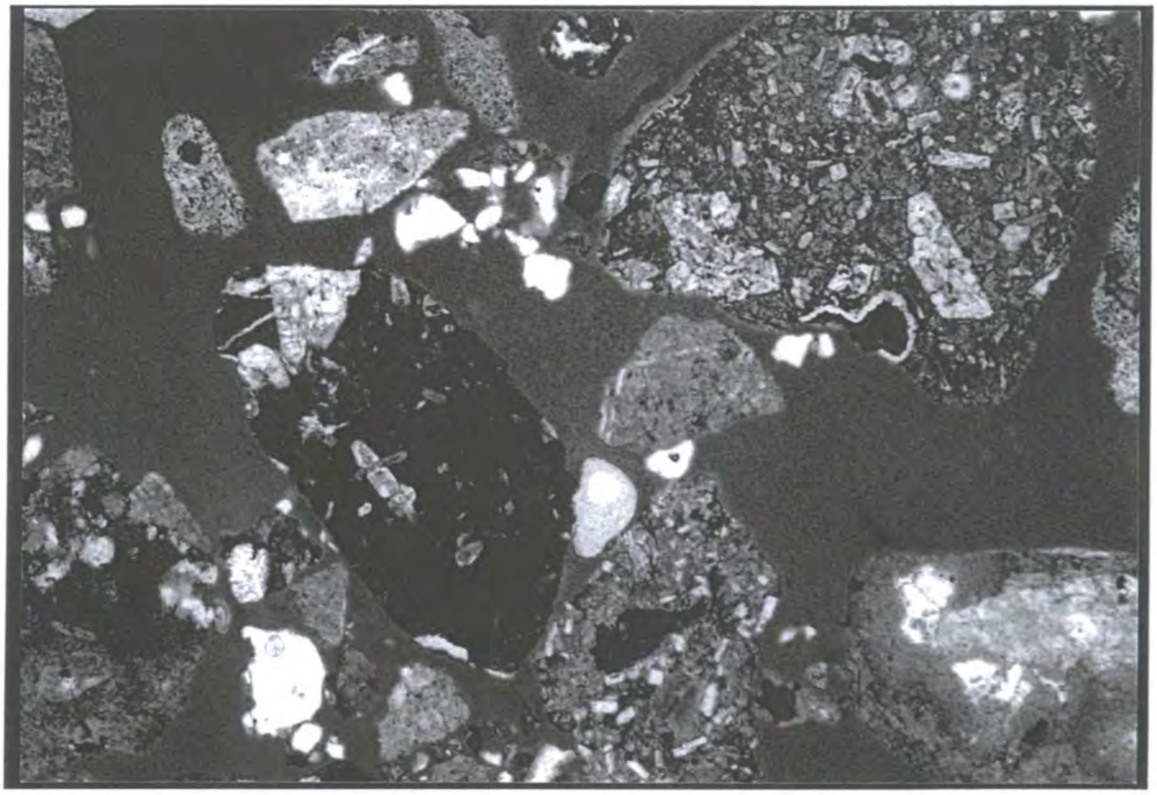

Plate 4.14. Thin-section of sandy fine gravel (x 25 magnification).

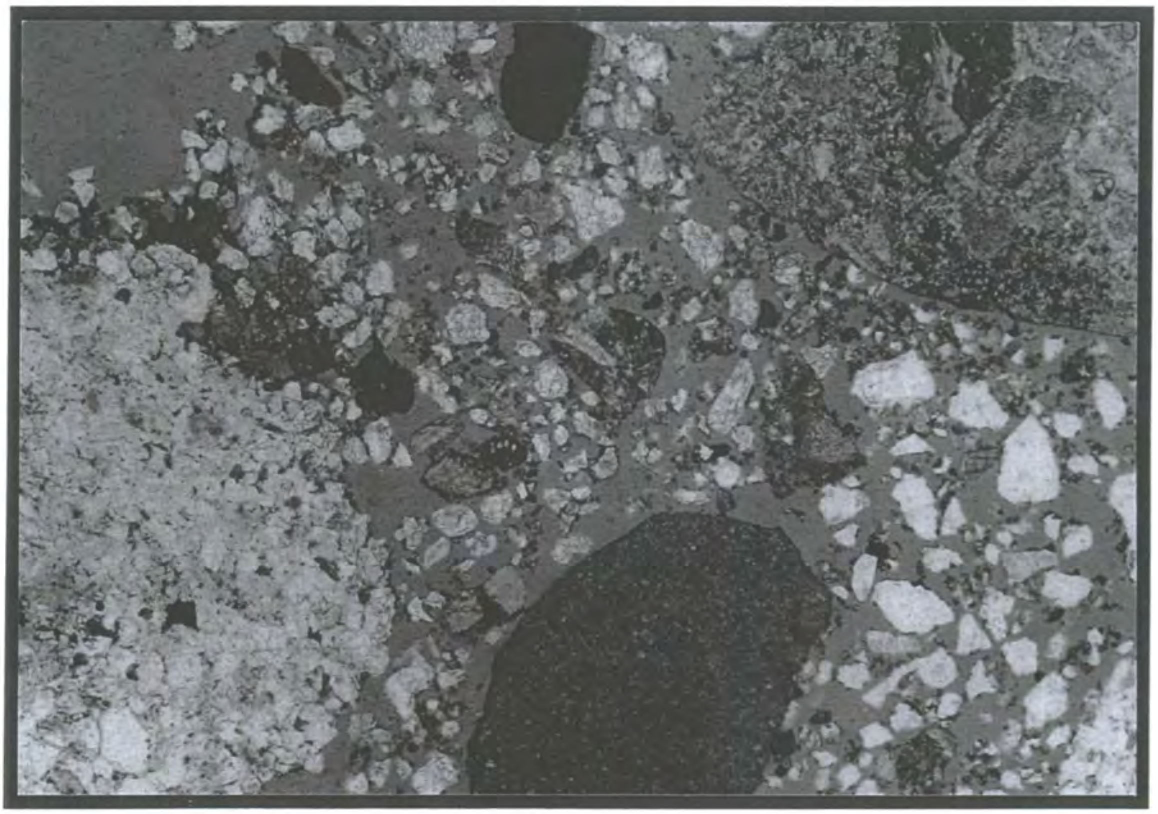

Plate 4.15. Thin-section of sandy fine to medium gravel (x 25 magnification).

CHAPTER 5
RESULTS AND APPLICATIONS

5.1 Introduction

This chapter presents and describes over two hundred laboratory vibration tests. The tests are grouped into soil and frequency specific results and show sample settlement induced by vibration (i.e. 'vibratory settlement') as a percentage decrease in initial (statically loaded) sample height with increasing acceleration, at four maintained effective stress levels. Because much of the soil in Britain is saturated, the majority of the tests were performed in the saturated state. A limited number of vibration tests were performed using dried and partially saturated material to account for the full range of *in-situ* moisture contents (Section 5.2).

To observe the effects that test variables have on vibratory settlement; the data was processed to evolve trends (Section 5.3). The influences of acceleration, static load and soil type are presented graphically. A soil type parameter was identified and used with trend data to develop basic predictive capabilities (Section 5.4). The settlements predicted using the trend data are compared with the equivalent test specific data.

Equations are presented that combine the soil type parameter, acceleration, relative density and static stress for accelerations up to 6.0*g* (Section 5.5). The equations are used to generate settlement values that are compared with test specific data. The effects of frequency, vibration time and moisture content are demonstrated. A procedure is presented that demonstrates how to calculate vibration induced ground compaction settlement using the equations derived from data analysis.

A number of basic examples are presented for typical site conditions, in terms of; vibrodriver operating frequency, energy per cycle and ground conditions which are modified to demonstrate, *inter alia*, the influence of stand-off distance, soil type, relative density and moisture content (Section 5.6).

The penultimate section examines categories that group; soils, site conditions and vibration induced surface settlement into concise categories of settlement *potential*, *risk* and *severity* (Section 5.7). This data presents the laboratory work and derived equations in summary tables that are in a convenient form for the practising engineer.

5.2 Test Results

This section summarises the laboratory test results in tabular and graphical form. An overview of the laboratory programme is presented below:

Test type	Number performed
Saturated at 25Hz, 9 soils, 10, 20, 50, 100 kPa	36
Saturated at 40Hz, 9 soils, 10, 20, 50, 100 kPa	36
Dried at 25Hz, 4 soils, 10 kPa	4
Partial saturated at 25Hz, 1 soil, 10 kPa	4
Dry-partial saturation-saturated at 25Hz, 1 soil, 10 kPa	3
High acceleration tests	92
Saturated at 120Hz, 1 soil, 10, 20, 50, 100kPa	4
Tests of fixed time length, saturated at 25Hz, 1 soil	6
Tests of different vibration orientation at 25Hz, 2 soils	10
Tests of increasing initial acceleration at 25Hz, 1 soil	6
Total	201

The compaction of each soil is presented in terms of acceleration and of maintained static stress levels in Figures 5.1.1 to 5.1.9 for accelerations up to 1.0g. Figures 5.3.1 to 5.3.10 present data for acceleration up to 5.0g. Result tables are presented, in the first instance, to show the settlement responses of soil types to acceleration and static stress for 25Hz (Table 5.1a) and 40Hz (Table 5.1b). Secondly, the data is presented to allow convenient examination of individual soil response to acceleration, static load and frequency (Tables 5.2a, 5.2b and 5.2c). Low vibration test data tables include settlement data for all the acceleration magnitudes (i.e. up to, and including, the 2.0g values). However, graphical data presents the values to 1.0g, which is more appropriate to vibropiling activities.

5.2.1 Vibration Test Settlement Results on Saturated Soil Samples

Tables 5.1.a and 5.1.b are grouped into four sections showing the percentage settlement obtained for the four static stresses (10, 20, 50 and 100kPa) that were used during the laboratory test programme. The term 'static stress' (used throughout the text) refers to the consolidation pressure that was applied to equilibrate the samples prior to (and maintained during) the vibration test that modelled the geostatic stress that acts on *in-situ* equivalent soils. Under each static stress, it can be seen that; for a given soil type, vibratory settlement (i.e. percentage decrease in initial (static) sample height due to vibration) increases with increasing acceleration. However, note that as static stress is increased, the magnitude of the increase in settlement with acceleration is reduced. For example, under 10kPa, the medium sharp sand settled 0.94% at 0.8*g*. At 100kPa, for the same acceleration, the settlement is decreased to 0.02%.

In addition, settlement response related to static stress is presented in terms of the relationship between static stress and the minimum level of acceleration required to initiate settlement response. The data shows that with static stress of 10kPa, medium sharp sand experienced an initial settlement at 0.3*g*. Under 100kPa, the minimum acceleration necessary to induce settlement was 0.8*g*.

Table 5.1.a and 5.1.b demonstrate that the soils responded differently under given test conditions. An acceleration of 1.0*g* at 25Hz, and a static load of 20kPa caused the fine uniform sand, medium uniform sand and the sandy fine to medium gravel to settle 1.26%, 0.34% and 1.88%, respectively.

The data is also summarised in Tables 5.2 (a, b, c), which group the data into soil specific settlement. This allows a convenient comparison of particular soil response to combinations of acceleration and stress under frequencies of 25Hz and 40Hz.

The graphical presentation of the data shows each single soil type experiencing acceleration of up to and including 1.0g, for static stresses of 10, 20, 50, and 100kPa. The graphs show that as acceleration increases monotonically, the sample settlement tends to be greater for each unit increase in acceleration. This produces a settlement curve of increasing gradient (see Figures 5.1.1 to 5.1.9).

5.2.2 Partially Saturated and Dried Acceleration Tests

The results in this section summarise the effect that variation in moisture content has on the settlement response of four soils (medium uniform sand, coarse Leighton Buzzard sand, medium sharp sand and sandy fine to medium gravel). The tests were performed under the same static stress and acceleration conditions as the standard tests on saturated samples. The results are summarised in Table 5.3.1.

	ACCL, *g*	SFS	FUS	GMS	MUS	MLB	CLB	MSS	SFG	SFMG
10kPa	**0.0**	-	-	-	-	-	-	-	-	-
	0.1	-	-	-	-	-	-	-	-	-0.01
	0.2	-	-0.06	-	-	-0.01	-	-	-	-0.01
	0.3	-	-0.27	-0.12	-	-0.05	-0.01	-0.11	-0.03	-0.34
	0.4	-	-0.48	-0.24	-	-0.08	-0.01	-0.21	-0.05	-0.67
	0.5	-	-0.81	-0.40	-0.02	-0.13	-0.02	-0.40	-0.18	-1.03
	0.6	-0.05	-1.09	-0.54	-0.04	-0.18	-0.05	-0.63	-0.37	-1.37
	0.8	-0.11	-1.46	-0.84	-0.15	-0.35	-0.16	-0.94	-0.68	-2.57
	1.0	-0.24	-2.52	-1.29	-0.37	-0.76	-0.44	-1.12	-1.21	-3.52
	2.0	-2.27	-7.98	-4.49	-2.54	-4.30	-3.79	-6.42	-9.80	-9.07
20kPa	**0.0**	-	-	-	-	-	-	-	-	-
	0.1	-	-	-	-	-	-	-	-	-0.01
	0.2	-0.01	-	-	-	-	-	-	-	-0.01
	0.3	-0.16	-0.07	-0.02	-	-0.03	-0.01	-0.04	-	-0.14
	0.4	-0.31	-0.13	-0.03	-	-0.06	-0.01	-0.08	-	-0.26
	0.5	-0.51	-0.23	-0.07	-	-0.11	-0.03	-0.21	-0.09	-0.47
	0.6	-0.64	-0.42	-0.12	-0.03	-0.15	-0.06	-0.42	-0.21	-0.67
	0.8	-0.85	-0.74	-0.28	-0.15	-0.24	-0.21	-0.77	-0.43	-1.16
	1.0	-1.13	-1.26	-0.60	-0.34	-0.44	-0.58	-1.03	-0.77	-1.88
	2.0	-4.56	-6.15	-3.72	-1.75	-4.03	-4.43	-6.39	-10.11	-6.37
50kPa	**0.0**	-	-	-	-	-	-	-	-	-
	0.1	-	-	-	-	-	-	-	-	-
	0.2	-	-	-	-	-	-	-	-	-
	0.3	-	-	-	-	-	-	-	-	-
	0.4	-	-	-	-	-0.01	-	-	-	-0.01
	0.5	-0.04	-0.01	-0.01	-0.01	-0.04	-0.01	-	-	-0.01
	0.6	-0.10	-0.01	-0.02	-0.01	-0.07	-0.01	-0.23	-	-0.01
	0.8	-0.23	-0.06	-0.08	-0.02	-0.14	-0.04	-0.50	-0.07	-0.11
	1.0	-0.41	-0.21	-0.26	-0.03	-0.29	-0.11	-0.87	-0.32	-3.77
	2.0	-2.83	-3.48	-2.34	-1.34	-3.04	-2.14	-5.48	-8.13	-7.32
100kPa	**0.0**	-	-	-	-	-	-	-	-	-
	0.1	-	-	-	-	-	-	-	-	-
	0.2	-	-	-	-	-	-	-	-	-
	0.3	-	-	-	-	-	-	-	-	-
	0.4	-	-0.01	-	-	-	-	-	-	-
	0.5	-0.01	-0.02	-0.01	-	-	-0.01	-	-	-
	0.6	-0.19	-0.06	-0.02	-	-	-0.01	-	-	-
	0.8	-1.08	-0.12	-0.05	-	-0.01	-0.02	-0.02	-	-0.02
	1.0	-1.64	-0.19	-0.11	-	-0.11	-0.02	-0.06	-0.01	-0.18
	2.0	-3.53	-1.76	-0.99	-0.08	-2.61	-1.99	-3.32	-4.50	-5.62

Table 5.1a. 25Hz saturated vibratory test data (presented as percentage settlements), for all soils tested, for effective stresses of 10 - 100kPa, vibrated up to 2.0g. Hyphens represent acceleration increments that produced no sample settlement.

Where: SFS = silty fine sand; FUS = fine uniform sand; GMS = Garside medium sand; MUS = medium uniform sand; MLB = medium Leighton Buzzard sand; CLB = coarse Leighton Buzzard sand; MSS = medium sharp sand: SFG = sandy fine gravel; SFMG = sandy fine to medium gravel.

	ACCL, *g*	SFS	FUS	GMS	MUS	MLB	CLB	MSS	SFG	SFMG
10kPa	**0.0**	-	-	-	-	-	-	-	-	-
	0.1	-	-	-	-	-	-	-	-	-
	0.2	-	-	-0.03	-	-	-	-0.07	-	-
	0.3	-0.03	-0.17	-0.12	-	-0.06	-	-0.39	-	-0.31
	0.4	-0.07	-0.21	-0.19	-	-0.09	-	-0.71	-0.29	-0.53
	0.5	-0.19	-0.49	-0.30	-	-0.20	-	-0.99	-0.51	-0.86
	0.6	-0.35	-0.85	-0.42	-	-0.36	-0.01	-1.35	-0.82	-1.33
	0.8	-0.76	-1.34	-0.71	-0.01	-0.63	-0.02	-1.88	-1.39	-1.80
	1.0	-1.67	-2.38	-1.00	-0.28	-0.95	-0.05	-2.46	-2.02	-2.99
	2.0	-4.23	-5.24	-3.96	-2.17	-5.58	-1.63	-6.50	-8.99	-9.25
20kPa	**0.0**	-	-	-	-	-	-	-	-	-
	0.1	-	-	-	-	-	-	-	-	-
	0.2	-	-	-	-	-	-	-	-	-
	0.3	-	-0.05	-0.01	-	-0.03	-	-	-	-0.04
	0.4	-	-0.12	-0.07	-	-0.05	-	-0.10	-	-0.22
	0.5	-0.12	-0.33	-0.13	-0.02	-0.10	-0.02	-0.27	-	-0.45
	0.6	-0.24	-0.91	-0.20	-0.06	-0.15	-0.04	-0.50	-	-0.65
	0.8	-0.56	-1.43	-0.39	-0.17	-0.24	-0.10	-0.85	-0.16	-1.08
	1.0	-0.83	-1.69	-0.69	-0.47	-0.47	-0.28	-1.36	-0.50	-1.72
	2.0	-2.38	-4.67	-3.05	-2.18	-3.59	-2.01	-4.90	-7.09	-6.83
50kPa	**0.0**	-	-	-	-	-	-	-	-	-
	0.1	-	-	-	-	-	-	-	-	-
	0.2	-	-	-	-	-	-	-	-	-
	0.3	-	-	-	-	-0.02	-	-	-	-
	0.4	-0.05	-	-0.01	-	-0.02	-0.01	-0.01	-	-
	0.5	-0.11	-	-0.03	-0.01	-0.06	-0.02	-0.02	-	-0.09
	0.6	-0.34	-0.04	-0.06	-0.01	-0.10	-0.02	-0.05	-	-0.17
	0.8	-0.60	-0.14	-0.15	-0.03	-0.23	-0.04	-0.16	-0.04	-0.40
	1.0	-0.95	-0.29	-0.31	-0.10	-0.44	-0.20	-0.38	-0.17	-0.71
	2.0	-2.52	-2.54	-2.25	-1.39	-4.14	-2.10	-3.86	-6.71	-5.45
100kPa	**0.0**	-	-	-	-	-	-	-	-	-
	0.1	-	-	-	-	-	-	-	-	-
	0.2	-	-	-	-	-	-	-	-	-
	0.3	-	-	-	-	-	-	-	-	-
	0.4	-	-	-	-	-0.02	-	-	-	-
	0.5	-	-	-0.02	-	-0.02	-	-	-	-
	0.6	-	-0.05	-0.02	-	-0.03	-0.01	-0.01	-	-0.03
	0.8	-0.01	-0.42	-0.03	-0.01	-0.05	-0.01	-0.07	-	-0.24
	1.0	-0.04	-0.71	-0.05	-0.02	-0.10	-0.01	-0.17	-0.03	-0.50
	2.0	-1.020	-2.728	-1.149	-0.562	-1.670	-0.548	-3.206	-4.410	-4.492

Table 5.1a. 40Hz saturated vibratory test data (presented as percentage settlements), for all soils tested, for effective stresses of 10 - 100kPa, vibrated up to 2.0*g*. Hyphens represent acceleration increments that produced no sample settlement.

Where: SFS = silty fine sand; FUS = fine uniform sand; GMS = Garside medium sand; MUS = medium uniform sand; MLB = medium Leighton Buzzard sand; CLB = coarse Leighton Buzzard sand; MSS = medium sharp sand: SFG = sandy fine gravel; SFMG = sandy fine to medium gravel.

Silty Fine Sand

ACCEL	25Hz				40Hz			
(g)	10kPa	20kPa	50kPa	100kPa	10kPa	20kPa	50kPa	100kPa
0.0	-	-	-	-	-	-	-	-
0.1	-	-	-	-	-	-	-	-
0.2	-	-0.01	-	-	-	-	-	-
0.3	-	-0.16	-	-	-0.03	-	-	-
0.4	-	-0.31	-	-	-0.07	-	-0.05	-
0.5	-	-0.51	-0.04	-0.01	-0.19	-0.12	-0.11	-
0.6	-0.05	-0.64	-0.10	-0.19	-0.35	-0.24	-0.34	-
0.8	-0.11	-0.85	-0.23	-1.08	-0.76	-0.56	-0.60	-0.01
1.0	-0.24	-1.13	-0.41	-1.64	-1.67	-0.83	-0.95	-0.04
2.0	-2.27	-4.56	-2.83	-3.53	-4.23	-2.38	-2.52	-1.02

Garside Medium Sand

ACCEL	25Hz				40Hz			
(g)	10kPa	20kPa	50kPa	100kPa	10kPa	20kPa	50kPa	100kPa
0.0	-	-	-	-	-	-	-	-
0.1	-	-	-	-	-	-	-	-
0.2	-	-	-	-	-0.03	-	-	-
0.3	-0.12	-0.02	-	-	-0.12	-0.01	-	-
0.4	-0.24	-0.03	-	-	-0.19	-0.07	-0.01	-
0.5	-0.40	-0.07	-0.01	-0.01	-0.30	-0.13	-0.03	-0.02
0.6	-0.54	-0.12	-0.02	-0.02	-0.42	-0.20	-0.06	-0.02
0.8	-0.84	-0.28	-0.08	-0.05	-0.71	-0.39	-0.15	-0.03
1.0	-1.29	-0.60	-0.26	-0.11	-1.00	-0.69	-0.31	-0.05
2.0	-4.49	-3.72	-2.34	-0.99	-3.96	-3.05	-2.25	-1.15

Medium Leighton Buzzard Sand

ACCEL	25Hz				40Hz			
(g)	10kPa	20kPa	50kPa	100kPa	10kPa	20kPa	50kPa	100kPa
0.0	-	-	-	-	-	-	-	-
0.1	-	-	-	-	-	-	-	-
0.2	-0.01	-	-	-	-	-	-	-
0.3	-0.05	-0.03	-	-	-0.06	-0.03	-0.02	-
0.4	-0.08	-0.06	-0.01	-	-0.09	-0.05	-0.02	-0.02
0.5	-0.13	-0.11	-0.04	-	-0.20	-0.10	-0.06	-0.02
0.6	-0.18	-0.15	-0.07	-	-0.36	-0.15	-0.10	-0.03
0.8	-0.35	-0.24	-0.14	-0.01	-0.63	-0.24	-0.23	-0.05
1.0	-0.76	-0.44	-0.29	-0.11	-0.95	-0.47	-0.44	-0.10
2.0	-4.30	-4.03	-3.04	-2.61	-5.58	-3.59	-4.14	-1.67

Table 5.2a. Test specific data, presented as percentage settlements.

Fine Uniform Sand

ACCEL	25Hz				40Hz			
(g)	10kPa	20kPa	50kPa	100kPa	10kPa	20kPa	50kPa	100kPa
0.0	-	-	-	-	-	-	-	-
0.1	-	-	-	-	-	-	-	-
0.2	-0.06	-	-	-	-	-	-	-
0.3	-0.27	-0.07	-	-	-0.17	-0.05	-	-
0.4	-0.48	-0.13	-	-0.01	-0.21	-0.12	-	-
0.5	-0.81	-0.23	-0.01	-0.02	-0.49	-0.33	-	-
0.6	-1.09	-0.42	-0.01	-0.06	-0.85	-0.91	-0.04	-0.05
0.8	-1.46	-0.74	-0.06	-0.12	-1.34	-1.43	-0.14	-0.42
1.0	-2.52	-1.26	-0.21	-0.19	-2.38	-1.69	-0.29	-0.71
2.0	-7.98	-6.15	-3.48	-1.76	-5.24	-4.67	-2.54	-2.73

Medium Uniform Sand

ACCEL	25Hz				40Hz			
(g)	10kPa	20kPa	50kPa	100kPa	10kPa	20kPa	50kPa	100kPa
0.0	-	-	-	-	-	-	-	-
0.1	-	-	-	-	-	-	-	-
0.2	-	-	-	-	-	-	-	-
0.3	-	-	-	-	-	-	-	-
0.4	-	-	-	-	-	-	-	-
0.5	-0.02	-	-0.01	-	-	-0.02	-0.01	-
0.6	-0.04	-0.03	-0.01	-	-	-0.06	-0.01	-
0.8	-0.15	-0.15	-0.02	-	-0.01	-0.17	-0.03	-0.01
1.0	-0.37	-0.34	-0.03	-	-0.28	-0.47	-0.10	-0.02
2.0	-2.54	-1.75	-1.34	-0.08	-2.17	-2.18	-1.39	-0.56

Coarse Leighton Buzzard Sand

ACCEL	25Hz				40Hz			
(g)	10kPa	20kPa	50kPa	100kPa	10kPa	20kPa	50kPa	100kPa
0.0	-	-	-	-	-	-	-	-
0.1	-	-	-	-	-	-	-	-
0.2	-	-	-	-	-	-	-	-
0.3	-0.01	-0.01	-	-	-	-	-	-
0.4	-0.01	-0.01	-	-	-	-	-0.01	-
0.5	-0.02	-0.03	-0.01	-0.01	-	-0.02	-0.02	-
0.6	-0.05	-0.06	-0.01	-0.01	-0.01	-0.04	-0.02	-0.01
0.8	-0.16	-0.21	-0.04	-0.02	-0.02	-0.10	-0.04	-0.01
1.0	-0.44	-0.58	-0.11	-0.02	-0.05	-0.28	-0.20	-0.01
2.0	-3.79	-4.43	-2.14	-1.99	-1.63	-2.01	-2.10	-0.55

Table 5.2b. Test specific data, presented as percentage settlements.

Medium Sharp Sand

ACCEL	25Hz				40Hz			
(g)	10kPa	20kPa	50kPa	100kPa	10kPa	20kPa	50kPa	100kPa
0.0	-	-	-	-	-	-	-	-
0.1	0.00	-	-	-	-	-	-	-
0.2	0.00	0.00	-	-	-0.07	-	-	-
0.3	-0.11	-0.04	-	-	-0.39	-	-	-
0.4	-0.21	-0.08	-	-	-0.71	-0.10	-0.01	-
0.5	-0.40	-0.21	-	-	-0.99	-0.27	-0.02	0.00
0.6	-0.63	-0.42	-0.23	-	-1.35	-0.50	-0.05	-0.01
0.8	-0.94	-0.77	-0.50	-0.02	-1.88	-0.85	-0.16	-0.07
1.0	-1.12	-1.03	-0.87	-0.06	-2.46	-1.36	-0.38	-0.17
2.0	-6.42	-6.39	-5.48	-3.32	-6.50	-4.90	-3.86	-3.21

Sandy Fine Gravel

ACCEL	25Hz				40Hz			
(g)	10kPa	20kPa	50kPa	100kPa	10kPa	20kPa	50kPa	100kPa
0.0	-	-	-	-	-	-	-	-
0.1	-	-	-	-	-	-	-	-
0.2	-	-	-	-	-	-	-	-
0.3	-0.03	-	-	-	-	-	-	-
0.4	-0.05	-	-	-	-0.29	-	-	-
0.5	-0.18	-0.09	-	-	-0.51	-	-	-
0.6	-0.37	-0.21	-	-	-0.82	-	-	-
0.8	-0.68	-0.43	-0.07	0.00	-1.39	-0.16	-0.04	0.00
1.0	-1.21	-0.77	-0.32	-0.01	-2.02	-0.50	-0.17	-0.03
2.0	-9.80	-10.11	-8.13	-4.50	-8.99	-7.09	-6.71	-4.41

Sandy Fine to Medium Gravel

ACCEL	25Hz				40Hz			
(g)	10kPa	20kPa	50kPa	100kPa	10kPa	20kPa	50kPa	100kPa
0.0	-	-	-	-	-	-	-	-
0.1	-0.01	-0.01	-	-	-	-	-	-
0.2	-0.01	-0.01	-	-	0.00	-	-	-
0.3	-0.34	-0.14	-	-	-0.31	-0.04	-	-
0.4	-0.67	-0.26	-0.01	-	-0.53	-0.22	-	-
0.5	-1.03	-0.47	-0.01	-	-0.86	-0.45	-0.09	0.00
0.6	-1.37	-0.67	-0.01	0.00	-1.33	-0.65	-0.17	-0.03
0.8	-2.57	-1.16	-0.11	-0.02	-1.80	-1.08	-0.40	-0.24
1.0	-3.52	-1.88	-3.77	-0.18	-2.99	-1.72	-0.71	-0.50
2.0	-9.07	-6.37	-7.32	-5.62	-9.25	-6.83	-5.45	-4.49

Table 5.2c. Test specific data, presented as percentage settlements.

In contrast to the equivalent saturated test data, it can be seen that; for accelerations up to and including 1.0*g*, the settlements achieved are much reduced. Note that the dried data for the clean sands show a very marked increase in settlement at an acceleration of 2.0*g* (which is not observed for the sandy fine to medium gravel). This behaviour is not observed for the equivalent partially saturated tests that demonstrate no particular sensitivity to the increase of 1.0*g* to 2.0*g*. Additionally, the acceleration required to induce initial settlement of the partially saturated samples is higher than that required under saturated test conditions.

Figures 5.2.1 to 5.2.4 present the dried and partially saturated test data in chart form. Figure 5.2.3 shows the general effect of moisture content on vibratory settlement response. The dried and partially saturated settlement values are an order of magnitude less than the settlement obtained for equivalent saturated tests. The influence that the degree of saturation has on vibratory sample settlement, for given test conditions, is demonstrated in Figure 5.2.4. The chart shows that as a fully saturated (medium sharp sand) sample begins to lose moisture, a decrease in settlement of approximately 90% occurs over a 10% reduction in saturation. As the degree of saturation continues to reduce, the vibratory settlement tends towards a minimum value. The settlement is then seen to increase when saturation falls below 15%, to a dried 'maximum' that is approximately 10% of the saturated value.

5.2.3 High Acceleration Vibration Tests.

Vibration tests were performed in increments of 1.0*g* to a maximum of 6.0*g* in order to observe the settlement response of granular material under vibration magnitudes that are much higher than those generated by vibropiling operations at distances of more than 2m from the pile. However, soils within 500mm of a pile may encounter vibrations in the order of several times gravitational acceleration (e.g. Selby, 1989 and Dowding, 1994) and experience liquefaction. The tests allow the observation of the fundamental behaviour of granular material, extending the description of settlement behaviour which is beyond that focused on the narrow range of acceleration appropriate to vibropiling conditions. In addition, the high acceleration tests have application to the process of dynamic compaction techniques that increase the density of granular fills before commencement of construction.

ACCEL	DRIED DATA				PARTIAL SATURATION DATA			
(g)	MUS	CLB	MSS	SFMG	MUS	CLB	MSS	SFMG
0.1	-	-	-	-	-	-	-	-
0.2	-	-	-	-	-	-	-	-
0.3	-	-	-	-	-	-	-	-
0.4	-	-	-	-	-	-	-	-
0.5	-0.01	-	-	-0.01	-	-	-	-
0.6	-0.02	-	-	-0.01	-	-	-	-
0.8	-0.05	-0.20	-	-0.01	-0.02	-	-	-
1.0	-0.05	-0.24	-0.01	-0.01	-0.02	-0.01	-	-
2.0	-2.86	-3.27	-3.25	-0.05	-0.05	-0.29	-0.04	-0.04

Table 5.3.1. Vibratory settlement data for dried and partially saturated tests (saturated, 25Hz, 10kPa).

ACCEL	DEGREE OF SATURATION					
(g)	0%	15%	58%	65%	92%	100%
0.1	-	-	-	-	-	-
0.2	-	-	-	-	-	-
0.3	-	-	-	-	-	-
0.4	-	-	-	-	-	-
0.5	-0.01	-	-	-	-	-0.02
0.6	-0.02	-	-	-	-	-0.04
0.8	-0.05	-	-0.02	-	-	-0.15
1.0	-0.05	-	-0.02	-	-0.03	-0.37
2.0	-2.86	-0.02	-0.05	-0.27	-0.21	-2.54

Table 5.3.2. The effects of the degree of saturation on vibratory settlement response (for medium uniform sand, 25Hz).

ACCEL (g)	Sat (%)	Dried (%)	P. Sat (%)	Dried (% of sat)	P. Sat (% of sat)
0.1	-	-	-	-	-
0.2	-	-	-	-	-
0.3	-0.11	-	-	0.65	-
0.4	-0.22	-	-	0.87	-
0.5	-0.37	-0.01	-	1.73	-
0.6	-0.53	-0.01	-	1.62	-
0.8	-0.95	-0.07	-	6.93	0.46
1.0	-1.36	-0.08	-0.01	5.62	0.59
2.0	-5.46	-2.36	-0.11	43.19	1.93

Table 5.3.3. Comparison of the effect of moisture content on settlement (using mean values of MUS, CLB, MSS and SFMG).

	Soil Type	Acceleration					
		1.0*g*	**2.0*g***	**3.0*g***	**4.0*g***	**5.0*g***	**6.0*g***
10kPa	**SFS**	-0.04	-2.79	-3.39	-4.01	-4.34	-
	FUS	-0.27	-1.66	-2.70	-3.82	-4.63	-
	GMS	-0.23	-0.74	-1.25	-1.52	-1.77	-
	MUS	-	-2.05	-4.52	-6.22	-	-
	MLB	-0.07	-1.80	-2.94	-3.65	-4.28	-
	CLB	-0.37	-3.18	-4.32	-4.79	-4.99	-5.29
	MSS	-0.16	-2.57	-6.29	-7.20	-8.50	-8.98
	CSS63	-0.25	-8.00	-10.03	-10.34	-	-
	CSS	-0.01	-3.32	-5.62	-8.00	-	-
	SFMG	-1.65	-8.31	-11.29	-13.05	-13.85	-14.45
20kPa	**SFS**	-0.65	-1.99	-2.36	-3.05	-3.55	-
	FUS	-0.09	-1.43	-2.74	-3.58	-3.79	-
	GMS	-0.10	-0.72	-1.04	-1.18	-1.27	-
	MUS	-0.06	-2.01	-2.23	-2.56	-	-
	MLB	-0.11	-2.40	-4.05	-4.85	-5.43	-
	CLB	-0.28	-3.69	-5.18	-5.43	-5.72	-6.03
	MSS	-0.28	-8.71	-9.96	-10.82	-11.11	-11.28
	CSS63	-	-7.59	-10.23	-10.78	-	-
	CSS	-0.08	-2.65	-5.73	-6.66	-	-
	SFMG	-1.07	-7.30	-9.58	-10.23	-11.11	-11.55
50kPa	**SFS**	-0.11	-0.75	-1.36	-2.21	-3.91	-
	FUS	-0.05	-0.56	-2.22	-3.16	-3.90	-
	GMS	-0.07	-0.43	-0.58	-0.88	-1.09	-
	MUS	-	-1.29	-2.10	-2.45	-	-
	MLB	-0.14	-1.76	-2.94	-3.86	-4.27	-
	CLB	-0.01	-2.02	-3.11	-3.49	-3.84	-4.43
	MSS	-0.91	-5.01	-6.81	-7.61	-8.91	-9.12
	CSS63	-0.12	-6.51	-10.10	-10.67	-	-
	CSS	-0.01	-3.69	-5.13	-6.24	-	-
	SFMG	-0.38	-5.66	-8.14	-8.98	-10.12	-10.41
100kPa	**SFS**	-0.07	-1.55	-2.25	-3.15	-4.35	-
	FUS	-0.08	-1.06	-2.04	-2.36	-2.50	-
	GMS	-0.05	-0.57	-0.93	-1.16	-1.35	-
	MUS	-	-	-	-	-	-
	MLB	-0.03	-1.13	-2.01	-2.57	-2.86	-
	CLB	-	-0.61	-1.15	-1.36	-1.75	-2.33
	MSS	-0.16	-1.37	-3.11	-4.47	-5.03	-5.03
	CSS63	-	-	-	-	-	-
	CSS	-	-	-	-	-	-
	SFMG	-0.06	-1.70	-5.76	-6.93	-7.49	-8.37

Table 5.4.1. High acceleration vibration saturated test results (25Hz) for effective stresses of 10 -100kPa and vibrations up to 6.0g. Hyphens indicate missing data points which occurred in preliminary tests and where no settlement occurred.

Where: CSS = coarse sharp sand; CSS63 = coarse sharp sand sieved to remove the <63μ fraction.

	Soil Type	Test Type	Acceleration					
			1*g*	2*g*	3*g*	4*g*	5*g*	6*g*
10kPa	MSS	DRIED	-0.03	-0.66	-5.93	-7.55	-7.85	-8.02
	MSS	PSAT	-0.08	-0.11	-0.16	-0.19	-0.25	-0.34
	SFS	DRIED	-	-1.05	-2.38	-2.55	-6.20	-6.20
	MUS	DRIED	-0.03	-0.22	-0.64	-3.03	-3.03	-3.03
	MUS	PSAT	-0.03	-0.04	-0.06	-0.28	-0.28	-0.28
	MLB	DRIED	-0.19	-9.03	-9.37	-9.47	-9.57	-9.67
	MLB	PSAT	-0.01	-0.54	-1.05	-1.21	-2.09	-2.39
	GMS	DRY	-0.07	-3.88	-4.50	-4.84	-5.01	-5.01
	CSS63	DRIED	-0.49	-11.72	-12.50	-12.96	-12.96	-12.96
	CSS63	PSAT	-0.35	-1.18	-1.93	-2.66	-2.66	-2.66
	CSS	DRIED	-0.09	-11.17	-11.34	-12.07	-12.07	-12.07
	CSS	PSAT	-0.42	-1.22	-1.51	-2.11	-2.11	-2.11
20kPa	MSS	DRIED	-0.01	-0.59	-4.12	-4.55	-4.85	-4.85
	MSS	PSAT	-0.03	-0.22	-0.46	-0.62	-0.99	-1.14
	SFS	DRIED	-0.02	-4.41	-4.72	-5.33	-6.33	-6.33
	MUS	DRIED	-0.02	-4.64	-5.91	-6.48	-6.48	-6.48
	MUS	PSAT	-0.01	-0.03	-0.04	-0.65	-0.65	-0.65
	MLB	DRIED	-0.01	-7.36	-7.71	-7.89	-7.96	-8.09
	MLB	PSAT	-0.07	-1.06	-1.60	-1.87	-2.25	-2.49
	GMS	DRY	-0.07	-4.18	-5.01	-5.19	-5.26	-5.32
	CSS63	DRIED	-0.40	-11.78	-12.24	-12.71	-12.71	-12.71
	CSS63	PSAT	-0.19	-0.31	-0.88	-1.38	-1.38	-1.38
	CSS	DRIED	-0.03	-12.52	-13.57	-13.60	-13.60	-13.60
	CSS	PSAT	-0.31	-0.58	-0.98	-1.22	-1.22	-1.22
50kPa	MSS	DRIED	-0.03	-0.44	-2.27	-2.49	-3.32	-3.32
	MSS	PSAT	-0.01	-0.03	-0.04	-0.07	-0.11	-0.16
	SFS	DRIED	-	-0.06	-4.87	-5.09	-5.36	-5.36
	MUS	DRIED	-0.02	-4.33	-4.93	-5.17	-5.17	-5.17
	MUS	PSAT	-	-0.01	-0.04	-0.06	-0.06	-0.06
	MLB	DRIED	-0.12	-8.17	-8.58	-8.91	-9.04	-9.04
	MLB	PSAT	-	-0.53	-0.85	-1.07	-1.37	-1.51
	GMS	DRY	-	-0.84	-1.43	-1.93	-2.29	-2.29
	CSS63	DRIED	-0.01	-10.78	-12.54	-12.89	-12.89	-12.89
	CSS63	PSAT	-	-0.03	-0.15	-0.34	-0.34	-0.34
	CSS	DRIED	-	-	-12.71	-12.79	-12.79	-12.79
	CSS	PSAT	-0.02	-0.28	-0.43	-0.65	-0.65	-0.65
100kPa	MSS	DRIED	-	-2.27	-3.57	-5.06	-5.42	-5.42
	MSS	PSAT	-0.01	-0.01	-0.06	-0.10	-0.16	-0.18
	MLB	DRIED	-	-5.36	-5.75	-5.87	-6.01	-6.17
	GMS	DRY	-0.02	-1.39	-1.67	-1.91	-2.15	-2.15
	CSS	DRIED	-0.02	-11.14	-12.61	-12.89	-12.89	-12.89

Table 5.4.2. High acceleration vibration partially saturated and dried test results (25Hz) expressed as percentage settlements, for effective stresses of 10 -100kPa and vibrations up to 6.0g. Hyphens represent no sample settlement.

The settlement data of the low and high acceleration tests experience common accelerations of $1.0g$ and $2.0g$. Hence, the settlement trends in this range of acceleration are comparable; i.e. a clear increase in settlement is observed when acceleration is increased from $1.0g$ to $2.0g$. A unit increase in acceleration tends to produce a reduction in the rate of the increase of vibratory settlement; a decrease in the gradient of the settlement curve is observed (see Figures 5.3.1 to 5.3.10).

The influence of a fines fraction in a granular soil is demonstrated by the difference in settlement response of the coarse sharp sand and the same material with the $<63\mu$ removed. The data (see Table 5.4.1) demonstrates that, in general terms, the fines content allows approximately half the settlement generated by the coarse sharp sand without a fines fraction.

Two additional tests were performed (on the Garside medium sand) to observe the settlement response of (a), the resaturation of a previously (statically equilibrated) saturated material that was dried-back, and (b), the response of a granular material that experienced stress relief prior to vibration (see Figure 5.3.3). The resaturated sample settlement response is comparable to the standard saturated test (under 20kPa). The sample that was statically consolidated under 300kPa, and vibrated under 10kPa, shows less settlement below $2.0g$, and slightly increased settlement (by approximately 0.2%) at higher acceleration, but is essentially comparable to the test performed at only 10kPa.

Figure 5.3.6 compares the settlement obtained for the coarse Leighton Buzzard sand under 50kPa for a test performed at $6.0g$, with the settlement generated over a range of increasing acceleration to a maximum of $6.0g$. The settlements are very similar, i.e. approximately 4.2% for the $6.0g$ test, and 4.4% for the standard vibration test.

Figure 5.4.8 shows the general settlement trend of a granular material (the protosoil* under mean stress conditions) under the range of accelerations used for the low acceleration and high acceleration tests. Comparison of the $1g$ data for the high and low acceleration test programmes shows less settlement at $1g$ is generated for the high acceleration tests than the low acceleration tests. However, the dial gauge that was used during the high acceleration test (which was accurate to 0.01mm) did not allow the relatively small settlements that occured under $1.0g$ to be resolved. During low vibration

* 'protosoil' is a personal term used to describe the mean response of all the soils tested. This approach was used because of the unsuitable variation of individual tests.

testing, a dial gauge that was accurate to 0.002mm allowed the settlements below 1.0*g* to be defined.

5.2.4 Partially Saturated and Dried High Acceleration Tests

The partially saturated and dried high acceleration tests results (Figures 5.4.1 to 5.4.7) demonstrate different settlement behaviour compared to the equivalent saturated tests. For example, the dried silty fine sand (Figure 5.4.1) shows less vibratory settlement under 10kPa than the equivalent saturated test, up to an acceleration of 4.0*g*. However, at 5g, a rapid increase in settlement is observed, such that the settlement magnitudes under 10, 20 and 50kPa are comparable. On test completion, it was observed that 'nuggets' of intact cemented material (up to 3cms diameter) existed in a matrix of entirely disaggregated silty fine sand. The 'jumps' in the settlement response of the silty fine sand would be the result of the interaction between the effects of increase in acceleration, sample density and stress that causes a previously cemented and intact sample (which could be considered to be a 'weak rock') to break-down. This behaviour was not observed in the other samples that had a fines content. This does not imply that such behaviour did not occur; the other samples (medium sharp sand and the coarse sharp sands) had 1-2% fines (the silty fine sand had approximately 10%) which may have only very weakly cemented the dried samples.

All the tested sands, with exception of the silty fine sand, demonstrated greater settlement under an acceleration of 2*g* than the equivalent saturated tests. Higher accelerations produced only very little additional settlement increase, such that the ultimate accelerations of the equivalent saturated tests produced comparable settlements.

5.2.5 Miscellaneous Tests.

A range of tests were performed to examine additional aspects of granular soil response to vibration. These tests examined the effects of: horizontally propagating primary waves, and torsional shear vibration, compared to values obtained for the standard (vertical) vibration tests; high frequency tests performed under the same test conditions as the standard vibratory test, at 120Hz; the affect on settlement of fixed vibration duration per acceleration increment and tests that examined the assumption that using cumulative vibration settlement was a valid method.

	ACCEL	HORIZONTAL ACCELERATION				VERTICAL ACCELERATION			
	(g)	**10kPa**	**20kPa**	**50kPa**	**100kPa**	**10kPa**	**20kPa**	**50kPa**	**100kPa**
SFMG	**0.1**	-	-0.01	-	-	-	-	-	-
	0.2	-	-0.01	-	-	-	-	-	-
	0.3	-0.16	-0.05	-	-	-0.31	-0.04	-	-
	0.4	-0.32	-0.09	-0.03	-0.01	-0.53	-0.22	-	-
	0.5	-0.55	-0.33	-0.09	-0.02	-0.86	-0.45	-0.09	-
	0.6	-0.79	-0.52	-0.21	-0.03	-1.33	-0.65	-0.17	-0.03
	0.8	-1.59	-0.99	-0.44	-0.09	-1.80	-1.08	-0.40	-0.24
	1.0	-2.12	-1.65	-0.86	-0.26	-2.99	-1.72	-0.71	-0.50
	2.0	-6.32	-4.57	-2.75	-2.26	-9.25	-6.83	-5.45	-4.49
MLB	**0.1**	-	-	-	-	-	-	-	-
	0.2	-0.02	-	-	-0.01	-	-	-	-
	0.3	-0.07	-	-0.01	-0.01	-0.06	-0.03	-0.02	-
	0.4	-0.10	-	-0.03	-0.01	-0.09	-0.05	-0.02	-0.02
	0.5	-0.15	-	-0.03	-0.01	-0.20	-0.10	-0.06	-0.02
	0.6	-0.23	-	-0.03	-0.02	-0.36	-0.15	-0.10	-0.03
	0.8	-0.39	-0.03	-0.16	-0.02	-0.63	-0.24	-0.23	-0.05
	1.0	-0.92	-0.08	-0.35	-0.10	-0.95	-0.47	-0.44	-0.10
	2.0	-2.22	-0.99	-1.38	-0.37	-5.58	-3.59	-4.14	-1.67

Table 5.5.1. Comparison between vertical and horizontal vibration settlement

ACCEL	Vibration mode and frequency				
(g)	**25Hz v**	**40Hz v**	**40Hz h**	**120Hz v**	**40Hz sh**
0.1	-	-	-	-	-
0.2	-0.01	-	-	-	-
0.3	-0.12	-0.09	-0.05	-0.10	-0.01
0.4	-0.23	-0.19	-0.11	-0.22	-0.02
0.5	-0.38	-0.35	-0.25	-0.42	-0.02
0.6	-0.51	-0.55	-0.39	-0.72	-0.04
0.8	-0.96	-0.88	-0.78	-1.20	-0.05
1.0	-2.34	-1.48	-1.22	-1.92	
2.0	-7.09	-6.51	-3.97	-6.61	

Table 5.5.2. Comparison of vibration mode on the settlement response (of saturated sandy fine to medium gravel).

The horizontal vibration tests used two contrasting soil types; the medium Leighton Buzzard sand and the sandy fine to medium gravel. The results are given in Table 5.5.1 and Figure 5.5.2 (a, b). The data shows that the general form of settlement produced using horizontally acting vibration is comparable to the vertical vibration settlement trends. As acceleration increases, the gradient of the settlement curve becomes steeper, and increasing static stress reduces the magnitude of settlement. The clean uniform sand and the well-graded material tended to experience less magnitude of settlement under horizontally acting vibration than vertically acting vibration. The effect of propagating shear vibration was modelled using the sandy fine to medium gravel, and the results are given in Figure 5.5.2c. To allow convenient comparison, the general settlement response of the sandy fine to medium gravel under frequencies of 25, 40 and 120Hz (which is presented separately in Figure 5.5.1) and vertical, horizontal and shear vibrations are included in Figure 5.5.2c. The chart indicates the similarity of the vibratory settlement trends produced using vibration that models the action of primary waves. In comparison, the shear vibration settlement values are markedly reduced, by an order of magnitude. The shear vibration test data presents data to 0.8*g*, which was the maximum output possible using the linked pair of LDS DA100 series electromagnetic shakers vibrating at 40Hz. The maximum acceleration produced by the smaller shakers vibrating at 25Hz was reduced to approximately 0.25*g*, which was considered to be too low for useful testing.

Table 5.5.3 and Figure 5.5.3 summarise the fixed time length (high acceleration) vibration test results. The figure shows the general tendency for sample settlement to increase with increase in vibration duration. However the values for vibration of 1 and 2 minutes per acceleration increment are very similar after an acceleration of 3.0*g*. This is also seen for the 5 and 10 minute vibration settlement values.

A series of tests were carried out to examine the assumption that using the cumulative settlement generated over increasing acceleration increments to a maximum value produces the same settlement as a test performed at the maximum value only. Tests were performed on saturated medium sharp sand under 10kPa. The acceleration ranges used (with increments of 1.0*g*) were: 1.0*g* to 6.0*g*; 2.0*g* to 6.0*g*; 3.0*g* to 6.0*g*; 4.0*g* to 6.0*g*; 5.0*g* to 6.0*g* and 6.0*g*. The results (see Figure 5.5.4. Table 5.5.4) indicate that the ultimate acceleration produces a level of settlement that is independent of the effects of any preceding combination of lower levels of acceleration. For example, the settlement for each acceleration range is similar at 6.0*g*, regardless of the initial level of acceleration and number of increments. This response is apparent for settlement values at 5.0*g* and 4.0*g*. The settlement response of the 1.0*g* to 6.0*g* range shows greater settlement at 3.0*g* than the other acceleration ranges.

ACCEL (g)	1min	2min	5min	10min	20min	50min
0.0	-	-	-	-	-	-
1.0	-0.08	-0.03	-0.03	-0.07	-0.18	-0.29
2.0	-1.91	-1.58	-2.08	-2.30	-2.32	-3.25
3.0	-2.51	-2.34	-2.94	-3.08	-3.31	-4.71
4.0	-2.87	-2.78	-3.49	-3.58	-3.94	-5.26
5.0	-3.20	-3.22	-4.01	-3.99	-4.47	-5.90
6.0	-3.47	-3.62	-4.40	-4.43	-4.98	-6.21

Table 5.5.3 The effect of vibration duration on settlement response (of saturated coarse Leighton Buzzard sand, 25Hz, 50kPa).

Accel	Acceleration					
(g)	1g to 6g	2g to 6g	3g to 6g	4g to 6g	5g to 6g	6g
0.0	0.00	-	-	-	-	-
1.0	-0.13	0.00	-	-	-	-
2.0	-2.54	-1.18	0.00	-	-	-
3.0	-6.26	-2.82	-2.98	0.00	-	-
4.0	-7.18	-5.89	-6.19	-6.46	0.00	-
5.0	-8.47	-7.34	-8.76	-8.32	-6.73	0.00
6.0	-8.95	-8.70	-9.57	-9.02	-10.28	-10.91

Table 5.5.4. Settlement response of medium sharp sand to increasing initial acceleration (saturated, 25Hz, 10kPa).

5.3 Vibratory Settlement Trend Data.

To allow an overview of the test results in terms of the settlement response of soil types, and the influence of static stress on vibratory settlement, trend data are presented.

Figure 5.6.1(a,b) shows the settlement responses of the individual soil-types tested in the acceleration range of 0.1g to 1.0g. Note that mean stress values are used, i.e. the settlement data for a given soil type and acceleration, is the mean value of the sum of the settlements that were obtained for the 10, 20, 50 and 100kPa tests. This is a simple data treatment, but it allows a convenient comparison of general soil-type vibration settlement response. Table 5.6.1 presents the 25Hz and 40Hz data, and the sands are presented in order of increasing maximum particle size.

	ACCL, *g*	SFS	FUS	GMS	MUS	MLB	CLB	MSS	SFG	SFMG
25Hz	**0.0**	-	-	-	-	-	-	-	-	-
	0.1	-	-	-	-	-	-	-	-	-0.004
	0.2	-0.002	-0.015	-	-	-0.003	-0.001	-	-	-0.007
	0.3	-0.040	-0.084	-0.034	-	-0.019	-0.003	-0.036	-0.006	-0.119
	0.4	-0.079	-0.154	-0.069	-0.001	-0.038	-0.006	-0.072	-0.013	-0.233
	0.5	-0.140	-0.265	-0.122	-0.007	-0.070	-0.015	-0.153	-0.067	-0.378
	0.6	-0.244	-0.393	-0.174	-0.022	-0.100	-0.033	-0.319	-0.144	-0.514
	0.8	-0.567	-0.592	-0.311	-0.079	-0.184	-0.106	-0.557	-0.297	-0.965
	1.0	-0.856	-1.045	-0.565	-0.186	-0.399	-0.287	-0.769	-0.577	-2.337
	2.0	-3.301	-4.842	-2.886	-1.429	-3.496	-3.088	-5.405	-8.134	-7.093
40Hz	**0.0**	-	-	-	-	-	-	-	-	-
	0.1	-	-	-	-	-	-	-	-	-
	0.2	-	-	-0.007	-	-0.001	-	-0.018	-	-
	0.3	-0.007	-0.056	-0.032	-	-0.027	-	-0.097	-	-0.088
	0.4	-0.030	-0.083	-0.069	-	-0.045	-0.003	-0.204	-0.071	-0.186
	0.5	-0.103	-0.206	-0.119	-0.006	-0.094	-0.010	-0.321	-0.127	-0.350
	0.6	-0.231	-0.460	-0.178	-0.018	-0.160	-0.018	-0.477	-0.205	-0.545
	0.8	-0.484	-0.830	-0.320	-0.058	-0.287	-0.044	-0.738	-0.399	-0.880
	1.0	-0.875	-1.269	-0.511	-0.218	-0.492	-0.136	-1.093	-0.679	-1.482
	2.0	-2.538	-3.794	-2.602	-1.578	-3.744	-1.572	-4.614	-6.799	-6.506

Table 5.6.1. Comparison of soil settlement trends with acceleration (using mean stress values).

	25Hz				**40Hz**			
ACCL, *g*	10kPa	20kPa	50kPa	100kPa	10kPa	20kPa	50kPa	100kPa
0.0	-	-	-	-	-	-	-	-
0.1	-0.001	-0.001	-	-	-	-	-	-
0.2	-0.009	-0.003	-	-	-0.011	-	-	-
0.3	-0.101	-0.050	-	-	-0.119	-0.015	-0.002	-
0.4	-0.193	-0.098	-0.003	-0.002	-0.231	-0.063	-0.012	-0.002
0.5	-0.331	-0.192	-0.014	-0.004	-0.393	-0.159	-0.037	-0.005
0.6	-0.481	-0.301	-0.051	-0.032	-0.609	-0.305	-0.088	-0.016
0.8	-0.805	-0.537	-0.138	-0.146	-0.949	-0.554	-0.198	-0.094
1.0	-1.275	-0.891	-0.696	-0.258	-1.535	-0.890	-0.395	-0.182
2.0	-5.629	-5.281	-4.012	-2.711	-5.284	-4.077	-3.440	-2.198

Table 5.6.2. Affect of static load on the settlement of the protosoil.

The soil-type settlement data shows that, in general terms (i.e. without specific reference to static stress), granular soils experiencing a vibration of 25Hz tend to show initial settlement at $0.2g$ ($\pm 0.1g$). The 40Hz equivalent values show initial settlements at $0.3g$ ($\pm 0.1g$). Increase in maximum particle size from medium sands to the sandy fine to medium gravel tends to show an increase in vibratory settlement. Note that the settlement response of the silty fine sand and fine uniform sand (at $1.0g$, for example) is greater than the values for the preceding six soils.

The effect that specific static stress has on the settlement response of granular material is presented in Table 5.6.2 and Figures 5.6.2 (a, b) and 5.6.3 (a, b). To allow a convenient overview of the influence of static stress, the vibratory settlement data presented is the mean of the sum of the settlements of all the soils types for a particular static stress and level of acceleration. Treating the data in this way allows the description of granular soil behaviour in general terms. The term 'protosoil' is used to describe the mean of the sum of the soil specific settlements because it is a concise term and conceptually presents the idea that this settlement response is appropriate to a parent material from which the separate soil types may evolve, under a range of transportation and depositional environments.

Figure 5.6.2a presents stress specific protosoil settlement response in acceleration-settlement space (i.e. *g-Sv* space). Note that the decrease in settlement that occurs when static stress is increased from 10kPa to 20kPa is greater than the relative decrease in settlement when stress is increased from 20kPa to 50kPa. The reduction in settlement when stress is increased from 20kPa to 50kPa is of the same order as that produced for an increase from 50kPa to 100kPa. This response to static stress suggests that granular material is relatively more sensitive to increases in static stress at low stress than increases in static stress at higher stress levels. Figure 5.6.2b presents the same data that is shown in Figure 5.6.2a, but in three dimensional space (i.e. acceleration-stress-settlement (g-σ-Sv) space). The 3D chart allows an appreciation of the vibratory settlement surface. Figures 5.6.3(a, b) present the equivalent 40Hz data.

An additional trend that the data demonstrates is the relationship between static stress and the minimum magnitude of acceleration that is required to induce initial settlement (for the protosoil). Figure 5.6.4 shows, for example, that under a static stress of 10kPa, an acceleration of at least $0.2g$ is required to cause sample settlement. This minimum value is increased to 0.6*g* at 100kPa. Figure 5.6.5 shows the best relationship that was found between the minimum acceleration that was required to initiate settlement and specific soil types. The solid lines are regression trends and the R^2 values are in brackets for appropriate static stress. The regression lines are not specifically labelled because the soil specific-minimum acceleration relationship was poor, and the lines are only included to illustrate this. Other combinations of soil specific properties were used in addition to the coefficient of curvature (C_c) and the internal angle of friction (ϕ), such as e_{max}-e_{min}, D_r/U_c etc, but these produced even poorer results.

5.4 Identification of Vibration Test Related Parameters.

In addition to the process of data description and analysis that allow prediction of vibration induced ground surface settlement, the identification of descriptive parameters is required. It is necessary to be able to produce an estimate of vibratory settlement potential for any granular soil type under any static load.

The identification of a soil-type parameter is performed using the soil specific data (for mean stress conditions, as described earlier). Mean stress data is used, because; in the first instance, it reduces the size of the data set. Additionally, it smoothes out any variations in the settlement response of soils under particular static stress, that may occur as a result of actual soil behaviour and/or experimental error that occur due to slight inconsistencies in sample preparation and resultant relative density.

An examination of the settlement trend data (described earlier; see Figure 5.6.1(a,b) and Table 5.6.1), and knowledge of the soil grading characteristics, such as maximum particle size (D_{max}) and uniformity coefficient (U_c), suggests that vibratory settlement is a function of D_{max} and/or U_c. Figures 5.7.1(a, b) and 5.7.2(a, b) show the relationship between maximum particle size and vibratory settlement and uniformity coefficient and vibratory settlement, with acceleration (under mean stress conditions), respectively. The data points represent the actual (acceleration dependant) settlement values for particular values of D_{max} or U_c. The curved lines are best-fit regressions. In all cases, the regression line that is furthest from the *x*-axis represents the 1.0*g* data, and the regression lines approaching the *x*-axis represent the regressed data for 0.8*g*-0.1*g*, respectively.

The best-fit line for settlement related to D_{max} (Figure 5.7.1(a,b)) is of second order polynomial form. The regression suggests that settlement decreases as maximum grain size decreases, to a minimum settlement value around a D_{max} of approximately 3mm. As grain size continues to decrease the settlement is seen to increase. Figure 5.7.2(a,b), shows the relationship obtained using the uniformity coefficient as the soil parameter. A logarithmic best-fit regression is used for this data set. The R^2 values that correspond to the regression lines are presented in Table 5.6.3 and use values that correspond to vibratory settlements obtained for 1.0*g* (see Appendix 3, Table A3.12.1, for regression equations and R^2 values over the entire range of accelerations).

To improve the regressed relationship of vibratory settlement and soil related characteristic (i.e. improving the R^2 values), a soil-type parameter using different combinations of D_n* is developed. In the first instance, the optimum non-dimensional expression is evolved:

$$D_x = \frac{D_{30}^2}{(D_{60}.D_{20})} \qquad \text{(Equation 5.1)}$$

where: D_x = non-dimensional particle size distribution coefficient.

This expression (equation 5.1) improves the R^2 values (to 0.60 (for 25Hz data) at 1.0*g*, see Table 5.6.3), and the settlement relationship is given in Figure 5.7.3(a,b). The combination of D_x values that produce the best relationship between soil-type grading characteristics and vibratory settlement was found to be:

$$D_c = \frac{D_{90}}{(D_{60}\ D_{30})} \quad (\text{mm}^{-1}) \qquad \text{(Equation 5.2)}$$

Figure 5.7.4(a,b) presents the data using equation 5.2. The R^2 values are further improved using this expression (see Table 5.6.3). An additional improvement in the accuracy of the soil-type parameter, is achieved if the influence of relative density is accounted for. This produces the relationship:

$$S_f = \frac{D_c}{D_r} \quad (\text{mm}^{-1}) \qquad \text{(Equation 5.3)}$$

* Where D_n represents a value of particle size below which a percentage of the sample passes, such as D_{30}, D_{50} or D_{90} for example.

where: S_f = soil factor

D_r = relative density

The data showing the relationship between vibratory settlement and S_f are presented in Figure 5.7.5(a,b), and an improvement in the R^2 value to 0.85 (for 40Hz data), for an acceleration of 1.0g, is seen.

The soil parameter, S_f, allows an estimation of the settlement of any granular soil for the range of acceleration, 0.1g to 1.0g. However, the expression was derived using mean stress values. To improve settlement estimates, it is necessary to adjust settlement values (derived using S_f) for the influence of static stress. Figure 5.7.6(a,b) presents vibratory settlement data of the protosoil as a function of static stress, and uses exponential best-fit regression (and R^2 values in the order of 0.9 are typical (Table 5.6.3 and Appendix 3, Table A3.12.1)). The charts allow stress specific settlement for the protosoil to be obtained under the given levels of acceleration.

Soil Parameter	Frequency (Hz)	Regression Equation	R^2 value
D_{max}	25	$S_v = -0.02g^2 + 0.12(D_{\max}) - 0.60$	0.72
(mm)	40	$S_v = -0.02g^2 + 0.12(D_{\max}) - 0.72$	0.42
	25	$S_v = -0.17\ln(D_{\max}) - 0.60$	0.21
	40	$S_v = -0.10\ln(D_{\max}) - 0.71$	0.06
U_c	25	$S_v = -0.49\ln(U_c) - 0.12$	0.49
	40	$S_v = -0.44\ln(U_c) - 0.30$	0.39
D_x	25	$S_v = 0.33\ln(D_x) - 0.23$	0.60
	40	$S_v = 0.28\ln(D_x) - 0.37$	0.41
D_c	25	$S_v = -0.45\ln(D_c) + 0.06$	0.61
(mm)	40	$S_v = -0.55\ln(D_c) + 0.15$	0.88
S_f	25	$S_v = -0.41\ln(S_f) + 0.38$	0.75
(mm)	40	$S_v = -0.43\ln(S_f) + 0.34$	0.85
Stress	25	$S_v = 13.6(\sigma)^{-0.92}$	1.00
(kPa)	40	$S_v = 25.0(\sigma)^{-1.17}$	0.94

Table 5.6.3. Example regression relationships (using 1.0g values).

Using the trend data (regression equations and graphs) allows, (a) the estimation of vibratory settlement of any granular soil type, for mean stress conditions and, (b), the estimation of settlement under any stress of the protosoil. Figure 5.7.7(a,b) show the stress correction multiplication factor that the settlement values generated using the soil parameter (under mean stress), should be adjusted by to obtain vibratory settlement under a given static stress. The stress correction multiplication factor is a ratio of the settlement obtained for specific soil under mean stress conditions to the settlement obtained for the protosoil at 10, 20, 50 and 100kPa.

A difference is observed between the 25Hz and 40Hz data (see Figure 5.7.7(a,b)). For example, under 25Hz, the estimated settlement for a specific soil (under mean stress conditions) experiencing an acceleration of 1.0*g* requires multiplication by a factor of approximately 2.1 to correct for a static load of 10kPa, and multiplication by approximately 0.6 under a static load of 50kPa. The same soil experiencing vibrations of 0.2*g* will require multiplication by a factor of 3.3 to correct for a static load of 10kPa, and no settlement is generated when correcting for 50kPa. However, vibratory settlement is produced under 20kPa and requires multiplication by 0.65. For equivalent conditions under 40Hz: at 1.0*g* the multiplication factor is 2.0 for 20kPa, and 0.5 under 50kPa. For an acceleration of 0.2*g*, the multiplication factor required for a 10kPa adjustment is 4.0, and, as for 25Hz data, no settlement in generated under 50kPa. Unlike the 25Hz response under 20kPa, no settlement is produced for vibrations of 40Hz under a static stress of 20kPa.

This suggests that under 40Hz, and a stress of 10kPa, granular soils are more susceptible to the influence of low acceleration than for vibrations of 25Hz, i.e. at 40Hz, soils demonstrate relatively greater settlement under low acceleration than equivalent 25Hz conditions. However, the 40Hz data demonstrates greater sensitivity to the effects of increasing static stress than the 25Hz data, i.e. soils experiencing 40Hz will experience a greater rate and magnitude of settlement decrease with increasing stress than equivalent soils under vibrations of 25Hz.

A comparison between vibratory settlement values produced using trend data and the equivalent test specific data is given in Table 5.6.4(a,b) for values of acceleration up to and including 1.0*g*.

Soil	Stress	Acceleration (g)													
Type	(kPa)	0.2		0.3		0.4		0.5		0.6		0.8		1.0	
SFS	10	-	-	-	-0.2	-	-0.2	-	-0.3	**-0.1**	-0.5	**-0.1**	-0.9	**-0.2**	-1.4
	20	-	-	-	-	-	-0.1	**-0.5**	-0.2	**-0.6**	-0.3	**-0.8**	-0.6	**-1.1**	-1.1
	50	-	-	-	-	-	-	-	-	**-0.1**	-0.1	**-0.2**	-0.2	**-0.4**	-0.4
	100	-	-	-	-	-	-	-	-	**-0.2**	-	**-1.1**	-	**-1.6**	-0.1
FUS	10	**-0.1**	-	**-0.3**	-0.2	**-0.5**	-0.3	**-0.8**	-0.5	**-1.1**	-0.8	**-1.5**	-1.3	**-2.5**	-2.0
	20	-	-	**-0.1**	-0.1	**-0.1**	-0.2	**-0.2**	-0.3	**-0.4**	-0.5	**-0.7**	-0.9	**-1.3**	-1.5
	50	-	-	-	-	-	-	-	-0.1	-	-0.1	**-0.1**	-0.3	**-0.2**	-0.6
	100	-	-	-	-	-	-	-	-	**-0.1**	-	**-0.1**	-0.1	**-0.2**	-0.1
GMS	10	-	-	-	-0.1	-	-0.1	**-0.1**	-0.2	**-0.2**	-0.3	**-0.3**	-0.5	**-0.5**	-0.9
	20	-	-	-	-	-	-	**-0.1**	-0.1	**-0.1**	-0.2	**-0.3**	-0.4	**-0.6**	-0.7
	50	-	-	-	-	-	-	-	-	-	-	**-0.1**	-0.1	**-0.3**	-0.3
	100	-	-	-	-	-	-	-	-	-	-	-	-	**-0.1**	-0.1
MUS	10	-	-	-	-	-	-	-	-0.1	-	-0.2	**-0.1**	-0.3	**-0.4**	-0.7
	20	-	-	-	-	-	-	-	-0.1	-	-0.1	**-0.1**	-0.2	**-0.3**	-0.5
	50	-	-	-	-	-	-	-	-	-	-	-	-0.1	-	-0.2
	100	-	-	-	-	-	-	-	-	-	-	-	-	-	-
MLB	10	-	-	-	-	**-0.1**	-	**-0.1**	-0.1	**-0.2**	-0.1	**-0.3**	-0.3	**-0.8**	-0.6
	20	-	-	-	-	**-0.1**	-	**-0.1**	-	**-0.2**	-0.1	**-0.2**	-0.2	**-0.4**	-0.5
	50	-	-	-	-	-	-	-	-	**-0.1**	-	**-0.1**	-0.1	**-0.3**	-0.2
	100	-	-	-	-	-	-	-	-	-	-	-	-	**-0.1**	-
CLB	10	-	-	-	-	-	-	-	-	**-0.1**	-	**-0.2**	-0.1	**-0.4**	-0.4
	20	-	-	-	-	-	-	-	-	**-0.1**	-	**-0.2**	-0.1	**-0.6**	-0.3
	50	-	-	-	-	-	-	-	-	-	-	-	-	**-0.1**	-0.1
	100	-	-	-	-	-	-	-	-	-	-	-	-	-	-
MSS	10	-	-	**-0.1**	-0.2	**-0.2**	-0.3	**-0.4**	-0.5	**-0.6**	-0.8	**-0.9**	-1.3	**-1.1**	-2.0
	20	-	-	-	-0.1	**-0.1**	-0.2	**-0.2**	-0.3	**-0.4**	-0.5	**-0.8**	-0.9	**-1.0**	-1.5
	50	-	-	-	-	-	-	-	-0.1	**-0.2**	-0.1	**-0.5**	-0.3	**-0.9**	-0.6
	100	-	-	-	-	-	-	-	-	-	-	-	-0.1	**-0.1**	-0.1
SFG	10	-	-	-	-0.1	**-0.1**	-0.2	**-0.2**	-0.3	**-0.4**	-0.5	**-0.7**	-0.8	**-1.2**	-1.3
	20	-	-	-	-	-	-0.1	**-0.1**	-0.2	**-0.2**	-0.3	**-0.4**	-0.6	**-0.8**	-1.0
	50	-	-	-	-	-	-	-	-	-	-0.1	**-0.1**	-0.2	**-0.3**	-0.4
	100	-	-	-	-	-	-	-	-	-	-	-	-	-	-0.1
SFMG	10	-	-	**-0.3**	-0.3	**-0.7**	-0.3	**-1.0**	-0.6	**-1.4**	-0.9	**-2.6**	-1.6	**-3.5**	-2.3
	20	-	-	**-0.1**	-0.1	**-0.3**	-0.2	**-0.5**	-0.4	**-0.7**	-0.6	**-1.2**	-1.1	**-1.9**	-1.7
	50	-	-	-	-	-	-	-	-0.1	-	-0.2	**-0.1**	-0.4	**-3.8**	-0.7
	100	-	-	-	-	-	-	-	-	-	-	-	-0.1	**-0.2**	-0.2

Table 5.6.4a. A comparison of (25Hz) test data and equivalent regressed values. Results are expressed as percentage settlements; the test data is in bold type. Hyphens represent accelerations where no settlement occurred or is predicted.

Soil Type	Stress (kPa)	Acceleration (g)													
		0.2		0.3		0.4		0.5		0.6		0.8		1.0	
SFS	**10**	-	-	-	-0.2	**-0.1**	-0.2	**-0.2**	-0.3	**-0.4**	-0.5	**-0.8**	-0.9	**-1.7**	-1.3
	20	-	-	-	-	-	-0.1	**-0.1**	-0.2	**-0.2**	-0.4	**-0.6**	-0.7	**-0.8**	-1.1
	50	-	-	-	-	**-0.1**	-	**-0.1**	-0.1	**-0.3**	-0.1	**-0.6**	-0.3	**-0.9**	-0.6
	100	-	-	-	-	-	-	-	-	-	-	-	-0.1	-	-0.2
FUS	**10**	-	-0.1	**-0.2**	-0.2	**-0.2**	-0.3	**-0.5**	-0.5	**-0.8**	-0.8	**-1.3**	-1.2	**-2.4**	-1.9
	20	-	-	**-0.1**	-	**-0.1**	-0.2	**-0.3**	-0.3	**-0.9**	-0.5	**-1.4**	-0.9	**-1.7**	-1.5
	50	-	-	-	-	-	-	-	-0.1	-	-0.2	**-0.1**	-0.4	**-0.3**	-0.8
	100	-	-	-	-	-	-	-	-	-	-	**-0.4**	-0.1	**-0.7**	-0.3
GMS	**10**	-	-	-	-0.1	**-0.2**	-0.1	**-0.3**	-0.2	**-0.4**	-0.3	**-0.7**	-0.5	**-1.0**	-0.8
	20	-	-	-	-	**-0.1**	-0.1	**-0.1**	-0.1	**-0.2**	-0.2	**-0.4**	-0.4	**-0.7**	-0.6
	50	-	-	-	-	-	-	-	-	**-0.1**	-0.1	**-0.1**	-0.2	**-0.3**	-0.3
	100	-	-	-	-	-	-	-	-	-	-	-	-	-	-0.1
MUS	**10**	-	-	-	-0.1	-	-0.1	-	-0.1	-	-0.2	-	-0.4	**-0.3**	-0.7
	20	-	-	-	-	-	-	-	-0.1	**-0.1**	-0.1	**-0.2**	-0.3	**-0.5**	-0.5
	50	-	-	-	-	-	-	-	-	-	-0.1	-	-0.1	**-0.1**	-0.3
	100	-	-	-	-	-	-	-	-	-	-	-	-	-	-0.1
MLB	**10**	-	-	**-0.1**	-0.1	**-0.1**	-0.1	**-0.2**	-0.1	**-0.4**	-0.2	**-0.6**	-0.3	**-1.0**	-0.6
	20	-	-	-	-	-	-	**-0.1**	-0.1	**-0.1**	-0.1	**-0.2**	-0.2	**-0.5**	-0.5
	50	-	-	-	-	-	-	**-0.1**	-	**-0.1**	-	**-0.2**	-0.1	**-0.4**	-0.2
	100	-	-	-	-	-	-	-	-	-	-	-	-	**-0.1**	-0.1
CLB	**10**	-	-	-	-	-	-	-	-	-	0.1	-	-0.2	**-0.1**	-0.4
	20	-	-	-	-	-	-	-	-	-	0.1	**-0.1**	-0.2	**-0.3**	-0.3
	50	-	-	-	-	-	-	-	-	-	-	-	-0.1	**-0.2**	-0.2
	100	-	-	-	-	-	-	-	-	-	-	-	-	-	-0.1
MSS	**10**	**-0.1**	-0.1	**-0.4**	-0.2	**-0.7**	-0.3	**-1.0**	-0.5	**-1.4**	-0.8	**-1.9**	-1.3	**-2.5**	-2.0
	20	-	-	-	-	**-0.1**	-0.2	**-0.3**	-0.3	**-0.5**	-0.6	**-0.9**	-1.0	**-1.4**	-1.6
	50	-	-	-	-	-	-	-	-0.1	-	-0.2	**-0.2**	-0.4	**-0.4**	-0.8
	100	-	-	-	-	-	-	-	-	-	-	**-0.1**	-0.1	**-0.2**	-0.3
SFG	**10**	-	-	-	-0.1	**-0.3**	-0.2	**-0.5**	-0.3	**-0.8**	-0.5	**-1.4**	-0.8	**-2.0**	-1.3
	20	-	-	-	-	-	-0.1	-	-0.2	-	-0.4	**-0.2**	-0.6	**-0.5**	-1.0
	50	-	-	-	-	-	-	-	-0.1	-	-0.1	-	-0.3	**-0.2**	-0.5
	100	-	-	-	-	-	-	-	-	-	-	-	-0.1	**-0.0**	-0.2
SFMG	**10**	-	-0.1	**-0.3**	-0.3	**-0.5**	-0.4	**-0.9**	-0.6	**-1.3**	-1.0	**-1.8**	-1.6	**-3.0**	-2.4
	20	-	-	-	-0.1	**-0.2**	-0.2	**-0.4**	-0.4	**-0.7**	-0.7	**-1.1**	-1.2	**-1.7**	-1.9
	50	-	-	-	-	-	-	**-0.1**	-0.1	**-0.2**	-0.3	**-0.4**	-0.5	**-0.7**	-1.0
	100	-	-	-	-	-	-	-	-	-	-	**-0.2**	-0.1	**-0.5**	-0.3

Table 5.6.4b. A comparison of (40Hz) test data and equivalent regressed values.
Results are expressed as percentage settlements; the test data is in bold type.
Hyphens represent accelerations where no settlement occurred or is predicted.

Figure 5.8.1 shows the relationship between specific static stress and high acceleration vibration settlement (for the protosoil). The lines show the test specific values, and the data points are the equivalent regression derived values. Note that the agreement is generally good; however the regression data tends to overestimate settlement values as acceleration decreases (for 20kPa). The opposite trend is indicated by the 100kPa data, where the low vibration data is slightly underestimated and the high acceleration values are slightly overestimated.

5.5 Vibration Settlement Equations

Using the previous data processing and analysis, equations were developed that allow the predictive estimate of ground surface settlement caused by vibrations generated during vibropiling activity. The equations relate the variables: soil distribution coefficient (D_c); acceleration (g); relative density (D_r) and static stress (σ) to produce a good relationship that allows predictive estimates of vibratory percentage settlement to be performed. Table 5.6.5 provides typical soil specific parameter values.

Soil type	Relative Density, *Dr*	Distribution Coefficient, *Dc*	Soil Factor, *Sf*	Settlement, *Sv* (%)
SFS	0.59	9.0	15.4	0.77
FUS	0.38	10.9	29.0	1.01
GMS	0.44	3.0	6.8	0.45
MUS	0.50	2.5	5.1	0.33
MLB	0.47	2.2	4.6	0.29
CLB	0.49	1.8	3.7	0.21
MSS	0.37	11.4	30.9	1.04
SFG	0.23	6.1	26.1	0.97
SFMG	0.26	13.6	52.3	1.24

Table 5.6.5. Values of relative density, distribution coefficient, soil factor and settlement (values are mean stress data for 1.0*g*).

5.5.1 Equation For Maximum Acceleration of 1.0*g*

The relationship between soil specific settlement, under mean stress conditions, and an acceleration of 1.0*g*, is described by the (regression) equation:

$$S_v = 0.39\ln(S_f) - 0.3 \qquad \text{equation 5.1}$$

where S_v = Vibratory settlement (%)

S_f = soil factor = $\frac{D_c}{D_r}$ (mm^{-1})

For convenience, this approximates to:

$$S_v = 0.32\ln(S_f) \qquad \text{equation 5.2}$$

The regression equation describing the particular relationship between accelerations up to and including 1g and settlement for the protosoil under a static stress of 10kPa is:

$$S_v = -1.4g^2 - 0.08g + 0.02 \qquad \text{equation 5.3}$$

where g = acceleration in gravitation units

This approximates to: $S_v = -1.4g^2$ equation 5.4

A regression equation that combines (a) the relationship between soil type and settlement (without specific reference to static stress, at an acceleration of 1.0g) and (b) the relationship between acceleration and settlement (for the protosoil under a static stress of 10kPa) produces the expression:

$$S_v = 0.32\ln(S_f).g^2 \qquad \text{equation 5.5}$$

The above equation generates settlements for any soil type up to a maximum acceleration of 1.0g, under the specific static stress of 10kPa. Finally, factoring in the influence of static stress, produces the expression:

$$S_{v\ max} = \frac{0.32\ln(S_f)g^2}{0.06\sigma_v} \qquad \text{equation 5.6i}$$

or,

$$S_{v\ max} = \frac{5.33\ln(S_f)g^2}{\sigma_v} \qquad \text{Equation 5.6ii}$$

where $S_{v\,max}$ = maximum estimated vibration settlement (%)

S_f = soil factor = $\frac{D_c}{D_r}$ (mm^{-1})

g = acceleration in gravitation units

σ_v = static stress, i.e. surcharge and/or overburden (kPa)

The above equation (5.6ii) was generated using settlement trend and parameter data (described earlier). The soil parameter, S_f, (the product of the distribution coefficient divided by relative density) was a convenient parameter to use during trend observation and regression analysis. However, to demonstrate more clearly the relationship between; the various parameters (specifically the influence of stress and density), and vibratory settlement, equation (6.2ii) was reworked to give the expression:

$$S_{v\ max} = \frac{0.5\ln(D_c)\,g^2}{0.18(D_r\,\sigma_v)} \qquad \text{equation 5.7}$$

or,

$$S_{v\ max} = \frac{2.8\ln(D_c)\,g^2}{D_r\,\sigma_v} \qquad \text{equation 5.8a}$$

In addition, if the coefficient of uniformity (U_c) is preferred to the distribution coefficient (D_c), then the optimum relationship that may be used to derive vibratory settlement is:

$$S_{v\ max} = \frac{3.3\ln(U_c)\,g^2}{D_r\,\sigma_v} \qquad \text{equation 5.8b}$$

Note however, that the regression equations that used U_c produced lower R^2 values than the equivalent data that used D_c (see Table 5.6.3) as the soil type parameter.

If SPT-N values are known, they may be converted to equivalent relative density values by using:

$$D_r = \sqrt{\frac{N.0.05}{1+(\sigma_v\ a)}}$$

(after Bazara, 1967)

where

D_r = relative density

N = SPT-N value (blows/30cm)

a = factor, $a = 0.04$ for $\sigma_v < 75$kPa and $a = 0.03$ for $\sigma_v > 75$kPa

5.5.2 Settlement Equation For Accelerations Greater than 1.0*g*

Regression analysis of the high acceleration test results identified relations that allowed the development of a vibration settlement equation for accelerations above 1*g*. It was found that U_c was the optimum soil specific parameter:

$$S_v = 4.3(\ln(U_c)) + 0.7\,, \quad \text{(for } 4.0g,\ R^2{=}0.85\text{)} \qquad \text{equation 5.9a}$$

and,

$$S_v = 5.0(\ln(U_c)) + 0.7\,, \quad \text{(for } 6.0g,\ R^2{=}0.73\text{)} \qquad \text{equation 5.9b}$$

Equations 5.9a and 5.9b describe the soil specific settlement trend for mean stress conditions. Equation 5.9a using the 4.0*g* settlement data was used in the generation of the settlement equation because not all soils were tested up to 6.0*g*, but all soils were tested at 4.0*g*.

Because it appears that a static stress of 20kPa tended to allow greater vibratory settlement than 10kPa (which is less clearly observed for the low acceleration data), the relationship between the protosoil and specific acceleration (for mean stress) used the 20kPa settlement data to give:

$$S_v = 4.5(\ln(g)) \qquad \text{equation 5.10a}$$

The effect of specific stress on the protosoil was determined to be:

$$S_v = 0.015(\sigma_v) + 0.8 \qquad \text{equation 5.10b}$$

The influence of relative density was best described by:

$$Sv = \frac{1}{(1 - D_r)} \qquad \text{equation 5.10c}$$

Combining the above expressions obtained by regression analysis to produce the equation that best described the relationship between soil type, acceleration, static stress and relative density, for the saturated condition, gave:

$$S_v = \frac{4(\ln(U_c) + 0.7).\ln(g)}{(0.01(\sigma_v) + 0.75).(1 - D_r)} \qquad \text{equation 5.11}$$

5.5.3 The Influence of Vibration Duration, Frequency and Saturation

To modify the maximum estimate of vibration induced surface settlement for the effects of; vibration time length, vibrodriver operating frequency and moisture state, the following time based, frequency dependant expression may be used:

$$S_v = \ln(t).\frac{S_{v\ max}}{\ln(t_{max})}.\frac{1}{f'}.m \qquad \text{equation 5.12}$$

where

S_v = estimated vibration settlement (%)

$\frac{S_{v\ max}}{\ln(t_{max})}$ = slope of the log plot

t_{max} = duration of laboratory vibration test increment (minutes)

t = duration of ground vibration (minutes)

f' = ratio of the vibrodriver frequency to laboratory test frequency

m = a function of saturation. Where

$S_r = 1$, m = 1

$S_r = 0$, m = 0.06

$0 < S_r > 1$, m = 0.01

A comparison between laboratory generated test specific data and the equivalent vibratory settlement evolved using the vibration settlement equation is presented in Tables 5.7.1 (low acceleration, 25Hz data), 5.7.2 (low acceleration, 40Hz data), 5.7.3 (high acceleration, protosoil data) and Figures 5.8.2, 5.9.1a-5.9.1d (silty fine sand, medium Leighton Buzzard sand, medium sharp sand and sandy fine to medium gravel). In general, there is good agreement between test specific and equation generated vibratory settlement data. The differences that occur between the data sets (note the silty fine sand data) may reflect minor aberrations in sample preparation and/or small inconsistencies in the standard laboratory test (BS 1377: 1990) data that describes the physical properties of the soils, and hence cause inherent error in the calculation of relative density, for example. Additionally, the vibration settlement equation assumes that all soils are equally sensitive to the effects of increasing levels of acceleration, which is not seen to occur if the laboratory test data is examined.

Soil Type	Stress (kPa)	Acceleration (g)													
		0.2		0.3		0.4		0.5		0.6		0.8		1.0	
SFS	10	-	-0.1	-	-0.1	-	-0.2	-	-0.4	**-0.1**	-0.5	**-0.1**	-0.9	**-0.2**	-1.4
	20	-	-	**-0.2**	-	**-0.3**	-0.1	**-0.5**	-0.1	**-0.6**	-0.2	**-0.8**	-0.4	**-1.1**	-0.6
	50	-	-	-	-	-	-	-	-0.1	**-0.1**	-0.1	**-0.2**	-0.1	**-0.4**	-0.2
	100	-	-	-	-	-	-	-	-	**-0.2**	-	**-1.1**	-	**-1.6**	-0.1
FUS	10	**-0.1**	-0.1	**-0.3**	0.2	**-0.5**	-0.4	**-0.8**	0.7	**-1.1**	-1.0	**-1.5**	-1.7	**-2.5**	-2.7
	20	-	-	**-0.1**	-0.1	**-0.1**	-0.2	**-0.2**	-0.3	**-0.4**	-0.4	**-0.7**	-0.8	**-1.3**	-1.2
	50	-	-	-	-	-	-0.1	-	-0.1	-	-0.1	**-0.1**	-0.2	**-0.2**	-0.3
	100	-	-	-	-	-	-	-	-	**-0.1**	-0.1	**-0.1**	-0.1	**-0.2**	-0.1
GMS	10	-	-	-	-0.1	-	-0.1	**-0.1**	-0.2	**-0.2**	-0.3	**-0.3**	-0.5	**-0.5**	-0.8
	20	-	-	-	-	-	-0.1	**-0.1**	-0.1	**-0.1**	-0.1	**-0.3**	-0.3	**-0.6**	-0.4
	50	-	-	-	-	-	-	-	-	-	-0.1	**-0.1**	-0.1	**-0.3**	-0.2
	100	-	-	-	-	-	-	-	-	-	-	-	-	**-0.1**	-0.1
MUS	10	-	-	-	-0.1	-	-0.1	-	-0.2	-	-0.2	**-0.1**	-0.4	**-0.4**	0.6
	20	-	-	-	-	-	-0.1	-	-0.1	-	-0.1	**-0.1**	-0.3	**-0.3**	-0.4
	50	-	-	-	-	-	-	-	-	-	-	-	-0.1	-	-0.1
	100	-	-	-	-	-	-	-	-	-	-	-	-	-	-
MLB	10	-	-	-	-	**-0.1**	-0.1	**-0.1**	-0.1	**-0.2**	-0.2	**-0.3**	-0.4	**-0.8**	-0.6
	20	-	-	-	-	**-0.1**	-	**-0.1**	-0.1	**-0.2**	-0.1	**-0.2**	-0.2	**-0.4**	-0.3
	50	-	-	-	-	-	-	-	-	**-0.1**	-	**-0.1**	-0.1	**-0.3**	-0.1
	100	-	-	-	-	-	-	-	-	-	-	-	-	**-0.1**	-
CLB	10	-	-	-	-	-	-0.1	-	-0.1	**-0.1**	-0.2	**-0.2**	-0.3	**-0.4**	-0.5
	20	-	-	-	-	-	-	-	-0.1	**-0.1**	-0.1	**-0.2**	-0.1	**-0.6**	-0.2
	50	-	-	-	-	-	-	-	-	-	-	-	-	**-0.1**	-0.1
	100	-	-	-	-	-	-	-	-	-	-	-	-	-	-
MSS	10	-	-0.1	**-0.1**	-0.2	**-0.2**	-0.3	**-0.4**	-0.5	**-0.6**	-0.7	**-0.9**	-1.3	**-1.1**	-2.0
	20	-	-	-	-0.1	**-0.1**	-0.2	**-0.2**	-0.3	**-0.4**	-0.4	**-0.8**	-0.7	**-1.0**	-1.1
	50	-	-	-	-	-	-0.1	-	-0.1	**-0.2**	-0.1	**-0.5**	-0.2	**-0.9**	-0.4
	100	-	-	-	-	-	-	-	-	-	-0.1	-	-0.1	**-0.1**	-0.2
SFG	10	-	-0.1	-	-0.1	**-0.1**	-0.2	**-0.2**	-0.3	**-0.4**	-0.5	**-0.7**	-0.8	**-1.2**	-1.3
	20	-	-	-	-0.1	-	-0.1	**-0.1**	-0.2	**-0.2**	-0.2	**-0.4**	-0.4	**-0.8**	-0.7
	50	-	-	-	-	-	-	-	-0.1	-	-0.1	**-0.1**	-0.1	**-0.3**	-0.2
	100	-	-	-	-	-	-	-	-	-	-	-	-0.1	-	-0.1
SFMG	10	-	-0.1	**-0.3**	-0.3	**-0.7**	-0.6	**-1.0**	-0.9	**-1.4**	-1.3	**-2.6**	-2.4	**-3.5**	-3.7
	20	-	-0.1	**-0.1**	-0.2	**-0.3**	-0.3	**-0.5**	-0.4	**-0.7**	-0.6	**-1.2**	-1.1	**-1.9**	-1.8
	50	-	-	-	-	-	-0.1	-	-0.1	-	-0.2	**-0.1**	-0.3	**-3.8**	-0.5
	100	-	-	-	-	-	-	-	-0.1	-	-0.1	-	-0.2	**-0.2**	-0.3

Table 5.7.1. A comparison of (25Hz) test data and values generated using the vibration settlement equation (5.8a). Values are expressed as percentage settlements; the test data are in bold type.

Soil Type	Stress (kPa)	Acceleration (g)													
		0.2		0.3		0.4		0.5		0.6		0.8		1.0	
SFS	**10**	-	-	-	-0.1	**-0.1**	-0.2	**-0.2**	-0.3	**-0.4**	-0.4	**-0.8**	-0.7	**-1.7**	-1.1
	20	-	-	-	-0.1	-	-0.1	**-0.1**	-0.2	**-0.2**	-0.2	**-0.6**	-0.4	**-0.8**	-0.6
	50	-	-	-	-	**-0.1**	-	**-0.1**	-0.1	**-0.3**	-0.1	**-0.6**	-0.1	**-0.9**	-0.2
	100	-	-	-	-	-	-	-	-	-	-	-	-0.1	-	-0.1
FUS	**10**	-	-0.1	**-0.2**	-0.2	**-0.2**	-0.3	**-0.5**	-0.5	**-0.8**	-0.8	**-1.3**	-1.3	**-2.4**	-2.1
	20	-	-	**-0.1**	-0.1	**-0.1**	-0.2	**-0.3**	-0.3	**-0.9**	-0.4	**-1.4**	-0.7	**-1.7**	-1.1
	50	-	-	-	-	-	-0.1	-	-0.1	-	-0.1	**-0.1**	-0.2	**-0.3**	-0.3
	100	-	-	-	-	-	-	-	-	-	-0.1	**-0.4**	-0.1	**-0.7**	-0.1
GMS	**10**	-	-	-	-0.1	**-0.2**	-0.1	**-0.3**	-0.2	**-0.4**	-0.3	**-0.7**	-0.6	**-1.0**	-0.9
	20	-	-	-	-	**-0.1**	-0.1	**-0.1**	-0.1	**-0.2**	-0.1	**-0.4**	-0.2	**-0.7**	-0.4
	50	-	-	-	-	-	-	-	-	**-0.1**	-	**-0.1**	-0.1	**-0.3**	-0.1
	100	-	-	-	-	-	-	-	-	-	-	-	-	-	-0.1
MUS	**10**	-	-	-	-	-	-0.1	-	-0.1	-	-0.2	-	-0.3	**-0.3**	-0.5
	20	-	-	-	-	-	-0.1	-	-0.1	**-0.1**	-0.1	**-0.2**	-0.2	**-0.5**	-0.4
	50	-	-	-	-	-	-	-	-	-	-	-	-0.1	**-0.1**	-0.1
	100	-	-	-	-	-	-	-	-	-	-	-	-	-	-
MLB	**10**	-	-	**-0.1**	-0.1	**-0.1**	-0.1	**-0.2**	-0.2	**-0.4**	-0.3	**-0.6**	-0.6	**-1.0**	-0.9
	20	-	-	-	-	-	-0.1	**-0.1**	-0.1	**-0.1**	-0.1	**-0.2**	-0.2	**-0.5**	-0.4
	50	-	-	-	-	-	-	**-0.1**	-0.1	**-0.1**	-0.1	**-0.2**	-0.2	**-0.4**	-0.2
	100	-	-	-	-	-	-	-	-	-	-	-	-	**-0.1**	-0.1
CLB	**10**	-	-	-	-	-	-	-	-0.1	-	-0.1	-	-0.2	**-0.1**	-0.3
	20	-	-	-	-	-	-	-	-0.1	-	-0.1	**-0.1**	-0.1	**-0.3**	-0.2
	50	-	-	-	-	-	-	-	-	-	-	-	-	**-0.2**	-0.1
	100	-	-	-	-	-	-	-	-	-	-	-	-	-	-
MSS	**10**	**-0.1**	-0.1	**-0.4**	-0.3	**-0.7**	-0.4	**-1.0**	-0.7	**-1.4**	-1.0	**-1.9**	-1.8	**-2.5**	-2.8
	20	-	-	-	-0.1	**-0.1**	-0.2	**-0.3**	-0.3	**-0.5**	-0.4	**-0.9**	-0.7	**-1.4**	-1.1
	50	-	-	-	-	-	-0.1	-	-0.1	-	-0.1	**-0.2**	-0.2	**-0.4**	-0.4
	100	-	-	-	-	-	-	-	-	-	-0.1	**-0.1**	-0.1	**-0.2**	-0.2
SFG	**10**	-	-0.1	-	-0.2	**-0.3**	-0.3	**-0.5**	-0.5	**-0.8**	-0.6	**-1.4**	-1.2	**-2.0**	-1.8
	20	-	-	-	-0.1	-	-0.1	-	-0.1	-	-0.2	**-0.2**	-0.4	**-0.5**	-0.6
	50	-	-	-	-	-	-	-	-0.1	-	-0.1	-	-0.1	**-0.2**	-0.2
	100	-	-	-	-	-	-	-	-	-	-	-	-0.1	-	-0.1
SFMG	**10**	-	-0.1	**-0.3**	-0.3	**-0.5**	-0.5	**-0.9**	-0.8	**-1.3**	-1.1	**-1.8**	-1.9	**-3.0**	-3.0
	20	-	-0.1	-	-0.1	**-0.2**	-0.3	**-0.4**	-0.4	**-0.7**	-0.6	**-1.1**	-1.0	**-1.7**	-1.6
	50	-	-	-	-	-	-0.1	**-0.1**	-0.1	**-0.2**	-0.2	**-0.4**	-0.3	**-0.7**	-0.5
	100	-	-	-	-	-	-	-	-0.1	-	-0.1	**-0.2**	-0.1	**-0.5**	-0.2

Table 5.7.2. A comparison of (40Hz) test data and values generated using the vibration settlement equation (5.8a). Values are expressed as percentage settlements; the test data are in bold type.

Soil Type	Stress (kPa)	Acceleration (g)											
		1g		2g		3g		4g		5g		6g	
SFS	**10.0**	**-0.0**	-0.4	**-2.8**	-2.7	**-3.4**	-4.3	**-4.0**	-5.4	**-4.3**	-6.3	-	-7.0
	20.0	**-0.7**	-0.3	**-2.0**	-2.2	**-2.4**	-3.5	**-3.0**	-4.4	**-3.6**	-5.1	-	-5.7
	50.0	**-0.1**	-0.2	**-0.7**	-1.5	**-1.4**	-2.3	**-2.2**	-2.9	**-3.9**	-3.4	-	-3.8
	100.0	**-0.1**	-0.2	**-1.5**	-1.6	**-2.2**	-2.6	**-3.1**	-3.3	**-4.4**	-3.8	-	-4.2
FUS	**10.0**	**-0.3**	-0.2	**-1.7**	-1.6	**-2.7**	-2.6	**-3.8**	-3.3	**-4.6**	-3.8	-	-4.3
	20.0	**-0.1**	-0.3	**-1.4**	-2.1	**-2.7**	-3.4	**-3.6**	-4.3	**-3.8**	-4.9	-	-5.5
	50.0	**-0.1**	-0.2	**-0.6**	-1.4	**-2.2**	-2.2	**-3.2**	-2.8	**-3.9**	-3.2	-	-3.6
	100.0	**-0.1**	-0.1	**-1.1**	-0.8	**-2.0**	-1.3	**-2.4**	-1.6	**-2.5**	-1.9	-	-2.1
GMS	**10.0**	**-0.2**	-0.3	**-0.7**	-2.4	**-1.3**	-3.8	**-1.5**	-4.8	**-1.8**	-5.6	-	-6.2
	20.0	**-0.1**	-0.2	**-0.7**	-1.8	**-1.0**	-2.8	**-1.2**	-3.6	**-1.3**	-4.2	-	-4.6
	50.0	**-0.1**	-0.2	**-0.4**	-1.1	**-0.6**	-1.7	**-0.9**	-2.2	**-1.1**	-2.6	-	-2.8
	100.0	**-0.1**	-0.2	**-0.6**	-1.2	**-0.9**	-1.9	**-1.2**	-2.4	**-1.4**	-2.7	-	-3.1
MUS	**10.0**	**-0.0**	-0.3	**-2.0**	-2.4	**-4.5**	-3.7	**-6.2**	-4.7	-	-5.5	-	-6.1
	20.0	**-0.1**	-0.2	**-2.0**	-1.4	**-2.2**	-2.2	**-2.6**	-2.7	-	-3.2	-	-3.5
	50.0	**-0.0**	-0.2	**-1.3**	-1.4	**-2.1**	-2.2	**-2.5**	-2.8	-	-3.2	-	-3.6
	100.0	-	-0.1	-	-0.7	-	-1.0	-	-1.3	-	-1.5	-	-1.7
MLB	**10.0**	**-0.1**	-0.4	**-1.8**	-2.6	**-2.9**	-4.1	**-3.6**	-5.1	**-4.3**	-6.0	-	-6.7
	20.0	**-0.1**	-0.4	**-2.4**	-2.6	**-4.1**	-4.1	**-4.8**	-5.1	**-5.4**	-6.0	-	-6.6
	50.0	**-0.1**	-0.3	**-1.8**	-2.3	**-2.9**	-3.6	**-3.9**	-4.6	**-4.3**	-5.3	-	-5.9
	100.0	**-0.0**	-0.2	**-1.1**	-1.3	**-2.0**	-2.1	**-2.6**	-2.6	**-2.9**	-3.0	-	-3.4
CLB	**10.0**	**-0.4**	-0.4	**-3.2**	-2.6	**-4.3**	-4.1	**-4.8**	-5.1	**-5.0**	-5.9	**-5.3**	-6.6
	20.0	**-0.3**	-0.3	**-3.7**	-2.3	**-5.2**	-3.7	**-5.4**	-4.6	**-5.7**	-5.4	**-6.0**	-6.0
	50.0	**-0.0**	-0.2	**-2.0**	-1.4	**-3.1**	-2.2	**-3.5**	-2.8	**-3.8**	-3.3	**-4.4**	-3.6
	100.0	**-0.0**	-0.1	**-0.6**	-0.6	**-1.2**	-0.9	**-1.4**	-1.2	**-1.7**	-1.4	**-2.3**	-1.5
MSS	**10.0**	**-0.2**	-0.5	**-2.6**	-3.8	**-6.3**	-6.1	**-7.2**	-7.7	**-8.5**	-8.9	**-9.0**	-9.9
	20.0	**-0.3**	-0.6	**-8.7**	-4.4	**-10.0**	-7.1	**-10.8**	-8.9	**-11.1**	-10.3	**-11.3**	-11.5
	50.0	**-0.9**	-0.5	**-5.0**	-3.4	**-6.8**	-5.4	**-7.6**	-6.8	**-8.9**	-7.9	**-9.1**	-8.8
	100.0	**-0.2**	-0.4	**-1.4**	-2.7	**-3.1**	-4.3	**-4.5**	-5.4	**-5.0**	-6.3	**-5.0**	-7.0
CSS63	**10.0**	**-0.2**	-0.5	**-8.0**	-3.9	**-10.0**	-6.2	**-10.3**	-7.9	-	-9.1	-	-10.2
	20.0	**-0.0**	-0.6	**-7.6**	-4.5	**-10.2**	-7.1	**-10.8**	-9.0	-	-10.4	-	-11.6
	50.0	**-0.1**	-0.4	**-6.5**	-2.9	**-10.1**	-4.6	**-10.7**	-5.8	-	-6.7	-	-7.5
	100.0	-	-0.2	-	-1.7	-	-2.8	-	-3.5	-	-4.0	-	-4.5
CSS	**10.0**	**-0.0**	-0.4	**-3.3**	-2.7	**-5.6**	-4.2	**-8.0**	-5.3	-	-6.2	-	-6.9
	20.0	**-0.1**	-0.3	**-2.7**	-2.3	**-5.7**	-3.7	**-6.7**	-4.7	-	-5.4	-	-6.0
	50.0	**-0.0**	-0.5	**-3.7**	-3.3	**-5.1**	-5.2	**-6.2**	-6.6	-	-7.6	-	-8.5
	100.0	-	-0.2	-	-1.7	-	-2.8	-	-3.5	-	-4.0	-	-4.5
SFMG	**10.0**	**-1.6**	-0.7	**-8.3**	-5.0	**-11.3**	-8.0	**-13.0**	-10.1	**-13.9**	-11.7	**-14.5**	-13.0
	20.0	**-1.1**	-0.6	**-7.3**	-4.4	**-9.6**	-7.0	**-10.2**	-8.9	**-11.1**	-10.3	**-11.5**	-11.5
	50.0	**-0.4**	-0.7	**-5.7**	-5.4	**-8.1**	-8.6	**-9.0**	-10.8	**-10.1**	-12.6	**-10.4**	-14.0
	100.0	**-0.1**	-0.3	**-1.7**	-2.2	**-5.8**	-3.5	**-6.9**	-4.5	**-7.5**	-5.2	**-8.4**	-5.8

Table 5.7.3. A comparison of (high acceleration) test data and values generated using the vibration settlement equation (5.11). Values are expressed as percentage settlements; the test data are in bold type.

Layer no.	Mid-layer depth (m)	Unit weight (kN/m2)	Mid-layer stress (kPa)	Vibe time (mins)	Relative density (Dr)	Distribution coefficient (Dc)	Accel. (g)	Max vibe. settlement (Sv%)	Vibe settlement Sv(t,f)%	Layer thickness (m)	Surface Sv (mm)	Water table (m)
1	0.50	17.70	3.95	120	0.25	2.0	0.86	1.51	1.68	1.00	16.75	16.75
2	1.50	18.10	12.44	120	0.30	5.0	0.86	0.93	1.03	1.00	10.29	10.29
3	3.00	18.80	26.97	120	0.35	10.0	0.86	0.52	0.58	3.00	17.45	17.45
4	5.25	18.10	43.52	120	0.40	5.0	0.86	0.20	0.22	0.50	1.10	1.10
5	7.00	17.70	55.23	120	0.65	2.0	0.86	0.04	0.05	3.00	1.38	1.38
6	10.25	18.10	84.97	120	0.80	5.0	0.86	0.05	0.06	3.50	1.98	1.98
								tmax	Freq		total	
								120	25		48.94	48.94

Table 5.7.4. An example of a ground surface settlement data table.

5.6 Applications.

5.6.1 Using the Vibratory Settlement Equation(s)

To apply the vibratory settlement equation(s) the following procedure should be followed:

1) Divide the soil profile into layers. The layer thickness should be defined by changes in soil-type and relative density.

2) The mid-layer overburden stress should then be calculated.

3) From knowledge of soil gradings calculate values of distribution coefficient (or U_c).

4) Obtain values of relative density.

5) Explicit ground vibration data should be used, or estimated using the attenuation expression derived by Attewell *et al.* (1992) (see Equation 2.6) and converted into acceleration values.

6) For a given value of acceleration, input the pertinent values of overburden stress, relative density and distribution coefficient into the appropriate vibratory settlement

equation: for accelerations up to and including $1g$ use equation 5.8a; equation 5.8b if U_c data only is available and Equation 5.11 for accelerations above $1g$.

7) The vibration induced ground surface compaction settlement is the sum of the reduction in thickness of all the layers. Table 5.7.4 gives an example of a settlement calculation data-sheet.

8) The above will produce the ground surface settlement of a point at a given stand-off distance from the vibration source. If a settlement profile is required, then the above should be repeated for values of acceleration over the appropriate stand-off range.

9) The ground surface settlement profile generated by the above steps produces an upperbound estimate for saturated soil. A time based, frequency dependant estimate with the water table at some depth can be generated using equation 5.12.

5.6.2 Demonstration of the Vibratory Settlement Equation(s)

To demonstrate the use of the vibration settlement equation, and the relative influence of various ground conditions, a range of settlement profiles are presented. The data describes fictitious sites where vibropiling is being performed. Unless otherwise stated, the vibrodriver is rated at 3kJ/cycle and runs at 25Hz. Tables 5.8.1 to 5.8.5 present a range of ground conditions in terms of soil type (distribution coefficient, unit weight, relative density), in varied layer thickness and depths. The default ground condition is 1.1, and subtypes (in this case ground condition 1.2 and 1.3) differ in terms of soil type, layer thickness and depth position. Other ground conditions present different soil profiles and demonstrate the relative influences on vibration induced surface settlement of vibrodriver power, vibration time, position of water table and layer resolution.

<u>Ground Condition 1.1</u> A medium uniform sand (with a distribution coefficient of D_c = 2), a coarse sand (D_c = 5) and a gravelly sand (D_c = 10) occur in six discrete layers to a depth of 12m, below which is bed rock. Ground conditions 1.2 and 1.3 are soil profiles that contain the same soil types, layer thickness and depths, but the order in which the soils occur is altered (see Table 5.8.1).

<u>Ground Condition 2.1</u> This example has a uniform coarse sand (D_c = 1.5), a sandy fine gravel (D_c = 6), a medium uniform sand (D_c = 3) and a sandy fine to medium gravel (D_c =14) to a depth of 20m divided into layer thickness of 5m (see Table 5.8.2).

Soil layer no.	Depth to layer base (m)	Layer thickness (m)	Distribution coefficient (D_c)	Unit weight (kN/m^3)	Relative density (D_r)
			<u>Ground condition 1.1</u>		
1	1.0	1.0	2	17.7	0.25
2	2.0	1.0	5	18.1	0.30
3	5.0	3.0	10	18.8	0.35
4	5.5	0.5	5	18.1	0.50
5	8.5	3.0	2	17.7	0.65
6	12.0	3.5	5	18.1	0.80
			<u>Ground condition 1.2</u>		
1	1.0	1.0	5	18.1	0.25
2	2.0	1.0	10	18.8	0.30
3	5.0	3.0	5	18.1	0.35
4	5.5	0.5	2	17.7	0.50
5	8.5	3.0	5	18.1	0.65
6	12.0	3.5	2	17.7	0.80
			<u>Ground condition 1.3</u>		
1	1.0	1.0	5	18.1	0.25
2	2.0	1.0	2	17.7	0.30
3	5.0	3.0	5	18.1	0.35
4	5.5	0.5	2	17.7	0.50
5	8.5	3.0	5	18.1	0.65
6	12.0	3.5	10	18.8	0.80

Table 5.8.1. Example soil profile (from surface to given depth): <u>Ground condition 1.1</u> and sub-types 1.2, 1.3. Vibrodriver power is 3kJ/cycle, running at 25Hz.

Soil Layer no.	Depth to layer base (m)	Layer thickness (m)	Distribution coefficient (D_c)	Unit weight (kN/m^3)	Relative density (D_r)
1	5.0	5.0	1.5	19.1	0.25
2	10.0	5.0	6	18.6	0.40
3	15.0	5.0	3	19.5	0.60
4	20.0	5.0	14	19.9	0.80

Table 5.8.2. Example soil profile (from surface to given depth): <u>Ground condition 2.1.</u> Vibrodriver power is 3kJ/cycle, running at 25Hz.

<u>Ground Condition 3.1</u> A ground profile containing a sandy medium gravel (D_c = 15), a medium uniform sand (D_c = 2), a stiff clay and a coarse sand (D_c =5) are presented in this example. The soils occur in four layers to a depth of 25m, above bedrock. Ground condition 3.2 is identical to 3.1, except that the sandy medium gravel (soil layer no.1) is replaced by the same stiff clay that occurs in layer no.3 (see Table 5.8.3).

Ground Condition 4.1 Two soils occur in layers 10m thick: a fine uniform sand (D_c = 2) and medium sharp sand (D_c = 10). Ground conditions 4.2, 4.3, and 4.4 contain the same soil types and positions, however, for settlement calculation purposes, the soil profile is split into 4 layers (5m thick), 10 layers (2m thick) and 20 layers (each 1m thick), respectively (see Table 5.8.4).

Ground Condition 5.1 Twenty metres of a sandy gravel (D_c = 15) occur above bed rock. For calculation purposes the soil profile is divided into 1m strata. Ground condition 5.2 and 5.3 are the same as 5.1, but the first 1m depth and 2m depth are ignored in the surface settlement calculation (Table 5.8.5).

Soil layer no.	Depth to layer base (m)	Layer thickness (m)	Distribution coefficient (D_c)	Unit weight (kN/m^3)	Relative density (D_r)
1	5.0	5.0	15	19.9	0.25
2	10.0	5.0	2	19.5	0.40
3	15.0	5.0	clay	18.5	stiff
4	25.0	10.0	5	19.0	0.80

Table 5.8.3. Example soil profile (from surface to given depth). Ground condition 3.1. Vibrodriver power is 3kJ/cycle, running at 25Hz.

Soil layer no.	Depth to layer base (m)	Layer thickness (m)	Distribution coefficient (D_c)	Unit weight (kN/m^3)	Relative density (D_r)
1	10.0	10.0	2.5	19.3	0.30
2	20.0	10.0	10	19.2	0.70

Table 5.8.4. Example soil profile (from surface to given depth). Ground condition 4.1. Vibrodriver power is 3kJ/cycle, running at 25Hz. Ground conditions 4.2, 4.3, 4.4 have number of layers increased to 4, 10 and 20 respectively.

Nine vibration induced surface settlement examples based on the above soil profiles are presented and described. Each example demonstrates the relative influence that a change in the ground condition or piling operation could have on the magnitude of surface settlement. The data is presented as vibration induced surface settlement (mm) with stand-off distance (m). The acceleration magnitude and attenuation is generated using:

$$ppv = \frac{1 \times w^{0.5}}{r} \quad (r > 2\text{m}) \qquad \text{equation 5.13}$$

(after Attewell, Selby and O'Donnel, 1992)

where ppv = peak particle velocity (mm/s)

w = vibrodriver input energy (kJ/cycle)

r = distance from source (m)

Soil layer no.s	Depth to layer base (m)	Layer thickness (m)	Distribution coefficient (D_c)	Unit weight (kN/m^3)	Relative density (D_r)
1	20.0	1.0	15.0	19.0	0.50

Table 5.8.5. Example soil profile (from surface to given depth). Ground condition 5.1. Vibrodriver power is 3kJ/cycle, running at 25Hz. 'Worst case' condition, with 20 layer resolution. Ground condition 5.2 as 5.1, but first 1m is ignored. Ground condition 5.3 as 5.1, but first 2m are ignored in the calculation.

Peak particle velocity is converted to values of acceleration using:

$$g = \frac{ppv}{10^4} . (2\pi f) \qquad \text{equation 5.14}$$

where g = acceleration in gravitation units

f = frequency of ground vibrations (mm/s) (see Table 5.8.6)

Figure 5.10.1 shows the form of the attenuation of acceleration using three hammers (rated at 2, 3 and 4kJ/cycle, see Table 5.8.6) running at 25Hz. Unless otherwise stated, the vibration settlement calculations use the acceleration values (with stand-off) generated by a vibrodriver rated at 3kJ/cycle. Figure 5.10.2 presents the surface settlement with stand-off for ground condition 1.1 for three vibrodriver energies. The data shows a rapid decrease in surface settlement over the first few metres stand-off. For clarity of presentation, settlement profiles will be presented in the first instance, as log-log plots, which allows clear definition of the settlement values of less than 1mm. Secondly, to allow an appreciation of the curved nature of ground surface settlements, the same data is presented as log of settlement verses monotonic increase in stand-off distance.

Stand-off distance (m)	Hammer energy (kJ/cycle) 2	3	4
	g	g	g
1	0.70	0.86	0.99
2	0.35	0.43	0.50
5	0.14	0.17	0.20
7	0.10	0.12	0.14
10	0.07	0.09	0.10
15	0.05	0.06	0.07
20	0.04	0.04	0.05

Table 5.8.6. Ground acceleration with stand-off distance for vibrodrivers rated at 2,3 and 4 kJ/cycle.

The first example (Figure 5.11.1(a,b), shows the influence of vibrodriver energy on surface settlement. At a stand-off distance of 1m, the magnitude of surface settlement is seen to decrease from 65mm (for the vibrodriver rated at 4kJ/cycle) to less than 0.2mm at 20m stand-off. Note that a settlement of 1mm occurs at a stand-off of 8m, 7m and 6m for the 4kJ/cycle, 3kJ/cycle and 2kJ/cycle hammers, respectively.

The effect of increasing and decreasing relative density (of ground condition 1.1) by ± 0.1 is shown in Figure 5.11.2(a,b). At 1m stand-off, a decrease in relative density values (by 0.1) produces an increase in the surface settlement of approximately 20mm. A decrease in the relative density values of ground condition 1.1 decreases the surface settlement by approximately 15mm.

Figure 5.11.3(a,b) demonstrates the effect of placing 50kPa and 100kPa surcharges (over the entire stand-off distance) on the surface settlement of ground condition 1.1. At 1m, the 50kPa surcharge has caused a decrease in settlement from 50mm to 11mm (an approximate decrease of 80%). An additional 50kPa load reduces the settlement to 7.5mm (a decrease of 85%). Without surcharge, 1mm of settlement occurs at a distance of 7m. Surcharges of 50kPa and 100kPa produce settlement of 1mm at stand-offs of 3.75m and 2.75m, respectively.

The influence that vibration time has on surface settlement is demonstrated in Figure 5.11.4(a,b). Vibration times of 120, 30 and 2 minutes are used. At 1m stand-off, these vibration durations cause settlements of 50mm, 25mm (a 50% decrease) and 5.5mm (a 90% decrease in surface settlement), respectively. The corresponding distance at which 1mm of settlement occurs is 7m, 5m and 2.5m respectively.

The effect that the position of the water table has on surface settlement is presented in Figure 5.11.5(a,b). The ground surface settlement calculation in this example, includes the settlement response of dried and partially saturated soils. Initially, the water table occurs at the surface, and is then seen to move to a depth of 1m, 2m and 5m. When the water table is at 1m, the soil above the saturated zone soil is assumed to be partially saturated. The water table at 2m depth allows a 1m layer of partially saturated soil, above which 1m of dried soil occurs. The water table at 5m has 2m of partially saturated soil, beneath 3m of dried soil. At 1m stand-off, water table depths of 0m, 1m, 2m and 5m generate settlements of 50mm, 35mm (a 30% decrease), 22mm (45% decrease) and 5mm (90% decrease), respectively. The stand-off at which 1mm of settlement occurs ranges between 7m, for saturated soil at the ground surface, to 1m for the water table at a 5m depth.

Figure 5.11.6(a,b) shows a comparison between surface settlement produced for ground conditions 1.1, 1.2 and 1.3. This example shows the relative contribution to surface settlement that different depth and thickness of a soil type, with much greater settlement potential than the surrounding soil, produces. In ground condition 1.1, the sandy medium gravel occurs as a 3m stratum to a depth of 5m, in ground condition 1.2 it occurs as a 1m stratum to 2m depth, and in ground condition 1.3, a 3.5m stratum to 12m depth. At 1m stand-off, the surface settlements of 1.1, 1.2 and 1.3 are 50mm, 60mm and 65mm, respectively.

The settlement of ground conditions 1.1, 2.1, 3.1 and 3.2 are given in Figure 5.11.7(a,b). This chart shows the effect of clay strata on vibration induced surface settlement. Ground conditions 1.1 and 1.2 are presented as examples of soil profiles that contain no clay layers. Ground condition 3.1 has a single clay layer, and 3.2 has two layers (see Table 5.8.3). Clay is assumed not to experience compaction related ground surface settlement during pile driving operations. The presence of clay layers (in these examples), is seen to significantly reduce surface settlement.

The effect of layer resolution (on ground condition 4.1) is demonstrated in Figure 5.11.8(a,b). The method of calculating settlement uses the static stress value at the mid-point of a given soil layer. Thus, in the example, where two soil types are present (in two layers), the static stresses at 5m and 15m are used in the settlement calculation, and a settlement of 20mm at 1m stand-off, is estimated. Dividing the soils into 2 equidimensional layers (i.e. 4 layers, and four stress values) produces a settlement value of 30mm at 1m distance, an increase of 50%. Increasing the layer resolution to 10 layers (2m per stratum) and 20 layers (1m per stratum), generates surface settlements of 65mm (an increase of 225%) and 85mm (an increase of 325%), respectively. The stand-off distance at which 1mm of settlement occurs for 2, 4, 10 and 20 layers is 5.75m, 6m, 8.2m and 8.7m, respectively.

The final example uses a 'worst case' scenario (ground condition 5.1), i.e. 20m of sandy gravel ($D_c = 15$), using a layer resolution of 1m, and relative density increasing from 0.1 (at 0.5m) to 1.0 at depth. The settlement profile is given in Figure 5.11.9(a,b). Also presented are the effects that ignoring the first 1m (ground condition 5.2) and 2m (ground condition 5.3) of soil has on the calculated surface settlement for the same ground condition. Ground condition 5.1 estimates approximately 250mm of settlement at a 1m stand-off, this value is reduced to 100mm and 55mm, for ground condition 5.2 and 5.3, respectively.

Figure 5.11.10(a,b) demonstrates the high acceleration settlement equation for ground condition 1.1, within a stand-off of 1m. The settlement profile assumes accelerations of 1.5*g*, 2.5*g*, 3.0*g* and 5.0*g* for stand-offs of 0.6m, 0.25m, 0.2m and 0.1m, respectively. The profile (which includes low acceleration settlement, shown in Figure 5.11.2(a,b)) assumes that the pile driving operation did not cause additional soil movements, such as localised soil 'plugging'.

5.7 Categories of Vibration Settlement.

The results of the vibratory tests, trend data, parameter identification, development of the vibration settlement equation and example applications allow the data to be grouped into categories of settlement *potential*, *risk* and *severity*. Such categories allow a convenient appreciation of surface settlement potential under a range of soil and piling conditions. Settlement risk to buildings is a function of deflection ratio/angular distortion and of building type. These parameters are not included in the definition of '*severity*' used here.

The settlement *potential* of a soil describes the relative magnitude of vibratory settlement response demonstrated under given conditions. Settlement potential is related to the distribution coefficient (D_c) of soils. For example, a sandy gravel (with a $D_c = 15$) will have greater settlement potential than a coarse uniform sand (which may have a $D_c = 2$), i.e. increase in D_c produces an increase in settlement potential. Note also that increasing values of the coefficient of uniformity (U_c) and/or maximum particle size, will similarly increase settlement potential. Table 5.9.1 suggests settlement potential categories.

Category number	Distribution coefficient (D_c)	Settlement Potential	Settlement (%) 1.0g	Settlement (%) 0.5g
1	< 2	very slight	~ 0.25	~ 0.01
2	2 - 5	slight	0.25 - 0.5	0.01 - 0.10
3	5 - 10	moderate	0.5 - 1.0	0.10 - 0.25
4	10 - 15	high	1.0 - 2.5	0.25 - 0.35
5	> 15	very high	>2.5	>0.35

Table 5.9.1. Categories of settlement potential based on distribution coefficient.

Risk Category	Acceleration (g)	Stand-off (m)	Risk
1	< 0.1	> 10	negligible
2	0.1 - 0.2	5 - 10	slight
3	0.2 - 0.5	2 - 5	possible
4	0.5 - 0.8	1 - 2	probable
5	0.8 - 1.5	1 - 0.5	definite
6	> 1.5	< 0.5	absolute

Table 5.9.2 Categories of settlement risk.

Settlement *risk* describes the influence of site conditions upon the potential of ground surface settlement. The site conditions are related to the soil profile and piling activities. For example, settlement risk decreases with increasing relative density, static stress and stand-off distance (i.e. attenuation of acceleration). A soil with a distribution coefficient of 10 (*high* settlement potential) is at more risk of settlement induced by vibropiling activity at a depth of 1m and a stand-off of 1m than the same soil at 10m depth and stand-off.

A soil with a high settlement potential under a highly likely risk of settlement (adjacent to pile driving activities) may be moved into a lower risk category if the soil unit is partially saturated or dry, or has been surcharged. More specifically, with consideration of settlement data and vibration magnitude, settlement *severity* may be described. If a surface settlement of less than 1mm is described as '*negligible*', then granular soil beyond a stand-off distance of 10m is not at risk from vibration induced ground surface settlement. Assuming radial symmetry, the soil at a depth of 10m below the pile base will not suffer appreciable settlement (especially if the influence of increasing relative density and static stress is considered).

Settlement category	Settlement (mm)	Stand-off distance (m)	Settlement severity
1	< 1	> 10	negligible
2	1 - 3	5 - 10	slight
3	3 - 10	2 - 5	moderate
4	10 - 50	1 - 2	significant
5	50 - 100	1 - 0.5	severe
6	> 100	< 0.5	very severe

Table 5.9.3. Categories of surface settlement severity.

		Distribution Coefficient, *Dc* (Uniformity Coefficient, *Uc*)				
Accel. (*g*)	Stand-off (m)	< 2 (1)	2 - 5 (1 - 2)	5 - 10 (2 - 5)	10 - 15 (5 - 10)	> 15 (> 10)
<0.1	>10	1	1	1	1	2
0.1-0.2	5-10	1	1	2	2	3
0.2-0.5	2-5	1	2	3	3	4
0.5-0.8	1-2	2	3	4	5	5
0.8-1.5	1-0.5	3	4	5	5	6
>1.5	<0.5	5	6	6	6	6

Table 5.9.4. Estimating settlement magnitude *severity* (Table 5.9.3), based on *potential* (Table 5.9.1) and *risk* (Table 5.9.2). For a saturated, 'green-field' site.

A surface settlement between 1mm-3mm, which may be described as '*slight*' tends to occur at a stand-off distance of approximately 10m-5m, and corresponds to ground vibrations between 0.1*g*-0.2*g*. '*Moderate*' surface settlement of between 3mm-

10mm is seen to occur for stand-offs between 5m-2m, and corresponds to accelerations of $0.2g$-$0.5g$. The term '*significant*' surface settlement may be described as settlement in the order of 10mm-50mm and is seen to occur at 1m-2m stand-off distance, and corresponds to ground vibrations of $0.5g$-$0.8g$ '*Severe*' settlement (50-100mm) is seen to occur at 100-50cms stand-off, and under vibrations of 0.8-$1.5g$ ($\pm 0.1g$). '*Very severe*' describes settlement of greater than 100mm, at stand-off of less than 50cms and vibrations greater than $1.5g$.

When the presence of clay layers, depth of the water table and presence of surcharge is considered, the above relationship between stand-off distance and surface settlement is less well defined. However the categories of settlement severity (i.e., '*negligible*', '*slight*', '*moderate*', '*significant*' and '*severe*') will still apply.

		Distribution Coefficient, *Dc* (Uniformity Coefficient, *Uc*)				
Accel. (g)	Stand-off (m)	< 2 (1)	2 - 5 (1 - 2)	5 - 10 (2 - 5)	10 - 15 (5 - 10)	> 15 (> 10)
<0.1	>10	1	1	1	1	1
0.1-0.2	5-10	1	1	1	1	2
0.2-0.5	2-5	1	1	2	2	3
0.5-0.8	1-2	1	2	3	4	4
0.8-1.5	1-0.5	2	3	4	4	5
>1.5	<0.5	4	5	5	5	5

Table 5.9.5. Modification of Table 5.9.4, accounting for variations in ground conditions such as dry soil, clay layer(s) and surcharge.

5.8 Summary

The vibratory settlement data enabled a number of settlement trends to be identified, which ultimately enabled an equation to be derived. This equation allows the estimation of ground surface settlement under a range of conditions such as; soil type, relative density, overburden and acceleration magnitude. For accelerations up to and including $1g$, the proposed equation to estimate the settlement of a discrete soil layer is:

$$S_{v\,\max} = \frac{2.8\ln(D_c)g^2}{D_r\sigma_v}$$

Where:

S_{vmax} = maximum estimated settlement of a discrete soil layer (%)

D_c = distribution coefficient

g = acceleration in gravitation units

D_r = relative density

σ_v = static stress (kPa)

For accelerations above 1.0g the relationhip becomes:

$$S_{v\,max} = \frac{4(\ln(U_c) + 0.7).\ln(g)}{0.01(\sigma_v) + 0.75.(1 - D_r)}$$

With consideration of vibration time length, operating frequency and moisture state, the following expression is proposed:

$$S_v = \ln(t).\frac{S_{v\,max}}{\ln(t_{max})}.\frac{1}{f'}.m$$

where:

S_v = estimated settlement (%)

$\frac{S_{v\,max}}{\ln(t_{max})}$ = slope of the log plot

t_{max} = duration of laboratory vibration test increment (minutes)

t = duration of ground vibration (minutes)

f' = ratio of the vibrodriver frequency to laboratory test frequency (Hz)

m = a function of saturation. Where

Sr = 1, m = 1

Sr = 0, m = 0.06

$0 < Sr > 1$, m = 0.01

The site investigation data may not always include all the data that is necessary to perform settlement calculations. If this occurs, then values have to be assumed. For example, if the vibration data is absent, the settlement severity summary table may be consulted (Section 5.10, Table 5.9.4), where typical values of acceleration with stand-off distance are presented, and may be used. If soil specific data is absent and the soils are only described as 'sandy', or a range of sands are anticipated, then using a distribution coefficient (D_c) of 7.5 is suggested. However, if slightly more information is available, such as 'uniform sands' and 'gravelly sands' then D_c values of 2 and 12, respectively are recommended. If relative density values (or SPT-N values) are unknown, then a value of 0.4 may be used. Note that the effects of increase in static load with depth will tend to be more significant than variations in relative density, so using a particular value of relative density is not critical (and values of 0.3 or 0.5 may be considered). Finally, a flow diagram that demonstrates the use of the vibratory settlement equation(s) during the construction process is given below:

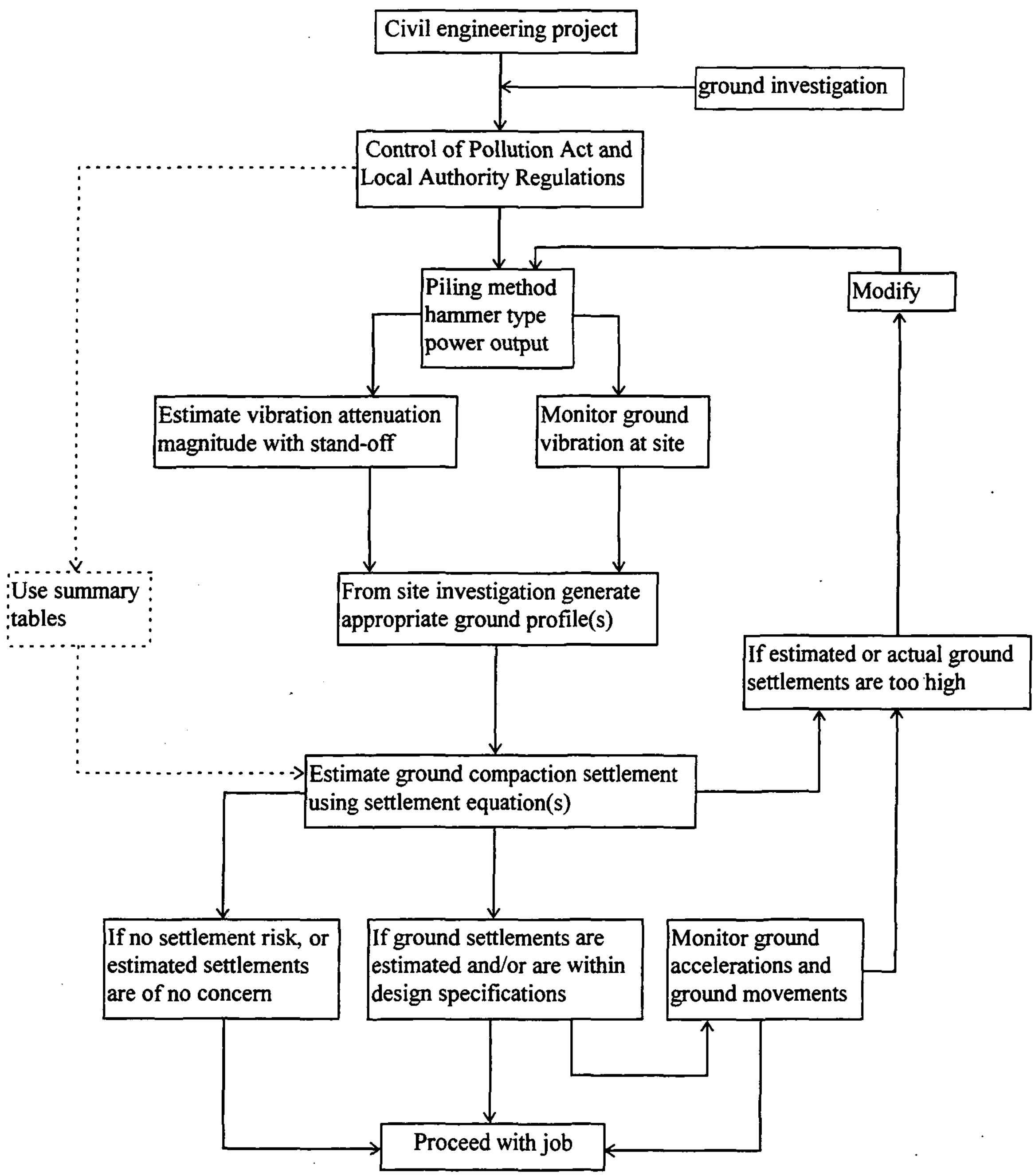

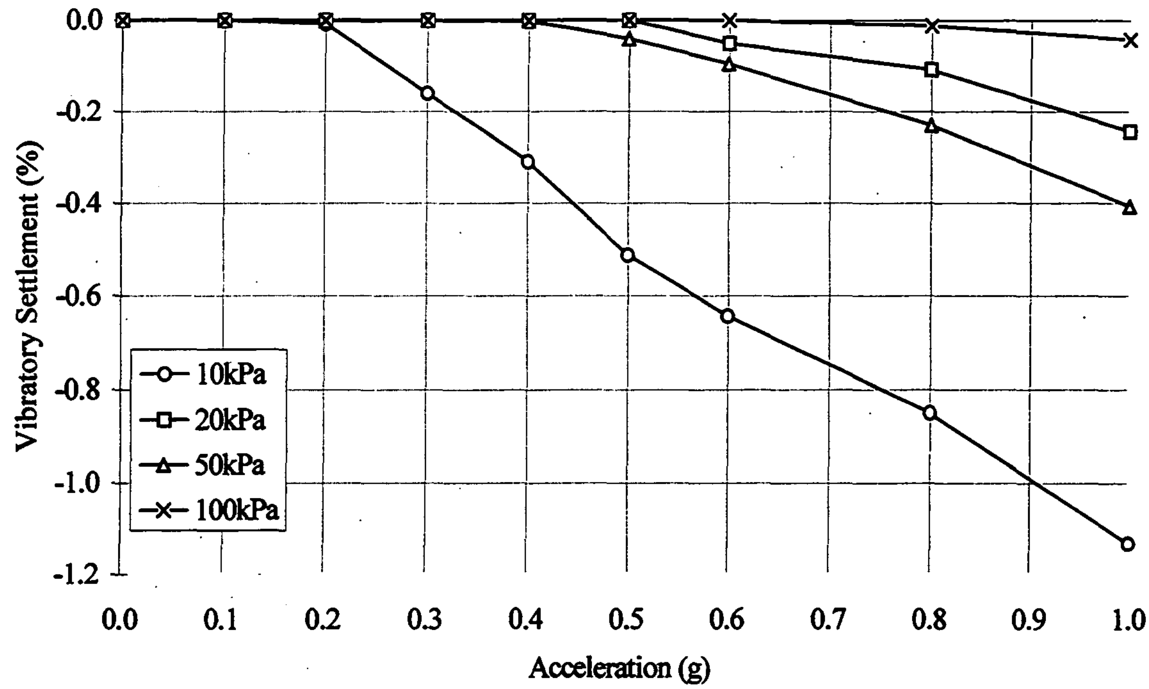

Figure 5.1.1a. Silty fine sand vibration test settlement results. Saturated, at 25Hz (see Appendix 3: Table A3.1.1, for test data sheet).

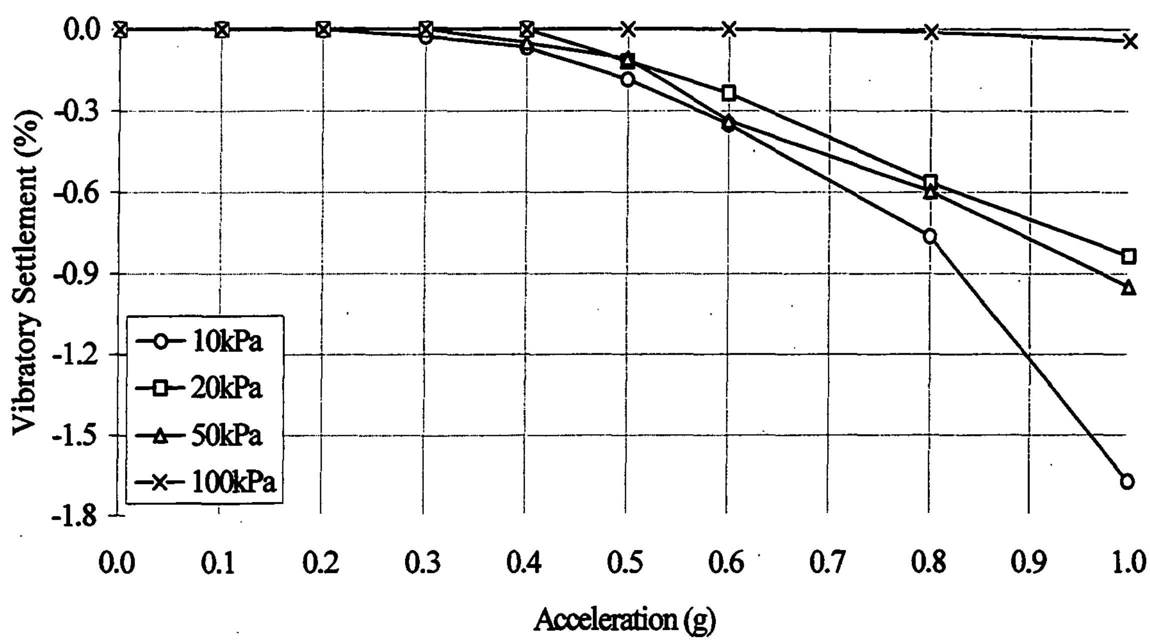

Figure 5.1.1b. Silty fine sand vibration test settlement results. Saturated, at 40Hz (see Appendix 3: Table A3.1.2, for test data sheet).

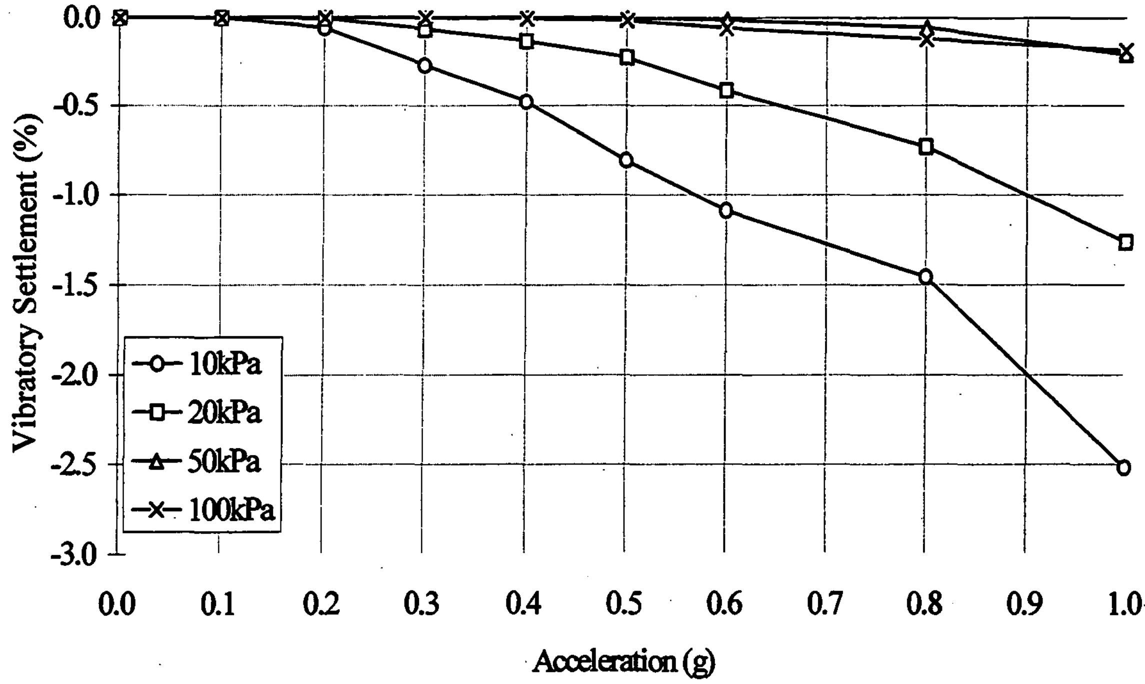

Figure 5.1.2a. Fine uniform sand vibration test settlement results. Saturated, at 25Hz (see Appendix 3: Table A3.2.1, for test data sheet).

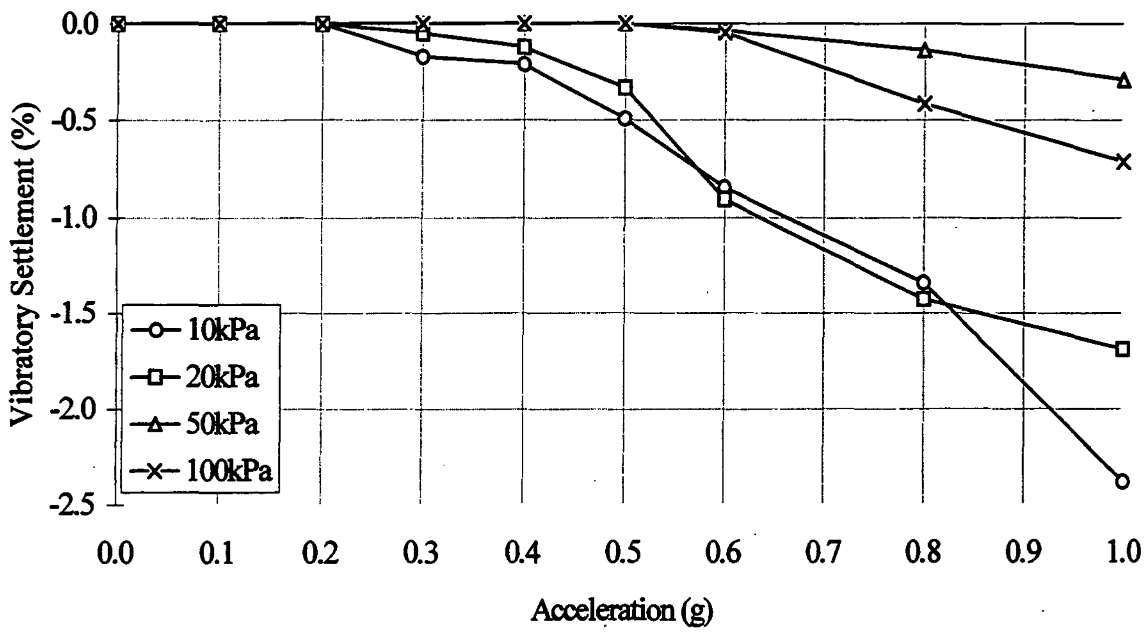

Figure 5.1.2b. Fine uniform sand vibration test settlement results. Saturated, at 40Hz (see Appendix 3: Table A3.2.2, for test data sheet).

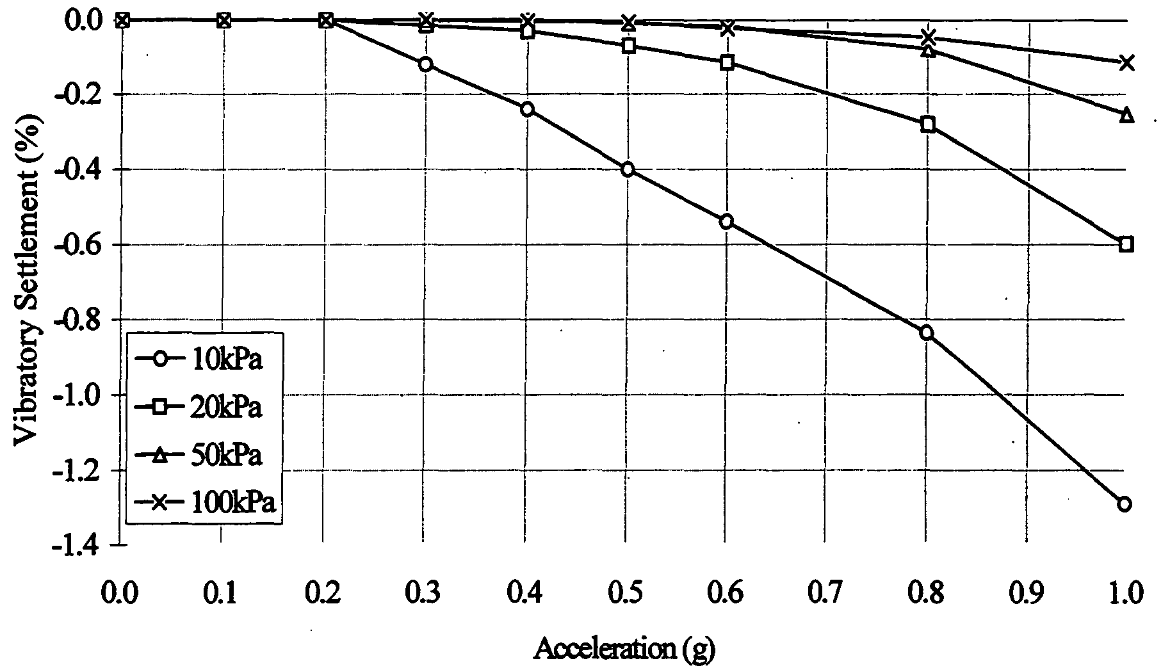

Figure 5.1.3a. Garside medium sand vibration test settlement results. Saturated, at 25Hz (see Appendix 3: Table A3.3.1, for test data sheet).

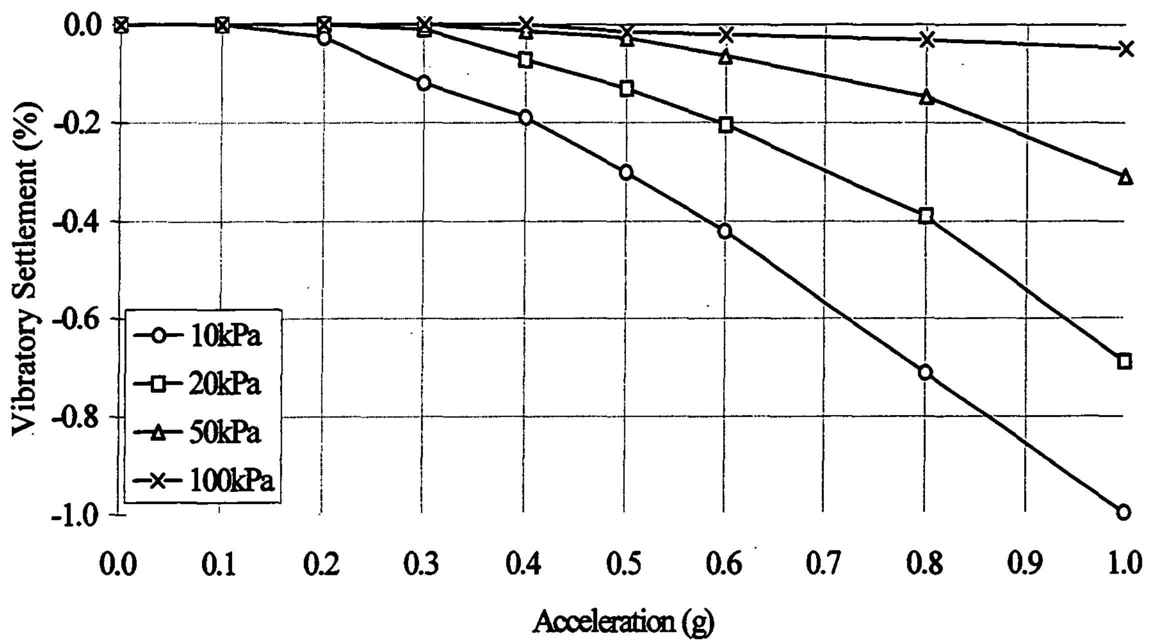

Figure 5.1.3b. Garside medium sand vibration test settlement results. Saturated, at 40Hz (see Appendix 3: Table 3.3.2, for test data sheet).

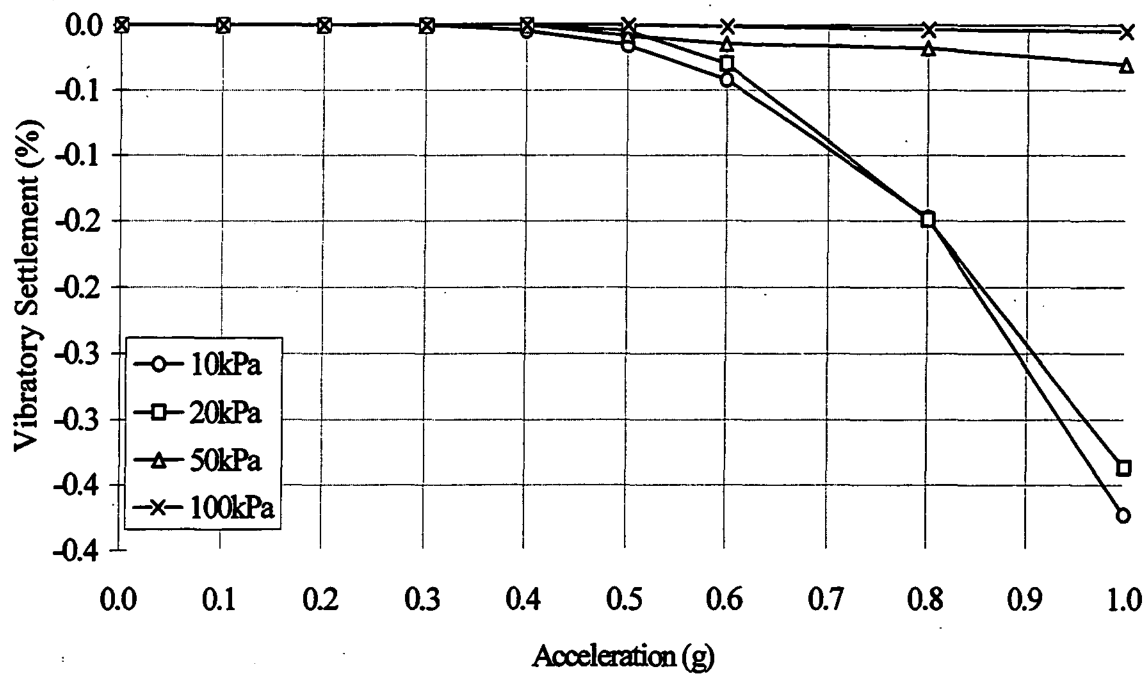

Figure 5.1.4a. Medium uniform sand vibration test settlement results. Saturated, at 25Hz (see Appendix 3: Table A3.4.1, for test data sheet).

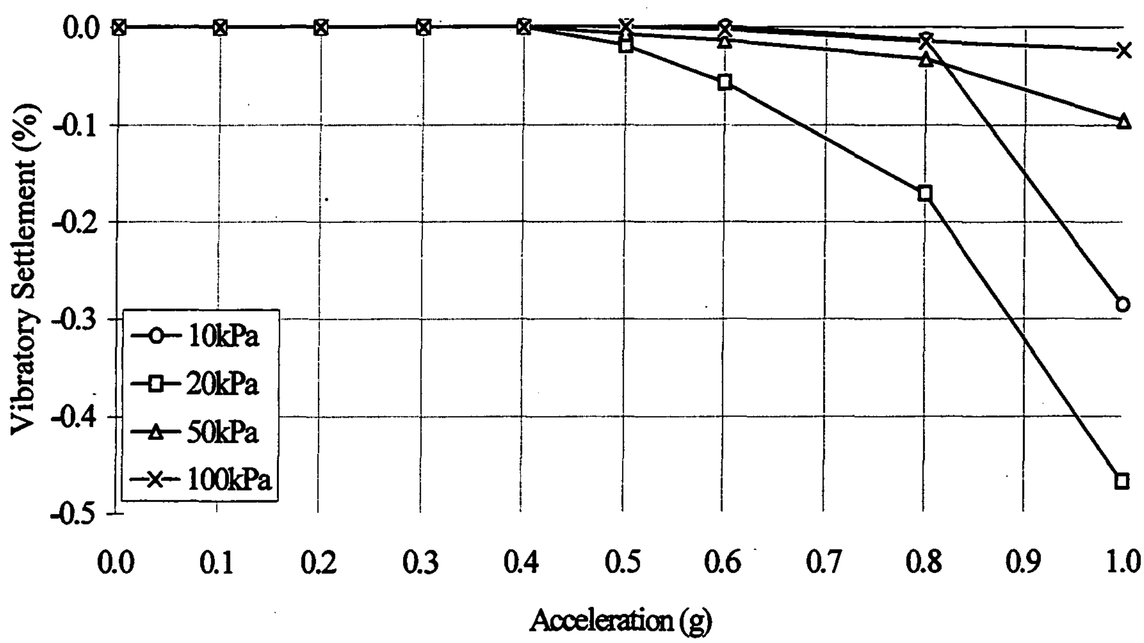

Figure 5.1.4b. Medium uniform sand vibration test settlement results. Saturated, at 40Hz (see Appendix 3: Table A3.4.2, for test data sheet).

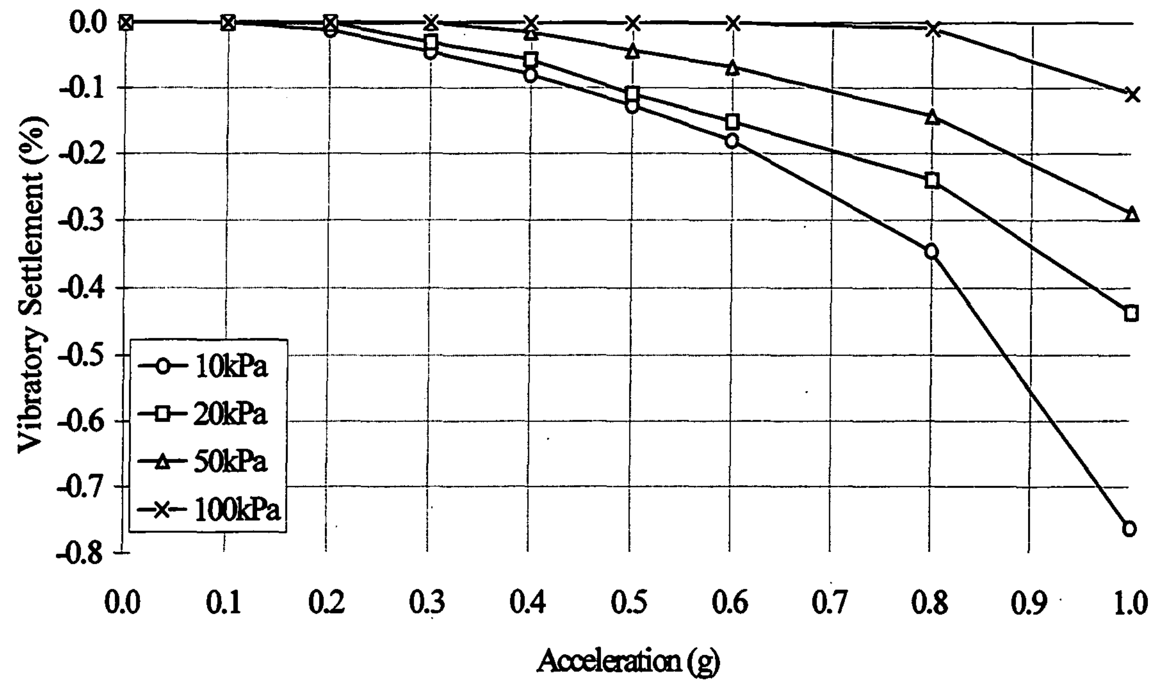

Figure 5.1.5a. Medium Leighton Buzzard sand vibration test settlement results. Saturated, at 25Hz (see Appendix 3: Table A3.5.1, for test data sheet).

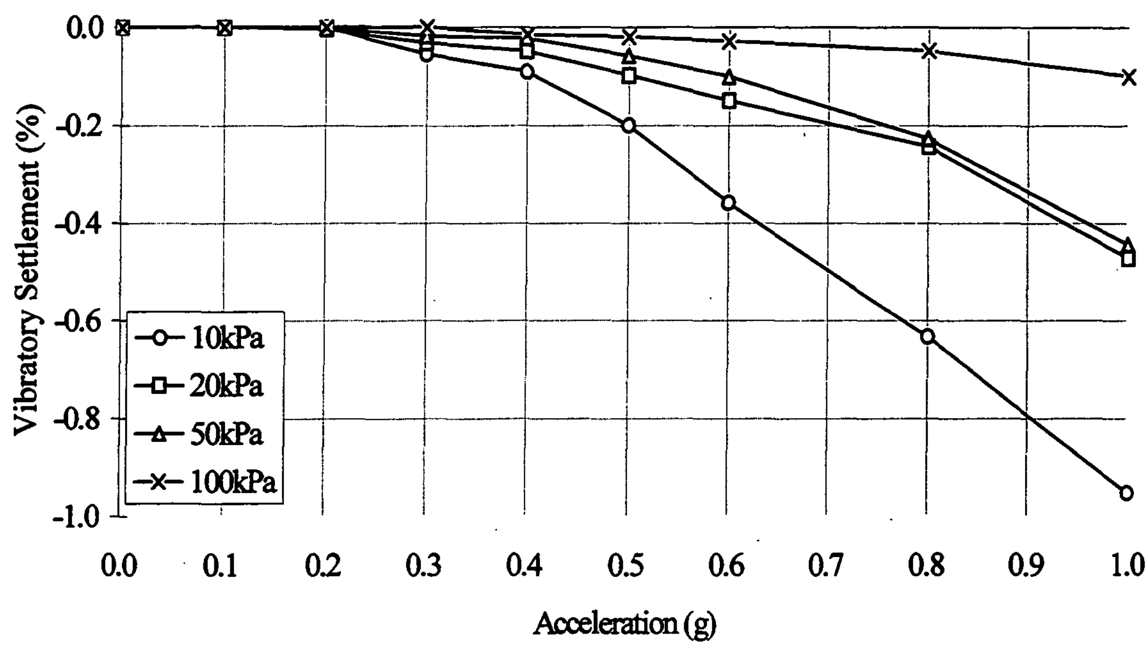

Figure 5.1.5b. Medium Leighton Buzzard sand vibration test settlement results. Saturated, at 40Hz (see Appendix 3: Table A3.5.2, for test data sheet).

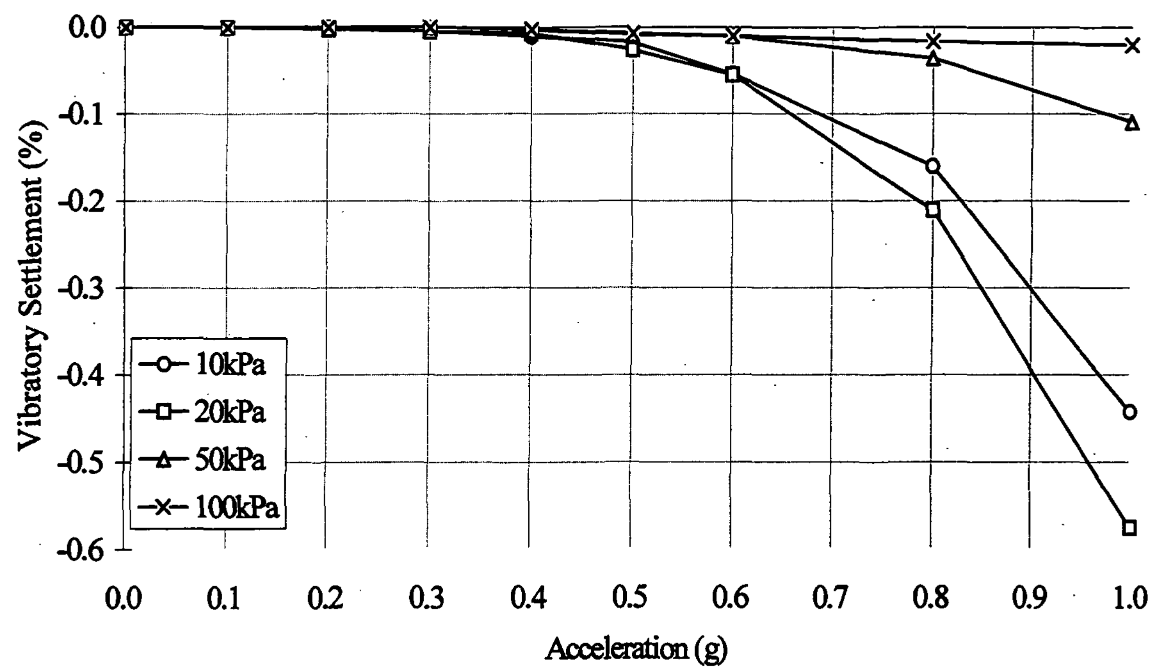

Figure 5.1.6a. Coarse Leighton Buzzard sand vibration test settlement results.
Saturated, at 25Hz (see Appendix 3: Table A3.6.1, for test data sheet).

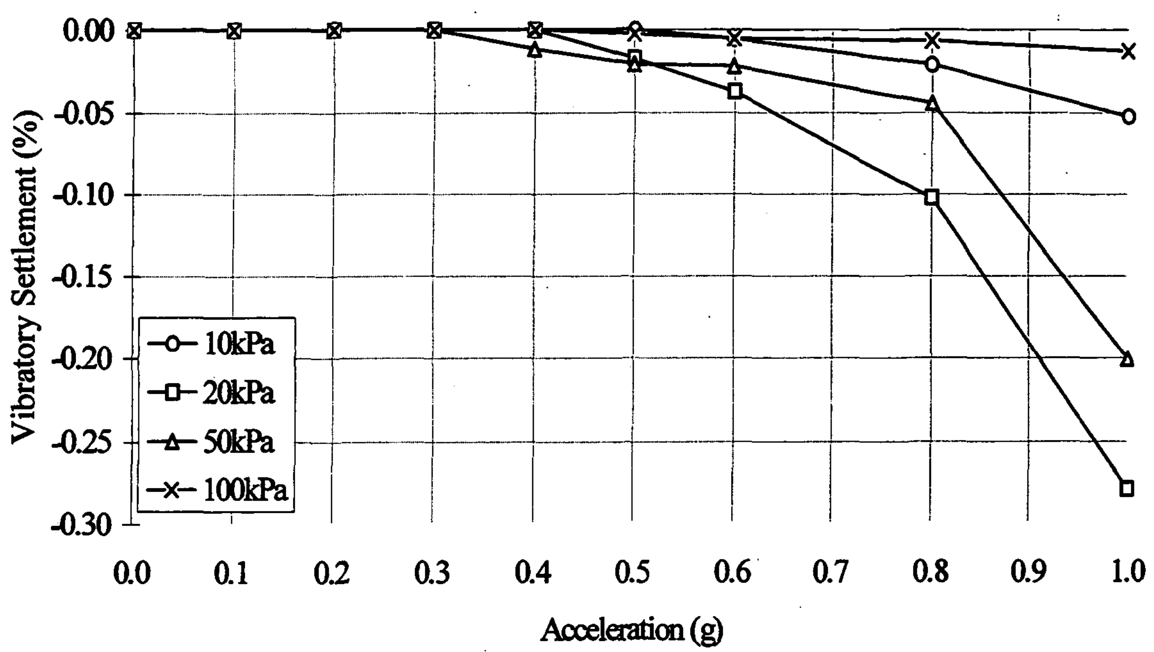

Figure 5.1.6b. Coarse Leighton Buzzard sand vibration test settlement results.
Saturated, at 40Hz (see Appendix 3: Table A3.6.2, for test data sheet).

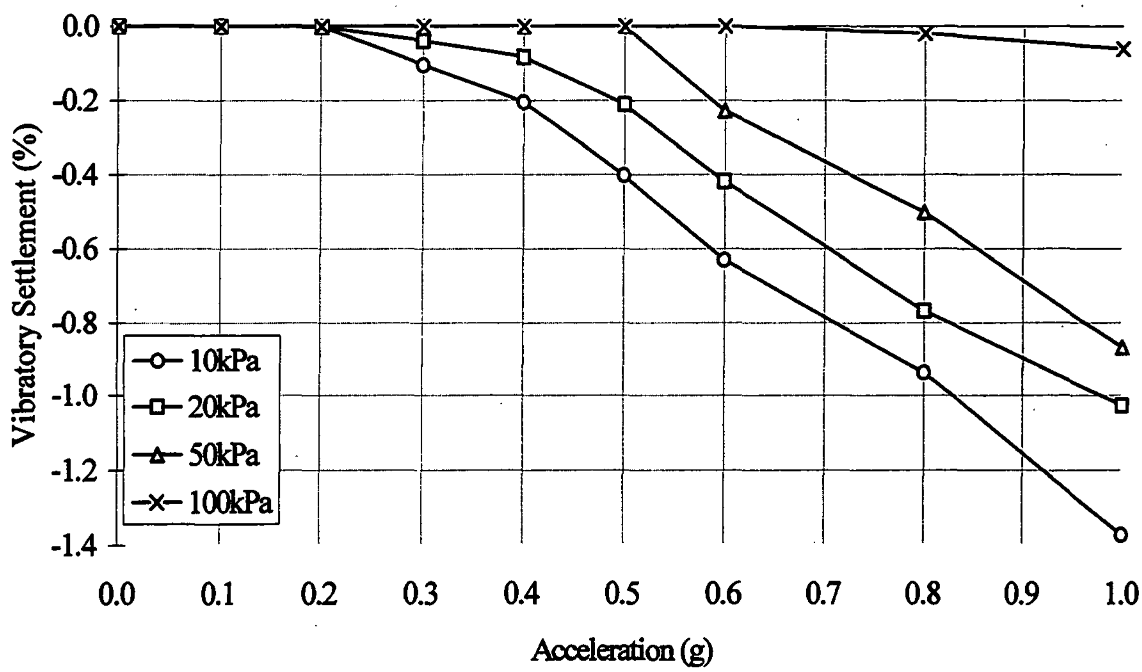

Figure 5.1.7a. Medium sharp sand vibration test settlement results. Saturated, at 25Hz (see Appendix 3: Table A3.7.1, for test data sheet).

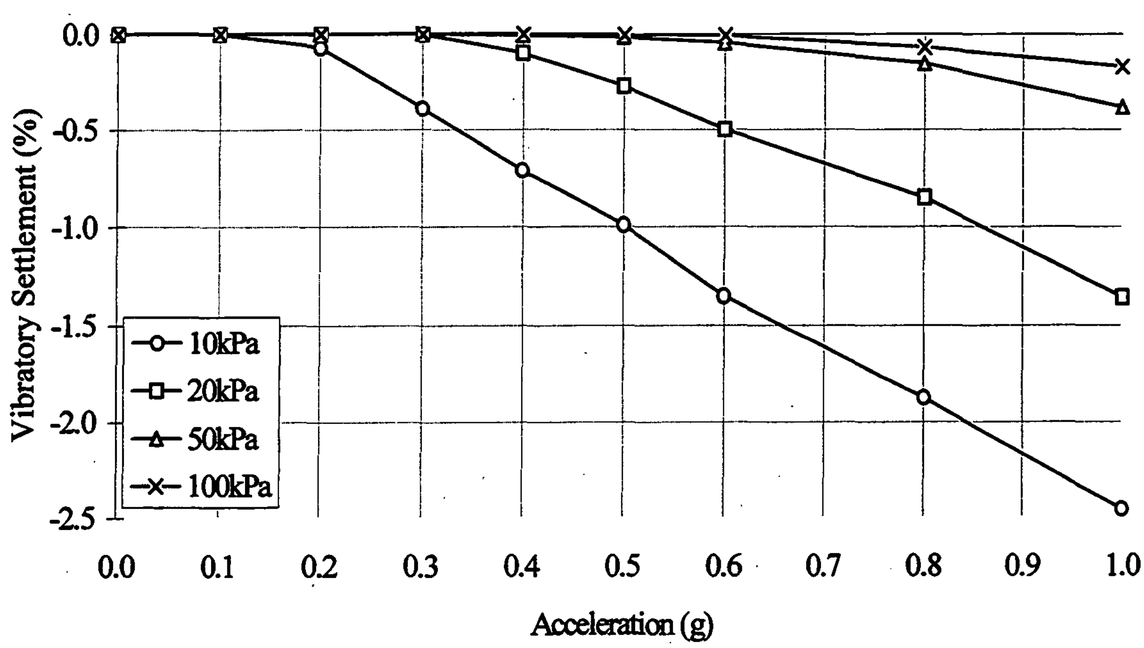

Figure 5.1.7b. Medium sharp sand vibration test settlement results. Saturated, at 40Hz (see Appendix 3: Table A3.7.2, for test data sheet).

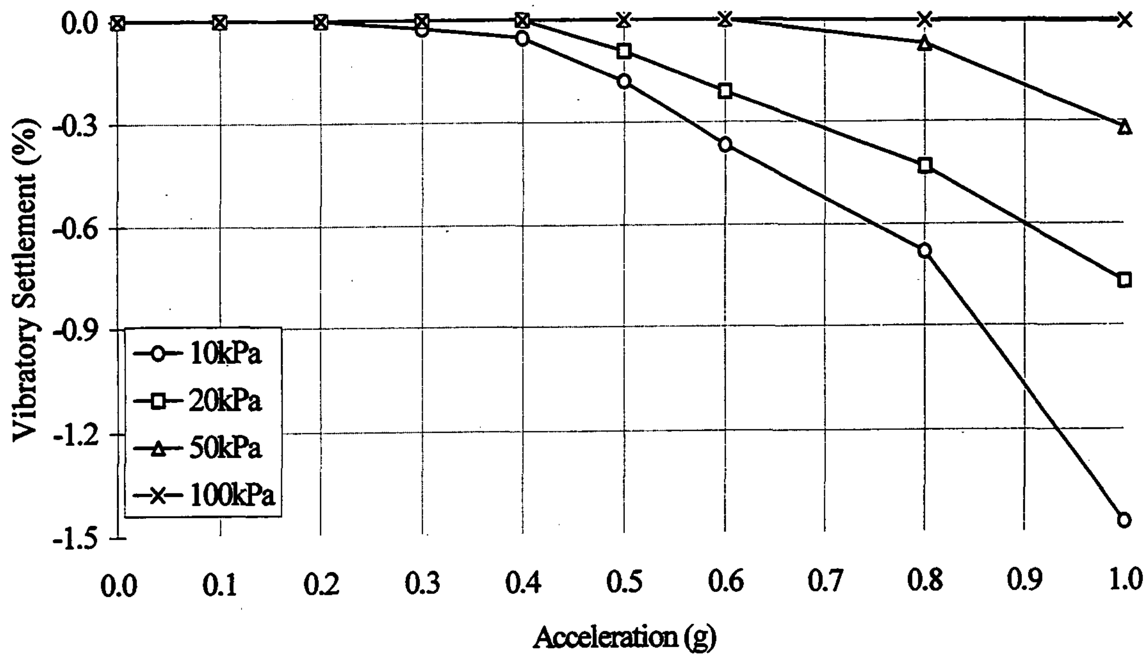

Figure 5.1.8a. Sandy fine gravel vibration test settlement results. Saturated, at 25Hz (see Appendix 3: Table A3.10.1, for test data sheet).

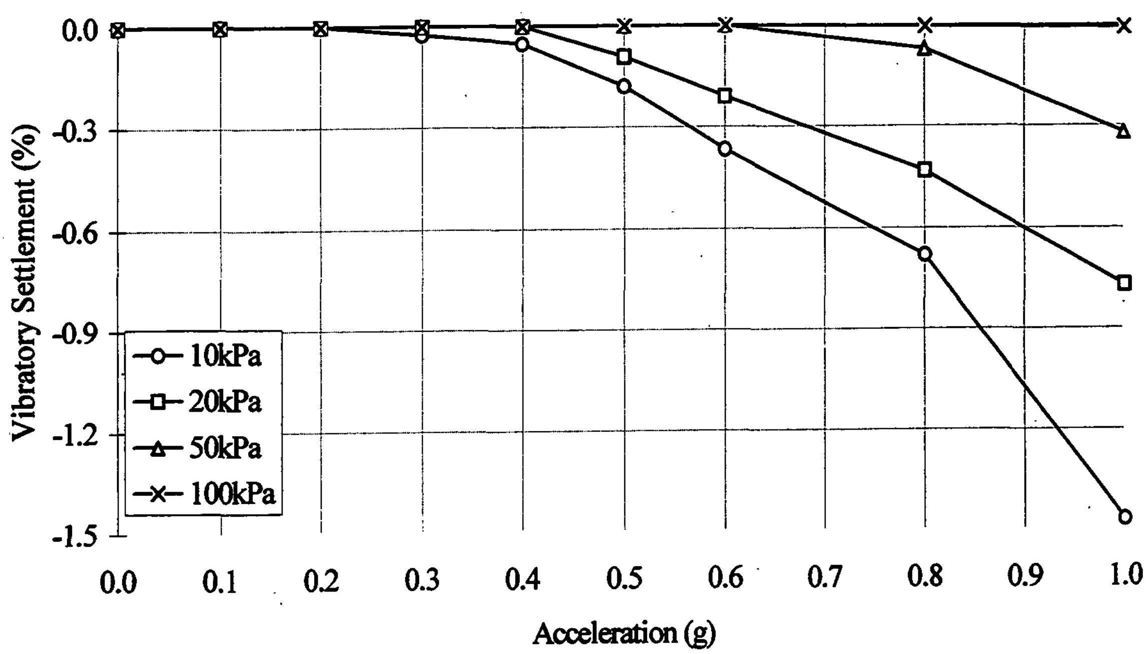

Figure 5.1.8b. Sandy fine gravel vibration test settlement results. Saturated, at 40Hz (see Appendix 3: Table A3.10.2, for test data sheet).

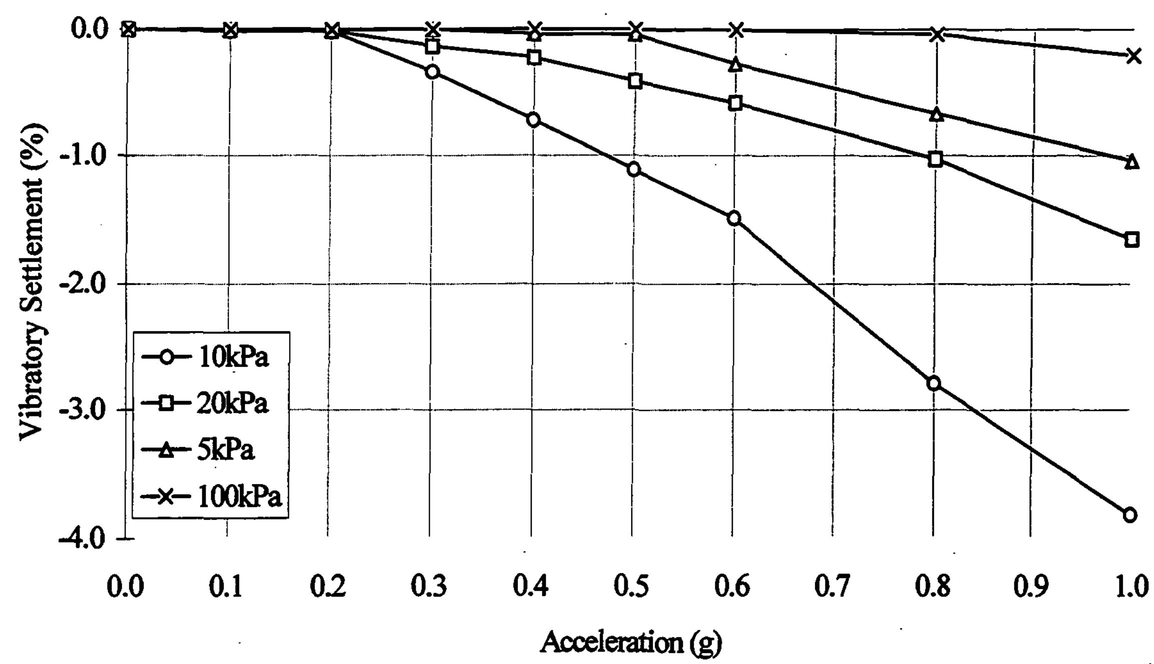

Figure 5.1.9a. Sandy fine to medium gravel vibration test settlement results. Saturated, at 25Hz. (see Appendix 3: Table A3.11.1, for test data sheet).

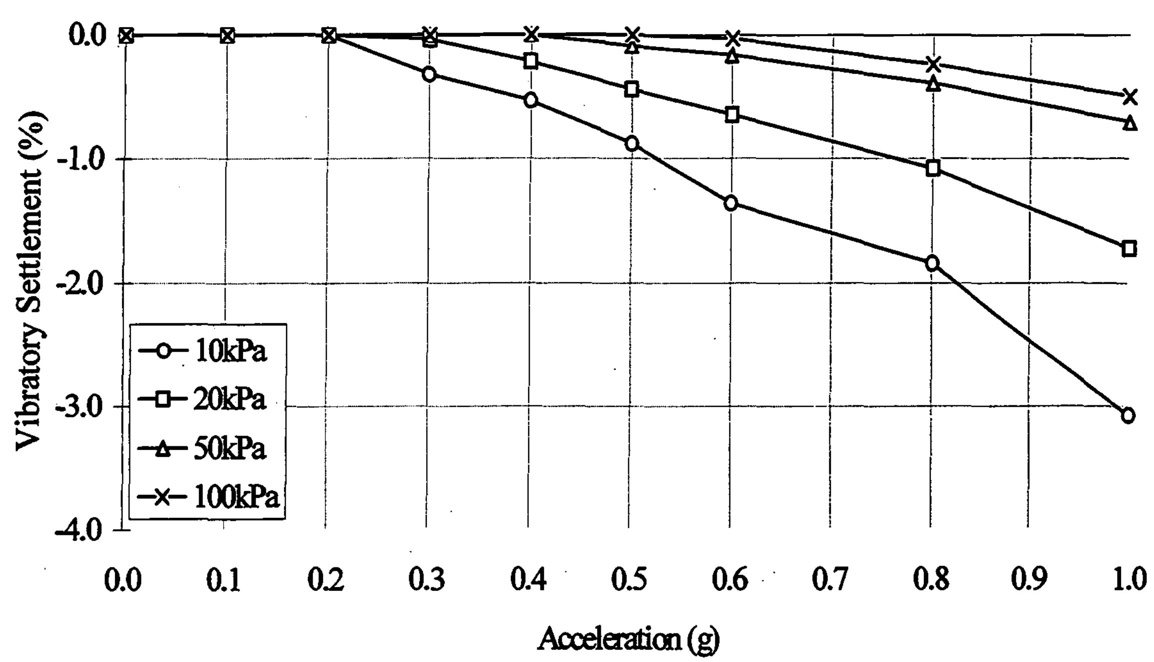

Figure 5.1.9b. Sandy fine to medium gravel vibration test settlement results. Saturated, at 40Hz (see Appendix 3: Table 3.11.2, for test data sheet).

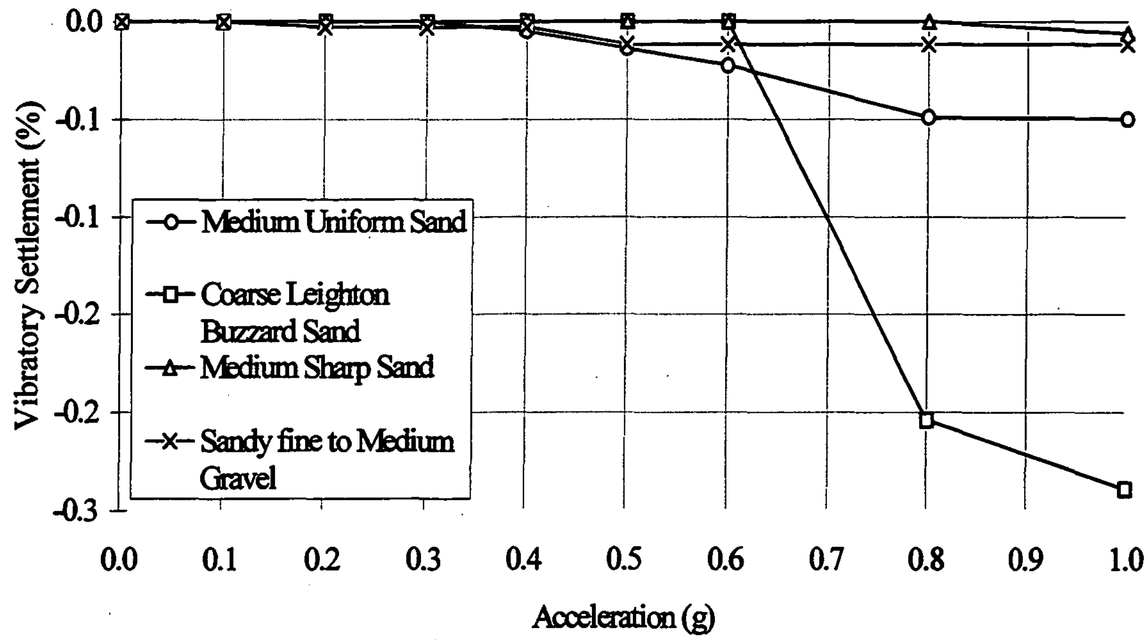

Figure 5.2.1. Dried vibration test settlement results, at 25Hz and 10kPa (see Appendix 3: Table A3.4.4; A3.6.3; A3.7.4; A3.11.5 for test data sheet).

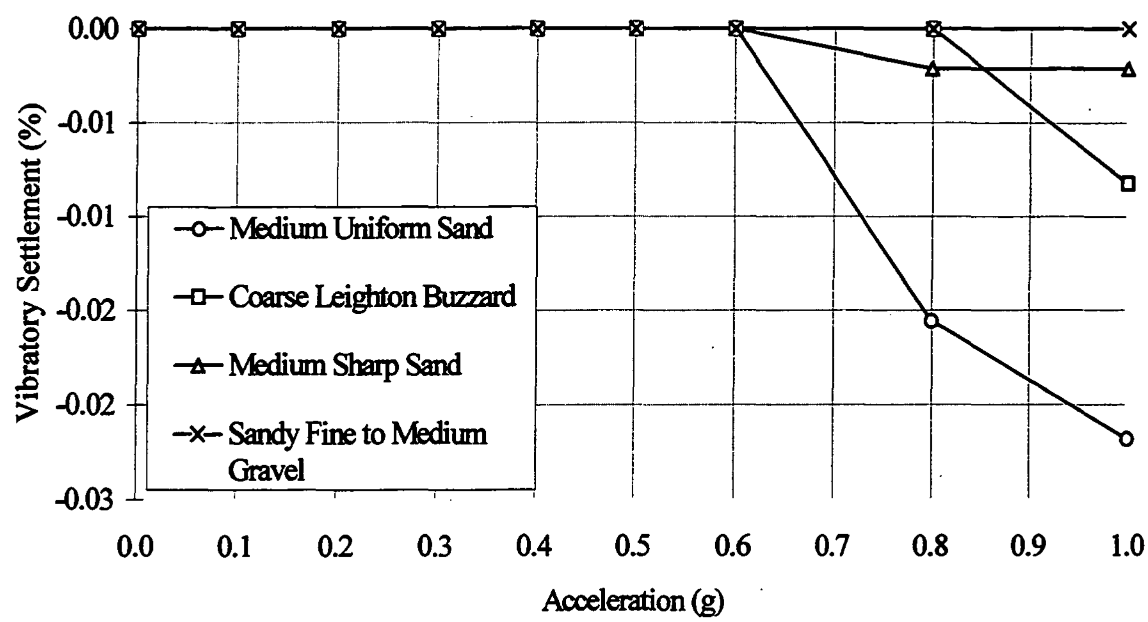

Figure 5.2.2. Partially saturated vibration test settlement results, at 25Hz and 10kPa (see Appendix 3: Table A3.4.3; A3.6.4; A3.7.3, A3.11.6 for test data sheet).

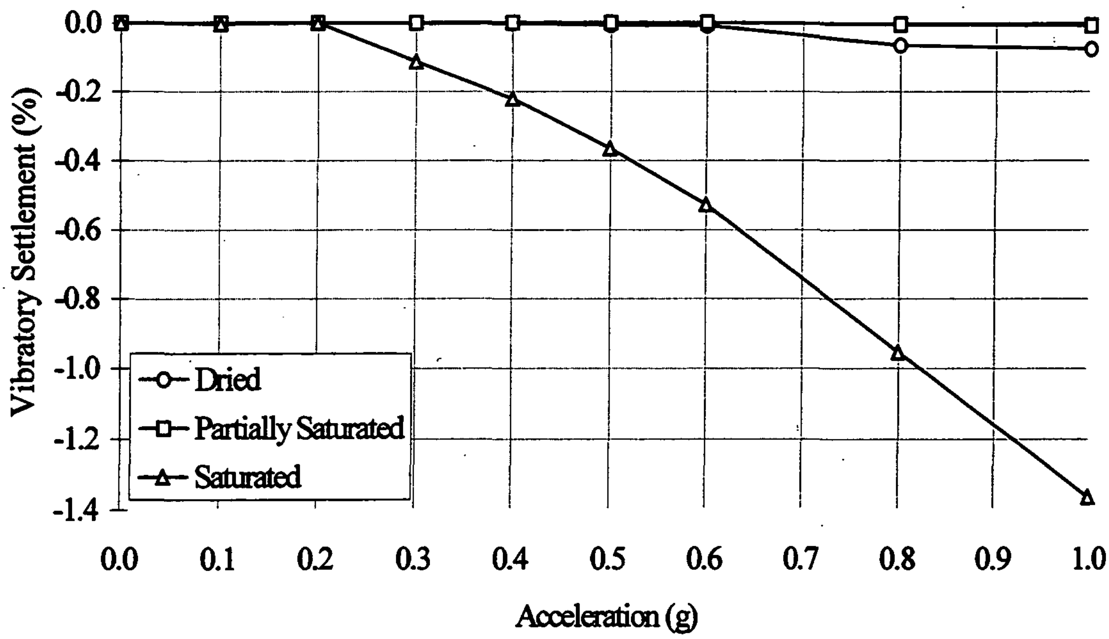

Figure 5.2.3. General comparison of saturated, partially saturated and dried vibration test results (using mean stress values, 25Hz, 10kPa).

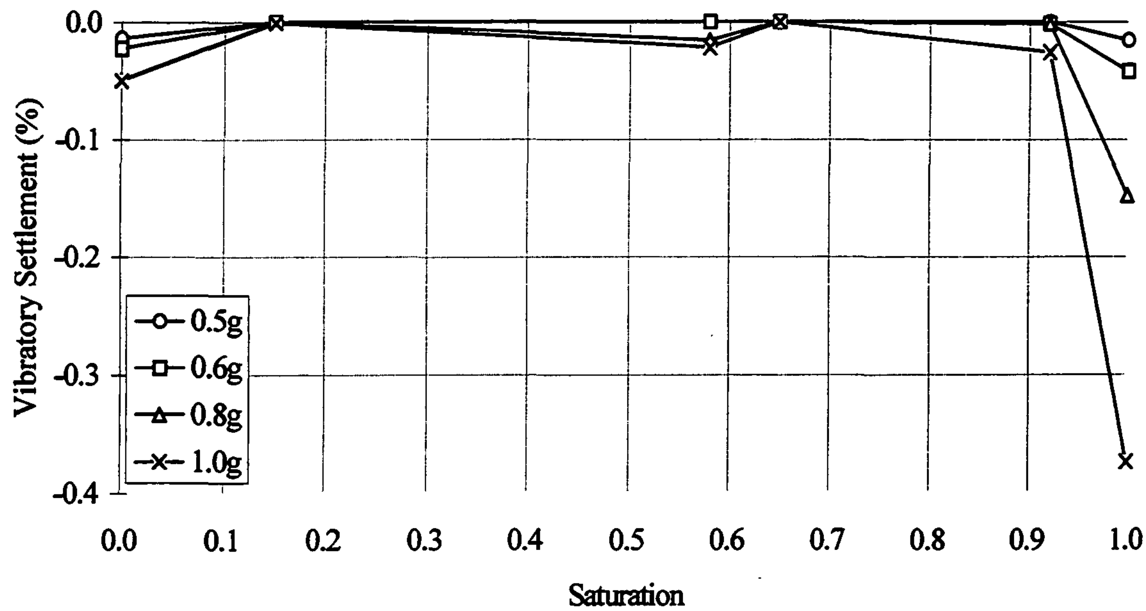

Figure 5.2.4. Influence of degree of saturation on medium uniform sand vibration test settlement results (25Hz, 10kPa) (see Appendix A3.4.3, for test data sheet).

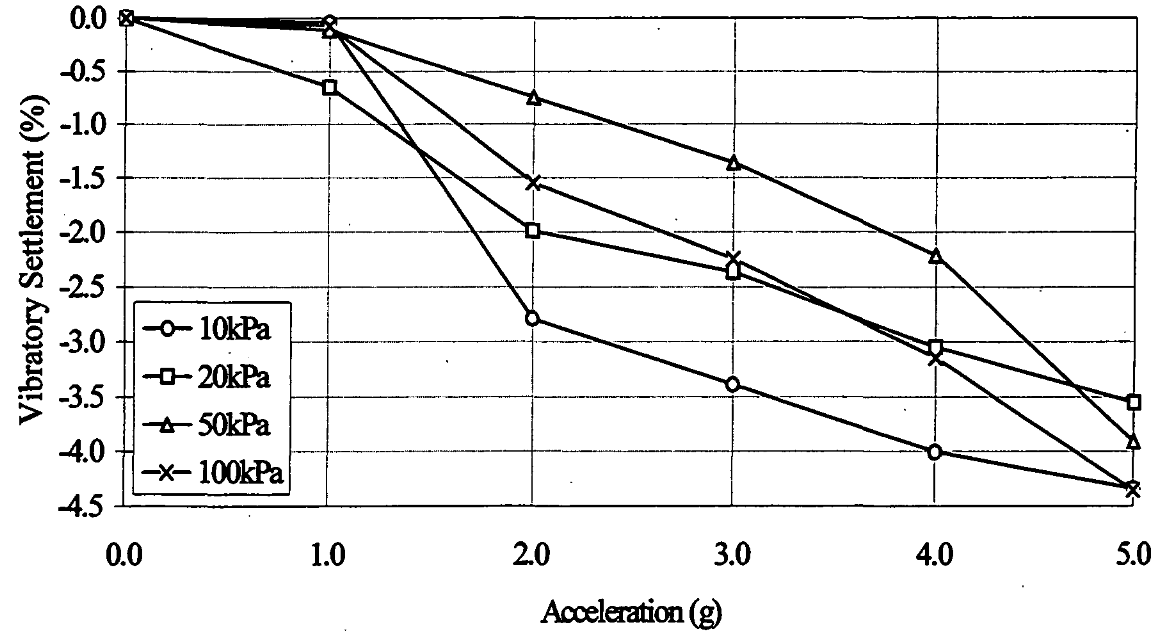

Figure 5.3.1. Silty fine sand, high acceleration vibration test settlement results. Saturated, at 25Hz (see Appendix 3: Table A3.1.3, for test data sheet).

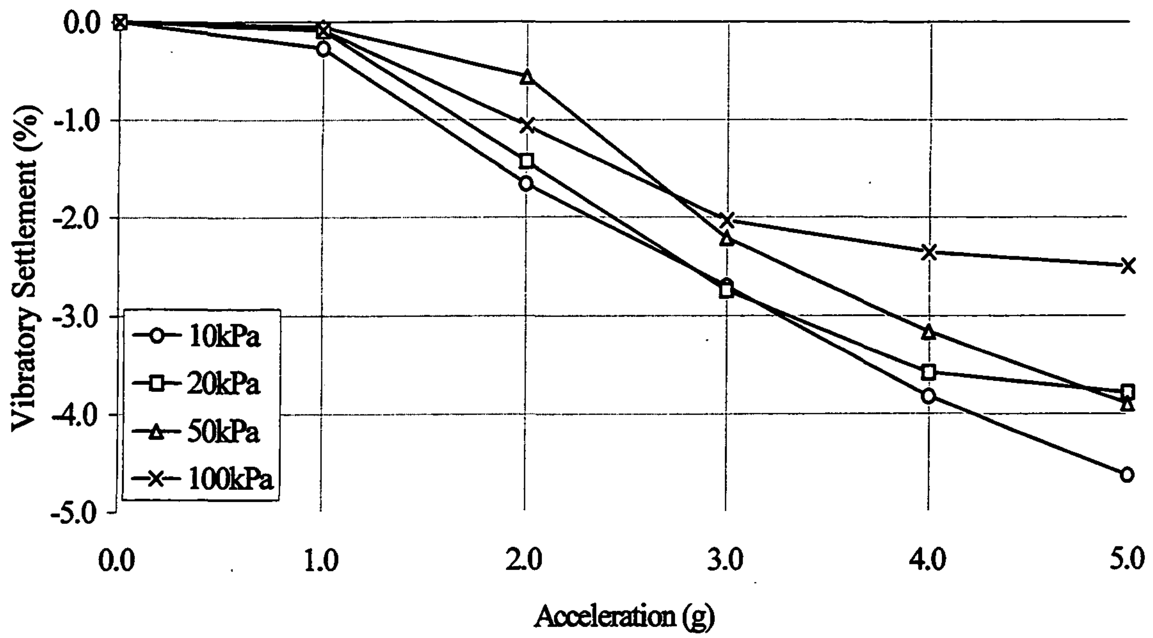

Figure 5.3.2. Fine uniform sand, high acceleration vibration test settlement results. Saturated, at 25Hz (see Appendix 3: Table A3.2.3, for test data sheet).

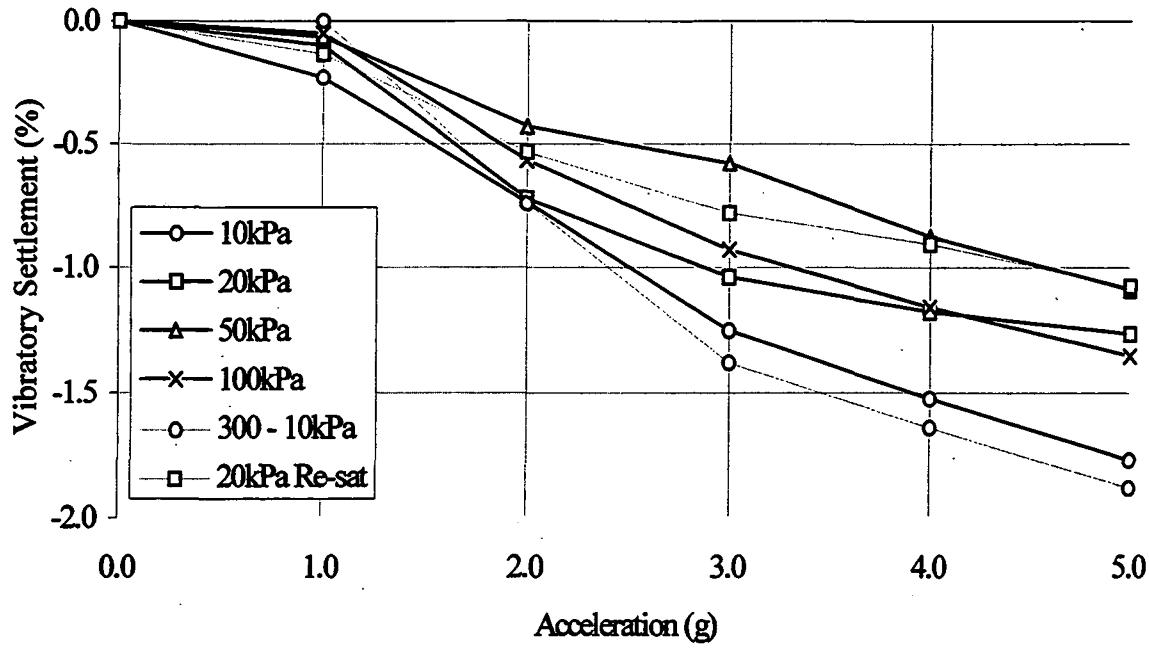

Figure 5.3.3. Garside medium sand, high acceleration vibration test settlement results. Saturated, at 25Hz (see Appendix 3: A3.3.3, for test data sheet).

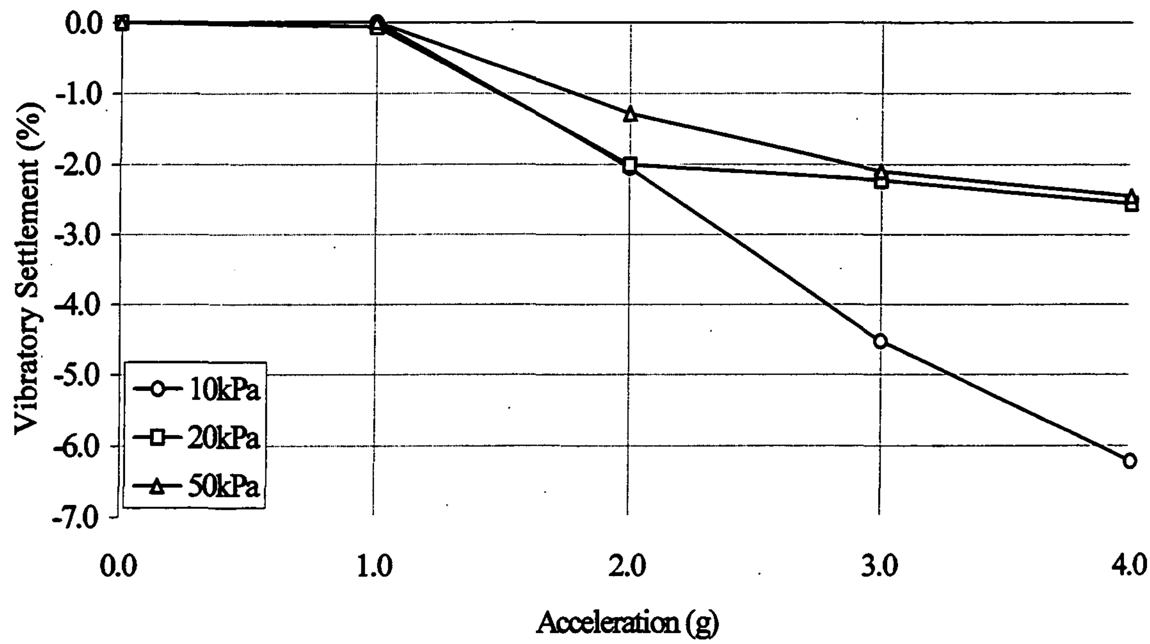

Figure 5.3.4. Medium uniform sand, high acceleration test settlement results. Saturated, at 25Hz (see Appendix 3: Table A3.4.5, for test data sheet).

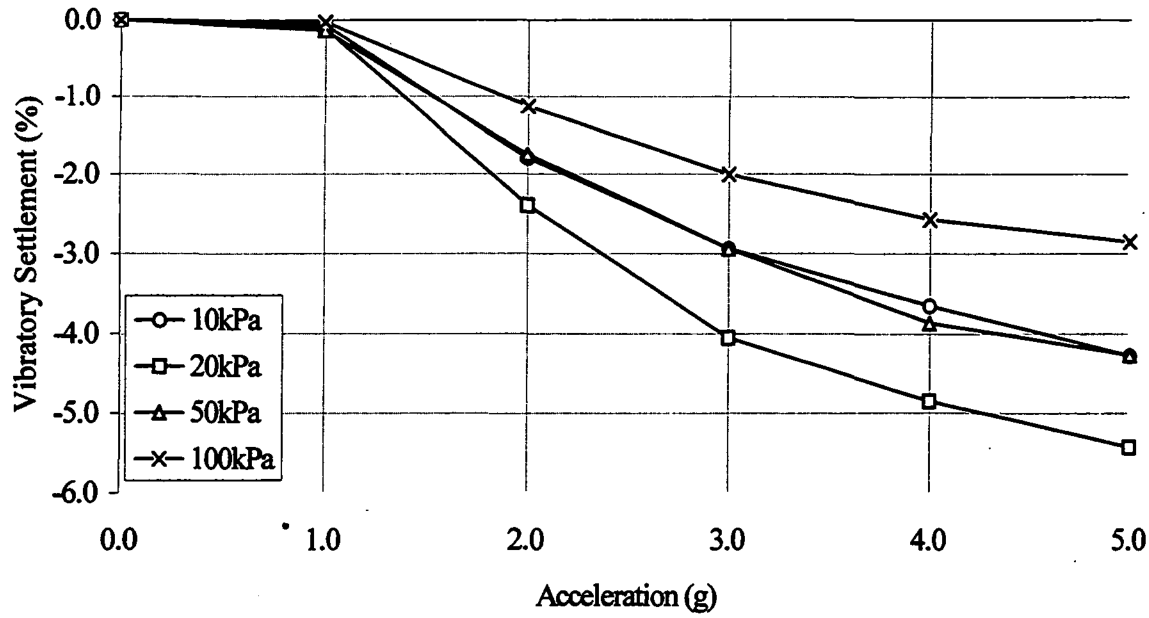

Figure 5.3.5. Medium Leighton Buzzard sand, high acceleration vibration test settlement results. Saturated, at 25Hz (see Appendix 3: Table A3.5.4, for test data sheet).

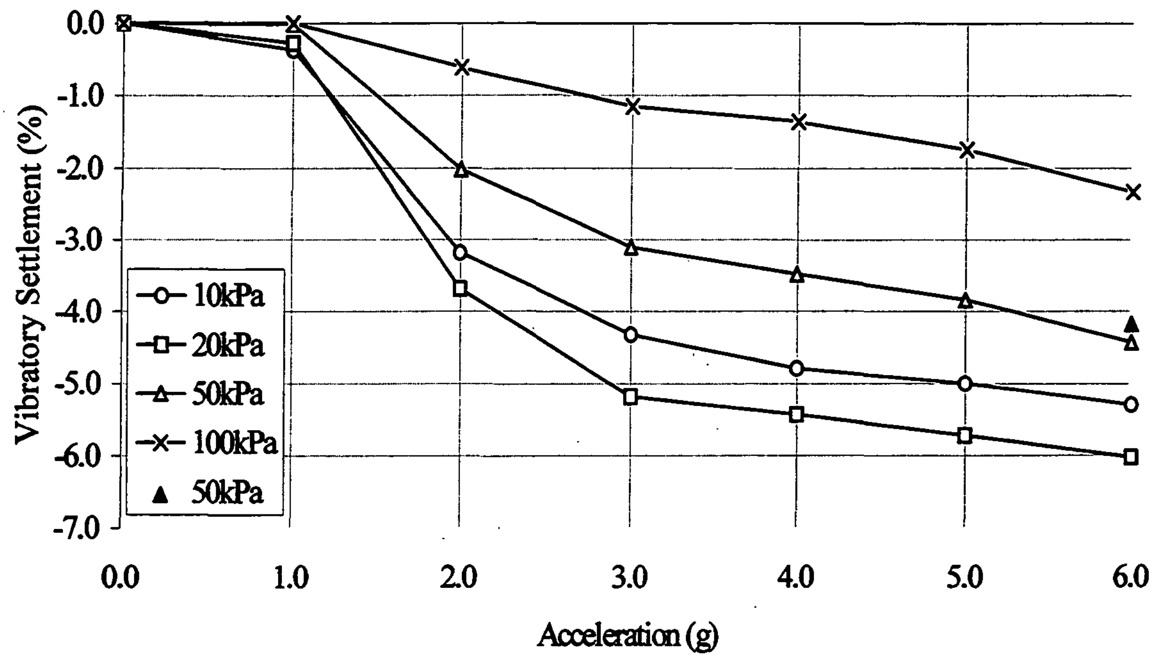

Figure 5.3.6. Coarse Leighton Buzzard sand, high acceleration vibration test settlement results. Saturated, at 25Hz (see Appendix 3: Table A3.6.5, for test data sheet).

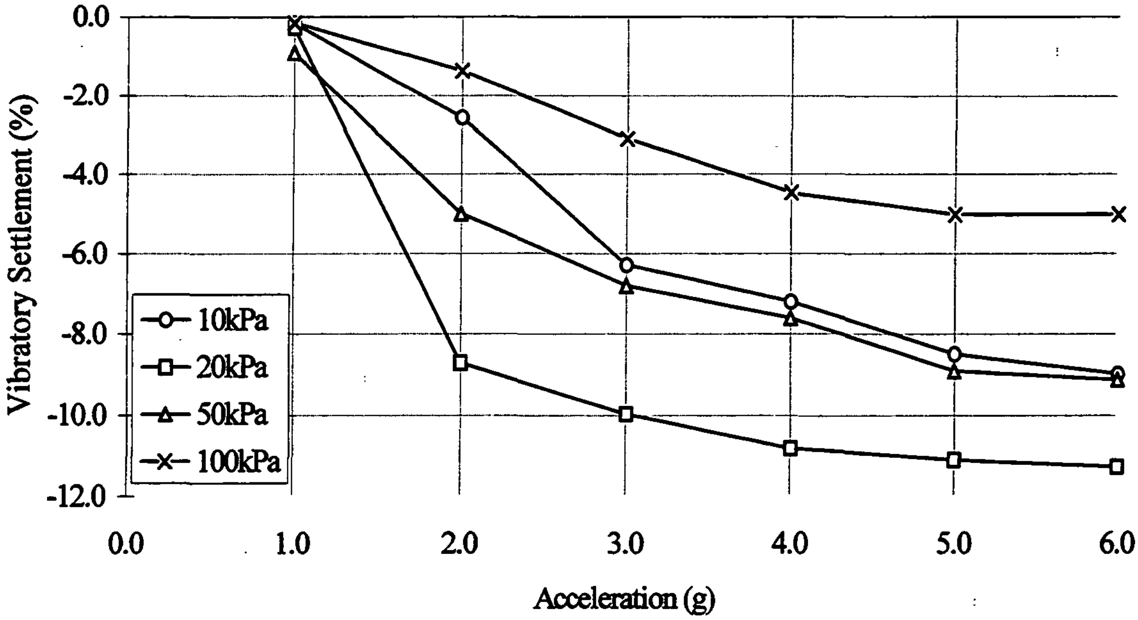

Figure 5.3.7. Medium sharp sand, high acceleration vibration test settlement results. Saturated, at 25Hz (see Appendix 3: Table A3.7.5, for test data sheet).

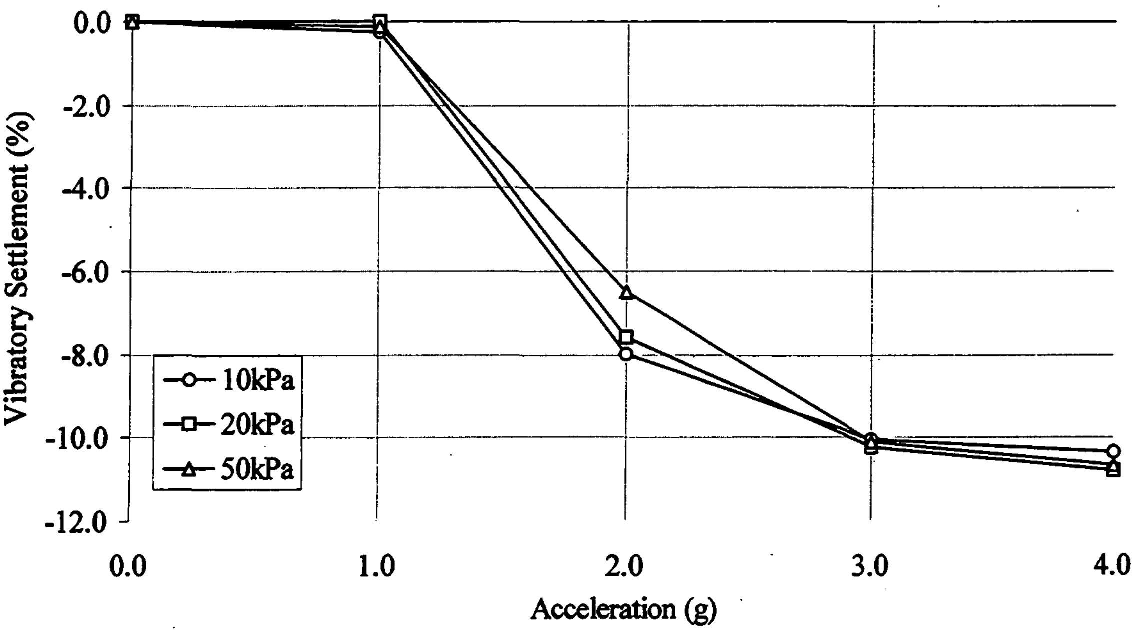

Figure 5.3.8. Coarse sharp sand >63μ, high acceleration vibration test settlement results. Saturated, at 25Hz (see Appendix 3: Table A3.8.1, for test data sheet).

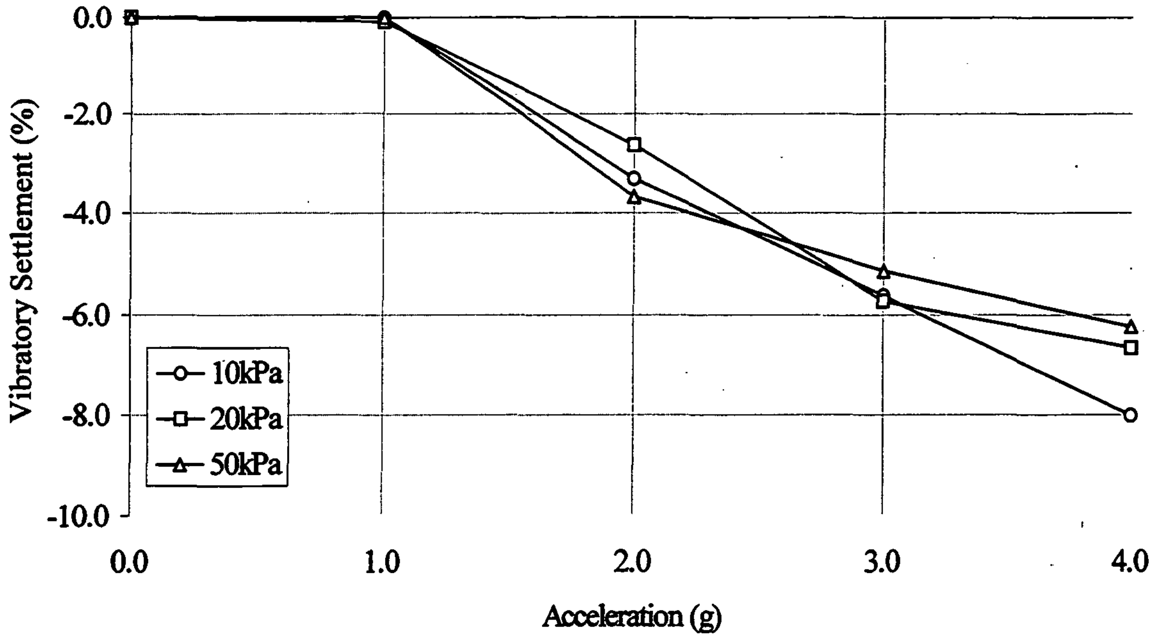

Figure 5.3.9. Coarse sharp sand , high acceleration vibration test settlement results. Saturated, at 25Hz (see Appendix 3; Table A3.9.1, for test data sheet).

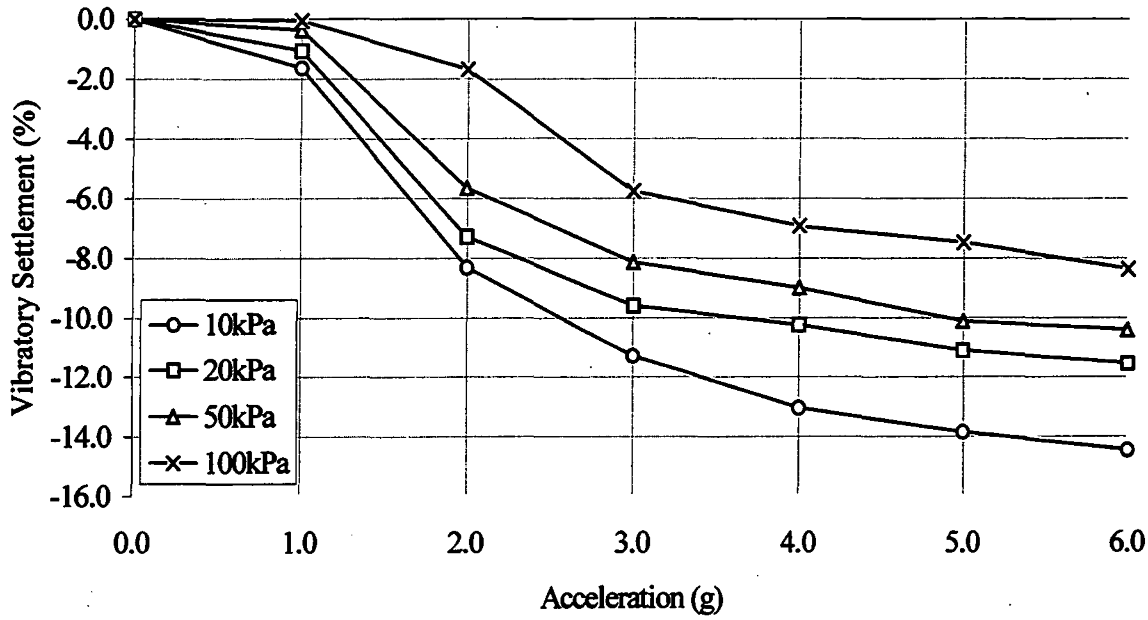

Figure 5.3.10. Sandy fine to medium gravel, high acceleration vibration test settlement results. Saturated, at 25Hz (see Appendix 3: Table A3.11.8, for test data sheet).

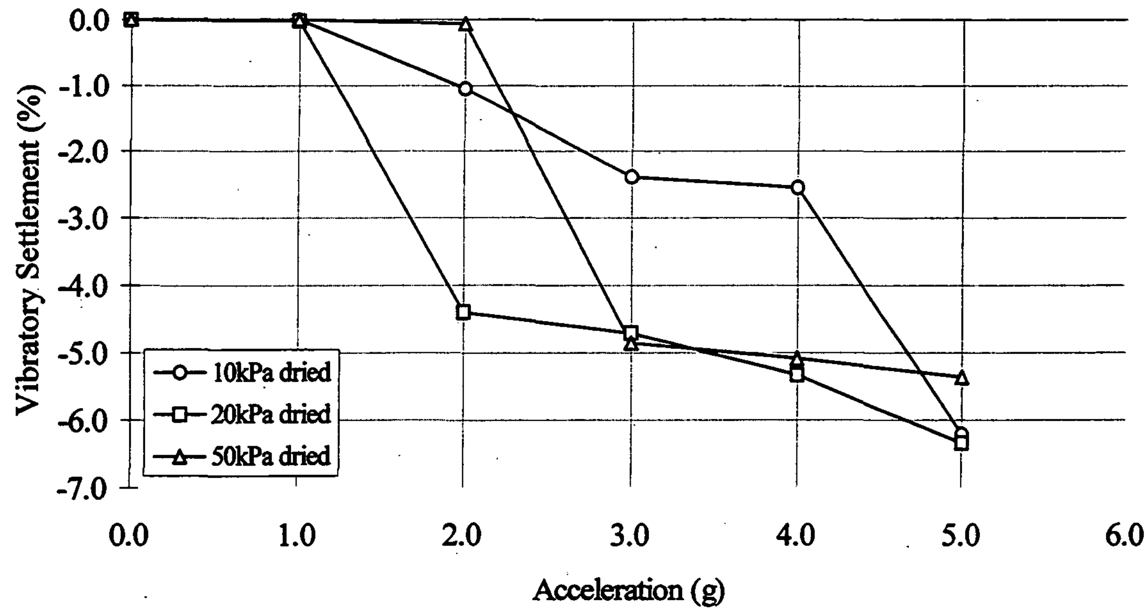

Figure 5.4.1. Silty fine sand dried high acceleration vibration test settlement results, at 25Hz.(see Appendix 3: Table A3.1.4, for test data sheet).

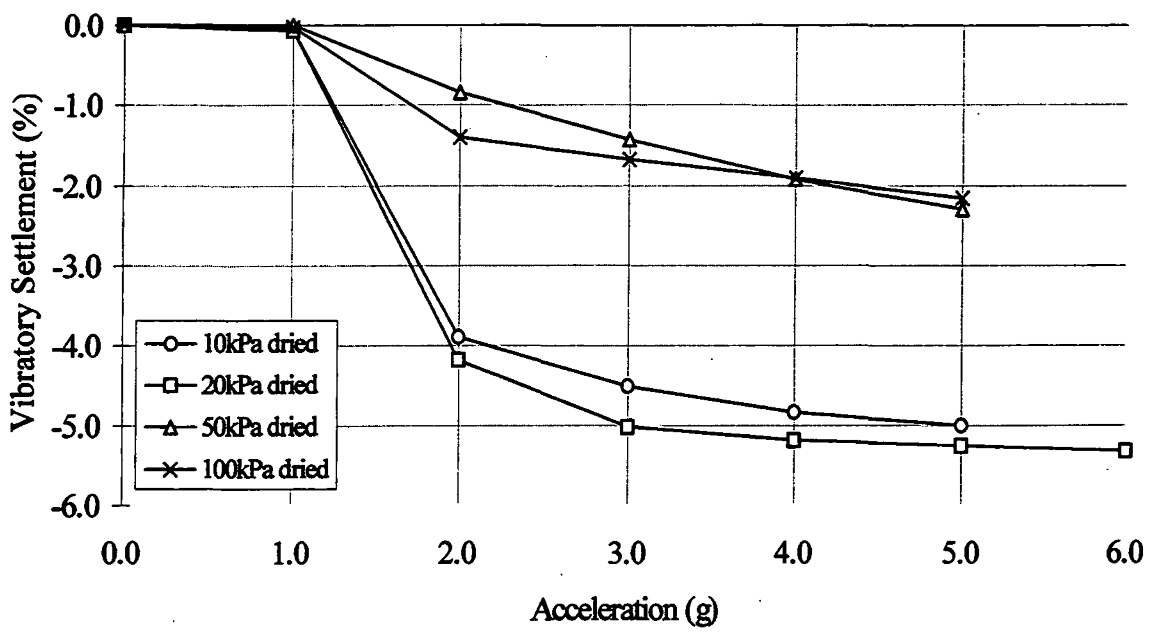

Figure 5.4.2. Garside medium sand dried high acceleration vibration test settlement results at 25Hz (see Appendix 3: Table A3.3.4, for test data sheet).

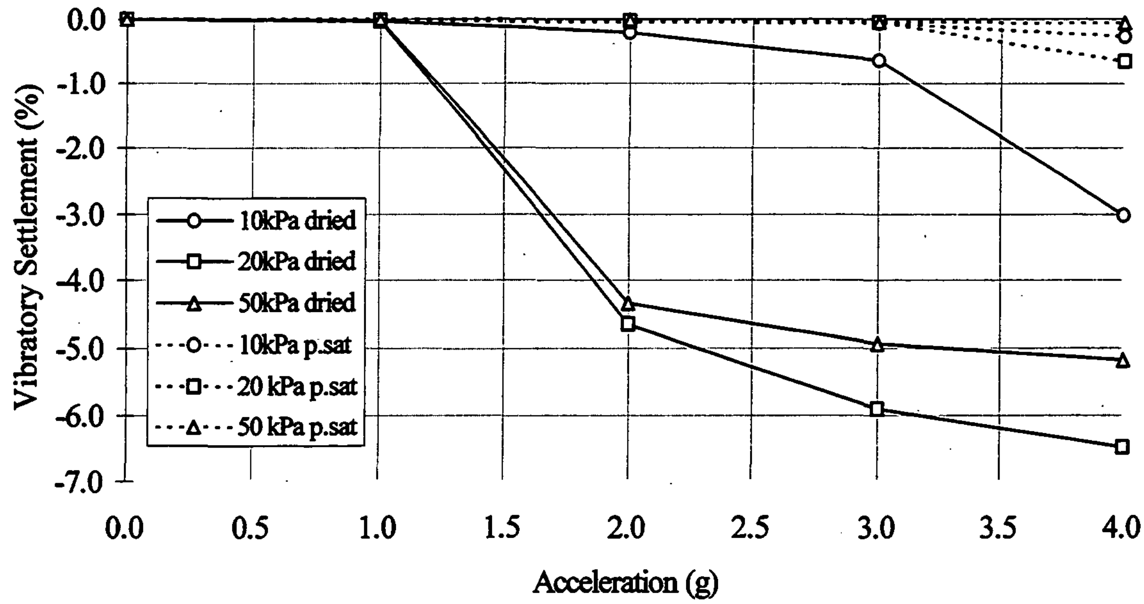

Figure 5.4.3. Medium uniform sand partially saturated and dried high acceleration vibration test settlement results at 25Hz (see Appendix 3: Table A3.4.6; A3.4.7, for test data sheet).

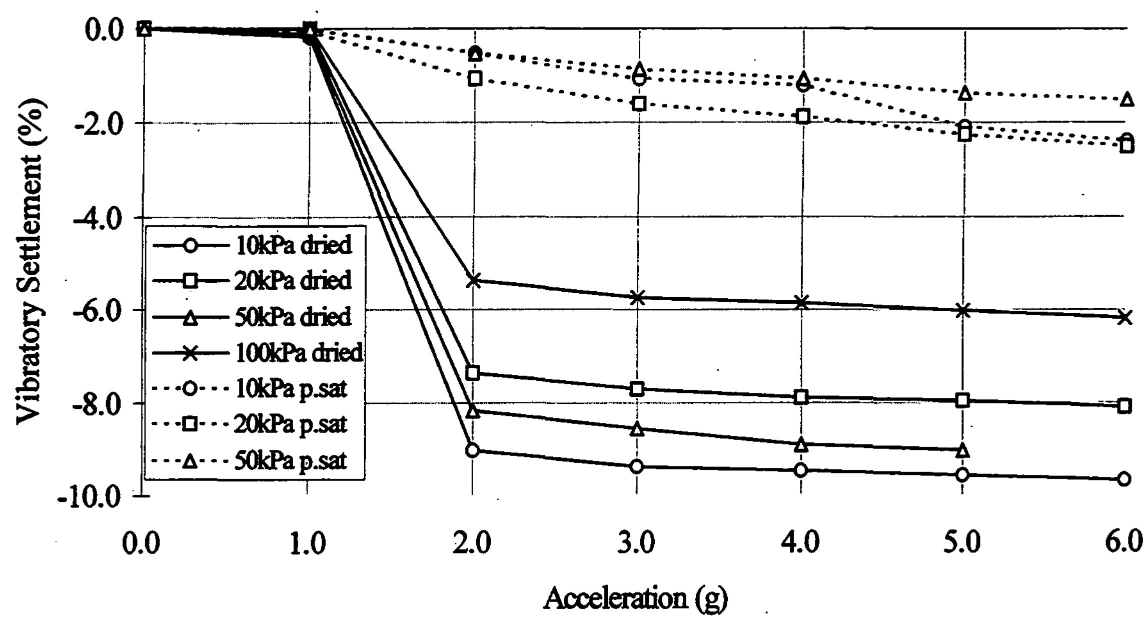

Figure 5.4.4. Medium Leighton Buzzard sand partially saturated and dried high acceleration vibration test settlement results at 25Hz (see Appendix 3: Table A3.5.5; A3.5.6, for test data sheet).

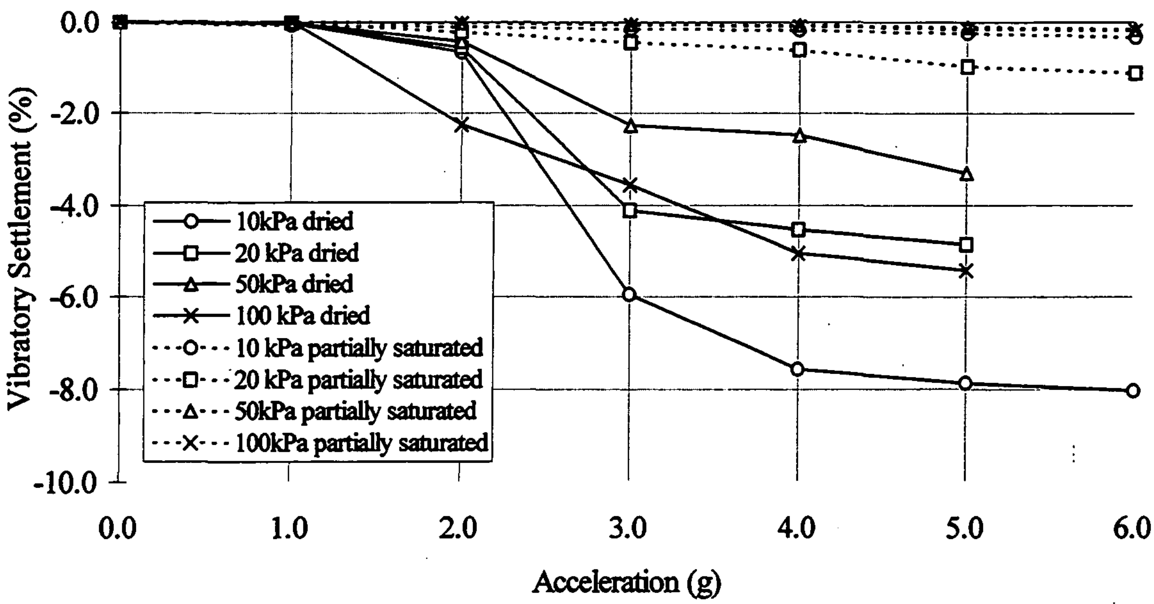

Figure 5.4.5. Medium sharp sand partially saturated and dried high acceleration vibration test settlement results at 25Hz (see Appendix 3: Table A3.7.7; A3.7.8, for test data sheet).

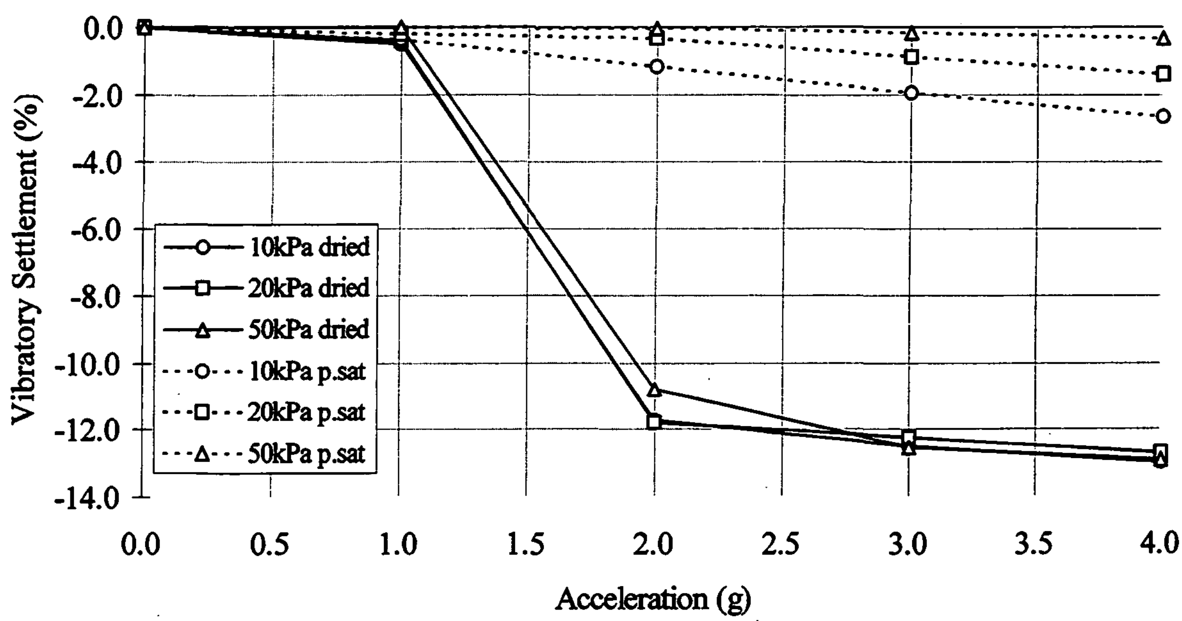

Figure 5.4.6. Coarse sharp sand >63μ partially saturated and dried high acceleration vibration test settlement results at 25Hz (see Appendix 3: Table A3.8.2; A3.8.3, for test data sheet).

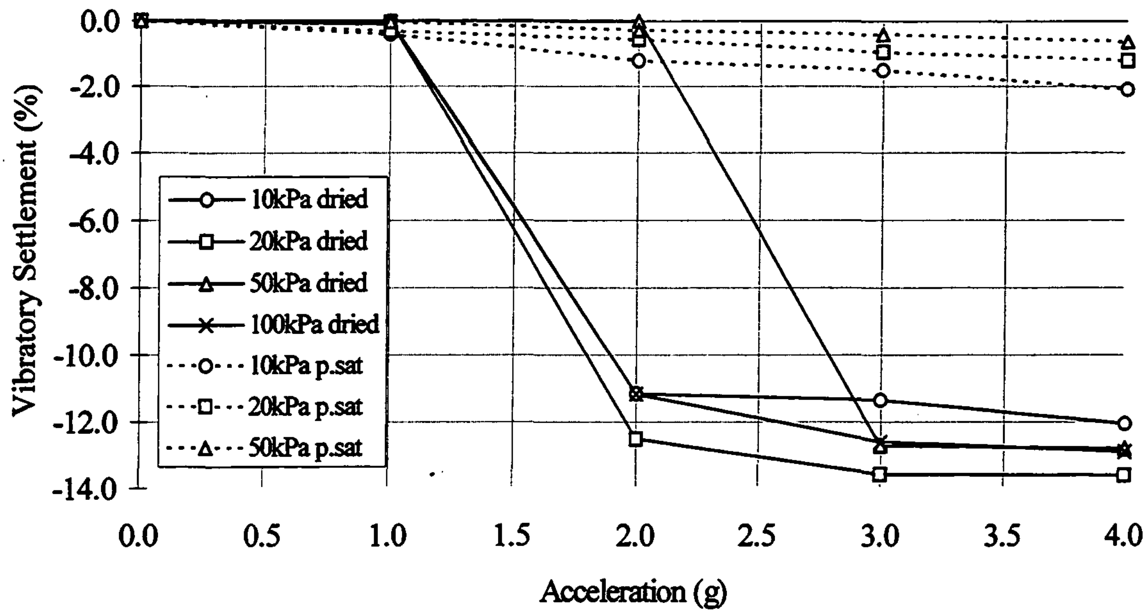

Figure 5.4.7. Coarse sharp sand partially saturated and dried high acceleration vibration test settlement results at 25Hz (see Appendix 3: Table A3.9.1; A3.9.2, for test data sheet).

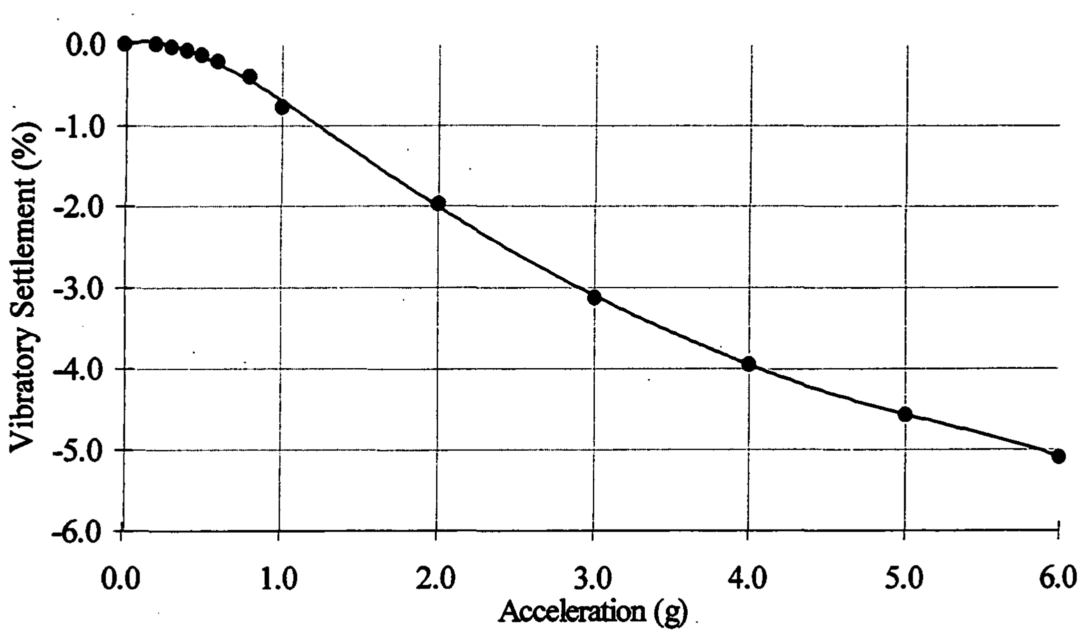

Figure 5.4.8. General trend of saturated vibration test settlement results (mean stress and mean soil-type data) at 25Hz.

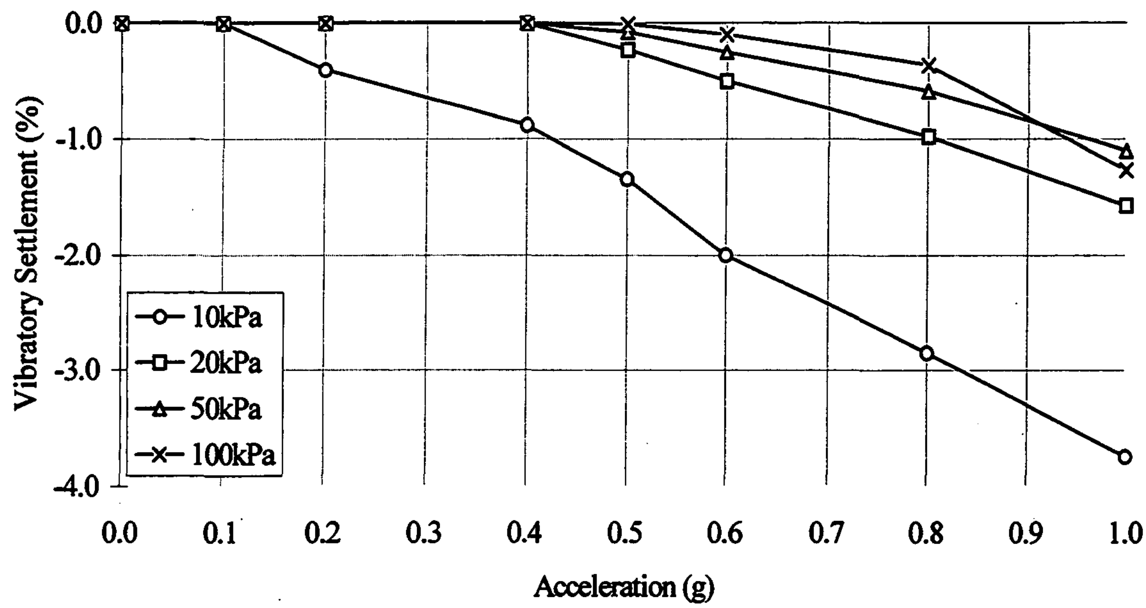

Figure 5.5.1. Sandy fine to medium gravel vibration test settlement results. Saturated, at 120Hz (see Appendix 3: Table A3.11.3, for test data sheet).

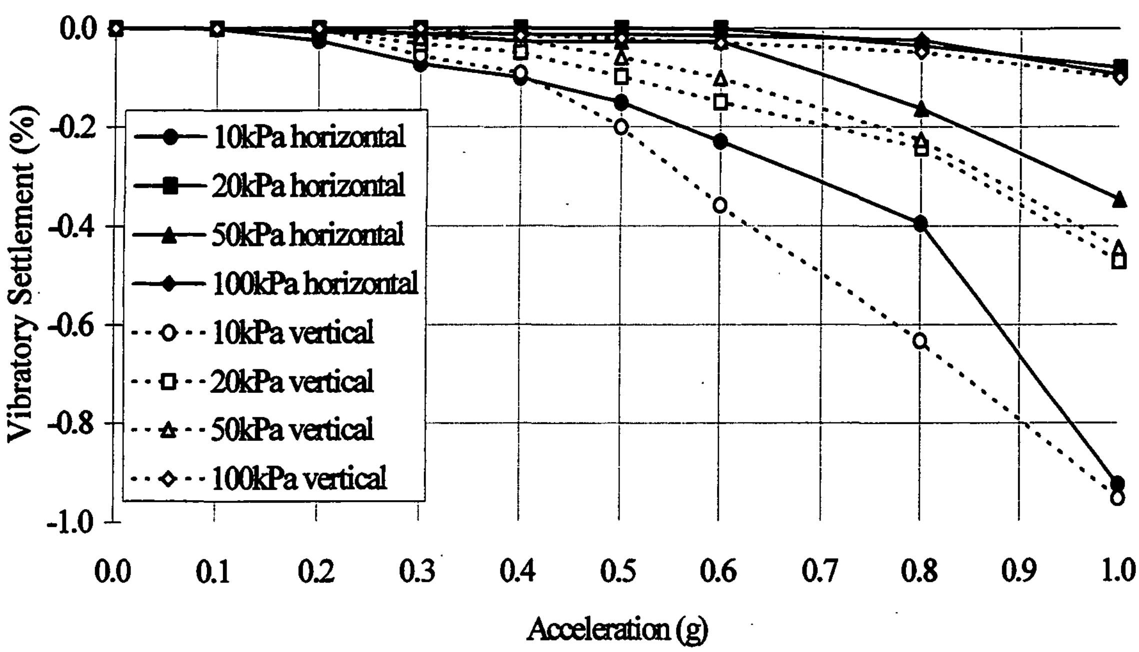

Figure 5.5.2a. Medium Leighton Buzzard sand, comparison of horizontal and vertical vibration orientation (40Hz, saturated) settlement tests (see Appendix 3: Table A3.5.2; A3.5.3, for test data sheet).

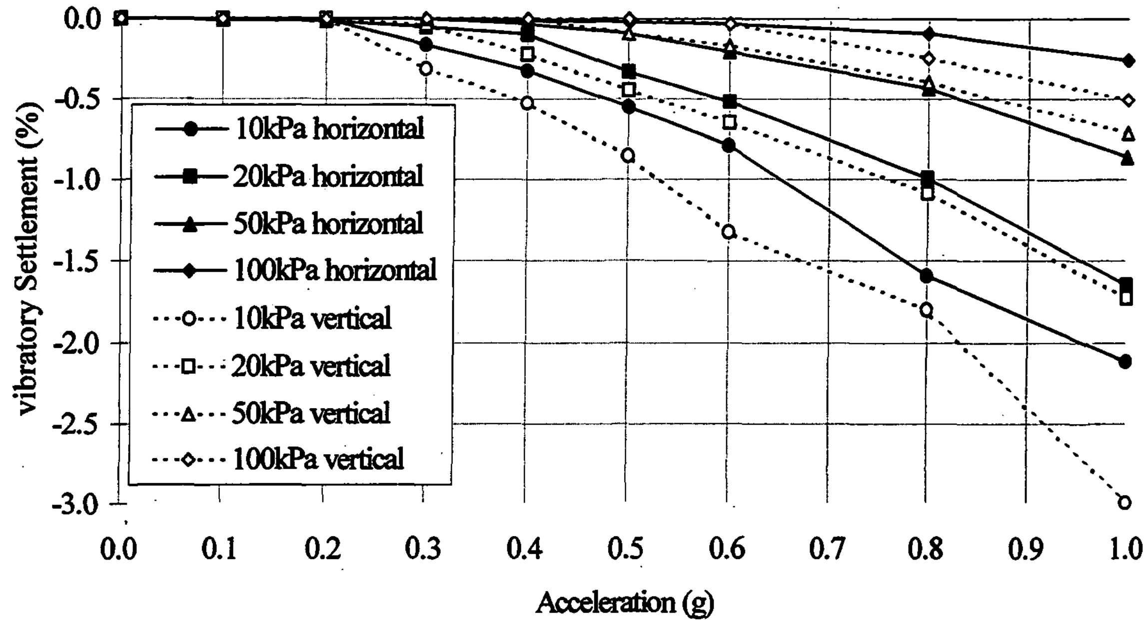

Figure 5.5.2b Sandy fine to medium gravel, comparison of horizontal and vertical vibration orientation (40Hz, saturated) settlement tests (see Appendix 3: Table A3.11.2; A3.11.4, for test data sheet).

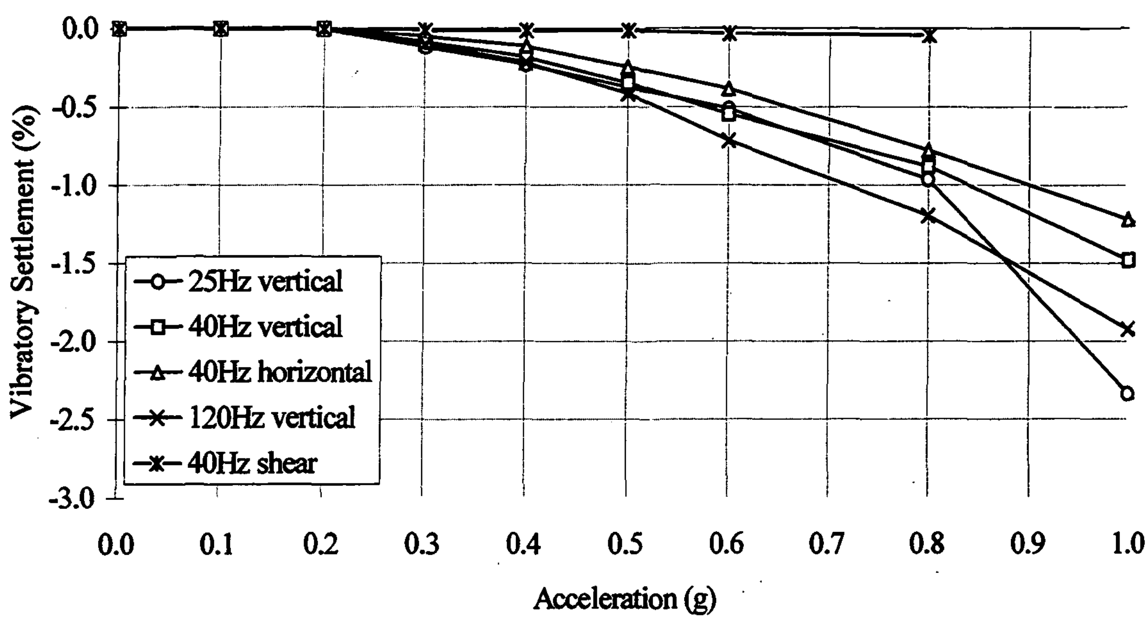

Figure 5.5.2c. Sandy fine to medium gravel settlement response to different vibration frequency and orientation (see Appendix 3: Table A3.11.7, for test data sheet).

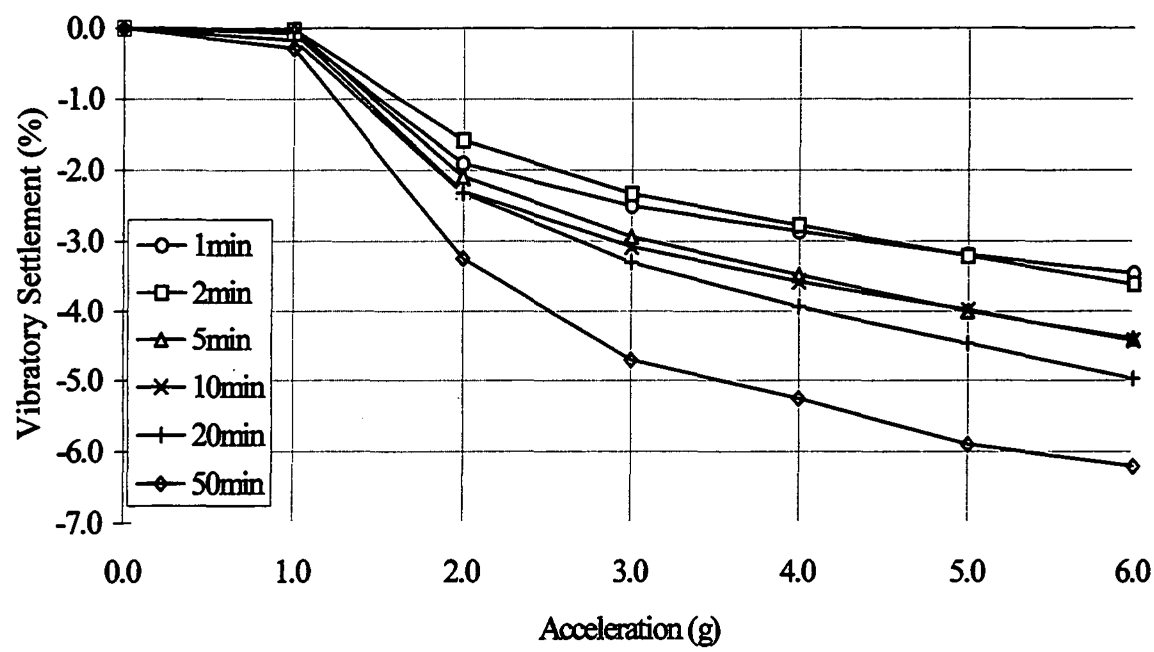

Figure 5.5.3. Coarse Leighton Buzzard sand settlement response to tests of fixed time length per acceleration increment (saturated, 50kPa, 25Hz) (see Appendix A3.6.6, for test data sheet).

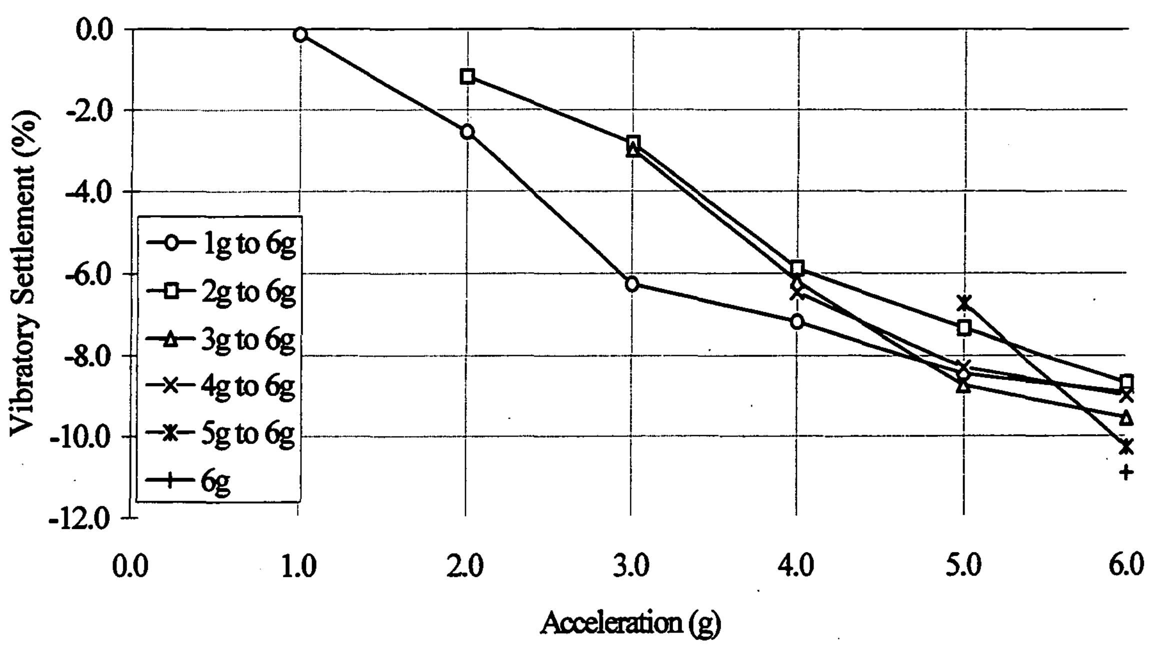

Figure 5.5.4. Medium sharp sand settlement response to increase in initial acceleration magnitude (saturated, 10kPa, 25Hz) (see Appendix 3: Table A3.7.6, for test data sheet).

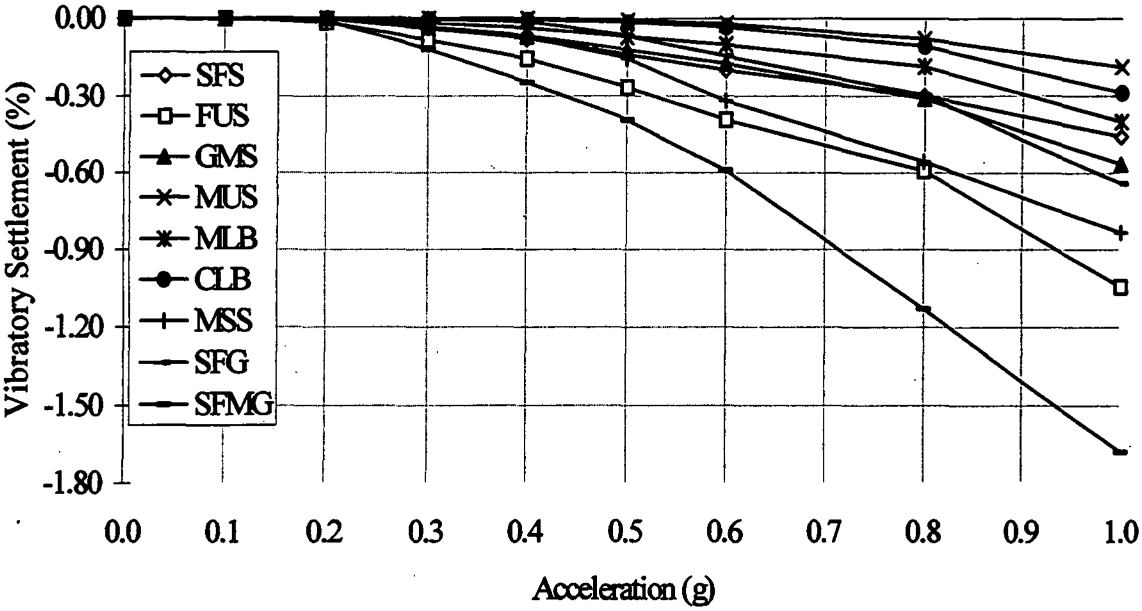

Figure 5.6.1a. Comparison of the vibration settlement response of all soils tested, using mean stress values (saturated, at 25Hz).

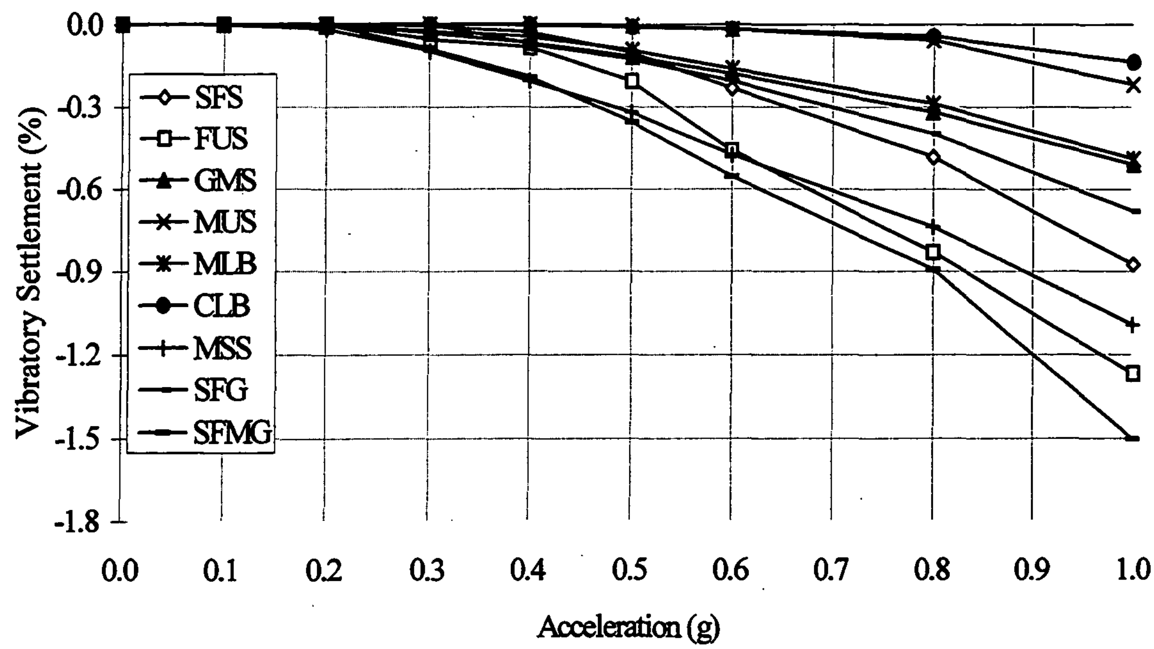

Figure 5.6.1b. Comparison of the vibration settlement response of all soils tested, using mean stress values (saturated, at 40Hz).

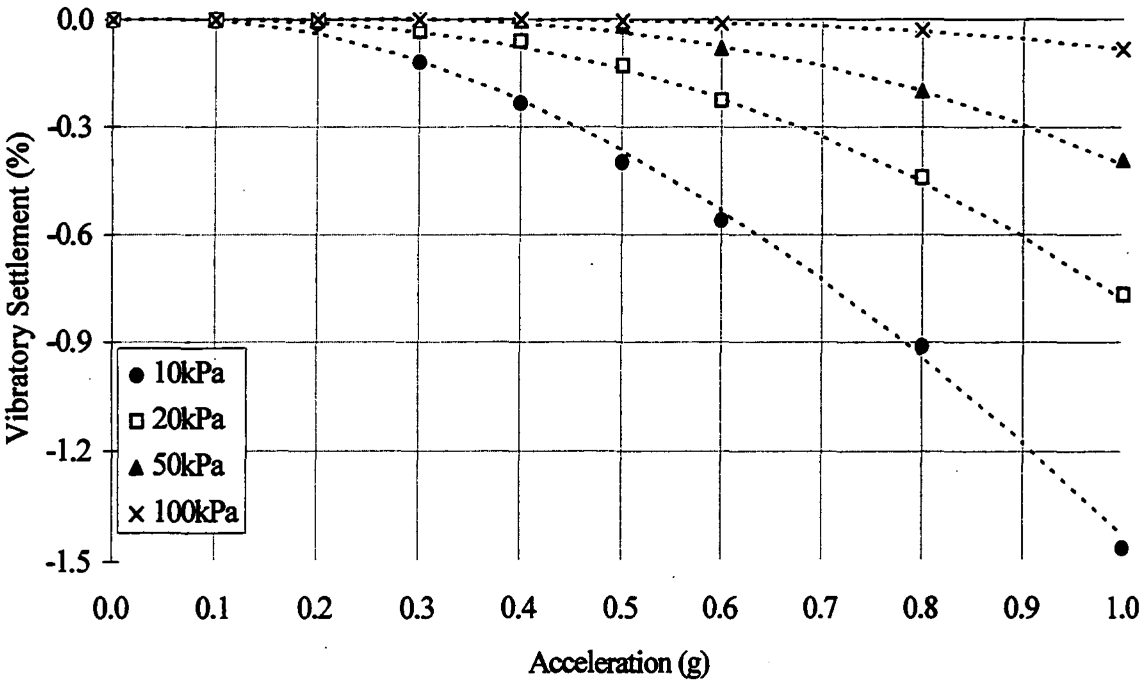

Figure 5.6.2a. Vibration settlement response of a protosoil to static stress (saturated, 25Hz).

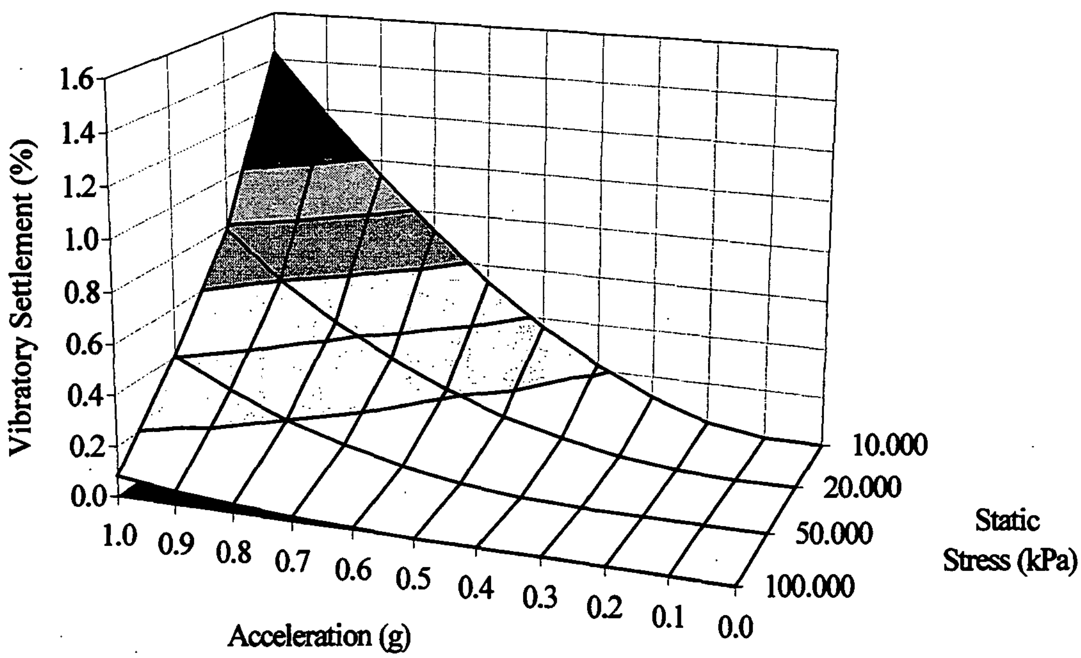

Figure 5.6.2b. Three-dimensional view of Figure 5.6.2a.

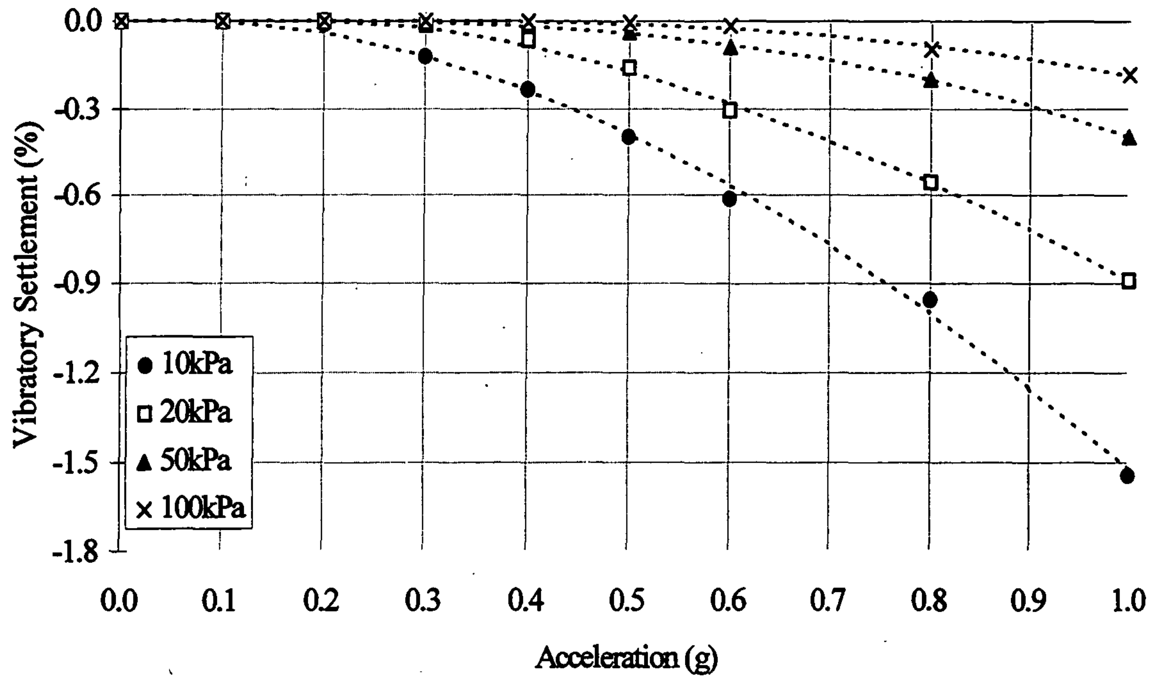

Figure 5.6.3a. Vibration settlement response of a protosoil to static stress (saturated, 40Hz).

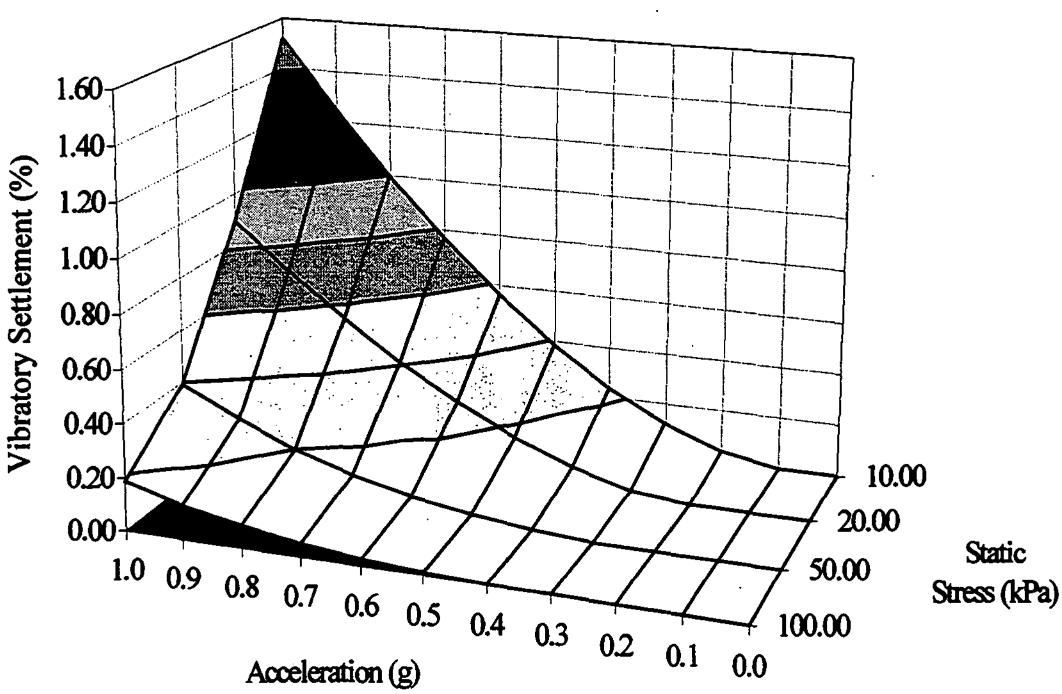

Figure 5.6.3b. Three-dimensional view of Figure 5.6.3a.

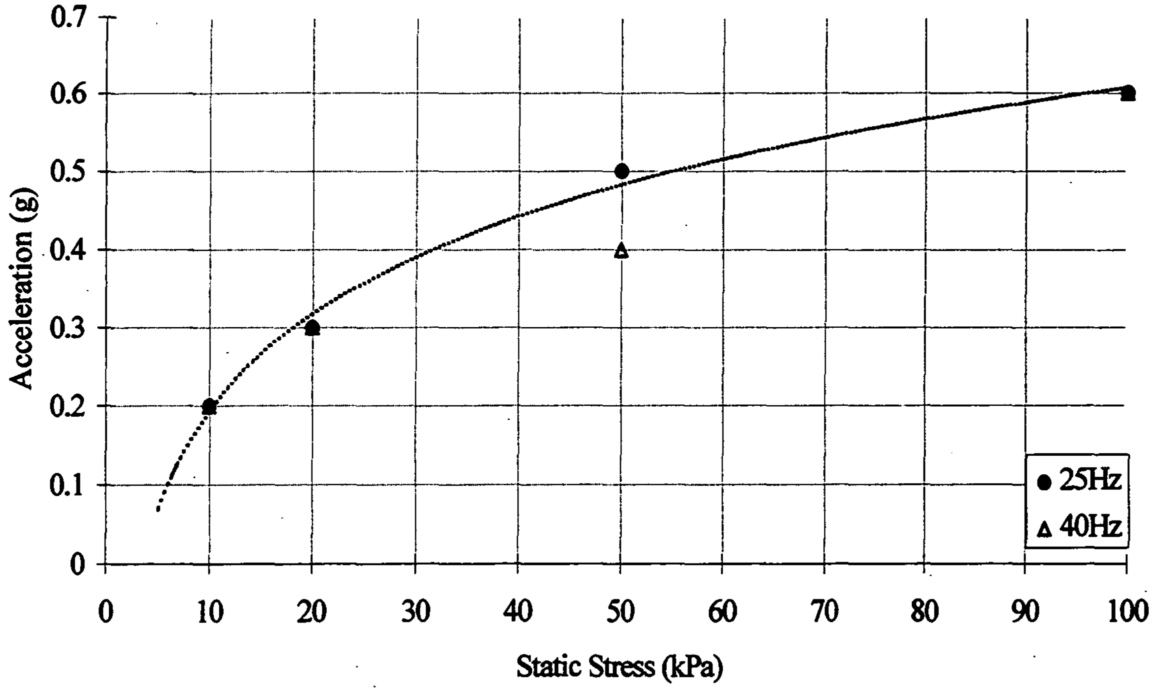

Figure 5.6.4. Minimum level of acceleration that induces initial soil settlement (protosoil, saturated).

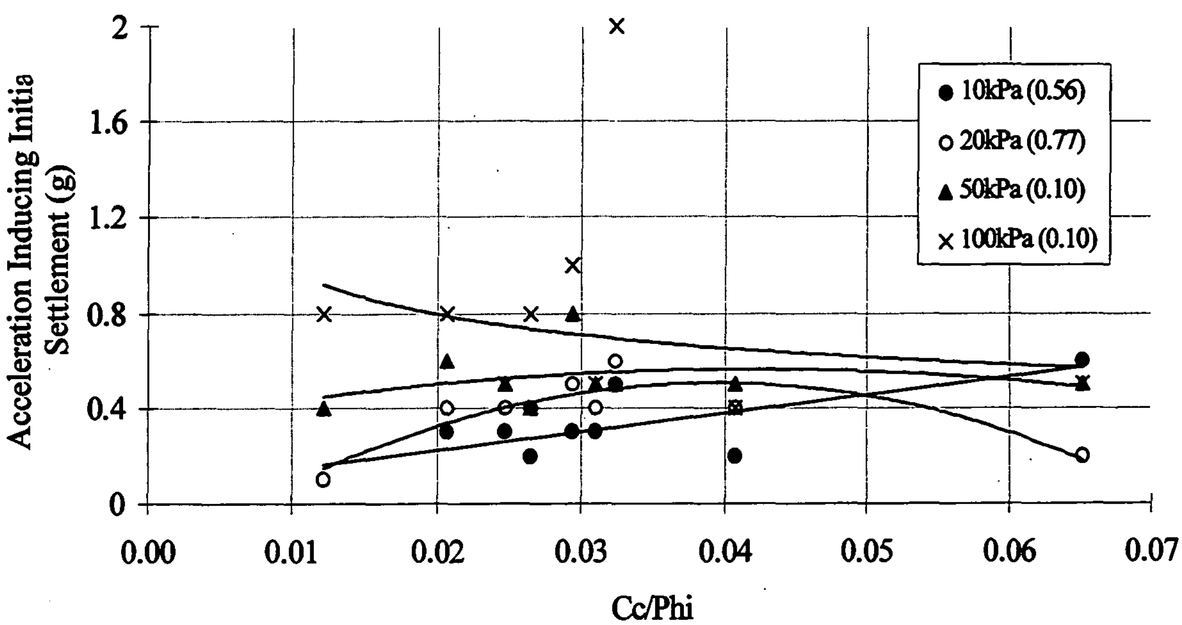

Figure 5.6.5. Best relationship between soil-type and minimum acceleration required to induce initial settlement (saturated, 25Hz). Data in brackets are best R^2 values.

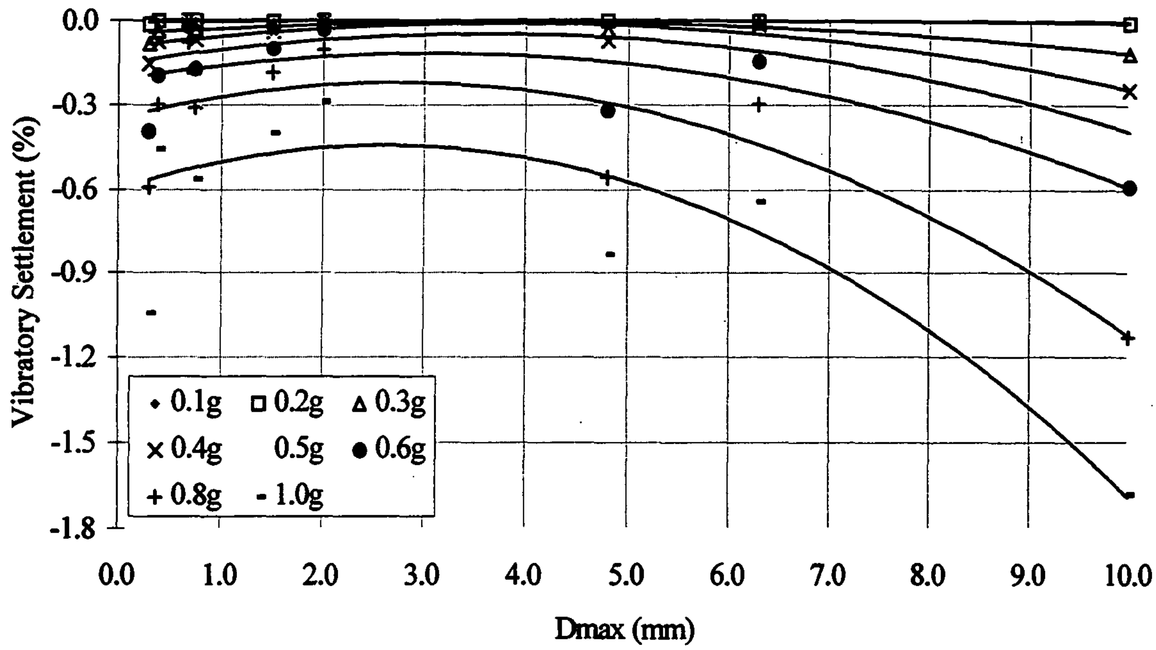

Figure 5.7.1a. Relationship between maximum particle size (D_{max}) and settlement (mean stress values, saturated, 25Hz).

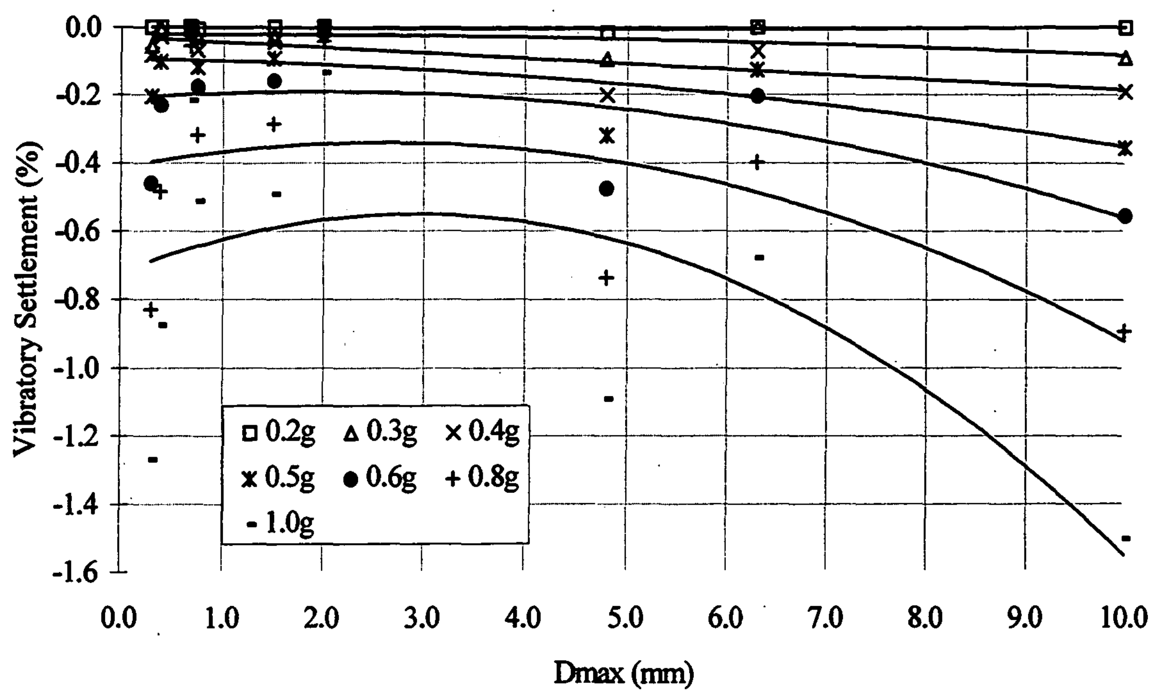

Figure 5.7.1b. Relationship between maximum particle size (D_{max}) and settlement (mean stress values, saturated, 40Hz).

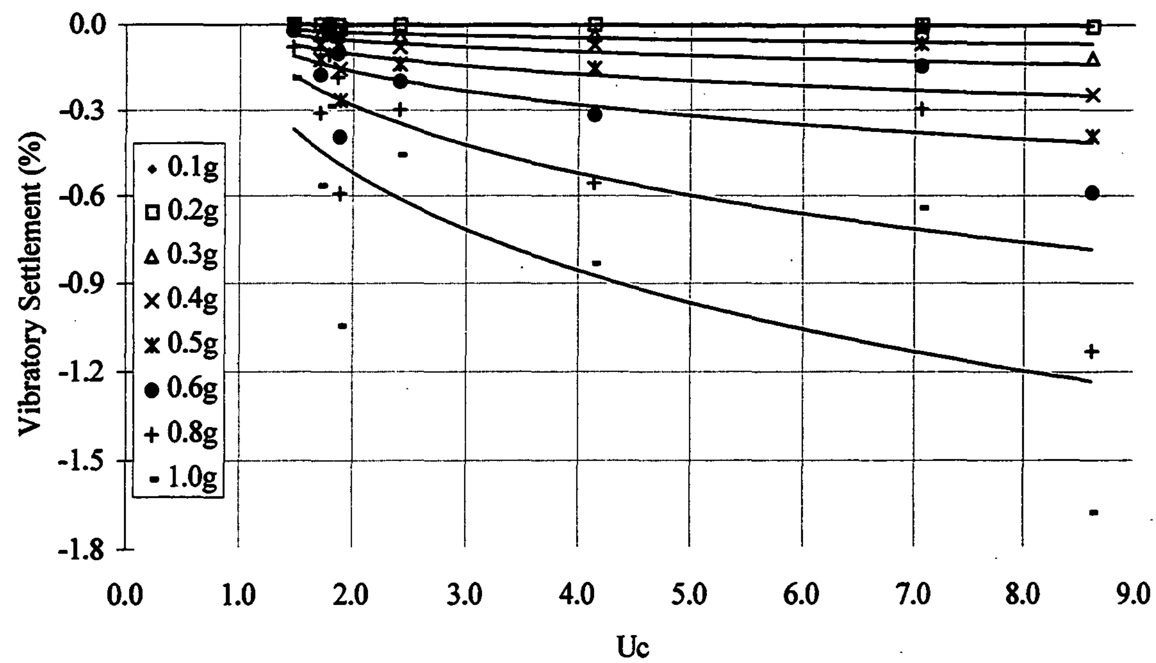

Figure 5.7.2a. Relationship between uniformity coefficient (U_c) and settlement (mean stress values, saturated, 25Hz).

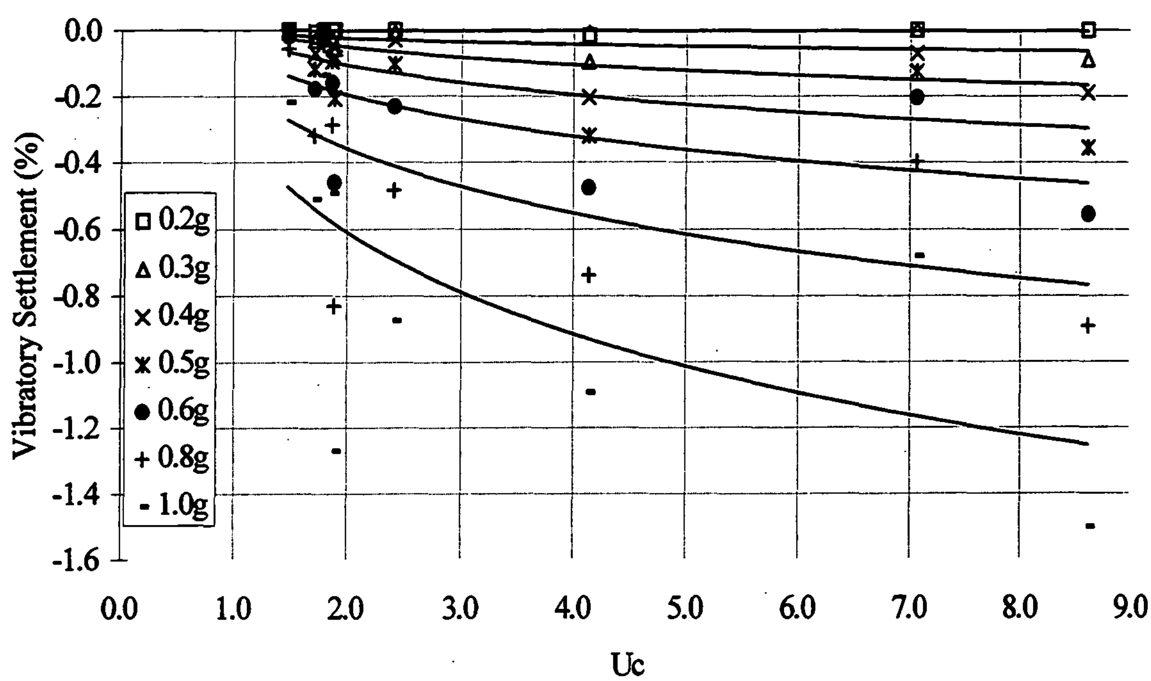

Figure 5.7.2b. Relationship between uniformity coefficient (U_c) and settlement (mean stress values, saturated, 40Hz).

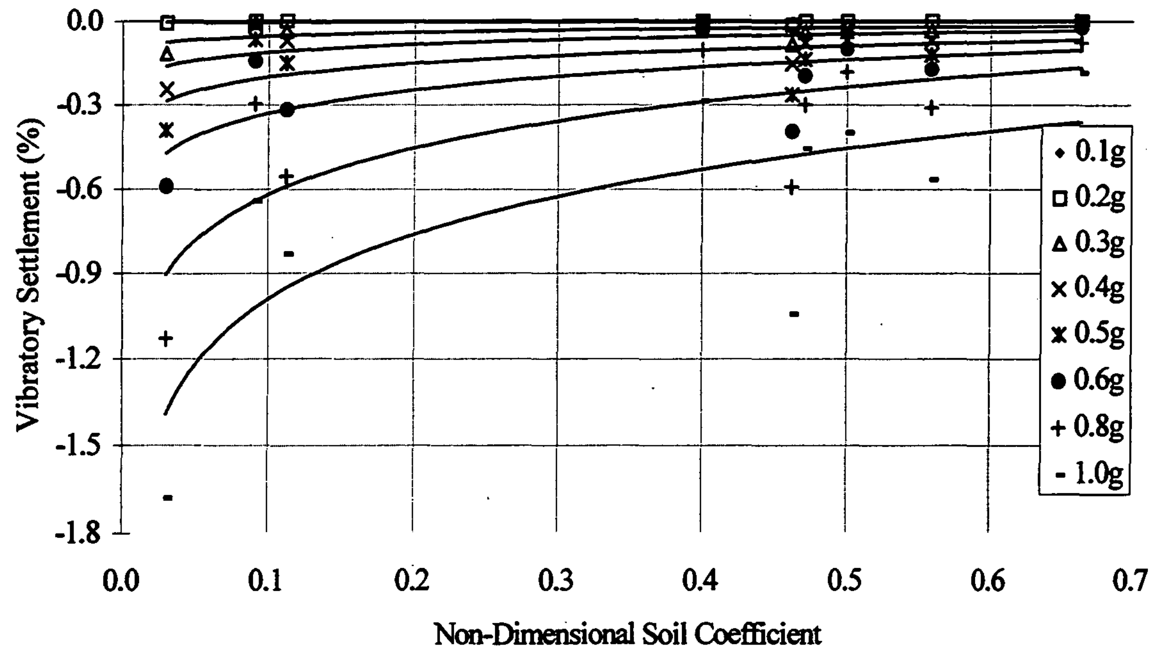

Figure 5.7.3a. Relationship between the non-dimensional coefficient (D_x) and settlement (mean stress values, saturated, 25Hz).

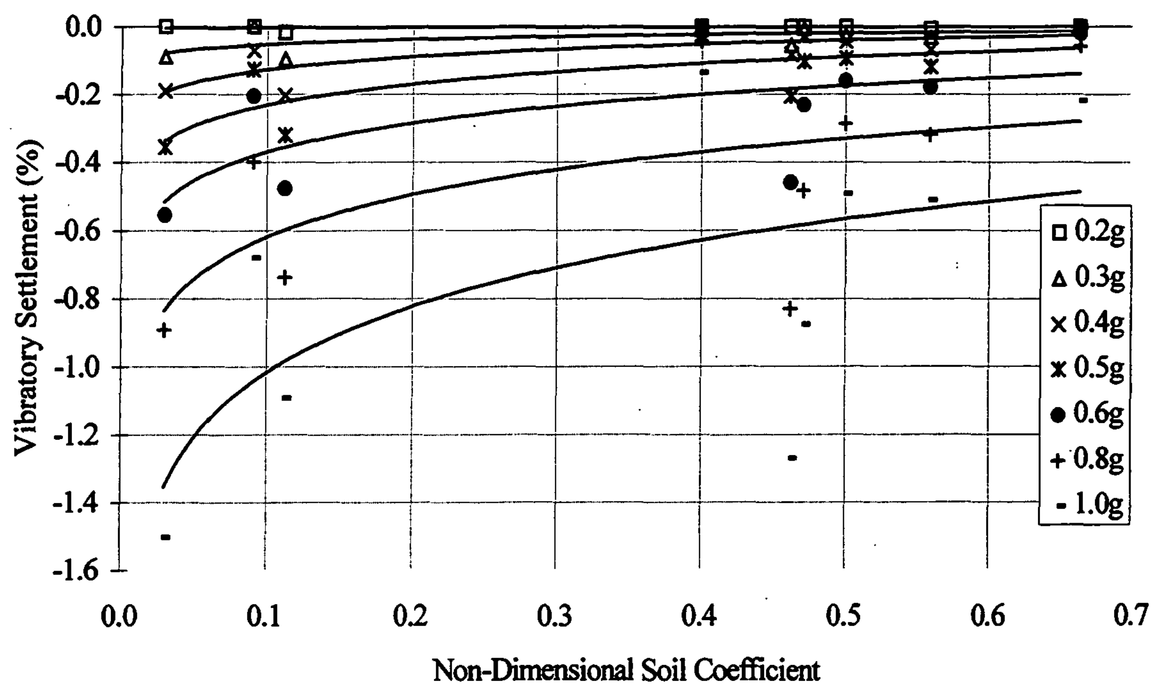

Figure 5.7.3b. Relationship between the non-dimensional coefficient (D_x) and settlement (mean stress values, saturated, 40Hz).

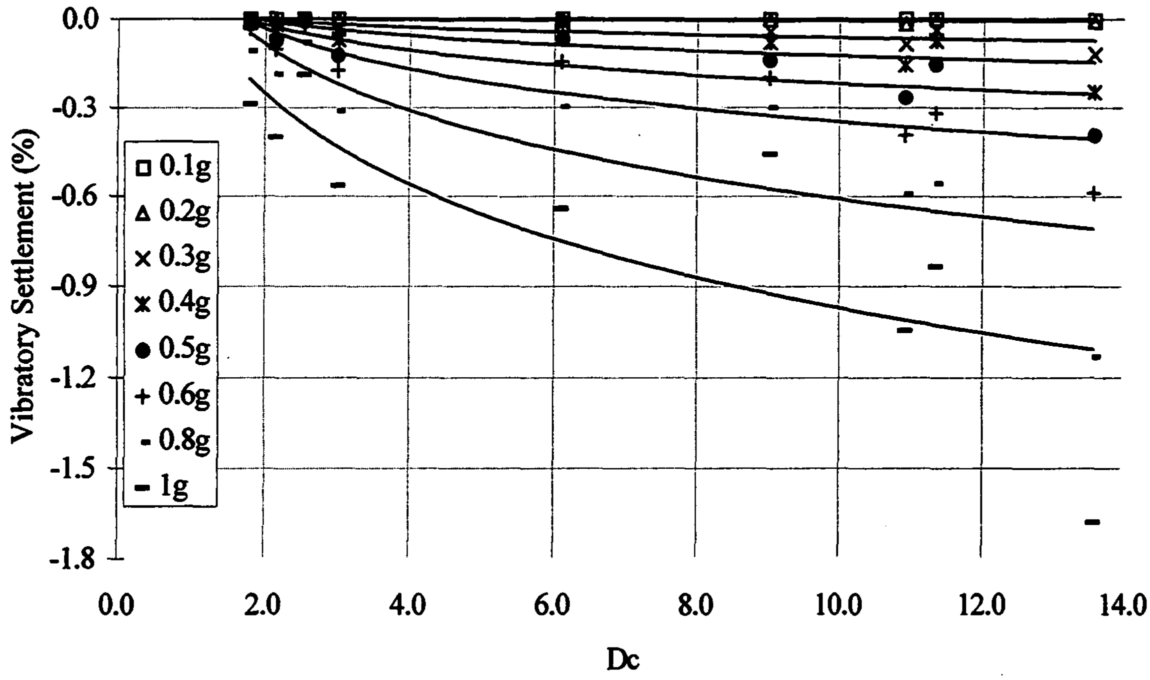

Figure 5.7.4a. Relationship between distribution coefficient (D_c) and settlement (mean stress values, saturated, 25Hz).

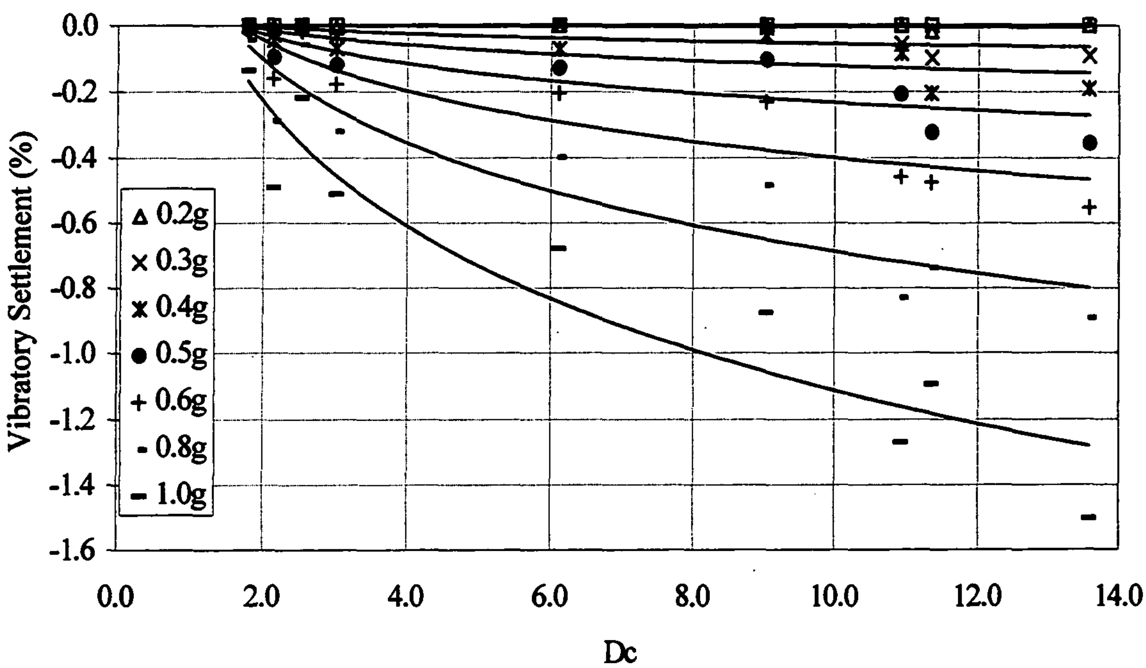

Figure 5.7.4b. Relationship between distribution coefficient (D_c) and settlement (mean stress values, saturated, 40Hz).

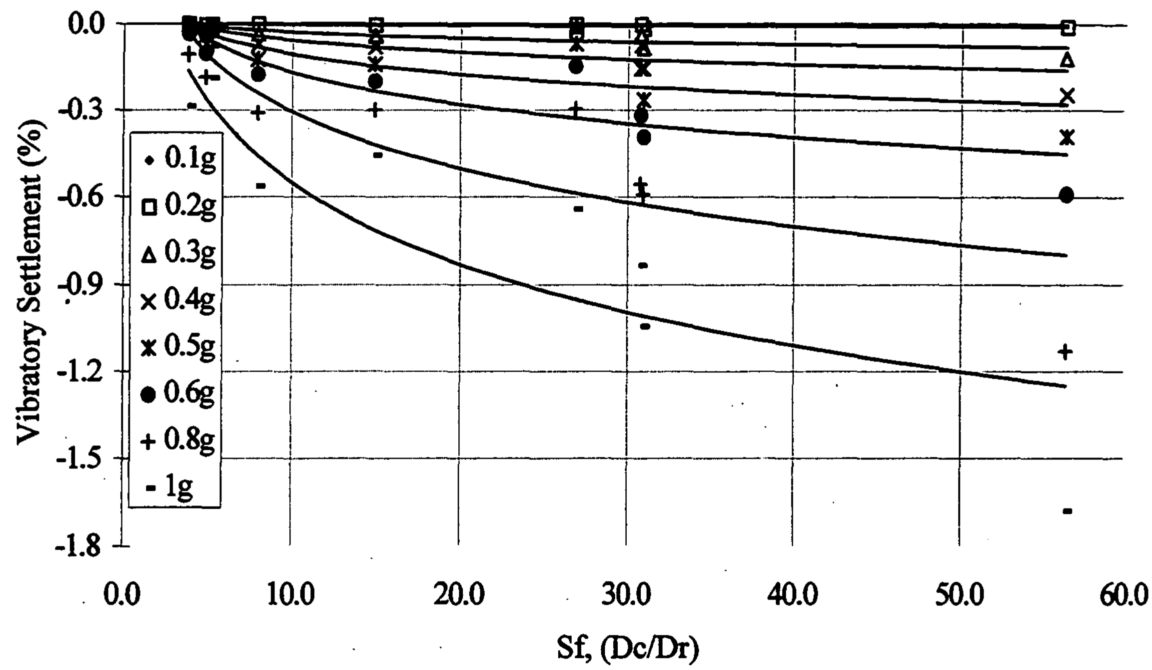

Figure 5.7.5a. Relationship between soil parameter (S_f) and settlement (mean stress values, saturated, 25Hz).

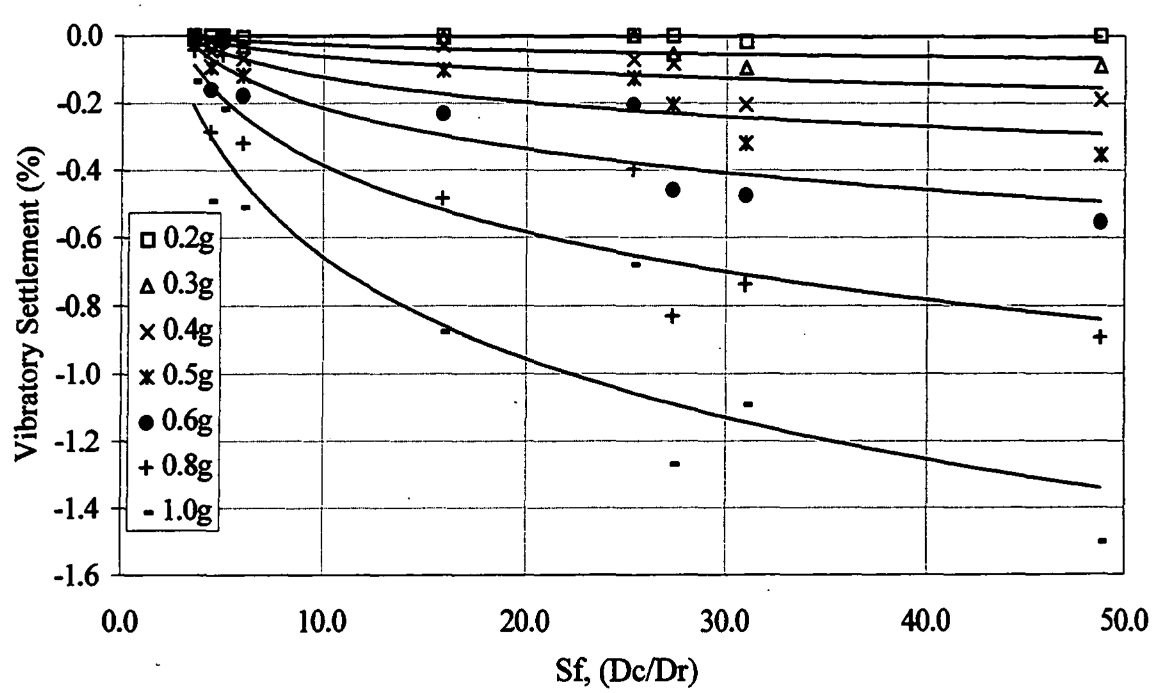

Figure 5.7.5b. Relationship between soil parameter (S_f) and settlement (mean stress values, saturated, 40Hz).

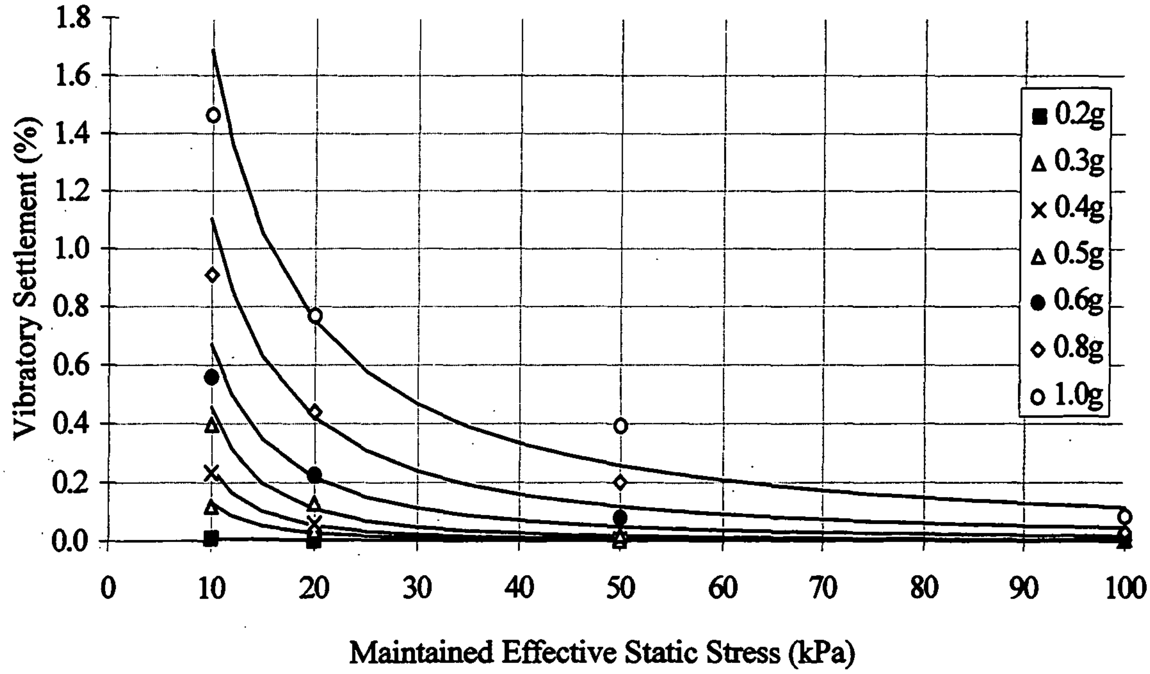

Figure 5.7.6a. General relationship between maintained effective static stress and settlement (protosoil values, saturated, 25Hz).

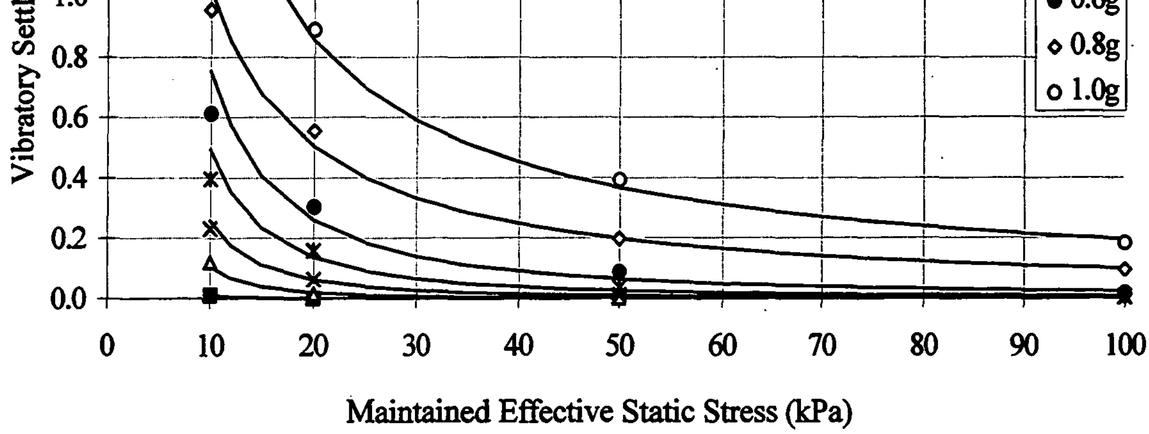

Figure 5.7.6b. General relationship between maintained effective static stress and settlement (protosoil values, saturated, 40Hz).

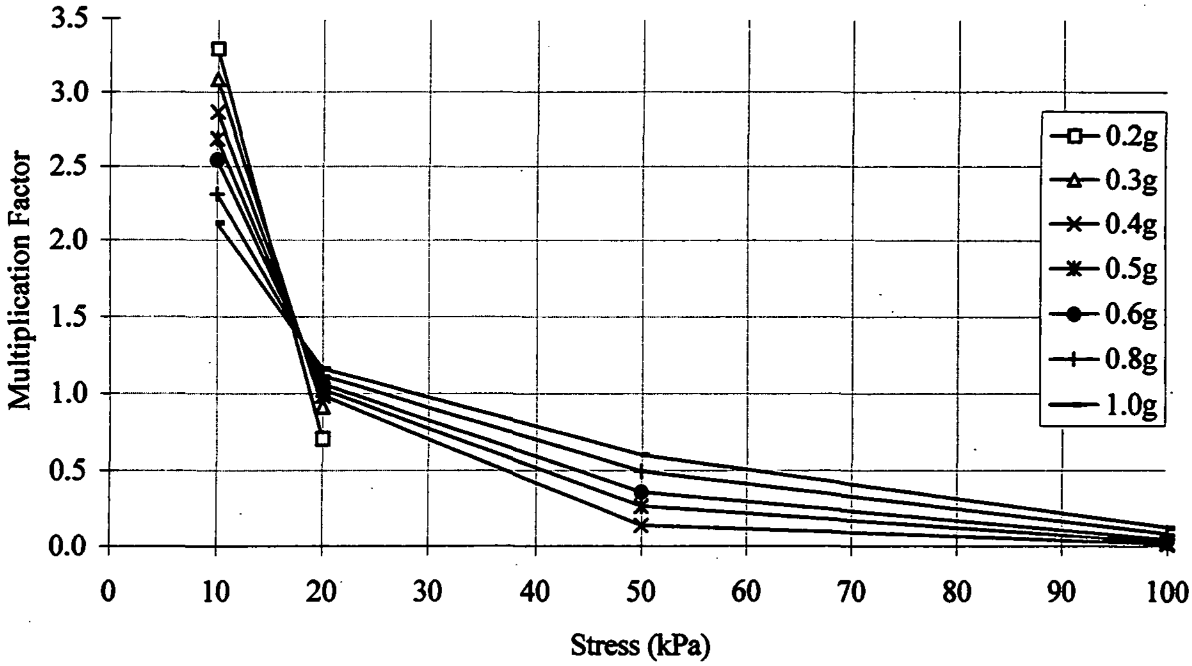

Figure 5.7.7a. Stress correction multiplication factor (using protosoil values, saturated, 25Hz).

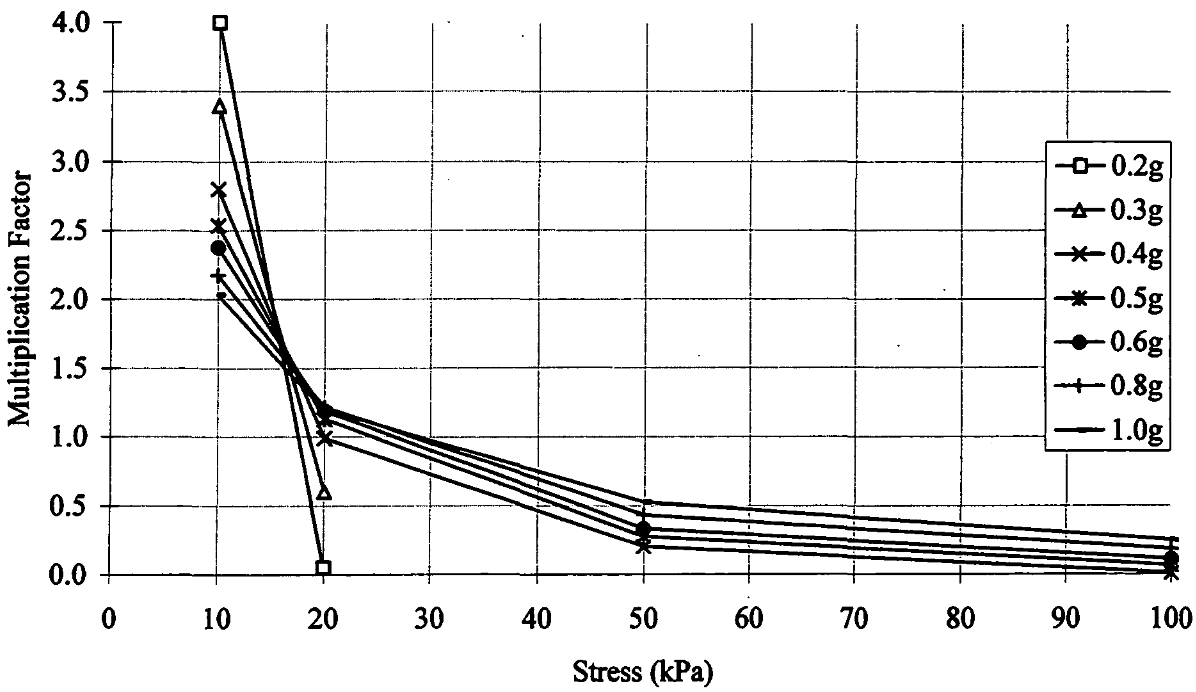

Figure 5.7.7b. Stress correction multiplication factor (using protosoil values, saturated, 40Hz).

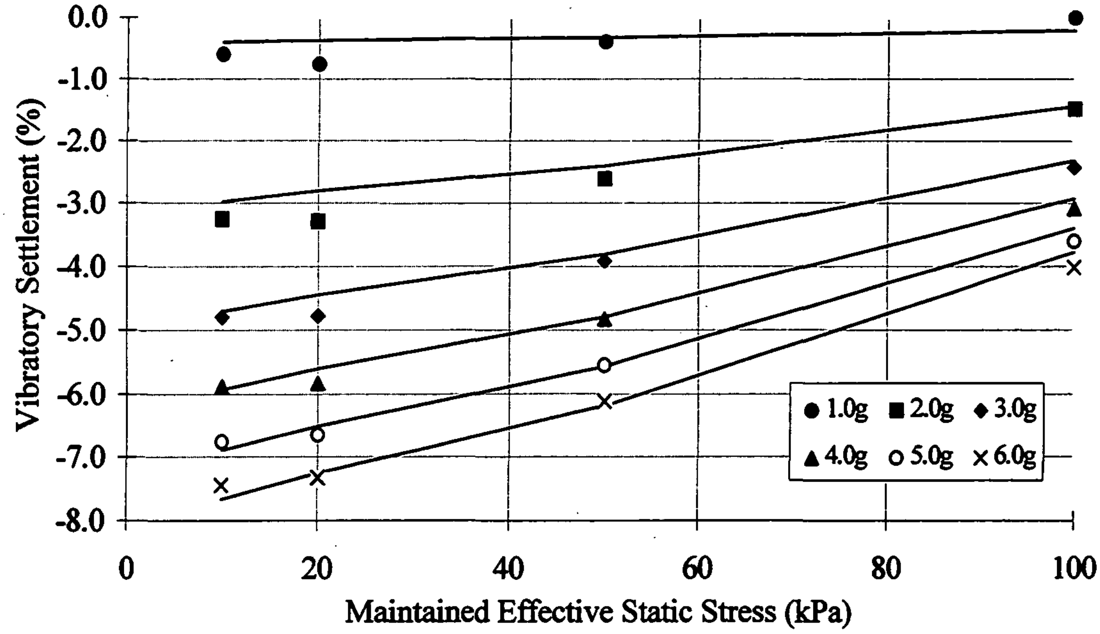

Figure 5.8.1. General relationship between static stress and high acceleration vibration settlement (protosoil values, saturated, 25Hz).

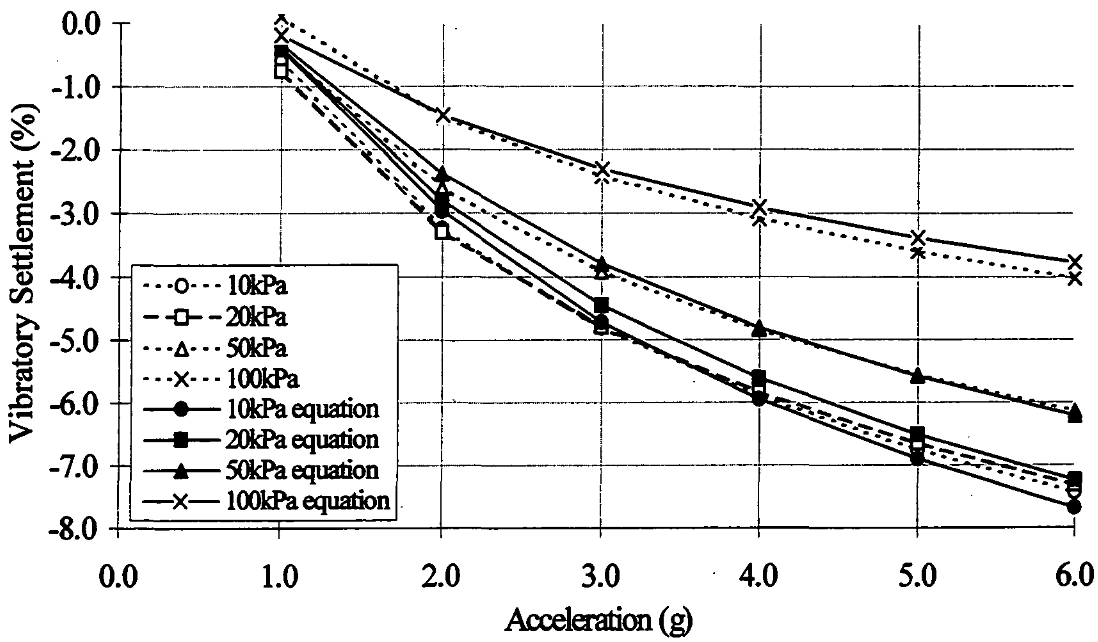

Figure 5.8.2. Comparison between high acceleration vibration test settlement and derived equivalent values (protosoil, saturated, 25Hz).

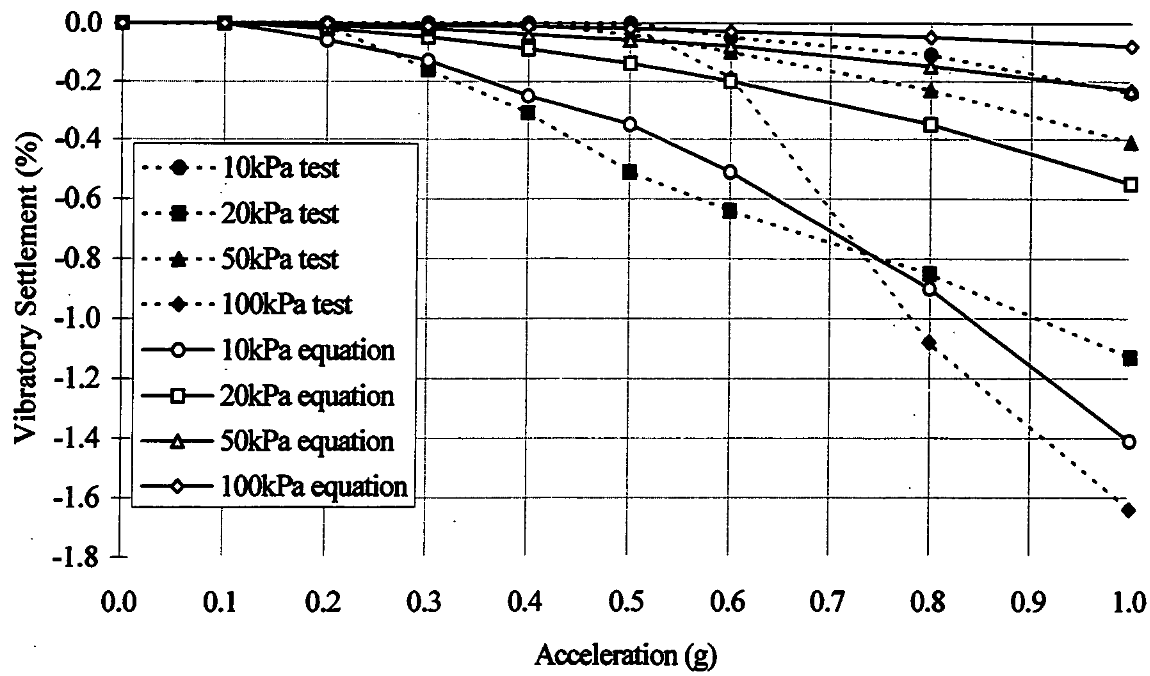

Figure 5.9.1a. Comparison between vibration test settlement and derived equivalent values (silty fine sand, saturated, 25Hz).

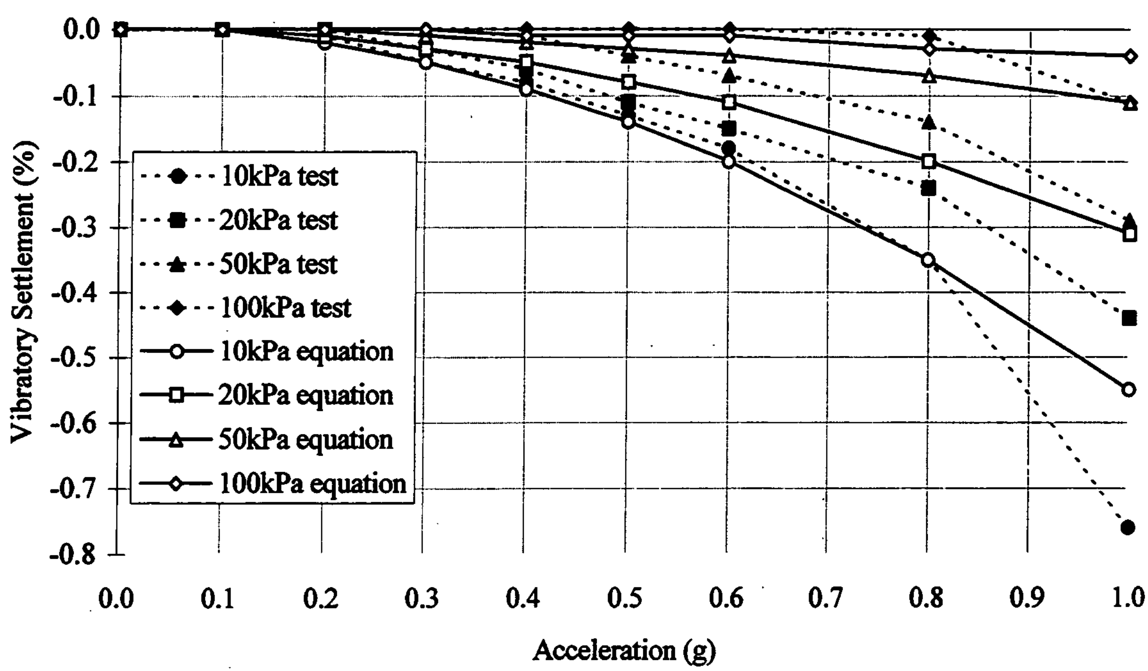

Figure 5.9.1b. Comparison between vibration test settlement and derived equivalent values (medium Leighton Buzzard sand, saturated, 40Hz).

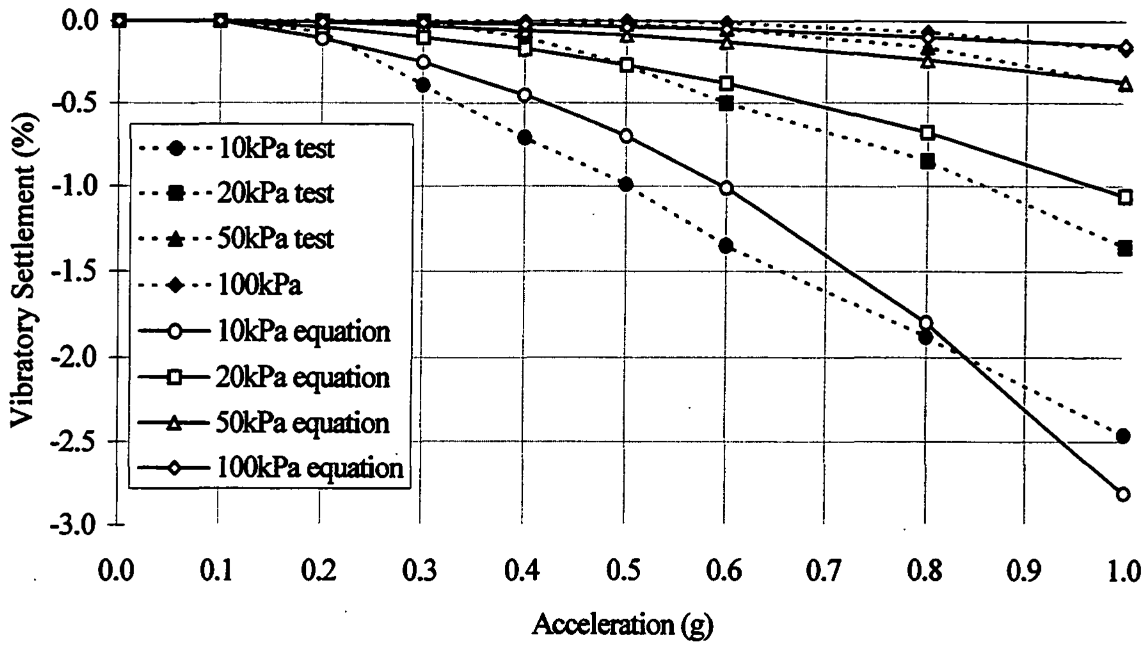

Figure 5.9.1c. Comparison between vibration test settlement and derived equivalent values (medium sharp sand, saturated, 25Hz).

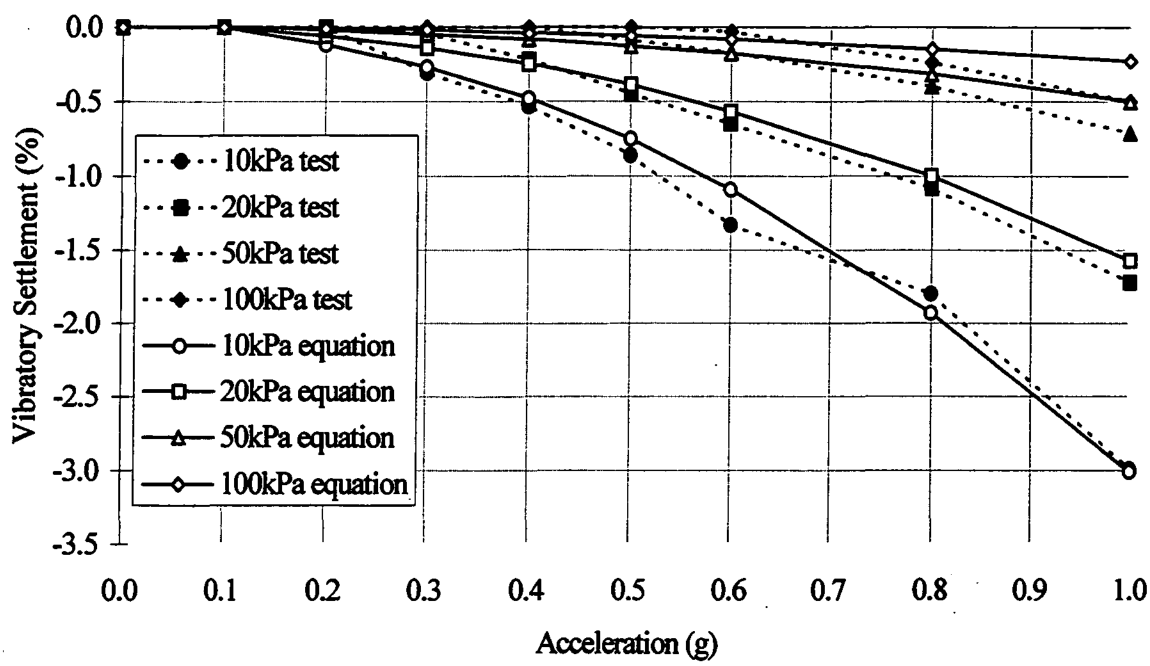

Figure 5.9.1d. Comparison between vibration test settlement and derived equivalent values (sandy fine to medium gravel, saturated, 40Hz).

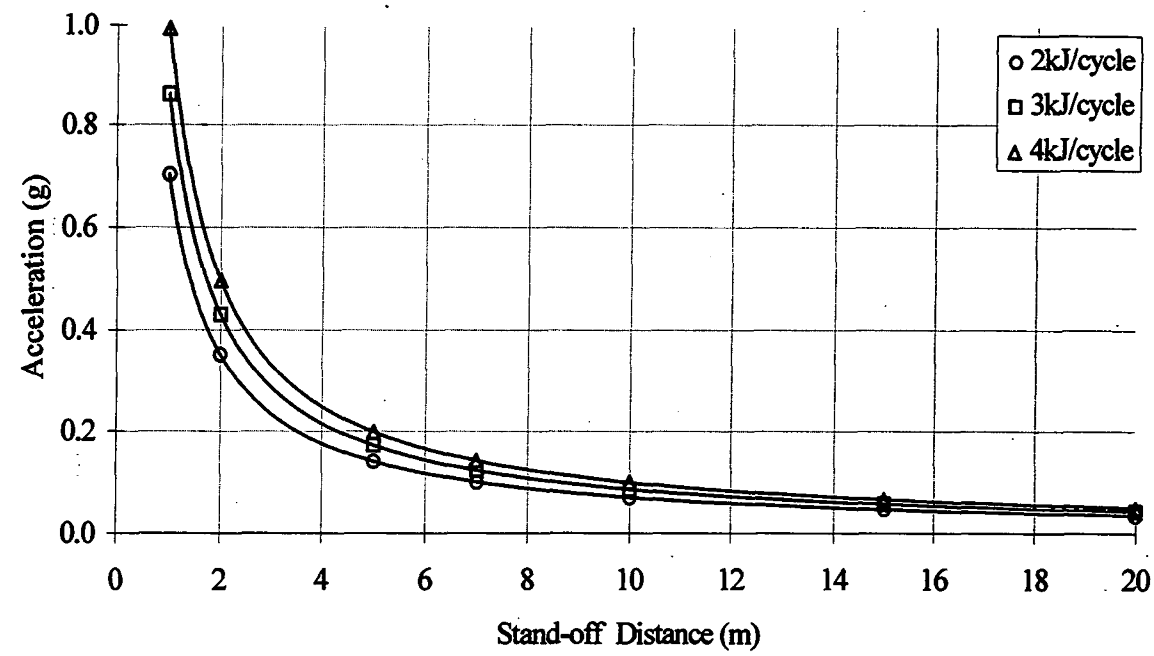

Figure 5.10.1. Attenuation of ground vibration with stand-off distance, using Equation 5.13.

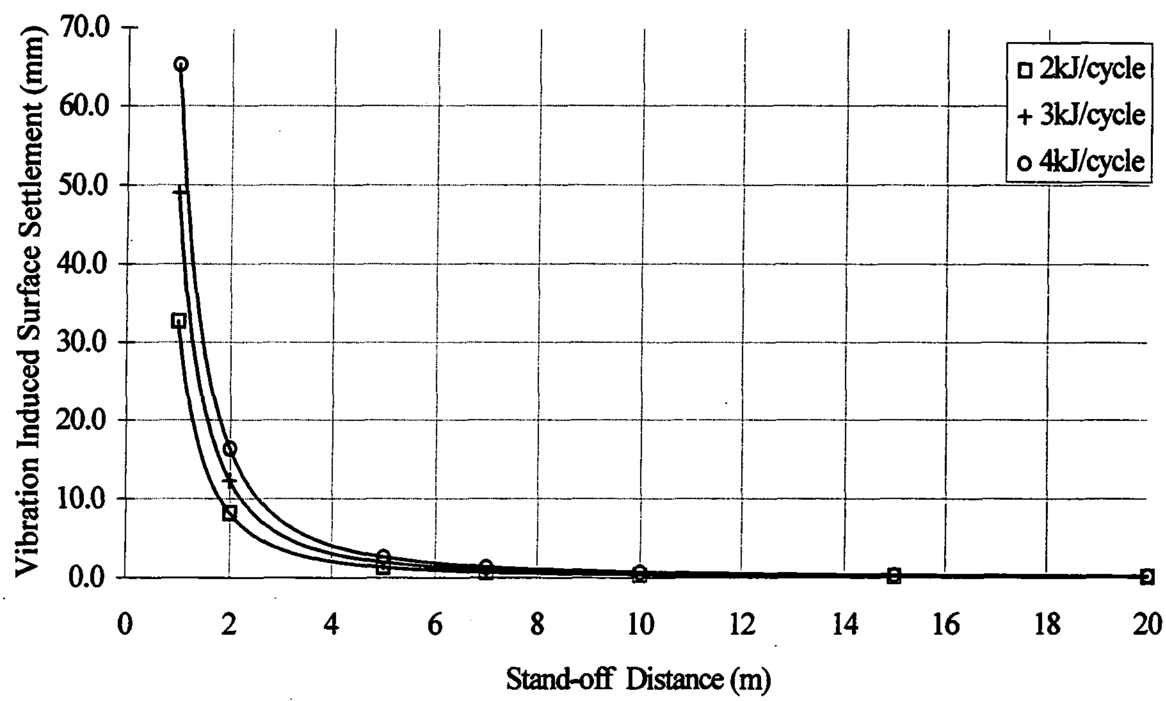

Figure 5.10.2. Surface settlement generated using Equation 5.13 and the vibration settlement equation, 5.8a (see Appendix 4: Table 4.1.1, for test data sheet).

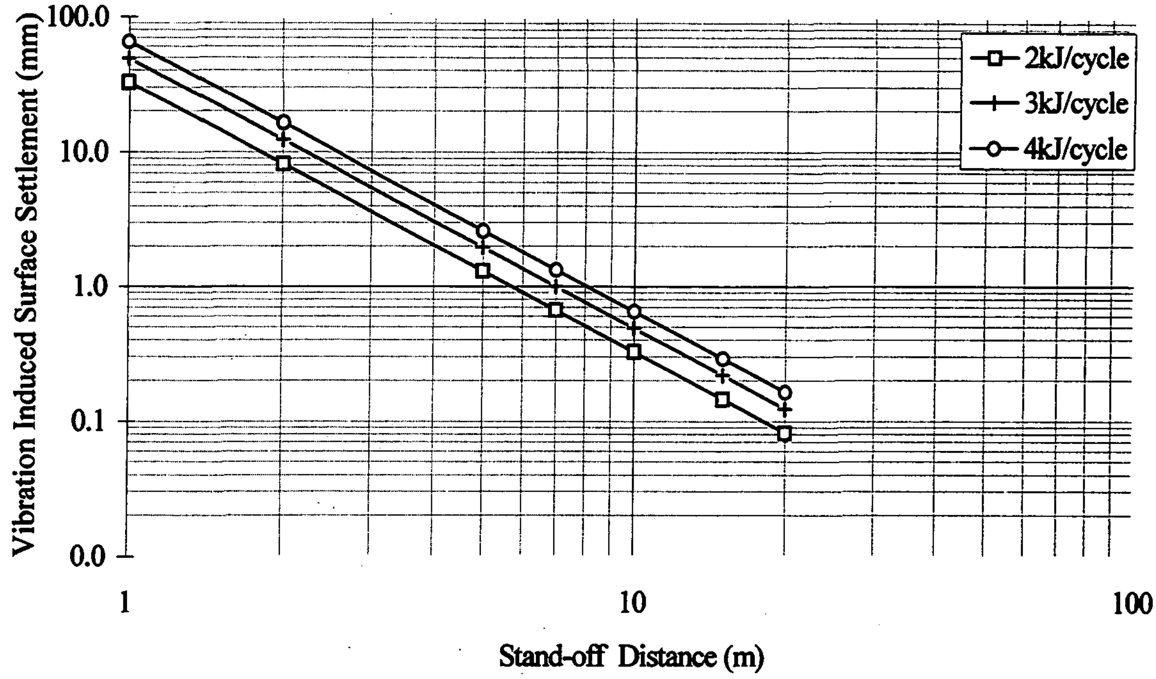

Figure 5.11.1a. Effect of vibrodriver (running at 25Hz) input energy on surface settlement (ground condition 1.1) (see Appendix 4: Table 4.1.1, for test data sheet).

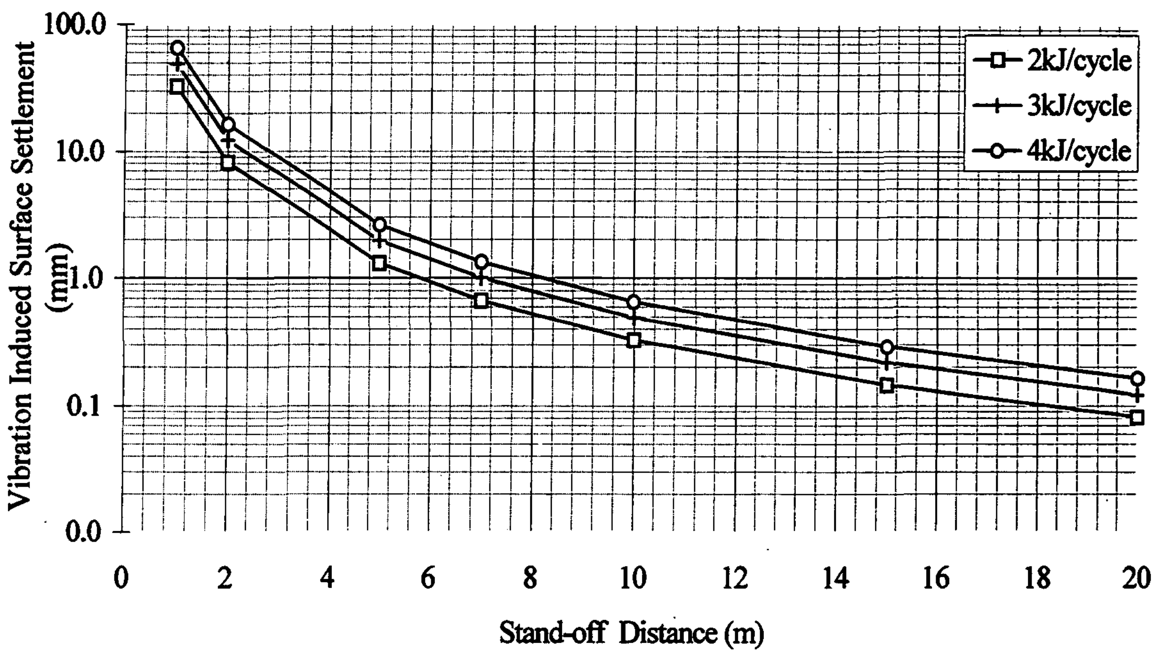

Figure 5.11.1b. As Figure 5.11.1a, semi-log plot.

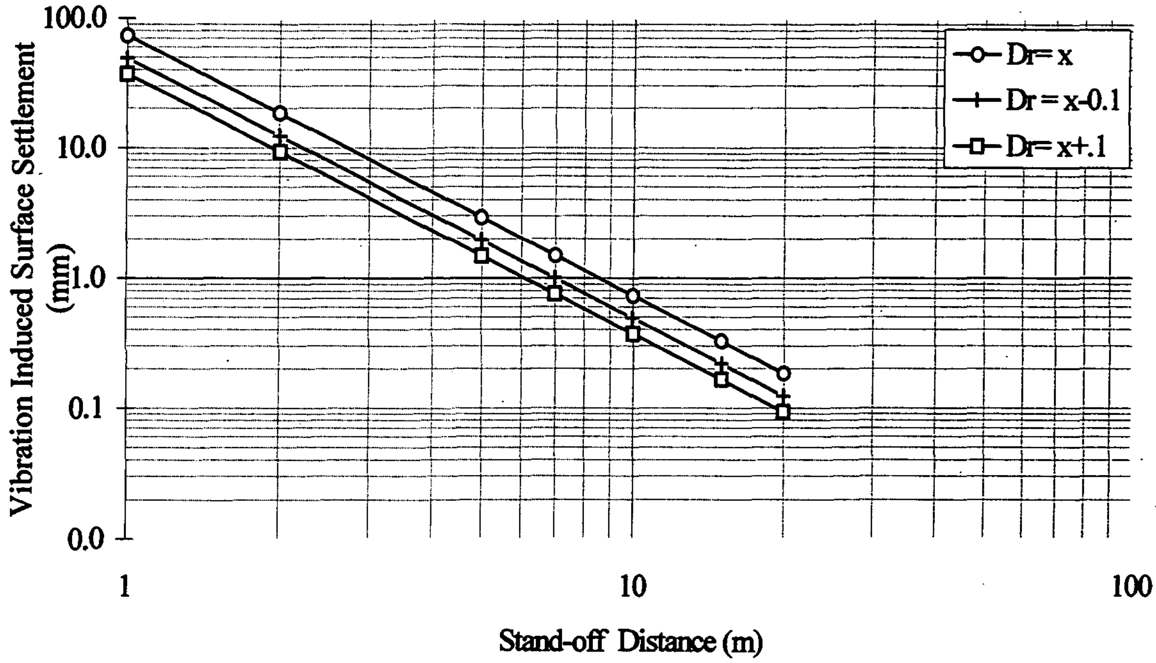

Figure 5.11.2a. Effect of varying relative density on surface settlement (ground condition 1.1, vibrodriver 1) (see Appendix 4: Table 4.1.1, for test data sheet).

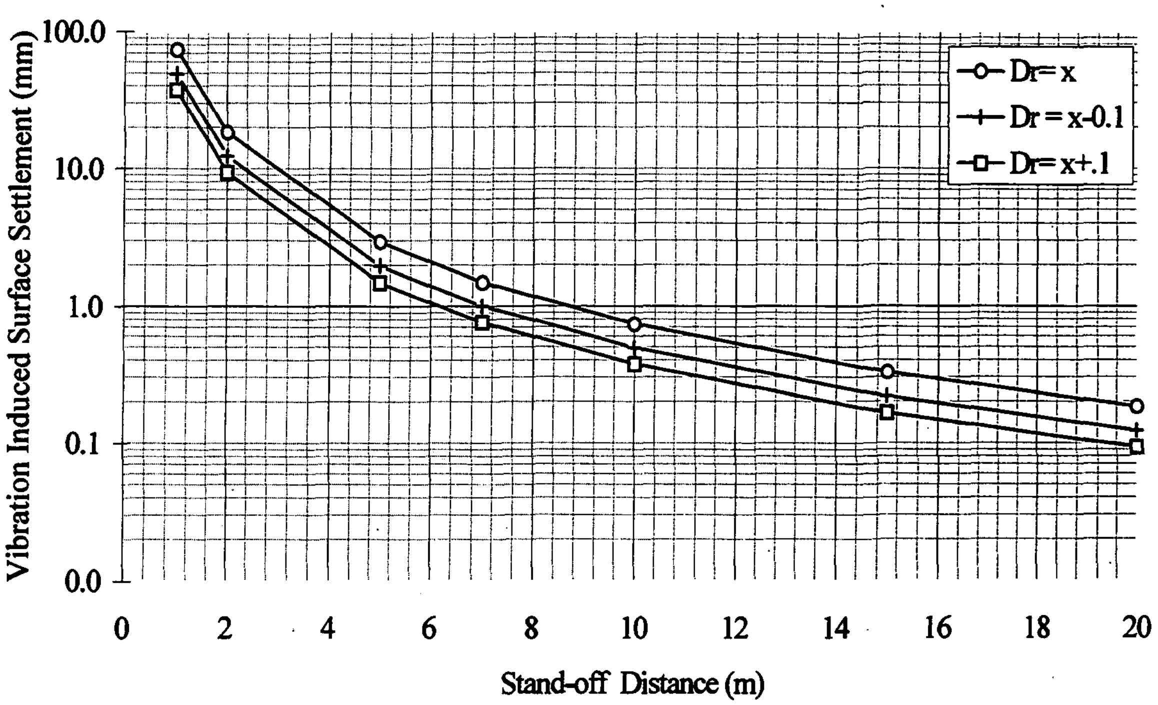

Figure 5.11.2b. As Figure 5.11.2a, semi-log plot.

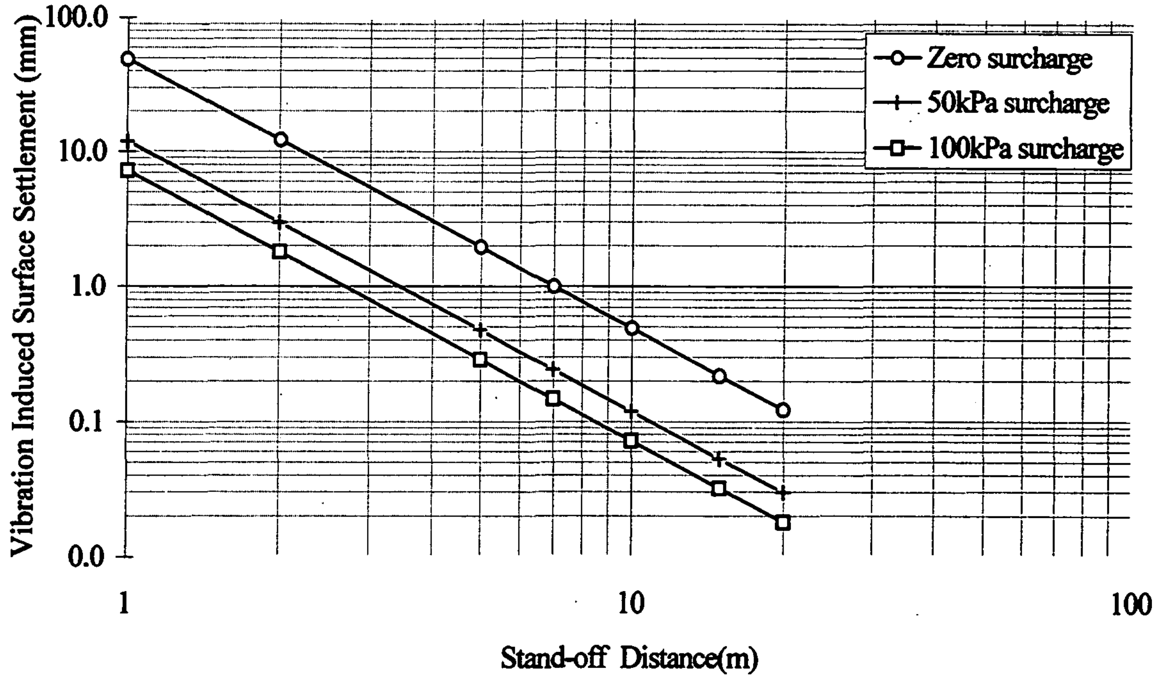

Figure 5.11.3a. Effect of varying surcharge on surface settlement (ground condition 1.1, vibrodriver 1) (see Appendix 4: Table 4.1.1, for test data sheet).

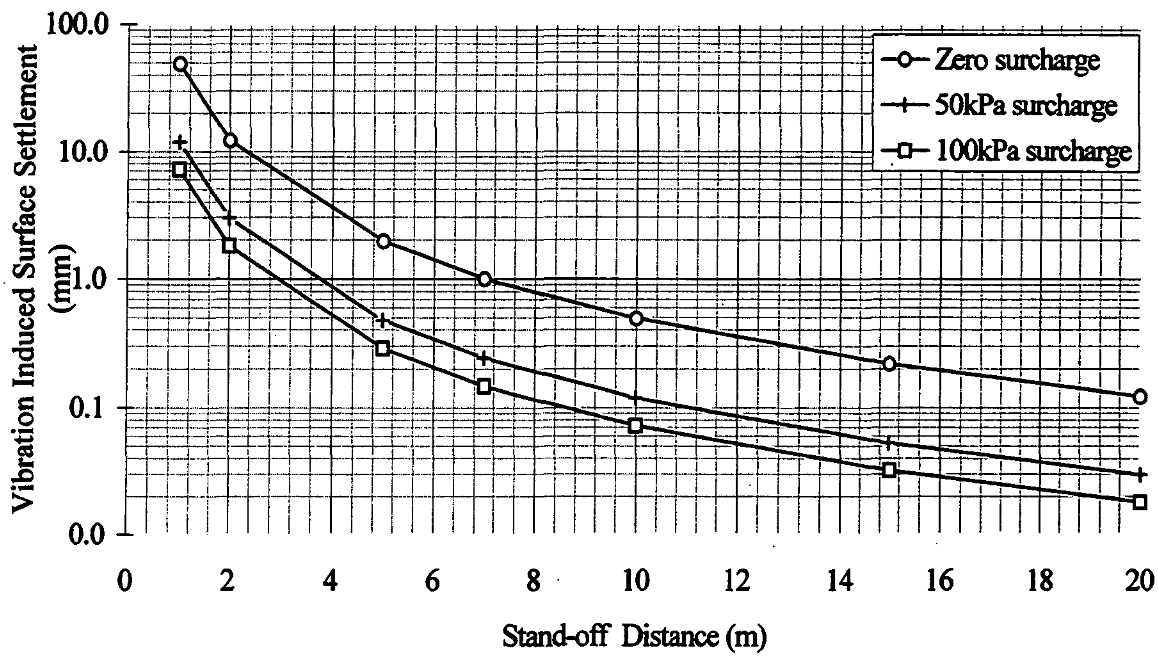

Figure 5.11.3b. As Figure 5.11.3a, semi-log plot.

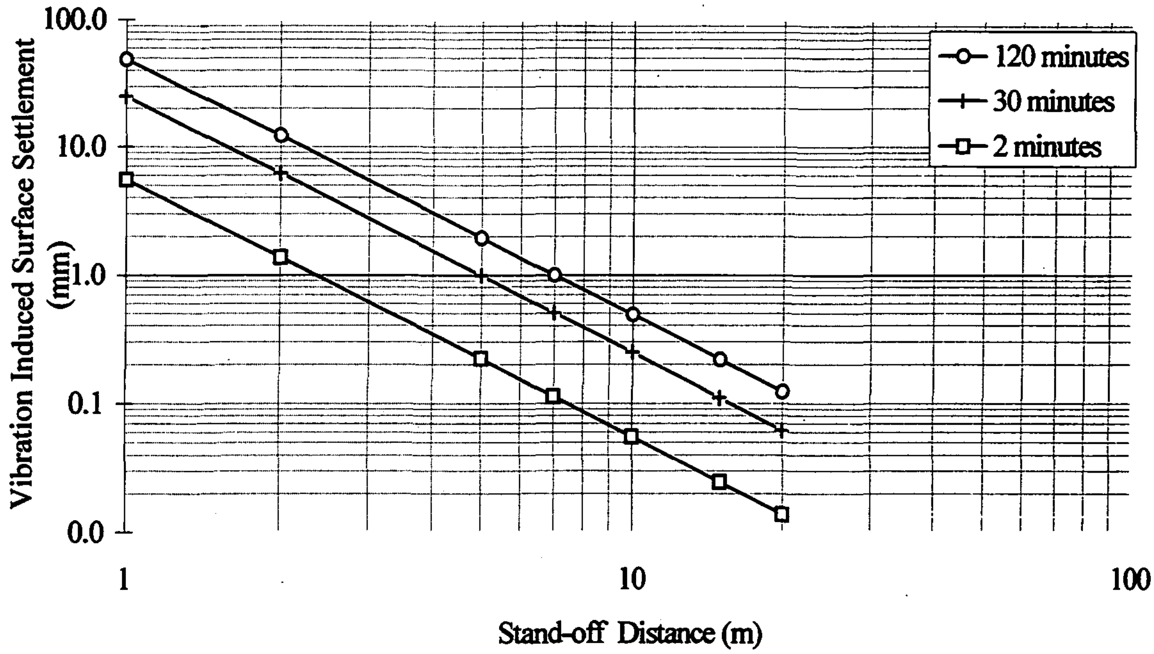

Figure 5.11.4a. Effect of varying vibration time on surface settlement (ground condition 1.1, vibrodriver 1) (see Appendix 4: Table 4.1.1, for test data sheet).

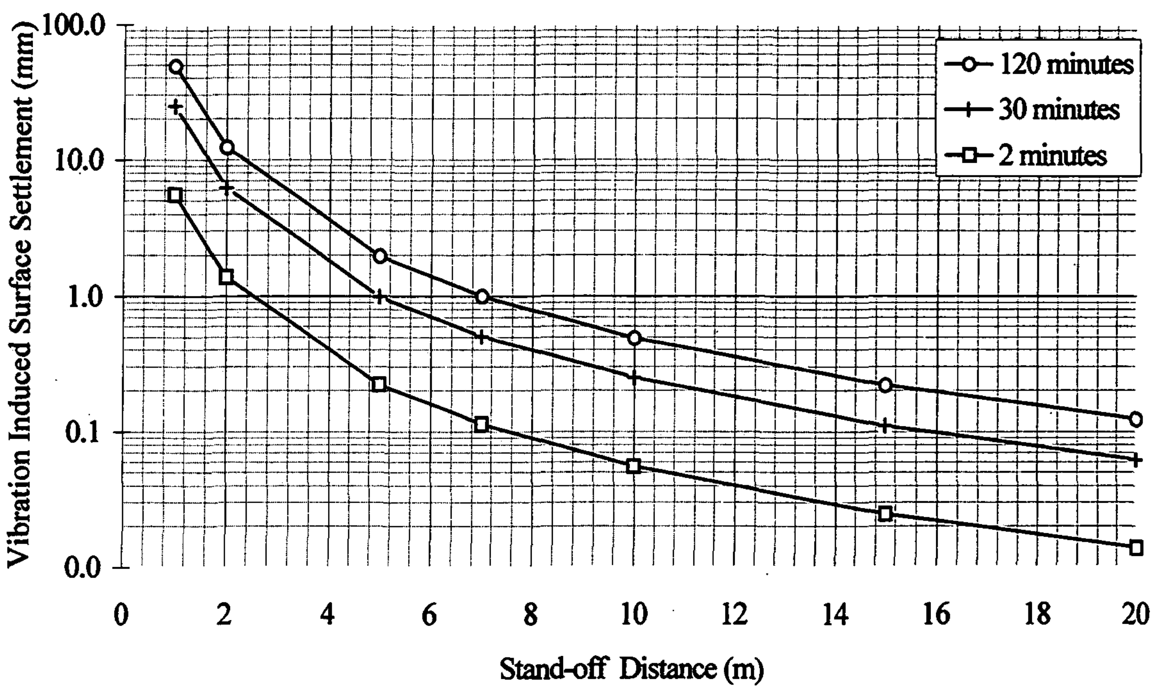

Figure 5.11.4b. As Figure 5.11.4a, semi-log plot.

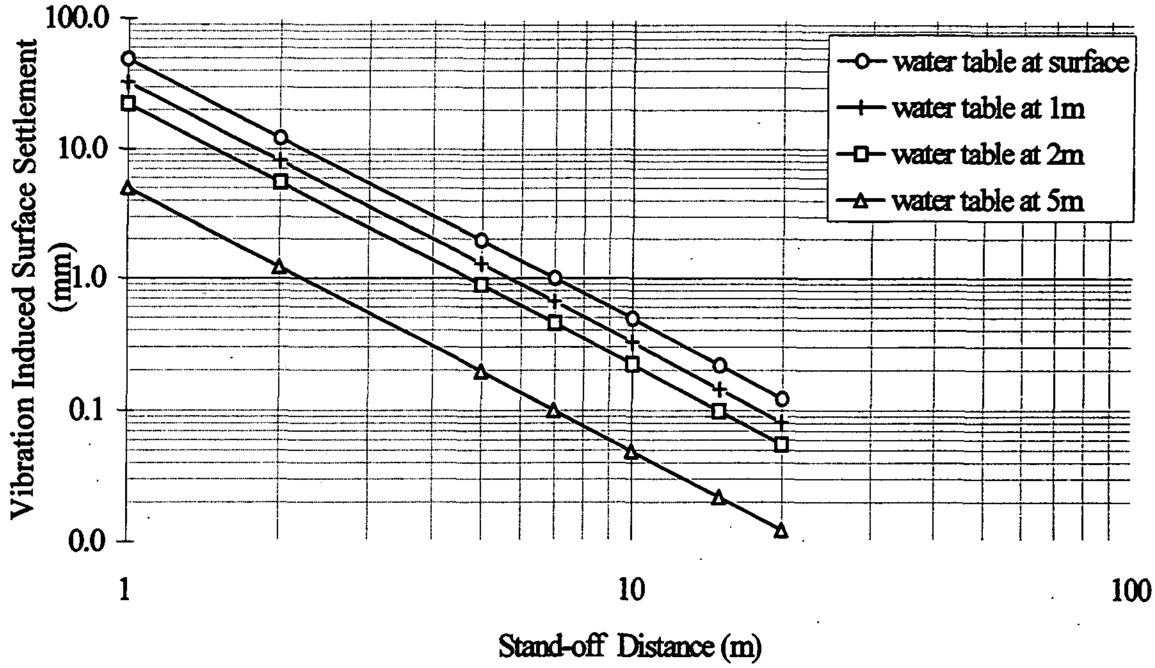

Figure 5.11.5a. Effect of varying water table position on surface settlement (ground condition 1.1, vibrodriver 1) (see Appendix 4: Table 4.1.1, for test data sheet).

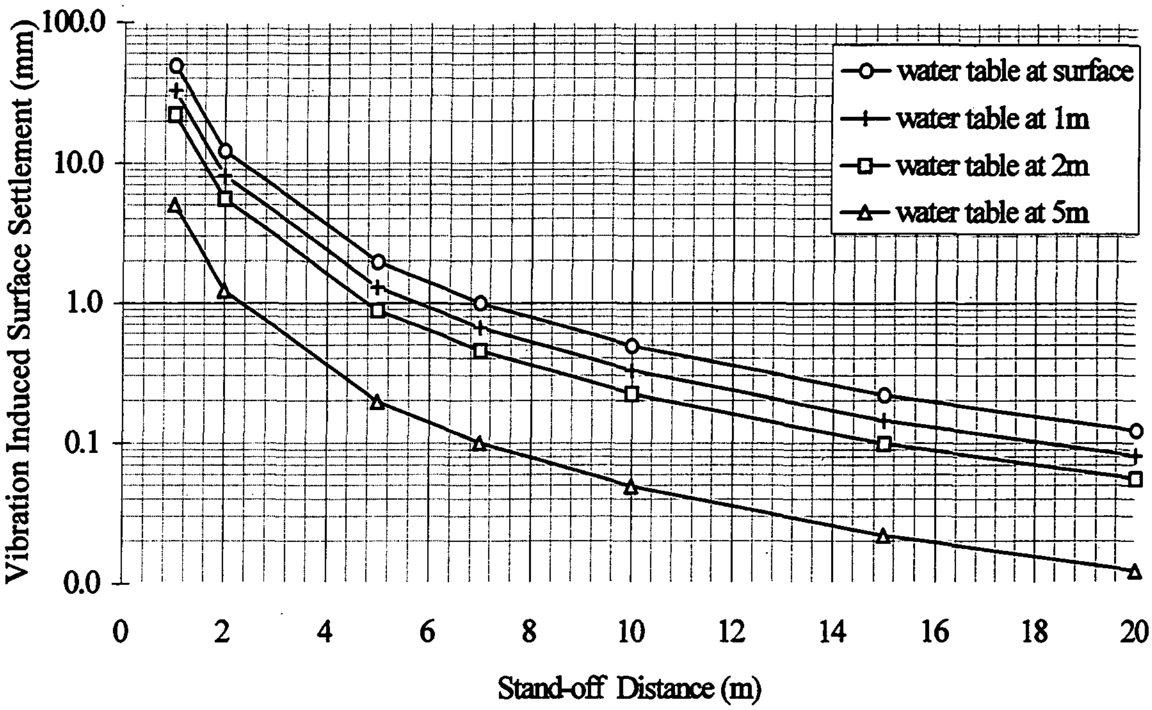

Figure 5.11.5b. As Figure 5.11.5a, semi-log plot.

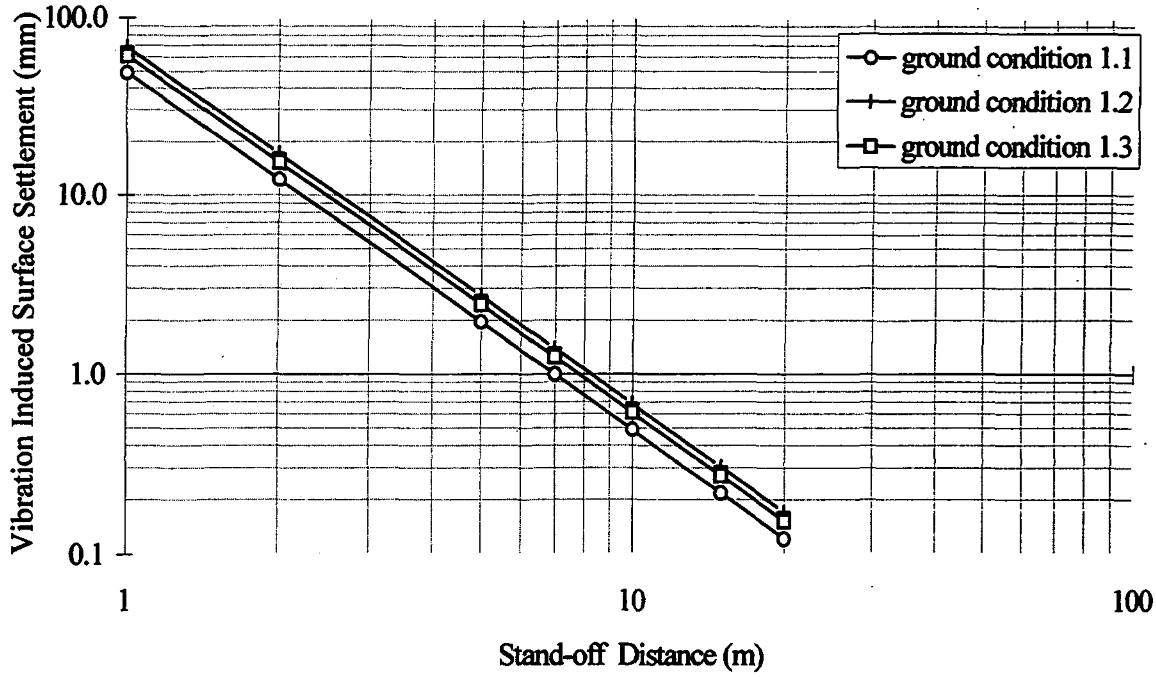

Figure 5.11.6a. Effect of varying ground condition 1.1 on surface settlement (vibrodriver 1) (see Appendix 4: Tables 4.1.1 - 4.1.3 for test data sheets).

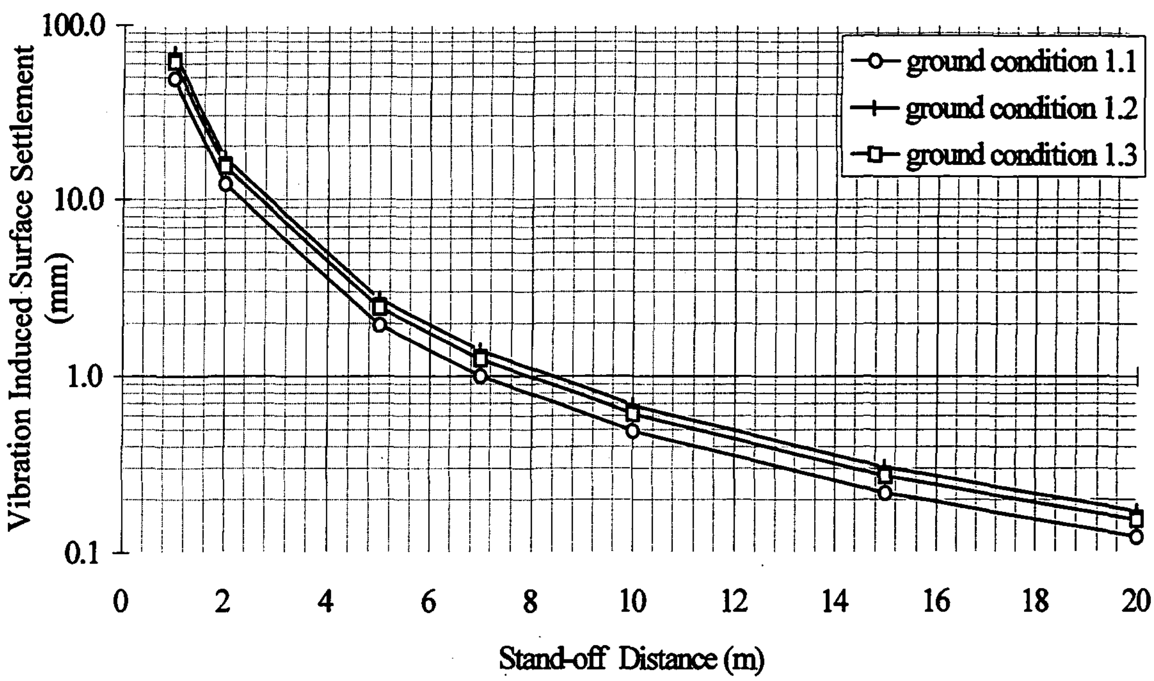

Figure 5.11.6b. As Figure 5.11.6a, semi-log plot.

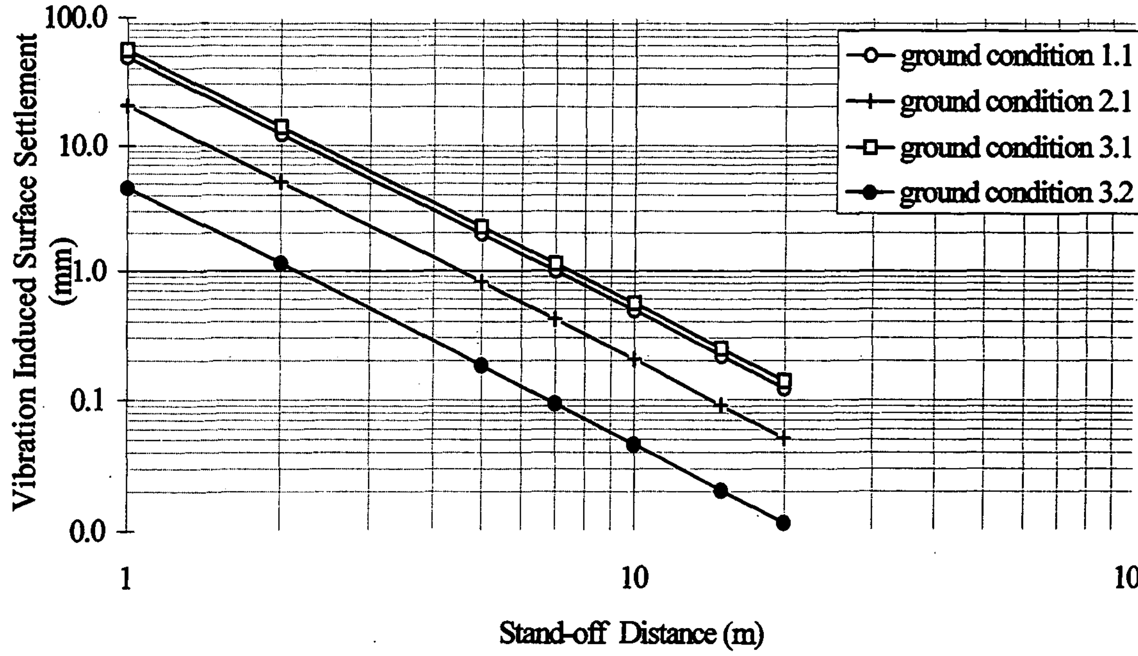

Figure 5.11.7a. Effect of varying ground conditions on surface settlement vibrodriver 1) (see Appendix 4: Tables 4.1.1, 4.1.4, 4.1.5 for test data sheets).

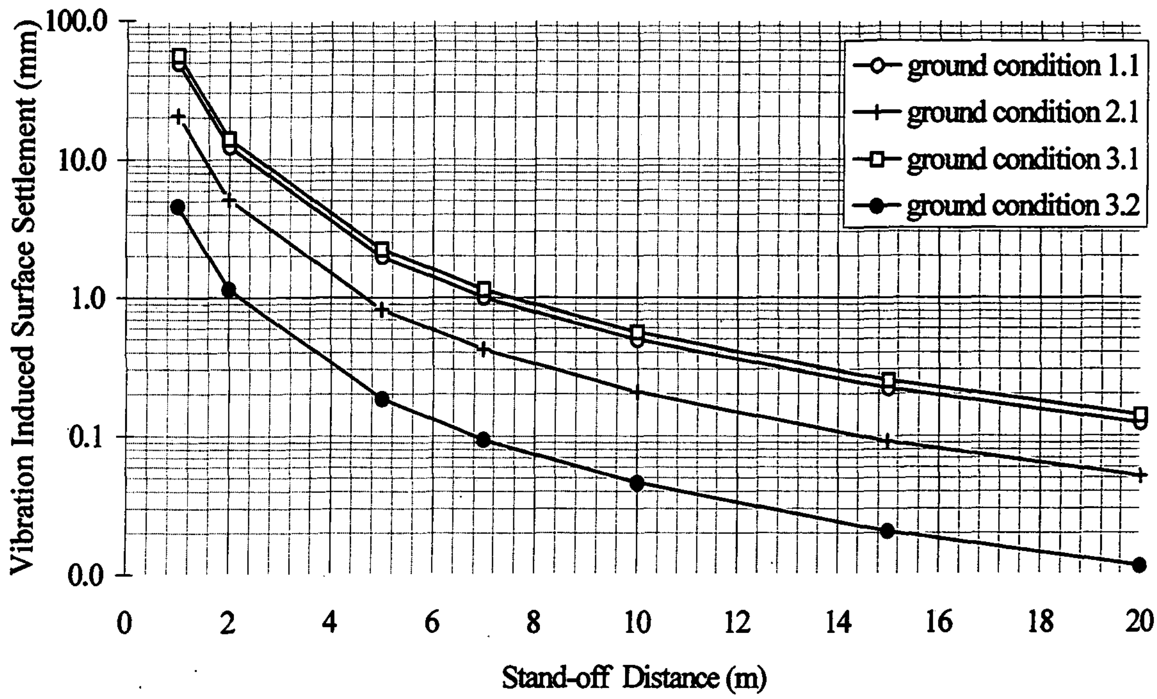

Figure 5.11.7b. As Figure 5.11.7a, semi-log plot.

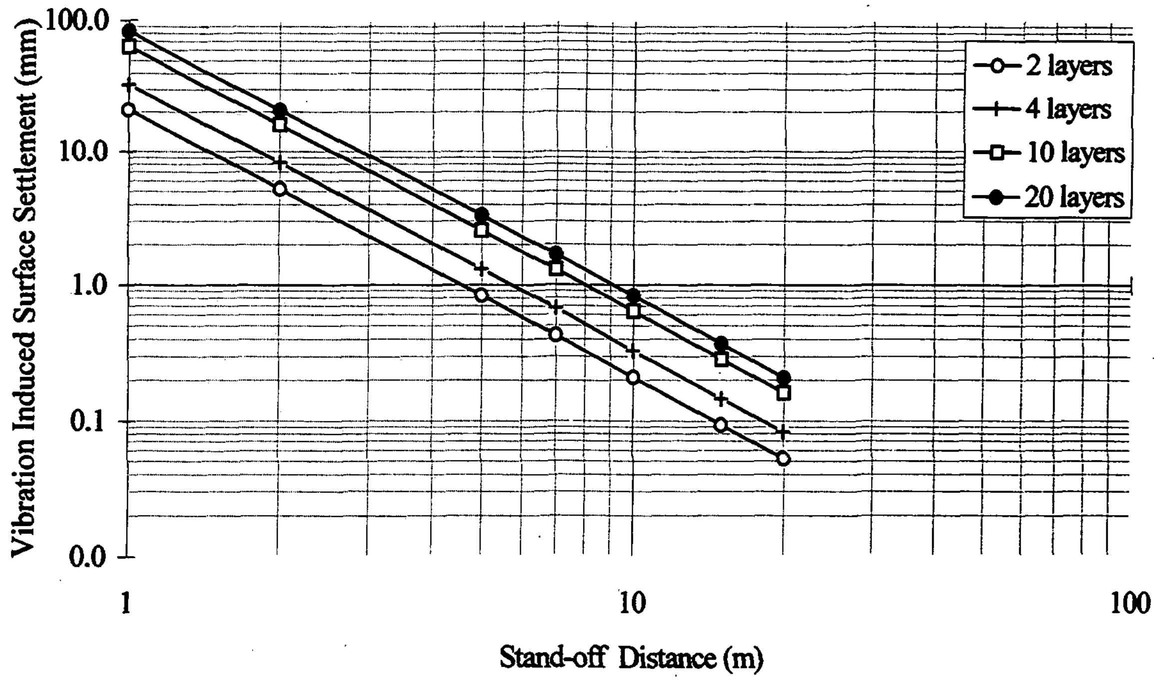

Figure 5.11.8a. Effect of layer resolution on surface settlement (ground condition 4.1, vibrodriver 1) (see Appendix 4: Tables 4.1.6, 4.1.7 for test data sheet).

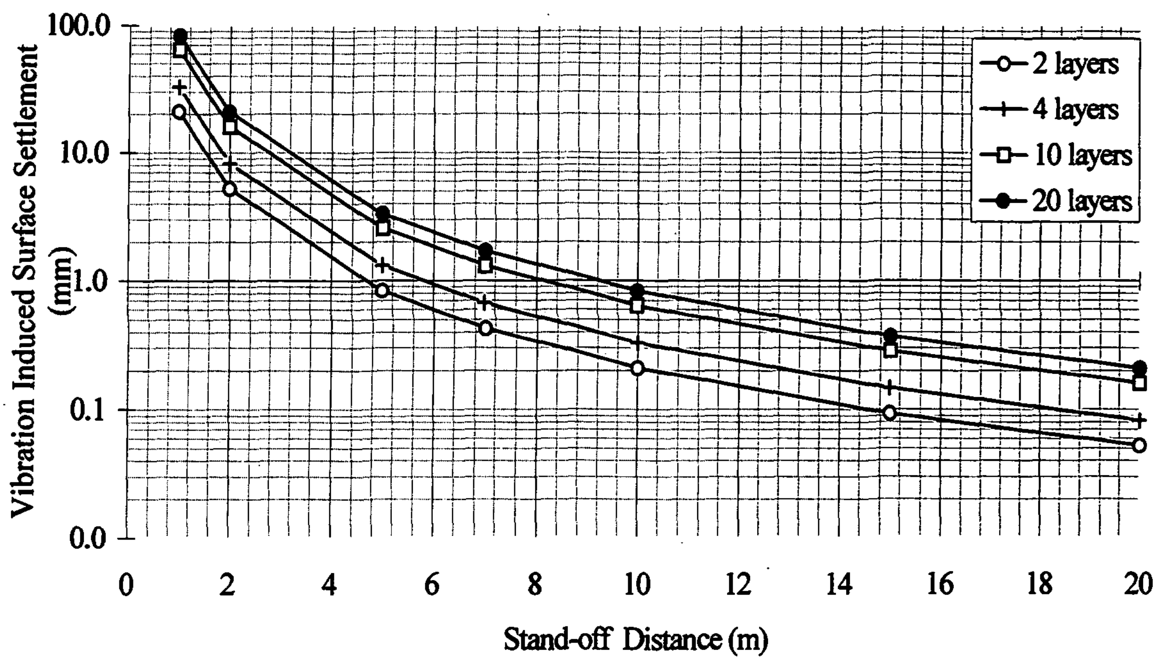

Figure 5.11.8b. As Figure 5.11.8a, semi-log plot.

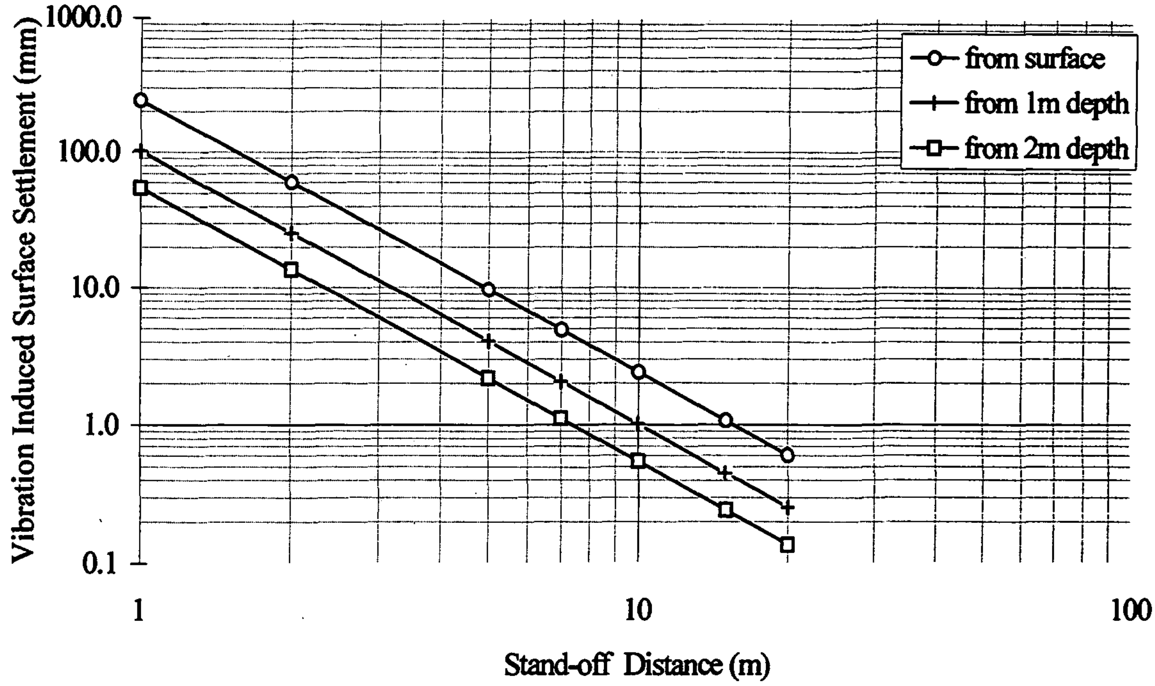

Figure 5.11.9a. Effect of depth below which settlement in calculated (ground condition 5, vibrodriver 1) (see Appendix 4: Table 4.1.8, for test data sheet).

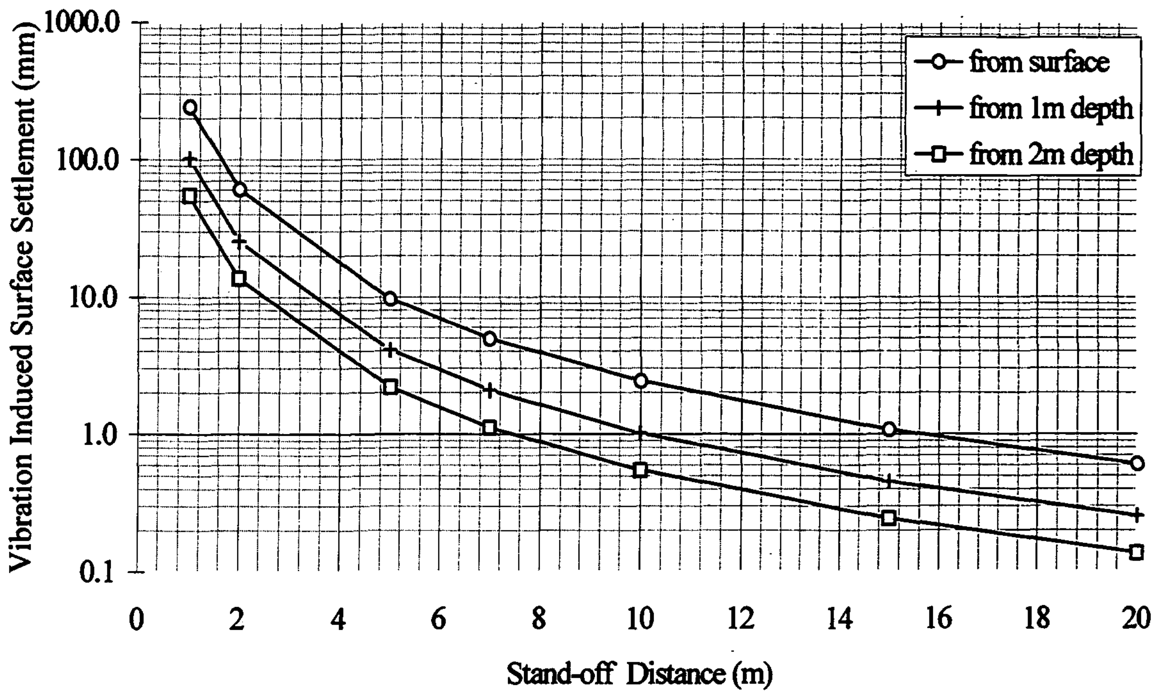

Figure 5.11.9b. As Figure 5.11.9a, semi-log plot.

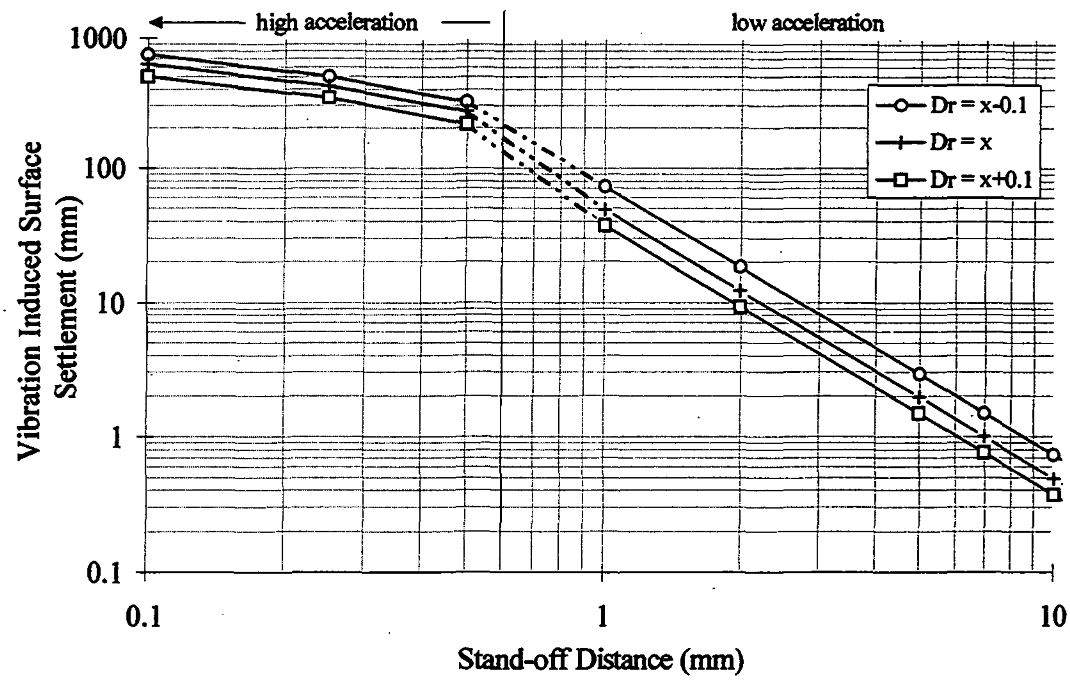

Figure 5.11.10a. Demonstrating the settlement generated using the high acceleration equation (ground condition 1.1) (see Appendix 4: Table 4.1.1, for test data sheet).

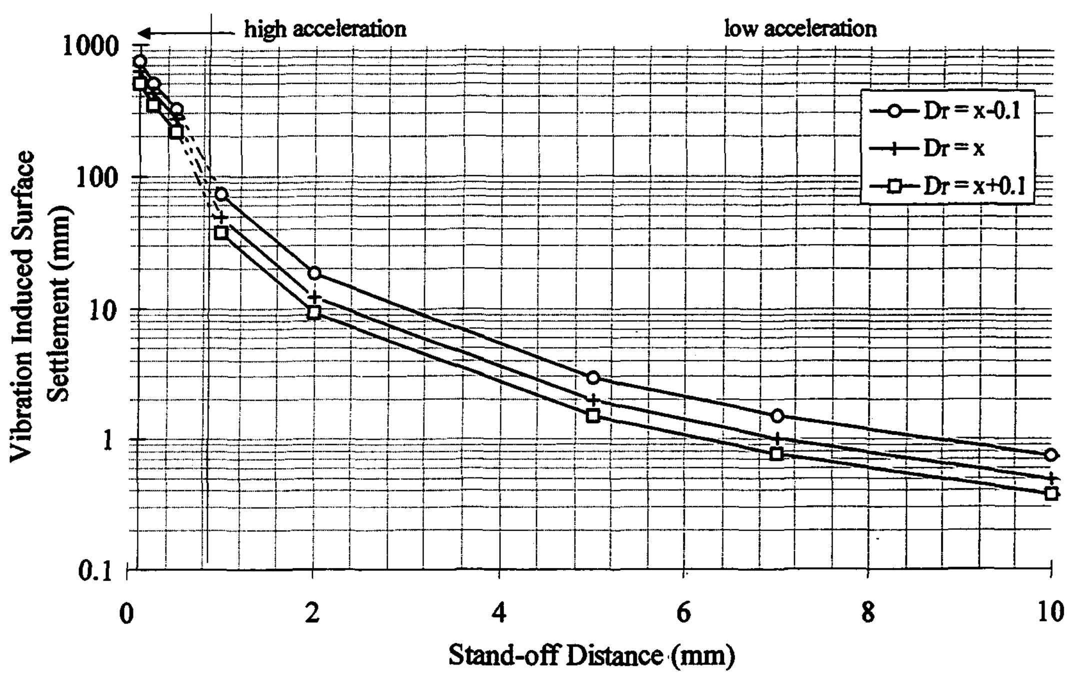

Figure 5.11.10b. As Figure 5.11.10a, semi-log plot.

CHAPTER 6
DISCUSSION

6.1 Introduction

The preceding two chapters detailed the laboratory apparatus, test procedure, results and analysis. This chapter discusses the laboratory programme and the data analysis that generated the research product which enables predictive estimates to be made of vibration induced ground compaction settlements. A number of ground settlement case studies from site work and the literature are compared with settlements 'predicted' using data that was abstracted from the case studies and used in the vibratory settlement equations. In addition, recommendations for further work are specified concerning adaptations of apparatus and test method: broad suggestions for further work are summarised in the following chapter.

No standard or novel laboratory test method can exactly represent the stress conditions experienced by equivalent *in-situ* soils. However, techniques such as the simple shear, triaxial or consolidation tests impose conditions that are representative of *in-situ* values, and force samples to behave in such a way that adequately models the behaviour of the *in-situ* soil. In addition, the way in which a sample is prepared can strongly affect stress-strain behaviour. With consideration of these factors, the laboratory method is discussed in terms of the use of the Rowe cell (see Section 6.2), side-wall friction, the difference between laboratory samples and *in-situ* equivalents and the sample preparation technique. The vibratory part of the test procedure is discussed in the context of different vibration orientations.

The influence of the test conditions that produced the observed sample behaviour is discussed in Section 6.3. The specific values of acceleration and static stress that were used during this research, forced the samples to behave in a way which might not be demonstrated by soils under 'free' conditions.

The regression data and selected parameters that enabled the derivation of the settlement equations are discussed in Sections 6.4. to 6.7. The application of the settlement summary tables that combined categories of settlement potential, risk and severity is discussed in Section 6.8.

Case studies are presented in order to demonstrate the reliability of the research (see Section 6.9). Comparisons are made between measured and estimated settlements, and reasons are suggested to account for the differences. Other mechanisms that account for or contribute to ground settlements associated with piling operations are highlighted.

6.2 Laboratory Method

6.2.1 Use of the Rowe Cell

Existing dynamic laboratory tests such as the resonant column, cyclic triaxial and cyclic shear tests are designed to model the effects of earthquakes, traffic and wind loading on soil. Such vibrations, in terms of duration and magnitude of frequency, acceleration and strains are of a different order than the ground vibrations that are generated during piling activities. Comparison of the influence of imposed test conditions and physical characteristics of test samples for cyclic tests and vibratory tests demonstrates that certain factors are common to both while some factors are different. For example, when describing (dry and free draining saturated) cyclic shear tests, Sawicki (1987) stated that: compaction depends on cyclic strain amplitude; compaction rate decreases with increase in number of cycles; compaction is independent of the frequency of cyclic load; compaction does not depend on the value of confining pressure and compaction is dependant on the initial value of relative density. However, Silver and Seed (1971b) considered that vertical stress may affect strains below 300kPa and strains that are less than 0.05%. In contrast, the results of this research programme demonstrated that vertical settlement is highly dependant on vertical stress, which was also reported by Oteo (1983). In addition, the acceleration that was required to initiate settlement increased with increase in static load, which was reported by authors such as Krizeck and Fernadez (1971) and New (1978a). On initial appraisal, it appeared that there was a fundamental difference in the behaviour of granular material that experiences cyclic stress-strain compared to granular material that experiences vibration. An examination of the literature suggests that the difference in behaviour can be attributed to the influence of stress and strain magnitude. When dynamic stresses are small compared to static loads, negligible compaction occurs (see Figure 3.10). This relationship is also dependant on acceleration magnitude, e.g. Whitman and Ortigosa

(1969) concluded that when dynamic stresses are small, compaction was negligible below acceleration of approximately 1.0*g*.

This research is fulfilling the need to examine the compaction effects that vibrations of the frequencies and accelerations appropriate to pile driving have on granular soil. The Rowe cell was used as the central apparatus of the laboratory test programme because loose sand samples could be brought to equilibration under appropriate static effective stresses. The standard cell required modification, and a novel sample preparation technique was developed that allowed good control during sample preparation. With the cell mounted on a powerful electromagnetic shaker, samples were vibrated unidirectionally at representative accelerations, and allowed to compact due to the action of the vibration and the maintained static load. The Rowe cell enabled the sample to experience the same disturbance, in terms of direct strain, wavelength and amplitude that an equivalent *in-situ* laboratory sized volume of sand would experience. The research generated upperbound estimates of ground compaction settlement, so the vibration tests were performed over an extended duration that also allowed the option of observing time dependant settlement behaviour.

In support of the research method, others workers such as d'Appolonia (1970), Krizek and Fernandez (1971), Brummund and Leonards (1972), Pyke *et al.* (1975), New (1978a), Oteo (1983), Kim *et al.* (1994), Kattis *et al.* (1995), have used direct vertical and/or horizontal sinusoidal vibration when modelling the effects of ground vibrations.

6.2.3 Side Wall Friction

In the Rowe cell, it is probable that not all the imposed vertical stress that is applied to the upper surface of a sample is transmitted to the base of the sample; there will be loss of vertical stress due to friction between the cell wall and the sample generated by the resulting horizontal component of stress. If the coefficient of earth pressure at rest (K_o) as taken as 0.5 (representative of a loose to medium dense sand), then the horizontal component (i.e. $\sigma_v.K_o$) acting on the cell wall as a result of the applied static loads that were used during the laboratory test programme are given in Table 6.1.

A test was performed to investigate the stress that was being transmitted through the sample to the cell base. A Rowe cell diaphragm was inverted between a modified cell base and body. The diaphragm was carefully filled with water, ensuring that no air was trapped, and a pressure transducer was fitted to the pore water pressure line (see Figure 6.1). A medium sharp sand sample was loaded to 100kPa and allowed to equilibrate under the imposed static load. The stress transmitted to the sample base was measured by the pressure transducer which showed the pressure that the water in the inverted diaphragm was experiencing. The resulting inverted diaphragm pressure showed that there was a 5kPa loss of stress between the upper and lower sample surfaces.

Vertical Stress (σ_v)	Horizontal Stress (σ_h)
10 kPa	5 kPa
20 kPa	10 kPa
50 kPa	25 kPa
100kPa	50 kPa

Table 6.1. Vertical stress and corresponding horizontal stress.

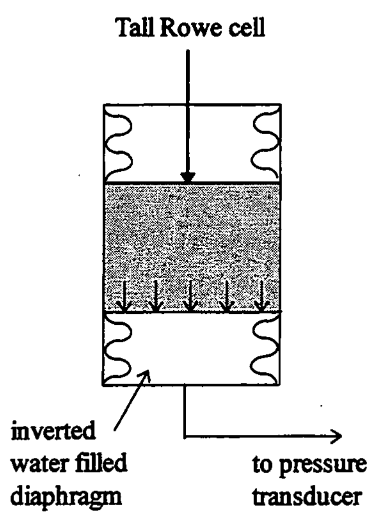

Figure 6.1. Testing the pressure applied to the base of the cell.

When performing standard Rowe cell tests on fine grained soils, it is suggested that to reduce the friction between the cell wall and sample to a negligible level, a thin layer of silicone grease should be applied to the internal surface of the cell body (BS 1377: Part 6: 1990). As part of standard shear box testing, a series of tests were performed that sheared sand samples against a cold rolled aluminium plate with and without a thin application of silicone grease, separated by a piece of sample confining bag (SCB) material. These tests were mainly performed on saturated samples, although a limited number of dry and partially saturated samples were tested (see Table 6.2).

Sample	Sand-sand	Sand-membrane-plate
FUS	29	27
SFS	33	26 (25)
GMS	30	27 (19)
MUS	32	26
MLB	37	22, 22, 19 (20)
CLB	32	24 (psat)
MSS	32	27 (19)(22)
SFG	-	-
SFMG	35	27
	Sand-membrane-plate	
	Silicone grease	Silicone spray
CLB	25, (21)	27, (19)

Table 6.2. Comparison of ϕ values for the soils, and the interface friction angle under various test conditions. Data in brackets represents data for dry samples (see Appendix 1).

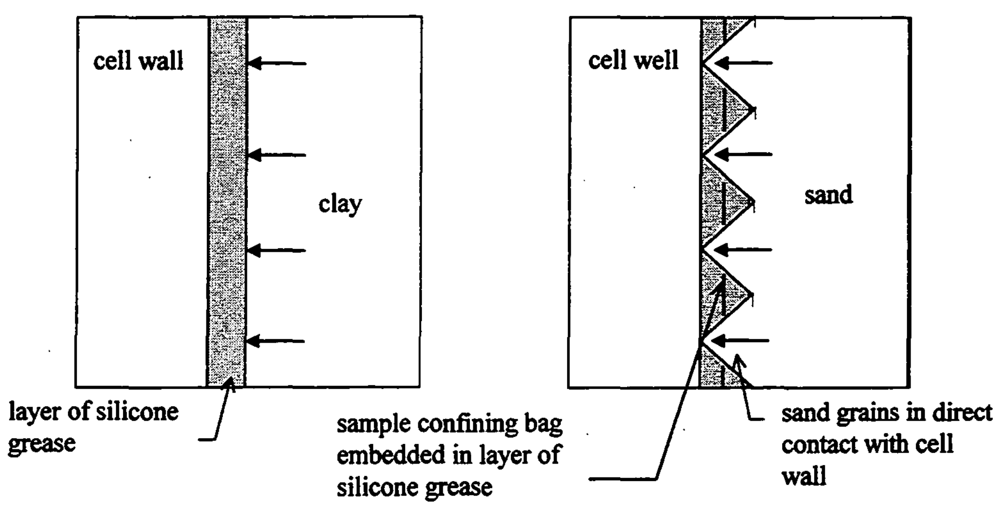

Figure 6.2. Comparison of the wall friction of fine grained soils and tests that use coarse grained soil.

The shear tests that modelled sample-SCB-cell wall friction demonstrated that the presence of the SCB material tended to generate an apparent friction angle of approximately 27° for saturated samples and about 19° for dry samples (dry samples were air pluviated, and not dried-back from saturated). The tests also suggested that the use of silicone grease or silicone spray, had a negligible effect on sample-cell wall friction. In addition, it was observed that the use of silicone grease tended to cause the SCB material to adhere to the aluminium plate, although no discernible values of cohesion were generated. Because the use of silicone grease (or spray) did not appear to reduce sample-cell wall friction, it was considered to be prudent not to use it in the bulk of the laboratory test programme. Using silicone grease could have created an unnecessary variable in the settlement behaviour of vibrated samples; for although in a static shear test it appeared to have no effect, it might or might not have had an influence on settlement during vibratory testing. Silicone grease is reported to work well with fine grained soils to reduce friction because the soil is presented to the cell wall as a smooth material. Because of the relatively large grain size of sand, discrete particles were pushed through the silicone grease to come into direct contact with the cell wall, maintaining the frictional contact that would have occurred without the application of silicone grease (see Figure 6.2.)

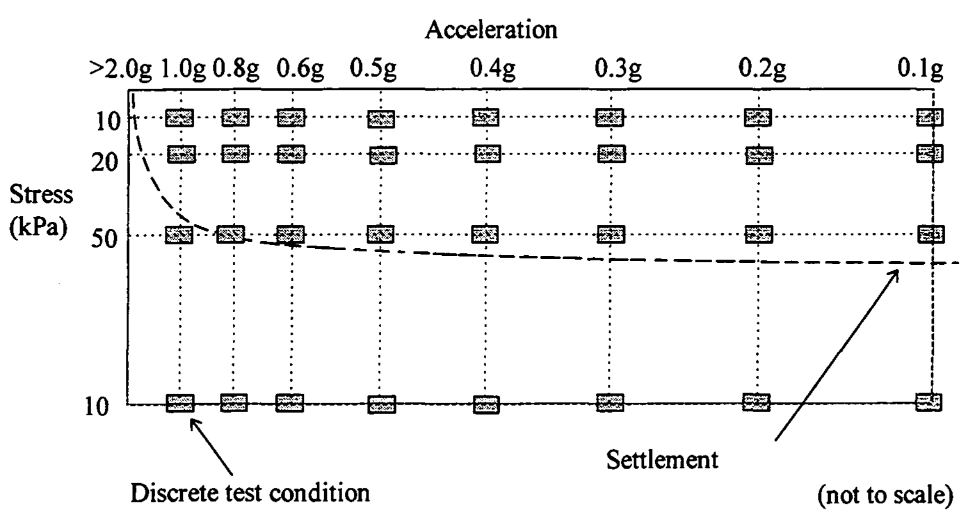

Figure 6.3. Illustrating the discrete points in a soil profile that the low acceleration laboratory test programme models.

6.2.3 Difference Between Laboratory Sample and *In-situ* Equivalent

In the laboratory test, samples settled as discrete units; in reality, settlement is experienced by single sand particles that are inter-relating with neighbouring particles during vibration. A particle that is nearer to the source will have more energy supplied to it and a greater potential for settlement. In a homogenous granular material, the net result of this would be a curved settlement surface, of increasing gradient towards the source. The laboratory testing models a grid of discrete *in-situ* laboratory sized samples (see Figure 6.3.), and identifies trends of settlement behaviour interpolated between specific test conditions.

The friction that an *in-situ* soil particle has to overcome in order to move relative to a neighbouring particle, for given conditions, is the internal angle of friction for that particular material. In the laboratory sample, the friction between the cell wall and the sample is less than the internal angle of friction of the sample. The laboratory sample is laterally confined, allowing no horizontal strains to develop. It is assumed that this condition applies to the *in-situ* soil, although in certain construction operations, lateral strains are developed (see Section 6.12) for example, when sheet piles suffer lateral movement.

Laboratory samples may have demonstrated a non-uniform variation in stress gradient. However, the value of relative density of a sample represented the sample of soil as a whole and did not define changes in density on the smaller scale. In addition, the vibratory settlement equations did not assume that relative density was dependent on the magnitude of applied vertical stress, but that settlement was inversely proportional to the product of stress and relative density. This is consistent with *in-situ* granular soils; if a number of soil profiles are compared at specific depths, a variety of relative density values will be observed. If there is a variation in the density of the laboratory sample as a result of say, arching; the net value of relative density is the product of those parts of the sample that are less dense and/or less stressed (with more settlement potential) and the more dense and/or stressed parts (with less settlement potential).

In addition to the consideration given to small-scale sample stress-density variation, observation of the large scale, *in-situ* condition, should also be made. The percentage settlements that were obtained from laboratory samples in the order of 70mm in height, are applied to much greater volumes of *in-situ* soil, where the potential for local variations in stress and density (and soil type) exists. Since such variations cannot reasonably be quantified, their specific effects on surface settlement are an unknown, i.e. site investigation data is assumed to provide reasonably accurate and representative data of ground conditions that may have greater variation than indicated. Like all laboratory testing, the assumption was made that the settlement behaviour of a small volume of soil can be used to predict the behaviour of *in-situ* volumes of soil that are orders of magnitude larger.

6.2.4 Sample Preparation Technique

Tests were performed on saturated, dried and partially saturated samples of several granular soils. The sample preparation techniques that are available such as tamping, pluviation and the slurry technique are described in Section 3.5.4 (e.g. Lambe 1957, Keurbis and Vaid, 1988). The initial laboratory tests were performed using air or water pluviation. Pluviation was performed in order to form samples that were as loose as possible, prior to the application of static load. The vibratory settlement obtained for these samples was considered to be very high, and unlikely to represent a naturally deposited sand; laboratory samples formed using the simple at-moisture-state technique were assumed to be representative of recently placed fill material. Additionally, the naturally occurring dry or partially saturated soils that are encountered in civil engineering practice in the UK are unlikely to have been deposited in their present moisture state.

The sample preparation method was modified to model soil formation that most closely matched natural soil formation process. All samples were water pluviated to allow initial consolidation in the saturated state, which modelled fluvial depositional process, i.e. initial deposition in a river system, and subsequent burial (and static consolidation) by later material. Samples that required testing in the dry or partially saturated state were allowed to dry-back to the required moisture content. These samples were then subject to re-application of the appropriate static load, prior to vibratory testing. It was proposed that this method modelled a granular material that was deposited in water, consolidated and then subjected to drying-back, due to a changing river course, and climatic or seasonal variation.

These early tests incurred a high failure rate and it was considered that too much time was being spent performing repeat tests. The main form of test 'failure' was due to the jamming and partial vertical rotation of the load drainage disc, as a result of particle migration. It was necessary to ensure, in the first instance, that vibratory sample settlement was due solely to a reduction in the void spaces, and not due to loss of material from the sample mass. In addition, the reduction in the sample height should be uniform and horizontal, and not due to deformation and compaction caused by load/drainage disc rotation (see Figure 6.4).

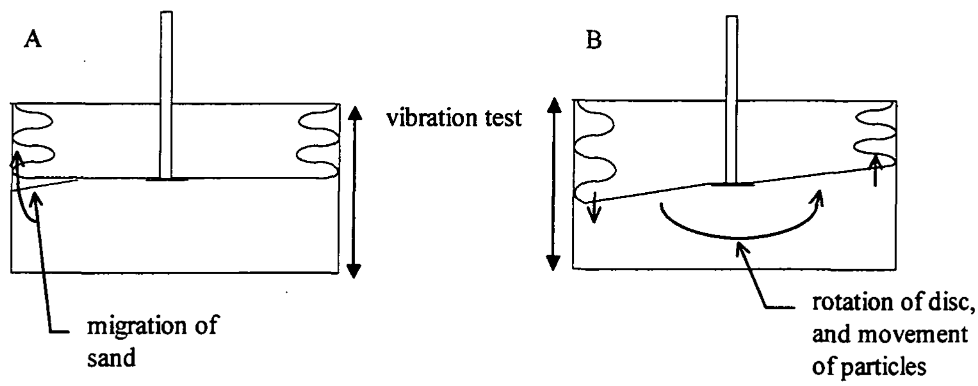

Figure 6.4. Illustrating the problem of sample migration and disc rotation.

A method that prevented sample migration was required and Section 4.6.2 details its development. The use of a novel disc-in-place sample confining bag technique was considered to be the optimal method for the research programme. Krizek and Fernandez (1971) used a rubber or felt gasket (or 'collar') to seal the load disc against the cell wall to prevent migration of dry clayey sand during vertical vibration tests. Such a seal was not required for partially saturated vibratory tests. In the present research programme, all samples were initially consolidated in the saturated state, so a rubber/felt collar would be required in all cases. It was also considered that a rubber gasket would have introduced additional and unnecessary friction between the sample and cell wall, which could have adversely affected sample sensitivity to low vibration levels. In addition, it was considered that use of a felt gasket was not appropriate because its use may have only *reduced* and not *prevented* sample migration.

The sample preparation technique that was used during the laboratory research programme combined elements of water pluviation and the slurry technique. When testing samples, it was required that each sample was identical to all the others, so that when different test conditions are imposed, such as static load and vibration, the variation in soil response was due directly to the effects of the different test conditions and was not affected by variations in the samples that were being tested. The likelihood of sample variation increases as the fines content increases, the particle size distribution widens and sample size decreases. Thus it was conceivable that the silty fine sand, medium sharp sand, sandy fine gravel and the sandy fine to medium gravel would be more susceptible to sample variation than the uniform materials. However, because the wet mass of samples was in the order of 2.5-3.0kg and the bulk samples were thoroughly mixed prior to removal of a sub-sample, it was considered that any given sample had a particle size distribution that adequately represented that of the bulk sample.

During sample preparation, the placement of material into the sample confinement bag (SCB), and the subsequent removal of the confined sample to the cell, resulted in a degree of sample segregation in the susceptible materials. However, because the sample was confined by the SCB, the gross movement (potential) of the larger particles would be reduced. Similarly, finer particles would have had their potential for movement reduced locally by the presence of the larger particles. The movement of fines was subsequently demonstrated as cloudy water, that was observed moving along the back pressure line during initial application of static load, and under an acceleration of 3.0*g*. However, the cloudy water was assumed to have removed only a small fraction of fines from the sample and upon cell disassembly and removal of the sample for moisture content determination: the water draining from the sample appeared to be as cloudy as that prior to test preparation. In addition, it was considered that *in-situ*, when water is migrating through a granular soil containing a fines fraction, some of these fines would be removed by the passage of the water. Thus, rather than modelling an equivalent *in-situ* soil less accurately, because of the removal of 'cloudy water', a laboratory sample that experienced some fines migration may actually more closely approximate the *in-situ* process than a method that prevented fines migration.

Achieving the complete restriction of the movement of fines from samples would have created more problems than it would have solved. In the first instance, the flow rate of water from the sample would need to be very low in order to prevent disturbance of the fines. A fine filter material could have been used, which would have become blocked by the fines and reduced the flow rate of water from the sample. Such restriction on the free movement of water would have adversely affected the bulk response of a sample, in terms of causing erroneous pore water pressure generation and dissipation during initial consolidation. The subsequent vibratory settlement character would have been affected to some extent by restricted flow, i.e. the vibratory test would have effectively proceeded in the undrained condition, or caused the granular material to behave like a material with much lower permeability.

The problem of blockage caused by fines was encountered during preliminary testing. Initially, top and bottom sample drainage was used. It was found that the drainage point in the cell base became blocked when samples with fines were tested; the top drainage point remained clear. This effectively caused tests to proceed with top drainage only. This did not occur when the clean uniform sands were tested. However, in order to standardise the test method, all soils regardless of their fines content were tested in the same way, i.e. using top drainage only.

Although test samples were representative of their bulk samples, in terms of particle size distributions, the actual distribution of the particles within a test sample may not have been homogeneous. Producing identical samples in terms of particle size distributions was not possible. However, because vibratory settlement was seen to be a function of sample grading, it was considered that for a given soil-type, with a wide range of sample size, net settlement would have been the product of the settlement of the zones containing smaller particle size, with less settlement potential, and zones of larger particle sizes, with greater settlement potential. Any conclusions that were made regarding the behaviour of samples under particular test conditions were determined by the intrinsic properties of the discrete soil types, and not significantly affected by heterogeneity of the test sample or variations between samples.

6.2.5 Vibration Duration

The vibration time of laboratory tests were of the order of 1 hour per acceleration increment. Thus, after testing up to 2.0*g*, a maximum vibration time of up to 9 hours was imposed on the soils: the high acceleration tests which used fewer acceleration increments, took approximately 5 hours to complete. Under normal driving conditions, a pile may only take a minute (or less) to be driven to level. Thus, vibration time of 1 hour per acceleration increment may be considered excessive. However, if more than one pile is driven, a particular stand-off position may experience a range of vibration levels over a more prolonged period as the piling operation proceeds and the distance between a particular point on the ground surface varies. For example, at the start of a project, point (A) (see Figure 6.5) experiences an acceleration of approximately 1*g* at a stand-off distance of 0.5m. At a stand-off of 5m point (B) experiences 0.4*g* for one minute (i.e. the time to drive the first pile to level). As the piling operation proceeds, points (A) and (B) will receive progressively less vibration, and will not exhibit additional settlement because the soil is at equilibrium with the prevailing static loads and the higher energy levels of previous higher acceleration. Point (C) and (D) will experience increasing levels of vibration as the piling proceeds. Point (C) will not experience more vibration than point (B) (i.e. about 0.4*g*), whereas point (D) at 0.5m stand-off, will experience increasing levels of vibration of up to approximately 1.0*g*, and increasing levels of settlement. The laboratory test method, that uses increasingly higher acceleration increments, directly models the experience of the soil at point (D).

However, if driving conditions are difficult, then the vibration time per pile may increase to many minutes, for example, approximately 40 minutes per pile was reported by Todd (1994).

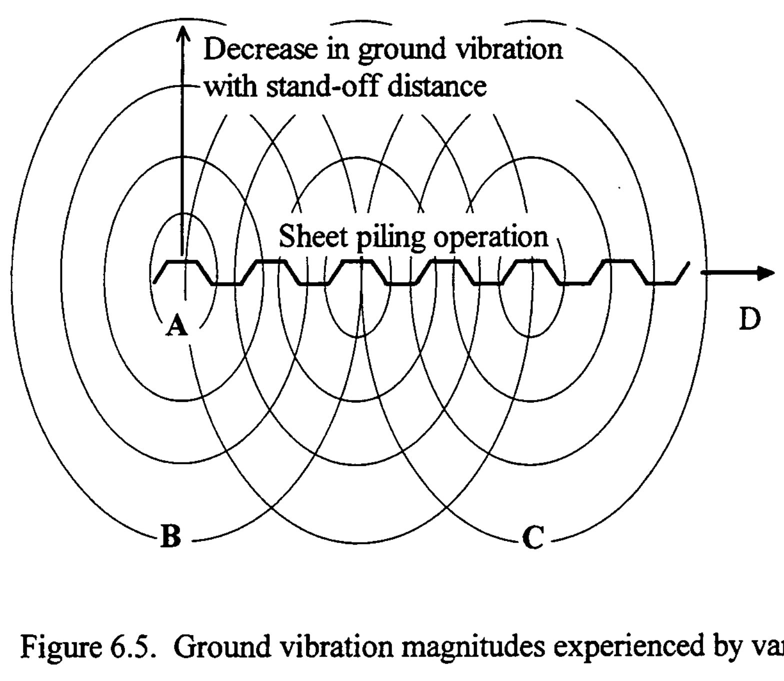

Figure 6.5. Ground vibration magnitudes experienced by various soil units.

Vibration tests that were performed using fixed time intervals of 1, 2, 5, 10, 20 and 50 minutes per acceleration increment on coarse Leighton Buzzard sand (see Section 5.2.4 and Figure 5.5.3) demonstrated the tendency for increasing soil settlement with time. However, there was some overlap in settlement values for the 1 and 2 minute data and the 5 and 10 minute data, which reflected minor sample variation. It was considered prudent to vibrate for a long duration with the objective of near to 100% potential compaction. If a sample vibrated for 1 minute demonstrated a reduction in sample height of 1mm (± 1mm), a sample that settles 10mm (± 1mm) in 1 hour, has less inherent error than the vibration test of shorter duration.

In addition, because sample settlement for a given vibration magnitude approximated to a log rate reduction, it was sensible to obtain a value of settlement after 5 minutes of vibration by interpolation of a vibration test that ran for 1 hour, than it was to obtain a value of settlement by extrapolating a vibration test result of 5 minutes duration to a value of settlement required for 1 hour of vibration. Performing prolonged vibration tests was judicious because maximum (upper bound) values of settlement were evolved and any differences that may have been relatively significant using a short vibration time due to initial variations in sample fabric and density were reduced.

The test procedure modelled the continuous sinusoidal vibrations that are generated during vibropiling activities. A useful extension to the research would be performing a test programme that uses discrete single pulses of vibration to model the effects that impact hammer vibration has on adjacent soil.

6.2.6 Test Procedure

A central assumption of the laboratory test programme was that a soil vibrated in increments of acceleration to a given maximum value, would settle to the same magnitude as a soil that only experienced this maximum value. A number of tests were performed to test this assumption using the medium sharp sand under a static load of 10kPa. Samples were subjected to an increase in initial vibration level, the increments of acceleration being the same, to a maximum vibration of 6.0*g* (see Section 5.2.4. and Figure 5.5.4). The data confirmed that the above assumption was valid.

The laboratory test procedure that imposed increasing increments of acceleration to a statically equilibrated material can be viewed directly in two ways (a), that such a pattern of acceleration increase modelled the vibrations experienced by a soil unit at a given depth which experienced increasing levels of vibration as a piling operation proceeded towards it and (b) that such a test programme modelled, for a given static load, the effects of vibration on soil units which had different values of relative density under the same values of static load, i.e. materials with higher values of relative density under the same static load will require higher levels of vibration to induce initial vibratory settlement.

There are additional treatments that can be applied to samples before and during vibratory testing. Such options for further work include :

a) Re-saturation - This may be performed on samples that have been dried back, to observe the effect of a series of wet-dry cycles on vibratory settlement response.

b) Vibration without drainage - It is reasonable to consider that, under certain conditions a layer of granular material may experience vibration when rapid removal of water is not possible. This condition may be represented by a sand deposit between two clay layers and may be modelled in the laboratory by closing the back pressure drainage valve prior to application of vibration, or by increasing the level of back pressure.

c) Desaturating and resaturation whilst vibrating - A unit of soil may experience alteration of moisture content that is not merely a function of vibratory induced compaction settlement. The water moving from this layer may cause a dry or partially saturated soil nearer to the surface to experience some degree of resaturation. Such layers may then behave differently, i.e. demonstrate greater settlement, to that which was expected based on their moisture state prior to vibration.

Removal of water (artificial desaturation) from a unit of soil experiencing vibration is also possible due to a site requiring pumping of water away from a current location of work.

6.2.7 Vertical Vibration

The majority of tests were performed using vertically orientated vibrations (see Section 4.6.4). These tests modelled a propagating compressive wave, emanating from the pile toe during pile driving activities, at short stand-off distance, when a spherically expanding compressive wave is nearly vertically orientated. As stand-off distance increases, the vertical component becomes less significant as the expanding wave tends towards a horizontal compressive wave (see Figure 6.6). Thus the use of vertical vibration in the laboratory is reasonable for strong vibrations.

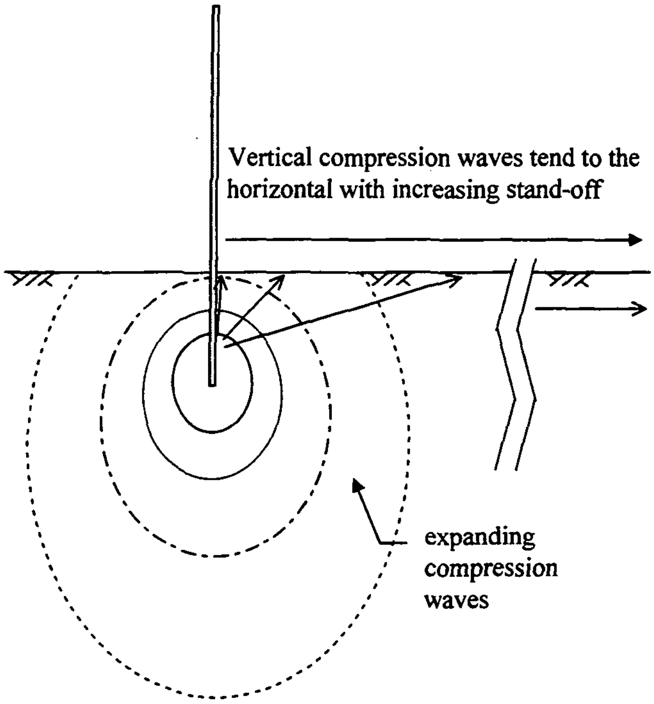

Figure 6.6 Compression waves.

6.2.8 Horizontal Vibration

A number of tests were performed using a horizontal vibration (details are given in Section 4.6.7). Two soils were tested; the medium Leighton Buzzard sand and the sandy fine to medium gravel because these soils were very different in terms of particle size distribution characteristics. It was considered that testing only one type of sand would not allow confident observations to be made, i.e. if only a uniform soil was vibrated in the horizontal direction, observations concerning the settlement response may not necessarily be attributable to other soil types. A comparison of the settlements due to vertical and horizontal vibration demonstrated that while the settlement tendencies were similar (i.e. an increase in the gradient of the settlement response curve with increasing acceleration) the vertical settlements tended to be slightly higher (in the order of approximately 0.25% for the sandy fine to medium gravel, and about 0.05% for the medium Leighton Buzzard sand (see Figure 5.5.2a,b). Note that the apparent correspondance between vertical and horizontal vibratory settlements may reflect the isotropic nature of the fabric induced by the sample preparation technique and the sands that were used.

The data also indicated that, in general, samples that are subjected to vertical acceleration suffer initial settlement at a lower value of acceleration (an average of approximately $0.1g$) than the equivalent horizontal vibration tests. The inference is that for conditions appropriate to pile driving, a soil unit that experiences vertical vibration tends to be more sensitive to lower accelerations and demonstrates slightly greater settlement than for horizontal vibrations. As the horizontal component becomes more significant, the vertical component may be of greater significance at greater stand-off distances than might be expected if a 1:1 assumption is made concerning the settlement caused by vertical and horizontal vibrations.

In addition, an expanding compression wavefront is still a unidirectional vibration, regardless of its orientation. If the settlements that were obtained for vertical and horizontal vibration orientation during testing are considered to be comparable, then any vibration orientation between the vertical and horizontal might be expected to produce the same settlement as equivalent vertical or horizontal vibration.

6.2.9 Shear Vibration

The laboratory modelling of spherically expanding shear waves was not readily accomplished with the laboratory apparatus that was designed for the bulk of the test programme. However, torsional shear was applied by modifying the existing Rowe cell design using a pair of opposing shakers (see Section 4.6.7). Performing torsional shear tests do not adequately represent *in-situ* shear waves, in terms of strain amplitude and strain density. However, subjecting samples to some form of shear excitation was considered necessary, at least to acknowledge the occurrence and gain some comparative insight into the effects of shear waves on soil compaction for the particular application of this research.

Two tests were performed: at 10kPa negligible settlements were observed, and no vibratory settlement was observed for at test performed using 20kPa. Additional testing at higher stresses was not considered to be of value. An initial appraisal of the torsional shear test results (see Table 5.5.2) suggested that (on their own) shear waves induce negligible vibratory settlements compared to the equivalent compressive wave tests. The results were unexpected: the shear strains in the laboratory sample were an order of magnitude higher than those which may be encountered *in-situ*, and other authors have reported that shear waves can cause significant strains in soil (see Section 3.6.3). Such observations were made for different applications (such as earthquake modelling), and were appropriate for different levels of acceleration, frequency, duration and strains than those used in this research programme.

The very small values of torsionally induced vibratory settlement may reflect a failure of the test method. Factors that could have contributed to test failure include: the possibility that the rotating central spindle failed to transmit the rotation to the load sample disc; or that the friction between the diaphragm and the cell was too great; a preferred shear plane may have developed between the load disc and sample, and/or between the sandy fine to medium gravel sample and the cell base. Examination of the spindle rotation when the cell top was attached to the cell body demonstrated that, without pressure within the diaphragm and no sample to bear down upon, the vibrations were transmitted to the integral load disc. Also no shear damage was observed between the rotating arm and the spindle head. On test disassembly, the holes on the load/drainage disc were clogged with material, which suggested intimate contact between the sample and the disc; no evidence of a preferred shear surface was observed.

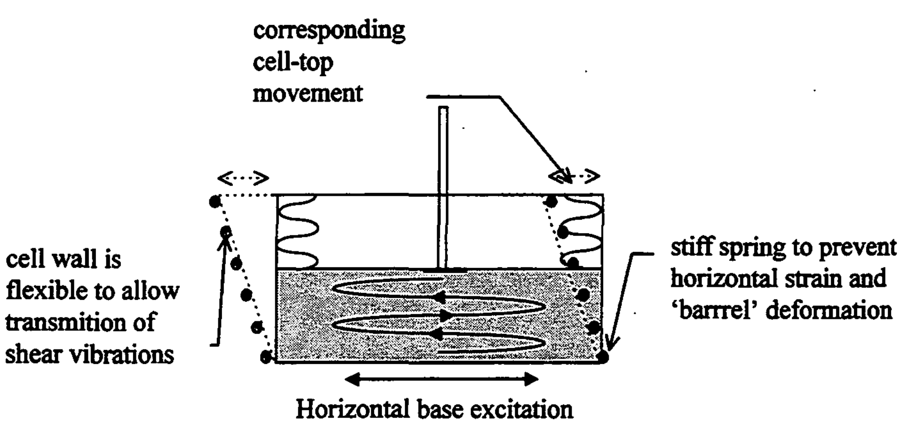

Figure 6.7. Illustrating Rowe cell modification to enable simple shear wave testing.

It could be argued that (assuming the test method worked and that torsional shear adequately models the *in-situ* conditions), the shear wave component of ground vibrations that are generated during vibratory pile driving have negligible effect on ground strain. However, due to the limited number of tests that were performed, any conclusions based on the data are at best, tentative.

The design of apparatus was considered that would enable the effects of shear vibrations to be investigated (see Figure 6.7). However, due to time constraints this technique was not possible to implement, and is recommended as further work. The method required that the aluminium cell wall is replaced by a polythene copy (a clear plastic would allow direct observation of the sample) that was flexible enough to allow the transmission of horizontally acting shear wave vibration, but stiff enough to ensure that 'barrel' deformation was resisted. This would allow the investigation of ground compaction settlement induced by shear wave transmission at accelerations and frequencies appropriate to piling operations. The use of confining springs of different stiffness could be used to impose different stress-strain characteristics on the samples, modelling different *in-situ* densities and strength characteristics. Such confining springs would need calibration and a separate programme of testing.

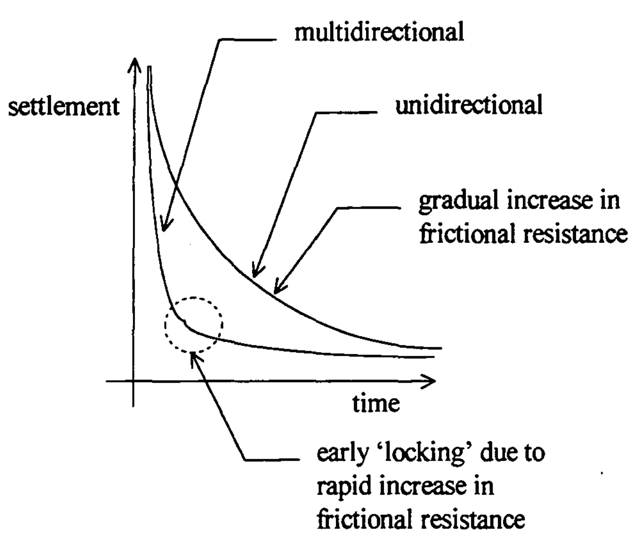

Figure 6.8. Multidirectional and unidirectional shaking.

more dense configuration. Thus, the ultimate density of a sample that is produced by unidirectional shaking may actually be greater than the ultimate density achievable under multidirectional conditions.

However, multidirectional vibrations of 0.5g in the x, y and z directions will produce a resultant acceleration of 0.87g, i.e. a higher acceleration than the equivalent unidirectional test performed at 0.5g, and thus, greater settlement potential is inferred. It may be appropriate to use resultant acceleration values if *in-situ* records contain such data. If only vertical (or horizontal) vibrations are recorded, then assumed resultant acceleration values could be used by increasing the unidirectional values, at a given stand-off distance, by a factor of approximately 2. It appears that impact hammers and vibrodrivers may produce vibrations that have different characteristics at the ground surface with respect to the depth of the pile toe, and the stand-off distance (see Appendix 5).

6.2.11 Working at Low Pressures

Most standard laboratory testing is carried out at stresses of hundreds of kilo Pascals. The hydrostatic pressure systems are designed to work well at such stress levels. The pressures that were used in this research were at the lower end of the operational capability of the pressure systems. The test gauges that are used to measure pressures that are typical of those used in standard testing are not recommended for use below 100kPa. Thus a digital volt meter was used to monitor pressures during testing.

In addition, when the volume change devices required value changes, a change in supplied pressure was observed in the order of 1kPa. Such a small change in pressure is negligible if pressures of, for example, 500kPa are being used. However, during testing under the low pressures of this research, a change of 1kPa was potentially significant. During preliminary testing, a 'kick' in the volume change response was observed during vibratory sample settlement. Under high acceleration levels, where vibratory settlements were large, a 'kick' in sample settlement during one acceleration increment was not considered to significantly affect the results. However, during the low acceleration testing, a settlement 'kick' due to a pressure change during volume change valve turning was more significant because of the small settlements that occurred. However, careful pre-test set-up ensured that a volume change valve turn was necessary only during an acceleration of 2.0g, i.e. when settlement magnitude was more significant.

An LVDT and dial gauges (reading to 0.01mm and 0.002mm) were used to record sample height change. At low acceleration, when Rowe cell amplitude was slight, accurate reading of the dial gauge was possible. However, as acceleration magnitude and amplitude increased, some lateral vibration of the LVDT-dial gauge assembly occurred. This was translated as a blurred arc of the dial gauge needle, and unsteady LVDT output on the digital volt meter. However, judicious use of a clamp system reduced the lateral shake, and solved the problem.

6.3 Influence of Test Conditions

6.3.1 Range and Values of Acceleration

In general, the data showed that for accelerations below 2.0g, as acceleration magnitude increases, the settlement magnitude increased, producing a curve of increasing gradient (a second order polynomial relation). The data for accelerations up to 6.0g again demonstrated that increasing acceleration produces increase in settlement. However, in this case, the increase in settlement per acceleration increment was seen to reduce in magnitude, thus reducing the gradient of settlement response. This suggested that a different behaviour was occurring for acceleration levels around the 2.0g value.

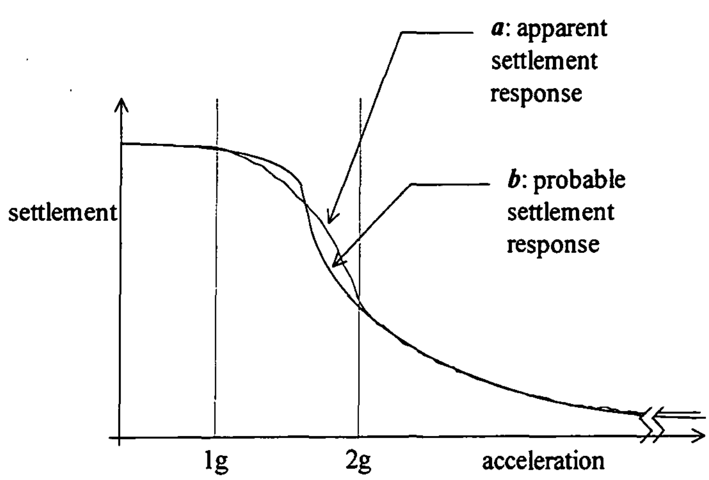

Figure 6.9. Settlement response between 1g and 2g.

The specific acceleration values that were used forced the soils to respond to the imposed test conditions. The behaviour up to $1g$ is considered to be well represented by the acceleration increments used (i.e. 0.1, 0.2, 0.3, 0.4, 0.5, 0.6, 0.8, and $0.9g$), because the rate of change of settlement response was gradual over the range $0.1\text{-}1.0g$. This confidence in the results representing 'free' soil behaviour was also appropriate to accelerations greater than $2.0g$. The data showed that the greatest rate of change in settlement increase occurred at $2.0g$. In practice, the acceleration level at which the sample behaviour changed was observed to be between $1.4g\text{-}1.6g$, depending on the soil type and test condition (and possibly on the rate of increase in acceleration, i.e. how quickly the function generator dial was turned to increase the signal from $1.0g$ to $2.0g$). Because of the lay-out of the laboratory apparatus, this behaviour was observed by chance. Thus, the response to increasing acceleration may be more realistically represented by curve *b* (see Figure 6.9) than by curve *a*. This behaviour was also described by Rodger and Littlejohn (1980), who stated that abrupt change in settlement (or strain) magnitude occurred at approximately $1.5g$. Closer examination of the laboratory settlement data indicated that greater increase in settlement occurred at $0.8g$ and again at $1.0g$ than at lower accelerations. The 'free' sample behaviour might have demonstrated an increase of settlement rate at any acceleration between $0.6g\text{-}0.8g$ and $0.8g\text{-}1.0g$ which would be soil type, stress and density dependant.

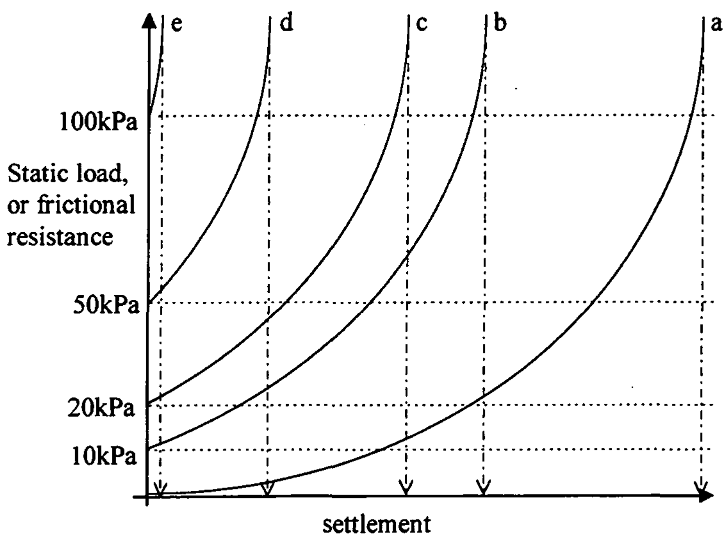

Figure 6.10. Illustrating the influence of static load and frictional resistance on the settlement potential of a soil (for a given density and acceleration).

The overall settlement response indicates that the resistance to vibratory compaction due to the internal frictional resistance was not significantly reduced until the energy level attained a value of approximately 1.5*g* (in theory, the energy required is 1.0*g*, but because of friction it is not seen in practice, see Section 3.10). The increase in density that occurred at about 1.5*g* (forced at 2.0*g* in this case) dramatically altered the fabric of the sample (the density), and hence the internal frictional resistance of the material.

With consideration of the above, it is recommended that the equation that was developed to predict settlement of up to 1.0*g* is also applied to vibrations with a maximum acceleration of 1.5*g*. Similarly, the equation for accelerations of greater than 2.0*g* should be applied to accelerations that are greater than 1.5*g*.

6.3.2 Static Load

Unconfined dry sand has been demonstrated to experience a dramatic increase in settlement when acceleration reaches 1*g* (see Section 3.8.2 and Figure 3.16). With the presence of an applied load, the frictional resistance is greater, the particle movements are restricted and the acceleration level that is necessary to induce initial settlement must increase. This behaviour was demonstrated by the results which showed settlement decrease with static stress increase from 10kPa to 100kPa. Also, the acceleration required to initiate settlement was greater with increasing static stress. It was assumed that the amount of applied stress that was necessary to produce a settlement response of a soil that was 'confined' is very small, i.e. just enough to increase the stress level above that generated by the self-weight of the sample, and to prevent the free upward movement of particles during vibration. This suggested that if tests were performed using a static load of 5kPa, settlements would initially occur at a lower acceleration, and settlement magnitudes would be greater than for tests performed under higher maintained static loads.

Figure 6.10 demonstrates that a soil under a minimal stress and at a given vibration (e.g. curve (a), a soil under 1kPa) will reduce in volume and settle with time. The curve demonstrates that settlement potential decreases as the magnitude of initial static stress increases and as frictional resistance increases as the sample compacts and densifies under the influence of vibration. Soil (b), (at the same relative density as soil (a)) due to an initial static load of 10kPa, already has a greater degree of frictional resistance prior to the onset of vibration, than soil (a). As vibration proceeds, soil (a) increases its frictional resistance until a value equivalent to that generated under a static load of 10kPa is achieved. Because the frictional resistance of samples (a) and (b) are equivalent, the rate of settlement for these two samples is assumed to be equivalent. However, because soil (a) initially had less frictional resistance, it has already suffered a degree of settlement whilst increasing its frictional resistance to a level that is equivalent to the frictional resistance demonstrated by soil (b) prior to the start of vibration. Hence, soil (a) has greater settlement potential than soil (b). As vibration continues, both soils are settling and increasing their frictional resistance until a value equivalent to that generated by a stress of 20kPa is achieved. The soils (a), (b), (c) have the same internal frictional resistance (a function of static load and density), and settlement rate is common to all three soils.

The above behaviour is a generalisation and variation will occur when the results of several soil types are compared. However, increasing the initial static load and/or relative density tended to produce less settlement. Note that the variation in vibratory settlement attributed to the effects of initial relative density was accounted for by later data processing, trend observation and settlement equations. A more detailed appraisal of the laboratory results indicates that certain materials did not show this monotonic stress-settlement tendency; for example, the silty fine sand, medium uniform sand and the coarse Leighton Buzzard sand (see Table 6.3).

Soil type	Settlement magnitude (decreasing left to right) kPa			
general response	10	20	50	100
SFS, 25Hz	10	50	20	100
SFS, 40Hz	10	50	20	100
MUS, 40Hz	20	50	10	100
CLB, 25Hz	20	10	50	100
CLB, 40Hz	20	50	10	100

Table 6.3. Showing the soils which did not demonstrate the trend of decrease in settlement magnitude with increase in static load.

Such variation in settlement response might reflect the sensitivity of soil behaviour to initial variations caused during sample preparation. Other variations in the data reflected different sensitivity to the effect of increase in static load. In general, the greatest change in soil settlement response occurred between 10 to 20kPa and the smallest was between 50 to 100kPa. Again, variation is seen across the soil types and for the 25Hz and 40Hz data (see Table 6.4).

Soil type	Greatest difference in settlement
general response	10 -20 kPa
SFS, 40Hz	20 - 100kPa
FUS, 40Hz	20 - 50 kPa
MUS, 25Hz	20 - 50kPa
CLB, 25Hz	20 - 50 kPa
CLB, 40Hz	50 - 10 kPa
MSS, 25Hz	50 - 100 kPa

Table 6.4. The soil types which did not demonstrate greatest decrease for static load increase from 10kPa to 20kPa.

There was also variation in settlement response to static load with increase in acceleration, i.e. some soils showed greatest difference between 20-50kPa up to a given value of acceleration, e.g. 0.8*g* (for SFG at 25Hz and 40Hz), and above this acceleration the greatest difference was observed between 10-20kPa, than previously indicated by the 20-50kPa (see Figure 5.2.8a,b).

With consideration of the observations that were made concerning soil-stress sensitivity, and the work of Oteo (1983), it is possible that a critical depth may be defined for maximum settlement potential, which will vary with soil type, density, frequency and acceleration, e.g. for the same conditions, one soil may be more sensitive to the action of a particular acceleration-stress combination than another soil. Thus, the stress-settlement trend that was identified for the results of this research may simplify the actual specific soil response. Figure 6.11 modifies the stress-settlement trend that is given in Figure 6.10, for the above considerations.

Further work would be required that specifically seeks to describe and quantify the more complex stress sensitivity. Because the 10, 20, 50 and 100kPa response has been investigated, testing under maintained static loads of 5, 15, 35, 75 and 150kPa would enable more confident observations to be made of soil specific response to static stress.

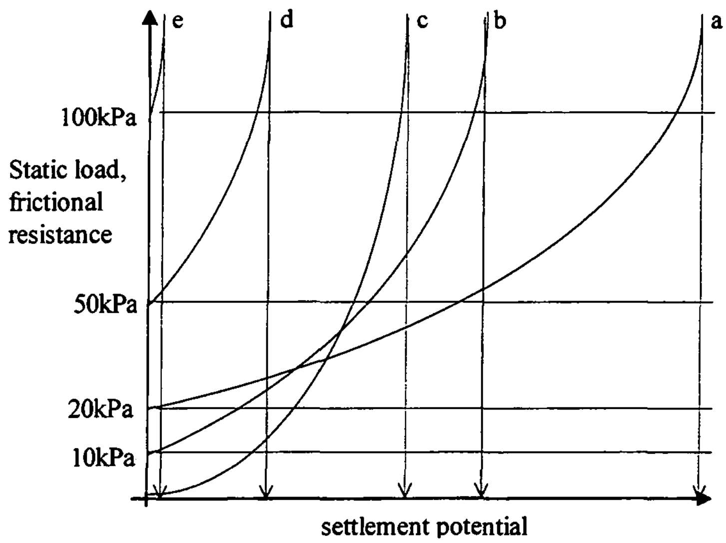

Figure 6.11. Modification of Figure 6.10, accounting for the optimum superposition of the influences of soil type, density, acceleration, frequency and static load.

6.3.3 Moisture Content

Partially saturated and dried tests in the 0.1-2.0g acceleration range, were performed on four soils: the medium uniform sand; coarse Leighton Buzzard; medium sharp sand and sandy fine to medium gravel under a static stress of 10kPa. Because soils in the UK are normally saturated or partially saturated with few deposits of totally dry material, a limited number of tests were considered adequate because, since dry and partially saturated soils are less prone to vibratory induced settlement than saturated equivalents, dried and partially saturated soils do not present as great a risk of settlement. Hence, less tests were performed. Additionally, because the settlement magnitudes were so slight, any variation in settlement response across the soil types was negligible, hence, fewer soils required testing. The four soils chosen were considered to represent adequately the range of soils that were tested in the saturated condition.

A static load of 10kPa was used because the saturated tests that were performed under 10kPa tended to generate maximum settlements. Additional testing at higher stress levels would have been carried out if significant vibratory settlements were evolved using 10kPa. In any case, the data that were produced for partially saturated and dried 10kPa tests was considered amenable to modification by the settlement trends that were developed with respect to stress influence, for the saturated test data. A frequency of 25Hz was used because, as demonstrated during saturated tests, settlement occurred at a faster rate than at higher frequencies.

The most apparent difference in the settlement behaviour of dried and partially saturated samples compared to saturated equivalent data was the very marked difference in settlement magnitude, especially for those vibration levels that were more appropriate to piling operations (i.e. up to 1.0*g*). The high acceleration tests demonstrated that settlement magnitudes for dried tests were comparable with the equivalent saturated values, although the partially saturated soils continued to show less settlement.

The difference between the settlement response of dried materials and the saturated equivalent was due to the absence of water. It is probable that the dried material had greater frictional resistance because water acts as a lubricant. In addition, the dried samples were cemented to some degree by the presence of any fines, which would have tended to accumulate at the interstices between particles as water was progressively lost through evaporation during oven drying. Thus, frictional resistance was increased at particle-particle contacts due to the presence of a small clay fraction, acting in a the manner of a 'cementing agent'. Up to and including 1.0*g*, dried sample settlements were negligible (although the coarse Leighton Buzzard sand showed about 0.25%), there was then a marked increase in settlement at 2.0*g*, for the medium uniform sand, coarse Leighton Buzzard sand and the medium sharp sand, but not the sandy fine to medium gravel. On test disassembly, the medium uniform sand and coarse Leighton Buzzard sand demonstrated no particle cementation, which implied that the dried behaviour of these clean sands was modified only by the absence of water, which caused an increase in frictional resistance. The medium sharp sand and the sandy fine to medium gravel settlement results demonstrated the effects of particle cementation. The medium sharp sand, which settled more than the sandy fine to medium gravel, exhibited 'nuggets' of intact material within a matrix of completely disaggregated material. The sandy fine to medium gravel sample was entirely cemented, and only showed slight break-down, and hence, negligible settlement even under 2.0*g*. Examination of particle size distributions suggested that the greater proportion of larger particles of the sandy fine to medium gravel interlocked to form a more robust soil skeleton than was possible for the medium sharp sand, and hence, was able to resist compaction at higher acceleration. The dried tests that were performed under higher accelerations demonstrated similar behaviour, i.e. a varied degree of sample break-down due to the presence of cementing fines. Additionally, the data demonstrated that: with increasing stress, acceleration; reduction in uniformity coefficient and percentage fines and decrease in relative density, more breakdown occurred (see Figure 6.12).

Although the above behaviour is interesting and required comment, such behaviour does not have much significance to *in-situ* conditions. In the UK, even during the summer months, dried material tends to occur only as a thin crust (so data for 20-100kPa has little relevance to site conditions). Because minimal settlements were obtained in the laboratory under accelerations appropriate to those that are generated during pile driving, a mean value of the soil specific settlements could be used in settlement estimations. Additionally, since such data have negligible impact on settlement estimations it can be ignored in any subsequent settlement calculations.

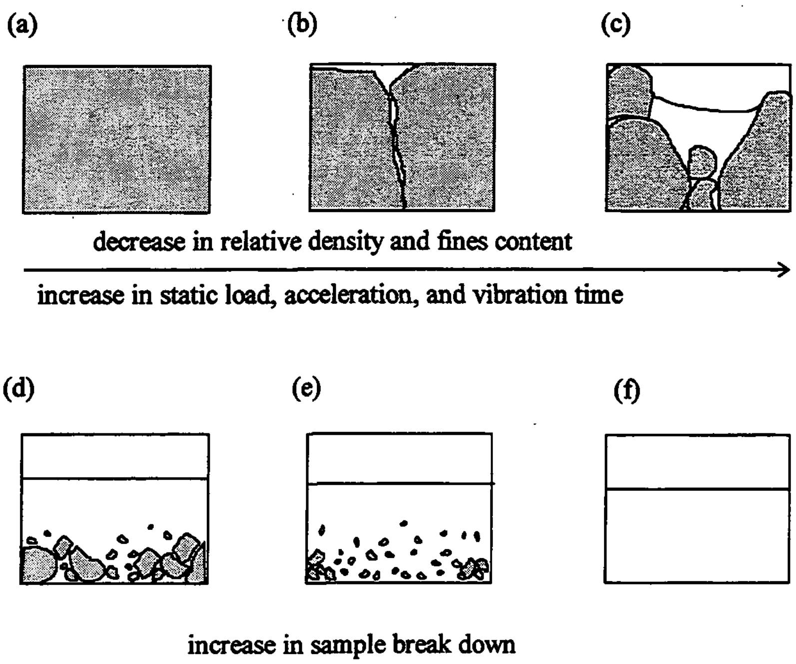

Figure 6.12. The mode of dried sample break-down under the effects of acceleration, stress and time.

Similar behaviour was demonstrated by the partially saturated tests. However, the mechanism that caused the increase in resistance to settlement was the presence of suction forces, rather than an increase in frictional resistance due to the complete absence of water and the cementing action of fines. An apparent cohesion was generated in the samples that resisted the effects of acceleration to an even greater extent than the equivalent dried tests. The data suggested that the contribution of partially saturated material to vibration settlement is negligible and can be discounted in settlement estimation calculations. However, consideration of the broader application of the data suggests that in more arid regions, where substantial deposits of dried and partially saturated granular material occur, the dried and partially saturated test data would have a greater significance than for conditions in the UK.

There must be some value of moisture content at which dried material starts to behave as a partially saturated material, and a value of partial saturation above which, material behaves as if effectively saturated. Medium uniform sand was selected for a series of vibratory tests that were carried out under a static stress of 10kPa, using different levels of moisture content. Previous tests had provided three data points, i.e. dried, partially saturated (at about 12.5% moisture content) and saturated: three additional moisture contents were used. The data (see Figure 5.5.5) showed that as moisture content increased towards complete saturation or completely dried, the corresponding vibratory settlements increased. However, because the data demonstrated an order of magnitude decrease over the 100-92% saturation level, it was assumed that the 'critical' value of moisture content is closer to complete saturation rather than the lower value. Soils less than 100% saturated are considered to be partially saturated, and hence, assumed to demonstrate negligible vibratory settlement. Note that change from occluded to continuous air voids occurs at approximately 90-95% (Toll, 1996)

Different soils having different densities will display different partial saturation (suction) behaviour. Well-graded soil will tend to demonstrate a less abrupt response to moisture content change, than a more uniform soil, because the suction forces will tend to break down at a more uniform rate (Toll, 1991). Hence, the use of the medium uniform sand for these tests is more appropriate than a soil with a wider grading character, because a more abrupt settlement response allowed more precise observation of the critical moisture contents. Further work should be performed on a range of soils with increasingly wider particle distributions to enable more confident observations to be made concerning the vibratory critical moisture content of soils.

6.4 Results and Applications

6.4.1 Introduction

The basic laboratory data were amenable to a number of levels of processing and application. For example, specific laboratory settlement results may be applied very directly to site conditions, e.g. the settlement demonstrated by the medium uniform sand is used to estimate the settlement for any *in-situ* medium uniform sand. Specific values of overburden and vibration levels are inferred by linear interpolation of the specific test data.

The next level of data processing and application would use specific parameters of the test results. Instead of using the medium uniform sand settlement data for all *in-situ* medium uniform sands, a (common) physical characteristic may be used that most closely matches that of the laboratory data, such as similar values of maximum particle size, coefficient of uniformity, coefficient of distribution or relative density.

However, more useful than relying on discrete values within a large data set to estimate vibration compaction settlement, greater flexibility would be allowed if settlement estimations could be performed for any soil type under a range of *in-situ* conditions. An initial processing step was achieved by identifying settlement trends based on specific soil type response to combinations of acceleration and maintained static load. Regression relations could be used to perform a settlement estimation, e.g. quantifying settlement trends for specific soils and modifying a given value by the general response of granular soils to specific stress (overburden).

The most versatile and convenient product that could be employed to perform settlement estimations are the equations that combined the significant parameters such as soil type, acceleration, density and overburden and additionally accounted for the influence of frequency, vibration time and moisture content.

To allow convenient and rapid assessment of the potential magnitude of vibration induced ground compaction settlement, summary tables that were derived from all the laboratory data and subsequent processing could be consulted by an engineer to allow informed decisions to be made concerning piling.

6.4.2 Data Processing

The data handling and archiving method was developed to enable the convenient and logical structure for data input and processing. The data sheets in Appendix 3 allowed the test data to be entered manually, in a few minutes. The spreadsheet records test number and stress level followed by the acceleration increments of a given test. The next section calculated percentage settlement from raw settlement data at each level of acceleration and the initial sample height (h_o) after static equilibration. The cumulative decrease in sample height, decremented from h_o, and the equivalent percentage decrease in height was calculated for the increasing acceleration levels.

The sample height calculations were checked by the next section of the data sheet, which calculated the equivalent sample volume changes (using a sample area of $0.0182m^2$). The moisture content and density calculations required the manual entry of the wet sample mass after test completion, and the dry sample mass after oven drying. The volume change data of the previous section was then used to perform back-calculations of sample moisture content and density to enable values to be appropriately generated for given acceleration increments.

In the final section, additional physical properties were calculated such as void ratios, relative densities and equivalent SPT-N and relative compaction values values.

The spreadsheets contain all the relevant information for the vibration tests, for particular soils, over the range of static stresses and acceleration increments. Data analysis and trend observation used the settlement data in the above form as a convenient database of information.

6.4.3 Identification of Trends

Because of the number of tests performed (i.e. 200 tests with 1500 acceleration increments, and some 15000 individual settlement increment values), and the number of inter-dependent variables, it was considered to be reasonable to simplify and reduce the size of the data set. This was appropriate if initial identification of basic settlement trends were to be made. Initially, the data were examined from two different view points. These were: the response of specific granular soils to a non-specific overburden stress and the influence of specific overburden stress on a non-specific granular soil (the protosoil) (see Section 5.3.1).

The data also indicated that the 40Hz data demonstrated less sensitivity to very low acceleration levels than the equivalent 25Hz data. Norman-Gregory and Sellig (1989), stated that lower frequencies allowed more time for particles to move (and so attain a smaller volume) per cycle than under higher frequency.

Taking the mean settlement of all the soils tested for specific stress levels enabled the general settlement response of the protosoil (or 'mixed' soil) to specific values of overburden stress to be observed. This simple data treatment generated the simulated response of a material, the net response of which demonstrated the properties of all the specific soil types. In addition, the surficial deposits of the UK are frequently mixed in nature. Averaging the soil specific data generated data that would be appropriate to the parent material from which the specific soils could be considered to have evolved from. Data generation for the protosoil allowed an insight into the general behaviour trend of granular material to static load under a range of acceleration.

It was assumed that the nine soils that were tested will produce the same mean soil type response and static stress trend as any nine (or more) granular soils that were randomly chosen from Britain. Testing more soils was not feasible within the time-frame of the research programme. In any case, if the heterogeneous nature of soil deposits is considered along with any experimental error that might occur during sample preparation, discerning the possible settlement variation under specific stress that any other 10 randomly selected soils may demonstrate, compared to the soils that were used in this case, may not be significant or discernible.

Treating the data to reduce the size of the data set, and simplifying the data allowed convenient appreciation of the general trends (see Figures 5.6.2 to 5.6.4). Identification of settlement trends allowed the development of test parameters by subsequent regression analysis.

6.5 Identification of Parameters

6.5.1 Soil Parameter

The data demonstrated that the use of standard soil parameters and combinations of standard parameters, was not appropriate in this case. Using the uniformity coefficient and maximum particle size, or any combination of the above, produce reasonable regressions for some of the soils. However, the vibratory settlement of the silty fine sand and the fine uniform sand did not follow such trends. These soils had the smallest grain sizes and demonstrated disproportionally high vibratory settlement results. Ignoring the silty fine sand and fine uniform sand data would discount the time taken in the laboratory to perform the tests and ignore the effects of such soils *in-situ*. The data for these soils could be assumed to be invalid because they did not fit the trend shown by the other soils. However, because the 25Hz and 40Hz data showed the same settlement response, it was unlikely that these 16 tests demonstrated erroneous settlement values.

A parameter was required that effectively represented the specific soil behaviour of all the soils tested. As demonstrated (in Section 5.4.1) a non-dimensional expression was initially developed after various combinations of size ranges were tried. However, it was found that the optimum soil type parameter was a dimensional expression (R^2 values are presented in Table 5.6.3). Compare the regression equation R^2 values of 0.60 and 0.41 that were obtained for the non-dimensional expression under 25 and 40Hz respectively, with the equivalent dimensional expression that produced R^2 values of 0.61 and 0.88. It was found that the soil type parameter was improved when the relative density was incorporated into the expression, i.e. vibratory induced settlement was a product of relative density and the overburden pressure.

It was sensible to consider the possibility that if more soils were tested, more scatter in the settlement data would occur. This behaviour could lead to the observation that using a soil parameter based on standard criteria, such as U_c or D_{max} could produce regression relations that were as good as the distribution coefficient that was derived for the nine granular soils that were tested. Note that the high acceleration data (1.0*g* to 6.0*g*) showed U_c to be the most appropriate parameter to use.

This difference in the soil parameter; D_c for the low acceleration test data and U_c for the high acceleration tests is interesting. It could be argued that U_c was the appropriate parameter to use when attempting to predict soil compaction response to levels of acceleration. Other authors have used U_c as a soil type parameter, although D_{max}, D_{10} and D_{50} have also been used in conjunction with the density characteristics of soils. However, the need to use D_c instead of U_c in the acceleration tests up to and including 1.0*g* may illustrate a subtle change in soil type response to acceleration magnitude. The distribution coefficient (D_c) was developed because sample settlement was seen to be a function of maximum particle size (as observed by other workers) and also U_c (which has been used in other research).

Up to and including accelerations of 1.0*g*, the particle size range(s) that determines settlement response was given by D_c. Under higher accelerations, the necessary use of U_c to produce the best settlement prediction demonstrated that the particle size range(s) that were dominant under lower accelerations are no longer as influential. This led to the conclusion that different size ranges of soil grading control the settlement response above and below an acceleration of 1.0*g*. For example, below 1.0*g* it appeared that the larger particle size of a given soil was most influential; but under higher accelerations it appeared that maximum particle size was not as important as the size range of the smaller fraction of a soil.

Note that the use of mean data to generate regression equations when determining the optimal soil parameter had two effects. Firstly, any errors that occurred as a result of variation in the sample preparation technique were reduced. However, any subtle soil-stress specific variations were also lost. For example, as particle size distribution increases, the potential for developing a wider range of relative density is possible.

6.5.2 Stress Correction

The relationship between the protosoil under specific stress and acceleration has been demonstrated for any stress up to 100kPa and accelerations up to and including 6.0*g*. It was proposed that the vibratory settlement values that were obtained for a specific soil (under mean stress) are multiplied by the specific stress correction factor that was generated for the protosoil (see Figure 5.7.7.a,b). This graph was derived by dividing the protosoil specific stress for discrete acceleration values (see Figure 5.7.6.a,b) by the mean stress value of the protosoil, to obtain the stress multiplication factor for discrete accelerations and any stress.

This pragmatic approach was valid because the stress correction factor was based on the ratio between the mean stress data to the specific values (for the protosoil). Figure 5.7.7.a,b graphically presents the value by which a mean stress settlement value should be multiplied by in order to obtain the value that would be generated under a specific stress, of say 10kPa at 1.0*g* (approximately 2.1) and under 50kPa (about 0.2).

Thus, stress values above the mean stress (for specific soils) multiply the soil specific data by values greater than unity, and for stress below the mean stress value of soil specific settlement multiply the settlement by a value less than unity. Figures 5.7.7.a,b suggested that the mean stress value is approximately 17kPa, which reflected the disproportional contribution of the lower stress values to settlement. Table 5.6.4.a,b presents a comparison between the regression trend data and the test specific data (using mean values of relative density).

Other methods of stress correction were considered. For example, another way of performing stress correction involved taking ratios of mean (protosoil) data to soil specific data under specific stress values and evolving a correction factor in this way, i.e. by how much did a specific soil vary from the mean value of settlement at 10kPa and other specific stresses. However, this method produced a wide range of soil specific relations which were not amenable to treatment in terms of stress correlation with particular soil type properties.

6.5.3 Minimum Acceleration

It was clear from the vibratory test settlement data (see Table 5.1a,b and 5.2a,b,c) that (depending on test conditions) soils had different sensitivity to low acceleration. That is, soils demonstrate initial settlement under various lower values of acceleration. For example, Table 5.6.1 indicates that in general, the silty fine sand tended to show initial settlement at about 0.2g. In contrast, the medium uniform sand showed initial settlement at about 0.4g (for 25Hz).

Figure 5.6.4a demonstrated the relationship between static stress and the minimum acceleration magnitude that was required to initialise settlement for 25Hz and 40Hz for the protosoil. This chart showed that in general, granular materials required at least 0.2g to cause settlement under 10kPa, and at least 0.6g to induce settlement under 100kPa. Extrapolation suggested that under 5kPa, 0.1g would be required to induce initial vibration settlement. Interestingly, the data suggest very similar behaviour between the 25Hz data and the 40Hz data, except under 50kPa, where the 40Hz data appears to require 0.1g less acceleration to cause initial settlement than the 25Hz data (under 40Hz, there is a greater maximum-minimum range of soil sensitivity than under 25Hz).

Quantifying the initial soil specific settlement response with acceleration would be more useful than merely describing the general response. However, because of the variation in the data, making the relationship that is shown in Figure 5.6.4 more specific was not practicable with data generated by the test programme. Solution of the problem was attempted by using a range of soil type characteristics, such as particle size distribution, density and settlement properties. Initially, it was considered that 'settlement gradient' might have been a useful parameter. Settlement gradient (i.e. the acceleration required to induce initial settlement divided by the ultimate settlement magnitude) was combined with various density and acceleration values, such as e_{min}-e_{max}, e_{max}/e_{min}, initial relative density for mean stress and specific stresses. However, any combination of variables generated 'measles' plots (see Figure 5.6.4b).

It was apparent that with the data available, no specific relationship between soil type and the minimum acceleration required to induce settlement was possible. An examination of the data, however, does allow a reason for such behaviour to be suggested. It is apparent that the granular soils responded differently to the same stress-acceleration conditions. It is likely that the specific values of acceleration used (i.e. 0.1, 0.2, 0.3, 0.4, 0.5, 0.6, 0.8 and 1.0*g*) were too coarse to allow more specific soil response to be observed. Using Table 5.6.1 (specific soil settlements under mean stress) the initial settlement for silty fine sand and the fine uniform sand occurred under 0.2*g* for both materials. The magnitudes of settlement are different (approximately 0.002% and 0.015%, respectively). This could merely reflect soil type response, i.e. that fine uniform sand settles more than silty fine sand. However, because of the difference in settlements, it is possible that the fine uniform sand could show observable settlement under a lower level of acceleration, less than 0.2*g* but more that 0.1*g*. This is likely to be true for all the soils tests, i.e. it is unlikely that *in-situ*, granular soils only settle under accelerations in units of 0.1*g*. That is, the acceleration values that were used in the laboratory testing programme were too coarse. Thus, when soil specific minimum acceleration trends were attempted, the soil types were artificially 'grouped' into acceleration values that were not fine enough to allow the resolution of any specific soil response.

The limited study of vibratory settlement performed by New (1978) on 5 soils, reported that accelerations of 0.05*g*, 0.1*g* and 0.2*g* caused initial settlement response. More rigorous tests would be required to identify the relationship between the minimum acceleration that is required to initiate settlements for specific soils under given stress and density conditions.

6.5.4 Comparison Between Trend and Test Data

A comparison between regression generated settlements and the test specific equivalents did show comparable sensitivity to the minimum acceleration required to induce initial settlement (see Table 5.6.4 and 5.6.5). The good agreements support the use of the soil specific (mean stress) values of settlement-stress corrected regression method. The difference between the test specific data and the equivalent regression values may be attributed to a number of factors. Firstly, there will be a degree of experimental error. This could be (in part) related to variations in relative density values which were later accounted for by the vibration settlement equation. The regressed data also assumed that soils respond in the same way to static load, and that the soils were equally sensitive to the minimum acceleration necessary to induce initial settlement. Clearly, it can be seen (by examination of the test specific data) that soils had different values of relative density, responded differently in terms of settlement magnitude and required different minimum acceleration to induce settlement.

With the consideration of the above, the regressed settlement values and the equivalent test specific data show good agreement. If the overall differences between the derived and actual settlements are summed, the regressed values demonstrated an overestimation of 0.05%. Thus, even though some of the data did not demonstrate particularly good agreement, overall, using the regression data was a reasonable nextstep in the data processing and analysis.

6.6 Settlement Equations

The data analysis used trend data generated values that were reasonably consistent with the equivalent test specific data. However, a single expression that identifies a good relation between static stress, density, soil type, acceleration and also accounts for the influence of frequency, vibration time and moisture content was considered to be preferable.

The vibration settlement equation presented in Section 5.5.1 (equation 5.8) was based on the previous trend data and successfully demonstrated the relationship between the various test parameters for accelerations up to and including 1.0g. The high acceleration data uses Equation 5.9 to estimate vibration induced surface settlement estimations. In addition, because site investigation data often uses SPT-N values, rather than relative density, the relationship between D_r and N-values (after Bazara, 1967) is provided.

Because the coefficient of uniformity (U_c) is the standard expression that is used to describe the soil grading characteristic, an expression that uses U_c as the soil parameter (rather than the distribution coefficient, D_c) is presented (note the earlier discussion on the use of U_c, Section 6.8.1). Note however that because the regression analysis that used U_c evolved lower R^2 values than the D_c (see earlier), the corresponding settlements demonstrated poorer correlation agreement between derived values and the test specific data.

To account for the influence of vibration time, frequency and moisture content Equation 5.10 (Section 5.5.5) modifies values of settlement generated that describe the maximum settlement. Note that for dried and partially saturated sand multiply any settlement estimate by 0.06 and 0.01, respectively (being mean difference between the dried and partially saturated tests to the equivalent saturated data). Because the settlements generated for dried and partially saturated sands were so small, such material may be discounted in *in-situ* settlement estimation calculations. The expression that accounts for the time length uses a log settlement rate decrease with time, and a linear relationship between ratio of test frequency to vibrodriver frequency. Because only two frequencies were used, the relationship is a tentative one. Performing additional tests at of frequencies such as 15 and 75Hz would be useful.

6.7 Influence of Parameters and Site Conditions

To demonstrate the use of the settlement equation, a selection of fictitious ground conditions were presented that experienced ground vibrations which were generated using the attenuation equation in Section 5.6.1. The attenuation equation is demonstrated in Figure 5.9.1 for three vibrodrivers (operating at 2, 3, and 4kJ/cycle) running at 25Hz. Note that the attenuation equation is derived for stand-off distances greater than 2m. However, the relationship is extrapolated to a stand-off of 1m, since no better relationship exists (Selby, 1995). Figure 5.9.2 demonstrated the estimated vibration induced ground surface settlement (for ground condition 1.1, and 25Hz, 3kJ/cycle). Using a linear scale, the reduction in ground surface settlement with stand-off is very rapid, especially over the first 2m. Difference in the settlement response influenced by different ground-piling conditions is not very clear after approximately 5m. Thus, log-log scale and the equivalent log-monotonic linear scales were used to enable the differences to be resolved with increasing stand-off distance.

6.8 Risk Table Development

The development of the risk tables served a number of purposes. Firstly, the tables allowed initial appraisal of ground compaction settlement. Secondly, it is proposed that categories that define settlement are inherently contractually significant, i.e. if a 'slight' risk of settlement is stated, which implies ground acceleration of 0.1g-0.2g, with a resulting surface settlement of between 1-3mm for soils with a moderate settlement potential. Knowledge of such vibratory settlement under given conditions may result in the decision to use one construction technique instead of another.

Additionally, the settlement tables allow an appreciation that settlement severity is a function of the interaction between 'potential', which describes saturated soil settlement potential and 'risk', which depends on the vibration characteristics, stand-off distance and site conditions. When potential and risk are combined, the resultant settlement magnitude can then be known.

The tables are presented because they summarise the results of this research in a form that allows a rapid appreciation of the application of the work. The settlement potential table groups soils into 5 categories based on distribution coefficient. The categories show that as distribution coefficient increases, the range of settlements under 1.0g, for a given category, increases. This indicates that more variation in settlement occurred at higher accelerations and higher D_c values. The categories for lower settlement (0.5g is used in the table) imply a different trend: range of settlement decreases with increase of D_c, which reflects the relatively small impact on surface settlement of soil-specific variation under low acceleration.

The categories that define settlement risk indicate the relative importance of acceleration magnitude (which tends to amplify the difference in the settlement response of soils). As stand-off distance decreases, the extent of the categories decreases from 5m for the 'slight risk' category to 0.5m, for the 'definite risk' category.

Basing a settlement estimation solely on the summary tables is not recommended. The tables may be used to give an immediate response to a query, or used in order to decide if a more detailed settlement estimation calculation is required and whether monitoring of ground vibration and ground level is considered to be appropriate. However, if ground acceleration data are not known, or a confident estimation is not possible because, for example, vibrodriver information is absent, or soil types are not confidently defined, then the tables may be used to give a cautious settlement estimate, on which further action may be recommended.

6.9 Case Studies

6.9.1 Introduction

The following section presents case studies of the sites that were visited during the research, and examples taken from the literature. The case studies that were taken from the literature show a bias towards examples from the USA. This suggests that in America, the problem occurs more frequently; that very different soils occur; construction methods are subject to less control, or that the legal system is different.

In the first instance, the case studies are presented to demonstrate that vibration induced ground compaction settlements of granular soils does occur. Secondly, they are used as a source from which data can be abstracted and used in the vibratory settlement equations to make settlement 'predictions', which are then compared with the reported settlements presented in the case studies. The comparisons are discussed, and where estimates differ, reasons are given to account for this. Note that no reference is made to the possible influnce of arching and bulk modulus in these comparisons.

6.9.2 Example Sites

Case Study 1: Durham University Biology Site.

A line of sheet piles was driven to form a retaining wall behind a new building development. The piles were driven by an ABI-1400 vibrodriver, which produced a maximum acceleration of 0.3*g* at 2m stand-off on the level ground (see Table A5.1.1), and approximately 0.9*g* on the slope (see Figure 6.13).

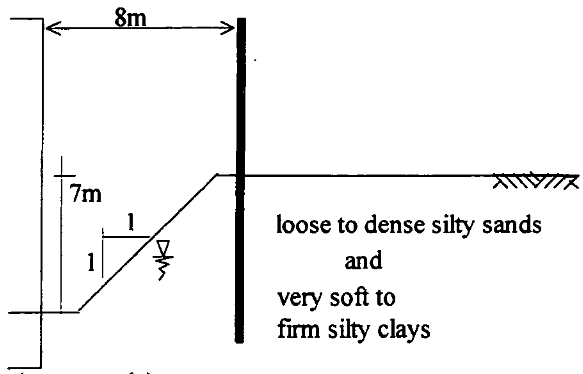

Figure 6.13. Cross-section of a retaining wall, Durham (Case Study 1).

Ground levelling measurements indicated that settlement occurred at two points on the level ground. One levelling pin settled 96mm and the other settled 77mm (see Table A5.1.2) at a distance of 9.7m from the vibration source. However, the site was heavily trafficked, and the settlements were observed for pins at the end of levelling lines, rather than near to the source. Using the vibratory settlement equation, estimated settlements in the order of 1mm on the level ground (at 0.3*g*) for stand-off of 2.5m, and about 10mm on the slope (with 0.9*g*) at the same distance, are generated (see Table A4.2.1 for the ground profile data sheet). The observed settlements were attributed to direct disturbance of the ground surface by site plant, rather than by ground vibrations.

Case Study 2: Walshford to Dishforth, A1 Widening Scheme, Bridge 04.

An 11km, £54 million, carriage-way widening scheme constructed an additional 3 lanes on the west side (north bound) of the existing dual carriage-way. At Bridge 04 (B04), three bridge piers were constructed. Vertical and raked H-piles were driven approximately 20m through fine to coarse, medium dense to dense sands, clayey silty sands and silty clays to bedrock. A 6 tonne hydraulic drop hammer produced ground vibrations of 0.45*g* at 2.5m stand-off (see Table A5.2.1). No positive settlements resulting from vibrations were recorded (see Table A52.2). Using the settlement equation, approximately 2mm of settlement was estimated for a stand-off distance of 2.5m (see Table A4.2.2 for the ground profile data sheet).

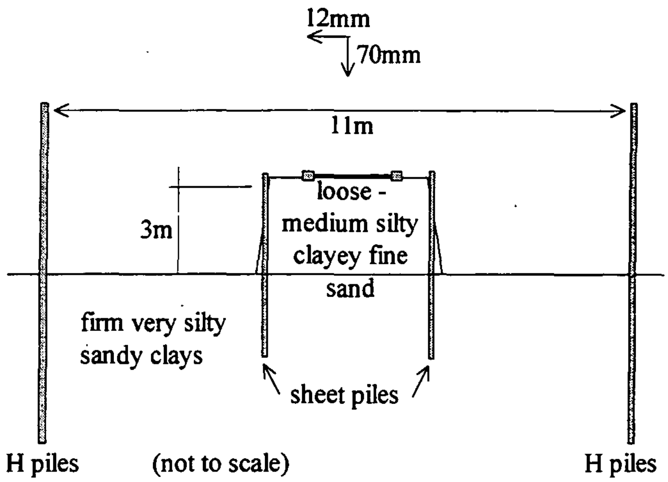

Figure 6.14. Cross-section of railway bridge construction (Case Study 3).

<u>Case Study 3: Walshford to Dishforth, A1 Widening Scheme, Railway Bridge.</u>

Track movement was experienced when driving H-piles during bridge pier construction (see Figure 6.14). Track movement included elements of settlement and lateral deflection (of 12mm). The lateral deflection tended towards the side which was undergoing piling. Track settlements reached a maximum of 70mm (see Table A5.4.3). Maximum ground acceleration of 0.65*g* was recorded at 2m stand-off from the H-piling, for a 6 tonne drop hammer (see Table A5.4.1). A geophone placed adjacent to the sheet piles recorded an acceleration of 0.13*g*. If 0.65*g* is used in the calculation to estimate ground settlement, then some 80mm of settlement is predicted (see Table A4.2.3). However, the piling was carried out some 6m from the sheet piles, at which distance 0.13*g* was recorded, which estimated 4mm of settlement.

Lowering the water table could have been a contributory factor to ground movements. Initially, settlement was attributed to a reduction of artesian water pressure and consequent consolidation in the sands and gravels. However, inclinometer deflections indicated any or all of the following factors: consolidation in the boulder clay because of dissipation of excess pore water pressure caused by piling; settlement in the clay and upper levels of sand demonstrated by large inclinometer deflections; settlements due to the migration of fine sands with artesian water up the pile faces; consolidation of material at higher levels due to plant trafficking (incremental deflection graphs suggested that settlements occurred at depth). Assessment of likely settlements induced by excess pore water pressure indicated only minor track settlement, and not of the order recorded on the track. Additionally, consolidation caused by lowering of the ground water table would have been completed prior to the commencement of piling operations. In addition, track settlement started when piling commenced, and not when pumping commenced. It was concluded that track settlement was probably associated with the compaction of near surface sands caused by vibrations during H-piling.

However, the difference between the recorded and calculated estimate suggests that an additional mechanism contributed to ground settlement. It is probable that the sheet piles suffered lateral deflection; possibly outward movement at the pile-toe, and ground movements occurred as a result.

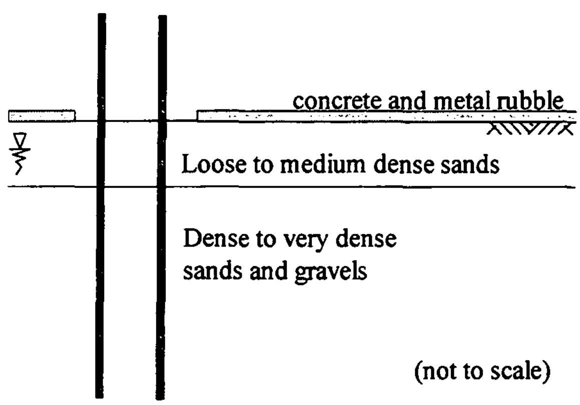

Figure 6.15. Cross-section of pile trials, Flitwick (Case Study 4).

Case Study 4: Dawson's Yard, Flitwick.

Ground vibration and ground levelling was performed during wider pile driving trials in granular soils. A range of vibrodrivers and drop hammers were used to drive a range of sheet piles. Fine sands, increasing in density (N-values of approximately 10 near the surface) to 15m depth where SPT-N values of 80 to 100 were recorded.

Maximum ground acceleration of 0.9*g* was recorded at 2m stand-off (0.5*g* at 5m) when a BSP HH-357 (in 5 tonne mode) drop hammer was driving 15m long Frodingham piles (see Table A5.3.1). A PTC 13HF1 vibrodriver driving 9m Larssen piles produced a maximum acceleration of 0.35*g* at 2m (0.06*g* at 5m). Using 0.9*g* in the settlement estimate calculation produces 10mm, and 0.35*g* predicts less than 2mm at 2m stand-off (see Table A4.2.4). The site was heavily trafficked by site plant, and most of the ground surface was covered in dense concrete and metal rubble (see Figure 6.15). Ground settlements between 2-7mm were recorded (see A5.3.2), showing good correlation with the estimated values.

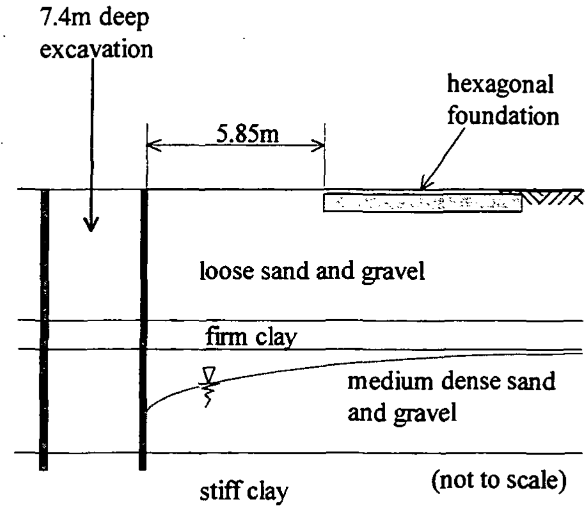

Figure 6.16. Cross-section of cofferdam (Case Study 5).

Case Study 5: Cofferdam, Walton on Thames.

Concern was expressed that the construction of a sheet piled cofferdam 6m from the base of a communications tower that was founded in loose sands could cause settlement of the sand and hence, differential settlement of the tower (see Figure 6.16). Ground vibration induced surface settlement estimation assuming the water table to be at the surface predicted 7mm of settlement on the near side of the tower foundation. However, as indicated by site investigation data, the water table was measured at a depth of 6m, and the settlement calculation that accounted for this predicted that there would be less than 1mm settlement on the near side of the tower foundation, and none on the far side (see Table A4.2.5). Pile driving using a PTC 15HF1 generated an estimated 0.3g at the front of the foundation. No settlement of the sands or differential settlement of the communications tower was recorded, producing good correlation with the predicted settlement estimate.

6.9.3 Pile Driving and Compaction Settlement: A National Survey

A questionnaire was distributed to 230 members of the construction industry, such as consultants, contractors, piling specialists and local authorities. A very low level of response was obtained. Only 14 replies were received: 4 related directly to compaction settlement induced during pile driving activities; 9 replies effectively or explicitly reported no experience of the phenomenon. This low response may be attributed to:

a) The problem is not common, so many engineers had nothing to contribute

b) The cases in which the problem had occurred were subject to contractual negotiations or even to arbitration/litigation.

c) Companies with experience of the problem prefer to keep any information private, for commercial advantage.

Because an element of contractual negotiation occurred in the reported cases, and since the questionnaire offered shared benefits to participants, there is some justification in proposing that the primary reason for the low response is a very low frequency of occurrence of the problem in the UK construction industry. Lacy and Gould (1985) related that the settlement effects of pile driving at thousands of sites occurred in a small percentage of cases. However, where settlement was recorded, costly damage to structures did result.

The examples of vibration induced ground compaction settlement are presented; the full report (Selby and Tuck, 1995) is presented elsewhere:

<u>Example #1: Temporary Sheet Pile Wall</u>

A temporary sheet pile wall was driven to approximately 8m by a BSP 7000N air hammer to allow the excavation and construction of a concrete retaining wall (see Figure 6.17). During extraction of the sheet piles by a PTC 13HF1 vibrodriver, the newly constructed wall tilted into the retained soil by some 20mm. It was noted that the pans of the extracted piles were filled with clay over the bottom 2m of their length. Additionally, running sands were noted emerging from the weep holes in the concrete wall.

If an acceleration of 2.0g is assumed for the back of the wall, and 0.4g is assumed for the front of the wall, then settlements of 22mm and 0.3mm, are predicted, respectively (see Table 4.3.1). The report did not relate measured settlement magnitude, and expressed ground movements in terms of a top-of-wall tilt.

The primary cause of the tilting was probably due to ground loss on extraction of the piles. However, ground vibrations probably exacerbated the problem, with some local liquefaction of the saturated loose sands. If the sheet piles had been left in place, and used as part of a permanent retaining wall, no settlement problems would have occurred.

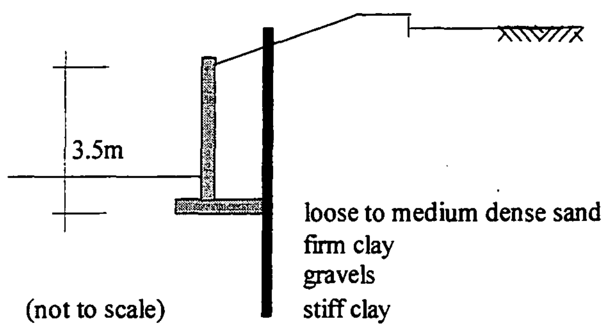

Figure 6.17. Cross-section of temporary works (Example #1).

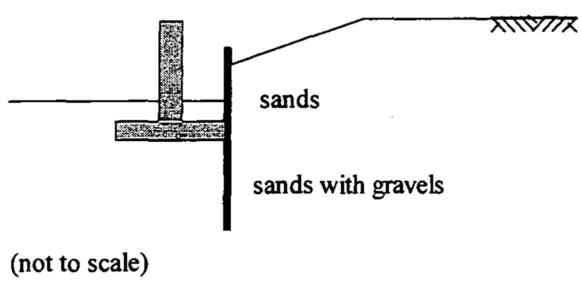

Figure 6.18. Cross-section of the pier construction (Example #2).

Example #2: Temporary Sheet Pile Wall

A temporary sheet pile was used to support a slope to allow the construction of a pier base (see Figure 6.18). The piles were extracted by vibrodriver (of unknown power, running at 30Hz) and caused the near side of the base to settle 50mm, and the far side by

5mm. If 2.0g is assumed for the near side of the pier base, and 0.2g is assumed for the far side of the pier base, a settlement of 57mm and <1mm for the near and far sides, respectively, is predicted (see Table A4.3.2) which produces a good correlation with the observed settlements.

Site investigation showed dry sands, generally medium dense, but with layers of very loose sands below the base of the north pier.

The severe differential settlement of the pier base was attributed directly to vibratory compaction of loose dry sands during prolonged and severe vibratory extraction of the sheet piles.

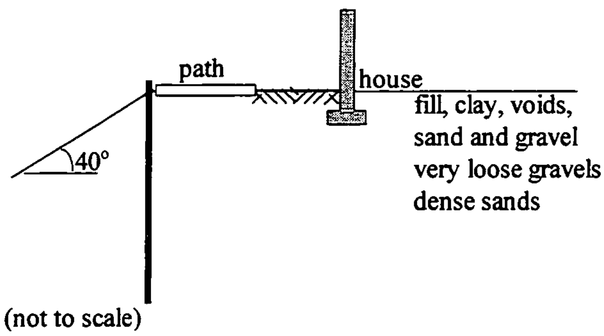

Figure 6.19. Cross-section of sheet pile works (Example #3).

Example #3: Damage to a Structure

This case is not directly related to vibratory compaction settlement, but it is cited because settlements are described that were caused by pile installation (see Figure 6.19). A row of piles was installed to a depth of 9m at the top of a steep bank of very weak soils to prevent further slips and damage to exiting housing at the top of the bank. Piles were installed by a Giken 'vibrationless' driver.

Settlements at the ground surface were recorded at 41mm at 3m from the piling, 10mm at 6m and 0.5mm at 10mm distance. In the 2 storey house some 3m back from the line of piles, existing cracks opened further and new cracks were caused. At ground level, tension cracks opened at 2-3m back from the pile line.

Example #4: Cofferdam

Severe settlements of a basement compensated raft foundation to a pumping station occurred during vibro-extraction of sheet piles in a cofferdam, which lasted for several weeks (see Figure 6.20). Maximum settlements of the foundation slab of 95mm were recorded, although settlements of approximately 70mm were characteristic. These values are conservative, in that some settlement probably occurred before the records began, and during discontinuity of measurements. Performing a settlement estimate calculation assuming 0.9*g* at 1.5m, predicts a maximum settlement of 32mm (see Table A4.3.3) with the water table at 2m depth, and 73mm if the water table is assumed to be at the surface.

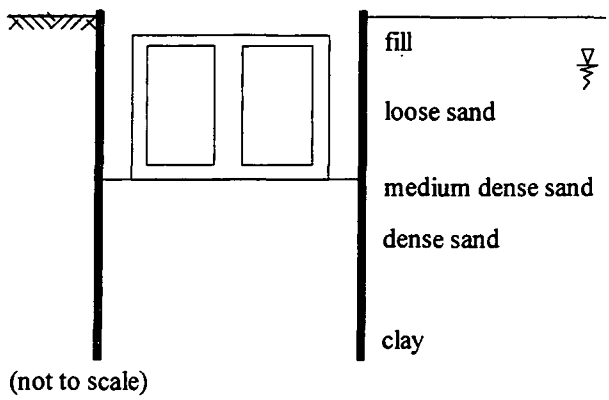

Figure 6.20. Cross-section of raft foundation (Example #4).

An interesting aspect of this example is to question why the sands were not compacted during the installation of the piles, so that once compacted, the sands should not have been susceptible to compaction by further vibrations, i.e. during pile extraction. However, a heavy inflow of water when the excavation was at its deepest must be assumed to have re-loosened the sands to some depth. Thus, subsequent pile extraction led to the severe settlements. Other possible mechanisms which could have contributed to the settlements include: ground loss due to filling of the pans of the sheet piles, but no report was made of this; liquefaction over a wide area, however liquefaction occurs immediately adjacent to vibro-driven piles and this rarely extends beyond about 0.5m;

seepage flow combined with vibrations might have caused a more widespread liquefaction of the loose sands. Whilst there is strong evidence to link the observed settlements with sheet pile extraction, the exact mechanism is not absolutely clear.

6.9.4 Examples from the Literature

The following section provides examples of vibration induced ground movements abstracted from the literature.

Paper #1: Picornell and del Monte (1982)

Steel H-piles that were driven adjacent to existing pier foundations for factory construction caused settlements of approximately 25cm (see Figure 6.21). No ground settlement was detected at stand-off distances greater than 12m. The ground essentially consisted of loose to medium dense sands, gravel and sandy silts with frequent limestone boulders to very variable depths. The water table varied between 1 to 5m depth. Ground vibrations were assumed to be the same as those presented by Clough and Chameau (1980, see Paper #4). Settlement estimation calculation estimated 37mm (see Table A4.4.1) if hard driving is assumed to produce 0.5g at 2m stand-off. At 1m stand-off, hard driving is estimated to produce 0.88g, and a settlement of 149mm.

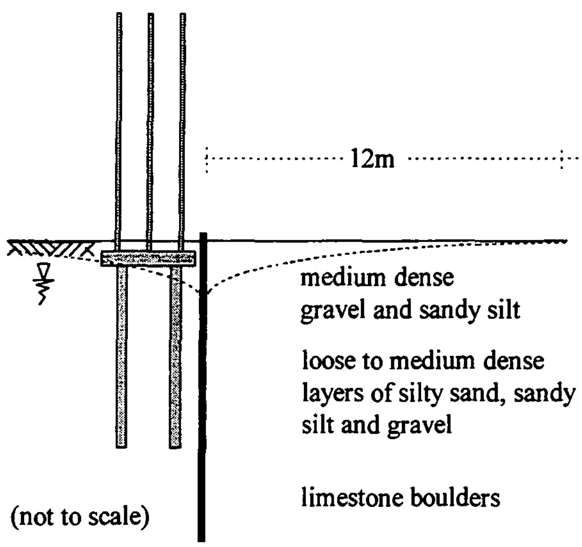

Figure 6.21. Cross-section of H-piles adjacent to existing structure (Paper #1).

The presence of boulders caused hard driving and an increase in the ground vibrations by an order of 2. It was noted that in one instance, the SPT sampler was driven 2m by 3 blows, indicating large void spaces, possibly associated with the presence of the boulders. Settlement was attributed to the dynamic compaction of the soil induced by the pile driving activities. The difference between observed and estimated settlement could be due to the very variable nature of the density of the deposits, which was not explicitly presented in the site investigation data.

Paper #2: Linehan *et al.* (1988)

A pressurised gas pipeline immediately adjacent to construction work for pile foundations of a bridge settled 50mm (see Figure 6.22). The ground essentially consisted of loose to medium dense sands and dense to very dense sands and gravels. Ground surface settlement was greatest over the centre-line of the pipe. Vibrodriving generated peak particle velocities of 100mm/s at 1.5m, 10mm/s at 4m and 2mm/s at approximately 20m. The primary cause of the settlement was attributed to vibratory densification and loss of lateral support. The ground settlement equation predicted 50mm settlement using 3.0*g* estimated during the driving of the east wall of the cofferdam, some 600mm from the pipe. The ground vibrations (0.4*g*) from the west side, 3m from the pipe, generate 15mm (see Table A4.4.2). However, if 2.0g is used in the settlement estimation, then 21mm of settlement are estimated, and an additional mechanism is required to cause the settlements that were observed. It was reported that the settlements that occurred were also influenced by lateral pile movements.

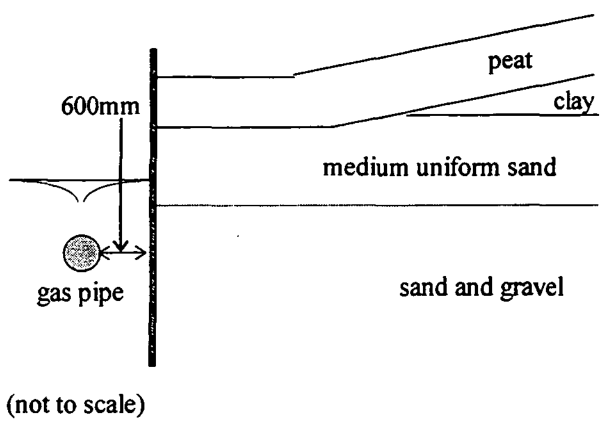

Figure 6.22. Cross-section of cofferdam construction (Paper #2).

Paper #3: Holloway *et al.* (1980)

This paper describes the effects of driving H-piles near an existing series of locks and dams founded on 9-11m timber piles (see Figure 6.23). The ground consisted of 30m of alluvial sands; glacial sands and gravels on limestone bedrock. All piles within 15m of the monolithic structure caused at least 5mm displacement. A Foster 400 vibro-hammer, MKT DE-70B single acting air hammer and a Vulcan 010 single acting air hammer were used and vibrodriving was reported to have caused greater displacements than impact driving for given conditions. Maximum settlement recorded was 35mm for 0.39g at 3m stand-off from the piling. Using the settlement estimation equation predicts 32mm of settlement (see Table A4.4.3) for an acceleration of 0.39g.

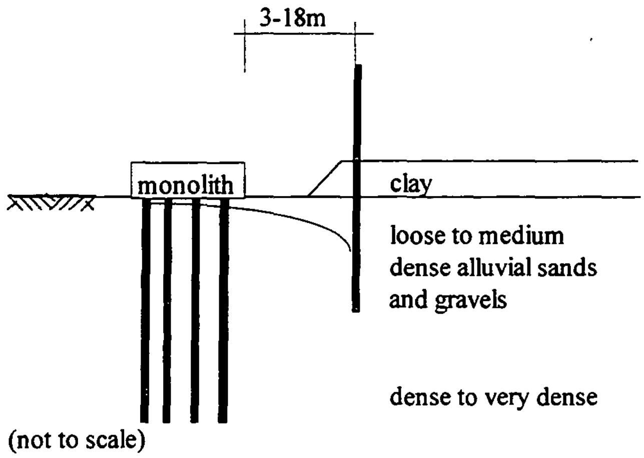

Figure 6.23. Cross-section of piling near existing structure (Paper #3).

Paper #4: Clough and Chameau (1980)

An extensive series of (4.5-12m deep) sewer outfall systems was constructed between a built-up area and a yacht harbour (see Figure 6.24). Sheet pile walls were driven by an ICE 812 vibrodriver running at 18Hz. The soils of the area consist of Bay mud and loose sands, overlain by approximately 7-10m of rubble-sand fill. The water table was generally at a depth of 1.5-3m.

Ground accelerations at 2m stand-off, were in the range of 0.4-0.5g for hard driving into the rubble fill and 0.2-0.3g for normal driving. At 12m stand-off 0.02g was recorded and beyond 12m no measurements were made because of interference from traffic. The data suggested that settlements would be very small as long as accelerations are less than $0.1g$. Driving the sheet piles into the rubble and rock caused substantial densification of the sands. Settlements of 152mm were recorded adjacent to the piles and these reduced to zero at 12m stand-off. A settlement of 24mm is estimated using an acceleration of $0.45g$ at 2m, and 61mm using $0.72g$ at a 1m stand-off (see TableA4.4.4). If the water table is assumed to be at the surface, then the settlement caused by $0.72g$ is increased to 137mm.

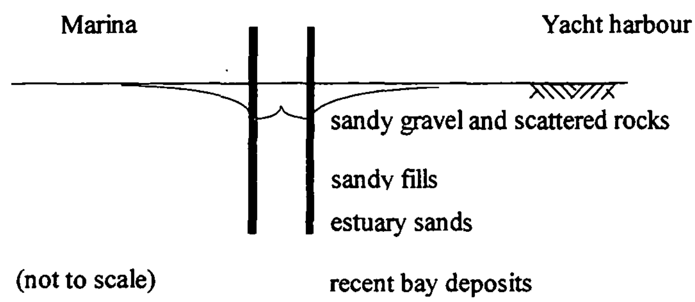

Figure 6.24. Cross-section of sewer culvert (Paper #4).

Paper #5: Lucas and Gill (1992)

Driving of H-piles for a building foundation, movements occurred in the adjacent structures and street (see Figure 6.25) The upper 12.2m of the soil deposits were loose very uniform angular fine to medium sand with trace amounts of silt becoming increasingly dense with depth. The sands fall within the gradings that are considered to be most sensitive to liquefaction from earthquakes. The water table was at approximately 1m depth. When driving the piles it was noted that the water would temporarily rise up to the surface, and returned to its original position a few hours later.

During the driving of the first 50 piles, vertical and lateral deformations of adjacent buildings and streets were observed approximately 6.0-7.5m west of piling operations. The cracks were approximately 10-15mm wide and a water main failed. A building supported on shallow foundations, some 3.0-4.5m stand-off settled 64mm and the exterior wall displaced approximately 51mm. A settlement estimation calculation predicts 63mm settlement (see Table A4.4.5) which correlates well with the observed settlement.

When piling resumed on lines 2 and 3 the sheet-piling along the edge of the excavation displaced a total of 127-152mm laterally in the direction of the piles. There was a vertical movement of soil of a similar order of magnitude. Midway between the piles in line 2 and 3 ground settlements were measured of 0.76-0.91m. Between pile groups the settlements were in the order of 0.4m. These large settlements were attributed to liquefaction of the soil.

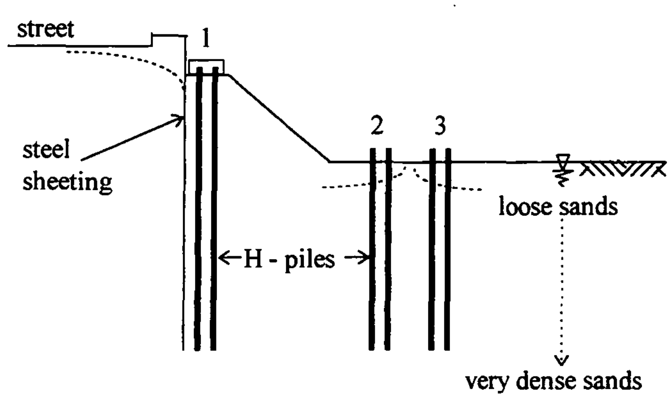

Figure 6.25. Cross-section of H-piles for a building foundation (Paper #5).

Compaction grouting was undertaken under the portions of the structures immediately adjacent to the site to increase the relative density of the soil to minimise further ground movements. The remaining piling to be installed within 15.5m of existing structures was to be jetted to reduce the ground vibrations and number of repetitive blows. The jetted piles generated ground accelerations about 0.5 times of those for non-grouted piles and a third of the hammer blows.

The piles were installed by a HC Hydrohammer, Model S-70 (delivering a maximum of 70kNm/blow). Driving energy increased with pile penetration (as the ground density increased) and ground accelerations were seen to vary widely, e.g. 0.04-0.3g at 15m.

Paper #6: Examples from Lacy and Gould (1985)

Case A: Foley Square, New York City: Bearing piles for high rise structure were driven 24m (over nine months) into bouldery till which was overlain by fine sand and varved silt. A 35kJ hammer was used to drive the piles, and settlements were caused in adjacent buildings. After 25mm of settlement was observed for an adjacent building, under pinning was carried out (see Figure 6.26) with shallow jacked piles. As settlements continued, pile driving was switched to vibrodrivers, on the assumption that less total energy and time would be required to advance the piles. However, settlements continued to a maximum of 76mm. Peak ground accelerations recorded were approximately 0.1g at 6m. The increase in pore water pressure was believed to have propagated over a wide area and contributed to the settlements observed. Whilst the deformation of the glacial sediments ($D_r \approx 45\%$) under static loads was low, densification under prolonged vibrations was significant.

Settlement estimation produces less than 1mm settlement under 0.1g (see Table A4.5.1). However, if liquefaction is assumed to have occurred below 20m, and the corresponding effective static stress is reduced to an average of 0.2kPa, then the settlement calculated is increased to 69mm (see Table A4.5.2).

Case B: Southern Brooklyn, New York City: Expanding a treatment plant required the construction of a new structure (see Figure 6.27) that extended 6-9m below grade and required lowering the ground water by as much as 7.5m. After the first 100 piles had be driven (3.0-24m from the aeration tanks), significant settlements were noted. Settlement continued until driving was halted after 220 piles were driven. After the first 25mm of settlement, all fluid was removed from the tanks, but the rate of settlement of the structure was unaffected, reaching a maximum of 76mm. Peak accelerations measured adjacent to the building were 0.35g. However, two hammers were used to drive the piles for several days, and when hammer strikes became synchronous the accelerations increased to approximately 0.8g at 3m stand-off. A settlement of 72mm is estimated (see Table A4.5.4), if 1.1g is assumed at a stand-off distance of 2m. There was no indication of the generation of excess pore water pressure during driving; it was believed that the dewatering operation prevented pore pressure increase. Augercast piles were substituted for the remaining 300 pipe piles. However, augering piles immediately adjacent to the sheeting along the aeration tank caused an additional 50mm settlement of the tank. However, this later settlement was not attributed to vibrations, but was caused by the reduction in passive resistance beneath the cantilever sheeting.

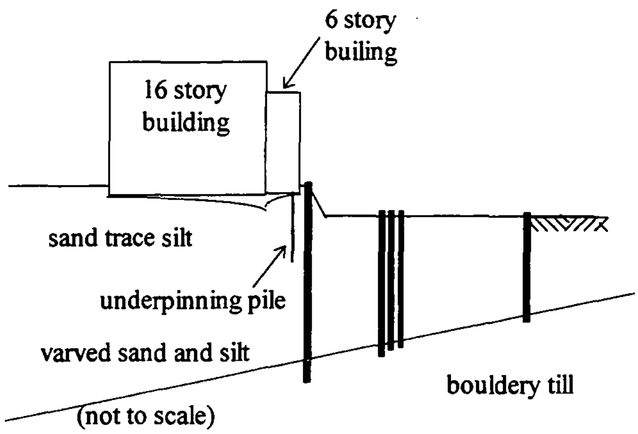

Figure 6.26. Cross-section of settlement of structure (Case A).

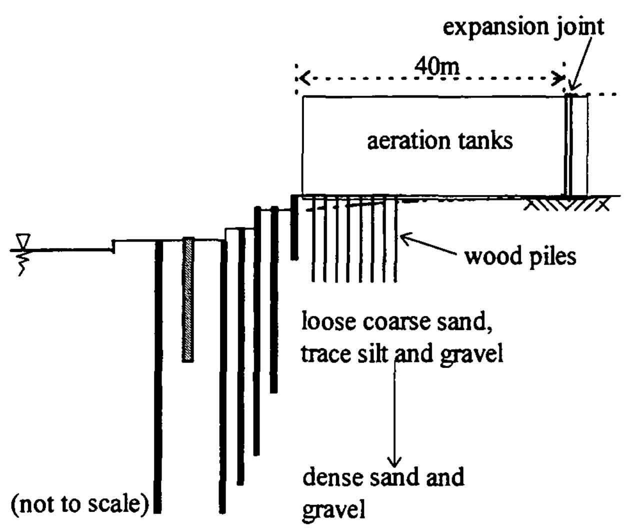

Figure 6.27. Cross-section of treatment plant expansion (Case B).

<u>Case C</u>: Lower Connecticut River: The construction of river pier foundations required the placement of sheet pile cofferdams (see Figure 6.28). Sheet piles were driven to 24m through a homogeneous stratum of uniform sand ($D_r \approx 40\%$). It was found that an average settlement of 0.84m had occurred between the piles. Settlement estimation

using 1.0g and 3.0g generates 99mm and 837mm, respectively (see Table A4.5.5). There was no transmission of this settlement from pier to pier. The experience was typical of sand compaction by deep vibration (such as the 'Terraprobe' technique).

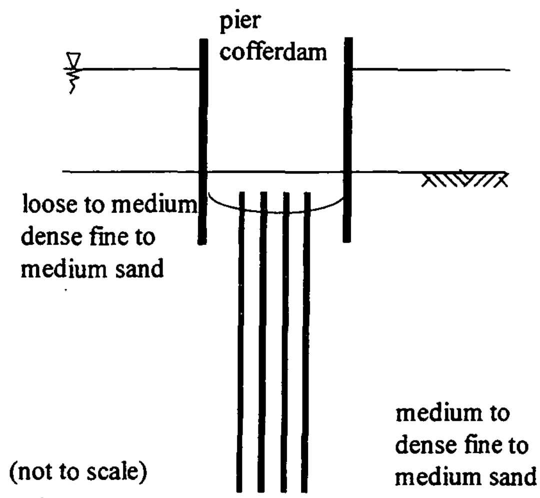

Figure 6.28. Cross-section of bridge pier (Case C).

Case D: Western Brooklyn, New York City: Sheet piling was being driven by an ICE 812 vibrodriver, to allow an excavation next to a warehouse (see Figure 6.29). The wall of the building, at 0.9m stand-off, settled 76mm. The warehouse was demolished and reconstructed after the near structure was completed. Assuming an acceleration of 0.85g, a settlement of 46mm is estimated.

Case E: North Syracuse, New York: Sheet piling was installed by an ICE 416 vibrodriver for a bridge cofferdam (see Figure 6.30). Boils developed due to dewatering difficulties that were attributed to the coarse permeable sands underlying very loose fine sands and silts. During construction, an access ramp settled, a joint in the sewer opened and surrounding soil was washed through the sewer causing a large area to settle to a maximum of 0.9m. The sheet piles were extracted which caused an additional 38mm of settlement on the edge of the access ramp. This case study provides an example of ground settlements and ground loss that can be indirectly caused by piling.

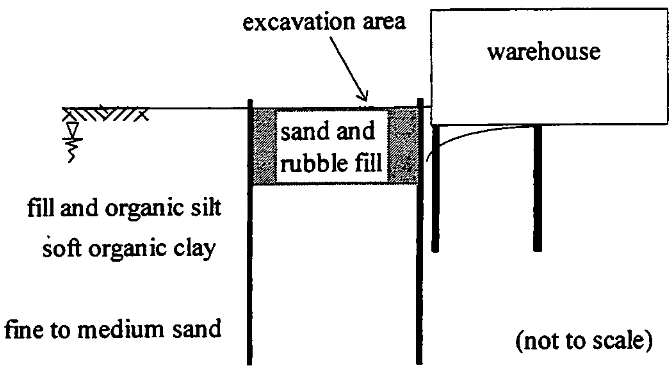

Figure 6.29. Cross-section of excavation adjacent to structure (Case D).

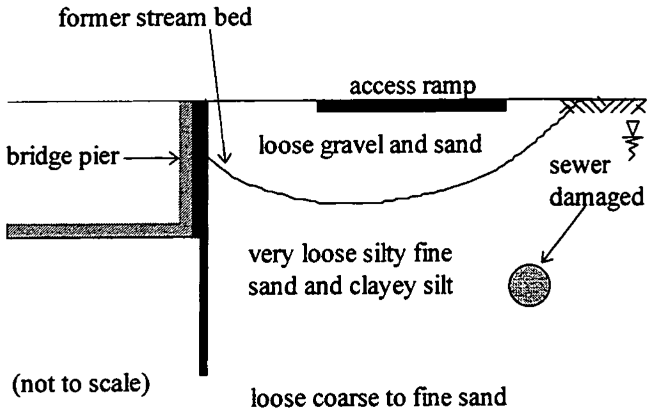

Figure 6.30. Cross-section of bridge cofferdam (Case E).

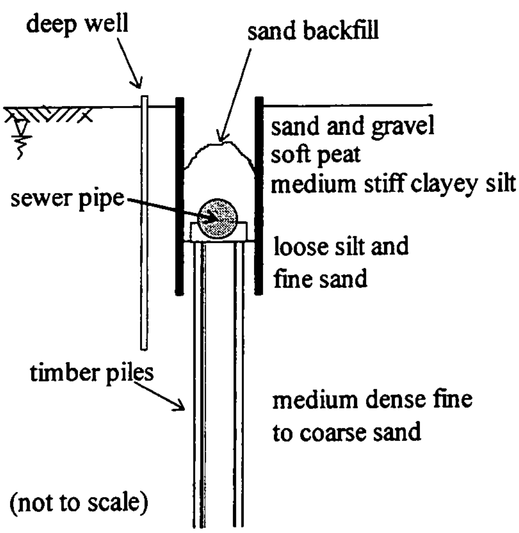

Figure 6.31. Cross-section of sewer repair (Case F).

Case F: Syracuse, New York: Repair work was carried out to an existing sewer, where a joint had opened that allowed silt and fine sand to enter. Sheet piles were driven to allow excavation to expose the damaged pipe (see Figure 6.31). After repairs, a 30m section of the sheet piles were extracted, and the sewer settled 150mm. Using an acceleration of 1.5g, settlement of 144mm was estimated for sewer settlement. It was considered that loosening of the soil beneath the pipe, due to previous soil loss into the damage pipe, contributed to the settlement of the newly installed pipe.

6.9.5 General Comments

The settlement values 'predicted' using the settlement equations showed agreement with reported measurements in many cases. The differences that are observed may be attributed to two reasons; that specific data values were absent, and assumed values were not those that actually occurred, resulting in calculation error, or that a second mechanism or combination of mechanisms contributed to the recorded settlements. Such mechanisms were identified as lateral movements of sheet piles, and increase in pore water pressure under low acceleration. Situations that appear to be susceptible to potential liquefaction include clayey silty fine sands, especially when inter-layered with clay. However, whilst this has been reported by the geotechnical press of the USA, few, if any records are to be found in the UK. In addition, it appears that a major cause of ground settlement is the extraction of piles by vibrodriver.

A serendipitous aspect of the vibration settlement equation allows the effects of liquefaction under low acceleration to be crudely estimated. The stress-settlement trend allows settlement to continue to increase as stress is reduced to zero. Liquefaction settlement under acceleration of 0.1g can be modelled if the settlement calculation uses an average effective stress value of say, 0.2kPa for those layers that experience liquefaction.

In order to prevent the potential consequences of ground vibrations, a number of options are worth considering. It was seen that vibration settlement of granular soils is highly dependent on acceleration, stress and moisture content. Any process that decreases the acceleration received by a soil unit, increases the static load or decreases the level of saturation, should be considered. Using the smallest vibrodriver that satifies particular construction requirements would be beneficial. However, any activities that change the stress experienced by a given unit of soil, may actually cause as much consequential ground movements as those which were predicted for a vibropiling operation. For example; artificially increasing the depth of the water table to create more partially saturated soil, would reduce vibratory ground settlements. However, the resulting increase in static stress could cause significant static ground settlement.

6.10 Summary

This chapter discussed aspects of the test programme that was designed to model the ground compaction settlements that are induced by vibrodriving of piles in granular materials. It was important that, in the first instance, a sample preparation technique was developed to model *in-situ* soil and enable good sample control and behaviour during subsequent static loading and testing. It was argued that the assumptions that were made during testing were reasonable.

Various aspects of the vibratory tests were discussed, such as vibration duration and orientation. The influence of test conditions were examined with a view to highlighting subtle sample behaviour which was masked by the particular values of acceleration and static stress that were used. The results of the laboratory programme were discussed and the data processing that evolved trends, regression relations, parameters and the equations that were developed were subject to comment.

Case studies were presented that allowed the settlement equations to be applied to actual examples of ground settlement induced during piling operations. Good correlation was observed in many cases. However, some cases demonstrated that other mechanisms contribute to settlement such as build-up of pore water pressure and lateral movements of piles. In addition, the vibro-extraction of piles was seen to be as important mechanism that causes ground settlement. Any procedures that are performed in order to prevent or minimise vibratory ground settlement should be applied with consideration of the site geometry and of the ground movements that could result as a consequence.

CHAPTER 7
CONCLUSIONS AND FURTHER WORK

7.1 Introduction

This thesis has described a programme of over two hundred laboratory tests that were performed on a range of granular soils under conditions that equivalent soils would experience in the field. The main emphasis was on observing the vibratory settlement behaviour of the soils under conditions of simulated ground acceleration that were representative of those that would occur in the ground during vibropiling activity. Settlement trends and parameters were defined that allowed empirical equations to be derived showing a good relationship between the various parameters. The tests were performed to investigate the most severe potential settlements, i.e. those which would occur at an undisturbed 'green field' site, with the water table at the ground surface. However, if sites are heavily trafficked, the water table is at a few metres depth or clay layer are present, then settlement may be decreased to negligible levels

7.2 Conclusions

A number of trends were identified from analyses of the vibratory test settlement results. These trends were:

- Increase in static pressure towards 100kPa caused a decrease in vibratory settlement magnitude to very small values, i.e. vibratory compaction settlement is highly dependant on vertical stress. The high acceleration data suggests that a monotonic decrease in settlement with increasing static load may not occur for some soils under certain circumstances.
- The type and grading of the soil influences compaction. In general, well-graded soils showed greater compaction than uniform soils. However, decrease in grain size does not necessarily imply that a decrease in settlement will occur. A distribution coefficient was developed for use as the soil parameter, which is given by:

$$D_c = \frac{D_{90}}{D_{60}.D_{30}}$$

- Compaction was seen to increase with increase in acceleration. The soil settlement response to acceleration below 1.0g was relatively small compared to the increase in settlement for accelerations of 2.0g and above. Because soil settlement behaviour did not show a uniform response over the acceleration range used, two equations were required to describe soil settlement under low and high acceleration ranges.
- The frequency of vibration had little effect on ultimate settlements for equal peak accelerations. However, frequency affected the rate of settlement, in that higher frequencies took longer to achieve a given settlement.
- Vibration may be defined in terms of frequency and displacement, velocity or acceleration. The results demonstrate that for the case of vibratory compaction, acceleration is the correct parameter for vibration, as settlement behaviour was dependant on acceleration magnitude, regardless of frequency.
- It was demonstrated that moisture content was a significant parameter. Saturated soils compacted significantly more than equivalent partially saturated and dried soils for accelerations up to 1.0g. During high acceleration tests the saturated and dried samples showed comparable settlement magnitude, while the partially saturated samples continued to show much smaller settlement.
- Evaluation of the results of the laboratory programme compared well with the reported case studies in many cases. In addition, the comparisons showed that in some cases, two or more contributory effects can be identified when damaging settlements occur. It is important to consider the other mechanisms that could cause or contribute to observed ground settlements.
- A risk strategy is proposed which takes into account settlement potential, categories of risk and settlement severity. The categories are summarised in two tables that may be consulted by the engineer as the means to perform an initial assessment of the potential ground settlement. The initial assessment can then be used as a basis to decide if a more detailed settlement estimation calculation is necessary and if monitoring of ground vibrations and settlements is required. The tables may also be used if data are unavailable that would allow a more detailed settlement estimation.

- Reports of recent problems in the UK identified vibro-extraction as a troublesome mechanism. In addition, commercial secrecy is a factor that influences the apparent extent of vibration induced settlement.

The data required to enable an estimation of ground compaction settlement to be made are: a knowledge of the soil grading(s) so that the distribution coefficient (D_c) can be calculated for low acceleration conditions, and uniformity coefficient (U_c) can be calculated as the soil parameter to be to used for high acceleration settlement calculation; values of ground acceleration (directly measured or estimated) for increasing stand-off distance to generate a settlement profile; the relative density (D_r) of each soil layer is required, in addition to the overburden stress (σ_v) calculated for the midpoint of each defined layer.

To estimate an upperbound vibration induced ground compaction settlement (S_v), for a discrete saturated soil layer, the following empirical equation is recommended for accelerations of less than 1.5g:

$$S_v = \frac{2.8\ln(D_c)\,g^2}{D_r\,\sigma_v}$$

If site investigation data characterises soils in terms of the coefficient of uniformity (U_c) only, then the following equation may be used instead, but note that the S_v-U_c settlement relationship is not as strong as the S_v-D_c relationship, for low accelerations:

$$S_v = \frac{3.3\ln(U_c)\,g^2}{D_r\,\sigma_v}$$

For ground acceleration above 1.5g, the following is recommended:

$$S_v = \frac{4\left(\ln(U_c) + 0.7\right)\,\ln(g)}{\left(0.01(\sigma_v) + 0.75\right)\left(1 - D_r\right)}$$

To account for the influence of vibration duration, frequency and level of saturation, the following equation is recommended:

$$S_v\,(t,f,m) = \ln(t).\frac{S_v}{\ln(t_{\max})}.\frac{1}{f'}.m$$

Note that because of the complex nature of ground vibrations, the variability of piling operations, the variable quality of site investigation data, the heterogeneity of natural soil deposits, site geometry and size of construction operation, it is difficult to make absolutely confident recommendations of predictive equations. It would be prudent that where settlements are estimated and are of concern, continuous monitoring of vibration, ground level and adjacent structures is performed. In addition, where settlements are of concern, the contract and construction method should be subject to modification as and when required; i.e. at the design stage, a number of options should be planned that may be used when certain site conditions are manifested, such as unlikely but possible ground vibration at a given stand-off distance, which could cause severe instead of moderate ground settlement.

7.3 Further Work Summary

A number of specific recommendations have been made for further work that concerned the modification of test equipment, the test programme and the grading characteristics of the soils. The following recommendations refer to the wider issues of additional lines of research.

It would be beneficial to perform vibratory tests at different specific stresses in order to identify more confidently the relationship between static load and the vibratory settlement observed for specific soils. It would be useful to perform vibratory tests specifically to enable the relationship between soil type, static load and the minimum acceleration that is required to initiate vibratory settlement response to be quantified. Similarly, it would be useful if tests were performed to identify the transition acceleration at which a soil begins to settle under high acceleration, i.e. at what level of acceleration between 1.0*g* and 2.0*g* does a particular soil demonstrate, for various test conditions, a marked increase in settlement.

Also, an investigation into the applicability of using resultant values of ground accelerations and comparison with multidirectional settlement data would be of use. The use of discrete, repetitive vibration impulses to model the effects of impact hammers should be performed.

In addition, performing vibratory tests on more cohesive soils, or tests where drainage is restricted or prevented would expand the application of this research. Such tests would simulate the situation where a granular soil is bounded by soil(s) with low permeability, and where pore water pressures are generated which could ultimately lead to liquefaction at accelerations well below 1.0*g*. To complement such tests, it would be valuable to be able to identify, for various test conditions, what percentage of cohesive material is required to make a non-cohesive material respond like a cohesive material, i.e. show no settlement during vibration. It would be interesting to gain insight into the effect of ground water chemistry on vibratory settlement, i.e. what level of cohesive material and what concentration of salts or other chemicals are required to significantly affect granular soil vibratory settlement response.

Additional work that examines the effect of shear waves and/or constant shear stress and combinations of direct and shear waves would be advantageous. A modified Rowe cell design has been suggested that would be a useful next-step to examine the influence of shear waves. Also, performing tests that model the case of a soil settling under vibration, that experiences horizontal stress variation due to say, the horizontal movements of an adjacent retaining wall, would complement the field measurement work that has been performed.

It is recommended that a local 'dedicated site', where the properties of granular soils can be controlled, is used to conduct full-scale vibrodriving trials to validate the vibratory settlement equations that were produced. Money could be obtained from piling companies and an application made to EPSRC for support of a three year research project.

REFERENCES

Alyoshin, A.S. (1994) "Influence of Strong Dynamic Impacts on Physical-Mechanical Properties of Dispersive Grounds." *7th Internationl IAEG Congress*, Balkema, Rotterdam, ISBN 90-5410-5038.

Ambraseys, N. and Jackson, J. (1984) "Seismic Movements." *Ground Movements and Their Effects on Structures*, Chp 12, ed. Attewell, P.B. and Taylor, R., Surrey University Press, pp. 353-355.

Amini, F., Tawfiq, K.S. and Aggour, M.S. (1988) "Cohesionless Soil Behaviour Under Random Excitation Conditions." *Journal of Geotechnical Engineering*, Vol. 144, No. 8, August, pp. 896-914.

Arulanandan, K. and Sybico, J. (1993) "Post-Liquefaction Settlement of Sands." *Predictive Soil Mechanics*, Ed. Houlsby and Schofield., ISBN 0-7277-19165.

Atkinson, J.H. (1993) "An Introduction to the Mechanics of Soils and Foundations: through critical state soil mechanics." London: New York: McGraw-Hill Book Co. ISBN 007707713x.

Attewell, P.B. and Farmer, I. A. (1973) "Attenuation of Ground Vibration From Pile Driving" *Ground Engineering*, June, No.4, pp. 26-29.

Attewell, P.B. and Farmer, I.A. (1976) "Principles of Engineering Geology." London: Chapman and Hall, ISBN 0412114003.

Attewell, P.B., Selby, A.R. and Uromeihy, A. (1989) " Appraisal of Ground Vibration From Civil Engineering Construction." *Int. J. Min. and Geo. Eng.*, July, pp. 183-208, London.

Attewell, P.B., Oliver, A. and Selby, A.R. (1990) "Database Management and Analysis of Piling-Induced Ground Vibration Records." *AMSE Conf. "Signals and Systems*", Vol. 2, pp. 115-126, Rabat, Morocco.

Attewell, P.B., Selby, A.R. and O'Donnel, L (1992) "Estimation of Ground Vibration From Driven Piling Based on Statistical Analyses of Recorded Data." *Geotechnical and Geological Engineering*, 10, pp. 41-59.

Barkan, D.D (1960) "Dynamics of bases and Foundations." McGraw-Hill, New York.

Barton, M.E. and Brookes, A. (1989), "Lateral Shaking During Sedimentation." *Ground Engineering*, October, pp. 36-39.

Bazara, A.R.S, (1967) "Use of the Standard Penetration Test for Estimating Settlements of Shallow Foundations on Sand." PhD thesis, University of Illinois, Urbana.

Bhandri, R.K.M. (1981) "Dynamic Consolidation of Liquefiable Sands." *Proc. Int. Conf. Recent Adv. Geotech. Earthq. Engng and Soil Dynamics*. St.Loius, USA. pp. 857-860.

Bjerrum, L. (1963) Disscussion, Proc. Euro. Conf. Soil Mech. and Found Eng., Wiesbaden, Vol III, 135.

Blekhman, I. I. (1954) "Investigation of the Process of Vibration Driving of Piles." *Inzhenerniyi Sbornik Akad. Nauk.* SSR 10. Translated by Assoc. Techn. Services Inc., New York, RJ-4524.

Bolton, M.D. and Wilson, J.M.R. (1990) "Soil Stiffness and Damping." *Proc. European Conf. on Structural Dynamics*, Eurodyn '90, pp. 209-216, Bochum.

Boscardin, M.D. and Cording, E.J. (1989) "Building Response to Excavation Induced Settlement." *J. Geotech. Engng*, Vol 115, No. 1, January, pp. 1-21.

Bouckovalas,G., Whitman, R.V. and Marr, W.A. (1984) "Permanent Displacement of Sand with Cyclic Loading." *Journal of Geotechnical Engineering*, Vol. 110, No, 11, November, pp. 1606-1623.

Boyle, S. (1990) "The Effects of Piling Operations in the Vicinity of Computing Systems." *Ground Engineering*, June, pp. 23-27.

BRE Digest 353 (1990) "Damage to Structures From Ground-Bourne Vibration." HMSO, ISBN 0-85125-457-8.

Brumund, W.F. and Leonards, G.A. (1972) "Subsidence of Sand due to Surface Vibration." *J. Soil Mech. Found. Div.*, ASCE, 98(SM1), pp. 27-42.

BS 1377, (1990) "Methods of Testing Soils for Civil Engineering Purposes" *British Standards Institution*, London.

BS 6472, (1984) "Guide to the evaluation of Human Exposure to Vibration in Buildings (1-80Hz)." *British Standards Institution*, London.

BS 5228:4, (1986) "Noise Control on Construction and Open Sites." Part 4: "Code of Practice for Noise Control Applicable to Piling Operations." *British Standard Institution*, London.

BS 5930, (1981) "Code of Practice for Site Investigation." *British Standard Institution*, London

BS 6841, (1987) "British Standard Guide to Measurement and Evaluation of Human Exposure to Whole-Body Mechanical Vibration and Repeated Shock." *British Standard Institution*, London.

Burland, J.B. and Wroth, C.P. (1975) "Settlement of Buildings and Associated Damage." *Proc COSOS*, Review Paper: Session V, Cambridge, pp. 611-654.

Casagrande, A. (1936) "Characteristics of Cohesionless Soils Affecting the Stability of Slopes and Earth Fills." *J. Boston Soc. Civ. Eng.*, Vol. 23, p. 13.

Cascone, E. and Maugeri, M. (1995) "Shaking Table Tests of Gravity Retaining Walls." Proceedings of the 7th International Conference on *Soil Dynamics and Earthquake Engineering VII*, Crete.

Chang, N.Y., Yey, S.T. and Kaufman, L.P. (1982) " Liquefaction Potential of Clean and Silty Sands." *Proc III Microzonation Conf.*, Seattle, pp. 1018-1032.

Chang, C.S. and Whitman, R.V. (1988), "Drained Permanent Deformation of Sand due to Cyclic Loading." *Journal of Geotechnical Engineering*, Vol. 114, No. 10, October, pp. 1164-1180.

Christian, J.T. and Swiger, W.F. (1975) "Statistics of Liquefaction and SPT Results." *J. Geotech. Engin. Div.*, ASCE, Vol. 101, GT11, pp. 1135-1150.

CIRIA Technical Note 142 (1992) "Ground-Bourne Vibrations Arising From Piling." ed. Head, J.M. and Jardine, F.M.

Clough, G.W (1973) "Performance of Tie-back Support Systems." *Procs. Conf. Performance of Earth and Earth Retaining Structures*, Purdue University, Lafayette, 3, pp. 259-64.

Clough, G.W. and Chameau, J.L. (1980) "Effects of Vibratory Sheetpile Driving: A Case Study." *ASCE Spec. Tech. Pub., Minimising Detrimental Construction Vibrations*, Preprint, pp. 27-61.

Clough, F. and O'Rourke, T.D. (1990) "Construction Induced Movements of *In-Situ* Walls." *Proc. of Speciality Conf. on Design and Performances of Earth Retaining Structures*, Cornell, ASCE Geotech Sp. Pub. No.25, eds Lambe, P.C. and Hansen, L.A.

Control of Pollution Act, (1974) Part III. HM Stationary Office, London.

Coop, M.R. and Lee, I.K. (1993) "The Behaviour of Granular Soils at Elevated Stresses." Proceedings of the 5th International Conference on *Soil Dynamics and Earthquake Engineering V*, Crete.

Craig, R.F. (1989) "Soil Mechanics." 4th Edition, Van Nostrand Reinhold Co. Ltd. ISBN 0-278-00019-3.

d'Appolonia, E. (1970) "Dynamic Loadings." *J. Soil Mech. Found. Div.*, ASCE, 96(SM1), pp. 49-72.

d'Appolonia, D.J. and d'Appolonia, E. (1967) "Determination of the Maximum Dry Density of Cohesionless Soils." *Procs. III Asian Regional Conference on Soil Mech. and Found. Engng.*, Haifa, Israel, Vol. 1, pp 266.

d'Appolonia, D.J., Whitman, R.V. and d'Appolonia, E. (1969), "Sand Compaction with Vibratory Rollers." *Journal of the Soil Mechanics and Foundations Division, ASCE*, SM1, pp. 263-284.

Daramola, O. (1980) "Effect of Consolidation Age on Stiffness of Sand." *Geotechnique*, 30(2), pp. 213-216.

Das, B.M. (1983) "Fundamentals of Soil Dynamics." Elsevier Science Publishing Co., Inc. ISBN 0-4444-00705-9.

DIN 4150: Part 3: 1986. "Structural Vibration in Buildings. Effects on Structures."

Dowding, C.H. (1994) "Permanent Displacement and Pile Driving Vibrations" *Pile Buck*, Second August Issue, pp. 11-24.

Dowding, C.H. and Hyrciw, R.D. (1986) " A Laboratory Study of Blast Densification of Saturated Sand." *J. Geotech. Engrg.*, ASCE, 112(2), pp. 187-199.

Drnevich, V.P., Hall, J.R. and Richart, F.E. (1967) "Effects of the Amplitude of Vibration on the Shear Modulus of Sand." *Procs. Int. Symp.on Wave Propagation and Dynamic Properties of Earth Materials,* University of New Mexico Press, pp. 189-199.

Erten, D. and Maher, M.H. (1995) "Liquefaction Potential of Silty Soils. Proceedings of the 7th International Conference on *Soil Dynamics and Earthquake Engineering VII*, Crete.

Finn, W.D.L., Pickering, D.J. and Bransby, P.L. (1971) "Sand Liquefaction in Triaxial and Simple Shear Tests." *J. Soil Mechs. and Foundtn Div.*, ASCE, Vol.97, No.SM4, pp. 639-659.

Finn, W.D.L. (1982) "Dynamic Response Analysis of Saturated Sands." *Soil Mechanics-Transient and Cyclic Loads*, ed. Pande, G.N. and Zienkiewicz, O.C., John Wiley and Sons, 105.

Florin, V.A. and Ivanov, P.L. (1961) "Liquefaction of Saturated Sandy Soils." *Proc. V Int. Conf. Soil Mech. Found. Engin.*, Paris, Vol. 4, pp. 107-111.

Fukutake, K., Ohtsuki, A., Sato, M. and Shamoto, Y. (1990), "Analysis of Saturated Dense Sand-Structure System and Comparison with Results from Shaking Table Test." *Earthquake Engineering and Structural Dynamics*, Vol. 19, pp. 977-992.

Gibbs, H.J. and Holtz, W.G. (1957) " Research on Determining the Density of Sands by Spoon Penetration Testing." *Proc. 4th Int. Conf. Soil Mech. Fdn. Engng.* London 1, pp. 35-39.

Haldar, A. and Miller, F.J. (1984) "Statistical Evaluation of Cyclic Strength of Sand." *Journal of Geotechnical Engineering*, Vol. 110, No. 12, December, pp. 1785-1802.

Harris, F. (1983) "Ground Engineering Equipment and Methods." Granada.

Hardin, B.O. and Richart, F.E. (1963) " Elastic Wave Velocities in Granular Soils." *J. Soil Mechs. and Found. Div.*, ASCE, 94(SM2), pp. 371-389.

Head, K.H. (1984) "Manual of Soil Laboratory Testing." ELE International Ltd, Pentech Press, London.

Hencher, S.R. and Acar, I.A. (1995) "The Erzincan Earthquake, Friday, 13th March, 1992." *Quarterly Journal of Engineering Geology*, 28, pp. 313-316.

Holloway, D.M., Moriwaki, Y., Demsky, M., Moore, F. and Perez, J. (1980) "Field Study of Pile Driving Effects on Nearby Structures" *ASCE Spec. Tech. Pub.*, Minimising Detrimental Construction Vibration, pp. 63-100.

Horne, M.R. (1965) "The Behaviour of an Assembly of Rotund, Rigid, Cohesionless Particles. Part II." *Proc. Roy. Soc. Av.*, Vol. 286, pp. 79-97.

Ishihara, K. and Towhata, I. (1982) "Dynamic Reponse Analysis of Level Ground Based on the Effective Stress Method." *Soil Mechanics-Transient and Cyclic Loads*, ed. Pande, G.N. and Zienkiewicz, O.C., John Wiley and Sons, 133.

Jonker, G (1995) *personal communication.*

Jumikis, A.R. (1969) "Theoretical Soil Mechanics." Von Nostrand, American Book Co.

Kattis, S.E., Polyzos, D. and Beskos, D.E. (1995) "Structural Vibration Isolation by Rows of Piles." Proceedings of the 7th International Conference on *Soil Dynamics and Earthquake Engineering VII*, Crete.

Kim. D., Drabkin, S., Rokhvarger, A. and Laefer, D. (1994) "Prediction of Low Level Vibration Induced Settlement." Vertical and Horizontal Deformations of Foundations and Embankments, *Proc. Settlement '94*, ed. Yeung, A.T. and Felio, G.Y., ASCE, Texas, Vol. 1, pp. 806-817.

Krizek, J.K. and Fernandez, J.I. (1971) "Vibratory Densification of Damp Clayey Sands." *Journal of the Soil Mechanics and Foundations Div., Procs ASCE*, SM8, August, pp. 1069-1078.

Kuerbis, R. and Vaid, Y.P. (1988) "Sand Sample Preparation - The Slurry Deposition Method." *Soils and Foundations*, Vol. 28, No. 4, Dec., pp. 107-188.

Lacy, H.S. and Gould, J.P. (1985) "Settlement From Pile Driving in Sands" *ASCE Spec. Tech. Pub.*, Vibration Problems in Geotechnical Engineering, pp. 153-173.

LaFosse, U. and Gelormino, T.A. (1991) "Soil Improvement by Deep Blasting: A Case Study." *Proc. Explos. Blast Tech. Annual Conf. Soc. Explos. Engineers*, Vol.1, pp. 205-211.

Lambe, T.W. (1951) "Soil Testing for Engineers." John Wiley and Sons, Inc., New York.

Lee, K.L. and Seed, H.B. (1967) "Cyclic Stress Conditions Causing liquefaction of Sand." *Journal of the Soil Mechanics and Foundations Division, ASCE*, SM1, pp. 47-70.

Lee, K.L. and Fitton, J.A. (1969) "Factors Affecting the Cyclic Loading strength of Soil." *Vibration Effects of Earthquakes*, pp. 71-95.

Lee, K.L. and Albaisa, A. (1974) "Earthquake Induced Settlements in Saturated Sands." *J. Geotech. Eng.* Div., ASCE, Vol. 100, No GT4, April, pp. 387-405.

Lee, I.K., White, W. and Ingles, O.G. (1983) "Geotechnical Engineering." Pitman Books Ltd. ISBN 0-273-01756-X.

Leonards, G.A. and Girault, P. (1961) "A Study of the One-Dimensional Consolidation Test." Proc. 5th Int. Conference of *Soil Mechanics & Foundation Eng. V*, Paris. Vol.1, Paper 1/36, pp. 213-218.

Linehan, P.W., Longinow, A. and Dowding, C.H. (1988) "Pipe Response to Pile Driving and Adjacent Excavation." *J. Geotech. Eng.*, ASCE, Vol. 118, No. 2, pp. 300-316.

Little, J.A., Symons, I.F. and Williams, S.G.O. (1987) "Comparison of Methods for Measuring Horizontal Movements on an Anchored Sheet Pile Wall." Proceedings of *International Conference on Foundations and Tunnels*, London, 2, pp. 137-45.

Lo, K.Y., Bozozuk, M. and Law, K.T. (1976) "Settlement Analysis of the Gloucester Test Fill." *Canadian Geotechnical Journal*, Vol. 13: 339, Nov.

Lowe, J., Zaccheo, P.F. and Feldman, H.S. (1964) "Consolidation Testing With Back Pressure" *J.Soil Mech. Fdn. Div. ASCE*, Vol. 90, SM5:69.

Lukas, R.G. and Gill, S.A. (1992) "Ground Movements From Piling Vibrations." Procs. *Conf. Piling: European Practice and Worldwide Trends*, ICE, London, pp. 163-169.

Marcuson, W.F. and Gilbert, P.A. (1972) "Earthquake Liquefaction Potential at Patoka Dam, Indiana." Army Engineer Waterways Experimental Station, Misc. Paper S-72-42.

Martin, P.P. and Seed, H.B. (1982) "One-Dimensional Dynamic Ground Response Analyses." *J. Geotech. Engng. Div.*, 108, GT7, 935.

McGown, A., Barden, L and Lee, K.L. (1974) "Sample Disturbance in Soft Alluvial Clyde Estuary Clay." *Canadian Geotechnical Journal*, Vol. 11: 651, Nov.

Meissner, H. and Becker, A. (1995) "Dynamic Behaviour of Partially Saturated Sand." Proceedings of the 7th International Conference on *Soil Dynamics and Earthquake Engineering VII*, Crete.

Mesri, G., Feng, T.W. and Benak, J.M. (1990) "Postdensificaton Penetration Resistance of Clean Sands." *Journal of Geotechnical Engineering*, Vol. 116, No. 7, July, pp. 1095-1115.

Mitchel, J.K. (1976) "Fundamentals of Soil Behaviour." John Wiley and Sons LTD, ISBN 0-471-61168-9.

Mitchell, J.K. and Solymar, Z.V. (1984) "Time-Dependent Strength Gain in Freshly Deposited or Densified Sand." *Journal of Geotechnical Engineering*, Vol. 110, No. 11, November, pp. 1559-1576.

Ming, K.J., Kee, K.K. and Tim, L.S. (1989) "Some Observations and Simple Theoretical Model of Vibrations Caused by Pile Driving." *Piletalk International*, March, Kuala Lumpur, Malaysia.

Muira, S. and Toki, S. (1982) " A Sample Preparation Method and its Effect on Static and Cyclic Deformation-Strength Properties of Sand." *Soils and Foundations*, Vol.22. No.1, pp. 61-77.

Mulilis, J.P., Seed, H.B., Chan, C.K., Mitchell, J.K. and Arulanandan, K. (1977) "The Effects of Method of Sample Preparation on Sand Liquefaction." *J. Geotech. Engrg. Div.*, ASCE, 103, (GT2), pp. 91-108.

Neimark, Y.I. (1953) "Theory of Vibration Driving." *Tech. Pap. Acad. Science* (USSR) 5, 15. Translated by B.L.L.

Nemat-Nasser, S. and Takahashi, T. (1984) "Liquefaction and Fabric of Sand. " *Journal of Geotechnical Engineering*, Vol. 110, No. 9, September, pp. 1291-1306.

New, B.M. (1978a) "The Effects of Ground Vibration During Bentonite Shield Tunnelling at Warrington." TRRL Laboratory Report 860.

New, B.M. (1978b) "A Note on the Relationship Between Penetration Resistance and Density of Sand." *Ground Engineering*, July.

New, B.M. and O'Reilly, M.P. (1991) " Tunelling Induced Ground Movements; Predicting Their Magnitude and Effects." Invited Review Paper to *4th Int. Conf. on Ground Movements and Structures*, Cardiff, july.

Norman-Gregory, G.M. and Sellig, E.T. (1989) "Volume Change Behaviour of Vibrated Sand Columns." *Journal of Geotechnical Engineering*, Vol. 115, No. 3, March, pp. 289-303.

Oda, M. (1978), "Significance of Fabric in Granular Mechanics." Procs. U.S.-Japan Seminar on Continuum-Mechanical and Statistical Approaches in the Mechanics of Granular Materials. pp. 7-26.

Ohasaki, Y. (1970) "Effects of Sand Comapction on Liquefaction During the Tokachioki Earthquake." *Soil Found* (Tokyo), Vol. 10, no. 2, pp. 112-128, June.

Oliver, A and Selby, A.R. (1991) "Estimation of Piling-Induced Vibrations." *Int. Conf. on Earthquake, Blast and Impact*, SECED, UMIST, Elsevier.

O'Neil, M.W., Vipulanandan, C. and Wong, D. (1990) "A Laboratory Model Of Vibro-driven Piles." *Journal of Geotechnical Engineering*, Vol 116, no. 8, August, pp. 1190-1209.

Orlova, O.A. (1989) "Behaviour of Soil Under A Brief Dynamic Load." *Gidrotekhnicheskoe Stroitrl'stvo*, No.11, November, pp. 20-26.

Oteo, C.S. (1983) "Prediction of Settlements after Deep Vibration in Granular Fills." 8th European Conference on *Soil Mechanics and Foundation Engineering VIII*, Helsinki. Vol. 1, pp. 283-287.

Parsons, A.W. (1992) "Compaction of Soils and Granular Materials: a Review of Research Performed at the Transport Research Laboratory." TRL, HMSO, London.

Peacock, W.H. and Seed, H.B. (1968) "Sand Liquefaction under Cyclic Loading Simple Shear Conditions." *J. Soil Mech.Found. Div.*, ASCE, Vol.94, SM3, pp.689-708.

Picornell, M. and del Monto, E. (1982) "Pile Driving Induced Settlements of a Pier Foundation." ASCE Spec. Tech. Pub. *Vibration Problems in Geotechnical Engineering*, pp. 174-186.

Prakash, S. (1981) "Soil Dynamics." McGraw-Hill, Inc. ISBN 0-07-050658-2.

Prakash, S. and Gupta, M.K. (1970) "Report on Dynamic Properties of Soil for Diesel Power House Nakodar." Earthquake Engineering Studies, School of Research and Training in Earthquake Engineering, University of Roorkee, India.

PTC (1986) "Vibrofonceur." France.

Pyke, R.M., Seed, H.B. and Chan, C.K. (1975) "Settlement of Sands Under Multidirectional Shaking." *J. Geot. Engg. Div., ASCE*, Vol. 101, No. GT 4, pp. 379-398.

Redhead. D, (1986) " Pile Driving Equipment Developments." *Civil Engineering* 5, pp. 21-29, London.

Richards, R., Elms, D.G. and Budhu, M. (1990) "Dynamic Fluidization of Soils." *Journal of Geotechnical Engineering*, Vol. 116, No. 5, May, pp. 740-759.

Richart, F.E., Hall.J.R. and Woodes, R.D. (1970) "Vibrations of Soils and Foundations." Prentice-Hall, Englewood Cliffs, N.J.

Rodger, A.A. and Littlejohn, G.S. (1980), "A Study of Vibratory Driving in Granular Soils." *Geotechnique*, 30, No. 3, pp. 269-293.

Rowe, P.W. (1954) "A Stress-Strain Theory for Cohesionless Soil, with Applications to Earth Pressure at Rest and Moving Walls." *Geotechnique*, 4:2:70.

Rowe, P.W. (1968) "The Influence of Geological Features of Clay Deposits on the Design and Performance of Sand Drains." Proc. I.C.E. Supplimentary Paper No. 7058S.

Rowe, P.W. (1972) "The Relevance of Soil Fabric to Site Investigation Practice." Twelfth Rankine Lecture. *Geotechnique*, 22:2:195.

Rowe, P.W and Barden, L. (1966) "A New Consolidation cell." *Geotechnique*, 16:2:162.

Salas, J.A. and Oteo C.S. (1978) "The Compressibility of Lapilli Fills in the Canary Island." *Proc Third Int Congress Engineering Geology* Section 2, Vol.1, pp. 200-210.

Sawicki, A. (1987) "An Engineering Model for Compaction of Sand Under Cyclic Loading." *Engineering Transactions*, 35, 4, pp. 677-693.

Sawicki, A. and Swidzinski, W. (1990) "Compaction Beneath Flexible Pavement due to Traffic." *Journal of Geotechnical Engineering*, Vol. 116, No.11, November, pp. 1738-1743.

Seed, H.B. (1976) "Evaluation of Soil Liquefaction Effects on Level Ground During Earthquakes." State of the Art Paper, *Symp. Soil Liquefaction*, ASCE Convention, Philadelphia, pp. 1-104.

Seed, H.B. (1979) "Soil Liquefaction and Cyclic Mobility Evaluation for Level Ground During Earthquakes." *J. Geotech. Engrg. Div.*, ASCE, 105(2), pp .201-255.

Seed, H.B. and Lee, K.L. (1966) "Liquefaction of Saturated Sands During Cyclic Loadings." *Proc. ASCE, J. Soil Mech. Found. Div.*, 92, SM6, pp. 105-134.

Seed, H.B. and Idriss, I.M. (1971) "Simplified Procedure for Evaluating Soil Liquefaction Potential." *J. Soil Mech. and Found. Div.*, ASCE, Vol. 97, No. SM9, Sept., pp. 1249-1273.

Seed, H.B. and Silver, M.L. (1972) "Settlement of Dry Sands During Earthquakes." *J.Soil Mech. Found. Div., ASCE*, SM4, April, pp. 831-397.

Selby, A.R. (1988) "Surface Movements Caused by Tunelling in Two-layer Soil." *Engineering Geology of Underground Movements*, Geol. Soc. Spec. Pub., no. 5, Bell, F.G., Culshaw, M.G., Cripps, J.C. and Lovell, M.A. (eds), pp. 71-77

Selby, A.R. (1989) "Acquisition by Microcomputer of Some Ground Vibration Data During Pile Driving." *Proc. Int. Symp. on Computer Modelling in Geotechnical Engineering*, Dec., Balkema, Rotterdam, pp. 133-147.

Selby, A.R. (1996) *personal communication.*

Selby A.R. and Attewell, P.B. (1987) "Estimation of Ground Movements and Their Effects Caused by Tumelling in Compressible Soils." *Procs. Int. Conf. Foundations and Tunnels*, London, pp. 323-330.

Selby, A.R. and Tuck, C. (1995) "Pile Driving and Compaction Settlement: A National Survey." Joint report by School of Engineering, University of Durham and Piling Technical Division, British Steel, Scunthorpe.

Shimming, W., Gray, D.H. and Richart, F.E. (1984), "Capillary Effects on Dynamic Modulus of Sands." *Journal of Geotechnical Engineering*, Vol. 110, No. 9, September, pp. 1188-1203.

Silver, M.S. and Seed, H.B. (1971a) " Deformation Characteristics of Sands Under Cyclic Loading." *Journal of the Soil Mechanics and Foundations Divisions, ASCE*, SM8, pp .1081-1089.

Silver, M.S. and Seed, H.B. (1971b) "Volume Changes in Sands During Cyclic Loading." *Journal of the Soil Mechanics and Foundations Division, ASCE*, SM9, pp. 1171-1182.

Simons, N.E. and Beng, T.S. (1969) "A Note on the One-Dimensional Consolidation of Saturated Clays." Technical Note, *Geotechnique*, 19:1:140.

Skempton, A.W. (1986) "Standard Penetration Test Procedures and the Effects in Sands of Overburden Pressure, Relative Density, Particle Size, Ageing and Overconsolidation." *Geotechnique*, 36, No. 3, pp. 425-447.

Skempton, A.W. and MacDonald, D.H. (1956) "Allowable Settlement of Buildings." *Proc. Instn. Civ. Engrs*, pt III, Vol. 5, pp. 727-768.

Skip, B. (1984) "Dynamic Ground Movements, Man-Made Vibrations." *Ground Movements and Their Effects on Structures*, Chp13, ed. Attewell, P.B. and Taylor, R., Surrey University Press, pp. 382-395.

Sladen, J.A., D'Hollander, R.D. and Krahn, J. (1985) "The Liquefaction of Sands, a Collapse Surface Approach." *Canadian Geotech. Journal*, Vol.22, pp. 564-578.

SN 640 312:1978 "Effects of Vibrations on Buildings."

Solymar, Z.V. (1984) "Compaction of Alluvial Sands by Deep Blasting." *Can. Geotech. J.*, 21, pp. 305-321.

Symons, I.F., Little, J.A. and Carder, D.R. (1988) "Ground Movements and Deflections of an Anchored Sheet Pile Wall in Granular Soil." Geological Society Engineering Geology Special Publication No. 5, pp. 117-127.

Tatsuoka, F., Sakamoto, M., Kawamura, T. and Fukushima, S. (1986) "Some Factors Affecting Cyclic Undrained Triaxial Strength of Sand." *Soils and Foundations*, Vol.26, No.3, pp. 99-116.

Terzaghi, K. and Peck, R.B. (1948) "Soil Mechanics in Engineering Practice." New York: Wiley.

Timmerman, D.H. and Wu, T.H. (1969) "Behaviour of Dry Sands Under Cyclic Loading." *Journal of the Soil Mechanics and Foundations Division, ASCE*, SM1, pp. 1097-1112.

Todd, A. (1994) "Berwick River Walls: An Unique Scheme to Safeguard a Historic Part of Berwick-upon-Tweed" Parkman Consulting Engineers.

Tokimatsu, K. and Seed, H.B. (1987) "Evaluation of Settlements in Sands Due to Earthquake Shaking." *J.Geotech. Engng.*, ASCE, Vol. 113, No. 8, pp. 861-878.

Tokue, T. (1979) " Deformation Behaviours of Dry Sand Under Cyclic Loading and a Stress-Dilatancy Model." *Soils and Foundations*, Vol. 19, No. 2, June 1979, pp. 63-77.

Toll, D.G. (1991) "Towards Understanding the Behaviour of Naturally-Occurring Road Construction Materials." *Geotechnical and Geological Engineering*, 9, pp. 197-217.

Toll, D.G. (1996) *personal communication..*

Toll, D.G., Hight, D.W. and Shaw H.F. (1987) "The Role of Soil Fabric in Determining the Engineering Behaviour of Compacted Lateritic and Quartzitic Gravels." *Z. Geomorph.* Suppl. Bd.64, pp. 133-144, Berlin.

Tomlinson, M.J. (1977) "Pile Design and Construction Practice." Viewpoint Publication, London.

Ueng, T. and Lee, C. (1990) "Deformation Behaviour of Sand Under Shear - Particulate Approach." *Journal of Geotechnical Engineering*, Vol. 116, No. 11, November, pp. 1625-1640.

Uromeihy, A. (1990) "Ground Vibration Measurements With Special Reference to Pile Driving." PhD Thesis, University of Durham, UK.

Vaid, Y.P. and Negussey, D. (1984) "Relative Density of Air and Water Pluviated Sand Sand." *Soils and Foundations*, Vol.24,No.2, pp. 101-105.

Vaid, Y.P., Fisher, J.M., Kuerbis, R.H. and Negusey, D. (1990) "Particle Gradation and Liquefaction." *Journal of Geotechnical Engineering*, Vol. 116, No. 4, April, pp. 699-703.

Vasquez-Herrera, A., Vucetic, M., Dobry, R. and Mohamad, R. (1985) "Liquefaction low Failure Characteristics of Some Silty Sands." Proceedings of the 2nd International Conference on *Soil Dynamics and Earthquake Engineering II*, p.(3-85)-(3-96).

Voznesensky, E.A. (1994) "Dynamic Instability of Soils and Rocks." *7th International IAEG Congress.*, Balkema, Rotterdam, ISBN 90-5410-5038.

Whitman, R.V. and Ortigoas, P.O. (1969) "Densification of Sand by Vertical Vibrations." *Procs. IV World Conf. on Earthquake Engng.*, Santiago, Chile, Feb.

Whyley, P.J. and Sarsby, R.W. (1992) "Ground Borne Vibration From Piling." *Ground Engineering*, May, pp. 32-37.

Woodley, S.L. (1994) "Protection of Buried Structures From Groundshock: Pendine Field Trials, 1993." *BGS Young Geotech. Eng. Symp.III*, Cardiff.

Yasuda, S *et al.*, (1995) "A Study on the Mechanism of the Floatation of Buried Pipes Due to Liquefaction." Proceedings of the 7th International Conference on *Soil Dynamics and Earthquake Engineering VII*, Crete.

Zhang, X.J. and Aggour, M.S. (1995) "Young's Modulus of Sands Under Different Types of Loading." Proceedings of the 7th International Conference *on Soil Dynamics and Earthquake Engineering VII*, Crete.

Zienkiewicz, O.C., Chang, C.T. and Hinton, E. (1978) "Nonlinear Seismic Response and Liquefaction" *Int. J. Num. and Analytical Meth. in Geomech.*, **2**, pp. 381-404.

Appendix 1

Standard Laboratory Soil Tests

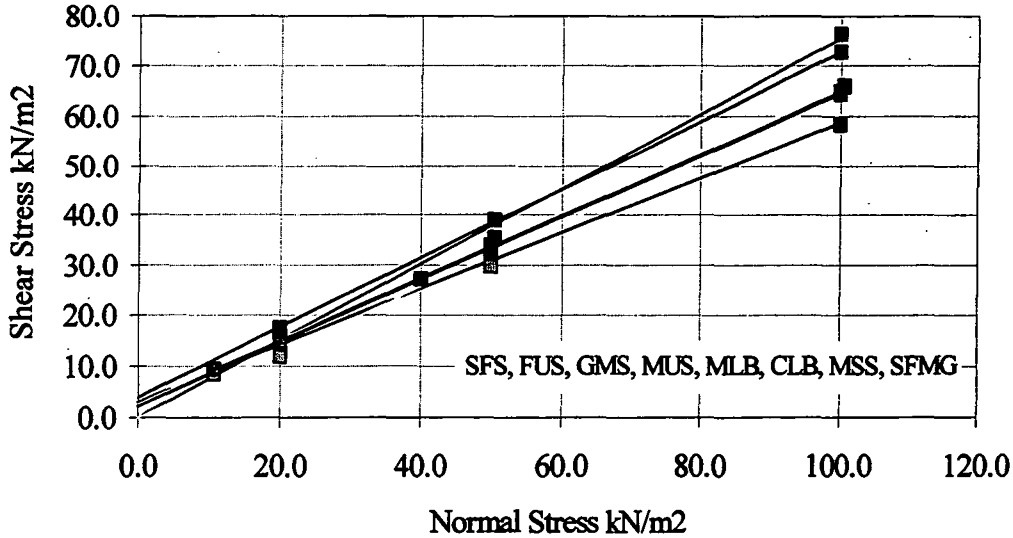

Figure A1.1.1. Standard shear box test results.

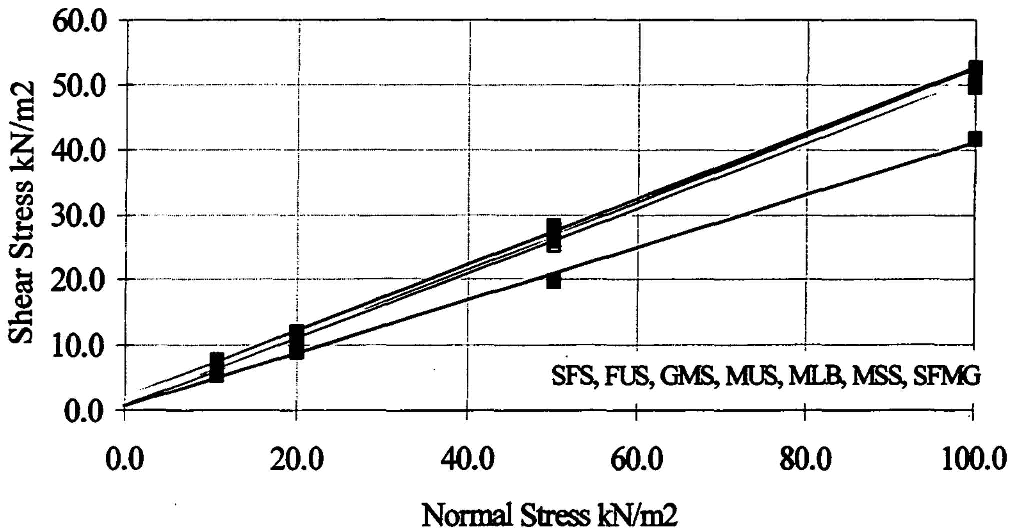

Figure A1.1.2. Saturated shear box test results. Shearing sand against sample confining bag material and cold-rolled aluminium plate.

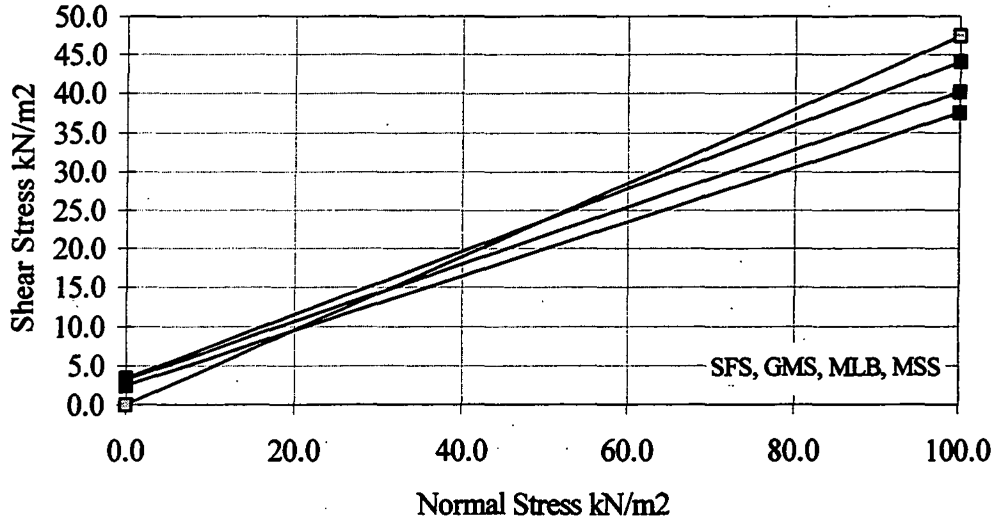

Figure A1.1.3. Dry shear box test results. Shearing sand against sample confining bag material and cold-rolled aluminium plate.

Soil type	Test	Stress	Stress (kPa)			
SFS	Soil-soil	Normal stress	10.6	20.0	50.0	100.0
		Stress at failure	8.3	11.8	29.7	64.5
	Sat+mem	Normal stress	10.6	20.0	50.0	100.0
		Stress at failure	7.6	11.3	26.8	51.3
	Dry+mem	Normal stress	10.6	20.0	50.0	100.0
		Stress at failure	4.5	9.1	23.5	46.9
FUS	Soil-soil	Normal stress	0.0	20.0	50.0	100.0
		Stress at failure	2.9	13.2	32.3	58.2
	Sat+mem	Normal stress	10.6	20.0	50.0	100.0
		Stress at failure	6.3	11.0	25.4	51.2
GMS	Soil-soil	Normal stress	10.6	20.0	50.0	100.0
		Stress at failure	8.3	14.7	33.8	64.2
	Sat+mem	Normal stress	10.6	20.0	50.0	100.0
		Stress at failure	5.6	10.9	28.3	51.9
	Dry+mem	Normal stress	10.0	20.0	50.0	100.0
		Stress at failure	7.0	8.5	19.5	37.5
MUS	Soil-soil	Normal stress	10.0	20.0	50.0	10.0
		Stress at failure	8.0	15.0	28.0	60.5
	Sat+mem	Normal stress	10.6	20.0	50.0	100.0
		Stress at failure	6.0	10.6	25.9	49.7
MLB	Soil-soil	Normal stress	10.6	20.0	40.0	100.0
		Stress at failure	9.3	14.2	27.1	76.4
	Sat+mem	Normal stress	10.6	20.0	50.0	100.0
		Stress at failure	3.7	8.4	19.1	34.6
	Dry+mem	Normal stress	10.0	20.0	50.0	100.0
		Stress at failure	6.5	9.5	21.5	40.3

Soil type	Test	Stress	Stress (kPa)			
CLB	Soil-soil	Normal stress	10.6	20.0	50.0	100.0
		Stress at failure	9.2	14.6	33.4	64.8
	Sat+mem	Normal stress	10.0	20.0	50.0	100.0
		Stress at failure	5.5	12.0	26.5	47.0
	PSat+mem	Normal stress	10.0	20.0	50.0	100.0
		Stress at failure	6.0	9.5	23.0	44.0
	Dry+mem	Normal stress	10.0	20.0	50.0	100.0
	(spray)	Stress at failure	4.8	7.0	18.0	33.5
	Dry+mem	Normal stress	10.0	20.0	50.0	100.0
	(grease)	Stress at failure	4.7	9.5	19.0	38.0
MSS	Soil-soil	Normal stress	0.0	20.0	50.5	100.6
		Stress at failure	2.6	14.7	35.2	65.7
	Sat+mem	Normal stress	10.6	20.0	50.0	100.0
		Stress at failure	6.2	11.4	26.9	50.9
	Dry+mem	Normal stress	10.6	20.0	50.0	100.0
		Stress at failure	8.5	11.3	22.7	44.6
SFMG	Soil-soil	Normal stress	0.0	20.0	50.5	100.0
		Stress at failure	3.8	17.4	38.9	72.6
	Sat+mem	Normal stress	10.6	20.0	50.0	100.0
		Stress at failure	7.5	11.9	27.7	52.6

Table A1.1.1. Data sheet: standard shearbox tests, and cell-wall-sample-confing-bag-sand tests.

Soil Type	Bot.no	Bot+soil+wtr (g)	Bot+soil (g)	Bot+wtr (g)	Bottle (g)	Soil (g)	wtr full bot (g)	wtr used (g)	vol soil (ml)	*Gs*	Accpted *Gs*
SFS	77.00	152.98	57.37	146.71	47.31	10.06	99.40	95.61	3.79	2.65	
	82.00	152.40	55.81	146.30	46.02	9.78	100.27	69.59	3.68	2.66	2.66
	84.00	149.67	54.94	143.00	44.25	10.69	68.75	94.74	4.01	2.66	
FUS	77.00	153.03	55.66	146.01	45.16	10.07	99.44	95.66	3.78	2.66	
	78.00	154.30	59.99	146.87	45.95	13.17	100.89	95.96	4.94	2.67	2.67
	82.00	152.68	55.99	144.04	44.59	10.15	100.31	96.50	3.81	2.67	
FUS	78.00	152.61	55.66	146.01	45.16	10.49	100.85	96.96	3.89	2.70	
	70.00	155.62	59.99	146.87	45.94	14.05	100.93	95.62	5.30	2.65	2.67
	72.00	151.17	55.99	144.04	44.59	11.40	99.45	95.19	4.27	2.67	
GMS	77.00	153.34	57.83	146.81	47.30	10.54	99.52	95.51	4.00	2.63	
	74.00	152.64	59.61	146.10	44.24	15.36	98.86	93.03	5.82	2.64	2.63
	78.00	155.08	59.53	146.13	45.16	14.37	1003.97	95.55	5.43	2.65	
MUS	70.00	155.40	59.58	146.98	45.94	13.65	101.05	95.81	5.24	2.63	
	82.00	154.59	59.58	146.42	46.02	13.27	100.40	98.31	5.10	2.64	2.64
	72.00	153.07	59.04	144.16	44.58	14.46	99.58	94.03	5.55	2.65	
MLB	77.00	155.05	60.65	146.76	47.30	13.34	99.46	94.41	5.05	2.64	
	74.00	149.95	55.41	143.05	44.26	11.15	98.79	94.54	4.25	2.63	2.64
	72.00	151.98	57.30	144.09	44.59	12.71	99.50	94.68	4.82	2.64	
CLB	82.00	154.06	58.46	146.36	46.03	12.44	100.33	95.59	4.74	2.63	
	70.00	156.13	60.81	146.93	45.94	14.86	100.98	95.32	5.66	2.62	2.63
	78.00	155.04	59.60	146.07	45.17	14.44	100.91	95.44	5.47	2.64	
MSS	70.00	152.90	55.68	146.90	45.95	9.74	100.95	97.22	3.74	2.60	
	72.00	151.70	56.74	144.08	44.51	12.23	99.57	94.95	4.62	2.65	2.65
	74.00	153.29	60.61	146.03	44.26	16.35	98.77	92.68	6.09	2.68	
MSS	72.00	151.33	56.26	144.04	44.58	11.68	99.46	95.07	4.38	2.64	
	74.00	153.12	60.42	143.03	44.25	16.18	98.79	92.69	6.06	2.66	2.65
	77.00	159.14	67.26	146.75	47.31	19.95	99.44	91.88	7.56	2.64	
SFG	70.00	160.08	67.33	146.84	45.95	21.39	100.89	92.75	8.14	2.63	2.63
	77.00	159.93	6+8.702	146.67	47.31	21.40	99.36	91.23	8.13	2.63	
SFMG	1.00	1903.80	983.30	1655.40	583.10	920.50	1072.30	400.20	151.80	2.64	2.63
	2.00	1899.40	985.10	1650.70	583.90	914.30	1066.80	401.20	152.50	2.63	

Table A1.1.2.Data sheet: specific gravity calculation.

Soil	Property	1	2	3	mean	Gs	emax	emin
SFS	mass (g)	282.70	403.40	550.40	412.17			
	vol (ml)	225.00	315.00	425.00	321.67			
	density	1.26	1.28	1.30	1.28	2.66	1.082	0.65
FUS	mass	287.30	411.50	600.40	433.07			
	vol	217.00	306.00	445.00	322.67			
	density	1.32	1.34	1.35	1.34	2.67	0.994	0.64
GMS	mass	303.40	512.50	687.40	501.10			
	vol	205.00	345.00	467.00	339.00			
	density	1.48	1.49	1.47	1.48	2.64	0.785	0.56
MUS	mass	208.10	385.20	639.30	410.87			
	vol	140.00	260.00	423.00	274.33			
	density	1.49	1.48	1.51	1.49	2.61	0.748	0.62
MLB	mass	414.20	581.70	669.00	554.97			
	vol	287.00	405.00	465.00	385.67			
	density	1.44	1.44	1.44	1.44	2.64	0.834	0.61
CLB	mass	284.50	437.00	605.40	442.30			
	vol	195.00	295.00	400.00	296.67			
	density	1.46	1.48	1.51	1.48	2.63	0.772	0.60
MSS	mass	336.35	494.40	675.90	502.22			
	vol	235.00	347.00	468.00	350.00			
	density	1.43	1.42	1.44	1.43	2.65	0.849	0.43
SFG	mass	288.10	464.90	670.40	474.47			
	vol	215.00	330.00	474.00	339.67			
	density	1.34	1.41	1.41	1.39	2.63	0.895	0.60
SFMG	mass	382.70	575.40	717.80	558.63			
	vol	235.00	355.00	440.00	343.33			
	density	1.63	1.62	1.63	1.63	2.63	0.617	0.25

Table A1.1.3. Data sheet: void ratio calculation.

SFS		Sample mass	131.0		
Sieve	Mass	Sieve +Soil	Soil	Mass Pass	% Passing
1.4	450.9	451.1	0.2	130.8	99.8
600.0	353.6	353.6	0.0	130.8	99.8
425.0	391.2	391.5	0.3	130.5	99.6
300.0	338.8	339.3	0.5	130.0	99.2
212.0	361.5	367.5	6.0	124.0	94.7
150.0	309.9	349.5	39.6	84.4	64.4
90.0	0.0	0.0	0.0	0.0	0.0
63.0	297.0	367.5	70.5	14.0	10.7

FUS		Sample mass	85		
Sieve	Mass	Sieve+ Soil	Soil	Mass Pass	% Passing
600.0	353.8	353.9	0.1	84.9	99.0
425.0	386.6	386.7	0.1	84.8	99.8
300.0	335.0	334.9	0.1	84.9	99.9
212.0	376.7	387.3	10.6	74.3	87.4
150.0	309.5	344.1	34.6	39.7	46.7
75.0	305.2	342.6	37.4	2.3	2.7
63.0	300.7	301.5	0.8	1.5	1.8

GMS		Sample mass	267.0		
Sieve	Mass	Sieve+ Soil	Soil	Mass Pass	% Passing
1.4	450.8	387.4	0.0	267.0	100.0
710.0	414.1	336.0	0.2	266.5	99.8
425.0	353.5	387.8	215.7	62.0	23.2
300.0	391.4	340.8	44.9	9.1	3.4
212.0	338.7	344.1	5.4	0.7	0.3
150.0	361.3	301.2	0.7	0.0	0.0
63.0	309.8	301.2	0.0	0.0	0.0

MUS		Sample mass	251.0		
Sieve	Mass	Sieve+ Soil	Soil	Mass Pass	% Passing
1.4	450.8	387.4	0.0	251.0	100.0
710.0	414.1	336.0	0.2	249.7	99.5
425.0	353.5	387.8	201.7	48.0	19.1
300.0	391.4	340.8	41.9	6.1	2.4
212.0	338.7	344.1	5.4	0.7	0.3
150.0	361.3	301.2	0.7	0.0	0.0
63.0	309.8	301.2	0.0	0.0	0.0

MLB		Sample mass	200.4		
Sieve	Mass	Sieve+ Soil	Soil	Mass Pass	% Passing
2.0	463.9	463.9	0.0	200.4	100.0
1.4	467.3	467.4	0.1	200.3	100.0
600.0	353.8	497.5	143.7	56.6	28.2
420.0	386.7	430.3	43.6	13.0	6.5
300.0	335.1	344.9	9.8	3.2	1.6
212.0	377.0	379.2	2.2	1.0	0.5
150.0	310.5	311.0	0.5	0.5	0.2
63.0	300.7	301.1	0.4	0.1	0.0

CLB		Sample mass	154.1		
Sieve	Mass	Sieve+ Soil	Soil	Mass Pass	% Passing
3.4	475.4	475.3	-0.1	154.2	100.1
2.8	502.7	502.6	-0.1	154.3	100.1
2.0	475.9	476.7	0.8	153.5	99.6
1.4	450.8	497.2	46.4	107.1	69.5
600.0	353.6	460.7	107.1	0.0	0.0

Table A1.1.4. Data sheet: particle size distribution raw data

MSS		Sample mass		200.9	
Sieve	Mass	Sieve+ Soil	Soil	Mass Pass	% Passing
4.0	506.3	510.7	4.4	196.5	97.8
3.4	474.5	478.1	3.6	192.9	96.0
2.8	502.4	507.0	4.6	188.3	93.7
1.4	450.8	469.1	18.3	170.0	84.6
710.0	414.2	449.3	35.1	134.9	67.1
600.0	353.5	364.7	11.2	123.7	61.6
425.0	391.3	412.8	21.5	102.2	50.9
300.0	338.6	362.3	23.7	78.5	39.1
212.0	361.3	386.2	24.9	53.6	26.7
150.0	309.8	340.2	30.4	23.2	11.5
63.0	300.8	320.1	19.3	3.9	1.9

CSS		Sample mass		307.0	
Sieve	Mass	Sieve+ Soil	Soil	Mass Pass	% Passing
4.0	506.5	511.2	4.7	302.3	98.5
2.8	498.5	538.1	39.6	262.7	85.6
1.4	467.5	563.3	95.8	166.9	54.4
710.0	414.3	484.3	70.0	96.9	31.6
500.0	414.4	441.6	27.2	69.7	22.7
5425.0	391.8	397.7	5.9	63.8	20.8
300.0	338.6	355.0	16.4	47.4	15.4
212.0	361.3	372.8	11.5	35.9	11.7
150.0	309.6	324.8	15.2	20.7	6.7
63.0	298.0	316.0	18.0	2.7	0.9

CSS>63		Sample mass		197.0	
Sieve	Mass	Sieve+ Soil	Soil	Mass Pass	% Passing
4.0	506.4	510.1	3.7	193.3	98.1
3.4	474.8	486.5	11.7	181.6	92.2
2.8	502.5	519.0	16.5	165.1	83.8
1.4	450.8	509.7	58.9	106.2	53.9
710.0	414.1	457.5	43.4	62.8	31.9
600.0	353.5	362.1	8.6	54.2	27.5
425.0	391.4	405.2	13.8	40.4	20.5
300.0	338.7	351.0	12.3	28.1	14.3
212.0	361.3	369.8	8.5	19.6	9.9
150.0	309.8	319.3	9.5	10.1	5.1
63.0	300.8	310.5	9.7	0.4	0.2

SFG		Sample mass		1000.0	
Sieve	Mass	Sieve+ Soil	Soil	Mass Pass	% Passing
3.4	476.5	550.9	74.4	925.6	92.6
2.8	502.3	567.8	65.5	860.1	86.0
1.4	450.6	680.4	229.8	630.3	63.0
600.0	353.6	601.3	247.7	382.6	38.3
420.0	399.7	497.4	97.7	284.9	28.5
300.0	338.9	420.3	81.4	203.5	20.4
212.0	361.1	434.4	73.3	130.2	13.0
150.0	309.6	372.4	62.8	67.4	6.7
63.0	297.6	351.9	54.3	13.1	1.3
base	324.0	336.6	12.6	0.5	0.1

SFMG		Sample mass		900.0	
Sieve	Mass	Sieve+ Soil	Soil	Mass Pass	% Passing
10.0	874.0	874.8	0.8	899.2	99.9
6.4	1334.5	1463.8	129.3	769.9	77.0
4.0	506.3	582.6	76.3	693.6	69.4
3.4	475.4	503.5	28.1	665.5	66.6
2.0	476.0	542.9	66.9	598.6	59.9
1.4	450.7	493.8	43.1	555.5	55.6
710.0	414.8	518.6	103.8	451.7	45.2
600.0	353.7	386.0	32.3	419.4	41.9
425.0	391.9	465.8	73.9	345.5	34.6
300.0	338.5	421.7	83.2	262.3	26.2
212.0	361.3	451.0	89.7	172.6	17.3
150.0	308.9	395.7	86.8	85.8	8.6
63.0	296.7	360.4	63.7	22.1	2.2

Table A1.1.4 (cont). Data sheet: particle size distribution raw data.

Appendix 2

Diaphragm Calibration

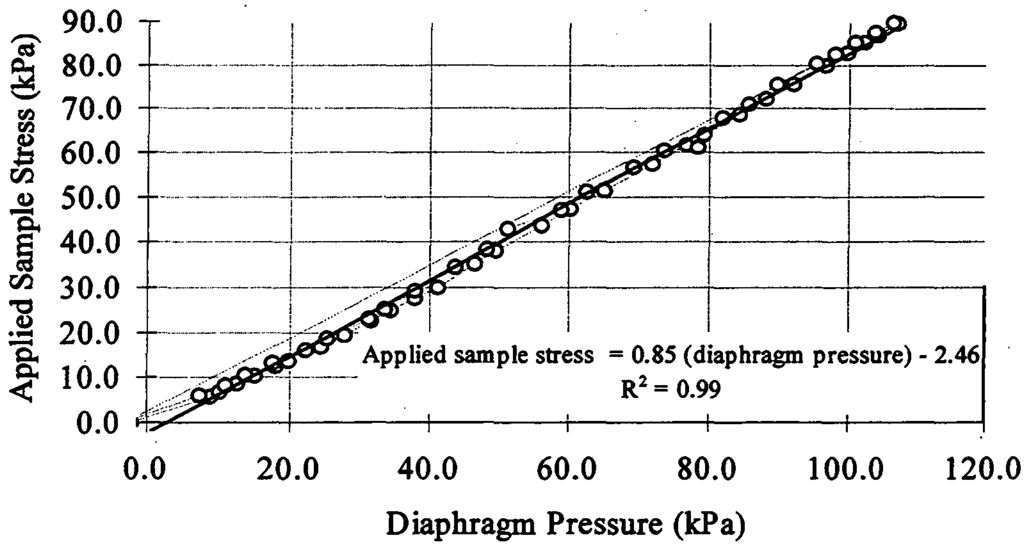

Figure A2.1.1. Diaphragm calibration graph (see Table A2.1.1a).

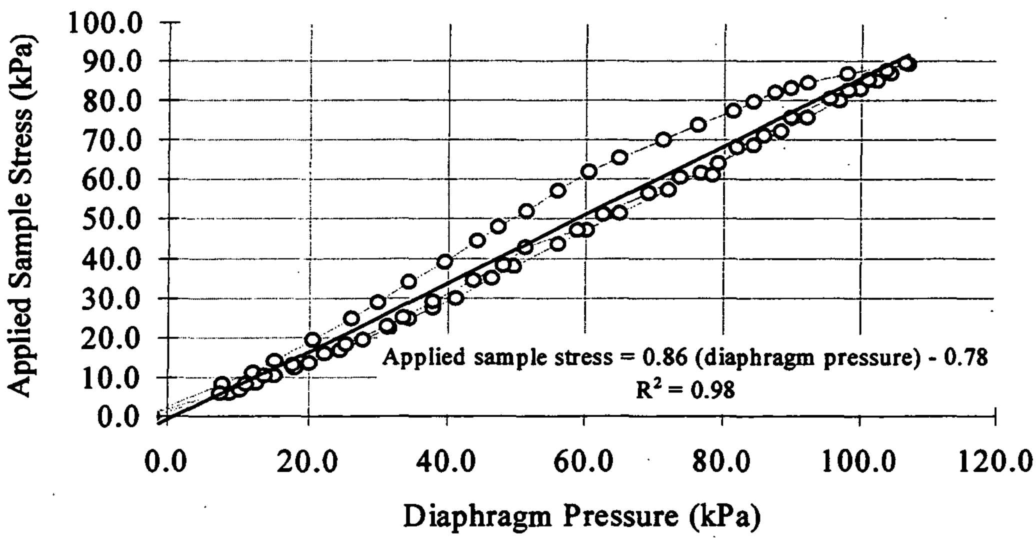

Figure A2.1.2. Diaphragm calibration graph (see Table A2.1.1b).

Calibration was performed using a CBR Test machine and load frame, and was based on the calibration procedure in BS 1377: Part 6:1990. The diaphragm calibration used during testing was that shown in Figure A2.1.1. Figure A2.1.2 was the data obtained during preliminary calibration testing.

A

DIAPH' PRESS (KPa)	SAMPLE STRESS (KPa)
-2.16	0.00
8.89	5.77
10.27	6.63
12.76	8.55
15.25	10.34
18.01	12.39
19.95	13.79
24.37	16.83
27.69	19.49
31.55	22.60
34.32	24.99
37.91	27.64
41.23	30.09
46.48	35.19
49.52	38.11
56.15	43.74
60.30	47.26
65.00	51.37
71.91	57.46
76.61	61.57
79.09	64.09
84.34	68.66
88.21	72.24
92.08	75.49
96.78	79.86
99.82	82.91
102.31	85.10
104.24	86.89
107.01	89.41
-2.72	0.20
7.51	5.90
11.10	8.22
13.87	10.47
17.74	13.12
22.16	16.17
25.20	18.62
31.28	23.06
33.49	25.12
37.91	29.23
43.72	34.46
48.14	38.37
51.18	42.88
58.92	47.12
62.51	51.10
69.14	56.67
73.57	60.51
78.26	61.24
81.86	68.00
85.73	71.12
89.87	75.49
95.40	80.33
98.16	82.58
100.93	85.23
103.69	87.69
106.45	89.67

B

DIAPH' PRESS (KPa)	SAMPLE STRESS (KPa)
-2.2	0.0
8.9	5.8
10.3	6.6
12.8	8.5
15.2	10.3
18.0	12.4
19.9	13.8
24.4	16.8
27.7	19.5
31.6	22.6
34.3	25.0
37.9	27.6
41.2	30.1
46.5	35.2
49.5	38.1
56.2	43.7
60.3	47.3
65.0	51.4
71.9	57.5
76.6	61.6
79.1	64.1
84.3	68.7
88.2	72.2
92.1	75.5
96.8	79.9
99.8	82.9
102.3	85.1
104.2	86.9
107.0	89.4
97.9	86.9
92.4	84.5
89.9	83.0
87.4	81.9
84.3	79.7
81.3	77.3
76.1	73.7
71.1	70.0
65.0	65.5
60.6	61.8
56.2	57.1
51.5	52.1
47.3	47.9
44.3	44.4
39.6	39.2
34.3	33.9
29.9	28.9
26.0	24.9
20.5	19.6
15.2	14.3
12.2	11.3
7.8	8.4

(B cont.)

DIAPH' PRESS (KPa)	SAMPLE STRESS (KPa)
-2.7	0.2
7.5	5.9
11.1	8.2
13.9	10.5
17.7	13.1
22.2	16.2
25.2	18.6
31.3	23.1
33.5	25.1
37.9	29.2
43.7	34.5
48.1	38.4
51.2	42.9
58.9	47.1
62.5	51.1
69.1	56.7
73.6	60.5
78.3	61.2
81.9	68.0
85.7	71.1
89.9	75.5
95.4	80.3
98.2	82.6
100.9	85.2
103.7	87.7
106.5	89.7

Table A2.1.1 Data sheet: diaphragm calibration values (A), see Figure A2.1.1 and (B), see Figure A2.1.2.

Appendix 3

Vibratory Test Data Sheets and Parameter Regression Data

TEST	ACCEL	TIME incr.	TIME cum.	SET inc.	SET cum.	HEIGHT	SET	VOL inc.	VOL cum.	VOL	VOL	WET MASS	WATER MASS	M	M CHANGE	BULK DENSE	DRY DENSE	VOID RATIO	VOID CHANGE	POROS	SAT	REL DENSE	REL COMP	PENE. RESIST
	(g)	(mins)	(mins)	(mm)	(mm)	(mm)	(%)	(ml)	(ml)	(ml)	(%)	(g)	(g)	(%)	(%)	(Mg/m2)	(Mg/m2)	(e)	(%)	(n)	(Sr)	(Dr)	(Cr)	(N)
1	(static)					(h0)								(cmc)										
	0.0	0.0	0.0	0.000	0.000	$\boxed{77.84}$	0.000	0.00	0.00	1418.79	0.00	2702.76	684.76	33.93	0.00	1.905	1.422	0.884	0.000	0.469	1.028	0.450	0.890	5.75
TT1DA	0.1	5.0	5.0	0.000	0.000	77.838	0.000	0.00	0.00	1418.79	0.00	2702.76	684.76	33.93	0.00	1.905	1.422	0.884	0.000	0.469	1.028	0.450	0.890	5.75
	0.2	5.0	10.0	0.006	0.006	77.833	-0.007	0.10	0.10	1418.69	0.01	2702.66	684.66	33.93	-0.01	1.905	1.422	0.884	-0.015	0.469	1.028	0.450	0.890	5.75
10 kPa	0.4	15.0	25.0	0.236	0.241	77.597	-0.310	4.29	4.39	1414.40	0.31	2698.37	680.37	33.72	-0.64	1.908	1.427	0.878	-0.660	0.468	1.029	0.463	0.893	6.09
	0.5	25.0	50.0	0.158	0.399	77.439	-0.513	2.88	7.27	1411.52	0.51	2695.49	677.49	33.57	-1.06	1.910	1.430	0.875	-1.092	0.467	1.029	0.472	0.894	6.33
	0.6	105.0	155.0	0.102	0.501	77.337	-0.644	1.86	9.13	1409.66	0.64	2693.63	675.63	33.48	-1.33	1.911	1.432	0.872	-1.372	0.466	1.029	0.478	0.896	6.48
	0.8	85.0	240.0	0.160	0.661	77.177	-0.849	2.92	12.05	1406.74	0.85	2690.71	672.71	33.34	-1.76	1.913	1.435	0.868	-1.810	0.465	1.029	0.487	0.897	6.72
	1.0	125.0	365.0	0.220	0.881	76.957	-1.132	4.01	16.06	1402.73	1.13	2686.70	668.70	33.14	-2.35	1.915	1.439	0.863	-2.412	0.463	1.029	0.499	0.900	7.07
	2.0	120.0	485.0	2.672	3.553	74.285	-4.565	48.70	64.76	1354.03	4.56	2638.00	620.00	30.72	-9.46	1.948	1.490	0.798	-9.727	0.444	1.032	0.648	0.930	11.90
						(h1)						2638.00	2018.00											
2	(static)					(h0)								(cmc)										
	0.0	0.0	0.0	0.000	0.00	$\boxed{79.869}$	0.00	0.00	0.00	1455.80	0.00	2807.06	674.06	31.60	0.00	1.928	1.465	0.829	0.000	0.453	1.021	0.577	0.915	12.22
TT1DB	0.1	5.0	5.0	0.000	0.00	79.87	0.00	0.00	0.00	1455.80	0.00	2807.06	674.06	31.60	0.00	1.928	1.465	0.829	0.000	0.453	1.021	0.577	0.915	12.22
	0.2	15.0	20.0	0.000	0.00	79.87	0.00	0.00	0.00	1455.80	0.00	2807.06	674.06	31.60	0.00	1.928	1.465	0.829	0.000	0.453	1.021	0.577	0.915	12.22
20 kPa	0.4	80.0	100.0	0.000	0.00	79.87	0.00	0.00	0.00	1455.80	0.00	2807.06	674.06	31.60	0.00	1.928	1.465	0.829	0.000	0.453	1.021	0.577	0.915	12.22
	0.5	180.0	280.0	0.000	0.00	79.87	0.00	0.00	0.00	1455.80	0.00	2807.06	674.06	31.60	0.00	1.928	1.465	0.829	0.000	0.453	1.021	0.577	0.915	12.22
	0.6	90.0	370.0	0.040	0.04	79.83	-0.05	0.73	0.73	1455.07	0.05	2806.33	673.33	31.57	-0.11	1.929	1.466	0.828	-0.110	0.453	1.021	0.579	0.916	12.31
	0.8	105.0	475.0	0.047	0.09	79.78	-0.11	0.85	1.58	1454.23	0.11	2805.48	672.48	31.53	-0.23	1.929	1.467	0.827	-0.239	0.453	1.021	0.581	0.916	12.41
	1.0	95.0	570.0	0.109	0.20	79.67	-0.24	1.98	3.55	1452.25	0.24	2803.50	670.50	31.43	-0.53	1.930	1.469	0.825	-0.539	0.452	1.022	0.587	0.917	12.66
	2.0	85.0	655.0	1.619	1.81	78.06	-2.27	29.50	33.06	1422.75	2.27	2774.00	641.00	30.05	-4.90	1.950	1.499	0.788	-5.009	0.441	1.023	0.672	0.934	16.60
						(h1)						2774.00	2133.00											
3	(static)					(h0)								(cmc)										
	0.0	0.0	0.0	0.000	0.00	$\boxed{78.79}$	0.00	0.00	0.00	1436.11	0.00	2750.70	656.70	31.36	0.00	1.915	1.458	0.838	0.000	0.456	1.003	0.556	0.911	19.11
TT1DC	0.1	5.0	5.0	0.000	0.00	78.79	0.00	0.00	0.00	1436.11	0.00	2750.70	656.70	31.36	0.00	1.915	1.458	0.838	0.000	0.456	1.003	0.556	0.911	19.11
	0.2	5.0	10.0	0.001	0.00	78.79	0.00	0.02	0.02	1436.09	0.00	2750.68	656.68	31.36	0.00	1.915	1.458	0.838	-0.003	0.456	1.003	0.556	0.911	19.12
50 kPa	0.4	5.0	15.0	0.000	0.00	78.79	0.00	0.00	0.02	1436.09	0.00	2750.68	656.68	31.36	0.00	1.915	1.458	0.838	-0.003	0.456	1.003	0.556	0.911	19.12
	0.5	30.0	45.0	0.031	0.03	78.76	-0.04	0.57	0.58	1435.53	0.04	2750.12	656.12	31.33	-0.09	1.916	1.459	0.837	-0.089	0.456	1.003	0.558	0.912	19.23
	0.6	45.0	90.0	0.043	0.08	78.71	-0.10	0.78	1.37	1434.74	0.10	2749.33	655.33	31.30	-0.21	1.916	1.459	0.836	-0.209	0.455	1.003	0.560	0.912	19.39
	0.8	100.0	190.0	0.106	0.18	78.61	-0.23	1.93	3.30	1432.81	0.23	2747.40	653.40	31.20	-0.50	1.917	1.461	0.834	-0.504	0.455	1.003	0.566	0.913	19.79
	1.0	120.0	310.0	0.140	0.32	78.47	-0.41	2.55	5.85	1430.26	0.41	2744.85	650.85	31.08	-0.89	1.919	1.464	0.831	-0.894	0.454	1.003	0.574	0.915	20.32
	2.0	100.0	410.0	1.912	2.23	76.56	-2.83	34.85	40.70	1395.41	2.83	2710.00	616.00	29.42	-6.20	1.942	1.501	0.786	-6.216	0.440	1.003	0.676	0.935	28.23
						(h1)						2710.00	2094.00											
4	(static)			0.000		(h0)								(cmc)										
	0.0	0.0	0.0	0.000	0.00	$\boxed{69.00}$	0.00	0.00	0.00	1257.70	0.00	2575.86	613.86	31.29	0.00	2.048	1.560	0.718	0.000	0.418	1.168	0.832	0.966	59.49
TT1DD	0.1	5.0	5.0	0.000	0.00	69.00	0.00	0.00	0.00	1257.70	0.00	2575.86	613.86	31.29	0.00	2.048	1.560	0.718	0.000	0.418	1.168	0.832	0.966	59.49
	0.2	5.0	10.0	0.000	0.00	69.00	0.00	0.00	0.00	1257.70	0.00	2575.86	613.86	31.29	0.00	2.048	1.560	0.718	0.000	0.418	1.168	0.832	0.966	59.49
100 kPa	0.4	5.0	15.0	0.000	0.00	69.00	0.00	0.00	0.00	1257.70	0.00	2575.86	613.86	31.29	0.00	2.048	1.560	0.718	0.000	0.418	1.168	0.832	0.966	59.49
	0.5	5.0	20.0	0.000	0.00	69.00	0.00	0.00	0.00	1257.70	0.00	2575.86	613.86	31.29	0.00	2.048	1.560	0.718	0.000	0.418	1.168	0.832	0.966	59.49
	0.6	55.0	75.0	0.000	0.00	69.00	0.00	0.00	0.00	1257.70	0.00	2575.86	613.86	31.29	0.00	2.048	1.560	0.718	0.000	0.418	1.168	0.832	0.966	59.49
	0.8	225.0	300.0	0.008	0.01	68.99	-0.01	0.15	0.15	1257.55	0.01	2575.71	613.71	31.28	-0.02	2.048	1.560	0.718	-0.028	0.418	1.168	0.833	0.967	59.55
	1.0	120.0	420.0	0.021	0.03	68.97	-0.04	0.39	0.54	1257.16	0.04	2575.32	613.32	31.26	-0.09	2.049	1.561	0.717	-0.102	0.418	1.168	0.834	0.967	59.73
	2.0	115.0	535.0	0.676	0.71	68.29	-1.02	12.32	12.86	1244.84	1.02	2563.00	601.00	30.63	-2.09	2.059	1.576	0.700	-2.447	0.412	1.172	0.873	0.975	65.40
						(h1)						2563.00	1962.00											

Table A3.1.1. Data sheet: silty fine sand, saturated, 25Hz.

TEST	ACCEL (g)	TIME incr.	TIME cum.	SET inc. (mm)	SET cum. (mm)	HEIGHT (mm)	SET (%)	VOL inc. (ml)	VOL cum. (ml)	VOL (ml)	VOL (%)	WET MASS (g)	WATER MASS (g)	M (%)	M CHANGE (%)	BULK DENSE (Mg/m2)	DRY DENSE (Mg/m2)	VOID RATIO (e)	VOID CHANGE (%)	POROS (n)	SAT (Sr)	REL DENSE (Dr)	REL COMP (Cr)	PENE. RESIST (N)
1	(static)					(h0)								(cmc)										
	0.0	0.0	0.0	0.000	0.000	63.415	0.000	0.00	0.00	1155.90	0.00	2242.92	551.92	32.64	0.00	1.940	1.463	0.832	0.000	0.454	1.051	0.570	0.914	9.23
TT1DE	0.1	5.0	5.0	0.000	0.000	63.415	0.000	0.00	0.00	1155.90	0.00	2242.92	551.92	32.64	0.00	1.940	1.463	0.832	0.000	0.454	1.051	0.570	0.914	9.23
	0.2	5.0	10.0	0.001	0.001	63.414	-0.002	0.02	0.02	1155.88	0.00	2242.90	551.90	32.64	0.00	1.940	1.463	0.832	-0.003	0.454	1.051	0.570	0.914	9.23
	0.3	120.0	130.0	0.016	0.017	63.398	-0.027	0.29	0.31	1155.59	0.03	2242.61	551.61	32.62	-0.06	1.941	1.463	0.831	-0.059	0.454	1.051	0.571	0.914	9.26
10 kPa	0.4	120.0	130.0	0.042	0.043	63.372	-0.067	0.76	0.78	1155.12	0.07	2242.15	551.15	32.59	-0.14	1.941	1.464	0.831	-0.148	0.454	1.052	0.573	0.915	9.32
	0.5	120.0	250.0	0.075	0.118	63.298	-0.185	1.37	2.14	1153.76	0.19	2240.78	549.78	32.51	-0.39	1.942	1.466	0.829	-0.408	0.453	1.052	0.578	0.916	9.48
	0.6	120.0	370.0	0.105	0.222	63.193	-0.350	1.90	4.05	1151.85	0.35	2238.88	547.88	32.40	-0.73	1.944	1.468	0.826	-0.771	0.452	1.052	0.585	0.917	9.71
	0.8	120.0	490.0	0.263	0.485	62.931	-0.764	4.78	8.83	1147.07	0.76	2234.09	543.09	32.12	-1.60	1.948	1.474	0.818	-1.682	0.450	1.052	0.602	0.920	10.30
	1.0	120.0	610.0	0.577	1.061	62.354	-1.674	10.52	19.35	1136.55	1.67	2223.58	532.58	31.49	-3.51	1.956	1.488	0.801	-3.686	0.445	1.053	0.641	0.928	11.65
	2.0	120.0	730.0	1.623	2.684	60.731	-4.232	29.58	48.92	1106.97	4.23	2194.00	503.00	29.75	-8.86	1.982	1.528	0.754	-9.320	0.430	1.057	0.749	0.950	15.89
						(hl)						2194.00	1691.00											
2	(static)					(h0)								(cmc)										
	0.0	0.0	0.0	0.000	0.00	70.97	0.000	0.00	0.00	1293.59	0.00	2431.78	566.78	30.39	0.00	1.880	1.442	0.859	0.000	0.462	0.948	0.508	0.902	9.49
TT1DF	0.1	5.0	5.0	0.000	0.00	70.97	0.000	0.00	0.00	1293.59	0.00	2431.78	566.78	30.39	0.00	1.880	1.442	0.859	0.000	0.462	0.948	0.508	0.902	9.49
	0.2	5.0	10.0	0.000	0.00	70.97	0.000	0.00	0.00	1293.59	0.00	2431.78	566.78	30.39	0.00	1.880	1.442	0.859	0.000	0.462	0.948	0.508	0.902	9.49
	0.3	5.0	15.0	0.000	0.00	70.97	0.000	0.00	0.00	1293.59	0.00	2431.78	566.78	30.39	0.00	1.880	1.442	0.859	0.000	0.462	0.948	0.508	0.902	9.49
20 kPa	0.4	15.0	25.0	0.000	0.00	70.97	0.000	0.00	0.00	1293.59	0.00	2431.78	566.78	30.39	0.00	1.880	1.442	0.859	0.000	0.462	0.948	0.508	0.902	9.49
	0.5	120.0	145.0	0.084	0.08	70.88	-0.119	1.53	1.53	1292.06	0.12	2430.24	565.24	30.31	-0.27	1.881	1.443	0.857	-0.256	0.461	0.948	0.513	0.903	9.68
	0.6	120.0	265.0	0.084	0.17	70.80	-0.237	1.53	3.06	1290.53	0.24	2428.71	563.71	30.23	-0.54	1.882	1.445	0.854	-0.512	0.461	0.948	0.518	0.904	9.87
	0.8	120.0	385.0	0.232	0.40	70.57	-0.564	4.24	7.30	1286.29	0.56	2424.48	559.48	30.00	-1.29	1.885	1.450	0.848	-1.221	0.459	0.948	0.532	0.906	10.41
	1.0	120.0	505.0	0.192	0.59	70.38	-0.835	3.50	10.80	1282.79	0.83	2420.98	555.98	29.81	-1.90	1.887	1.454	0.843	-1.806	0.458	0.947	0.544	0.909	10.87
	2.0	120.0	625.0	1.096	1.69	69.28	-2.379	19.98	30.78	1262.81	2.38	2401.00	536.00	28.74	-5.43	1.901	1.477	0.815	-5.149	0.449	0.945	0.610	0.922	13.67
						(hl)						2401.00	1865.00											
3	(static)					(h0)								(cmc)										
	0.0	0.0	0.0	0.000	0.00	69.08	0.000	0.00	0.00	1259.16	0.00	2410.76	571.76	31.09	0.00	1.915	1.461	0.835	0.000	0.455	0.998	0.563	0.913	19.62
TT1DG	0.1	0.0	0.0	0.000	0.00	69.08	0.000	0.00	0.00	1259.16	0.00	2410.76	571.76	31.09	0.00	1.915	1.461	0.835	0.000	0.455	0.998	0.563	0.913	19.62
	0.2	0.0	0.0	0.000	0.00	69.08	0.000	0.00	0.00	1259.16	0.00	2410.76	571.76	31.09	0.00	1.915	1.461	0.835	0.000	0.455	0.998	0.563	0.913	19.62
	0.3		0.0	0.000	0.00	69.08	0.000	0.00	0.00	1259.16	0.00	2410.76	571.76	31.09	0.00	1.915	1.461	0.835	0.000	0.455	0.998	0.563	0.913	19.62
50 kPa	0.4	120.0	120.0	0.035	0.04	69.04	-0.051	0.65	0.65	1258.51	0.05	2410.11	571.11	31.06	-0.11	1.915	1.461	0.834	-0.113	0.455	0.998	0.565	0.913	19.77
	0.5	120.0	240.0	0.040	0.08	69.00	-0.109	0.73	1.37	1257.78	0.11	2409.39	570.39	31.02	-0.24	1.916	1.462	0.833	-0.240	0.454	0.998	0.568	0.914	19.94
	0.6	120.0	360.0	0.158	0.23	68.85	-0.338	2.89	4.26	1254.90	0.34	2406.50	567.50	30.86	-0.74	1.918	1.465	0.829	-0.743	0.453	0.998	0.578	0.916	20.63
	0.8	120.0	480.0	0.179	0.41	68.67	-0.598	3.27	7.53	1251.63	0.60	2403.23	564.23	30.68	-1.32	1.920	1.469	0.824	-1.314	0.452	0.998	0.588	0.918	21.41
	1.0	120.0	600.0	0.242	0.65	68.43	-0.948	4.41	11.94	1247.22	0.95	2398.82	559.82	30.44	-2.09	1.923	1.474	0.818	-2.083	0.450	0.998	0.603	0.921	22.50
	2.0	120.0	720.0	1.087	1.74	67.34	-2.522	19.82	31.76	1227.40	2.52	2379.00	540.00	29.36	-5.55	1.938	1.498	0.789	-5.543	0.441	0.998	0.670	0.934	27.73
						(hl)						2379.00	1839.00											
4	(static)					(h0)								(cmc)										
	0.0	0.0	0.0	0.000	0.00	69.16	0.00	0.00	0.00	1260.58	0.00	2409.86	537.86	28.73	0.00	1.912	1.485	0.805	0.000	0.446	0.957	0.633	0.927	34.40
TT1DH	0.1	0.0	0.0	0.000	0.00	69.16	0.00	0.00	0.00	1260.58	0.00	2409.86	537.86	28.73	0.00	1.912	1.485	0.805	0.000	0.446	0.957	0.633	0.927	34.40
	0.2	0.0	0.0	0.000	0.00	69.16	0.00	0.00	0.00	1260.58	0.00	2409.86	537.86	28.73	0.00	1.912	1.485	0.805	0.000	0.446	0.957	0.633	0.927	34.40
	0.3	0.0	0.0	0.000	0.00	69.16	0.00	0.00	0.00	1260.58	0.00	2409.86	537.86	28.73	0.00	1.912	1.485	0.805	0.000	0.446	0.957	0.633	0.927	34.40
100 kPa	0.4	5.0	5.0	0.000	0.00	69.16	0.00	0.00	0.00	1260.58	0.00	2409.86	537.86	28.73	0.00	1.912	1.485	0.805	0.000	0.446	0.957	0.633	0.927	34.40
	0.5	5.0	10.0	0.000	0.00	69.16	0.00	0.00	0.00	1260.58	0.00	2409.86	537.86	28.73	0.00	1.912	1.485	0.805	0.000	0.446	0.957	0.633	0.927	34.40
	0.6	5.0	15.0	0.000	0.00	69.16	0.00	0.00	0.00	1260.58	0.00	2409.86	537.86	28.73	0.00	1.912	1.485	0.805	0.000	0.446	0.957	0.633	0.927	34.40
	0.8	120.0	135.0	0.008	0.01	69.15	-0.01	0.15	0.15	1260.43	0.01	2409.71	537.71	28.72	-0.03	1.912	1.485	0.804	-0.026	0.446	0.957	0.633	0.927	34.46
	1.0	120.0	255.0	0.021	0.03	69.13	-0.04	0.39	0.54	1260.04	0.04	2409.32	537.32	28.70	-0.10	1.912	1.486	0.804	-0.095	0.446	0.957	0.635	0.927	34.60
	2.0	120.0	375.0	0.676	0.71	68.45	-1.02	12.32	12.86	1247.72	1.02	2397.00	525.00	28.04	-2.39	1.921	1.500	0.786	-2.288	0.440	0.956	0.675	0.935	39.16
						(hl)						2397.00	1872.00											

Table A3.1.2. Data sheet: silty fine sand, saturated, 40Hz.

TEST	ACCEL (g)	TIME incr. (mins)	TIME cum. (mins)	SET inc. (mm)	SET cum. (mm)	HEIGHT (mm)	SET (%)	VOL inc. (ml)	VOL cum. (ml)	VOL (ml)	VOL (%)	WET MASS (g)	WATER MASS (g)	M (%)	M CHANGE (%)	BULK DENSE (Mg/m2)	DRY DENSE (Mg/m2)	VOID RATIO (e)	VOID CHANGE (%)	POROS (n)	SAT (Sr)	REL DENSE (Dr)	REL COMP (Cr)	PENE RESIST (N)
1	(static)					(h0)								(cmc)										
	0.0	0.0	0.0	0.000	0.000	107.750	0.000	0.00	0.00	1964.01	0.00	3411.95	863.95	33.91	0.00	1.737	1.297	1.050	0.000	0.512	0.859	0.068	0.814	0.132
T1DA	1.0	20.0	20.0	0.760	0.760	106.990	-0.705	13.85	13.85	1950.16	0.71	3398.10	850.10	33.36	-1.60	1.742	1.307	1.036	-1.377	0.509	0.857	0.101	0.820	0.292
	2.0	216.0	236.0	4.200	4.960	102.790	-4.603	76.56	90.41	1873.61	4.64	3321.54	773.54	30.36	-10.46	1.773	1.360	0.956	-8.986	0.489	0.845	0.285	0.857	2.307
10kPa	3.0	88.0	324.0	1.560	6.520	101.230	-6.051	28.43	118.84	1845.17	6.09	3293.11	745.11	29.24	-13.76	1.785	1.381	0.926	-11.812	0.481	0.840	0.353	0.871	3.543
	4.0	81.0	405.0	1.490	8.010	99.740	-7.434	27.16	146.00	1818.01	7.49	3265.95	717.95	28.18	-16.90	1.796	1.402	0.898	-14.511	0.473	0.835	0.419	0.884	4.970
	5.0	54.0	459.0	1.610	9.620	98.130	-8.928	29.35	175.35	1788.67	8.99	3236.60	688.60	27.03	-20.30	1.810	1.425	0.867	-17.428	0.464	0.829	0.489	0.898	6.783
	6.0	0.0	459.0	0.000	9.620	98.130	-8.928	0.00	175.35	1788.67	8.99	3236.60	688.60	27.03	-20.30	1.810	1.425	0.867	-17.428	0.464	0.829	0.489	0.898	6.783
						(h1)						3236.60	2548.00											
2	(static)					(h0)								(cmc)										
	0.0	0.0	0.0	0.000	0.000	93.450	0.000	0.00	0.00	1703.36	0.00	3028.52	595.52	24.48	0.00	1.778	1.428	0.862	0.000	0.463	0.755	0.500	0.900	9.202
T1DB	1.0	30.0	30.0	0.610	0.610	92.840	-0.653	11.12	11.12	1692.24	0.66	3017.40	584.40	24.02	-1.87	1.783	1.438	0.850	-1.410	0.459	0.752	0.528	0.906	10.258
	2.0	70.0	100.0	1.250	1.860	91.590	-1.990	22.78	33.90	1669.46	2.00	2994.61	561.61	23.08	-5.69	1.794	1.457	0.825	-4.299	0.452	0.744	0.586	0.917	12.602
20kPa	3.0	30.0	130.0	0.350	2.210	91.240	-2.365	6.38	40.28	1663.08	2.38	2988.23	555.23	22.82	-6.76	1.797	1.463	0.818	-5.107	0.450	0.742	0.602	0.920	13.302
	4.0	40.0	170.0	0.640	2.850	90.600	-3.050	11.67	51.95	1651.41	3.07	2976.57	543.57	22.34	-8.72	1.802	1.473	0.805	-6.587	0.446	0.738	0.631	0.926	14.630
	5.0	53.0	223.0	0.470	3.320	90.130	-3.553	8.57	60.52	1642.85	3.58	2968.00	535.00	21.99	-10.16	1.807	1.481	0.796	-7.673	0.443	0.735	0.653	0.931	15.645
	6.0	0.0	223.0	0.000	3.320	90.130	-3.553	0.00	60.52	1642.85	3.58	2968.00	535.00	21.99	-10.16	1.807	1.481	0.796	-7.673	0.443	0.735	0.653	0.931	15.645
						(h1)						2968.00	2433.00											
3	(static)					(h0)								(cmc)										
	0.0	0.0	0.0	0.000	0.000	116.135	0.000	0.00	0.00	2116.85	0.00	3894.75	826.75	26.95	0.00	1.840	1.449	0.835	0.000	0.455	0.858	0.562	0.912	19.537
T1DC	1.0	15.0	15.0	0.130	0.130	116.005	-0.112	2.37	2.37	2114.48	0.11	3892.38	824.38	26.87	-0.29	1.841	1.451	0.833	-0.246	0.455	0.858	0.567	0.913	19.866
	2.0	37.0	52.0	0.740	0.870	115.265	-0.749	13.49	15.86	2100.99	0.75	3878.89	810.89	26.43	-1.92	1.846	1.460	0.822	-1.646	0.451	0.856	0.594	0.919	21.794
50kPa	3.0	47.0	99.0	0.710	1.580	114.555	-1.360	12.94	28.80	2088.05	1.36	3865.95	797.95	26.01	-3.48	1.851	1.469	0.810	-2.989	0.448	0.854	0.620	0.924	23.728
	4.0	62.0	161.0	0.990	2.570	113.565	-2.213	18.05	46.84	2070.01	2.22	3847.91	779.91	25.42	-5.67	1.859	1.482	0.795	-4.862	0.443	0.851	0.656	0.931	26.562
	5.0	60.0	221.0	1.970	4.540	111.595	-3.909	35.91	82.75	2034.10	3.91	3812.00	744.00	24.25	-10.01	1.874	1.508	0.764	-8.589	0.433	0.845	0.727	0.945	32.675
	6.0	0.0	221.0	0.000	4.540	111.595	-3.909	0.00	82.75	2034.10	3.91	3812.00	744.00	24.25	-10.01	1.874	1.508	0.764	-8.589	0.433	0.845	0.727	0.945	32.675
						(h1)						3812.00	3068.00											
4	(static)					(h0)								(cmc)										
	0.0	0.0	0.0	0.000	0.000	94.380	0.000	0.00	0.00	1720.31	0.00	3094.92	741.92	31.53	0.00	1.799	1.368	0.945	0.000	0.486	0.888	0.311	0.862	8.300
T1DD	1.0	15.0	15.0	0.070	0.070	94.310	-0.074	1.28	1.28	1719.04	0.07	3093.64	740.64	31.48	-0.17	1.800	1.369	0.943	-0.153	0.485	0.888	0.314	0.863	8.478
	2.0	55.0	70.0	1.390	1.460	92.920	-1.547	25.34	26.61	1693.70	1.55	3068.30	715.30	30.40	-3.59	1.812	1.389	0.915	-3.184	0.478	0.884	0.380	0.876	12.404
100kPa	3.0	45.0	115.0	0.660	2.120	92.260	-2.246	12.03	38.64	1681.67	2.25	3056.27	703.27	29.89	-5.21	1.817	1.399	0.901	-4.624	0.474	0.882	0.411	0.882	14.529
	4.0	58.0	173.0	0.850	2.970	91.410	-3.147	15.49	54.14	1666.18	3.15	3040.78	687.78	29.23	-7.30	1.825	1.412	0.884	-6.478	0.469	0.880	0.452	0.890	17.513
	5.0	65.0	238.0	1.140	4.110	90.270	-4.355	20.78	74.92	1645.40	4.36	3020.00	667.00	28.35	-10.10	1.835	1.430	0.860	-8.964	0.462	0.877	0.506	0.901	21.951
	6.0	0.0	238.0	0.000	4.110	90.270	-4.355	0.00	74.92	1645.40	4.36	3020.00	667.00	28.35	-10.10	1.835	1.430	0.860	-8.964	0.462	0.877	0.506	0.901	21.951
						(h1)						3020.00	2353.00											

Table A3.1.3. Data sheet: silty fine sand, high acceleration,saturated, 25Hz.

TEST	ACCEL (g)	TIME incr. (mins)	TIME cum. (mins)	SET inc. (mm)	SET cum. (mm)	HEIGHT (mm)	SET (%)	VOL inc. (ml)	VOL cum. (ml)	VOL (ml)	VOL (%)	WET MASS (g)	WATER MASS (g)	M (%)	M CHANGE (%)	BULK DENSE (Mg/m2)	DRY DENSE (Mg/m2)	VOID RATIO (e)	VOID CHANGE (%)	POROS (n)	SAT (Sr)	AIR CONT (A)	REL DENSE (Dr)	REL COMP (Cr)	PENE. RESIST (N)
1	(static)					(h0)								(cmc)											
	0.0	0.0	0.0	0.00	0.00	111.48	0.00	0.00	0.00	2031.91	0.00	2918.00	4.00	0.14	0.00	1.436	1.434	0.869	0.000	0.465	0.004	0.463	0.486	0.897	6.69
T1DE	1.0	5.0	5.0	0.00	0.00	111.48	0.00	0.00	0.00	2031.91	0.00	2918.00	4.00	0.14	0.00	1.436	1.434	0.869	0.000	0.465	0.004	0.463	0.486	0.897	6.69
	2.0	43.0	48.0	1.17	1.17	110.31	-1.05	21.33	21.33	2010.59	1.05	2918.00	4.00	0.14	0.00	1.451	1.449	0.849	-2.258	0.459	0.004	0.457	0.531	0.906	7.99
10	3.0	54.0	102.0	1.48	2.65	108.83	-2.38	26.98	48.30	1983.61	2.38	2918.00	4.00	0.14	0.00	1.471	1.469	0.824	-5.114	0.452	0.004	0.450	0.588	0.918	9.80
	4.0	18.0	120.0	0.19	2.84	108.64	-2.55	3.46	51.77	1980.15	2.55	2918.00	4.00	0.14	0.00	1.474	1.472	0.821	-5.480	0.451	0.004	0.449	0.595	0.919	10.05
	5.0	93.0	213.0	4.07	6.91	104.57	-6.20	74.19	125.95	1905.96	6.20	2918.00	4.00	0.14	0.00	1.531	1.529	0.753	-13.334	0.430	0.005	0.427	0.752	0.950	16.04
	6.0	0.0	213.0	0.00	6.91	104.57	-6.20	0.00	125.95	1905.96	6.20	2918.00	4.00	0.14	0.00	1.531	1.529	0.753	-13.334	0.430	0.005	0.427	0.752	0.950	16.04
						(h1)						2918.00	2914.00												
2	(static)					(h0)								(cmc)											
	0.0	0.0	0.0	0.00	0.00	108.33	0.00	0.00	0.00	1974.59	0.00	2772.00	9.00	0.33	0.00	1.404	1.399	0.915	0.000	0.478	0.010	0.473	0.379	0.876	5.27
T1DF	1.0	10.0	10.0	0.02	0.02	108.31	-0.02	0.36	0.36	1974.22	0.02	2772.00	9.00	0.33	0.00	1.404	1.400	0.915	-0.039	0.478	0.010	0.473	0.380	0.876	5.29
	2.0	100.0	110.0	4.76	4.78	103.55	-4.41	86.76	87.13	1887.46	4.41	2772.00	9.00	0.33	0.00	1.469	1.464	0.831	-9.233	0.454	0.011	0.449	0.573	0.915	12.06
20	3.0	53.0	163.0	0.33	5.11	103.22	-4.72	6.02	93.14	1881.44	4.72	2772.00	9.00	0.33	0.00	1.473	1.469	0.825	-9.871	0.452	0.011	0.447	0.586	0.917	12.63
	4.0	45.0	208.0	0.66	5.77	102.56	-5.33	12.03	105.17	1869.41	5.33	2772.00	9.00	0.33	0.00	1.483	1.478	0.813	-11.146	0.449	0.011	0.444	0.613	0.923	13.81
	5.0	49.0	257.0	1.09	6.86	101.47	-6.33	19.87	125.04	1849.55	6.33	2772.00	9.00	0.33	0.00	1.499	1.494	0.794	-13.251	0.443	0.011	0.438	0.658	0.932	15.88
	6.0	0.0	257.0	0.00	6.86	101.47	-6.33	0.00	125.04	1849.55	6.33	2772.00	9.00	0.33	0.00	1.499	1.494	0.794	-13.251	0.443	0.011	0.438	0.658	0.932	15.88
						(h1)						2772.00	2763.00												
3	(static)					(h0)								(cmc)											
	0.0	0.0	0.0	0.00	0.00	78.93	0.00	0.00	0.00	1438.70	0.00	2226.00	6.00	0.27	0.00	1.547	1.543	0.737	0.000	0.424	0.010	0.420	0.789	0.958	38.44
T1DG	1.0	10.0	10.0	0.00	0.00	78.93	0.00	0.00	0.00	1438.70	0.00	2226.00	6.00	0.27	0.00	1.547	1.543	0.737	0.000	0.424	0.010	0.420	0.789	0.958	38.44
	2.0	14.0	24.0	0.05	0.05	78.88	-0.06	0.91	0.91	1437.79	0.06	2226.00	6.00	0.27	0.00	1.548	1.544	0.736	-0.149	0.424	0.010	0.420	0.791	0.958	38.69
50	3.0	73.0	97.0	3.79	3.84	75.09	-4.87	69.08	69.99	1368.70	4.87	2226.00	6.00	0.27	0.00	1.626	1.622	0.652	-11.468	0.395	0.011	0.390	0.983	0.997	59.70
	4.0	29.0	126.0	0.18	4.02	74.91	-5.09	3.28	73.27	1365.42	5.09	2226.00	6.00	0.27	0.00	1.630	1.626	0.648	-12.006	0.393	0.011	0.389	0.992	0.998	60.81
	5.0	40.0	166.0	0.21	4.23	74.70	-5.36	3.83	77.10	1361.59	5.36	2226.00	6.00	0.27	0.00	1.635	1.630	0.644	-12.633	0.392	0.011	0.387	1.003	1.001	62.12
	6.0	0.0	166.0	0.00	4.23	74.70	-5.36	0.00	77.10	1361.59	5.36	2226.00	6.00	0.27	0.00	1.635	1.630	0.644	-12.633	0.392	0.011	0.387	1.003	1.001	62.12
						(h1)						2226.00	2220.00												

Table A3.1.4. Data sheet: silty fine sand, high acceleration,dried 25Hz.

TEST	ACCEL (g)	TIME incr. (mins)	TIME cum. (mins)	SET inc. (mm)	SET cum. (mm)	HEIGHT (mm)	SET (%)	VOL inc. (ml)	VOL cum. (ml)	VOL (ml)	VOL (%)	WET MASS (g)	WATER MASS (g)	M (%)	M CHANGE (%)	BULK DENSE (Mg/m2)	DRY DENSE (Mg/m2)	VOID RATIO (e)	VOID CHANGE (%)	POROS (n)	SAT (Sr)	REL DENSE (Dr)	REL COMP (Cr)	PENE. RESIST (N)
1	(static)					(h0)								(cmc)										
	0.0	0.0	0.0	0.000	0.000	71.00	0.000	0.00	0.00	1294.15	0.00	2439.55	623.55	34.34	0.00	1.885	1.403	0.903	0.000	0.474	1.016	0.256	0.851	1.85
TT1ZD	0.1	5.0	5.0	0.000	0.000	71.000	0.000	0.00	0.00	1294.15	0.00	2439.55	623.55	34.34	0.00	1.885	1.403	0.903	0.000	0.474	1.016	0.256	0.851	1.85
	0.2	65.0	70.0	0.041	0.041	70.959	-0.058	0.75	0.75	1293.41	0.06	2438.80	622.80	34.30	-0.12	1.886	1.404	0.902	-0.122	0.474	1.016	0.259	0.852	1.90
10 kPa	0.4	120.0	190.0	0.299	0.340	70.660	-0.479	5.45	6.20	1287.96	0.48	2433.35	617.35	34.00	-0.99	1.889	1.410	0.894	-1.009	0.472	1.016	0.281	0.856	2.25
	0.5	130.0	320.0	0.237	0.577	70.423	-0.813	4.32	10.52	1283.64	0.81	2429.03	613.03	33.76	-1.69	1.892	1.415	0.887	-1.713	0.470	1.016	0.299	0.860	2.54
	0.6	115.0	435.0	0.198	0.775	70.225	-1.092	3.61	14.13	1280.03	1.09	2425.42	609.42	33.56	-2.27	1.895	1.419	0.882	-2.301	0.469	1.016	0.315	0.863	2.81
	0.8	105.0	540.0	0.262	1.037	69.963	-1.461	4.78	18.90	1275.25	1.46	2420.65	604.65	33.30	-3.03	1.898	1.424	0.875	-3.078	0.467	1.016	0.334	0.867	3.17
	1.0	115.0	655.0	0.756	1.793	69.207	-2.525	13.78	32.68	1261.47	2.53	2406.87	590.87	32.54	-5.24	1.908	1.440	0.855	-5.323	0.461	1.016	0.392	0.878	4.35
	2.0	150.0	805.0	3.888	5.681	65.319	-8.001	70.87	103.55	1190.60	8.00	2336.00	520.00	28.63	-16.61	1.962	1.525	0.751	-16.865	0.429	1.019	0.687	0.937	13.39
						(h1)						2336.00	1816.00											
2	(static)					(h0)								(cmc)										
	0.0	0.0	0.0	0.000	0.000	82.746	0.000	0.00	0.00	1508.25	0.00	2822.76	692.76	32.52	0.00	1.872	1.412	0.891	0.000	0.471	0.975	0.290	0.858	3.09
TT1ZB	0.1	5.0	5.0	0.000	0.000	82.746	0.000	0.00	0.00	1508.25	0.00	2822.76	692.76	32.52	0.00	1.872	1.412	0.891	0.000	0.471	0.975	0.290	0.858	3.09
	0.2	5.0	10.0	0.003	0.003	82.743	-0.004	0.05	0.05	1508.20	0.00	2822.71	692.71	32.52	-0.01	1.872	1.412	0.891	-0.008	0.471	0.975	0.290	0.858	3.09
20 kPa	0.4	60.0	70.0	0.107	0.110	82.636	-0.133	1.95	2.01	1506.25	0.13	2820.75	690.75	32.43	-0.29	1.873	1.414	0.888	-0.282	0.470	0.975	0.297	0.859	3.24
	0.5	55.0	125.0	0.078	0.188	82.558	-0.227	1.42	3.43	1504.83	0.23	2819.33	689.33	32.36	-0.49	1.874	1.415	0.886	-0.482	0.470	0.975	0.302	0.860	3.35
	0.6	80.0	205.0	0.156	0.344	82.402	-0.416	2.84	6.27	1501.98	0.42	2816.49	686.49	32.23	-0.91	1.875	1.418	0.883	-0.883	0.469	0.975	0.312	0.862	3.58
	0.8	172.0	377.0	0.265	0.609	82.137	-0.736	4.83	11.10	1497.15	0.74	2811.66	681.66	32.00	-1.60	1.878	1.423	0.877	-1.562	0.467	0.975	0.329	0.866	3.99
	1.0	95.0	472.0	0.437	1.046	81.700	-1.264	7.97	19.07	1489.19	1.26	2803.69	673.69	31.63	-2.75	1.883	1.430	0.867	-2.683	0.464	0.974	0.358	0.872	4.70
	2.0	130.0	602.0	4.043	5.089	77.657	-6.150	73.69	92.76	1415.49	6.15	2730.00	600.00	28.17	-13.39	1.929	1.505	0.774	-13.056	0.436	0.971	0.619	0.924	14.09
						(h1)						2730.00	2130.00											
3	(static)					(h0)								(cmc)										
	0.0	0.0	0.0	0.000	0.000	69.265	0.000	0.00	0.00	1262.53	0.00	2414.93	594.93	32.69	0.00	1.913	1.442	0.852	0.000	0.460	1.024	0.399	0.880	9.83
TT1AC	0.1	5.0	5.0	0.000	0.000	69.265	0.000	0.00	0.00	1262.53	0.00	2414.93	594.93	32.69	0.00	1.913	1.442	0.852	0.000	0.460	1.024	0.399	0.880	9.83
	0.2	10.0	15.0	0.000	0.000	69.265	0.000	0.00	0.00	1262.53	0.00	2414.93	594.93	32.69	0.00	1.913	1.442	0.852	0.000	0.460	1.024	0.399	0.880	9.83
50 kPa	0.4	15.0	30.0	0.000	0.000	69.265	0.000	0.00	0.00	1262.53	0.00	2414.93	594.93	32.69	0.00	1.913	1.442	0.852	0.000	0.460	1.024	0.399	0.880	9.83
	0.5	65.0	95.0	0.004	0.004	69.262	-0.005	0.06	0.06	1262.46	0.01	2414.86	594.86	32.68	-0.01	1.913	1.442	0.852	-0.011	0.460	1.024	0.399	0.880	9.84
	0.6	30.0	125.0	0.004	0.008	69.258	-0.011	0.07	0.14	1262.39	0.01	2414.79	594.79	32.68	-0.02	1.913	1.442	0.852	-0.024	0.460	1.024	0.400	0.880	9.86
	0.8	50.0	175.0	0.032	0.039	69.226	-0.056	0.57	0.71	1261.82	0.06	2414.22	594.22	32.65	-0.12	1.913	1.442	0.851	-0.122	0.460	1.024	0.402	0.880	9.98
	1.0	120.0	295.0	0.106	0.145	69.120	-0.209	1.93	2.64	1259.89	0.21	2412.29	592.29	32.54	-0.44	1.915	1.445	0.848	-0.455	0.459	1.024	0.410	0.882	10.38
	2.0	210.0	505.0	2.265	2.410	66.855	-3.479	41.29	43.93	1218.60	3.48	2371.00	551.00	30.27	-7.38	1.946	1.494	0.788	-7.562	0.441	1.026	0.582	0.916	20.88
						(h1)						2371.00	1820.00											
4	(static)					(h0)								(cmc)										
	0.0	0.0	0.0	0.000	0.000	71.311	0.000	0.00	0.00	1299.82	0.00	2486.89	582.89	30.61	0.00	1.913	1.465	0.823	0.000	0.451	0.993	0.482	0.896	19.98
TT1ZD	0.1	5.0	5.0	0.000	0.000	71.311	0.000	0.00	0.00	1299.82	0.00	2486.89	582.89	30.61	0.00	1.913	1.465	0.823	0.000	0.451	0.993	0.482	0.896	19.98
	0.2	5.0	10.0	0.000	0.000	71.311	0.000	0.00	0.00	1299.82	0.00	2486.89	582.89	30.61	0.00	1.913	1.465	0.823	0.000	0.451	0.993	0.482	0.896	19.98
100 kPa	0.4	55.0	65.0	0.004	0.004	71.307	-0.006	0.07	0.07	1299.75	0.01	2486.82	582.82	30.61	-0.01	1.913	1.465	0.823	-0.012	0.451	0.993	0.483	0.897	20.00
	0.5	35.0	100.0	0.008	0.012	71.299	-0.017	0.15	0.22	1299.60	0.02	2486.68	582.68	30.60	-0.04	1.913	1.465	0.822	-0.037	0.451	0.993	0.483	0.897	20.05
	0.6	65.0	165.0	0.030	0.042	71.269	-0.059	0.55	0.77	1299.06	0.06	2486.13	582.13	30.57	-0.13	1.914	1.466	0.822	-0.130	0.451	0.993	0.485	0.897	20.23
	0.8	60.0	225.0	0.043	0.085	71.226	-0.119	0.78	1.55	1298.27	0.12	2485.34	581.34	30.53	-0.27	1.914	1.467	0.821	-0.264	0.451	0.993	0.488	0.898	20.49
	1.0	35.0	260.0	0.048	0.133	71.178	-0.187	0.87	2.42	1297.40	0.19	2484.47	580.47	30.49	-0.42	1.915	1.468	0.819	-0.413	0.450	0.993	0.492	0.898	20.78
	2.0	130.0	390.0	1.123	1.256	70.055	-1.761	20.47	22.89	1276.93	1.76	2464.00	560.00	29.41	-3.93	1.930	1.491	0.791	-3.902	0.442	0.993	0.573	0.915	28.22
						(h1)						2464.00	1904.00											

Table A3.2.1. Data sheet: fine uniform sand, saturated, 25Hz.

TEST	ACCEL (g)	TIME incr. (mins)	TIME cum. (mins)	SET inc. (mm)	SET cum. (mm)	HEIGHT (mm)	SET (%)	VOL inc. (ml)	VOL cum. (ml)	VOL (ml)	VOL (%)	WET MASS (g)	WATER MASS (g)	M (%)	M CHANGE (%)	BULK DENSE (Mg/m2)	DRY DENSE (Mg/m2)	VOID RATIO (e)	VOID CHANGE (%)	POROS (n)	SAT (Sr)	AIR CONT (A)	REL DENSE (Dr)	REL COMP (Cr)	PENE. RESIST (N)
1	(static)					(h0)								(cmc)											
	0.0	0.0	0.0	0.000	0.000	81.16	0.000	0.00	0.00	1479.31	0.00	2824.47	720.47	34.24	0.00	1.909	1.422	0.877	0.000	0.467	1.042	-0.020	0.328	0.866	3.05
TT1ZEb	0.1	5.0	5.0	0.000	0.000	81.158	0.000	0.00	0.00	1479.31	0.00	2824.47	720.47	34.24	0.00	1.909	1.422	0.877	0.000	0.467	1.042	-0.020	0.328	0.866	3.05
	0.2	5.0	10.0	0.000	0.000	81.158	0.000	0.00	0.00	1479.31	0.00	2824.47	720.47	34.24	0.00	1.909	1.422	0.877	0.000	0.467	1.042	-0.020	0.328	0.866	3.05
	0.3	120.0	130.0	0.139	0.139	81.019	-0.172	2.54	2.54	1476.77	0.17	2821.93	717.93	34.12	-0.35	1.911	1.425	0.874	-0.367	0.466	1.042	-0.020	0.337	0.867	3.22
10 kPa	0.4	120.0	250.0	0.171	0.171	80.987	-0.211	3.12	3.12	1476.18	0.21	2821.34	717.34	34.09	-0.43	1.911	1.425	0.873	-0.452	0.466	1.042	-0.020	0.339	0.868	3.26
	0.5	120.0	370.0	0.228	0.399	80.759	-0.492	4.16	7.28	1472.03	0.49	2817.19	713.19	33.90	-1.01	1.914	1.429	0.868	-1.053	0.465	1.043	-0.020	0.354	0.871	3.56
	0.6	120.0	490.0	0.287	0.687	80.472	-0.846	5.23	12.51	1466.80	0.85	2811.96	707.96	33.65	-1.74	1.917	1.434	0.861	-1.810	0.463	1.043	-0.020	0.373	0.875	3.94
	0.8	120.0	610.0	0.400	1.087	80.071	-1.339	7.30	19.81	1459.50	1.34	2804.66	700.66	33.30	-2.75	1.922	1.442	0.852	-2.866	0.460	1.043	-0.020	0.399	0.880	4.52
	1.0	120.0	730.0	0.847	1.934	79.224	-2.383	15.44	35.25	1444.05	2.38	2789.21	685.21	32.57	-4.89	1.932	1.457	0.833	-5.100	0.454	1.044	-0.020	0.455	0.891	5.86
	2.0	120.0	850.0	2.316	4.250	76.908	-5.237	42.21	77.47	1401.84	5.24	2747.00	643.00	30.56	-10.75	1.960	1.501	0.779	-11.206	0.438	1.048	-0.021	0.606	0.921	10.43
						(h1)						2747.00	2104.00												
2	(static)					(h0)								(cmc)											
	0.0	0.0	0.0	0.000	0.000	77.182	0.000	0.00	0.00	1406.84	0.00	2661.84	664.84	33.29	0.00	1.892	1.419	0.881	0.000	0.468	1.009	-0.004	0.317	0.863	3.70
TT1ZF	0.1	5.0	5.0	0.000	0.000	77.182	0.000	0.00	0.00	1406.84	0.00	2661.84	664.84	33.29	0.00	1.892	1.419	0.881	0.000	0.468	1.009	-0.004	0.317	0.863	3.70
	0.2	5.0	10.0	0.000	0.000	77.182	0.000	0.00	0.00	1406.84	0.00	2661.84	664.84	33.29	0.00	1.892	1.419	0.881	0.000	0.468	1.009	-0.004	0.317	0.863	3.70
	0.3	120.0	130.0	0.039	0.039	77.143	-0.051	0.72	0.72	1406.12	0.05	2661.13	664.13	33.26	-0.11	1.893	1.420	0.880	-0.109	0.468	1.009	-0.004	0.320	0.864	3.77
20 kPa	0.4	120.0	250.0	0.093	0.093	77.089	-0.120	1.69	1.69	1405.15	0.12	2660.15	663.15	33.21	-0.25	1.893	1.421	0.879	-0.256	0.468	1.009	-0.004	0.324	0.865	3.85
	0.5	120.0	370.0	0.161	0.253	76.929	-0.328	2.93	4.62	1402.22	0.33	2657.23	660.23	33.06	-0.69	1.895	1.424	0.875	-0.700	0.467	1.009	-0.004	0.335	0.867	4.12
	0.6	120.0	490.0	0.437	0.690	76.492	-0.894	7.97	12.58	1394.25	0.89	2649.26	652.26	32.66	-1.89	1.900	1.432	0.864	-1.910	0.464	1.009	-0.004	0.365	0.873	4.90
	0.8	120.0	610.0	0.396	1.087	76.096	-1.408	7.22	19.80	1387.03	1.41	2642.04	645.04	32.30	-2.98	1.905	1.440	0.854	-3.006	0.461	1.009	-0.004	0.392	0.878	5.66
	1.0	120.0	730.0	0.202	1.288	75.894	-1.669	3.67	23.48	1383.36	1.67	2638.36	641.36	32.12	-3.53	1.907	1.444	0.850	-3.563	0.459	1.009	-0.004	0.406	0.881	6.07
	2.0	120.0	850.0	2.269	3.557	73.625	-4.609	41.36	64.84	1341.99	4.61	2597.00	600.00	30.05	-9.75	1.935	1.488	0.794	-9.841	0.443	1.010	-0.004	0.563	0.913	11.65
						(h1)						2597.00	1997.00												
3	(static)					(h0)								(cmc)											
	0.0	0.0	0.0	0.000	0.000	84.584	0.000	0.00	0.00	1541.76	0.00	2947.16	726.16	32.70	0.00	1.912	1.441	0.853	0.000	0.460	1.023	-0.011	0.395	0.879	9.65
TT1ZG	0.1	5.0	5.0	0.000	0.000	84.584	0.000	0.00	0.00	1541.76	0.00	2947.16	726.16	32.70	0.00	1.912	1.441	0.853	0.000	0.460	1.023	-0.011	0.395	0.879	9.65
	0.2	5.0	10.0	0.000	0.000	84.584	0.000	0.00	0.00	1541.76	0.00	2947.16	726.16	32.70	0.00	1.912	1.441	0.853	0.000	0.460	1.023	-0.011	0.395	0.879	9.65
	0.3	10.0	20.0	0.000	0.000	84.584	0.000	0.00	0.00	1541.76	0.00	2947.16	726.16	32.70	0.00	1.912	1.441	0.853	0.000	0.460	1.023	-0.011	0.395	0.879	9.65
50 kPa	0.4	15.0	35.0	0.000	0.000	84.584	0.000	0.00	0.00	1541.76	0.00	2947.16	726.16	32.70	0.00	1.912	1.441	0.853	0.000	0.460	1.023	-0.011	0.395	0.879	9.65
	0.5	25.0	60.0	0.000	0.000	84.584	0.000	0.00	0.00	1541.76	0.00	2947.16	726.16	32.70	0.00	1.912	1.441	0.853	0.000	0.460	1.023	-0.011	0.395	0.879	9.65
	0.6	120.0	180.0	0.032	0.032	84.552	-0.038	0.59	0.59	1541.17	0.04	2946.57	725.57	32.67	-0.08	1.912	1.441	0.853	-0.083	0.460	1.023	-0.011	0.397	0.879	9.75
	0.8	120.0	300.0	0.085	0.117	84.467	-0.139	1.55	2.14	1539.62	0.14	2945.03	724.03	32.60	-0.29	1.913	1.443	0.851	-0.301	0.460	1.023	-0.011	0.403	0.881	10.01
	1.0	120.0	420.0	0.129	0.246	84.338	-0.291	2.34	4.48	1537.28	0.29	2942.68	721.68	32.49	-0.62	1.914	1.445	0.848	-0.631	0.459	1.023	-0.011	0.411	0.882	10.41
	2.0	120.0	540.0	1.903	2.149	82.436	-2.540	34.68	39.16	1502.59	2.54	2908.00	687.00	30.93	-5.39	1.935	1.478	0.806	-5.516	0.446	1.024	-0.011	0.529	0.906	17.27
						(h1)						2908.00	2221.00												
4	(static)					(h0)								(cmc)											
	0.0	0.0	0.0	0.000	0.000	74.217	0.000	0.00	0.00	1352.79	0.00	2619.91	635.91	32.05	0.00	1.937	1.467	0.821	0.000	0.451	1.043	-0.019	0.489	0.898	20.50
TT1ZH	0.1	5.0	5.0	0.000	0.000	74.217	0.000	0.00	0.00	1352.79	0.00	2619.91	635.91	32.05	0.00	1.937	1.467	0.821	0.000	0.451	1.043	-0.019	0.489	0.898	20.50
	0.2	5.0	10.0	0.000	0.000	74.217	0.000	0.00	0.00	1352.79	0.00	2619.91	635.91	32.05	0.00	1.937	1.467	0.821	0.000	0.451	1.043	-0.019	0.489	0.898	20.50
	0.3	5.0	15.0	0.000	0.000	74.217	0.000	0.00	0.00	1352.79	0.00	2619.91	635.91	32.05	0.00	1.937	1.467	0.821	0.000	0.451	1.043	-0.019	0.489	0.898	20.50
100 kPa	0.4	15.0	30.0	0.000	0.000	74.217	0.000	0.00	0.00	1352.79	0.00	2619.91	635.91	32.05	0.00	1.937	1.467	0.821	0.000	0.451	1.043	-0.019	0.489	0.898	20.50
	0.5	15.0	45.0	0.000	0.000	74.217	0.000	0.00	0.00	1352.79	0.00	2619.91	635.91	32.05	0.00	1.937	1.467	0.821	0.000	0.451	1.043	-0.019	0.489	0.898	20.50
	0.6	40.0	85.0	0.036	0.036	74.181	-0.049	0.66	0.66	1352.13	0.05	2619.25	635.25	32.02	-0.10	1.937	1.467	0.820	-0.108	0.450	1.043	-0.019	0.491	0.898	20.71
	0.8	120.0	205.0	0.273	0.309	73.908	-0.416	4.98	5.63	1347.16	0.42	2614.27	630.27	31.77	-0.89	1.941	1.473	0.813	-0.924	0.448	1.043	-0.019	0.510	0.902	22.34
	1.0	120.0	325.0	0.220	0.529	73.688	-0.712	4.00	9.64	1343.16	0.71	2610.27	626.27	31.57	-1.52	1.943	1.477	0.808	-1.580	0.447	1.044	-0.019	0.525	0.905	23.70
	2.0	120.0	445.0	1.496	2.025	72.192	-2.728	27.27	36.91	1315.89	2.73	2583.00	599.00	30.19	-5.80	1.963	1.508	0.771	-6.053	0.435	1.046	-0.020	0.629	0.926	34.00
						(h1)						2583.00	1984.00												

Table A3.2.2. Data sheet: fine uniform sand, saturated, 40Hz.

TEST	ACCEL (g)	TIME incr. (mins)	TIME cum. (mins)	SET inc. (mm)	SET cum. (mm)	HEIGHT (mm)	SET (%)	VOL inc. (ml)	VOL cum. (ml)	VOL (ml)	VOL (%)	WET MASS (g)	WATER MASS (g)	M (%)	M CHANGE (%)	BULK DENSE (Mg/m2)	DRY DENSE (Mg/m2)	VOID RATIO (e)	VOID CHANGE (%)	POROS (n)	SAT (Sr)	REL DENSE (Dr)	REL COMP (Cr)	PENE RESIST (N)
1	(static)					(h0)								(cmc)										
	0.0	0.0	0.0	0.000	0.000	89.255	0.000	0.00	0.00	1626.90	0.00	3207.28	718.28	28.86	0.00	1.971	1.530	0.745	0.000	0.427	1.034	0.702	0.940	13.979
T1ZA	1.0	30.0	30.0	0.240	0.240	89.015	-0.269	4.37	4.37	1622.52	0.27	3202.90	713.90	28.68	-0.61	1.974	1.534	0.741	-0.630	0.425	1.034	0.715	0.943	14.513
	2.0	20.0	50.0	1.240	1.480	87.775	-1.658	22.60	26.98	1599.92	1.66	3180.30	691.30	27.77	-3.76	1.988	1.556	0.716	-3.883	0.417	1.035	0.784	0.957	17.434
10kPa	3.0	40.0	90.0	0.930	2.410	86.845	-2.700	16.95	43.93	1582.97	2.71	3163.35	674.35	27.09	-6.12	1.998	1.572	0.698	-6.323	0.411	1.036	0.835	0.967	19.801
	4.0	59.0	149.0	1.000	3.410	85.845	-3.821	18.23	62.16	1564.74	3.83	3145.12	656.12	26.36	-8.65	2.010	1.591	0.679	-8.947	0.404	1.037	0.891	0.978	22.513
	5.0	70.0	219.0	0.720	4.130	85.125	-4.627	13.12	75.28	1551.62	4.64	3132.00	643.00	25.83	-10.48	2.019	1.604	0.664	-10.836	0.399	1.038	0.931	0.986	24.574
	6.0	0.0	219.0	0.000	4.130	85.125	-4.627	0.00	75.28	1551.62	4.64	3132.00	643.00	25.83	-10.48	2.019	1.604	0.664	-10.836	0.399	1.038	0.931	0.986	24.574
						(h1)						3132.00	2489.00											
3	(static)					(h0)								(cmc)										
	0.0	0.0	0.0	0.000	0.000	123.240	0.000	0.00	0.00	2246.36	0.00	4189.12	934.12	28.70	0.00	1.865	1.449	0.843	0.000	0.457	0.909	0.426	0.885	6.666
T1ZB	1.0	9.0	9.0	0.110	0.110	123.130	-0.089	2.01	2.01	2244.35	0.09	4187.12	932.12	28.64	-0.21	1.866	1.450	0.841	-0.195	0.457	0.909	0.431	0.886	6.812
	2.0	60.0	69.0	1.650	1.760	121.480	-1.428	30.08	32.08	2214.28	1.43	4157.04	902.04	27.71	-3.43	1.877	1.470	0.816	-3.123	0.449	0.906	0.501	0.900	9.203
20kPa	3.0	70.0	139.0	1.620	3.380	119.860	-2.743	29.53	61.61	2184.75	2.75	4127.51	872.51	26.81	-6.60	1.889	1.490	0.792	-5.997	0.442	0.904	0.569	0.914	11.899
	4.0	59.0	198.0	1.030	4.410	118.830	-3.578	18.77	80.38	2165.98	3.58	4108.74	853.74	26.23	-8.61	1.897	1.503	0.777	-7.825	0.437	0.902	0.613	0.923	13.793
	5.0	30.0	228.0	0.260	4.670	118.570	-3.789	4.74	85.12	2161.24	3.79	4104.00	849.00	26.08	-9.11	1.899	1.506	0.773	-8.286	0.436	0.901	0.624	0.925	14.293
	6.0	0.0	228.0	0.000	4.670	118.570	-3.789	0.00	85.12	2161.24	3.79	4104.00	849.00	26.08	-9.11	1.899	1.506	0.773	-8.286	0.436	0.901	0.624	0.925	14.293
						(h1)						4104.00	3255.00											
4	(static)					(h0)								(cmc)										
	0.0	0.0	0.0	0.000	0.000	73.040	0.000	0.00	0.00	1331.34	0.00	2691.95	608.95	29.23	0.00	2.022	1.565	0.707	0.000	0.414	1.105	0.812	0.962	40.678
T1ZC	1.0	10.0	10.0	0.040	0.040	73.000	-0.055	0.73	0.73	1330.61	0.05	2691.22	608.22	29.20	-0.12	2.023	1.565	0.706	-0.132	0.414	1.105	0.814	0.963	40.944
	2.0	28.0	38.0	0.370	0.410	72.630	-0.561	6.74	7.47	1323.86	0.56	2684.48	601.48	28.88	-1.23	2.028	1.573	0.697	-1.356	0.411	1.106	0.839	0.968	43.444
50kPa	3.0	53.0	91.0	1.210	1.620	71.420	-2.218	22.06	29.53	1301.81	2.22	2662.42	579.42	27.82	-4.85	2.045	1.600	0.669	-5.357	0.401	1.111	0.919	0.984	52.137
	4.0	62.0	153.0	0.690	2.310	70.730	-3.163	12.58	42.11	1289.23	3.16	2649.84	566.84	27.21	-6.91	2.055	1.616	0.653	-7.639	0.395	1.113	0.964	0.993	57.449
	5.0	61.0	214.0	0.540	2.850	70.190	-3.902	9.84	51.95	1279.39	3.90	2640.00	557.00	26.74	-8.53	2.063	1.628	0.640	-9.425	0.390	1.116	1.000	1.000	61.785
	6.0	0.0	214.0	0.000	2.850	70.190	-3.902	0.00	51.95	1279.39	3.90	2640.00	557.00	26.74	-8.53	2.063	1.628	0.640	-9.425	0.390	1.116	1.000	1.000	61.785
						(h1)						2640.00	2083.00											
5	(static)					(h0)								(cmc)										
	0.0	0.0	0.0	0.000	0.000	70.720	0.000	0.00	0.00	1289.05	0.00	2609.26	580.26	28.60	0.00	2.024	1.574	0.696	0.000	0.410	1.097	0.841	0.968	60.677
T1ZD	1.0	10.0	10.0	0.060	0.060	70.660	-0.085	1.09	1.09	1287.96	0.08	2608.17	579.17	28.54	-0.19	2.025	1.575	0.695	-0.207	0.410	1.097	0.845	0.969	61.267
	2.0	49.0	59.0	0.690	0.750	69.970	-1.061	12.58	13.67	1275.38	1.06	2595.59	566.59	27.92	-2.36	2.035	1.591	0.678	-2.584	0.404	1.099	0.892	0.978	68.257
100kPa	3.0	60.0	119.0	0.690	1.440	69.280	-2.036	12.58	26.25	1262.80	2.04	2583.02	554.02	27.30	-4.52	2.045	1.607	0.662	-4.961	0.398	1.102	0.938	0.988	75.625
	4.0	31.0	150.0	0.230	1.670	69.050	-2.361	4.19	30.44	1258.61	2.36	2578.82	549.82	27.10	-5.25	2.049	1.612	0.656	-5.753	0.396	1.103	0.954	0.991	78.165
	5.0	15.0	165.0	0.100	1.770	68.950	-2.503	1.82	32.26	1256.79	2.50	2577.00	548.00	27.01	-5.56	2.050	1.614	0.654	-6.097	0.395	1.103	0.961	0.992	79.283
	6.0	0.0	165.0	0.000	1.770	68.950	-2.503	0.00	32.26	1256.79	2.50	2577.00	548.00	27.01	-5.56	2.050	1.614	0.654	-6.097	0.395	1.103	0.961	0.992	79.283
						(h1)						2577.00	2029.00											

Table A3.2.3. Data sheet: fine uniform sand, high acceleration, saturated, 25Hz.

TEST	ACCEL (g)	TIME incr. (mins)	TIME cum. (mins)	SET inc. (mm)	SET cum. (mm)	HEIGHT (mm)	SET (%)	VOL inc. (ml)	VOL cum. (ml)	VOL (ml)	VOL (%)	WET MASS (g)	WATER MASS (g)	M (%)	M CHANGE (%)	BULK DENSE (Mg/m2)	DRY DENSE (Mg/m2)	VOID RATIO (e)	VOID CHANGE (%)	POROS (n)	SAT (Sr)	REL DENSE (Dr)	REL COMP (Cr)	PENE. RESIST (N)
1	(static)					(h0)								(cmc)										
	0.0	0.0	0.0	0.000	0.000	70.408	0.000	0.00	0.00	1283.35	0.00	2521.67	532.67	26.78	0.00	1.965	1.550	0.697	0.000	0.411	1.011	0.385	0.877	4.21
TT1EA	0.1	5.0	5.0	0.000	0.000	70.408	0.000	0.00	0.00	1283.35	0.00	2521.67	532.67	26.78	0.00	1.965	1.550	0.697	0.000	0.411	1.011	0.385	0.877	4.21
	0.2	5.0	10.0	0.000	0.000	70.408	0.000	0.00	0.00	1283.35	0.00	2521.67	532.67.	26.78	0.00	1.965	1.550	0.697	0.000	0.411	1.011	0.385	0.877	4.21
10 kPa	0.4	35.0	45.0	0.170	0.170	70.238	-0.241	3.10	3.10	1280.25	0.24	2518.57	529.57	26.63	-0.58	1.967	1.554	0.693	-0.588	0.409	1.011	0.403	0.881	4.61
	0.5	35.0	80.0	0.112	0.282	70.126	-0.400	2.03	5.13	1278.22	0.40	2516.54	527.54	26.52	-0.96	1.969	1.556	0.690	-0.973	0.408	1.011	0.415	0.883	4.89
	0.6	30.0	110.0	0.099	0.380	70.028	-0.540	1.80	6.93	1276.43	0.54	2514.75	525.75	26.43	-1.30	1.970	1.558	0.688	-1.314	0.408	1.011	0.426	0.885	5.14
	0.8	40.0	150.0	0.208	0.588	69.820	-0.835	3.79	10.72	1272.64	0.84	2510.95	521.95	26.24	-2.01	1.973	1.563	0.683	-2.033	0.406	1.011	0.448	0.890	5.69
	1.0	55.0	205.0	0.320	0.908	69.500	-1.290	5.83	16.55	1266.80	1.29	2505.12	516.12	25.95	-3.11	1.978	1.570	0.675	-3.140	0.403	1.011	0.482	0.896	6.59
	2.0	60.0	265.0	2.256	3.164	67.244	-4.494	41.12	57.67	1225.68	4.49	2464.00	475.00	23.88	-10.83	2.010	1.623	0.621	-10.942	0.383	1.012	0.723	0.945	14.81
						(h1)						2464.00	1989.00											
3	(static)					(h0)								(cmc)										
	0.0	0.0	0.0	0.000	0.000	78.245	0.000	0.00	0.00	1426.20	0.00	2789.11	604.11	27.65	0.00	1.956	1.532	0.717	0.000	0.417	1.015	0.298	0.860	5.48
TT1EB	0.1	5.0	5.0	0.000	0.000	78.245	0.000	0.00	0.00	1426.20	0.00	2789.11	604.11	27.65	0.00	1.956	1.532	0.717	0.000	0.417	1.015	0.298	0.860	5.48
	0.2	5.0	10.0	0.000	0.000	78.245	0.000	0.00	0.00	1426.20	0.00	2789.11	604.11	27.65	0.00	1.956	1.532	0.717	0.000	0.417	1.015	0.298	0.860	5.48
20 kPa	0.4	25.0	35.0	0.024	0.024	78.221	-0.031	0.44	0.44	1425.76	0.03	2788.68	603.68	27.63	-0.07	1.956	1.533	0.716	-0.073	0.417	1.015	0.300	0.860	5.57
	0.5	25.0	60.0	0.031	0.055	78.190	-0.070	0.57	1.00	1425.20	0.07	2788.11	603.11	27.60	-0.17	1.956	1.533	0.715	-0.168	0.417	1.015	0.303	0.861	5.68
	0.6	40.0	100.0	0.035	0.090	78.155	-0.115	0.64	1.64	1424.56	0.12	2787.47	602.47	27.57	-0.27	1.957	1.534	0.715	-0.276	0.417	1.015	0.307	0.861	5.81
	0.8	45.0	145.0	0.131	0.221	78.024	-0.282	2.39	4.03	1422.17	0.28	2785.09	600.09	27.46	-0.67	1.958	1.536	0.712	-0.677	0.416	1.015	0.319	0.864	6.30
	1.0	35.0	180.0	0.248	0.469	77.776	-0.599	4.52	8.55	1417.65	0.60	2780.57	595.57	27.26	-1.42	1.961	1.541	0.706	-1.436	0.414	1.015	0.343	0.869	7.29
	2.0	100.0	280.0	2.445	2.914	75.331	-3.724	44.57	53.11	1373.09	3.72	2736.00	551.00	25.22	-8.79	1.993	1.591	0.653	-8.921	0.395	1.016	0.581	0.916	20.84
						(h1)						2736.00	2185.00											
4	(static)					(h0)								(cmc)										
	0.0	0.0	0.0	0.000	0.000	80.604	0.000	0.00	0.00	1469.21	0.00	2886.38	600.38	26.26	0.00	1.965	1.556	0.690	0.000	0.408	1.001	0.415	0.883	14.76
TT1EC	0.1	5.0	5.0	0.000	0.000	80.604	0.000	0.00	0.00	1469.21	0.00	2886.38	600.38	26.26	0.00	1.965	1.556	0.690	0.000	0.408	1.001	0.415	0.883	14.76
	0.2	5.0	10.0	0.000	0.000	80.604	0.000	0.00	0.00	1469.21	0.00	2886.38	600.38	26.26	0.00	1.965	1.556	0.690	0.000	0.408	1.001	0.415	0.883	14.76
50 kPa	0.4	15.0	25.0	0.000	0.000	80.604	0.000	0.00	0.00	1469.21	0.00	2886.38	600.38	26.26	0.00	1.965	1.556	0.690	0.000	0.408	1.001	0.415	0.883	14.76
	0.5	30.0	55.0	0.008	0.008	80.596	-0.010	0.15	0.15	1469.06	0.01	2886.23	600.23	26.26	-0.02	1.965	1.556	0.690	-0.024	0.408	1.001	0.415	0.883	14.82
	0.6	20.0	75.0	0.007	0.015	80.590	-0.018	0.12	0.26	1468.95	0.02	2886.11	600.11	26.25	-0.04	1.965	1.556	0.690	-0.044	0.408	1.001	0.416	0.883	14.86
	0.8	30.0	105.0	0.050	0.064	80.540	-0.079	0.90	1.17	1468.04	0.08	2885.21	599.21	26.21	-0.19	1.965	1.557	0.689	-0.194	0.408	1.001	0.421	0.884	15.19
	1.0	45.0	150.0	0.142	0.206	80.398	-0.256	2.59	3.75	1465.46	0.26	2882.62	596.62	26.10	-0.63	1.967	1.560	0.686	-0.626	0.407	1.001	0.434	0.887	16.16
	2.0	55.0	205.0	1.680	1.886	78.718	-2.340	30.62	34.38	1434.83	2.34	2852.00	566.00	24.76	-5.73	1.988	1.593	0.651	-5.729	0.394	1.001	0.590	0.918	29.86
						(h1)						2852.00	2286.00											
5	(static)					(h0)								(cmc)										
	0.0	0.0	0.0	0.000	0.000	77.140	0.000	0.00	0.00	1406.07	0.00	2790.85	595.85	27.15	0.00	1.985	1.561	0.685	0.000	0.406	1.043	0.439	0.888	5.47
TT1ED	0.1	5.0	5.0	0.000	0.000	77.140	0.000	0.00	0.00	1406.07	0.00	2790.85	595.85	27.15	0.00	1.985	1.561	0.685	0.000	0.406	1.043	0.439	0.888	5.47
	0.2	5.0	10.0	0.000	0.000	77.140	0.000	0.00	0.00	1406.07	0.00	2790.85	595.85	27.15	0.00	1.985	1.561	0.685	0.000	0.406	1.043	0.439	0.888	5.47
100 kPa	0.4	10.0	20.0	0.003	0.003	77.137	-0.004	0.05	0.05	1406.02	0.00	2790.80	595.80	27.14	-0.01	1.985	1.561	0.685	-0.010	0.406	1.043	0.440	0.888	5.48
	0.5	20.0	40.0	0.002	0.005	77.135	-0.006	0.04	0.09	1405.98	0.01	2790.76	595.76	27.14	-0.02	1.985	1.561	0.685	-0.016	0.406	1.043	0.440	0.888	5.49
	0.6	35.0	75.0	0.013	0.018	77.122	-0.023	0.24	0.33	1405.74	0.02	2790.53	595.53	27.13	-0.06	1.985	1.561	0.684	-0.057	0.406	1.043	0.441	0.888	5.52
	0.8	60.0	135.0	0.019	0.037	77.103	-0.048	0.35	0.67	1405.40	0.05	2790.18	595.18	27.12	-0.11	1.985	1.562	0.684	-0.118	0.406	1.043	0.443	0.889	5.56
	1.0	50.0	185.0	0.051	0.088	77.052	-0.114	0.93	1.60	1404.47	0.11	2789.25	594.25	27.07	-0.27	1.986	1.563	0.683	-0.281	0.406	1.043	0.448	0.890	5.69
	2.0	55.0	240.0	0.672	0.760	76.380	-0.985	12.25	13.85	1392.22	0.99	2777.00	582.00	26.51	-2.33	1.995	1.577	0.668	-2.424	0.401	1.044	0.513	0.903	7.46
						(h1)						2777.00	2195.00											

Table A3.3.1. Data sheet: Garside medium sand, saturated, 25Hz.

TEST	ACCEL (g)	TIME incr. (mins)	TIME cum. (mins)	SET inc. (mm)	SET cum. (mm)	HEIGHT (mm)	SET (%)	VOL inc. (ml)	VOL cum. (ml)	VOL (ml)	VOL (%)	WET MASS (g)	WATER MASS (g)	M (%)	M CHANGE (%)	BULK DENSE (Mg/m2)	DRY DENSE (Mg/m2)	VOID RATIO (e)	VOID CHANGE (%)	POROS (n)	SAT (Sr)	REL DENSE (Dr)	REL COMP (Cr)	PENE. RESIST (N)
1	(static)					(h0)								(cmc)										
	0.0	0.0	0.0	0.000	0.000	79.470	0.000	0.00	0.00	1448.54	0.00	2877.03	633.03	28.21	0.00	1.986	1.549	0.704	0.000	0.413	1.058	0.353	0.871	3.54
TT1EF	0.1	5.0	5.0	0.000	0.000	79.470	0.000	0.00	0.00	1448.54	0.00	2877.03	633.03	28.21	0.00	1.986	1.549	0.704	0.000	0.413	1.058	0.353	0.871	3.54
	0.2	40.0	45.0	0.021	0.021	79.449	-0.026	0.38	0.38	1448.16	0.03	2876.65	632.65	28.19	-0.06	1.986	1.550	0.704	-0.064	0.413	1.058	0.355	0.871	3.58
	0.3	120.0	165.0	0.074	0.095	79.375	-0.119	1.35	1.73	1446.81	0.12	2875.30	631.30	28.13	-0.27	1.987	1.551	0.702	-0.289	0.413	1.058	0.362	0.872	3.72
10 kPa	0.4	120.0	165.0	0.056	0.150	79.320	-0.189	1.01	1.39	1445.80	0.10	2875.64	631.64	28.15	-0.22	1.989	1.552	0.701	-0.458	0.412	1.060	0.368	0.874	3.83
	0.5	120.0	285.0	0.088	0.239	79.231	-0.300	1.61	3.00	1444.19	0.21	2874.03	630.03	28.08	-0.47	1.990	1.554	0.699	-0.727	0.411	1.060	0.376	0.875	4.01
	0.6	120.0	405.0	0.096	0.334	79.136	-0.421	1.74	4.74	1442.45	0.33	2872.29	628.29	28.00	-0.75	1.991	1.556	0.697	-1.018	0.411	1.060	0.385	0.877	4.20
	0.8	120.0	525.0	0.231	0.566	78.904	-0.712	4.22	8.96	1438.23	0.62	2868.07	624.07	27.81	-1.42	1.994	1.560	0.692	-1.722	0.409	1.061	0.407	0.881	4.70
	1.0	120.0	645.0	0.226	0.792	78.678	-0.996	4.12	13.09	1434.11	0.90	2863.95	619.95	27.63	-2.07	1.997	1.565	0.687	-2.412	0.407	1.061	0.428	0.886	5.21
	2.0	120.0	765.0	2.356	3.148	76.322	-3.961	42.95	56.03	1391.16	3.87	2821.00	577.00	25.71	-8.85	2.028	1.613	0.637	-9.587	0.389	1.066	0.652	0.930	12.06
						(h1)						2821.00	2244.00											
2	(static)					(h0)								(cmc)										
	0.0	0.0	0.0	0.000	0.000	81.540	0.000	0.00	0.00	1486.27	0.00	2967.97	647.97	27.93	0.00	1.997	1.561	0.691	0.000	0.409	1.067	0.410	0.882	6.18
TT1EG	0.1	5.0	5.0	0.000	0.000	81.540	0.000	0.00	0.00	1486.27	0.00	2967.97	647.97	27.93	0.00	1.997	1.561	0.691	0.000	0.409	1.067	0.410	0.882	6.18
	0.2	5.0	10.0	0.000	0.000	81.540	0.000	0.00	0.00	1486.27	0.00	2967.97	647.97	27.93	0.00	1.997	1.561	0.691	0.000	0.409	1.067	0.410	0.882	6.18
	0.3	15.0	25.0	0.008	0.008	81.532	-0.010	0.15	0.15	1486.13	0.01	2967.83	647.83	27.92	-0.02	1.997	1.561	0.691	-0.024	0.409	1.067	0.411	0.882	6.21
20 kPa	0.4	50.0	60.0	0.051	0.059	81.481	-0.072	0.93	0.93	1485.20	0.06	2967.04	647.04	27.89	-0.14	1.998	1.562	0.690	-0.177	0.408	1.067	0.416	0.883	6.35
	0.5	45.0	105.0	0.047	0.106	81.434	-0.130	0.86	1.79	1484.34	0.12	2966.19	646.19	27.85	-0.28	1.998	1.563	0.689	-0.318	0.408	1.067	0.420	0.884	6.48
	0.6	55.0	160.0	0.060	0.166	81.374	-0.204	1.09	2.88	1483.25	0.19	2965.09	645.09	27.81	-0.44	1.999	1.564	0.688	-0.498	0.408	1.067	0.426	0.885	6.65
	0.8	55.0	215.0	0.151	0.317	81.224	-0.388	2.74	5.62	1480.50	0.38	2962.35	642.35	27.69	-0.87	2.001	1.567	0.685	-0.950	0.406	1.068	0.439	0.888	7.09
	1.0	120.0	335.0	0.243	0.559	80.981	-0.686	4.43	10.05	1476.08	0.68	2957.92	637.92	27.50	-1.55	2.004	1.572	0.680	-1.678	0.405	1.068	0.462	0.892	7.83
	2.0	120.0	455.0	1.916	2.475	79.065	-3.036	34.92	44.97	1441.15	3.03	2923.00	603.00	25.99	-6.94	2.028	1.610	0.640	-7.427	0.390	1.072	0.637	0.927	14.93
						(h1)						2923.00	2320.00											
3	(static)					(h0)								(cmc)										
	0.0	0.0	0.0	0.000	0.000	71.709	0.000	0.00	0.00	1307.08	0.00	2708.38	576.38	27.03	0.00	2.072	1.631	0.619	0.000	0.382	1.154	0.732	0.946	33.11
TT1EH	0.1	0.0	0.0	0.000	0.000	71.709	0.000	0.00	0.00	1307.08	0.00	2708.38	576.38	27.03	0.00	2.072	1.631	0.619	0.000	0.382	1.154	0.732	0.946	33.11
	0.2	0.0	0.0	0.000	0.000	71.709	0.000	0.00	0.00	1307.08	0.00	2708.38	576.38	27.03	0.00	2.072	1.631	0.619	0.000	0.382	1.154	0.732	0.946	33.11
	0.3	0.0	0.0	0.000	0.000	71.709	0.000	0.00	0.00	1307.08	0.00	2708.38	576.38	27.03	0.00	2.072	1.631	0.619	0.000	0.382	1.154	0.732	0.946	33.11
50 kPa	0.4	120.0	120.0	0.010	0.010	71.699	-0.014	0.18	0.18	1306.89	0.01	2708.20	576.20	27.03	-0.03	2.072	1.631	0.618	-0.036	0.382	1.154	0.733	0.947	33.20
	0.5	40.0	160.0	0.010	0.020	71.689	-0.028	0.18	0.36	1306.71	0.03	2708.02	576.02	27.02	-0.06	2.072	1.632	0.618	-0.073	0.382	1.154	0.734	0.947	33.29
	0.6	120.0	280.0	0.026	0.046	71.663	-0.064	0.48	0.84	1306.23	0.06	2707.54	575.54	27.00	-0.15	2.073	1.632	0.617	-0.169	0.382	1.154	0.737	0.947	33.53
	0.8	120.0	400.0	0.059	0.106	71.603	-0.147	1.08	1.92	1305.15	0.15	2706.46	574.46	26.94	-0.33	2.074	1.634	0.616	-0.385	0.381	1.155	0.743	0.949	34.07
	1.0	120.0	520.0	0.116	0.221	71.488	-0.308	2.11	4.03	1303.04	0.31	2704.35	572.35	26.85	-0.70	2.075	1.636	0.614	-0.807	0.380	1.155	0.754	0.951	35.14
	2.0	120.0	640.0	1.391	1.612	70.097	-2.248	25.35	29.38	1277.70	2.25	2679.00	547.00	25.66	-5.10	2.097	1.669	0.582	-5.882	0.368	1.164	0.893	0.979	49.27
						(h1)						2679.00	2132.00											
4	(static)					(h0)								(cmc)										
	0.0	0.0	0.0	0.000	0.000	74.170	0.000	0.00	0.00	1351.93	0.00	2696.54	562.54	26.36	0.00	1.995	1.578	0.672	0.000	0.402	1.035	0.493	0.899	20.91
TT1EI	0.1	0.0	0.0	0.000	0.000	74.170	0.000	0.00	0.00	1351.93	0.00	2696.54	562.54	26.36	0.00	1.995	1.578	0.672	0.000	0.402	1.035	0.493	0.899	20.91
	0.2	0.0	0.0	0.000	0.000	74.170	0.000	0.00	0.00	1351.93	0.00	2696.54	562.54	26.36	0.00	1.995	1.578	0.672	0.000	0.402	1.035	0.493	0.899	20.91
	0.3	5.0	5.0	0.000	0.000	74.170	0.000	0.00	0.00	1351.93	0.00	2696.54	562.54	26.36	0.00	1.995	1.578	0.672	0.000	0.402	1.035	0.493	0.899	20.91
100 kPa	0.4	5.0	5.0	0.000	0.000	74.170	0.000	0.00	0.00	1351.93	0.00	2696.54	562.54	26.36	0.00	1.995	1.578	0.672	0.000	0.402	1.035	0.493	0.899	20.91
	0.5	120.0	125.0	0.012	0.012	74.158	-0.016	0.22	0.22	1351.71	0.02	2696.31	562.31	26.35	-0.04	1.995	1.579	0.672	-0.041	0.402	1.035	0.495	0.899	21.01
	0.6	40.0	165.0	0.004	0.016	74.154	-0.022	0.07	0.29	1351.64	0.02	2696.24	562.24	26.35	-0.05	1.995	1.579	0.672	-0.054	0.402	1.035	0.495	0.899	21.04
	0.8	120.0	285.0	0.007	0.023	74.147	-0.032	0.13	0.43	1351.51	0.03	2696.11	562.11	26.34	-0.08	1.995	1.579	0.672	-0.078	0.402	1.035	0.496	0.899	21.10
	1.0	120.0	405.0	0.013	0.036	74.134	-0.049	0.23	0.66	1351.27	0.05	2695.88	561.88	26.33	-0.12	1.995	1.579	0.672	-0.121	0.402	1.035	0.497	0.899	21.21
	2.0	120.0	525.0	0.816	0.852	73.318	-1.149	14.88	15.54	1336.40	1.15	2681.00	547.00	25.63	-2.76	2.006	1.597	0.653	-2.858	0.395	1.036	0.578	0.916	28.73
						(h1)						2681.00	2134.00											

Table A3.3.2. Data sheet: Garside medium sand, saturated, 40Hz.

TEST	ACCEL (g)	TIME incr. (mins)	TIME cum. (mins)	SET inc. (mm)	SET cum. (mm)	HEIGHT (mm)	SET (%)	VOL inc. (ml)	VOL cum. (ml)	VOL (ml)	VOL (%)	WET MASS (g)	WATER MASS (g)	M (%)	M CHANGE (%)	BULK DENSE (Mg/m2)	DRY DENSE (Mg/m2)	VOID RATIO (e)	VOID CHANGE (%)	POROS (n)	SAT (Sr)	REL DENSE (Dr)	REL COMP (Cr)	PENE RESIST (N)
2	(static)					(h0)								(cmc)										
	0.0	0.0	0.0	0.00	0.00	77.41	0.00	0.00	0.00	1410.99	0.00	2728.97	537.97	24.55	0.00	1.934	1.553	0.700	0.000	0.412	0.926	0.371	0.874	3.905
T2EA	1.0	11.0	11.0	0.18	0.18	77.23	-0.23	3.28	3.28	1407.71	0.23	2725.69	534.69	24.40	-0.61	1.936	1.556	0.696	-0.565	0.410	0.925	0.389	0.878	4.282
	2.0	24.0	35.0	0.39	0.57	76.84	-0.74	7.11	10.39	1400.60	0.74	2718.58	527.58	24.08	-1.93	1.941	1.564	0.688	-1.788	0.407	0.924	0.426	0.885	5.159
10kPa	3.0	43.0	78.0	0.40	0.97	76.44	-1.25	7.29	17.68	1393.31	1.26	2711.29	520.29	23.75	-3.29	1.946	1.573	0.679	-3.043	0.404	0.924	0.465	0.893	6.142
	4.0	27.0	105.0	0.21	1.18	76.23	-1.52	3.83	21.51	1389.48	1.53	2707.46	516.46	23.57	-4.00	1.949	1.577	0.674	-3.702	0.403	0.923	0.486	0.897	6.693
	5.0	15.0	120.0	0.19	1.37	76.04	-1.77	3.46	24.97	1386.02	1.77	2704.00	513.00	23.41	-4.64	1.951	1.581	0.670	-4.298	0.401	0.923	0.504	0.901	7.211
						(h1)						2704.00	2191.00											
3	(static)					(h0)								(cmc)										
	0.0	0.0	0.0	0.00	0.00	78.88	0.00	0.00	0.00	1437.69	0.00	2828.23	564.23	24.92	0.00	1.967	1.575	0.676	0.000	0.404	0.973	0.476	0.895	8.317
T1EB	1.0	12.0	12.0	0.08	0.08	78.80	-0.10	1.46	1.46	1436.24	0.10	2826.77	562.77	24.86	-0.26	1.968	1.576	0.675	-0.251	0.403	0.973	0.483	0.897	8.582
	2.0	41.0	53.0	0.49	0.57	78.31	-0.72	8.93	10.39	1427.31	0.72	2817.84	553.84	24.46	-1.84	1.974	1.586	0.664	-1.791	0.399	0.972	0.529	0.906	10.297
20kPa	3.0	35.0	88.0	0.25	0.82	78.06	-1.04	4.56	14.95	1422.75	1.04	2813.28	549.28	24.26	-2.65	1.977	1.591	0.659	-2.576	0.397	0.972	0.553	0.911	11.232
	4.0	14.0	102.0	0.11	0.93	77.95	-1.18	2.01	16.95	1420.74	1.18	2811.28	547.28	24.17	-3.00	1.979	1.594	0.657	-2.922	0.396	0.972	0.563	0.913	11.656
	5.0	15.0	117.0	0.07	1.00	77.88	-1.27	1.28	18.23	1419.47	1.27	2810.00	546.00	24.12	-3.23	1.980	1.595	0.655	-3.142	0.396	0.972	0.570	0.914	11.930
						(h1)						2810.00	2264.00											
4	(static)					(h0)								(cmc)										
	0.0	0.0	0.0	0.00	0.00	74.25	0.00	0.00	0.00	1353.39	0.00	2690.76	530.76	24.57	0.00	1.988	1.596	0.654	0.000	0.395	0.992	0.575	0.915	24.905
T1EC	1.0	2.0	2.0	0.05	0.05	74.20	-0.07	0.91	0.91	1352.48	0.07	2689.85	529.85	24.53	-0.17	1.989	1.597	0.653	-0.170	0.395	0.992	0.580	0.916	25.334
	2.0	27.0	29.0	0.27	0.32	73.93	-0.43	4.92	5.83	1347.56	0.43	2684.93	524.93	24.30	-1.10	1.992	1.603	0.647	-1.090	0.393	0.992	0.606	0.921	27.715
50kPa	3.0	13.0	42.0	0.11	0.43	73.82	-0.58	2.01	7.84	1345.55	0.58	2682.93	522.93	24.21	-1.48	1.994	1.605	0.645	-1.464	0.392	0.992	0.617	0.923	28.715
	4.0	20.0	62.0	0.22	0.65	73.60	-0.88	4.01	11.85	1341.54	0.88	2678.92	518.92	24.02	-2.23	1.997	1.610	0.640	-2.214	0.390	0.992	0.639	0.928	30.770
	5.0	20.0	82.0	0.16	0.81	73.44	-1.09	2.92	14.76	1338.63	1.09	2676.00	516.00	23.89	-2.78	1.999	1.614	0.636	-2.759	0.389	0.991	0.654	0.931	32.308
						(h1)						2676.00	2160.00											
5	(static)					(h0)								(cmc)										
	0.0	0.0	0.0	0.00	0.00	77.56	0.00	0.00	0.00	1413.63	0.00	2755.14	562.14	25.63	0.00	1.949	1.551	0.702	0.000	0.412	0.964	0.364	0.873	11.368
T1ED	1.0	5.0	5.0	0.04	0.04	77.52	-0.05	0.73	0.73	1412.91	0.05	2754.41	561.41	25.60	-0.13	1.949	1.552	0.701	-0.125	0.412	0.964	0.368	0.874	11.612
	2.0	11.0	16.0	0.40	0.44	77.12	-0.57	7.29	8.02	1405.61	0.57	2747.12	554.12	25.27	-1.43	1.954	1.560	0.692	-1.376	0.409	0.964	0.407	0.881	14.194
100kPa	3.0	20.0	36.0	0.28	0.72	76.84	-0.93	5.10	13.12	1400.51	0.93	2742.02	549.02	25.03	-2.33	1.958	1.566	0.686	-2.251	0.407	0.963	0.434	0.887	16.156
	4.0	18.0	54.0	0.18	0.90	76.66	-1.16	3.28	16.40	1397.23	1.16	2738.73	545.73	24.89	-2.92	1.960	1.570	0.682	-2.814	0.405	0.963	0.451	0.890	17.484
	5.0	12.0	66.0	0.15	1.05	76.51	-1.35	2.73	19.14	1394.50	1.35	2736.00	543.00	24.76	-3.40	1.962	1.573	0.679	-3.283	0.404	0.963	0.466	0.893	18.631
						(h1)						2736.00	2193.00											
6	(static)					(h0)								(cmc)										
	0.0	0.0	0.0	0.00	0.00	57.94	0.00	0.00	0.00	1056.10	0.00	2067.87	395.87	23.68	0.00	1.958	1.583	0.668	0.000	0.400	0.936	0.515	0.903	7.534
T1EF	1.0	5.0	5.0	0.00	0.00	57.94	0.00	0.00	0.00	1056.10	0.00	2067.87	395.87	23.68	0.00	1.958	1.583	0.668	0.000	0.400	0.936	0.515	0.903	7.534
	2.0	21.0	26.0	0.43	0.43	57.51	-0.74	7.84	7.84	1048.26	0.74	2060.03	388.03	23.21	-1.98	1.965	1.595	0.655	-1.854	0.396	0.935	0.570	0.914	9.221
300kPa	3.0	31.0	57.0	0.37	0.80	57.14	-1.38	6.74	14.58	1041.52	1.38	2053.29	381.29	22.80	-3.68	1.971	1.605	0.645	-3.449	0.392	0.934	0.617	0.923	10.808
(10kPa)	4.0	25.0	82.0	0.15	0.95	56.99	-1.64	2.73	17.32	1038.79	1.64	2050.55	378.55	22.64	-4.37	1.974	1.610	0.640	-4.096	0.390	0.934	0.636	0.927	11.487
	5.0	25.0	107.0	0.14	1.09	56.85	-1.88	2.55	19.87	1036.23	1.88	2048.00	376.00	22.49	-5.02	1.976	1.614	0.636	-4.699	0.389	0.933	0.654	0.931	12.140
						(h1)						2048.00	1672.00											
6	(static)					(h0)								(cmc)										
	0.0	0.0	0.0	0.00	0.00	80.73	0.00	0.00	0.00	1471.42	0.00	3011.86	544.86	22.09	0.00	2.047	1.677	0.575	0.000	0.365	1.015	0.927	0.985	31.538
T1EH	1.0	20.0	20.0	0.11	0.11	80.62	-0.14	2.01	2.01	1469.41	0.14	3009.85	542.85	22.00	-0.37	2.048	1.679	0.572	-0.373	0.364	1.015	0.936	0.987	32.187
	2.0	20.0	40.0	0.32	0.43	80.30	-0.53	5.83	7.84	1463.58	0.53	3004.02	537.02	21.77	-1.44	2.053	1.686	0.566	-1.460	0.362	1.015	0.964	0.993	34.115
20kPa	3.0	20.0	60.0	0.20	0.63	80.10	-0.78	3.65	11.48	1459.93	0.78	3000.37	533.37	21.62	-2.11	2.055	1.690	0.562	-2.139	0.360	1.015	0.981	0.996	35.348
	4.0	15.0	75.0	0.10	0.73	80.00	-0.90	1.82	13.31	1458.11	0.91	2998.55	531.55	21.55	-2.44	2.056	1.692	0.560	-2.478	0.359	1.015	0.990	0.998	35.973
(RESAT)	5.0	20.0	95.0	0.14	0.87	79.86	-1.08	2.55	15.86	1455.56	1.08	2996.00	529.00	21.44	-2.91	2.058	1.695	0.558	-2.953	0.358	1.015	1.002	1.000	36.856
						(h1)						2996.00	2467.00											

Table A3.3.3. Data sheet: Garside medium sand, high acceleration, saturated, 25Hz. Includes resaturated and stress relief tests.

TEST	ACCEL (g)	TIME incr. (mins)	TIME cum. (mins)	SET inc. (mm)	SET cum. (mm)	HEIGHT (mm)	SET (%)	VOL inc. (ml)	VOL cum. (ml)	VOL (ml)	VOL (%)	WET MASS (g)	WATER MASS (g)	M (%)	M CHANGE (%)	BULK DENSE (Mg/m2)	DRY DENSE (Mg/m2)	VOID RATIO (e)	VOID CHANGE (%)	POROS (n)	SAT (Sr)	AIR CONT (A)	REL DENSE (Dr)	REL COMP (Cr)	PENE. RESIST (N)
1	(static)					(h0)								(cmc)											
	0.0	0.0	0.0	0.00	0.00	75.48	0.00	0.00	0.00	1375.72	0.00	2178.00	1.00	0.05	0.00	1.583	1.582	0.662	0.000	0.398	0.002	0.398	0.540	0.908	8.27
TIEG	1.0	10.0	10.0	0.05	0.05	75.43	-0.07	0.91	0.91	1374.81	0.07	2178.00	1.00	0.05	0.00	1.584	1.583	0.661	-0.166	0.398	0.002	0.397	0.545	0.909	8.42
	2.0	69.0	79.0	2.88	2.93	72.55	-3.88	52.50	53.41	1322.31	3.88	2178.00	1.00	0.05	0.00	1.647	1.646	0.597	-9.746	0.374	0.002	0.373	0.825	0.965	19.32
10	3.0	58.0	137.0	0.47	3.40	72.08	-4.50	8.57	61.97	1313.75	4.51	2178.00	1.00	0.05	0.00	1.658	1.657	0.587	-11.310	0.370	0.002	0.369	0.871	0.974	21.53
	4.0	27.0	164.0	0.25	3.65	71.83	-4.84	4.56	66.53	1309.19	4.84	2178.00	1.00	0.05	0.00	1.664	1.663	0.582	-12.141	0.368	0.002	0.367	0.896	0.979	22.75
	5.0	9.0	173.0	0.13	3.78	71.70	-5.01	2.37	68.90	1306.82	5.01	2178.00	1.00	0.05	0.00	1.667	1.666	0.579	-12.574	0.367	0.002	0.366	0.908	0.982	23.40
	6.0	0.0	173.0		3.78	71.70	-5.01	0.00	68.90	1306.82	5.01														
						(h1)						2178.00	2177.00												
2	(static)					(h0)								(cmc)											
	0.0	0.0	0.0	0.00	0.00	74.19	0.00	0.00	0.00	1352.30	0.00	2119.00	2.00	0.09	0.00	1.567	1.565	0.680	0.000	0.405	0.004	0.403	0.460	0.892	7.78
TIEH2	1.0	15.0	15.0	0.05	0.05	74.14	-0.07	0.91	0.91	1351.39	0.07	2119.00	2.00	0.09	0.00	1.568	1.567	0.679	-0.167	0.404	0.004	0.403	0.465	0.893	7.95
	2.0	85.0	100.0	3.05	3.10	71.09	-4.18	55.59	56.51	1295.79	4.18	2119.00	2.00	0.09	0.00	1.635	1.634	0.610	-10.323	0.379	0.004	0.377	0.771	0.954	21.83
20	3.0	65.0	165.0	0.62	3.72	70.47	-5.01	11.30	67.81	1284.49	5.02	2119.00	2.00	0.09	0.00	1.650	1.648	0.596	-12.388	0.373	0.004	0.372	0.833	0.967	25.49
	4.0	30.0	195.0	0.13	3.85	70.34	-5.19	2.37	70.18	1282.12	5.19	2119.00	2.00	0.09	0.00	1.653	1.651	0.593	-12.821	0.372	0.004	0.371	0.846	0.969	26.29
	5.0	10.0	205.0	0.05	3.90	70.29	-5.26	0.91	71.09	1281.21	5.26	2119.00	2.00	0.09	0.00	1.654	1.652	0.592	-12.987	0.372	0.004	0.370	0.851	0.970	26.60
	6.0	15.0	220.0	0.05	3.95	70.24	-5.32	0.91	72.00	1280.30	5.33	2119.00	2.00	0.09	0.00	1.655	1.654	0.591	-13.154	0.371	0.004	0.370	0.856	0.971	26.92
						(h1)						2119.00	2117.00												
3	(static)					(h0)								(cmc)											
	0.0	0.0	0.0	0.00	0.00	67.99	0.00	0.00	0.00	1239.29	0.00	2000.00	2.00	0.10	0.00	1.614	1.612		0.000	0.387	0.004	0.385	0.676	0.935	28.20
TIEI	1.0	15.0	15.0	0.01	0.01	67.98	-0.01	0.18	0.18	1239.11	0.01	2000.00	2.00	0.10	0.00	1.614	1.612	0.631	-0.038	0.387	0.004	0.385	0.677	0.935	28.29
	2.0	40.0	55.0	0.56	0.57	67.42	-0.84	10.21	10.39	1228.90	0.84	2000.00	2.00	0.10	0.00	1.627	1.626	0.618	-2.166	0.382	0.004	0.380	0.736	0.947	33.47
50	3.0	50.0	105.0	0.40	0.97	67.02	-1.43	7.29	17.68	1221.61	1.43	2000.00	2.00	0.10	0.00	1.637	1.636	0.608	-3.687	0.378	0.004	0.376	0.779	0.956	37.45
	4.0	45.0	150.0	0.34	1.31	66.68	-1.93	6.20	23.88	1215.41	1.93	2000.00	2.00	0.10	0.00	1.646	1.644	0.600	-4.979	0.375	0.004	0.373	0.815	0.963	41.00
	5.0	45.0	195.0	0.25	1.56	66.43	-2.29	4.56	28.43	1210.85	2.29	2000.00	2.00	0.10	0.00	1.652	1.650	0.594	-5.929	0.373	0.004	0.371	0.841	0.968	43.71
	6.0	0.0	195.0		1.56	66.43	-2.29	0.00	28.43	1210.85	2.29														
						(h1)						2000.00	1998.00												
4	(static)					(h0)								(cmc)											
	0.0	0.0	0.0	0.00	0.00	84.92	0.00	0.00	0.00	1547.88	0.00	2428.00	4.00	0.17	0.00	1.569	1.566	0.679	0.000	0.405	0.006	0.402	0.463	0.893	18.39
TIEJ	1.0	20.0	20.0	0.02	0.02	84.90	-0.02	0.36	0.36	1547.52	0.02	2428.00	4.00	0.17	0.00	1.569	1.566	0.679	-0.058	0.404	0.006	0.402	0.464	0.893	18.53
	2.0	55.0	75.0	1.16	1.18	83.74	-1.39	21.14	21.51	1526.37	1.39	2428.00	4.00	0.17	0.00	1.591	1.588	0.656	-3.435	0.396	0.007	0.394	0.566	0.913	27.51
100	3.0	35.0	110.0	0.24	1.42	83.50	-1.67	4.37	25.88	1522.00	1.67	2428.00	4.00	0.17	0.00	1.595	1.593	0.651	-4.133	0.394	0.007	0.392	0.587	0.917	29.59
	4.0	25.0	135.0	0.20	1.62	83.30	-1.91	3.65	29.53	1518.35	1.91	2428.00	4.00	0.17	0.00	1.599	1.596	0.647	-4.715	0.393	0.007	0.390	0.604	0.921	31.38
	5.0	35.0	170.0	0.21	1.83	83.09	-2.15	3.83	33.36	1514.52	2.16	2428.00	4.00	0.17	0.00	1.603	1.601	0.643	-5.327	0.391	0.007	0.389	0.623	0.925	33.32
	6.0	0.0	170.0		1.83	83.09	-2.15	0.00	33.36	1514.52	2.16														
						(h1)						2428.00	2424.00												

Table A3.3.4. Garside medium sand, high acceleration, dried, 25Hz.

TEST	ACCEL (g)	TIME incr. (mins)	TIME cum. (mins)	SET inc. (mm)	SET cum. (mm)	HEIGHT (mm)	SET (%)	VOL inc. (ml)	VOL cum. (ml)	VOL (ml)	VOL (%)	WET MASS (g)	WATER MASS (g)	M (%)	M CHANGE (%)	BULK DENSE (Mg/m2)	DRY DENSE (Mg/m2)	VOID RATIO (e)	VOID CHANGE (%)	POROS (n)	SAT (Sr)	REL DENSE (Dr)	REL COMP (Cr)	PENE. RESIST (N)
1	(static)					(h0)								(cmc)										
	0.0	0.0	0.0	0.000	0.0000	70.1135	0.000	0.00	0.00	1277.99	0.00	2527.51	526.51	26.31	0.00	1.978	1.566	0.692	0.000	0.409	1.007	0.444	0.889	5.59
TTIAA	0.1	0.0	0.0	0.000	0.0000	70.1135	0.000	0.00	0.00	1277.99	0.00	2527.51	526.51	26.31	0.00	1.978	1.566	0.692	0.000	0.409	1.007	0.444	0.889	5.59
	0.2	0.0	0.0	0.000	0.0000	70.1135	0.000	0.00	0.00	1277.99	0.00	2527.51	526.51	26.31	0.00	1.978	1.566	0.692	0.000	0.409	1.007	0.444	0.889	5.59
10 kPa	0.4	5.0	5.0	0.003	0.0030	70.1105	-0.004	0.05	0.05	1277.94	0.00	2527.45	526.45	26.31	-0.01	1.978	1.566	0.692	-0.010	0.409	1.007	0.445	0.889	5.61
	0.5	20.0	25.0	0.008	0.0110	70.1025	-0.016	0.15	0.20	1277.79	0.02	2527.31	526.31	26.30	-0.04	1.978	1.566	0.692	-0.038	0.409	1.007	0.446	0.889	5.65
	0.6	35.0	60.0	0.019	0.0295	70.0840	-0.042	0.34	0.54	1277.46	0.04	2526.97	525.97	26.29	-0.10	1.978	1.566	0.692	-0.103	0.409	1.007	0.450	0.890	5.74
	0.8	50.0	110.0	0.074	0.1035	70.0100	-0.148	1.35	1.89	1276.11	0.15	2525.62	524.62	26.22	-0.36	1.979	1.568	0.690	-0.361	0.408	1.007	0.464	0.893	6.11
	1.0	65.0	175.0	0.158	0.2615	69.8520	-0.373	2.88	4.77	1273.23	0.37	2522.74	521.74	26.07	-0.91	1.981	1.572	0.686	-0.912	0.407	1.007	0.495	0.899	6.94
	2.0	85.0	260.0	1.522	1.7835	68.3300	-2.544	27.74	32.51	1245.49	2.54	2495.00	494.00	24.69	-6.17	2.003	1.607	0.649	-6.217	0.394	1.007	0.788	0.958	17.64
						(h1)						2495.00	2001.00											
2	(static)					(h0)								(cmc)										
	0.0	0.0	0.0	0.000	0.000	77.223	0.000	0.00	0.00	1407.58	0.00	2751.57	564.57	25.81	0.00	1.955	1.554	0.706	0.000	0.414	0.970	0.339	0.868	4.23
TTIAB	0.1	5.0	5.0	0.000	0.000	77.223	0.000	0.00	0.00	1407.58	0.00	2751.57	564.57	25.81	0.00	1.955	1.554	0.706	0.000	0.414	0.970	0.339	0.868	4.23
	0.2	5.0	10.0	0.000	0.000	77.223	0.000	0.00	0.00	1407.58	0.00	2751.57	564.57	25.81	0.00	1.955	1.554	0.706	0.000	0.414	0.970	0.339	0.868	4.23
20 kPa	0.4	10.0	20.0	0.000	0.000	77.223	0.000	0.00	0.00	1407.58	0.00	2751.57	564.57	25.81	0.00	1.955	1.554	0.706	0.000	0.414	0.970	0.339	0.868	4.23
	0.5	25.0	45.0	0.004	0.004	77.220	-0.005	0.06	0.06	1407.52	0.00	2751.51	564.51	25.81	-0.01	1.955	1.554	0.705	-0.011	0.414	0.970	0.340	0.868	4.25
	0.6	60.0	105.0	0.020	0.023	77.200	-0.030	0.36	0.42	1407.16	0.03	2751.15	564.15	25.80	-0.07	1.955	1.554	0.705	-0.072	0.414	0.970	0.343	0.869	4.33
	0.8	80.0	185.0	0.092	0.115	77.108	-0.149	1.68	2.10	1405.49	0.15	2749.47	562.47	25.72	-0.37	1.956	1.556	0.703	-0.360	0.413	0.969	0.360	0.872	4.75
	1.0	80.0	265.0	0.145	0.260	76.963	-0.337	2.64	4.74	1402.84	0.34	2746.83	559.83	25.60	-0.84	1.958	1.559	0.700	-0.814	0.412	0.969	0.385	0.877	5.45
	2.0	75.0	340.0	1.088	1.348	75.875	-1.746	19.83	24.57	1383.01	1.75	2727.00	540.00	24.69	-4.35	1.972	1.581	0.676	-4.220	0.403	0.968	0.578	0.916	12.25
						(h1)						2727.00	2187.00											
3	(static)					(h0)								(cmc)										
	0.0	0.0	0.0	0.000	0.000	79.000	0.000	0.00	0.00	1439.97	0.00	2821.84	557.84	24.64	0.00	1.960	1.572	0.685	0.000	0.407	0.953	0.500	0.900	15.45
TTIAC	0.1	5.0	5.0	0.000	0.000	79.000	0.000	0.00	0.00	1439.97	0.00	2821.84	557.84	24.64	0.00	1.960	1.572	0.685	0.000	0.407	0.953	0.500	0.900	15.45
	0.2	5.0	10.0	0.000	0.000	79.000	0.000	0.00	0.00	1439.97	0.00	2821.84	557.84	24.64	0.00	1.960	1.572	0.685	0.000	0.407	0.953	0.500	0.900	15.45
50 kPa	0.4	5.0	15.0	0.000	0.000	79.000	0.000	0.00	0.00	1439.97	0.00	2821.84	557.84	24.64	0.00	1.960	1.572	0.685	0.000	0.407	0.953	0.500	0.900	15.45
	0.5	25.0	40.0	0.007	0.007	78.994	-0.008	0.12	0.12	1439.85	0.01	2821.72	557.72	24.63	-0.02	1.960	1.572	0.685	-0.020	0.407	0.953	0.501	0.900	15.52
	0.6	25.0	65.0	0.005	0.012	78.989	-0.015	0.09	0.21	1439.76	0.01	2821.63	557.63	24.63	-0.04	1.960	1.572	0.685	-0.036	0.407	0.953	0.502	0.900	15.57
	0.8	15.0	80.0	0.003	0.014	78.986	-0.018	0.05	0.26	1439.72	0.02	2821.59	557.59	24.63	-0.05	1.960	1.573	0.685	-0.044	0.407	0.953	0.503	0.901	15.60
	1.0	25.0	105.0	0.010	0.024	78.976	-0.030	0.18	0.44	1439.54	0.03	2821.40	557.40	24.62	-0.08	1.960	1.573	0.685	-0.075	0.407	0.953	0.504	0.901	15.70
	2.0	65.0	170.0	1.065	1.089	77.912	-1.378	19.40	19.84	1420.13	1.38	2802.00	538.00	23.76	-3.56	1.973	1.594	0.662	-3.388	0.398	0.951	0.686	0.937	29.06
						(h1)						2802.00	2264.00											
4	(static)					(h0)								(cmc)										
	0.0	5.0	0.0	0.000	0.000	74.267	0.000	0.00	0.00	1353.70	0.00	2673.13	518.13	24.04	0.00	1.975	1.592	0.665	0.000	0.399	0.959	0.667	0.933	38.19
TTIAD	0.1	5.0	5.0	0.000	0.000	74.267	0.000	0.00	0.00	1353.70	0.00	2673.13	518.13	24.04	0.00	1.975	1.592	0.665	0.000	0.399	0.959	0.667	0.933	38.19
	0.2	5.0	10.0	0.000	0.000	74.267	0.000	0.00	0.00	1353.70	0.00	2673.13	518.13	24.04	0.00	1.975	1.592	0.665	0.000	0.399	0.959	0.667	0.933	38.19
100 kPa	0.4	5.0	15.0	0.000	0.000	74.267	0.000	0.00	0.00	1353.70	0.00	2673.13	518.13	24.04	0.00	1.975	1.592	0.665	0.000	0.399	0.959	0.667	0.933	38.19
	0.5	5.0	20.0	0.000	0.000	74.267	0.000	0.00	0.00	1353.70	0.00	2673.13	518.13	24.04	0.00	1.975	1.592	0.665	0.000	0.399	0.959	0.667	0.933	38.19
	0.6	5.0	25.0	0.001	0.001	74.266	-0.001	0.02	0.02	1353.68	0.00	2673.11	518.11	24.04	0.00	1.975	1.592	0.665	-0.003	0.399	0.959	0.667	0.933	38.21
	0.8	5.0	30.0	0.002	0.003	74.265	-0.003	0.03	0.05	1353.66	0.00	2673.08	518.08	24.04	-0.01	1.975	1.592	0.665	-0.008	0.399	0.959	0.667	0.933	38.24
	1.0	5.0	35.0	0.001	0.004	74.264	-0.005	0.02	0.06	1353.64	0.00	2673.07	518.07	24.04	-0.01	1.975	1.592	0.665	-0.012	0.399	0.959	0.667	0.933	38.26
	2.0	45.0	80.0	0.059	0.062	74.205	-0.083	1.07	1.13	1352.57	0.08	2672.00	517.00	23.99	-0.22	1.975	1.593	0.663	-0.209	0.399	0.959	0.678	0.936	39.47
						(h1)						2672.00	2155.00											

Table A3.4.1. Data sheet: medium uniform sand, saturated, 25Hz.

TEST	ACCEL (g)	TIME incr. (mins)	TIME cum. (mins)	SET inc. (mm)	SET cum. (mm)	HEIGHT (mm)	SET (%)	VOL inc. (ml)	VOL cum. (ml)	VOL (ml)	VOL (%)	WET MASS (g)	WATER MASS (g)	M (%)	M CHANGE (%)	BULK DENSE (Mg/m2)	DRY DENSE (Mg/m2)	VOID RATIO (e)	VOID CHANGE (%)	POROS (n)	SAT (Sr)	REL DENSE (Dr)	REL COMP (Cr)	PENE. RESIST (N)
1	(static)					(h0)								(cmc)										
	0.0	0.0	0.0	0.000	0.0000	68.6940	0.000	0.00	0.00	1252.12	0.00	2466.22	496.22	25.19	0.00	1.970	1.573	0.684	0.000	0.406	0.975	0.509	0.902	7.36
TTIAE	0.1	5.0	5.0	0.000	0.0000	68.6940	0.000	0.00	0.00	1252.12	0.00	2466.22	496.22	25.19	0.00	1.970	1.573	0.684	0.000	0.406	0.975	0.509	0.902	7.36
	0.2	5.0	10.0	0.000	0.0000	68.6940	0.000	0.00	0.00	1252.12	0.00	2466.22	496.22	25.19	0.00	1.970	1.573	0.684	0.000	0.406	0.975	0.509	0.902	7.36
	0.3	10.0	20.0	0.000	0.0000	68.6940	0.000	0.00	0.00	1252.12	0.00	2466.22	496.22	25.19	0.00	1.970	1.573	0.684	0.000	0.406	0.975	0.509	0.902	7.36
10 kPa	0.4	10.0	20.0	0.000	0.0000	68.6940	0.000	0.00	0.00	1252.12	0.00	2466.22	496.22	25.19	0.00	1.970	1.573	0.684	0.000	0.406	0.975	0.509	0.902	7.36
	0.5	10.0	30.0	0.000	0.0000	68.6940	0.000	0.00	0.00	1252.12	0.00	2466.22	496.22	25.19	0.00	1.970	1.573	0.684	0.000	0.406	0.975	0.509	0.902	7.36
	0.6	20.0	50.0	0.000	0.0000	68.6940	0.000	0.00	0.00	1252.12	0.00	2466.22	496.22	25.19	0.00	1.970	1.573	0.684	0.000	0.406	0.975	0.509	0.902	7.36
	0.8	30.0	80.0	0.009	0.0091	68.6849	-0.013	0.17	0.17	1251.95	0.01	2466.06	496.06	25.18	-0.03	1.970	1.574	0.684	-0.033	0.406	0.975	0.511	0.902	7.41
	1.0	120.0	200.0	0.187	0.1957	68.4983	-0.285	3.40	3.57	1248.55	0.28	2462.66	492.66	25.01	-0.72	1.972	1.578	0.680	-0.701	0.405	0.975	0.548	0.910	8.51
	2.0	120.0	320.0	1.298	1.4935	67.2005	-2.174	23.66	27.22	1224.90	2.17	2439.00	469.00	23.81	-5.49	1.991	1.608	0.648	-5.351	0.393	0.974	0.802	0.960	18.26
						(h1)						2439.00	1970.00											
2	(static)					(h0)								(cmc)										
	0.0	0.0	0.0	0.000	0.000	70.480	0.000	0.00	0.00	1284.67	0.00	2509.02	511.02	25.58	0.00	1.953	1.555	0.704	0.000	0.413	0.963	0.353	0.871	4.57
TT1AF	0.1	5.0	5.0	0.000	0.000	70.480	0.000	0.00	0.00	1284.67	0.00	2509.02	511.02	25.58	0.00	1.953	1.555	0.704	0.000	0.413	0.963	0.353	0.871	4.57
	0.2	5.0	10.0	0.000	0.000	70.480	0.000	0.00	0.00	1284.67	0.00	2509.02	511.02	25.58	0.00	1.953	1.555	0.704	0.000	0.413	0.963	0.353	0.871	4.57
	0.3	5.0	15.0	0.000	0.000	70.480	0.000	0.00	0.00	1284.67	0.00	2509.02	511.02	25.58	0.00	1.953	1.555	0.704	0.000	0.413	0.963	0.353	0.871	4.57
20 kPa	0.4	5.0	15.0	0.000	0.000	70.480	0.000	0.00	0.00	1284.67	0.00	2509.02	511.02	25.58	0.00	1.953	1.555	0.704	0.000	0.413	0.963	0.353	0.871	4.57
	0.5	120.0	135.0	0.013	0.013	70.467	-0.018	0.24	0.24	1284.44	0.02	2508.79	510.79	25.57	-0.05	1.953	1.556	0.704	-0.044	0.413	0.963	0.355	0.871	4.64
	0.6	120.0	255.0	0.027	0.040	70.440	-0.057	0.49	0.73	1283.95	0.06	2508.30	510.30	25.54	-0.14	1.954	1.556	0.703	-0.137	0.413	0.963	0.361	0.872	4.78
	0.8	120.0	375.0	0.081	0.121	70.360	-0.171	1.47	2.20	1282.48	0.17	2506.83	508.83	25.47	-0.43	1.955	1.558	0.701	-0.414	0.412	0.963	0.376	0.875	5.20
	1.0	120.0	495.0	0.209	0.330	70.150	-0.468	3.81	6.01	1278.67	0.47	2503.02	505.02	25.28	-1.18	1.958	1.563	0.696	-1.132	0.410	0.962	0.417	0.883	6.38
	2.0	120.0	615.0	1.208	1.538	68.943	-2.181	22.02	28.02	1256.65	2.18	2481.00	483.00	24.17	-5.48	1.974	1.590	0.667	-5.281	0.400	0.961	0.650	0.930	15.53
						(h1)						2481.00	1998.00											
3	(static)					(h0)								(cmc)										
	0.0	0.0	0.0	0.000	0.000	68.088	0.000	0.00	0.00	1241.07	0.00	2445.29	485.29	24.76	0.00	1.970	1.579	0.678	0.000	0.404	0.968	0.560	0.912	19.38
TT1AG	0.1	5.0	5.0	0.000	0.000	68.088	0.000	0.00	0.00	1241.07	0.00	2445.29	485.29	24.76	0.00	1.970	1.579	0.678	0.000	0.404	0.968	0.560	0.912	19.38
	0.2	5.0	10.0	0.000	0.000	68.088	0.000	0.00	0.00	1241.07	0.00	2445.29	485.29	24.76	0.00	1.970	1.579	0.678	0.000	0.404	0.968	0.560	0.912	19.38
	0.3	5.0	15.0	0.000	0.000	68.088	0.000	0.00	0.00	1241.07	0.00	2445.29	485.29	24.76	0.00	1.970	1.579	0.678	0.000	0.404	0.968	0.560	0.912	19.38
50 kPa	0.4	5.0	15.0	0.000	0.000	68.088	0.000	0.00	0.00	1241.07	0.00	2445.29	485.29	24.76	0.00	1.970	1.579	0.678	0.000	0.404	0.968	0.560	0.912	19.38
	0.5	10.0	25.0	0.005	0.005	68.083	-0.007	0.09	0.09	1240.98	0.01	2445.20	485.20	24.76	-0.02	1.970	1.579	0.678	-0.018	0.404	0.968	0.561	0.912	19.45
	0.6	10.0	35.0	0.004	0.009	68.079	-0.014	0.08	0.17	1240.91	0.01	2445.12	485.12	24.75	-0.03	1.970	1.579	0.678	-0.034	0.404	0.968	0.562	0.912	19.50
	0.8	120.0	155.0	0.013	0.022	68.066	-0.033	0.24	0.40	1240.67	0.03	2444.89	484.89	24.74	-0.08	1.971	1.580	0.677	-0.081	0.404	0.968	0.565	0.913	19.68
	1.0	120.0	275.0	0.043	0.065	68.023	-0.095	0.77	1.18	1239.90	0.10	2444.11	484.11	24.70	-0.24	1.971	1.581	0.676	-0.235	0.403	0.968	0.573	0.915	20.27
	2.0	120.0	395.0	0.884	0.949	67.139	-1.393	16.11	17.29	1223.78	1.39	2428.00	468.00	23.88	-3.56	1.984	1.602	0.655	-3.448	0.396	0.967	0.747	0.949	34.48
						(h1)						2428.00	1960.00											
4	(static)					(h0)								(cmc)										
	0.0	5.0	0.0	0.000	0.000	74.460	0.000	0.00	0.00	1357.22	0.00	2679.62	524.62	24.34	0.00	1.974	1.588	0.669	0.000	0.401	0.964	0.632	0.926	34.33
TT1AH	0.1	5.0	5.0	0.000	0.000	74.460	0.000	0.00	0.00	1357.22	0.00	2679.62	524.62	24.34	0.00	1.974	1.588	0.669	0.000	0.401	0.964	0.632	0.926	34.33
	0.2	5.0	10.0	0.000	0.000	74.460	0.000	0.00	0.00	1357.22	0.00	2679.62	524.62	24.34	0.00	1.974	1.588	0.669	0.000	0.401	0.964	0.632	0.926	34.33
	0.3	5.0	15.0	0.000	0.000	74.460	0.000	0.00	0.00	1357.22	0.00	2679.62	524.62	24.34	0.00	1.974	1.588	0.669	0.000	0.401	0.964	0.632	0.926	34.33
100 kPa	0.4	5.0	15.0	0.000	0.000	74.460	0.000	0.00	0.00	1357.22	0.00	2679.62	524.62	24.34	0.00	1.974	1.588	0.669	0.000	0.401	0.964	0.632	0.926	34.33
	0.5	5.0	20.0	0.000	0.000	74.460	0.000	0.00	0.00	1357.22	0.00	2679.62	524.62	24.34	0.00	1.974	1.588	0.669	0.000	0.401	0.964	0.632	0.926	34.33
	0.6	10.0	30.0	0.002	0.002	74.458	-0.003	0.04	0.04	1357.18	0.00	2679.58	524.58	24.34	-0.01	1.974	1.588	0.669	-0.007	0.401	0.964	0.633	0.927	34.37
	0.8	120.0	150.0	0.009	0.011	74.449	-0.015	0.17	0.20	1357.02	0.01	2679.42	524.42	24.33	-0.04	1.974	1.588	0.669	-0.037	0.401	0.964	0.634	0.927	34.54
	1.0	120.0	270.0	0.006	0.017	74.443	-0.023	0.11	0.32	1356.91	0.02	2679.31	524.31	24.33	-0.06	1.975	1.588	0.669	-0.058	0.401	0.964	0.635	0.927	34.66
	2.0	120.0	390.0	0.401	0.418	74.042	-0.562	7.31	7.62	1349.60	0.56	2672.00	517.00	23.99	-1.45	1.980	1.597	0.660	-1.401	0.397	0.964	0.707	0.941	42.95
						(h1)						2672.00	2155.00											

Table A3.4.2. Data sheet: medium uniform sand, saturated, 40Hz.

TEST	ACCEL (g)	TIME incr. (mins)	TIME cum. (mins)	SET inc. (mm)	SET cum. (mm)	HEIGHT (mm)	SET (%)	VOL inc. (ml)	VOL cum. (ml)	VOL (ml)	VOL (%)	WET MASS (g)	WATER MASS (g)	M (%)	M CHANGE (%)	BULK DENSE (Mg/m2)	DRY DENSE (Mg/m2)	VOID RATIO (e)	VOID CHANGE (%)	POROS (n)	SAT (Sr)	REL DENSE (Dr)	REL COMP (Cr)	PENE. RESIST (N)
1	(static)					(h0)								(cmc)										
	0.0	0.0	0.0	0.000	0.000	64.200	0.000	0.00	0.00	1170.21	0.00	2069.00	271.00	15.07	0.00	1.768	1.536	0.699	0.000	0.411	0.563	0.395	0.879	4.42
TT1AJ	0.1	0.0	0.0	0.000	0.000	64.200	0.000	0.00	0.00	1170.21	0.00	2069.00	271.00	15.07	0.00	1.768	1.536	0.699	0.000	0.411	0.563	0.395	0.879	4.42
	0.2	5.0	5.0	0.000	0.000	64.200	0.000	0.00	0.00	1170.21	0.00	2069.00	271.00	15.07	0.00	1.768	1.536	0.699	0.000	0.411	0.563	0.395	0.879	4.42
10 kPa	0.4	5.0	5.0	0.000	0.000	64.200	0.000	0.00	0.00	1170.21	0.00	2069.00	271.00	15.07	0.00	1.768	1.536	0.699	0.000	0.411	0.563	0.395	0.879	4.42
	0.5	5.0	5.0	0.000	0.000	64.200	0.000	0.00	0.00	1170.21	0.00	2069.00	271.00	15.07	0.00	1.768	1.536	0.699	0.000	0.411	0.563	0.395	0.879	4.42
	0.6	5.0	5.0	0.000	0.000	64.200	0.000	0.00	0.00	1170.21	0.00	2069.00	271.00	15.07	0.00	1.768	1.536	0.699	0.000	0.411	0.563	0.395	0.879	4.42
	0.8	5.0	5.0	0.010	0.010	64.190	-0.016	0.18	0.18	1170.02	0.02	2069.00	271.00	15.07	0.00	1.768	1.537	0.698	-0.038	0.411	0.563	0.397	0.879	4.46
	1.0	5.0	5.0	0.004	0.014	64.186	-0.022	0.07	0.26	1169.95	0.02	2069.00	271.00	15.07	0.00	1.768	1.537	0.698	-0.053	0.411	0.563	0.397	0.879	4.48
	2.0	10.0	10.0	0.018	0.032	64.168	-0.050	0.33	0.58	1169.62	0.05	2069.00	271.00	15.07	0.00	1.769	1.537	0.698	-0.121	0.411	0.564	0.401	0.880	4.57
						(h1)						2069.00	1798.00											
2	(static)					(h0)								(cmc)										
	0.0	0.0	0.0	0.000	0.000	68.880	0.000	0.00	0.00	1255.51	0.00	2001.00	75.00	3.89	0.00	1.594	1.534	0.701	0.000	0.412	0.145	0.373	0.875	3.94
TT1Ak	0.1	0.0	0.0	0.000	0.000	68.880	0.000	0.00	0.00	1255.51	0.00	2001.00	75.00	3.89	0.00	1.594	1.534	0.701	0.000	0.412	0.145	0.373	0.875	3.94
	0.2	0.0	0.0	0.000	0.000	68.880	0.000	0.00	0.00	1255.51	0.00	2001.00	75.00	3.89	0.00	1.594	1.534	0.701	0.000	0.412	0.145	0.373	0.875	3.94
10 kPa	0.4	0.0	0.0	0.000	0.000	68.880	0.000	0.00	0.00	1255.51	0.00	2001.00	75.00	3.89	0.00	1.594	1.534	0.701	0.000	0.412	0.145	0.373	0.875	3.94
	0.5	0.0	0.0	0.000	0.000	68.880	0.000	0.00	0.00	1255.51	0.00	2001.00	75.00	3.89	0.00	1.594	1.534	0.701	0.000	0.412	0.145	0.373	0.875	3.94
	0.6	5.0	5.0	0.000	0.000	68.880	0.000	0.00	0.00	1255.51	0.00	2001.00	75.00	3.89	0.00	1.594	1.534	0.701	0.000	0.412	0.145	0.373	0.875	3.94
	0.8	5.0	10.0	0.000	0.000	68.880	0.000	0.00	0.00	1255.51	0.00	2001.00	75.00	3.89	0.00	1.594	1.534	0.701	0.000	0.412	0.145	0.373	0.875	3.94
	1.0	5.0	15.0	0.001	0.001	68.880	-0.001	0.01	0.01	1255.50	0.00	2001.00	75.00	3.89	0.00	1.594	1.534	0.701	-0.002	0.412	0.145	0.373	0.875	3.95
	2.0	20.0	35.0	0.012	0.012	68.868	-0.017	0.21	0.22	1255.29	0.02	2001.00	75.00	3.89	0.00	1.594	1.534	0.701	-0.042	0.412	0.145	0.375	0.875	3.99
						(h1)						2001.00	1926.00											
3	(static)					(h0)								(cmc)										
	0.0	0.0	0.0	0.000	0.000	66.850	0.000	0.00	0.00	1218.51	0.00	2246.20	325.00	16.92	0.00	1.843	1.577	0.655	0.000	0.396	0.674	0.741	0.948	15.58
TT1AL	0.1	0.0	0.0	0.000	0.000	66.850	0.000	0.00	0.00	1218.51	0.00	2246.20	325.00	16.92	0.00	1.843	1.577	0.655	0.000	0.396	0.674	0.741	0.948	15.58
	0.2	0.0	0.0	0.000	0.000	66.850	0.000	0.00	0.00	1218.51	0.00	2246.20	325.00	16.92	0.00	1.843	1.577	0.655	0.000	0.396	0.674	0.741	0.948	15.58
10 kPa	0.4	5.0	5.0	0.000	0.000	66.850	0.000	0.00	0.00	1218.51	0.00	2246.20	325.00	16.92	0.00	1.843	1.577	0.655	0.000	0.396	0.674	0.741	0.948	15.58
	0.5	0.0	5.0	0.000	0.000	66.850	0.000	0.00	0.00	1218.51	0.00	2246.20	325.00	16.92	0.00	1.843	1.577	0.655	0.000	0.396	0.674	0.741	0.948	15.58
	0.6	5.0	10.0	0.000	0.000	66.850	0.000	0.00	0.00	1218.51	0.00	2246.20	325.00	16.92	0.00	1.843	1.577	0.655	0.000	0.396	0.674	0.741	0.948	15.58
	0.8	5.0	15.0	0.000	0.000	66.850	0.000	0.00	0.00	1218.51	0.00	2246.20	325.00	16.92	0.00	1.843	1.577	0.655	0.000	0.396	0.674	0.741	0.948	15.58
	1.0	5.0	20.0	0.000	0.000	66.850	0.000	0.00	0.00	1218.51	0.00	2246.20	325.00	16.92	0.00	1.843	1.577	0.655	0.000	0.396	0.674	0.741	0.948	15.58
	2.0	60.0	80.0	0.178	0.178	66.673	-0.266	3.24	3.24	1215.27	0.27	2246.20	325.00	16.92	0.00	1.848	1.581	0.651	-0.671	0.394	0.678	0.776	0.955	17.09
						(h1)						2246.20	1921.20											
4	(static)					(h0)								(cmc)										
	0.0	5.0	0.0	0.000	0.000	65.705	0.000	0.00	0.00	1197.64	0.00	2313.00	446.00	23.89	0.00	1.931	1.559	0.674	0.000	0.403	0.925	0.590	0.918	9.87
TT1AM	0.1	0.0	0.0	0.000	0.000	65.705	0.000	0.00	0.00	1197.64	0.00	2313.00	446.00	23.89	0.00	1.931	1.559	0.674	0.000	0.403	0.925	0.590	0.918	9.87
	0.2	5.0	5.0	0.000	0.000	65.705	0.000	0.00	0.00	1197.64	0.00	2313.00	446.00	23.89	0.00	1.931	1.559	0.674	0.000	0.403	0.925	0.590	0.918	9.87
10 kPa	0.4	5.0	10.0	0.000	0.000	65.705	0.000	0.00	0.00	1197.64	0.00	2313.00	446.00	23.89	0.00	1.931	1.559	0.674	0.000	0.403	0.925	0.590	0.918	9.87
	0.5	0.0	10.0	0.000	0.000	65.705	0.000	0.00	0.00	1197.64	0.00	2313.00	446.00	23.89	0.00	1.931	1.559	0.674	0.000	0.403	0.925	0.590	0.918	9.87
	0.6	5.0	15.0	0.001	0.001	65.704	-0.002	0.02	0.02	1197.62	0.00	2313.00	446.00	23.89	0.00	1.931	1.559	0.674	-0.004	0.403	0.925	0.590	0.918	9.88
	0.8	5.0	20.0	0.000	0.001	65.704	-0.002	0.00	0.02	1197.62	0.00	2313.00	446.00	23.89	0.00	1.931	1.559	0.674	-0.004	0.403	0.925	0.590	0.918	9.88
	1.0	5.0	25.0	0.016	0.017	65.688	-0.026	0.29	0.31	1197.33	0.03	2313.00	446.00	23.89	0.00	1.932	1.559	0.674	-0.064	0.403	0.925	0.593	0.919	9.99
	2.0	5.0	30.0	0.124	0.141	65.565	-0.214	2.25	2.56	1195.08	0.21	2313.00	446.00	23.89	0.00	1.935	1.562	0.671	-0.531	0.401	0.930	0.619	0.924	10.86
						(h1)						2313.00	1867.00											

Table A3.4.3. Data table: medium uniform sand, partially saturated, 25Hz.

TEST	ACCEL (g)	TIME incr. (mins)	TIME cum. (mins)	SET inc. (mm)	SET cum. (mm)	HEIGHT (mm)	SET (%)	VOL (ml)	VOL cum. (ml)	VOL (ml)	VOL (%)	WET MASS (g)	WATER MASS (g)	M (%)	M CHANGE (%)	BULK DENSE (Mg/m2)	DRY DENSE (Mg/m2)	VOID RATIO (e)	VOID CHANGE (%)	POROS (n)	SAT (Sr)	REL DENSE (Dr)	REL COMP (Cr)	PENE. RESIST (N)
1	(static)					(h0)								(cmc)										
	0.0	0.0	0.0	0.000	0.0000	62.3500	0.000	0.00	0.00	1136.49	0.00	1761.00	0.00	0.00	0.00	1.550	1.550	0.684	0.000	0.406	0.000	0.509	0.902	7.34
TT1AI	0.1	0.0	0.0	0.000	0.0000	62.3500	0.000	0.00	0.00	1136.49	0.00	1761.00	0.00	0.00	0.00	1.550	1.550	0.684	0.000	0.406	0.000	0.509	0.902	7.34
	0.2	5.0	5.0	0.000	0.0000	62.3500	0.000	0.00	0.00	1136.49	0.00	1761.00	0.00	0.00	0.00	1.550	1.550	0.684	0.000	0.406	0.000	0.509	0.902	7.34
10 kPa	0.4	5.0	5.0	0.003	0.0030	62.3470	-0.005	0.05	0.05	1136.43	0.00	1761.00	0.00	0.00	0.00	1.550	1.550	0.684	-0.012	0.406	0.000	0.509	0.902	7.36
	0.5	5.0	5.0	0.006	0.0085	62.3415	-0.014	0.10	0.15	1136.33	0.01	1761.00	0.00	0.00	0.00	1.550	1.550	0.684	-0.034	0.406	0.000	0.511	0.902	7.40
	0.6	10.0	10.0	0.006	0.0140	62.3360	-0.022	0.10	0.26	1136.23	0.02	1761.00	0.00	0.00	0.00	1.550	1.550	0.684	-0.055	0.406	0.000	0.512	0.902	7.43
	0.8	5.0	5.0	0.017	0.0305	62.3195	-0.049	0.30	0.56	1135.93	0.05	1761.00	0.00	0.00	0.00	1.550	1.550	0.684	-0.120	0.406	0.000	0.515	0.903	7.54
	1.0	10.0	10.0	0.001	0.0310	62.3190	-0.050	0.01	0.57	1135.92	0.05	1761.00	0.00	0.00	0.00	1.550	1.550	0.684	-0.122	0.406	0.000	0.516	0.903	7.54
	2.0	60.0	60.0	1.750	1.7810	60.5690	-2.856	31.90	32.46	1104.02	2.86	1761.00	0.00	0.00	0.00	1.595	1.595	0.636	-7.030	0.389	0.000	0.894	0.979	22.66
						(h1)						1761.00	1761.00											

Table A3.4.4. Data sheet: medium uniform sand, dried, 25Hz.

TEST	ACCEL (g)	TIME incr. (mins)	TIME cum. (mins)	SET inc. (mm)	SET cum. (mm)	HEIGHT (mm)	SET (%)	VOL inc. (ml)	VOL cum. (ml)	VOL (ml)	VOL (%)	WET MASS (g)	WATER MASS (g)	M (%)	M CHANGE (%)	BULK DENSE (Mg/m2)	DRY DENSE (Mg/m2)	VOID RATIO (e)	VOID CHANGE (%)	POROS (n)	SAT (Sr)	REL DENSE (Dr)	REL COMP (Cr)	PENE RESIST (N)
1	(static)					(h0)								(cmc)										
	0.0	0.0	0.0	0.000	0.000	37.137	0.000	0.00	0.00	676.92	0.00	883.38	218.38	32.84	0.00	1.305	0.982	1.657	0.000	N/A	N/A	N/A	N/A	N/A
T1AD	1.0	15.0	15.0	0.000	0.000	37.137	0.000	0.00	0.00	676.92	0.00	883.38	218.38	32.84	0.00	1.305	0.982	1.657	0.000	N/A	N/A	N/A	N/A	N/A
	2.0	70.0	85.0	0.760	0.760	36.377	-2.046	13.85	13.85	663.06	2.05	869.53	204.53	30.76	-6.34	1.311	1.003	1.602	-3.282	N/A	N/A	N/A	N/A	N/A
5kPa	3.0	90.0	175.0	0.920	1.680	35.457	-4.524	16.77	30.62	646.29	4.52	852.76	187.76	28.23	-14.02	1.319	1.029	1.537	-7.254	N/A	N/A	N/A	N/A	N/A
	4.0	105.0	280.0	0.630	2.310	34.827	-6.220	11.48	42.11	634.81	6.22	841.28	176.28	26.51	-19.28	1.325	1.048	1.492	-9.975	N/A	N/A	N/A	N/A	N/A
	5.0	57.0	337.0	0.070	2.380	34.757	-6.409	1.28	43.38	633.53	6.41	840.00	175.00	26.32	-19.86	1.326	1.050	1.487	-10.277	N/A	N/A	N/A	N/A	N/A
	6.0	0.0	337.0	0.000	2.380	34.757	-6.409	0.00	43.38	633.53	6.41	840.00	175.00	26.32	-19.86	1.326	1.050	1.487	-10.277	N/A	N/A	N/A	N/A	N/A
						(h1)						840.00	665.00											
2	(static)					(h0)								(cmc)										
	0.0	0.0	0.0	0.000	0.000	126.955	0.000	0.00	0.00	2314.07	0.00	959.24	246.74	34.63	0.00	0.415	0.308	7.477	0.000	N/A	N/A	N/A	N/A	N/A
T1AI	1.0	10.0	10.0	0.080	0.080	126.875	-0.063	1.46	1.46	2312.62	0.06	957.78	245.28	34.43	-0.59	0.414	0.308	7.471	-0.071	N/A	N/A	N/A	N/A	N/A
	2.0	158.0	168.0	2.470	2.550	124.405	-2.009	45.02	46.48	2267.59	2.01	912.76	200.26	28.11	-18.84	0.403	0.314	7.307	-2.277	N/A	N/A	N/A	N/A	N/A
20kPa	3.0	102.0	270.0	0.280	2.830	124.125	-2.229	5.10	51.58	2262.49	2.23	907.66	195.16	27.39	-20.91	0.401	0.315	7.288	-2.527	N/A	N/A	N/A	N/A	N/A
	4.0	118.0	388.0	0.420	3.250	123.705	-2.560	7.66	59.24	2254.83	2.56	900.00	187.50	26.32	-24.01	0.399	0.316	7.260	-2.902	N/A	N/A	N/A	N/A	N/A
	5.0	0.0	388.0	0.000	3.250	123.705	-2.560	0.00	59.24	2254.83	2.56	900.00	187.50	26.32	-24.01	0.399	0.316	7.260	-2.902	N/A	N/A	N/A	N/A	N/A
	6.0	0.0	388.0	0.000	3.250	123.705	-2.560	0.00	59.24	2254.83	2.56	900.00	187.50	26.32	-24.01	0.399	0.316	7.260	-2.902	N/A	N/A	N/A	N/A	N/A
						(h1)						900.00	712.50											
3	(static)					(h0)								(cmc)										
	0.0	0.0	0.0	0.000	0.000	111.736	0.000	0.00	0.00	2036.67	0.00	3855.94	811.14	26.64	0.00	1.893	1.495	0.746	0.000	0.427	0.932	0.017	0.803	0.019
T1AH	1.0	15.0	15.0	0.000	0.000	111.736	0.000	0.00	0.00	2036.67	0.00	3855.94	811.14	26.64	0.00	1.893	1.495	0.746	0.000	0.427	0.932	0.017	0.803	0.019
	2.0	215.0	230.0	1.440	1.440	110.296	-1.289	26.25	26.25	2010.42	1.29	3829.70	784.90	25.78	-3.24	1.905	1.515	0.723	-3.017	0.420	0.930	0.197	0.839	2.405
50kPa	3.0	365.0	595.0	0.910	2.350	109.386	-2.103	16.59	42.83	1993.83	2.10	3813.11	768.31	25.23	-5.28	1.912	1.527	0.709	-4.923	0.415	0.929	0.311	0.862	5.977
	4.0	164.0	759.0	0.390	2.740	108.996	-2.452	7.11	49.94	1986.73	2.45	3806.00	761.20	25.00	-6.16	1.916	1.533	0.703	-5.740	0.413	0.928	0.360	0.872	7.997
	5.0	0.0	759.0	0.000	2.740	108.996	-2.452	0.00	49.94	1986.73	2.45	3806.00	761.20	25.00	-6.16	1.916	1.533	0.703	-5.740	0.413	0.928	0.360	0.872	7.997
	6.0	0.0	759.0	0.000	2.740	108.996	-2.452	0.00	49.94	1986.73	2.45	3806.00	761.20	25.00	-6.16	1.916	1.533	0.703	-5.740	0.413	0.928	0.360	0.872	7.997
						(h1)						3806.00	3044.80											

Table A3.4.5. Data sheet: medium uniform sand, high acceleration, saturated, 25Hz.

TEST	ACCEL (g)	TIME incr.	TIME cum.	SET inc. (mm)	SET cum. (mm)	HEIGHT (mm)	SET (%)	VOL inc. (ml)	VOL cum. (ml)	VOL (ml)	VOL (%)	WET MASS (g)	WATER MASS (g)	M (%)	M CHANGE (%)	BULK DENSE (Mg/m2)	DRY DENSE (Mg/m2)	VOID RATIO (e)	VOID CHANGE (%)	POROS (n)	SAT (Sr)	AIR CONT (A)	REL DENSE (Dr)	REL COMP (Cr)	PENE. RESIST (N)
1	(static)					(h0)								(cmc)											
	0.0	0.0	0.0	0.00	0.00	114.33	0.00	0.00	0.00	2083.95	0.00	3623.00	106.00	3.01	0.00	1.739	1.688	0.570	0.000	0.363	0.140	0.312	0.977	0.995	27.07
T1AJ	1.0	10.0	10.0	0.03	0.03	114.30	-0.03	0.55	0.55	2083.40	0.03	3623.00	106.00	3.01	0.00	1.739	1.688	0.570	-0.072	0.363	0.140	0.312	0.979	0.996	27.19
	2.0	5.0	15.0	0.02	0.05	114.28	-0.04	0.36	0.91	2083.04	0.04	3623.00	106.00	3.01	0.00	1.739	1.688	0.570	-0.120	0.363	0.140	0.312	0.981	0.996	27.28
10	3.0	11.0	26.0	0.02	0.07	114.26	-0.06	0.36	1.28	2082.68	0.06	3623.00	106.00	3.01	0.00	1.740	1.689	0.569	-0.169	0.363	0.140	0.312	0.982	0.996	27.36
	4.0	49.0	75.0	0.25	0.32	114.01	-0.28	4.56	5.83	2078.12	0.28	3623.00	106.00	3.01	0.00	1.743	1.692	0.566	-0.771	0.361	0.141	0.310	1.001	1.000	28.42
	5.0	0.0	75.0	0.00	0.32	114.01	-0.28	0.00	5.83	2078.12	0.28	3623.00	106.00	3.01	0.00	1.743	1.692	0.566	-0.771	0.361	0.141	0.310	1.001	1.000	28.42
	6.0	0.0	75.0	0.00	0.32	114.01	-0.28	0.00	5.83	2078.12	0.28	3623.00	106.00	3.01	0.00	1.743	1.692	0.566	-0.771	0.361	0.141	0.310	1.001	1.000	28.42
						(h1)						3623.00	3517.00												
2	(static)					(h0)								(cmc)											
	0.0	0.0	0.0	0.00	0.00	120.65	0.00	0.00	0.00	2199.15	0.00	3792.00	109.00	2.96	0.00	1.724	1.675	0.582	0.000	0.368	0.135	0.318	0.910	0.982	30.44
T1AN	1.0	15.0	15.0	0.01	0.01	120.64	-0.01	0.18	0.18	2198.97	0.01	3792.00	109.00	2.96	0.00	1.724	1.675	0.582	-0.023	0.368	0.135	0.318	0.911	0.982	30.49
	2.0	13.0	28.0	0.03	0.04	120.61	-0.03	0.55	0.73	2198.42	0.03	3792.00	109.00	2.96	0.00	1.725	1.675	0.582	-0.090	0.368	0.135	0.318	0.913	0.983	30.63
20	3.0	25.0	53.0	0.01	0.05	120.60	-0.04	0.18	0.91	2198.24	0.04	3792.00	109.00	2.96	0.00	1.725	1.675	0.582	-0.113	0.368	0.135	0.318	0.914	0.983	30.68
	4.0	42.0	95.0	0.74	0.79	119.86	-0.65	13.49	14.40	2184.75	0.65	3792.00	109.00	2.96	0.00	1.736	1.686	0.572	-1.779	0.364	0.137	0.314	0.967	0.993	34.36
	5.0	0.0	95.0	0.00	0.79	119.86	-0.65	0.00	14.40	2184.75	0.65	3792.00	109.00	2.96	0.00	1.736	1.686	0.572	-1.779	0.364	0.137	0.314	0.967	0.993	34.36
	6.0	0.0	95.0	0.00	0.79	119.86	-0.65	0.00	14.40	2184.75	0.65	3792.00	109.00	2.96	0.00	1.736	1.686	0.572	-1.779	0.364	0.137	0.314	0.967	0.993	34.36
						(h1)						3792.60	3683.00												
3	(static)					(h0)								(cmc)											
	0.0	0.0	0.0	0.00	0.00	120.65	0.00	0.00	0.00	2199.09	0.00	n/a	n/a	n/a	n/a	n/a	n/a		n/a	n/a	n/a	n/a	n/a	n/a	n/a
T1AO	1.0	13.0	13.0	0.00	0.00	120.65	0.00	0.00	0.00	2199.09	0.00	n/a	n/a	n/a	n/a	n/a	n/a	n/a	n/a	n/a	n/a	n/a	n/a	n/a	n/a
	2.0	59.0	72.0	0.01	0.01	120.64	-0.01	0.18	0.18	2198.91	0.01	n/a	n/a	n/a	n/a	n/a	n/a	n/a	n/a	n/a	n/a	n/a	n/a	n/a	n/a
50	3.0	73.0	145.0	0.04	0.05	120.60	-0.04	0.73	0.91	2198.18	0.04	n/a	n/a	n/a	n/a	n/a	n/a	n/a	n/a	n/a	n/a	n/a	n/a	n/a	n/a
	4.0	28.0	173.0	0.02	0.07	120.58	-0.06	0.36	1.28	2197.82	0.06	n/a	n/a	n/a	n/a	n/a	n/a	n/a	n/a	n/a	n/a	n/a	n/a	n/a	n/a
	5.0	0.0	173.0	0.00	0.07	120.58	-0.06	0.00	1.28	2197.82	0.06	n/a	n/a	n/a	n/a	n/a	n/a	n/a	n/a	n/a	n/a	n/a	n/a	n/a	n/a
	6.0	0.0	173.0	0.00	0.07	120.58	-0.06	0.00	1.28	2197.82	0.06	n/a	n/a	n/a	n/a	n/a	n/a	n/a	n/a	n/a	n/a	n/a	n/a	n/a	n/a
						(h1)						4333.20	4207.10												

Table A3.4.6. Data sheet: medium uniform sand, high acceleration, partially saturated, 25Hz.

TEST	ACCEL (g)	TIME incr. (mins.)	TIME cum. (mins)	SET inc. (mm)	SET cum. (mm)	HEIGHT (mm)	SET (%)	VOL inc. (ml)	VOL cum. (ml)	VOL (ml)	VOL (%)	WET MASS (g)	WATER MASS (g)	M (%)	M CHANGE (%)	BULK DENSE (Mg/m2)	DRY DENSE (Mg/m2)	VOID RATIO (e)	VOID CHANGE (%)	POROS (n)	SAT (Sr)	AIR CONT (A)	REL DENSE (Dr)	REL COMP (Cr)	PENE. RESIST (N)
1	(static)					(h0)								(cmc)											
	0.0	0.0	0.0	0.00	0.00	115.57	0.00	0.00	0.00	2106.46	0.00	3433.00	1.00	0.03	0.00	1.630	1.629	0.626	0.000	0.385	0.001	0.385	0.668	0.934	12.64
T1AL	1.0	14.0	14.0	0.03	0.03	115.54	-0.03	0.55	0.55	2105.92	0.03	3433.00	1.00	0.03	0.00	1.630	1.630	0.626	-0.067	0.385	0.001	0.385	0.670	0.934	12.73
	2.0	97.0	111.0	0.22	0.25	115.32	-0.22	4.01	4.56	2101.91	0.22	3433.00	1.00	0.03	0.00	1.633	1.633	0.623	-0.562	0.384	0.001	0.383	0.687	0.937	13.39
10	3.0	28.0	139.0	0.49	0.74	114.83	-0.64	8.93	13.49	2092.97	0.64	3433.00	1.00	0.03	0.00	1.640	1.640	0.616	-1.662	0.381	0.001	0.381	0.725	0.945	14.90
	4.0	77.0	216.0	2.76	3.50	112.07	-3.03	50.31	63.80	2042.67	3.03	3433.00	1.00	0.03	0.00	1.681	1.680	0.577	-7.863	0.366	0.001	0.365	0.938	0.988	24.97
	5.0	0.0	216.0	0.00	3.50	112.07	-3.03	0.00	63.80	2042.67	3.03	3433.00	1.00	0.03	0.00	1.681	1.680	0.577	-7.863	0.366	0.001	0.365	0.938	0.988	24.97
	6.0	0.0	216.0	0.00	3.50	112.07	-3.03	0.00	63.80	2042.67	3.03	3433.00	1.00	0.03	0.00	1.681	1.680	0.577	-7.863	0.366	0.001	0.365	0.938	0.988	24.97
						(h1)						3433.00	3432.00												
2	(static)					(h0)								(cmc)											
	0.0	0.0	0.0	0.00	0.00	122.03	0.00	0.00	0.00	2224.21	0.00	3466.20	2.00	0.06	0.00	1.558	1.557	0.701	0.000	0.412	0.002	0.411	0.256	0.851	2.40
T1AK	1.0	35.0	35.0	0.03	0.03	122.00	-0.02	0.55	0.55	2223.67	0.02	3466.20	2.00	0.06	0.00	1.559	1.558	0.701	-0.060	0.412	0.002	0.411	0.258	0.852	2.45
	2.0	100.0	135.0	5.63	5.66	116.37	-4.64	102.62	103.17	2121.04	4.64	3466.20	2.00	0.06	0.00	1.634	1.633	0.623	-11.251	0.384	0.002	0.383	0.689	0.938	17.46
20	3.0	105.0	240.0	1.55	7.21	114.82	-5.91	28.25	131.42	2092.79	5.91	3466.20	2.00	0.06	0.00	1.656	1.655	0.601	-14.332	0.375	0.003	0.374	0.808	0.962	23.99
	4.0	54.0	294.0	0.70	7.91	114.12	-6.48	12.76	144.18	2080.03	6.48	3466.20	2.00	0.06	0.00	1.666	1.665	0.591	-15.724	0.372	0.003	0.371	0.862	0.972	27.28
	5.0	0.0	294.0	0.00	7.91	114.12	-6.48	0.00	144.18	2080.03	6.48	3466.20	2.00	0.06	0.00	1.666	1.665	0.591	-15.724	0.372	0.003	0.371	0.862	0.972	27.28
	6.0	0.0	294.0	0.00	7.91	114.12	-6.48	0.00	144.18	2080.03	6.48	3466.20	2.00	0.06	0.00	1.666	1.665	0.591	-15.724	0.372	0.003	0.371	0.862	0.972	27.28
						(h1)						3466.20	3464.00												
3	(static)					(h0)								(cmc)											
	0.0	0.0	0.0	0.00	0.00	117.13	0.00	0.00	0.00	2135.01	0.00	3342.00	3.00	0.09	0.00	1.565	1.564	0.694	0.000	0.410	0.003	0.408	0.294	0.859	5.35
T1AM	1.0	9.0	9.0	0.02	0.02	117.11	-0.02	0.36	0.36	2134.64	0.02	3342.00	3.00	0.09	0.00	1.566	1.564	0.694	-0.042	0.410	0.003	0.408	0.296	0.859	5.40
	2.0	133.0	142.0	5.05	5.07	112.06	-4.33	92.05	92.41	2042.59	4.33	3342.00	3.00	0.09	0.00	1.636	1.635	0.621	-10.561	0.383	0.004	0.382	0.697	0.939	30.02
50	3.0	56.0	198.0	0.71	5.78	111.35	-4.93	12.94	105.35	2029.65	4.94	3342.00	3.00	0.09	0.00	1.647	1.645	0.611	-12.040	0.379	0.004	0.378	0.754	0.951	35.08
	4.0	27.0	225.0	0.27	6.05	111.08	-5.17	4.92	110.28	2024.73	5.17	3342.00	3.00	0.09	0.00	1.651	1.649	0.607	-12.603	0.378	0.004	0.376	0.775	0.955	37.11
	5.0	0.0	225.0	0.00	6.05	111.08	-5.17	0.00	110.28	2024.73	5.17	3342.00	3.00	0.09	0.00	1.651	1.649	0.607	-12.603	0.378	0.004	0.376	0.775	0.955	37.11
	6.0	0.0	225.0	0.00	6.05	111.08	-5.17	0.00	110.28	2024.73	5.17	3342.00	3.00	0.09	0.00	1.651	1.649	0.607	-12.603	0.378	0.004	0.376	0.775	0.955	37.11
						(h1)						3342.00	3339.00												

Table A3.4.7. Data sheet: medium uniform sand, high acceleration, dried, 25Hz.

TEST	ACCEL (g)	TIME incr. (mins)	TIME cum. (mins)	SET inc. (mm)	SET cum. (mm)	HEIGHT (mm)	SET (%)	VOL inc. (ml)	VOL cum. (ml)	VOL (ml)	VOL (%)	WET MASS (g)	WATER MASS (g)	M (%)	M CHANGE (%)	BULK DENSE (Mg/m2)	DRY DENSE (Mg/m2)	VOID RATIO (e)	VOID CHANGE (%)	POROS (n)	SAT (Sr)	REL DENSE (Dr)	REL COMP (Cr)	PENE. RESIST (N)
1	(static)					(h0)								(cmc)										
	0.0	0	0	0.000	0.000	79.665	0.000	0.00	0.00	1452.09	0.00	2821.16	619.16	28.12	0.00	1.943	1.516	0.741	0.000	0.426	1.002	0.273	0.855	2.12
TT1FA	0.1	5	5	0.000	0.000	79.665	0.000	0.00	0.00	1452.09	0.00	2821.16	619.16	28.12	0.00	1.943	1.516	0.741	0.000	0.426	1.002	0.273	0.855	2.12
	0.2	30	35	0.009	0.009	79.656	-0.011	0.16	0.16	1451.93	0.01	2820.99	618.99	28.11	-0.03	1.943	1.517	0.741	-0.027	0.426	1.002	0.274	0.855	2.13
10 kPa	0.4	35	70	0.054	0.063	79.602	-0.079	0.98	1.15	1450.95	0.08	2820.01	618.01	28.07	-0.19	1.944	1.518	0.740	-0.186	0.425	1.002	0.277	0.855	2.18
	0.5	35	105	0.038	0.101	79.564	-0.127	0.69	1.84	1450.25	0.13	2819.31	617.31	28.03	-0.30	1.944	1.518	0.739	-0.298	0.425	1.002	0.280	0.856	2.22
	0.6	55	160	0.042	0.143	79.522	-0.180	0.77	2.61	1449.49	0.18	2818.55	616.55	28.00	-0.42	1.945	1.519	0.738	-0.422	0.425	1.002	0.283	0.857	2.26
	0.8	40	200	0.131	0.274	79.391	-0.344	2.39	4.99	1447.10	0.34	2816.16	614.16	27.89	-0.81	1.946	1.522	0.735	-0.808	0.424	1.002	0.291	0.858	2.40
	1.0	60	260	0.330	0.604	79.061	-0.758	6.02	11.01	1441.09	0.76	2810.15	608.15	27.62	-1.78	1.950	1.528	0.728	-1.781	0.421	1.002	0.312	0.862	2.76
	2.0	80	340	2.806	3.410	76.255	-4.280	51.15	62.16	1389.94	4.28	2759.00	557.00	25.30	-10.04	1.985	1.584	0.666	-10.058	0.400	1.002	0.490	0.898	6.81
						(h1)						2759.00	2202.00											
2	(static)					(h0)								(cmc)										
	0.0	0	0	0.000	0.000	79.047	0.000	0.00	0.00	1440.83	0.00	2775.10	609.10	28.12	0.00	1.926	1.503	0.756	0.000	0.431	0.982	0.229	0.846	1.93
TT1FB	0.1	5	5	0.000	0.000	79.047	0.000	0.00	0.00	1440.83	0.00	2775.10	609.10	28.12	0.00	1.926	1.503	0.756	0.000	0.431	0.982	0.229	0.846	1.93
	0.2	10	15	0.000	0.000	79.047	0.000	0.00	0.00	1440.83	0.00	2775.10	609.10	28.12	0.00	1.926	1.503	0.756	0.000	0.431	0.982	0.229	0.846	1.93
20 kPa	0.4	60	75	0.045	0.045	79.002	-0.057	0.82	0.82	1440.01	0.06	2774.28	608.28	28.08	-0.13	1.927	1.504	0.755	-0.132	0.430	0.982	0.232	0.846	1.98
	0.5	50	125	0.042	0.087	78.961	-0.109	0.76	1.58	1439.25	0.11	2773.52	607.52	28.05	-0.26	1.927	1.505	0.754	-0.254	0.430	0.982	0.235	0.847	2.03
	0.6	50	175	0.034	0.120	78.927	-0.152	0.61	2.19	1438.64	0.15	2772.91	606.91	28.02	-0.36	1.927	1.506	0.753	-0.353	0.430	0.982	0.237	0.847	2.06
	0.8	40	215	0.070	0.190	78.858	-0.240	1.27	3.45	1437.38	0.24	2771.65	605.65	27.96	-0.57	1.928	1.507	0.752	-0.557	0.429	0.982	0.241	0.848	2.14
	1.0	55	270	0.156	0.346	78.702	-0.437	2.84	6.30	1434.53	0.44	2768.80	602.80	27.83	-1.03	1.930	1.510	0.748	-1.015	0.428	0.982	0.252	0.850	2.32
	2.0	60	330	2.842	3.188	75.860	-4.032	51.80	58.10	1382.73	4.03	2717.00	551.00	25.44	-9.54	1.965	1.566	0.685	-9.365	0.407	0.980	0.435	0.887	6.95
						(h1)						2717.00	2166.00											
3	(static)					(h0)								(cmc)										
	0.0	0	0	0.000	0.000	74.677	0.000	0.00	0.00	1361.18	0.00	2624.32	562.32	27.27	0.00	1.928	1.515	0.743	0.000	0.426	0.969	0.268	0.854	4.44
TT1FC	0.1	5	5	0.000	0.000	74.677	0.000	0.00	0.00	1361.18	0.00	2624.32	562.32	27.27	0.00	1.928	1.515	0.743	0.000	0.426	0.969	0.268	0.854	4.44
	0.2	15	20	0.001	0.001	74.676	-0.001	0.02	0.02	1361.16	0.00	2624.30	562.30	27.27	0.00	1.928	1.515	0.743	-0.003	0.426	0.969	0.268	0.854	4.45
50 kPa	0.4	10	30	0.010	0.011	74.666	-0.015	0.18	0.20	1360.98	0.01	2624.12	562.12	27.26	-0.04	1.928	1.515	0.742	-0.035	0.426	0.969	0.269	0.854	4.47
	0.5	45	75	0.021	0.032	74.645	-0.043	0.38	0.58	1360.59	0.04	2623.74	561.74	27.24	-0.10	1.928	1.516	0.742	-0.101	0.426	0.969	0.270	0.854	4.52
	0.6	40	115	0.019	0.051	74.626	-0.068	0.35	0.93	1360.25	0.07	2623.39	561.39	27.23	-0.17	1.929	1.516	0.742	-0.160	0.426	0.969	0.272	0.854	4.56
	0.8	40	155	0.056	0.107	74.570	-0.143	1.02	1.95	1359.23	0.14	2622.37	560.37	27.18	-0.35	1.929	1.517	0.740	-0.336	0.425	0.969	0.275	0.855	4.69
	1.0	55	210	0.109	0.216	74.461	-0.289	1.99	3.94	1357.24	0.29	2620.38	558.38	27.08	-0.70	1.931	1.519	0.738	-0.679	0.425	0.969	0.283	0.857	4.94
	2.0	60	270	2.051	2.267	72.410	-3.036	37.38	41.32	1319.85	3.04	2583.00	521.00	25.27	-7.35	1.957	1.562	0.690	-7.123	0.408	0.967	0.422	0.884	11.00
						(h1)						2583.00	2062.00											
4	(static)					(h0)								(cmc)										
	0.0	0	0	0.000	0.000	72.999	0.000	0.00	0.00	1330.58	0.00	2611.79	563.79	27.53	0.00	1.963	1.539	0.715	0.000	0.417	1.016	0.348	0.870	10.42
TT1FD	0.1	5	5	0.000	0.000	72.999	0.000	0.00	0.00	1330.58	0.00	2611.79	563.79	27.53	0.00	1.963	1.539	0.715	0.000	0.417	1.016	0.348	0.870	10.42
	0.2	5	10	0.000	0.000	72.999	0.000	0.00	0.00	1330.58	0.00	2611.79	563.79	27.53	0.00	1.963	1.539	0.715	0.000	0.417	1.016	0.348	0.870	10.42
100 kPa	0.4	5	15	0.000	0.000	72.999	0.000	0.00	0.00	1330.58	0.00	2611.79	563.79	27.53	0.00	1.963	1.539	0.715	0.000	0.417	1.016	0.348	0.870	10.42
	0.5	15	30	0.001	0.001	72.998	-0.001	0.01	0.01	1330.57	0.00	2611.78	563.78	27.53	0.00	1.963	1.539	0.715	-0.002	0.417	1.016	0.348	0.870	10.42
	0.6	10	40	0.000	0.001	72.998	-0.001	0.00	0.01	1330.57	0.00	2611.78	563.78	27.53	0.00	1.963	1.539	0.715	-0.002	0.417	1.016	0.348	0.870	10.42
	0.8	40	80	0.006	0.007	72.992	-0.009	0.11	0.12	1330.46	0.01	2611.67	563.67	27.52	-0.02	1.963	1.539	0.715	-0.021	0.417	1.016	0.349	0.870	10.44
	1.0	60	140	0.073	0.080	72.919	-0.109	1.33	1.45	1329.13	0.11	2610.34	562.34	27.46	-0.26	1.964	1.541	0.713	-0.261	0.416	1.016	0.354	0.871	10.74
	2.0	75	215	1.829	1.909	71.090	-2.614	33.34	34.79	1295.79	2.61	2577.00	529.00	25.83	-6.17	1.989	1.580	0.670	-6.270	0.401	1.017	0.479	0.896	19.67
						(h1)						2577.00	2048.00											

Table A3.5.1. Data sheet: medium Leighton Buzzard sand, saturated, 25Hz.

TEST	ACCEL (g)	TIME incr. (mins)	TIME cum. (mins)	SET inc. (mm)	SET cum. (mm)	HEIGHT (mm)	SET (%)	VOL inc. (ml)	VOL cum. (ml)	VOL (ml)	VOL (%)	WET MASS (g)	WATER MASS (g)	M (%)	M CHANGE (%)	BULK DENSE (Mg/m2)	DRY DENSE (Mg/m2)	VOID RATIO (e)	VOID CHANGE (%)	POROS (n)	SAT (Sr)	REL DENSE (Dr)	REL COMP (Cr)	PENE. RESIST (N)
1	(static)					(h0)								(cmc)										
	0.0	0	0	0.000	0.000	79.741	0.000	0.00	0.00	1453.48	0.00	2838.49	643.49	29.32	0.00	1.953	1.510	0.748	0.000	0.428	1.034	0.252	0.850	1.81
TT1FA	0.1	5	5	0.000	0.000	79.741	0.000	0.00	0.00	1453.48	0.00	2838.49	643.49	29.32	0.00	1.953	1.510	0.748	0.000	0.428	1.034	0.252	0.850	1.81
	0.2	5	10	0.000	0.000	79.741	0.000	0.00	0.00	1453.48	0.00	2838.49	643.49	29.32	0.00	1.953	1.510	0.748	0.000	0.428	1.034	0.252	0.850	1.81
	0.3	55	65	0.044	0.044	79.698	-0.055	0.79	0.79	1452.69	0.05	2837.70	642.70	29.28	-0.12	1.953	1.511	0.747	-0.127	0.428	1.035	0.255	0.851	1.85
10 kPa	0.4	70	80	0.072	0.072	79.670	-0.090	1.30	1.30	1452.18	0.09	2837.19	642.19	29.26	-0.20	1.954	1.512	0.747	-0.210	0.427	1.035	0.257	0.851	1.87
	0.5	90	170	0.085	0.156	79.585	-0.196	1.54	2.84	1450.64	0.20	2835.65	640.65	29.19	-0.44	1.955	1.513	0.745	-0.457	0.427	1.035	0.262	0.852	1.95
	0.6	68	238	0.124	0.280	79.461	-0.351	2.26	5.10	1448.38	0.35	2833.39	638.39	29.08	-0.79	1.956	1.515	0.742	-0.820	0.426	1.035	0.270	0.854	2.07
	0.8	100	338	0.214	0.494	79.247	-0.620	3.90	9.00	1444.48	0.62	2829.49	634.49	28.91	-1.40	1.959	1.520	0.737	-1.448	0.424	1.035	0.284	0.857	2.29
	1.0	120	458	0.250	0.744	78.997	-0.933	4.56	13.56	1439.92	0.93	2824.93	629.93	28.70	-2.11	1.962	1.524	0.732	-2.180	0.423	1.035	0.300	0.860	2.55
	2.0	120	578	3.617	4.361	75.380	-5.469	65.93	79.49	1373.99	5.47	2759.00	564.00	25.69	-12.35	2.008	1.598	0.653	-12.779	0.395	1.040	0.530	0.906	7.98
						(h1)						2759.00	2195.00											
2	(static)					(h0)								(cmc)										
	0.0	0	0	0.000	0.000	81.788	0.000	0.00	0.00	1490.79	0.00	2915.45	642.45	28.26	0.00	1.956	1.525	0.731	0.000	0.422	1.020	0.301	0.860	3.33
TT1FB	0.1	5	5	0.000	0.000	81.788	0.000	0.00	0.00	1490.79	0.00	2915.45	642.45	28.26	0.00	1.956	1.525	0.731	0.000	0.422	1.020	0.301	0.860	3.33
	0.2	15	20	0.003	0.003	81.786	-0.003	0.05	0.05	1490.75	0.00	2915.41	642.41	28.26	-0.01	1.956	1.525	0.731	-0.007	0.422	1.020	0.301	0.860	3.33
	0.3	60	80	0.024	0.026	81.762	-0.032	0.43	0.47	1490.32	0.03	2914.98	641.98	28.24	-0.07	1.956	1.525	0.731	-0.075	0.422	1.020	0.302	0.860	3.36
20 kPa	0.4	90	80	0.038	0.040	81.748	-0.049	0.68	0.73	1490.06	0.05	2914.72	641.72	28.23	-0.11	1.956	1.525	0.731	-0.116	0.422	1.020	0.303	0.861	3.38
	0.5	89	169	0.041	0.081	81.708	-0.098	0.74	1.47	1489.32	0.10	2913.98	640.98	28.20	-0.23	1.957	1.526	0.730	-0.233	0.422	1.020	0.306	0.861	3.44
	0.6	90	259	0.042	0.123	81.666	-0.150	0.77	2.23	1488.56	0.15	2913.22	640.22	28.17	-0.35	1.957	1.527	0.729	-0.355	0.422	1.020	0.308	0.862	3.49
	0.8	90	349	0.076	0.199	81.590	-0.243	1.39	3.62	1487.17	0.24	2911.83	638.83	28.11	-0.56	1.958	1.528	0.727	-0.574	0.421	1.020	0.313	0.863	3.60
	1.0	120	469	0.187	0.386	81.403	-0.471	3.41	7.03	1483.76	0.47	2908.43	635.43	27.96	-1.09	1.960	1.532	0.723	-1.116	0.420	1.020	0.325	0.865	3.87
	2.0	120	589	2.547	2.933	78.856	-3.585	46.43	53.45	1437.34	3.59	2862.00	589.00	25.91	-8.32	1.991	1.581	0.669	-8.487	0.401	1.022	0.481	0.896	8.51
						(h1)						2862.00	2273.00											
3	(static)					(h0)								(cmc)										
	0.0	0	0	0.000	0.000	70.056	0.000	0.00	0.00	1276.95	0.00	2432.88	528.88	27.78	0.00	1.905	1.491	0.771	0.000	0.435	0.952	0.187	0.837	2.17
TT1FC	0.1	10	10	0.000	0.000	70.056	0.000	0.00	0.00	1276.95	0.00	2432.88	528.88	27.78	0.00	1.905	1.491	0.771	0.000	0.435	0.952	0.187	0.837	2.17
	0.2	10	20	0.000	0.000	70.056	0.000	0.00	0.00	1276.95	0.00	2432.88	528.88	27.78	0.00	1.905	1.491	0.771	0.000	0.435	0.952	0.187	0.837	2.17
	0.3	75	95	0.013	0.013	70.043	-0.019	0.24	0.24	1276.71	0.02	2432.64	528.64	27.76	-0.04	1.905	1.491	0.770	-0.043	0.435	0.952	0.188	0.838	2.19
50 kPa	0.4	75	95	0.016	0.016	70.040	-0.023	0.29	0.29	1276.65	0.02	2432.59	528.59	27.76	-0.06	1.905	1.491	0.770	-0.052	0.435	0.952	0.189	0.838	2.19
	0.5	60	155	0.025	0.041	70.015	-0.059	0.46	0.75	1276.20	0.06	2432.13	528.13	27.74	-0.14	1.906	1.492	0.770	-0.134	0.435	0.952	0.190	0.838	2.24
	0.6	85	240	0.030	0.071	69.985	-0.101	0.55	1.29	1275.65	0.10	2431.58	527.58	27.71	-0.24	1.906	1.493	0.769	-0.233	0.435	0.952	0.193	0.839	2.29
	0.8	110	350	0.088	0.159	69.897	-0.227	1.60	2.90	1274.05	0.23	2429.98	525.98	27.62	-0.55	1.907	1.494	0.767	-0.522	0.434	0.951	0.199	0.840	2.45
	1.0	135	485	0.152	0.311	69.745	-0.444	2.77	5.67	1271.28	0.44	2427.21	523.21	27.48	-1.07	1.909	1.498	0.763	-1.020	0.433	0.951	0.210	0.842	2.73
	2.0	160	645	2.590	2.901	67.155	-4.141	47.21	52.88	1224.07	4.14	2380.00	476.00	25.00	-10.00	1.944	1.555	0.697	-9.515	0.411	0.947	0.400	0.880	9.90
						(h1)						2380.00	1904.00											
4	(static)					(h0)								(cmc)										
	0.0	0	0	0.000	0.000	79.173	0.000	0.00	0.00	1443.13	0.00	2851.11	600.11	26.66	0.00	1.976	1.560	0.693	0.000	0.409	1.016	0.414	0.883	14.73
TT1FD	0.1	5	5	0.000	0.000	79.173	0.000	0.00	0.00	1443.13	0.00	2851.11	600.11	26.66	0.00	1.976	1.560	0.693	0.000	0.409	1.016	0.414	0.883	14.73
	0.2	5	10	0.000	0.000	79.173	0.000	0.00	0.00	1443.13	0.00	2851.11	600.11	26.66	0.00	1.976	1.560	0.693	0.000	0.409	1.016	0.414	0.883	14.73
	0.3	20	30	0.000	0.000	79.173	0.000	0.00	0.00	1443.13	0.00	2851.11	600.11	26.66	0.00	1.976	1.560	0.693	0.000	0.409	1.016	0.414	0.883	14.73
100 kPa	0.4	140	150	0.012	0.012	79.161	-0.015	0.22	0.22	1442.91	0.02	2850.89	599.89	26.65	-0.04	1.976	1.560	0.692	-0.037	0.409	1.016	0.415	0.883	14.79
	0.5	30	180	0.004	0.016	79.157	-0.020	0.07	0.29	1442.84	0.02	2850.81	599.81	26.65	-0.05	1.976	1.560	0.692	-0.049	0.409	1.016	0.415	0.883	14.80
	0.6	95	275	0.008	0.024	79.150	-0.030	0.14	0.43	1442.70	0.03	2850.68	599.68	26.64	-0.07	1.976	1.560	0.692	-0.073	0.409	1.016	0.416	0.883	14.84
	0.8	100	375	0.015	0.038	79.135	-0.048	0.26	0.69	1442.43	0.05	2850.41	599.41	26.63	-0.12	1.976	1.561	0.692	-0.117	0.409	1.016	0.417	0.883	14.90
	1.0	90	465	0.042	0.080	79.094	-0.100	0.76	1.45	1441.68	0.10	2849.66	598.66	26.60	-0.24	1.977	1.561	0.691	-0.245	0.409	1.016	0.419	0.884	15.09
	2.0	80	545	1.243	1.323	77.851	-1.670	22.66	24.11	1419.02	1.67	2827.00	576.00	25.59	-4.02	1.992	1.586	0.664	-4.082	0.399	1.017	0.496	0.899	21.16
						(h1)						2827.00	2251.00											

Table A3.5.2. Data Sheet: medium Leighton Buzzard sand, saturated, 40Hz.

TEST	ACCEL (g)	TIME incr. (mins)	TIME cum. (mins)	SET inc. (mm)	SET cum. (mm)	HEIGHT (mm)	SET (%)	VOL inc. (ml)	VOL cum. (ml)	VOL (ml)	VOL (%)	WET MASS (g)	WATER MASS (g)	M (%)	M CHANGE (%)	BULK DENSE (Mg/m2)	DRY DENSE (Mg/m2)	VOID RATIO (e)	VOID CHANGE (%)	POROS (n)	SAT (Sr)	REL DENSE (Dr)	REL COMP (Cr)	PENE. RESIST (N)
1	(static)					(h0)								(cmc)										
	0.0	0	0	0.000	0.000	70.920	0.000	0.00	0.00	1292.70	0.00	2459.63	535.63	27.84	0.00	1.903	1.488	0.774	0.000	0.436	0.950	0.276	0.855	2.16
TT1FH	0.1	5	5	0.001	0.001	70.920	-0.001	0.01	0.01	1292.69	0.00	2459.62	535.62	27.84	0.00	1.903	1.488	0.774	-0.002	0.436	0.950	0.276	0.855	2.16
	0.2	120	125	0.017	0.018	70.903	-0.025	0.31	0.32	1292.38	0.02	2459.31	535.31	27.82	-0.06	1.903	1.489	0.773	-0.057	0.436	0.950	0.278	0.856	2.19
	0.3	120	245	0.034	0.052	70.868	-0.073	0.62	0.94	1291.75	0.07	2458.69	534.69	27.79	-0.18	1.903	1.489	0.772	-0.167	0.436	0.950	0.282	0.856	2.25
10 kPa	0.4	120	245	0.054	0.072	70.849	-0.101	0.98	1.30	1291.39	0.10	2458.33	534.33	27.77	-0.24	1.904	1.490	0.772	-0.231	0.436	0.950	0.284	0.857	2.29
	0.5	120	365	0.035	0.107	70.813	-0.151	0.65	1.95	1290.75	0.15	2457.69	533.69	27.74	-0.36	1.904	1.491	0.771	-0.346	0.435	0.950	0.288	0.858	2.35
	0.6	120	485	0.056	0.163	70.757	-0.230	1.02	2.97	1289.73	0.23	2456.66	532.66	27.69	-0.55	1.905	1.492	0.770	-0.527	0.435	0.950	0.294	0.859	2.46
	0.8	120	605	0.117	0.280	70.640	-0.395	2.13	5.10	1287.59	0.39	2454.53	530.53	27.57	-0.95	1.906	1.494	0.767	-0.905	0.434	0.949	0.307	0.861	2.68
	1.0	120	725	0.376	0.656	70.264	-0.925	6.85	11.96	1280.74	0.92	2447.68	523.68	27.22	-2.23	1.911	1.502	0.757	-2.120	0.431	0.949	0.350	0.870	3.47
	2.0	120	845	0.915	1.571	69.349	-2.215	16.68	28.63	1264.06	2.22	2431.00	507.00	26.35	-5.35	1.923	1.522	0.734	-5.078	0.423	0.947	0.453	0.891	5.82
						(h1)						2431.00	1924.00											
2	(static)					(h0)								(cmc)										
	0.0	0	0	0.000	0.000	69.270	0.000	0.00	0.00	1262.62	0.00	2411.56	515.56	27.19	0.00	1.910	1.502	0.758	0.000	0.431	0.947	0.346	0.869	4.41
TT1FI	0.1	5	5	0.000	0.000	69.270	0.000	0.00	0.00	1262.62	0.00	2411.56	515.56	27.19	0.00	1.910	1.502	0.758	0.000	0.431	0.947	0.346	0.869	4.41
	0.2	5	10	0.000	0.000	69.270	0.000	0.00	0.00	1262.62	0.00	2411.56	515.56	27.19	0.00	1.910	1.502	0.758	0.000	0.431	0.947	0.346	0.869	4.41
	0.3	5	15	0.000	0.000	69.270	0.000	0.00	0.00	1262.62	0.00	2411.56	515.56	27.19	0.00	1.910	1.502	0.758	0.000	0.431	0.947	0.346	0.869	4.41
20 kPa	0.4	5	15	0.000	0.000	69.270	0.000	0.00	0.00	1262.62	0.00	2411.56	515.56	27.19	0.00	1.910	1.502	0.758	0.000	0.431	0.947	0.346	0.869	4.41
	0.5	5	20	0.000	0.000	69.270	0.000	0.00	0.00	1262.62	0.00	2411.56	515.56	27.19	0.00	1.910	1.502	0.758	0.000	0.431	0.947	0.346	0.869	4.41
	0.6	15	35	0.001	0.001	69.269	-0.001	0.02	0.02	1262.60	0.00	2411.54	515.54	27.19	0.00	1.910	1.502	0.758	-0.003	0.431	0.947	0.347	0.869	4.41
	0.8	15	50	0.023	0.024	69.246	-0.035	0.42	0.44	1262.18	0.03	2411.12	515.12	27.17	-0.08	1.910	1.502	0.757	-0.080	0.431	0.947	0.349	0.870	4.48
	1.0	12	62	0.032	0.056	69.214	-0.081	0.58	1.02	1261.60	0.08	2410.54	514.54	27.14	-0.20	1.911	1.503	0.757	-0.187	0.431	0.947	0.353	0.871	4.57
	2.0	120	182	0.633	0.689	68.581	-0.995	11.54	12.56	1250.06	0.99	2399.00	503.00	26.53	-2.44	1.919	1.517	0.741	-2.306	0.425	0.946	0.425	0.885	6.64
						(h1)						2399.00	1896.00											
3	(static)					(h0)								(cmc)										
	0.0	0	0	0.000	0.000	69.000	0.000	0.00	0.00	1257.70	0.00	2366.32	502.32	26.95	0.00	1.881	1.482	0.781	0.000	0.439	0.911	0.242	0.848	3.62
TT1FJ	0.1	5	5	0.000	0.000	69.000	0.000	0.00	0.00	1257.70	0.00	2366.32	502.32	26.95	0.00	1.881	1.482	0.781	0.000	0.439	0.911	0.242	0.848	3.62
	0.2	5	10	0.000	0.000	69.000	0.000	0.00	0.00	1257.70	0.00	2366.32	502.32	26.95	0.00	1.881	1.482	0.781	0.000	0.439	0.911	0.242	0.848	3.62
	0.3	120	130	0.008	0.008	68.992	-0.012	0.15	0.15	1257.55	0.01	2366.18	502.18	26.94	-0.03	1.882	1.482	0.781	-0.026	0.439	0.911	0.243	0.849	3.64
50 kPa	0.4	15	25	0.019	0.019	68.982	-0.027	0.34	0.34	1257.36	0.03	2365.98	501.98	26.93	-0.07	1.882	1.482	0.781	-0.061	0.438	0.911	0.244	0.849	3.68
	0.5	15	40	0.000	0.019	68.982	-0.027	0.00	0.34	1257.36	0.03	2365.98	501.98	26.93	-0.07	1.882	1.482	0.781	-0.061	0.438	0.911	0.244	0.849	3.68
	0.6	120	160	0.000	0.019	68.982	-0.027	0.00	0.34	1257.36	0.03	2365.98	501.98	26.93	-0.07	1.882	1.482	0.781	-0.061	0.438	0.911	0.244	0.849	3.68
	0.8	120	280	0.094	0.112	68.888	-0.162	1.71	2.04	1255.65	0.16	2364.28	500.28	26.84	-0.41	1.883	1.484	0.778	-0.370	0.438	0.910	0.255	0.851	4.02
	1.0	120	400	0.127	0.239	68.761	-0.347	2.31	4.36	1253.34	0.35	2361.96	497.96	26.71	-0.87	1.885	1.487	0.775	-0.790	0.437	0.910	0.270	0.854	4.49
	2.0	120	520	0.711	0.950	68.050	-1.377	12.96	17.32	1240.38	1.38	2349.00	485.00	26.02	-3.45	1.894	1.503	0.757	-3.140	0.431	0.908	0.352	0.870	7.67
						(h1)						2349.00	1864.00											
4	(static)					(h0)								(cmc)										
	0.0	0	0	0.000	0.000	70.513	0.000	0.00	0.00	1285.28	0.00	2501.77	527.77	26.74	0.00	1.946	1.536	0.719	0.000	0.418	0.982	0.523	0.905	23.48
TT1FK	0.1	5	5	0.000	0.000	70.513	0.000	0.00	0.00	1285.28	0.00	2501.77	527.77	26.74	0.00	1.946	1.536	0.719	0.000	0.418	0.982	0.523	0.905	23.48
	0.2	5	10	0.005	0.005	70.508	-0.007	0.09	0.09	1285.19	0.01	2501.68	527.68	26.73	-0.02	1.947	1.536	0.719	-0.017	0.418	0.982	0.523	0.905	23.53
	0.3	5	15	0.003	0.008	70.506	-0.011	0.05	0.14	1285.14	0.01	2501.63	527.63	26.73	-0.03	1.947	1.536	0.719	-0.025	0.418	0.982	0.524	0.905	23.56
100 kPa	0.4	5	15	0.002	0.009	70.504	-0.013	0.03	0.12	1285.11	0.01	2501.65	527.65	26.73	-0.02	1.947	1.536	0.719	-0.031	0.418	0.982	0.524	0.905	23.57
	0.5	5	20	0.000	0.009	70.504	-0.013	0.00	0.12	1285.11	0.01	2501.65	527.65	26.73	-0.02	1.947	1.536	0.719	-0.031	0.418	0.982	0.524	0.905	23.57
	0.6	10	30	0.002	0.011	70.502	-0.016	0.04	0.15	1285.08	0.01	2501.62	527.62	26.73	-0.03	1.947	1.536	0.719	-0.037	0.418	0.982	0.524	0.905	23.59
	0.8	15	45	0.006	0.017	70.496	-0.024	0.11	0.26	1284.97	0.02	2501.51	527.51	26.72	-0.05	1.947	1.536	0.718	-0.058	0.418	0.982	0.525	0.905	23.65
	1.0	120	165	0.050	0.067	70.446	-0.095	0.91	1.18	1284.06	0.09	2500.59	526.59	26.68	-0.22	1.947	1.537	0.717	-0.227	0.418	0.982	0.530	0.906	24.15
	2.0	120	285	0.197	0.264	70.249	-0.375	3.59	4.77	1280.46	0.37	2497.00	523.00	26.49	-0.90	1.950	1.542	0.712	-0.896	0.416	0.982	0.552	0.910	26.16
						(h1)						2497.00	1974.00											

Table A3.5.3. Data sheet: medium Leighton Buzzard sand, saturated, 40Hz, horizontal vibration.

TEST	ACCEL (g)	TIME incr. (mins)	TIME cum. (mins)	SET inc. (mm)	SET cum. (mm)	HEIGHT (mm)	SET (%)	VOL inc. (ml)	VOL cum. (ml)	VOL (ml)	VOL (%)	WET MASS (g)	WATER MASS (g)	M (%)	M CHANGE (%)	BULK DENSE (Mg/m2)	DRY DENSE (Mg/m2)	VOID RATIO (e)	VOID CHANGE (%)	POROS (n)	SAT (Sr)	REL DENSE (Dr)	REL COMP (Cr)	PENE RESIST (N)
1	(static)					(h0)								(cmc)										
	0.0	0.0	0.0	0.000	0.000	75.085	0.000	0.00	0.00	1368.61	0.00	2625.51	563.51	27.33	0.00	1.918	1.507	0.752	0.000	0.429	0.959	0.373	0.875	5.104
T1FA	1.0	15.0	15.0	0.050	0.050	75.035	-0.067	0.91	0.91	1367.70	0.07	2624.60	562.60	27.28	-0.16	1.919	1.508	0.751	-0.155	0.429	0.959	0.378	0.876	5.249
	2.0	45.0	60.0	1.300	1.350	73.735	-1.798	23.70	24.61	1344.01	1.80	2600.90	538.90	26.13	-4.37	1.935	1.534	0.721	-4.188	0.419	0.957	0.515	0.903	9.731
10kPa	3.0	43.0	103.0	0.860	2.210	72.875	-2.943	15.68	40.28	1328.33	2.95	2585.23	523.23	25.37	-7.15	1.946	1.552	0.701	-6.856	0.412	0.956	0.605	0.921	13.449
	4.0	35.0	138.0	0.530	2.740	72.345	-3.649	9.66	49.94	1318.67	3.65	2575.57	513.57	24.91	-8.86	1.953	1.564	0.688	-8.500	0.408	0.955	0.661	0.932	16.040
	5.0	40.0	178.0	0.470	3.210	71.875	-4.275	8.57	58.51	1310.10	4.28	2567.00	505.00	24.49	-10.38	1.959	1.574	0.677	-9.958	0.404	0.955	0.710	0.942	18.529
						(h1)						2567.00	2062.00											
2	(static)					(h0)								(cmc)										
	0.0	0.0	0.0	0.000	0.000	79.230	0.000	0.00	0.00	1444.17	0.00	2722.39	606.39	28.66	0.00	1.885	1.465	0.802	0.000	0.445	0.944	0.150	0.830	1.382
T1FB	1.0	15.0	15.0	0.090	0.090	79.140	-0.114	1.64	1.64	1442.53	0.11	2720.75	604.75	28.58	-0.27	1.886	1.467	0.800	-0.255	0.444	0.943	0.159	0.832	1.557
	2.0	55.0	70.0	1.810	1.900	77.330	-2.398	32.99	34.63	1409.53	2.40	2687.76	571.76	27.02	-5.71	1.907	1.501	0.759	-5.389	0.431	0.940	0.344	0.869	7.317
20kPa	3.0	55.0	125.0	1.310	3.210	76.020	-4.051	23.88	58.51	1385.66	4.06	2663.88	547.88	25.89	-9.65	1.922	1.527	0.729	-9.105	0.422	0.938	0.478	0.896	14.135
	4.0	55.0	180.0	0.630	3.840	75.390	-4.847	11.48	69.99	1374.17	4.85	2652.39	536.39	25.35	-11.54	1.930	1.540	0.714	-10.891	0.417	0.937	0.543	0.909	18.206
	5.0	50.0	230.0	0.460	4.300	74.930	-5.427	8.38	78.38	1365.79	5.43	2644.01	528.01	24.95	-12.93	1.936	1.549	0.704	-12.196	0.413	0.936	0.590	0.918	21.503
	6.0	20.0	250.0	0.220	4.520	74.710		4.01	82.39	1361.78	5.71	2640.00	524.00	24.76	-13.59	1.939	1.554	0.699	-12.820	0.411	0.935	0.613	0.923	23.177
						(h1)						2640.00	2116.00											
3	(static)					(h0)								(cmc)										
	0.0	0.0	0.0	0.000	0.000	71.700	0.000	0.00	0.00	1306.91	0.00	2431.78	510.78	26.59	0.00	1.861	1.470	0.796	0.000	0.443	0.882	0.175	0.835	1.899
T2FC	1.0	20.0	20.0	0.100	0.100	71.600	-0.139	1.82	1.82	1305.09	0.14	2429.95	508.95	26.49	-0.36	1.862	1.472	0.794	-0.315	0.442	0.881	0.187	0.837	2.152
	2.0	40.0	60.0	1.160	1.260	70.440	-1.757	21.14	22.97	1283.95	1.76	2408.81	487.81	25.39	-4.50	1.876	1.496	0.765	-3.965	0.433	0.877	0.318	0.864	6.227
50kPa	3.0	50.0	110.0	0.850	2.110	69.590	-2.943	15.49	38.46	1268.45	2.95	2393.32	472.32	24.59	-7.53	1.887	1.514	0.743	-6.640	0.426	0.873	0.413	0.883	10.557
	4.0	50.0	160.0	0.660	2.770	68.930	-3.863	12.03	50.49	1256.42	3.87	2381.29	460.29	23.96	-9.88	1.895	1.529	0.727	-8.716	0.421	0.870	0.488	0.898	14.703
	5.0	35.0	195.0	0.290	3.060	68.640	-4.268	5.29	55.78	1251.14	4.27	2376.00	455.00	23.69	-10.92	1.899	1.535	0.719	-9.629	0.418	0.869	0.521	0.904	16.741
						(h1)						2376.00	1921.00											
4	(static)					(h0)								(cmc)										
	0.0	0.0	0.0	0.000	0.000	67.210	0.000	0.00	0.00	1225.07	0.00	2345.50	506.50	27.54	0.00	1.915	1.501	0.759	0.000	0.431	0.958	0.344	0.869	10.154
T1FD	1.0	15.0	15.0	0.020	0.020	67.190	-0.030	0.36	0.36	1224.71	0.03	2345.13	506.13	27.52	-0.07	1.915	1.502	0.758	-0.069	0.431	0.958	0.346	0.869	10.293
	2.0	25.0	40.0	0.740	0.760	66.450	-1.131	13.49	13.85	1211.22	1.13	2331.64	492.64	26.79	-2.74	1.925	1.518	0.739	-2.621	0.425	0.957	0.433	0.887	16.133
100kPa	3.0	35.0	75.0	0.590	1.350	65.860	-2.009	10.75	24.61	1200.46	2.01	2320.89	481.89	26.20	-4.86	1.933	1.532	0.723	-4.656	0.420	0.956	0.503	0.901	21.726
	4.0	31.0	106.0	0.380	1.730	65.480	-2.574	6.93	31.53	1193.54	2.57	2313.96	474.96	25.83	-6.23	1.939	1.541	0.713	-5.967	0.416	0.956	0.548	0.910	25.767
	5.0	30.0	136.0	0.190	1.920	65.290	-2.857	3.46	35.00	1190.07	2.86	2310.50	471.50	25.64	-6.91	1.941	1.545	0.708	-6.622	0.415	0.955	0.570	0.914	27.917
	6.0	45.0	181.0	0.960	2.880	64.330		17.50	52.50	1172.58	4.29	2293.00	454.00	24.69	-10.36	1.956	1.568	0.683	-9.933	0.406	0.954	0.683	0.937	40.098
						(h1)						2293.00	1839.00											

Table A3.5.4. Data sheet: medium Leighton Buzzard sand, high acceleration, saturated, 25Hz.

TEST	ACCEL (g)	TIME incr. (mins)	TIME cum. (mins)	SET inc. (mm)	SET cum. (mm)	HEIGHT (mm)	SET (%)	VOL inc. (ml)	VOL cum. (ml)	VOL (ml)	VOL (%)	WET MASS (g)	WATER MASS (g)	M (%)	M CHANGE (%)	BULK DENSE (Mg/m2)	DRY DENSE (Mg/m2)	VOID RATIO (e)	VOID CHANGE (%)	POROS (n)	SAT (Sr)	AIR CONT (A)	REL DENSE (Dr)	REL COMP (Cr)	PENE. RESIST (N)
1	(static)					(h0)								(cmc)											
	0.0	0.0	0.0	0.00	0.00	77.85	0.00	0.00	0.00	1418.92	0.00	2555.00	312.00	13.91	0.00	1.801	1.581	0.670	0.000	0.401	0.548	0.181	0.479	0.896	6.52
T1FJ	1.0	10.0	10.0	0.01	0.01	77.84	-0.01	0.18	0.18	1418.74	0.01	2555.00	312.00	13.91	0.00	1.801	1.581	0.670	-0.032	0.401	0.548	0.181	0.480	0.896	6.54
	2.0	25.0	35.0	0.41	0.42	77.43	-0.54	7.47	7.66	1411.26	0.54	2555.00	312.00	13.91	0.00	1.810	1.589	0.661	-1.345	0.398	0.556	0.177	0.506	0.901	7.25
10	3.0	25.0	60.0	0.40	0.82	77.03	-1.05	7.29	14.95	1403.97	1.05	2555.00	312.00	13.91	0.00	1.820	1.598	0.652	-2.625	0.395	0.563	0.173	0.531	0.906	7.99
	4.0	20.0	80.0	0.12	0.94	76.91	-1.21	2.19	17.13	1401.79	1.21	2555.00	312.00	13.91	0.00	1.823	1.600	0.650	-3.010	0.394	0.565	0.171	0.538	0.908	8.21
	5.0	25.0	105.0	0.69	1.63	76.22	-2.09	12.58	29.71	1389.21	2.09	2555.00	312.00	13.91	0.00	1.839	1.615	0.635	-5.219	0.388	0.578	0.164	0.581	0.916	9.58
	6.0	25.0	130.0	0.23	1.86	75.99	-2.39	4.19	33.90	1385.02	2.39	2555.00	312.00	13.91	0.00	1.845	1.619	0.630	-5.955	0.387	0.583	0.161	0.595	0.919	10.06
						(h1)						2555.00	2243.00												
2	(static)					(h0)								(cmc)											
	0.0	0.0	0.0	0.00	0.00	61.41	0.00	0.00	0.00	1119.35	0.00	2216.00	287.00	14.88	0.00	1.980	1.723	0.532	0.000	0.347	0.738	0.091	0.881	0.976	28.51
T1FK	1.0	15.0	15.0	0.04	0.04	61.37	-0.07	0.73	0.73	1118.62	0.07	2216.00	287.00	14.88	0.00	1.981	1.724	0.531	-0.188	0.347	0.740	0.090	0.884	0.977	28.70
	2.0	30.0	45.0	0.61	0.65	60.76	-1.06	11.12	11.85	1107.50	1.06	2216.00	287.00	14.88	0.00	2.001	1.742	0.516	-3.048	0.340	0.762	0.081	0.928	0.986	31.65
20	3.0	25.0	70.0	0.33	0.98	60.43	-1.60	6.02	17.86	1101.49	1.60	2216.00	287.00	14.88	0.00	2.012	1.751	0.507	-4.596	0.337	0.774	0.076	0.952	0.990	33.30
	4.0	20.0	90.0	0.17	1.15	60.26	-1.87	3.10	20.96	1098.39	1.87	2216.00	287.00	14.88	0.00	2.017	1.756	0.503	-5.393	0.335	0.781	0.073	0.964	0.993	34.17
	5.0	20.0	110.0	0.23	1.38	60.03	-2.25	4.19	25.15	1094.20	2.25	2216.00	287.00	14.88	0.00	2.025	1.763	0.498	-6.472	0.332	0.790	0.070	0.981	0.996	35.36
	6.0	15.0	125.0	0.15	1.53	59.88	-2.49	2.73	27.89	1091.46	2.49	2216.00	287.00	14.88	0.00	2.030	1.767	0.494	-7.175	0.331	0.795	0.068	0.992	0.998	36.15
						(h1)						2216.00	1929.00												
3	(static)					(h0)								(cmc)											
	0.0	0.0	0.0	0.00	0.00	92.60	0.00	0.00	0.00	1687.87	0.00	2826.00	325.00	13.00	0.00	1.674	1.482	0.782	0.000	0.439	0.439	0.246	0.155	0.831	1.48
T1FL	1.0	15.0	15.0	-0.01	-0.01	92.61	0.01	-0.09	-0.09	1687.96	-0.01	2826.00	325.00	13.00	0.00	1.674	1.482	0.782	0.012	0.439	0.439	0.246	0.154	0.831	1.47
	2.0	30.0	45.0	0.50	0.49	92.11	-0.53	9.02	8.93	1678.94	0.53	2826.00	325.00	13.00	0.00	1.683	1.490	0.772	-1.206	0.436	0.444	0.242	0.182	0.836	2.05
50	3.0	30.0	75.0	0.30	0.79	91.81	-0.85	5.47	14.40	1673.47	0.85	2826.00	325.00	13.00	0.00	1.689	1.494	0.767	-1.944	0.434	0.448	0.240	0.199	0.840	2.44
	4.0	25.0	100.0	0.20	0.99	91.61	-1.07	3.65	18.05	1669.82	1.07	2826.00	325.00	13.00	0.00	1.692	1.498	0.763	-2.437	0.433	0.450	0.238	0.210	0.842	2.73
	5.0	30.0	130.0	0.28	1.27	91.33	-1.37	5.10	23.15	1664.72	1.37	2826.00	325.00	13.00	0.00	1.698	1.502	0.757	-3.126	0.431	0.453	0.236	0.226	0.845	3.15
	6.0	20.0	150.0	0.13	1.40	91.20	-1.51	2.37	25.52	1662.35	1.51	2826.00	325.00	13.00	0.00	1.700	1.504	0.755	-3.446	0.430	0.455	0.235	0.233	0.847	3.36
						(h1)						2826.00	2500.00												

Table A3.5.5. Data sheet: medium Leighton Buzzard sand, high acceleration, partially saturated, 25Hz.

TEST	ACCEL (g)	TIME incr.	TIME cum.	SET inc. (mm)	SET cum. (mm)	HEIGHT (mm)	SET (%)	VOL inc. (ml)	VOL cum. (ml)	VOL (ml)	VOL (%)	WET MASS (g)	WATER MASS (g)	M (%)	M CHANGE (%)	BULK DENSE (Mg/m2)	DRY DENSE (Mg/m2)	VOID RATIO (e)	VOID CHANGE (%)	POROS (n)	SAT (Sr)	AIR CONT (A)	REL DENSE (Dr)	REL COMP (Cr)	PENE. RESIST (N)
1	(static)					(h0)								(cmc)											
	0.0	0.0	0.0	0.00	0.00	58.72	0.00	0.00	0.00	1070.32	0.00	1666.00	1.00	0.06	0.00	1.557	1.556	0.697	0.000	0.411	0.002	0.410	0.401	0.880	4.56
T1FE	1.0	20.0	20.0	0.11	0.11	58.61	-0.19	2.01	2.01	1068.31	0.19	1666.00	1.00	0.06	0.00	1.559	1.559	0.694	-0.456	0.410	0.002	0.409	0.410	0.882	4.77
	2.0	80.0	100.0	5.19	5.30	53.42	-9.03	94.60	96.61	973.71	9.04	1666.00	1.00	0.06	0.00	1.711	1.710	0.544	-21.974	0.352	0.003	0.351	0.846	0.969	20.31
10	3.0	30.0	130.0	0.20	5.50	53.22	-9.37	3.65	100.25	970.07	9.38	1666.00	1.00	0.06	0.00	1.717	1.716	0.538	-22.803	0.350	0.003	0.349	0.863	0.973	21.13
	4.0	15.0	145.0	0.06	5.56	53.16	-9.47	1.09	101.34	968.97	9.49	1666.00	1.00	0.06	0.00	1.719	1.718	0.536	-23.052	0.349	0.003	0.348	0.868	0.974	21.38
	5.0	15.0	160.0	0.06	5.62	53.10	-9.57	1.09	102.44	967.88	9.59	1666.00	1.00	0.06	0.00	1.721	1.720	0.535	-23.301	0.348	0.003	0.347	0.873	0.975	21.62
	6.0	15.0	175.0	0.06	5.68	53.04	-9.67	1.09	103.53	966.79	9.69	1666.00	1.00	0.06	0.00	1.723	1.722	0.533	-23.549	0.348	0.003	0.347	0.878	0.976	21.87
						(h1)						1666.00	1665.00												
2	(static)					(h0)								(cmc)											
	0.0	0.0	0.0	0.00	0.00	69.95	0.00	0.00	0.00	1275.01	0.00	1879.00	1.00	0.05	0.00	1.474	1.473	0.792	0.000	0.442	0.002	0.441	0.124	0.825	0.56
T1FF	1.0	15.0	15.0	0.01	0.01	69.94	-0.01	0.18	0.18	1274.83	0.01	1879.00	1.00	0.05	0.00	1.474	1.473	0.792	-0.032	0.442	0.002	0.441	0.125	0.825	0.57
	2.0	85.0	100.0	5.14	5.15	64.80	-7.36	93.69	93.87	1181.14	7.36	1879.00	1.00	0.05	0.00	1.591	1.590	0.660	-16.654	0.398	0.002	0.397	0.508	0.902	9.46
20	3.0	40.0	140.0	0.24	5.39	64.56	-7.71	4.37	98.25	1176.77	7.71	1879.00	1.00	0.05	0.00	1.597	1.596	0.654	-17.430	0.395	0.002	0.395	0.525	0.905	10.14
	4.0	30.0	170.0	0.13	5.52	64.43	-7.89	2.37	100.62	1174.40	7.89	1879.00	1.00	0.05	0.00	1.600	1.599	0.651	-17.851	0.394	0.002	0.393	0.535	0.907	10.52
	5.0	15.0	185.0	0.05	5.57	64.38	-7.96	0.91	101.53	1173.49	7.96	1879.00	1.00	0.05	0.00	1.601	1.600	0.650	-18.012	0.394	0.002	0.393	0.539	0.908	10.67
	6.0	35.0	220.0	0.09	5.66	64.29	-8.09	1.64	103.17	1171.85	8.09	1879.00	1.00	0.05	0.00	1.603	1.603	0.647	-18.303	0.393	0.002	0.392	0.546	0.909	10.93
						(h1)						1879.00	1878.00												
3	(static)					(h0)								(cmc)											
	0.0	0.0	0.0	0.00	0.00	69.50	0.00	0.00	0.00	1266.81	0.00	2007.00	2.00	0.10	0.00	1.584	1.583	0.668	0.000	0.400	0.004	0.399	0.485	0.897	14.55
T1FH	1.0	15.0	15.0	0.08	0.08	69.42	-0.12	1.46	1.46	1265.35	0.12	2007.00	2.00	0.10	0.00	1.586	1.585	0.666	-0.287	0.400	0.004	0.398	0.491	0.898	14.89
	2.0	90.0	105.0	5.60	5.68	63.82	-8.17	102.07	103.53	1163.28	8.18	2007.00	2.00	0.10	0.00	1.725	1.724	0.532	-20.407	0.347	0.005	0.345	0.882	0.976	48.01
50	3.0	40.0	145.0	0.28	5.96	63.54	-8.58	5.10	108.64	1158.18	8.59	2007.00	2.00	0.10	0.00	1.733	1.731	0.525	-21.413	0.344	0.005	0.343	0.901	0.980	50.16
	4.0	30.0	175.0	0.23	6.19	63.31	-8.91	4.19	112.83	1153.98	8.92	2007.00	2.00	0.10	0.00	1.739	1.737	0.519	-22.239	0.342	0.005	0.340	0.917	0.983	51.96
	5.0	25.0	200.0	0.09	6.28	63.22	-9.04	1.64	114.47	1152.34	9.05	2007.00	2.00	0.10	0.00	1.742	1.740	0.517	-22.562	0.341	0.005	0.339	0.924	0.985	52.68
	6.0	15.0	215.0	0.00	6.28	63.22	-9.04	0.00	114.47	1152.34	9.05	2007.00	2.00	0.10	0.00	1.742	1.740	0.517	-22.562	0.341	0.005	0.339	0.924	0.985	52.68
						(h1)						2007.00	2005.00												
4	(static)					(h0)								(cmc)											
	0.0	0.0	0.0	0.00	0.00	74.99	0.00	0.00	0.00	1366.88	0.00	2084.00	1.00	0.05	0.00	1.525	1.524	0.732	0.000	0.423	0.002	0.422	0.298	0.860	7.64
T1FI	1.0	15.0	15.0	0.00	0.00	74.99	0.00	0.00	0.00	1366.88	0.00	2084.00	1.00	0.05	0.00	1.525	1.524	0.732	0.000	0.423	0.002	0.422	0.298	0.860	7.64
	2.0	85.0	100.0	4.02	4.02	70.97	-5.36	73.27	73.27	1293.61	5.36	2084.00	1.00	0.05	0.00	1.611	1.610	0.640	-12.680	0.390	0.002	0.389	0.568	0.914	27.73
100	3.0	35.0	135.0	0.29	4.31	70.68	-5.75	5.29	78.56	1288.32	5.75	2084.00	1.00	0.05	0.00	1.618	1.617	0.633	-13.595	0.388	0.002	0.387	0.588	0.918	29.67
	4.0	10.0	145.0	0.09	4.40	70.59	-5.87	1.64	80.20	1286.68	5.87	2084.00	1.00	0.05	0.00	1.620	1.619	0.631	-13.879	0.387	0.002	0.386	0.594	0.919	30.28
	5.0	15.0	160.0	0.11	4.51	70.48	-6.01	2.01	82.21	1284.67	6.01	2084.00	1.00	0.05	0.00	1.622	1.621	0.628	-14.226	0.386	0.002	0.385	0.601	0.920	31.04
	6.0	15.0	175.0	0.12	4.63	70.36	-6.17	2.19	84.39	1282.49	6.17	2084.00	1.00	0.05	0.00	1.625	1.624	0.625	-14.604	0.385	0.002	0.384	0.609	0.922	31.87
						(h1)						2084.00	2083.00												

Table A3.5.6. Data sheet: medium Leighton Buzzard sand, high acceleration, dried, 25Hz.

TEST	ACCEL (g)	TIME incr. (mins)	TIME cum. (mins)	SET inc. (mm)	SET cum. (mm)	HEIGHT (mm)	SET (%)	VOL inc. (ml)	VOL cum. (ml)	VOL (ml)	VOL (%)	WET MASS (g)	WATER MASS (g)	M (%)	M CHANGE (%)	BULK DENSE (Mg/m2)	DRY DENSE (Mg/m2)	VOID RATIO (e)	VOID CHANGE (%)	POROS (n)	SAT (Sr)	REL DENSE (Dr)	REL COMP (Cr)	PENE. RESIST (N)
1	(static)					(h0)								(cmc)										
	0.0	0	0	0.000	0.000	75.087	0.000	0.00	0.00	1368.64	0.00	2614.88	529.88	25.41	0.00	1.911	1.523	0.726	0.000	0.421	0.920	0.341	0.868	3.29
TT4GA	0.1	5	5	0.000	0.000	75.087	0.000	0.00	0.00	1368.64	0.00	2614.88	529.88	25.41	0.00	1.911	1.523	0.726	0.000	0.421	0.920	0.341	0.868	3.29
	0.2	10	15	0.000	0.000	75.087	0.000	0.00	0.00	1368.64	0.00	2614.88	529.88	25.41	0.00	1.911	1.523	0.726	0.000	0.421	0.920	0.341	0.868	3.29
10 kPa	0.4	10	25	0.008	0.008	75.079	-0.011	0.15	0.15	1368.49	0.01	2614.74	529.74	25.41	-0.03	1.911	1.524	0.726	-0.025	0.421	0.920	0.342	0.868	3.32
	0.5	10	35	0.005	0.013	75.074	-0.017	0.09	0.24	1368.40	0.02	2614.65	529.65	25.40	-0.04	1.911	1.524	0.726	-0.041	0.421	0.920	0.343	0.869	3.33
	0.6	20	55	0.028	0.041	75.046	-0.055	0.51	0.75	1367.89	0.05	2614.14	529.14	25.38	-0.14	1.911	1.524	0.725	-0.130	0.420	0.920	0.348	0.870	3.43
	0.8	25	80	0.080	0.121	74.966	-0.160	1.45	2.20	1366.44	0.16	2612.69	527.69	25.31	-0.41	1.912	1.526	0.724	-0.381	0.420	0.920	0.362	0.872	3.71
	1.0	45	125	0.212	0.333	74.754	-0.443	3.86	6.06	1362.58	0.44	2608.82	523.82	25.12	-1.14	1.915	1.530	0.719	-1.052	0.418	0.919	0.399	0.880	4.51
	2.0	65	190	2.514	2.847	72.240	-3.791	45.82	51.88	1316.76	3.79	2563.00	478.00	22.93	-9.79	1.946	1.583	0.661	-9.010	0.398	0.912	0.840	0.968	20.02
						(h1)						2563.00	2085.00											
2	(static)					(h0)								(cmc)										
	0.0	0	0	0.000	0.000	72.338	0.000	0.00	0.00	1318.54	0.00	2544.47	523.47	25.90	0.00	1.930	1.533	0.716	0.000	0.417	0.952	0.421	0.884	6.51
TT2GB	0.1	5	5	0.000	0.000	72.338	0.000	0.00	0.00	1318.54	0.00	2544.47	523.47	25.90	0.00	1.930	1.533	0.716	0.000	0.417	0.952	0.421	0.884	6.51
	0.2	25	30	0.002	0.002	72.337	-0.002	0.03	0.03	1318.51	0.00	2544.45	523.45	25.90	-0.01	1.930	1.533	0.716	-0.005	0.417	0.952	0.421	0.884	6.52
20 kPa	0.4	25	55	0.004	0.005	72.333	-0.007	0.06	0.09	1318.45	0.01	2544.38	523.38	25.90	-0.02	1.930	1.533	0.716	-0.017	0.417	0.952	0.422	0.884	6.54
	0.5	35	90	0.014	0.019	72.319	-0.026	0.26	0.35	1318.20	0.03	2544.13	523.13	25.88	-0.07	1.930	1.533	0.715	-0.063	0.417	0.952	0.424	0.885	6.61
	0.6	30	120	0.021	0.040	72.298	-0.055	0.38	0.73	1317.81	0.06	2543.74	522.74	25.87	-0.14	1.930	1.534	0.715	-0.133	0.417	0.952	0.428	0.886	6.73
	0.8	30	150	0.113	0.153	72.186	-0.211	2.05	2.78	1315.76	0.21	2541.69	520.69	25.76	-0.53	1.932	1.536	0.712	-0.505	0.416	0.951	0.448	0.890	7.39
	1.0	50	200	0.264	0.416	71.922	-0.575	4.80	7.58	1310.96	0.58	2536.89	515.89	25.53	-1.45	1.935	1.542	0.706	-1.378	0.414	0.951	0.496	0.899	9.04
	2.0	70	270	2.792	3.208	69.130	-4.435	50.89	58.47	1260.07	4.43	2486.00	465.00	23.01	-11.17	1.973	1.604	0.640	-10.630	0.390	0.946	1.002	1.000	36.86
						(h1)						2486.00	2021.00											
3	(static)					(h0)								(cmc)										
	0.0	0	0	0.000	0.000	75.950	0.000	0.00	0.00	1384.38	0.00	2679.67	542.67	25.39	0.00	1.936	1.544	0.704	0.000	0.413	0.949	0.513	0.903	16.28
TT2GC	0.1	5	5	0.000	0.000	75.950	0.000	0.00	0.00	1384.38	0.00	2679.67	542.67	25.39	0.00	1.936	1.544	0.704	0.000	0.413	0.949	0.513	0.903	16.28
	0.2	15	20	0.000	0.000	75.950	0.000	0.00	0.00	1384.38	0.00	2679.67	542.67	25.39	0.00	1.936	1.544	0.704	0.000	0.413	0.949	0.513	0.903	16.28
50 kPa	0.4	15	35	0.003	0.003	75.948	-0.003	0.05	0.05	1384.33	0.00	2679.62	542.62	25.39	-0.01	1.936	1.544	0.704	-0.008	0.413	0.949	0.514	0.903	16.30
	0.5	20	55	0.004	0.007	75.944	-0.009	0.07	0.12	1384.26	0.01	2679.55	542.55	25.39	-0.02	1.936	1.544	0.704	-0.021	0.413	0.949	0.514	0.903	16.35
	0.6	15	70	0.002	0.008	75.942	-0.011	0.03	0.15	1384.23	0.01	2679.52	542.52	25.39	-0.03	1.936	1.544	0.704	-0.026	0.413	0.949	0.515	0.903	16.36
	0.8	25	95	0.020	0.028	75.923	-0.036	0.36	0.50	1383.88	0.04	2679.16	542.16	25.37	-0.09	1.936	1.544	0.703	-0.088	0.413	0.949	0.518	0.904	16.58
	1.0	30	125	0.056	0.084	75.867	-0.110	1.02	1.52	1382.86	0.11	2678.14	541.14	25.32	-0.28	1.937	1.545	0.702	-0.266	0.412	0.949	0.528	0.906	17.19
	2.0	35	160	1.544	1.628	74.323	-2.143	28.14	29.67	1354.71	2.14	2650.00	513.00	24.01	-5.47	1.956	1.577	0.667	-5.188	0.400	0.946	0.792	0.958	38.74
						(h1)						2650.00	2137.00											
4	(static)					(h0)								(cmc)										
	0.0	0	0	0.000	0.000	72.479	0.000	0.00	0.00	1321.10	0.00	2574.23	521.23	25.39	0.00	1.949	1.554	0.692	0.000	0.409	0.964	0.600	0.920	30.92
TT1GD	0.1	5	5	0.000	0.000	72.479	0.000	0.00	0.00	1321.10	0.00	2574.23	521.23	25.39	0.00	1.949	1.554	0.692	0.000	0.409	0.964	0.600	0.920	30.92
	0.2	5	10	0.000	0.000	72.479	0.000	0.00	0.00	1321.10	0.00	2574.23	521.23	25.39	0.00	1.949	1.554	0.692	0.000	0.409	0.964	0.600	0.920	30.92
100 kPa	0.4	5	15	0.002	0.002	72.477	-0.003	0.04	0.04	1321.07	0.00	2574.19	521.19	25.39	-0.01	1.949	1.554	0.692	-0.007	0.409	0.964	0.600	0.920	30.95
	0.5	5	20	0.004	0.006	72.473	-0.008	0.06	0.10	1321.00	0.01	2574.13	521.13	25.38	-0.02	1.949	1.554	0.692	-0.019	0.409	0.964	0.601	0.920	31.02
	0.6	5	25	0.002	0.008	72.471	-0.010	0.04	0.14	1320.97	0.01	2574.09	521.09	25.38	-0.03	1.949	1.554	0.692	-0.025	0.409	0.964	0.601	0.920	31.05
	0.8	5	30	0.005	0.012	72.467	-0.017	0.08	0.22	1320.88	0.02	2574.01	521.01	25.38	-0.04	1.949	1.554	0.692	-0.040	0.409	0.964	0.602	0.920	31.14
	1.0	15	45	0.003	0.015	72.464	-0.021	0.05	0.27	1320.83	0.02	2573.96	520.96	25.38	-0.05	1.949	1.554	0.692	-0.051	0.409	0.964	0.603	0.921	31.19
	2.0	55	100	1.424	1.439	71.040	-1.985	25.96	26.23	1294.87	1.99	2548.00	495.00	24.11	-5.03	1.968	1.585	0.659	-4.853	0.397	0.963	0.856	0.971	63.00
						(h1)						2548.00	2053.00											

Table A3.6.1. Data sheet: coarse Leighton Buzzard sand, saturated, 25Hz.

TEST	ACCEL (g)	TIME incr. (mins)	TIME cum. (mins)	SET inc. (mm)	SET cum. (mm)	HEIGHT (mm)	SET (%)	VOL inc. (ml)	VOL cum. (ml)	VOL (ml)	VOL (%)	WET MASS (g)	WATER MASS (g)	M (%)	M CHANGE (%)	BULK DENSE (Mg/m2)	DRY DENSE (Mg/m2)	VOID RATIO (e)	VOID CHANGE (%)	POROS (n)	SAT (Sr)	REL DENSE (Dr)	REL COMP (Cr)	PENE. RESIST (N)
1	(static)					(h0)								(cmc)										
	0.0	0.0	0.0	0.000	0.000	70.938	0.000	0.00	0.00	1293.02	0.00	2524.09	492.09	24.22	0.00	1.952	1.572	0.674	0.000	0.402	0.946	0.573	0.915	9.32
TT1GE	0.1	5.0	5.0	0.000	0.000	70.938	0.000	0.00	0.00	1293.02	0.00	2524.09	492.09	24.22	0.00	1.952	1.572	0.674	0.000	0.402	0.946	0.573	0.915	9.32
	0.2	5.0	10.0	0.000	0.000	70.938	0.000	0.00	0.00	1293.02	0.00	2524.09	492.09	24.22	0.00	1.952	1.572	0.674	0.000	0.402	0.946	0.573	0.915	9.32
	0.3	60.0	70.0	0.000	0.000	70.938	0.000	0.00	0.00	1293.02	0.00	2524.09	492.09	24.22	0.00	1.952	1.572	0.674	0.000	0.402	0.946	0.573	0.915	9.32
10 kPa	0.4	60.0	70.0	0.000	0.000	70.938	0.000	0.00	0.00	1293.02	0.00	2524.09	492.09	24.22	0.00	1.952	1.572	0.674	0.000	0.402	0.946	0.573	0.915	9.32
	0.5	60.0	130.0	0.000	0.000	70.938	0.000	0.00	0.00	1293.02	0.00	2524.09	492.09	24.22	0.00	1.952	1.572	0.674	0.000	0.402	0.946	0.573	0.915	9.32
	0.6	60.0	190.0	0.004	0.004	70.934	-0.006	0.07	0.07	1292.95	0.01	2524.02	492.02	24.21	-0.01	1.952	1.572	0.673	-0.014	0.402	0.946	0.574	0.915	9.34
	0.8	60.0	250.0	0.011	0.015	70.923	-0.021	0.20	0.27	1292.75	0.02	2523.82	491.82	24.20	-0.06	1.952	1.572	0.673	-0.053	0.402	0.946	0.575	0.915	9.39
	1.0	60.0	310.0	0.022	0.037	70.901	-0.052	0.40	0.68	1292.35	0.05	2523.41	491.41	24.18	-0.14	1.953	1.572	0.673	-0.130	0.402	0.946	0.578	0.916	9.49
	2.0	60.0	370.0	1.120	1.157	69.781	-1.631	20.41	21.09	1271.93	1.63	2503.00	471.00	23.18	-4.29	1.968	1.598	0.646	-4.053	0.393	0.943	0.734	0.947	15.28
						(h1)						2503.00	2032.00											
2	(static)					(h0)								(cmc)										
	0.0	0.0	0.0	0.000	0.000	81.529	0.000	0.00	0.00	1486.07	0.00	2863.86	574.86	25.11	0.00	1.927	1.540	0.707	0.000	0.414	0.934	0.374	0.875	5.13
TT1GF	0.1	5.0	5.0	0.000	0.000	81.529	0.000	0.00	0.00	1486.07	0.00	2863.86	574.86	25.11	0.00	1.927	1.540	0.707	0.000	0.414	0.934	0.374	0.875	5.13
	0.2	5.0	10.0	0.000	0.000	81.529	0.000	0.00	0.00	1486.07	0.00	2863.86	574.86	25.11	0.00	1.927	1.540	0.707	0.000	0.414	0.934	0.374	0.875	5.13
	0.3	5.0	15.0	0.000	0.000	81.529	0.000	0.00	0.00	1486.07	0.00	2863.86	574.86	25.11	0.00	1.927	1.540	0.707	0.000	0.414	0.934	0.374	0.875	5.13
20 kPa	0.4	5.0	15.0	0.000	0.000	81.529	0.000	0.00	0.00	1486.07	0.00	2863.86	574.86	25.11	0.00	1.927	1.540	0.707	0.000	0.414	0.934	0.374	0.875	5.13
	0.5	60.0	75.0	0.014	0.014	81.515	-0.017	0.26	0.26	1485.81	0.02	2863.60	574.60	25.10	-0.04	1.927	1.541	0.707	-0.042	0.414	0.934	0.376	0.875	5.18
	0.6	60.0	135.0	0.016	0.030	81.499	-0.037	0.30	0.55	1485.52	0.04	2863.30	574.30	25.09	-0.10	1.927	1.541	0.707	-0.090	0.414	0.934	0.378	0.876	5.24
	0.8	60.0	195.0	0.053	0.083	81.446	-0.102	0.97	1.52	1484.55	0.10	2862.34	573.34	25.05	-0.26	1.928	1.542	0.706	-0.247	0.414	0.933	0.384	0.877	5.42
	1.0	60.0	255.0	0.144	0.227	81.302	-0.279	2.62	4.14	1481.93	0.28	2859.71	570.71	24.93	-0.72	1.930	1.545	0.703	-0.673	0.413	0.933	0.402	0.880	5.93
	2.0	60.0	315.0	1.411	1.638	79.891	-2.009	25.71	29.86	1456.21	2.01	2834.00	545.00	23.81	-5.19	1.946	1.572	0.673	-4.849	0.402	0.930	0.576	0.915	12.17
						(h1)						2834.00	2289.00											
3	(static)					(h0)								(cmc)										
	0.0	0.0	0.0	0.000	0.000	72.912	0.000	0.00	0.00	1329.00	0.00	2603.92	532.92	25.73	0.00	1.959	1.558	0.688	0.000	0.407	0.984	0.490	0.898	14.82
TT1GG	0.1	5.0	5.0	0.000	0.000	72.912	0.000	0.00	0.00	1329.00	0.00	2603.92	532.92	25.73	0.00	1.959	1.558	0.688	0.000	0.407	0.984	0.490	0.898	14.82
	0.2	5.0	10.0	0.000	0.000	72.912	0.000	0.00	0.00	1329.00	0.00	2603.92	532.92	25.73	0.00	1.959	1.558	0.688	0.000	0.407	0.984	0.490	0.898	14.82
	0.3	5.0	15.0	0.000	0.000	72.912	0.000	0.00	0.00	1329.00	0.00	2603.92	532.92	25.73	0.00	1.959	1.558	0.688	0.000	0.407	0.984	0.490	0.898	14.82
50 kPa	0.4	60.0	70.0	0.008	0.008	72.904	-0.012	0.15	0.15	1328.85	0.01	2603.76	532.76	25.72	-0.03	1.959	1.558	0.688	-0.028	0.407	0.984	0.491	0.898	14.89
	0.5	60.0	130.0	0.007	0.015	72.897	-0.021	0.12	0.28	1328.73	0.02	2603.64	532.64	25.72	-0.05	1.959	1.559	0.687	-0.051	0.407	0.984	0.492	0.898	14.94
	0.6	60.0	190.0	0.001	0.016	72.896	-0.022	0.02	0.30	1328.71	0.02	2603.62	532.62	25.72	-0.06	1.960	1.559	0.687	-0.055	0.407	0.984	0.492	0.898	14.95
	0.8	60.0	250.0	0.016	0.032	72.880	-0.044	0.30	0.59	1328.41	0.04	2603.33	532.33	25.70	-0.11	1.960	1.559	0.687	-0.109	0.407	0.984	0.494	0.899	15.09
	1.0	60.0	310.0	0.114	0.146	72.766	-0.201	2.07	2.66	1326.34	0.20	2601.25	530.25	25.60	-0.50	1.961	1.561	0.684	-0.492	0.406	0.984	0.510	0.902	16.05
	2.0	60.0	370.0	1.385	1.532	71.380	-2.101	25.25	27.92	1301.09	2.10	2576.00	505.00	24.38	-5.24	1.980	1.592	0.652	-5.155	0.395	0.983	0.698	0.940	30.12
						(h1)						2576.00	2071.00											
4	(static)					(h0)								(cmc)										
	0.0	0.0	0.0	0.000	0.000	74.487	0.000	0.00	0.00	1357.71	0.00	2655.45	517.45	24.20	0.00	1.956	1.575	0.670	0.000	0.401	0.950	0.593	0.919	30.22
TT1GH	0.1	5.0	5.0	0.000	0.000	74.487	0.000	0.00	0.00	1357.71	0.00	2655.45	517.45	24.20	0.00	1.956	1.575	0.670	0.000	0.401	0.950	0.593	0.919	30.22
	0.2	5.0	10.0	0.000	0.000	74.487	0.000	0.00	0.00	1357.71	0.00	2655.45	517.45	24.20	0.00	1.956	1.575	0.670	0.000	0.401	0.950	0.593	0.919	30.22
	0.3	5.0	15.0	0.000	0.000	74.487	0.000	0.00	0.00	1357.71	0.00	2655.45	517.45	24.20	0.00	1.956	1.575	0.670	0.000	0.401	0.950	0.593	0.919	30.22
100 kPa	0.4	5.0	15.0	0.000	0.000	74.487	0.000	0.00	0.00	1357.71	0.00	2655.45	517.45	24.20	0.00	1.956	1.575	0.670	0.000	0.401	0.950	0.593	0.919	30.22
	0.5	5.0	20.0	0.002	0.002	74.485	-0.003	0.04	0.04	1357.68	0.00	2655.41	517.41	24.20	-0.01	1.956	1.575	0.670	-0.007	0.401	0.950	0.593	0.919	30.25
	0.6	10.0	30.0	0.002	0.004	74.483	-0.005	0.04	0.07	1357.64	0.01	2655.37	517.37	24.20	-0.01	1.956	1.575	0.670	-0.013	0.401	0.950	0.594	0.919	30.28
	0.8	10.0	40.0	0.001	0.005	74.482	-0.007	0.02	0.09	1357.62	0.01	2655.35	517.35	24.20	-0.02	1.956	1.575	0.670	-0.017	0.401	0.950	0.594	0.919	30.29
	1.0	60.0	100.0	0.005	0.010	74.477	-0.013	0.08	0.17	1357.54	0.01	2655.27	517.27	24.19	-0.03	1.956	1.575	0.670	-0.032	0.401	0.950	0.594	0.919	30.35
	2.0	60.0	160.0	0.399	0.409	74.079	-0.548	7.27	7.45	1350.27	0.55	2648.00	510.00	23.85	-1.44	1.961	1.583	0.661	-1.367	0.398	0.949	0.647	0.929	35.96
						(h1)						2648.00	2138.00											

Table A3.6.2. Data sheet: coarse Leighton Buzzard sand, saturated, 40Hz.

TEST	ACCEL (g)	TIME incr. (mins)	TIME cum. (mins)	SET inc. (mm)	SET cum. (mm)	HEIGHT (mm)	SET (%)	VOL inc. (ml)	VOL cum. (ml)	VOL (ml)	VOL (%)	WET MASS (g)	WATER MASS (g)	M (%)	M CHANGE (%)	BULK DENSE (Mg/m2)	DRY DENSE (Mg/m2)	VOID RATIO (e)	VOID CHANGE (%)	POROS (n)	SAT (Sr)	AIR CONT (A)	REL DENSE (Dr)	REL COMP (Cr)	PENE. RESIST (N)
1	(static)					(h0)								(cmc)											
	0.0	0.0	0.0	0.000	0.000	61.260	0.000	0.00	0.00	1116.62	0.00	1708.00	0.00	0.00	0.00	1.530	1.530	0.719	0.000	0.418	0.000	0.418	0.304	0.861	2.62
TT1G1	0.1	5.0	5.0	0.000	0.000	61.260	0.000	0.00	0.00	1116.62	0.00	1708.00	0.00	0.00	0.00	1.530	1.530	0.719	0.000	0.418	0.000	0.418	0.304	0.861	2.62
	0.2	5.0	10.0	0.000	0.000	61.260	0.000	0.00	0.00	1116.62	0.00	1708.00	0.00	0.00	0.00	1.530	1.530	0.719	0.000	0.418	0.000	0.418	0.304	0.861	2.62
10 kPa	0.4	10.0	20.0	0.000	0.000	61.260	0.000	0.00	0.00	1116.62	0.00	1708.00	0.00	0.00	0.00	1.530	1.530	0.719	0.000	0.418	0.000	0.418	0.304	0.861	2.62
	0.5	5.0	25.0	0.000	0.000	61.260	0.000	0.00	0.00	1116.62	0.00	1708.00	0.00	0.00	0.00	1.530	1.530	0.719	0.000	0.418	0.000	0.418	0.304	0.861	2.62
	0.6	5.0	30.0	0.000	0.000	61.260	0.000	0.00	0.00	1116.62	0.00	1708.00	0.00	0.00	0.00	1.530	1.530	0.719	0.000	0.418	0.000	0.418	0.304	0.861	2.62
	0.8	15.0	45.0	0.125	0.125	61.135	-0.204	2.28	2.28	1114.34	0.20	1708.00	0.00	0.00	0.00	1.533	1.533	0.716	-0.488	0.417	0.000	0.417	0.324	0.865	2.98
	1.0	60.0	105.0	0.022	0.147	61.114	-0.239	0.39	2.67	1113.95	0.24	1708.00	0.00	0.00	0.00	1.533	1.533	0.715	-0.572	0.417	0.000	0.417	0.328	0.866	3.05
	2.0	60.0	165.0	1.859	2.006	59.255	-3.274	33.88	36.56	1080.06	3.27	1708.00	0.00	0.00	0.00	1.581	1.581	0.663	-7.825	0.399	0.000	0.399	0.635	0.927	11.43
						(h1)						1708.00	1708.00												

Table A3.6.4. Data sheet: coarse Leighton Buzzard sand, dried, 25Hz.

TEST STRESS MOIST	ACCEL (g)	TIME incr. (mins)	TIME cum. (mins)	SET inc. (mm)	SET cum. (mm)	HEIGHT (mm)	SET (%)	VOL inc. (ml)	VOL cum. (ml)	VOL (ml)	VOL (%)	WET MASS (g)	WATER MASS (g)	M (%)	M CHANGE (%)	BULK DENSE (Mg/m2)	DRY DENSE (Mg/m2)	VOID RATIO (e)	VOID CHANGE (%)	POROS (n)	SAT (Sr)	AIR CONT (A)	REL DENSE (Dr)	REL COMP (Cr)	PENE. RESIST (N)
1	(static)					(h0)								(cmc)				2.630							
	0.0	0.0	0.0	0.000	0.000	66.950	0.000	0.00	0.00	1220.33	0.00	2159.00	235.00	12.21	0.00	1.769	1.577	0.668	0.000	0.401	0.481	0.208	0.605	0.921	10.39
TT1GJ	0.1	5.0	5.0	0.000	0.000	66.950	0.000	0.00	0.00	1220.33	0.00	2159.00	235.00	12.21	0.00	1.769	1.577	0.668	0.000	0.401	0.481	0.208	0.605	0.921	10.39
	0.2	5.0	10.0	0.000	0.000	66.950	0.000	0.00	0.00	1220.33	0.00	2159.00	235.00	12.21	0.00	1.769	1.577	0.668	0.000	0.401	0.481	0.208	0.605	0.921	10.39
10 kPa	0.4	5.0	15.0	0.000	0.000	66.950	0.000	0.00	0.00	1220.33	0.00	2159.00	235.00	12.21	0.00	1.769	1.577	0.668	0.000	0.401	0.481	0.208	0.605	0.921	10.39
	0.5	5.0	20.0	0.000	0.000	66.950	0.000	0.00	0.00	1220.33	0.00	2159.00	235.00	12.21	0.00	1.769	1.577	0.668	0.000	0.401	0.481	0.208	0.605	0.921	10.39
	0.6	10.0	30.0	0.000	0.000	66.950	0.000	0.00	0.00	1220.33	0.00	2159.00	235.00	12.21	0.00	1.769	1.577	0.668	0.000	0.401	0.481	0.208	0.605	0.921	10.39
	0.8	10.0	40.0	0.000	0.000	66.950	0.000	0.00	0.00	1220.33	0.00	2159.00	235.00	12.21	0.00	1.769	1.577	0.668	0.000	0.401	0.481	0.208	0.605	0.921	10.39
	1.0	10.0	50.0	0.006	0.006	66.945	-0.008	0.10	0.10	1220.23	0.01	2159.00	235.00	12.21	0.00	1.769	1.577	0.668	-0.021	0.400	0.481	0.208	0.606	0.921	10.42
	2.0	60.0	110.0	0.192	0.197	66.753	-0.294	3.49	3.59	1216.74	0.29	2159.00	235.00	12.21	0.00	1.774	1.581	0.663	-0.735	0.399	0.484	0.206	0.634	0.927	11.40
						(h1)						2159.00	1924.00												

Table A3.6.3. Data sheet: coarse Leighton Buzzard sand, partially saturated, 25Hz.

TEST	ACCEL (g)	TIME incr. (mins)	TIME cum. (mins)	SET inc. (mm)	SET cum. (mm)	HEIGHT (mm)	SET (%)	VOL inc. (ml)	VOL cum. (ml)	VOL (ml)	VOL (%)	WET MASS (g)	WATER MASS (g)	M (%)	M CHANGE (%)	BULK DENSE (Mg/m2)	DRY DENSE (Mg/m2)	VOID RATIO (e)	VOID CHANGE (%)	POROS (n)	SAT (Sr)	REL DENSE (Dr)	REL COMP (Cr)	PENE RESIST (N)
1	(static)					(h0)								(cmc)										
	0.0	0.0	0.0	0.000	0.000	72.900	0.000	0.00	0.00	1328.79	0.00	2602.36	559.36	27.38	0.00	1.958	1.537	0.711	0.000	0.415	1.013	0.355	0.871	3.584
T1GG	1.0	10.0	10.0	0.270	0.270	72.630	-0.370	4.92	4.92	1323.86	0.37	2597.44	554.44	27.14	-0.88	1.962	1.543	0.704	-0.892	0.413	1.013	0.393	0.879	4.375
	2.0	38.0	48.0	2.050	2.320	70.580	-3.182	37.37	42.29	1286.50	3.19	2560.07	517.07	25.31	-7.56	1.990	1.588	0.656	-7.661	0.396	1.014	0.676	0.935	12.951
10kPa	3.0	50.0	98.0	0.830	3.150	69.750	-4.321	15.13	57.42	1271.37	4.34	2544.94	501.94	24.57	-10.26	2.002	1.607	0.637	-10.402	0.389	1.015	0.790	0.958	17.715
	4.0	30.0	128.0	0.340	3.490	69.410	-4.787	6.20	63.61	1265.17	4.81	2538.74	495.74	24.27	-11.37	2.007	1.615	0.629	-11.525	0.386	1.015	0.837	0.967	19.881
	5.0	15.0	143.0	0.150	3.640	69.260	-4.993	2.73	66.35	1262.44	5.01	2536.01	493.01	24.13	-11.86	2.009	1.618	0.625	-12.020	0.385	1.015	0.858	0.972	20.877
	6.0	20.0	163.0	0.220	3.860	69.040	-5.295	4.01	70.36	1258.43	5.31	2532.00	489.00	23.94	-12.58	2.012	1.623	0.620	-12.747	0.383	1.015	0.888	0.978	22.381
						(h1)						2532.00	2043.00											
2	(static)					(h0)								(cmc)										
	0.0	0.0	0.0	0.000	0.000	72.170	0.000	0.00	0.00	1315.48	0.00	2587.29	566.29	28.02	0.00	1.967	1.536	0.712	0.000	0.416	1.035	0.348	0.870	4.443
T1GH	1.0	10.0	10.0	0.200	0.200	71.970	-0.277	3.65	3.65	1311.83	0.28	2583.64	562.64	27.84	-0.64	1.969	1.541	0.707	-0.666	0.414	1.035	0.376	0.875	5.184
	2.0	35.0	45.0	2.460	2.660	69.510	-3.686	44.84	48.49	1266.99	3.70	2538.80	517.80	25.62	-8.56	2.004	1.595	0.649	-8.863	0.393	1.039	0.719	0.944	18.986
20kPa	3.0	50.0	95.0	1.080	3.740	68.430	-5.182	19.69	68.17	1247.31	5.20	2519.12	498.12	24.65	-12.04	2.020	1.620	0.623	-12.462	0.384	1.040	0.870	0.974	27.780
	4.0	25.0	120.0	0.180	3.920	68.250	-5.432	3.28	71.45	1244.03	5.45	2515.84	494.84	24.48	-12.62	2.022	1.625	0.619	-13.062	0.382	1.040	0.895	0.979	29.408
	5.0	20.0	140.0	0.210	4.130	68.040	-5.723	3.83	75.28	1240.20	5.74	2512.01	491.01	24.30	-13.29	2.025	1.630	0.614	-13.761	0.380	1.041	0.924	0.985	31.366
	6.0	25.0	165.0	0.220	4.350	67.820	-6.027	4.01	79.29	1236.19	6.04	2508.00	487.00	24.10	-14.00	2.029	1.635	0.609	-14.494	0.378	1.041	0.955	0.991	33.484
						(h1)						2508.00	2021.00											
3	(static)					(h0)								(cmc)										
	0.0	0.0	0.0	0.000	0.000	67.940	0.000	0.00	0.00	1238.38	0.00	2440.86	506.86	26.21	0.00	1.971	1.562	0.684	0.000	0.406	1.008	0.512	0.902	16.161
T1GJ	1.0	10.0	10.0	0.010	0.010	67.930	-0.015	0.18	0.18	1238.19	0.01	2440.68	506.68	26.20	-0.04	1.971	1.562	0.684	-0.036	0.406	1.008	0.513	0.903	16.253
	2.0	40.0	50.0	1.360	1.370	66.570	-2.016	24.79	24.97	1213.41	2.02	2415.89	481.89	24.92	-4.93	1.991	1.594	0.650	-4.964	0.394	1.008	0.711	0.942	31.246
50kPa	3.0	30.0	80.0	0.740	2.110	65.830	-3.106	13.49	38.46	1199.92	3.11	2402.40	468.40	24.22	-7.59	2.002	1.612	0.632	-7.646	0.387	1.008	0.819	0.964	41.445
	4.0	25.0	105.0	0.260	2.370	65.570	-3.488	4.74	43.20	1195.18	3.49	2397.67	463.67	23.97	-8.52	2.006	1.618	0.625	-8.588	0.385	1.008	0.857	0.971	45.370
	5.0	20.0	125.0	0.240	2.610	65.330	-3.842	4.37	47.57	1190.80	3.84	2393.29	459.29	23.75	-9.39	2.010	1.624	0.619	-9.458	0.382	1.008	0.892	0.978	49.150
	6.0	20.0	145.0	0.400	3.010	64.930	-4.430	7.29	54.86	1183.51	4.43	2386.00	452.00	23.37	-10.82	2.016	1.634	0.609	-10.907	0.379	1.009	0.950	0.990	55.787
						(h1)						2386.00	1934.00											
4	(static)					(h0)								(cmc)										
	0.0	0.0	0.0	0.000	0.000	70.350	0.000	0.00	0.00	1282.31	0.00	2559.89	518.89	25.42	0.00	1.996	1.592	0.652	0.000	0.395	1.025	0.698	0.940	41.828
T1GI	1.0	10.0	10.0	0.000	0.000	70.350	0.000	0.00	0.00	1282.31	0.00	2559.89	518.89	25.42	0.00	1.996	1.592	0.652	0.000	0.395	1.025	0.698	0.940	41.828
	2.0	30.0	40.0	0.430	0.430	69.920	-0.611	7.84	7.84	1274.47	0.61	2552.06	511.06	25.04	-1.51	2.002	1.601	0.642	-1.548	0.391	1.025	0.757	0.951	49.253
100kPa	3.0	25.0	65.0	0.380	0.810	69.540	-1.151	6.93	14.76	1267.54	1.15	2545.13	504.13	24.70	-2.85	2.008	1.610	0.633	-2.916	0.388	1.026	0.810	0.962	56.319
	4.0	15.0	80.0	0.150	0.960	69.390	-1.365	2.73	17.50	1264.81	1.36	2542.39	501.39	24.57	-3.37	2.010	1.614	0.630	-3.456	0.386	1.026	0.831	0.966	59.238
	5.0	20.0	100.0	0.270	1.230	69.120	-1.748	4.92	22.42	1259.89	1.75	2537.47	496.47	24.33	-4.32	2.014	1.620	0.623	-4.429	0.384	1.026	0.868	0.974	64.679
	6.0	25.0	125.0	0.410	1.640	68.710	-2.331	7.47	29.89	1252.41	2.33	2530.00	489.00	23.96	-5.76	2.020	1.630	0.614	-5.905	0.380	1.027	0.924	0.985	73.399
						(h1)						2530.00	2041.00											
5	(static)					(h0)								(cmc)										
	0.0	0.0	0.0	0.000	0.000	77.075	0.000	0.00	0.00	1404.89	0.00	2768.69	579.69	26.48	0.00	1.971	1.558	0.688	0.000	0.408	1.012	0.489	0.898	14.752
T1GK	1.0	0.0	0.0	0.000	0.000	77.075	0.000	0.00	0.00	1404.89	0.00	2768.69	579.69	26.48	0.00	1.971	1.558	0.688	0.000	0.408	1.012	0.489	0.898	14.752
	2.0	0.0	0.0	0.000	0.000	77.075	0.000	0.00	0.00	1404.89	0.00	2768.69	579.69	26.48	0.00	1.971	1.558	0.688	0.000	0.408	1.012	0.489	0.898	14.752
50kPa	3.0	0.0	0.0	0.000	0.000	77.075	0.000	0.00	0.00	1404.89	0.00	2768.69	579.69	26.48	0.00	1.971	1.558	0.688	0.000	0.408	1.012	0.489	0.898	14.752
	4.0	0.0	0.0	0.000	0.000	77.075	0.000	0.00	0.00	1404.89	0.00	2768.69	579.69	26.48	0.00	1.971	1.558	0.688	0.000	0.408	1.012	0.489	0.898	14.752
	5.0	0.0	0.0	0.000	0.000	77.075	0.000	0.00	0.00	1404.89	0.00	2768.69	579.69	26.48	0.00	1.971	1.558	0.688	0.000	0.408	1.012	0.489	0.898	14.752
	6.0	55.0	55.0	3.220	3.220	73.855	4.178	58.69	58.69	1346.19	4.18	2710.00	521.00	23.80	-10.12	2.013	1.626	0.617	-10.251	0.382	1.014	0.904	0.981	50.419
						(h1)						2710.00	2189.00											

TableA3.6.5. Data sheet: coarse Leighton Buzzard sand, high accelereation, saturated, 25Hz.

TEST	ACCEL (g)	TIME incr. (mins)	TIME cum. (mins)	SET inc. (mm)	SET cum. (mm)	HEIGHT (mm)	SET (%)	VOL inc. (ml)	VOL cum. (ml)	VOL (ml)	VOL (%)	WET MASS (g)	WATER MASS (g)	M (%)	M CHANGE (%)	BULK DENSE (Mg/m2)	DRY DENSE (Mg/m2)	VOID RATIO (e)	VOID CHANGE (%)	POROS (n)	SAT (Sr)	REL DENSE (Dr)	REL COMP (Cr)	PENE RESIST
1	(static)					(h0)								(cmc)										
1 MIN	0.0	0.0	0.0	0.000	0.000	74.990	0.000	0.00	0.00	1366.88	0.00	2674.39	573.39	27.29	0.00	1.957	1.537	0.711	0.000	0.416	1.009	0.353	0.871	7.683
T1GA	1.0	1.0	1.0	0.060	0.060	74.930	-0.080	1.09	1.09	1365.79	0.08	2673.30	572.30	27.24	-0.19	1.957	1.538	0.710	-0.193	0.415	1.009	0.361	0.872	8.038
	2.0	1.0	2.0	1.370	1.430	73.560	-1.907	24.97	26.07	1340.82	1.91	2648.33	547.33	26.05	-4.55	1.975	1.567	0.678	-4.589	0.404	1.010	0.545	0.909	18.319
50kPa	3.0	1.0	3.0	0.450	1.880	73.110	-2.507	8.20	34.27	1332.61	2.51	2640.12	539.12	25.66	-5.98	1.981	1.577	0.668	-6.033	0.401	1.010	0.605	0.921	22.608
	4.0	1.0	4.0	0.270	2.150	72.840	-2.867	4.92	39.19	1327.69	2.87	2635.20	534.20	25.43	-6.83	1.985	1.582	0.662	-6.899	0.398	1.010	0.641	0.928	25.397
	5.0	1.0	5.0	0.250	2.400	72.590	-3.200	4.56	43.75	1323.13	3.20	2630.65	529.65	25.21	-7.63	1.988	1.588	0.656	-7.701	0.396	1.010	0.675	0.935	28.125
	6.0	1.0	6.0	0.200	2.600	72.390	-3.467	3.65	47.39	1319.49	3.47	2627.00	526.00	25.04	-8.27	1.991	1.592	0.652	-8.343	0.395	1.010	0.702	0.940	30.407
						(h1)						2627.00	2101.00											
2	(static)					(h0)								(cmc)										
2 MIN	0.0	0.0	0.0	0.000	0.000	77.070	0.000	0.00	0.00	1404.79	0.00	2717.85	543.85	25.02	0.00	1.935	1.548	0.699	0.000	0.412	0.941	0.421	0.884	10.940
T1GB	1.0	2.0	2.0	0.020	0.020	77.050	-0.026	0.36	0.36	1404.43	0.03	2717.49	543.49	25.00	-0.07	1.935	1.548	0.699	-0.063	0.411	0.941	0.423	0.885	11.075
	2.0	2.0	4.0	1.200	1.220	75.850	-1.583	21.87	22.24	1382.56	1.58	2695.62	521.62	23.99	-4.09	1.950	1.572	0.673	-3.846	0.402	0.938	0.579	0.916	20.713
50kPa	3.0	2.0	6.0	0.580	1.800	75.270	-2.336	10.57	32.81	1371.98	2.34	2685.05	511.05	23.51	-6.03	1.957	1.585	0.660	-5.675	0.398	0.937	0.654	0.931	26.444
	4.0	2.0	8.0	0.340	2.140	74.930	-2.777	6.20	39.01	1365.79	2.78	2678.85	504.85	23.22	-7.17	1.961	1.592	0.652	-6.747	0.395	0.936	0.698	0.940	30.129
	5.0	2.0	10.0	0.340	2.480	74.590	-3.218	6.20	45.20	1359.59	3.22	2672.65	498.65	22.94	-8.31	1.966	1.599	0.645	-7.818	0.392	0.936	0.743	0.949	34.053
	6.0	2.0	12.0	0.310	2.790	74.280	-3.620	5.65	50.85	1353.94	3.62	2667.00	493.00	22.68	-9.35	1.970	1.606	0.638	-8.796	0.389	0.935	0.783	0.957	37.841
						(h1)						2667.00	2174.00											
3	(static)					(h0)								(cmc)										
5 MIN	0.0	0.0	0.0	0.000	0.000	73.390	0.000	0.00	0.00	1337.72	0.00	2649.87	572.87	27.58	0.00	1.981	1.553	0.694	0.000	0.410	1.045	0.454	0.891	12.709
T1GE	1.0	5.0	5.0	0.020	0.020	73.370	-0.027	0.36	0.36	1337.35	0.03	2649.51	572.51	27.56	-0.06	1.981	1.553	0.693	-0.067	0.409	1.045	0.456	0.891	12.861
	2.0	5.0	10.0	1.510	1.530	71.860	-2.085	27.52	27.89	1309.83	2.09	2621.99	544.99	26.24	-4.87	2.002	1.586	0.659	-5.089	0.397	1.048	0.661	0.932	27.013
50kPa	3.0	5.0	15.0	0.630	2.160	71.230	-2.943	11.48	39.37	1298.35	2.94	2610.50	533.50	25.69	-6.87	2.011	1.600	0.644	-7.185	0.392	1.049	0.747	0.949	34.452
	4.0	5.0	20.0	0.400	2.560	70.830	-3.488	7.29	46.66	1291.05	3.49	2603.21	526.21	25.34	-8.15	2.016	1.609	0.635	-8.515	0.388	1.050	0.801	0.960	39.644
	5.0	5.0	25.0	0.380	2.940	70.450	-4.006	6.93	53.59	1284.13	4.01	2596.29	519.29	25.00	-9.35	2.022	1.617	0.626	-9.779	0.385	1.050	0.853	0.971	44.915
	6.0	5.0	30.0	0.290	3.230	70.160	-4.401	5.29	58.87	1278.84	4.40	2591.00	514.00	24.75	-10.28	2.026	1.624	0.619	-10.744	0.382	1.051	0.892	0.978	49.158
						(h1)						2591.00	2077.00											

Table A3.6.6. Data sheet: coarse Leighton Buzzard sand, high acceleration, saturated, 25Hz. Fixed time length per vibration increment.

TEST	ACCEL (g)	TIME incr. (mins)	TIME cum. (mins)	SET inc. (mm)	SET cum. (mm)	HEIGHT (mm)	SET (%)	VOL inc. (ml)	VOL cum. (ml)	VOL (ml)	VOL (%)	WET MASS (g)	WATER MASS (g)	M (%)	M CHANGE (%)	BULK DENSE (Mg/m2)	DRY DENSE (Mg/m2)	VOID RATIO (e)	VOID CHANGE (%)	POROS (n)	SAT (Sr)	REL DENSE (Dr)	REL COMP (Cr)	PENE RESIST
4	(static)					(h0)								(cmc)										
10 MIN	0.0	0.0	0.0	0.000	0.000	74.240	0.000	0.00	0.00	1353.21	0.00	2676.97	586.97	28.08	0.00	1.978	1.544	0.703	0.000	0.413	1.051	0.401	0.880	9.927
T1GD	1.0	10.0	10.0	0.050	0.050	74.190	-0.067	0.91	0.91	1352.30	0.07	2676.06	586.06	28.04	-0.16	1.979	1.546	0.702	-0.163	0.412	1.051	0.408	0.882	10.264
	2.0	10.0	20.0	1.660	1.710	72.530	-2.303	30.26	31.17	1322.04	2.30	2645.80	555.80	26.59	-5.31	2.001	1.581	0.664	-5.581	0.399	1.054	0.632	0.926	24.640
50kPa	3.0	10.0	30.0	0.580	2.290	71.950	-3.085	10.57	41.74	1311.47	3.09	2635.23	545.23	26.09	-7.11	2.009	1.594	0.650	-7.473	0.394	1.055	0.710	0.942	31.124
	4.0	10.0	40.0	0.370	2.660	71.580	-3.583	6.74	48.49	1304.73	3.59	2628.48	538.48	25.76	-8.26	2.015	1.602	0.642	-8.681	0.391	1.056	0.760	0.952	35.655
	5.0	10.0	50.0	0.300	2.960	71.280	-3.987	5.47	53.95	1299.26	3.99	2623.02	533.02	25.50	-9.19	2.019	1.609	0.635	-9.660	0.388	1.056	0.800	0.960	39.555
	6.0	10.0	60.0	0.330	3.290	70.950	-4.432	6.02	59.97	1293.24	4.43	2617.00	527.00	25.22	-10.22	2.024	1.616	0.627	-10.737	0.386	1.057	0.845	0.969	44.079
						(h1)						2617.00	2090.00											
5	(static)					(h0)								(cmc)										
20 MIN	0.0	0.0	0.0	0.000	0.000	72.760	0.000	0.00	0.00	1326.23	0.00	2582.98	560.98	27.74	0.00	1.948	1.525	0.725	0.000	0.420	1.006	0.270	0.854	4.518
T2GF	1.0	20.0	20.0	0.130	0.130	72.630	0.179	2.37	2.37	1323.86	0.18	2580.61	558.61	27.63	-0.42	1.949	1.527	0.722	-0.425	0.419	1.006	0.289	0.858	5.144
	2.0	20.0	40.0	1.560	1.690	71.070	2.323	28.43	30.80	1295.43	2.33	2552.18	530.18	26.22	-5.49	1.970	1.561	0.685	-5.526	0.407	1.007	0.506	0.901	15.822
50kPa	3.0	20.0	60.0	0.720	2.410	70.350	3.312	13.12	43.93	1282.31	3.32	2539.06	517.06	25.57	-7.83	1.980	1.577	0.668	-7.881	0.400	1.007	0.607	0.921	22.722
	4.0	20.0	80.0	0.460	2.870	69.890	3.944	8.38	52.31	1273.92	3.95	2530.67	508.67	25.16	-9.33	1.987	1.587	0.657	-9.385	0.396	1.007	0.671	0.934	27.783
	5.0	20.0	100.0	0.380	3.250	69.510	4.467	6.93	59.24	1266.99	4.47	2523.74	501.74	24.81	-10.56	1.992	1.596	0.648	-10.628	0.393	1.007	0.724	0.945	32.347
	6.0	20.0	120.0	0.370	3.620	69.140	4.975	6.74	65.98	1260.25	4.98	2517.00	495.00	24.48	-11.76	1.997	1.604	0.639	-11.837	0.390	1.007	0.775	0.955	37.124
						(h1)						2517.00	2022.00											
6	(static)					(h0)								(cmc)										
50 MIN	0.0	0.0	0.0	0.000	0.000	68.960	0.000	0.00	0.00	1256.97	0.00	2436.74	499.74	25.80	0.00	1.939	1.541	0.707	0.000	0.414	0.960	0.378	0.876	8.842
T1GC	1.0	50.0	50.0	0.200	0.200	68.760	0.290	3.65	3.65	1253.32	0.29	2433.10	496.10	25.61	-0.73	1.941	1.545	0.702	-3.213	0.412	0.960	0.408	0.882	10.256
	2.0	50.0	100.0	2.040	2.240	66.720	3.248	37.18	40.83	1216.14	3.26	2395.91	458.91	23.69	-8.17	1.970	1.593	0.651	-10.177	0.394	0.957	0.704	0.941	30.652
50kPa	3.0	50.0	150.0	1.010	3.250	65.710	4.713	18.41	59.24	1197.73	4.73	2377.50	440.50	22.74	-11.85	1.985	1.617	0.626	-13.625	0.385	0.955	0.852	0.970	44.782
	4.0	50.0	200.0	0.380	3.630	65.330	5.264	6.93	66.17	1190.80	5.28	2370.58	433.58	22.38	-13.24	1.991	1.627	0.617	-14.922	0.382	0.954	0.907	0.981	50.789
	5.0	50.0	250.0	0.440	4.070	64.890	5.902	8.02	74.19	1182.78	5.92	2362.56	425.56	21.97	-14.84	1.997	1.638	0.606	-16.424	0.377	0.954	0.971	0.994	58.218
	6.0	50.0	300.0	0.210	4.280	64.680	6.206	3.83	78.01	1178.96	6.22	2358.73	421.73	21.77	-15.61	2.001	1.643	0.601	-17.140	0.375	0.953	1.001	1.000	61.942
						(h1)						2395.00	1937.00											

Table A3.6.6 (cont). Data sheet: coarse Leighton Buzzard sand, high acceleration, saturated, 25Hz. Fixed time length per vibration increment.

TEST	ACCEL. (g)	TIME incr. (mins)	TIME cum. (mins)	SET. inc. (mm)	SET. cum. (mm)	HEIGHT (mm)	SET. (%)	VOL. inc. (ml)	VOL. cum. (ml)	VOL. (ml)	VOL. (%)	WET MASS (g)	WATER MASS (g)	M (%)	M CHANGE (%)	BULK DENSE. (Mg/m2)	DRY DENSE. (Mg/m2)	VOID RATIO (e)	VOID CHANGE (%)	POROS. (n)	SAT. (Sr)	REL. DENSE. (Dr)	REL. COMP. (Cr)	PENE. RESIST. (N)
1	(static)					(h0)								(cmc)										
	0.0	0	0	0.000	0.000	81.372	0.000	0.00	0.00	1483.21	0.00	2922.26	613.26	26.56	0.00	1.970	1.557	0.702	0.000	0.413	1.002	0.350	0.870	3.48
TT1CA	0.1	25	25	0.001	0.001	81.372	-0.001	0.01	0.01	1483.20	0.00	2922.25	613.25	26.56	0.00	1.970	1.557	0.702	-0.001	0.413	1.002	0.350	0.870	3.48
	0.2	20	45	0.000	0.001	81.372	-0.001	0.00	0.01	1483.20	0.00	2922.25	613.25	26.56	0.00	1.970	1.557	0.702	-0.001	0.413	1.002	0.350	0.870	3.48
10 kPa	0.4	90	135	0.167	0.167	81.205	-0.205	3.03	3.04	1480.16	0.21	2919.21	610.21	26.43	-0.50	1.972	1.560	0.699	-0.497	0.411	1.002	0.359	0.872	3.65
	0.5	70	205	0.160	0.327	81.045	-0.402	2.92	5.96	1477.25	0.40	2916.30	607.30	26.30	-0.97	1.974	1.563	0.695	-0.974	0.410	1.002	0.367	0.873	3.82
	0.6	85	290	0.186	0.513	80.859	-0.630	3.39	9.35	1473.86	0.63	2912.91	603.91	26.15	-1.52	1.976	1.567	0.692	-1.528	0.409	1.002	0.376	0.875	4.01
	0.8	90	380	0.249	0.762	80.610	-0.936	4.54	13.89	1469.32	0.94	2908.37	599.37	25.96	-2.26	1.979	1.571	0.686	-2.270	0.407	1.002	0.389	0.878	4.28
	1.0	50	430	0.148	0.910	80.462	-1.118	2.70	16.59	1466.62	1.12	2905.67	596.67	25.84	-2.70	1.981	1.574	0.683	-2.711	0.406	1.002	0.396	0.879	4.45
	2.0	120	550	4.316	5.226	76.146	-6.422	78.67	95.26	1387.95	6.42	2827.00	518.00	22.43	-15.53	2.037	1.664	0.593	-15.568	0.372	1.003	0.613	0.923	10.66
						(h1)						2827.00	2309.00											
2	(static)					(h0)								(cmc)										
	0.0	0	0	0.000	0.000	75.386	0.000	0.00	0.00	1374.10	0.00	2679.85	558.85	26.35	0.00	1.950	1.544	0.717	0.000	0.418	0.974	0.315	0.863	3.65
TT1CB	0.1	10	10	0.000	0.000	75.386	0.000	0.00	0.00	1374.10	0.00	2679.85	558.85	26.35	0.00	1.950	1.544	0.717	0.000	0.418	0.974	0.315	0.863	3.65
	0.2	20	30	0.001	0.001	75.385	-0.001	0.02	0.02	1374.08	0.00	2679.83	558.83	26.35	0.00	1.950	1.544	0.717	-0.003	0.418	0.974	0.315	0.863	3.65
20 kPa	0.4	70	100	0.063	0.064	75.323	-0.084	1.14	1.16	1372.94	0.08	2678.69	557.69	26.29	-0.21	1.951	1.545	0.715	-0.202	0.417	0.974	0.319	0.864	3.73
	0.5	50	150	0.096	0.160	75.227	-0.212	1.75	2.91	1371.19	0.21	2676.94	555.94	26.21	-0.52	1.952	1.547	0.713	-0.507	0.416	0.974	0.324	0.865	3.86
	0.6	100	250	0.156	0.316	75.071	-0.419	2.84	5.75	1368.35	0.42	2674.10	553.10	26.08	-1.03	1.954	1.550	0.710	-1.002	0.415	0.974	0.333	0.867	4.06
	0.8	120	370	0.263	0.579	74.808	-0.767	4.79	10.54	1363.55	0.77	2669.30	548.30	25.85	-1.89	1.958	1.555	0.704	-1.838	0.413	0.974	0.347	0.869	4.42
	1.0	95	465	0.196	0.775	74.612	-1.027	3.57	14.12	1359.98	1.03	2665.73	544.73	25.68	-2.53	1.960	1.560	0.699	-2.461	0.411	0.973	0.358	0.872	4.70
	2.0	160	625	4.045	4.820	70.567	-6.393	73.73	87.85	1286.25	6.39	2592.00	471.00	22.21	-15.72	2.015	1.649	0.607	-15.312	0.378	0.969	0.579	0.916	12.32
						(h1)						2592.00	2121.00											
3	(static)					(h0)								(cmc)										
	0.0	0	0	0.000	0.000	72.663	0.000	0.00	0.00	1324.47	0.00	2609.60	541.60	26.19	0.00	1.970	1.561	0.697	0.000	0.411	0.995	0.362	0.872	8.11
TT1CC	0.1	10	10	0.000	0.000	72.663	0.000	0.00	0.00	1324.47	0.00	2609.60	541.60	26.19	0.00	1.970	1.561	0.697	0.000	0.411	0.995	0.362	0.872	8.11
	0.2	10	20	0.000	0.000	72.663	0.000	0.00	0.00	1324.47	0.00	2609.60	541.60	26.19	0.00	1.970	1.561	0.697	0.000	0.411	0.995	0.362	0.872	8.11
50 kPa	0.4	10	30	0.000	0.000	72.663	0.000	0.00	0.00	1324.47	0.00	2609.60	541.60	26.19	0.00	1.970	1.561	0.697	0.000	0.411	0.995	0.362	0.872	8.11
	0.5	185	215	0.000	0.000	72.663	0.000	0.00	0.00	1324.47	0.00	2609.60	541.60	26.19	0.00	1.970	1.561	0.697	0.000	0.411	0.995	0.362	0.872	8.11
	0.6	55	270	0.166	0.166	72.497	-0.228	3.03	3.03	1321.44	0.23	2606.57	538.57	26.04	-0.56	1.973	1.565	0.693	-0.556	0.409	0.995	0.372	0.874	8.54
	0.8	75	345	0.199	0.365	72.298	-0.502	3.63	6.65	1317.81	0.50	2602.95	534.95	25.87	-1.23	1.975	1.569	0.689	-1.223	0.408	0.995	0.383	0.877	9.06
	1.0	95	440	0.266	0.631	72.032	-0.868	4.85	11.50	1312.96	0.87	2598.10	530.10	25.63	-2.12	1.979	1.575	0.682	-2.114	0.406	0.995	0.398	0.880	9.78
	2.0	125	565	3.352	3.983	68.680	-5.481	61.10	72.60	1251.87	5.48	2537.00	469.00	22.68	-13.40	2.027	1.652	0.604	-13.343	0.377	0.995	0.586	0.917	21.22
						(h1)						2537.00	2068.00											
4	(static)					(h0)								(cmc)										
	0.0	0	0	0.000	0.000	76.947	0.000	0.00	0.00	1402.55	0.00	2779.61	543.61	24.31	0.00	1.982	1.594	0.662	0.000	0.398	0.973	0.447	0.889	17.12
TT1CD	0.1	5	5	0.000	0.000	76.947	0.000	0.00	0.00	1402.55	0.00	2779.61	543.61	24.31	0.00	1.982	1.594	0.662	0.000	0.398	0.973	0.447	0.889	17.12
	0.2	5	10	0.000	0.000	76.947	0.000	0.00	0.00	1402.55	0.00	2779.61	543.61	24.31	0.00	1.982	1.594	0.662	0.000	0.398	0.973	0.447	0.889	17.12
100 kPa	0.4	5	15	0.000	0.000	76.947	0.000	0.00	0.00	1402.55	0.00	2779.61	543.61	24.31	0.00	1.982	1.594	0.662	0.000	0.398	0.973	0.447	0.889	17.12
	0.5	5	20	0.000	0.000	76.947	0.000	0.00	0.00	1402.55	0.00	2779.61	543.61	24.31	0.00	1.982	1.594	0.662	0.000	0.398	0.973	0.447	0.889	17.12
	0.6	5	25	0.000	0.000	76.947	0.000	0.00	0.00	1402.55	0.00	2779.61	543.61	24.31	0.00	1.982	1.594	0.662	0.000	0.398	0.973	0.447	0.889	17.12
	0.8	30	55	0.016	0.016	76.932	-0.020	0.28	0.28	1402.27	0.02	2779.33	543.33	24.30	-0.05	1.982	1.595	0.662	-0.051	0.398	0.973	0.447	0.889	17.19
	1.0	35	90	0.033	0.048	76.899	-0.062	0.59	0.87	1401.68	0.06	2778.73	542.73	24.27	-0.16	1.982	1.595	0.661	-0.157	0.398	0.973	0.449	0.890	17.32
	2.0	150	240	2.509	2.557	74.390	-3.323	45.73	46.61	1355.94	3.32	2733.00	497.00	22.23	-8.57	2.016	1.649	0.607	-8.341	0.378	0.970	0.579	0.916	28.82
						(h1)						2733.00	2236.00											

Table.A3.7.1. Data sheet : medium sharp sand; 25Hz, saturated.

TEST	ACCEL (g)	TIME incr. (mins)	TIME cum. (mins)	SET inc. (mm)	SET cum. (mm)	HEIGHT (mm)	SET (%)	VOL inc. (ml)	VOL cum. (ml)	VOL (ml)	VOL (%)	WET MASS (g)	WATER MASS (g)	M (%)	M CHANGE (%)	BULK DENSE (Mg/m2)	DRY DENSE (Mg/m2)	VOID RATIO (e)	VOID CHANGE (%)	POROS (n)	SAT (Sr)	REL DENSE (Dr)	REL COMP (Cr)	PENE. RESIST (N)
1	(static)					(h0)								(cmc)										
	0.0	0.0	0.0	0.000	0.000	81.116	0.000	0.00	0.00	1478.54	0.00	2864.43	617.43	27.48	0.00	1.937	1.520	0.744	0.000	0.427	0.979	0.251	0.850	1.78
TT1CE	0.1	5.0	5.0	0.000	0.000	81.116	0.000	0.00	0.00	1478.54	0.00	2864.43	617.43	27.48	0.00	1.937	1.520	0.744	0.000	0.427	0.979	0.251	0.850	1.78
	0.2	120.0	125.0	0.057	0.057	81.059	-0.071	1.04	1.04	1477.50	0.07	2863.39	616.39	27.43	-0.17	1.938	1.521	0.742	-0.166	0.426	0.979	0.254	0.851	1.82
	0.3	120.0	245.0	0.254	0.311	80.805	-0.384	4.63	5.67	1472.87	0.38	2858.76	611.76	27.23	-0.92	1.941	1.526	0.737	-0.900	0.424	0.979	0.267	0.853	2.02
10 kPa	0.4	120.0	365.0	0.259	0.570	80.546	-0.703	4.72	5.77	1468.15	0.39	2858.67	611.67	27.22	-0.93	1.947	1.531	0.731	-1.648	0.422	0.986	0.280	0.856	2.23
	0.5	120.0	485.0	0.224	0.794	80.322	-0.979	4.08	9.85	1464.06	0.67	2854.58	607.58	27.04	-1.60	1.950	1.535	0.727	-2.296	0.421	0.986	0.292	0.858	2.41
	0.6	120.0	605.0	0.291	1.085	80.031	-1.338	5.30	15.15	1458.76	1.02	2849.28	602.28	26.80	-2.45	1.953	1.540	0.720	-3.137	0.419	0.986	0.307	0.861	2.67
	0.8	120.0	725.0	0.421	1.506	79.610	-1.857	7.67	22.83	1451.09	1.54	2841.61	594.61	26.46	-3.70	1.958	1.548	0.711	-4.354	0.416	0.986	0.329	0.866	3.06
	1.0	120.0	845.0	0.466	1.972	79.144	-2.431	8.49	31.32	1442.59	2.12	2833.11	586.11	26.08	-5.07	1.964	1.558	0.701	-5.701	0.412	0.986	0.353	0.871	3.53
	2.0	120.0	965.0	3.243	5.215	75.901	-6.429	59.11	90.43	1383.48	6.12	2774.00	527.00	23.45	-14.65	2.005	1.624	0.632	-15.074	0.387	0.984	0.520	0.904	7.68
						(h1)						2774.00	2247.00											
2	(static)					(h0)								(cmc)										
	0.0	0.0	0.0	0.000	0.000	78.821	0.000	0.00	0.00	1436.71	0.00	2811.34	587.34	26.41	0.00	1.957	1.548	0.712	0.000	0.416	0.983	0.327	0.865	3.93
TT1CF	0.1	5.0	5.0	0.000	0.000	78.821	0.000	0.00	0.00	1436.71	0.00	2811.34	587.34	26.41	0.00	1.957	1.548	0.712	0.000	0.416	0.983	0.327	0.865	3.93
	0.2	5.0	10.0	0.000	0.000	78.821	0.000	0.00	0.00	1436.71	0.00	2811.34	587.34	26.41	0.00	1.957	1.548	0.712	0.000	0.416	0.983	0.327	0.865	3.93
	0.3	35.0	45.0	0.000	0.000	78.821	0.000	0.00	0.00	1436.71	0.00	2811.34	587.34	26.41	0.00	1.957	1.548	0.712	0.000	0.416	0.983	0.327	0.865	3.93
20 kPa	0.4	120.0	130.0	0.079	0.079	78.742	-0.100	1.43	1.43	1435.28	0.10	2809.91	585.91	26.34	-0.24	1.958	1.550	0.710	-0.240	0.415	0.983	0.331	0.866	4.03
	0.5	120.0	250.0	0.136	0.215	78.606	-0.273	2.48	3.92	1432.80	0.27	2807.42	583.42	26.23	-0.67	1.959	1.552	0.707	-0.655	0.414	0.983	0.338	0.868	4.21
	0.6	120.0	370.0	0.179	0.394	78.427	-0.499	3.26	7.17	1429.54	0.50	2804.17	580.17	26.09	-1.22	1.962	1.556	0.703	-1.201	0.413	0.983	0.348	0.870	4.44
	0.8	120.0	490.0	0.278	0.671	78.150	-0.852	5.06	12.23	1424.48	0.85	2799.11	575.11	25.86	-2.08	1.965	1.561	0.697	-2.048	0.411	0.983	0.362	0.872	4.82
	1.0	120.0	610.0	0.400	1.071	77.750	-1.359	7.29	19.53	1417.18	1.36	2791.81	567.81	25.53	-3.32	1.970	1.569	0.689	-3.268	0.408	0.982	0.383	0.877	5.39
	2.0	120.0	730.0	2.788	3.859	74.962	-4.896	50.81	70.34	1366.37	4.90	2741.00	517.00	23.25	-11.98	2.006	1.628	0.628	-11.773	0.386	0.981	0.529	0.906	10.27
						(h1)						2741.00	2224.00											
3	(static)					(h0)								(cmc)										
	0.0	0.0	0.0	0.000	0.000	81.790	0.000	0.00	0.00	1490.83	0.00	2926.53	588.53	25.17	0.00	1.963	1.568	0.690	0.000	0.408	0.967	0.380	0.876	8.93
TT1CG	0.1	0.0	0.0	0.000	0.000	81.790	0.000	0.00	0.00	1490.83	0.00	2926.53	588.53	25.17	0.00	1.963	1.568	0.690	0.000	0.408	0.967	0.380	0.876	8.93
	0.2	0.0	0.0	0.000	0.000	81.790	0.000	0.00	0.00	1490.83	0.00	2926.53	588.53	25.17	0.00	1.963	1.568	0.690	0.000	0.408	0.967	0.380	0.876	8.93
	0.3	0.0	0.0	0.000	0.000	81.790	0.000	0.00	0.00	1490.83	0.00	2926.53	588.53	25.17	0.00	1.963	1.568	0.690	0.000	0.408	0.967	0.380	0.876	8.93
50 kPa	0.4	30.0	30.0	0.006	0.006	81.784	-0.007	0.11	0.11	1490.72	0.01	2926.43	588.43	25.17	-0.02	1.963	1.568	0.690	-0.018	0.408	0.967	0.381	0.876	8.95
	0.5	120.0	150.0	0.007	0.013	81.777	-0.016	0.13	0.24	1490.59	0.02	2926.29	588.29	25.16	-0.04	1.963	1.569	0.690	-0.040	0.408	0.967	0.381	0.876	8.97
	0.6	120.0	270.0	0.025	0.038	81.752	-0.047	0.46	0.70	1490.13	0.05	2925.84	587.84	25.14	-0.12	1.963	1.569	0.689	-0.114	0.408	0.967	0.382	0.876	9.02
	0.8	120.0	390.0	0.089	0.127	81.663	-0.155	1.62	2.31	1488.51	0.16	2924.22	586.22	25.07	-0.39	1.965	1.571	0.687	-0.380	0.407	0.967	0.387	0.877	9.23
	1.0	120.0	510.0	0.187	0.314	81.477	-0.383	3.40	5.71	1485.11	0.38	2920.82	582.82	24.93	-0.97	1.967	1.574	0.683	-0.939	0.406	0.967	0.396	0.879	9.68
	2.0	120.0	630.0	2.843	3.156	78.634	-3.859	51.82	57.53	1433.29	3.86	2869.00	531.00	22.71	-9.78	2.002	1.631	0.625	-9.454	0.384	0.964	0.537	0.907	17.82
						(h1)						2869.00	2338.00											
4	(static)					(h0)								(cmc)										
	0.0	0.0	0.0	0.000	0.000	80.480	0.000	0.00	0.00	1466.95	0.00	2926.03	577.03	24.56	0.00	1.995	1.601	0.655	0.000	0.396	0.994	0.464	0.893	18.50
TT1CH	0.1	0.0	0.0	0.000	0.000	80.480	0.000	0.00	0.00	1466.95	0.00	2926.03	577.03	24.56	0.00	1.995	1.601	0.655	0.000	0.396	0.994	0.464	0.893	18.50
	0.2	0.0	0.0	0.000	0.000	80.480	0.000	0.00	0.00	1466.95	0.00	2926.03	577.03	24.56	0.00	1.995	1.601	0.655	0.000	0.396	0.994	0.464	0.893	18.50
	0.3	0.0	0.0	0.000	0.000	80.480	0.000	0.00	0.00	1466.95	0.00	2926.03	577.03	24.56	0.00	1.995	1.601	0.655	0.000	0.396	0.994	0.464	0.893	18.50
100 kPa	0.4	5.0	5.0	0.000	0.000	80.480	0.000	0.00	0.00	1466.95	0.00	2926.03	577.03	24.56	0.00	1.995	1.601	0.655	0.000	0.396	0.994	0.464	0.893	18.50
	0.5	10.0	15.0	0.004	0.004	80.476	-0.004	0.07	0.07	1466.88	0.00	2925.96	576.96	24.56	-0.01	1.995	1.601	0.655	-0.011	0.396	0.994	0.464	0.893	18.51
	0.6	10.0	25.0	0.003	0.006	80.474	-0.008	0.05	0.12	1466.83	0.01	2925.91	576.91	24.56	-0.02	1.995	1.601	0.655	-0.020	0.396	0.994	0.464	0.893	18.52
	0.8	120.0	145.0	0.050	0.056	80.424	-0.070	0.91	1.02	1465.93	0.07	2925.00	576.00	24.52	-0.18	1.995	1.602	0.654	-0.176	0.395	0.994	0.467	0.893	18.72
	1.0	120.0	265.0	0.081	0.138	80.343	-0.171	1.48	2.51	1464.44	0.17	2923.52	574.52	24.46	-0.43	1.996	1.604	0.652	-0.432	0.395	0.994	0.471	0.894	19.05
	2.0	120.0	385.0	2.443	2.580	77.900	-3.206	44.52	47.03	1419.92	3.21	2879.00	530.00	22.56	-8.15	2.028	1.654	0.602	-8.101	0.376	0.993	0.592	0.918	30.06
						(h1)						2879.00	2349.00											

Table A3.7.2. Data sheet: medium sharp sand, 40Hz, saturated.

TEST STRESS MOIST	ACCEL (g)	TIME incr. (mins)	TIME cum. (mins)	SET inc. (mm)	SET cum. (mm)	HEIGHT (mm)	SET (%)	VOL inc. (ml)	VOL. cum. (ml)	VOL (ml)	VOL (%)	WET MASS (g)	WATER MASS (g)	M (%)	M CHANGE (%)	BULK DENSE (Mg/m2)	DRY DENSE (Mg/m2)	VOID RATIO (e)	VOID CHANGE (%)	POROS (n)	SAT (Sr)	REL DENSE (Dr)	REl COMP (Cr)	PENE. RESIST (N)
1	(static)					(h0)								(cmc)										
	0.0	0.0	0.0	0.000	0.000	70.650	0.000	0.00	0.00	1287.77	0.00	2365.00	334.00	16.45	0.00	1.837	1.577	0.680	0.000	0.405	0.641	0.403	0.881	4.61
TT1CI	0.1	5.0	5.0	0.000	0.000	70.650	0.000	0.00	0.00	1287.77	0.00	2365.00	334.00	16.45	0.00	1.837	1.577	0.680	0.000	0.405	0.641	0.403	0.881	4.61
	0.2	5.0	10.0	0.000	0.000	70.650	0.000	0.00	0.00	1287.77	0.00	2365.00	334.00	16.45	0.00	1.837	1.577	0.680	0.000	0.405	0.641	0.403	0.881	4.61
	0.3	5.0	15.0	0.000	0.000	70.650	0.000	0.00	0.00	1287.77	0.00	2365.00	334.00	16.45	0.00	1.837	1.577	0.680	0.000	0.405	0.641	0.403	0.881	4.61
10 kPa	0.4	5.0	20.0	0.000	0.000	70.650	0.000	0.00	0.00	1287.77	0.00	2365.00	334.00	16.45	0.00	1.837	1.577	0.680	0.000	0.405	0.641	0.403	0.881	4.61
	0.5	5.0	25.0	0.000	0.000	70.650	0.000	0.00	0.00	1287.77	0.00	2365.00	334.00	16.45	0.00	1.837	1.577	0.680	0.000	0.405	0.641	0.403	0.881	4.61
	0.6	5.0	30.0	0.000	0.000	70.650	0.000	0.00	0.00	1287.77	0.00	2365.00	334.00	16.45	0.00	1.837	1.577	0.680	0.000	0.405	0.641	0.403	0.881	4.61
	0.8	5.0	35.0	0.002	0.002	70.649	-0.002	0.03	0.03	1287.75	0.00	2365.00	334.00	16.45	0.00	1.837	1.577	0.680	-0.005	0.405	0.641	0.403	0.881	4.61
	1.0	5.0	40.0	0.000	0.002	70.649	-0.002	0.00	0.03	1287.75	0.00	2365.00	334.00	16.45	0.00	1.837	1.577	0.680	-0.005	0.405	0.641	0.403	0.881	4.61
	2.0	60.0	100.0	0.024	0.026	70.625	-0.036	0.44	0.46	1287.31	0.04	2365.00	334.00	16.45	0.00	1.837	1.578	0.680	-0.089	0.405	0.641	0.405	0.881	4.65
						(h1)						2365.00	2031.00											

Table A3.7.3. Data sheet: medium sharp sand, 25Hz, partially saturated.

TEST STRESS MOIST	ACCEL (g)	TIME incr. (mins)	TIME cum. (mins)	SET inc. (mm)	SET cum. (mm)	HEIGHT (mm)	SET (%)	VOL inc. (ml)	VOL cum. (ml)	VOL (ml)	VOL (%)	WET MASS (g)	WATER MASS (g)	M (%)	M CHANGE (%)	BULK DENSE (Mg/m2)	DRY DENSE (Mg/m2)	VOID RATIO (e)	VOID CHANGE (%)	POROS (n)	SAT (Sr)	REL DENSE (Dr)	REL COMP (Cr)	PENE. RESIST (N)
1	(static)					(h0)								(cmc)										
	0.0	0.0	0.0	0.000	0.000	80.860	0.000	0.00	0.00	1473.88	0.00	2313.00	2.00	0.09	0.00	1.569	1.568	0.690	0.000	0.408	0.003	0.380	0.876	4.09
TT1CI	0.1	5.0	5.0	0.000	0.000	80.860	0.000	0.00	0.00	1473.88	0.00	2313.00	2.00	0.09	0.00	1.569	1.568	0.690	0.000	0.408	0.003	0.380	0.876	4.09
	0.2	5.0	10.0	0.000	0.000	80.860	0.000	0.00	0.00	1473.88	0.00	2313.00	2.00	0.09	0.00	1.569	1.568	0.690	0.000	0.408	0.003	0.380	0.876	4.09
	0.3	5.0	15.0	0.000	0.000	80.860	0.000	0.00	0.00	1473.88	0.00	2313.00	2.00	0.09	0.00	1.569	1.568	0.690	0.000	0.408	0.003	0.380	0.876	4.09
10 kPa	0.4	5.0	20.0	0.000	0.000	80.860	0.000	0.00	0.00	1473.88	0.00	2313.00	2.00	0.09	0.00	1.569	1.568	0.690	0.000	0.408	0.003	0.380	0.876	4.09
	0.5	5.0	25.0	0.000	0.000	80.860	0.000	0.00	0.00	1473.88	0.00	2313.00	2.00	0.09	0.00	1.569	1.568	0.690	0.000	0.408	0.003	0.380	0.876	4.09
	0.6	5.0	30.0	0.000	0.000	80.860	0.000	0.00	0.00	1473.88	0.00	2313.00	2.00	0.09	0.00	1.569	1.568	0.690	0.000	0.408	0.003	0.380	0.876	4.09
	0.8	5.0	35.0	0.000	0.000	80.860	0.000	0.00	0.00	1473.88	0.00	2313.00	2.00	0.09	0.00	1.569	1.568	0.690	0.000	0.408	0.003	0.380	0.876	4.09
	1.0	5.0	40.0	0.005	0.005	80.855	-0.006	0.09	0.09	1473.79	0.01	2313.00	2.00	0.09	0.00	1.569	1.568	0.690	-0.015	0.408	0.003	0.380	0.876	4.09
	2.0	60.0	100.0	2.619	2.624	78.236	-3.245	47.74	47.83	1426.05	3.25	2313.00	2.00	0.09	0.00	1.622	1.621	0.635	-7.948	0.388	0.004	0.511	0.902	7.42
						(h1)						2313.00	2311.00											

Table A3.7.4. Data sheet: medium sharp sand, 25Hz, dried.

TEST	ACCEL (g)	TIME incr. (mins)	TIME cum. (mins)	SET inc. (mm)	SET cum. (mm)	HEIGHT (mm)	SET (%)	VOL inc. (ml)	VOL cum. (ml)	VOL (ml)	VOL (%)	WET MASS (g)	WATER MASS (g)	M (%)	M CHANGE (%)	BULK DENSE (Mg/m2)	DRY DENSE (Mg/m2)	VOID RATIO (e)	VOID CHANGE (%)	POROS (n)	SAT (Sr)	REL DENSE (Dr)	REL COMP (Cr)	PENE RESIST (N)
1	(static)					(h0)								(cmc)										
	0.0	0.0	0.0	0.000	0.000	75.540	0.000	0.00	0.00	1376.91	0.00	2707.58	528.58	24.26	0.00	1.966	1.583	0.675	0.000	0.403	0.953	0.417	0.883	4.933
TICA	1.0	4.0	4.0	0.120	0.120	75.420	-0.159	2.19	2.19	1374.72	0.16	2705.40	526.40	24.16	-0.41	1.968	1.585	0.672	-0.394	0.402	0.953	0.423	0.885	5.085
	2.0	86.0	90.0	1.820	1.940	73.600	-2.568	33.17	35.36	1341.54	2.57	2672.22	493.22	22.64	-6.69	1.992	1.624	0.632	-6.376	0.387	0.950	0.520	0.904	7.682
10	3.0	38.0	128.0	2.810	4.750	70.790	-6.288	51.22	86.58	1290.33	6.30	2621.00	442.00	20.28	-16.38	2.031	1.689	0.569	-15.610	0.363	0.944	0.670	0.934	12.739
	4.0	36.0	164.0	0.690	5.440	70.100	-7.201	12.58	99.16	1277.75	7.21	2608.42	429.42	19.71	-18.76	2.041	1.705	0.554	-17.878	0.356	0.943	0.707	0.941	14.175
	5.0	42.0	206.0	0.980	6.420	69.120	-8.499	17.86	117.02	1259.89	8.51	2590.56	411.56	18.89	-22.14	2.056	1.730	0.532	-21.098	0.347	0.940	0.759	0.952	16.347
	6.0	17.0	223.0	0.360	6.780	68.760	-8.975	6.56	123.58	1253.32	8.99	2584.00	405.00	18.59	-23.38	2.062	1.739	0.524	-22.281	0.344	0.940	0.778	0.956	17.183
						(h1)						2584.00	2179.00											
2	(static)					(h0)								(cmc)										
	0.0	0.0	0.0	0.000	0.000	64.630	0.000	0.00	0.00	1178.04	0.00	2255.88	468.88	26.24	0.00	1.915	1.517	0.747	0.000	0.428	0.931	0.243	0.849	2.167
TICG	1.0	15.0	15.0	0.180	0.180	64.450	-0.279	3.28	3.28	1174.76	0.28	2252.60	465.60	26.05	-0.70	1.917	1.521	0.742	-0.651	0.426	0.930	0.255	0.851	2.381
	2.0	95.0	110.0	5.450	5.630	59.000	-8.711	99.34	102.62	1075.42	8.74	2153.26	366.26	20.50	-21.89	2.002	1.662	0.595	-20.373	0.373	0.913	0.609	0.922	13.611
20	3.0	45.0	155.0	0.810	6.440	58.190	-9.964	14.76	117.39	1060.66	9.99	2138.49	351.49	19.67	-25.04	2.016	1.685	0.573	-23.304	0.364	0.910	0.661	0.932	16.067
	4.0	40.0	195.0	0.550	6.990	57.640	-10.815	10.03	127.41	1050.63	10.85	2128.47	341.47	19.11	-27.17	2.026	1.701	0.558	-25.295	0.358	0.907	0.697	0.939	17.850
	5.0	25.0	220.0	0.190	7.180	57.450	-11.109	3.46	130.87	1047.17	11.14	2125.01	338.01	18.91	-27.91	2.029	1.707	0.553	-25.982	0.356	0.907	0.709	0.942	18.488
	6.0	9.0	229.0	0.110	7.290	57.340	-11.280	2.01	132.88	1045.17	11.31	2123.00	336.00	18.80	-28.34	2.031	1.710	0.550	-26.380	0.355	0.906	0.717	0.943	18.863
						(h1)						2123.00	1787.00											
3	(static)					(h0)								(cmc)										
	0.0	0.0	0.0	0.000	0.000	51.520	0.000	0.00	0.00	939.08	0.00	1791.67	368.67	25.91	0.00	1.908	1.515	0.749	0.000	0.428	0.917	0.238	0.848	3.511
TICH	1.0	27.0	27.0	0.470	0.470	51.050	-0.912	8.57	8.57	930.51	0.92	1783.10	360.10	25.31	-2.32	1.916	1.529	0.733	-2.131	0.423	0.915	0.277	0.855	4.731
	2.0	88.0	115.0	2.110	2.580	48.940	-5.008	38.46	47.03	892.05	5.05	1744.64	321.64	22.60	-12.76	1.956	1.595	0.661	-11.695	0.398	0.906	0.449	0.890	12.448
50	3.0	57.0	172.0	0.930	3.510	48.010	-6.813	16.95	63.98	875.10	6.88	1727.69	304.69	21.41	-17.35	1.974	1.626	0.630	-15.911	0.386	0.901	0.525	0.905	17.011
	4.0	92.0	264.0	0.410	3.920	47.600	-7.609	7.47	71.45	867.63	7.68	1720.22	297.22	20.89	-19.38	1.983	1.640	0.616	-17.770	0.381	0.899	0.558	0.912	19.249
	5.0	46.0	310.0	0.670	4.590	46.930	-8.909	12.21	83.66	855.42	8.99	1708.01	285.01	20.03	-22.69	1.997	1.664	0.593	-20.807	0.372	0.895	0.613	0.923	23.204
	6.0	11.0	321.0	0.110	4.700	46.820	-9.123	2.01	85.67	853.41	9.21	1706.00	283.00	19.89	-23.24	1.999	1.667	0.589	-21.305	0.371	0.894	0.622	0.924	23.889
						(h1)						1706.00	1423.00											
4	(static)					(h0)								(cmc)										
	0.0	0.0	0.0	0.000	0.000	74.330	0.000	0.00	0.00	1354.85	0.00	2613.17	603.17	30.01	0.00	1.929	1.484	0.786	0.000	0.440	1.011	0.148	0.830	1.892
TICI	1.0	16.0	16.0	0.120	0.120	74.210	-0.161	2.19	2.19	1352.66	0.16	2610.98	600.98	29.90	-0.36	1.930	1.486	0.783	-0.367	0.439	1.011	0.155	0.831	2.073
	2.0	40.0	56.0	0.900	1.020	73.310	-1.372	16.40	18.59	1336.26	1.37	2594.58	584.58	29.08	-3.08	1.942	1.504	0.762	-3.118	0.432	1.012	0.207	0.841	3.693
100	3.0	112.0	168.0	1.290	2.310	72.020	-3.108	23.51	42.11	1312.75	3.11	2571.07	561.07	27.91	-6.98	1.959	1.531	0.731	-7.060	0.422	1.012	0.282	0.856	6.824
	4.0	65.0	233.0	1.010	3.320	71.010	-4.467	18.41	60.52	1294.34	4.47	2552.66	542.66	27.00	-10.03	1.972	1.553	0.706	-10.147	0.414	1.013	0.340	0.868	9.941
	5.0	40.0	273.0	0.420	3.740	70.590	-5.032	7.66	68.17	1286.68	5.04	2545.00	535.00	26.62	-11.30	1.978	1.562	0.696	-11.431	0.411	1.013	0.364	0.873	11.410
	6.0	0.0	273.0		3.740	70.590	-5.032	0.00	68.17	1286.68	5.04	2545.00	535.00	26.62	-11.30	1.978	1.562	0.696	-11.431	0.411	1.013	0.364	0.873	11.410
						(h1)						2545.00	2010.00											

Table A3.7.5. Data sheet: medium sharp sand, high acceleration, saturated, 25Hz.

TEST	ACCEL (g)	TIME incr. (mins)	TIME cum. (mins)	SET inc. (mm)	SET cum. (mm)	HEIGHT (mm)	SET (%)	VOL inc. (ml)	VOL cum. (ml)	VOL (ml)	VOL (%)	WET MASS (g)	WATER MASS (g)	M (%)	M CHANGE (%)	BULK DENSE (Mg/m2)	DRY DENSE (Mg/m2)	VOID RATIO (e)	VOID CHANGE (%)	POROS (n)	SAT (Sr)	REL DENSE (Dr)	REL COMP (Cr)	PENE RESIST (N)
1	(static)					(h0)								(cmc)										
1.0-6.0	0.0	0.0	0.0	0.000	0.000	75.540	0.000	0.00	0.00	1376.91	0.00	2707.22	528.22	24.24	0.00	1.966	1.583	0.675	0.000	0.403	0.952	0.417	0.883	4.933
T1CA	1.0	4.0	4.0	0.100	0.100	75.440	-0.132	1.82	1.82	1375.08	0.13	2705.40	526.40	24.16	-0.35	1.967	1.585	0.672	-0.329	0.402	0.952	0.422	0.884	5.060
	2.0	86.0	90.0	1.820	1.920	73.620	-2.542	33.17	35.00	1341.91	2.55	2672.22	493.22	22.64	-6.63	1.991	1.624	0.632	-6.310	0.387	0.949	0.519	0.904	7.650
10kPa	3.0	38.0	128.0	2.810	4.730	70.810	-6.262	51.22	86.22	1290.69	6.27	2621.00	442.00	20.28	-16.32	2.031	1.688	0.570	-15.544	0.363	0.944	0.669	0.934	12.698
	4.0	36.0	164.0	0.690	5.420	70.120	-7.175	12.58	98.79	1278.11	7.18	2608.42	429.42	19.71	-18.70	2.041	1.705	0.554	-17.812	0.357	0.942	0.706	0.941	14.132
	5.0	42.0	206.0	0.980	6.400	69.140	-8.472	17.86	116.66	1260.25	8.48	2590.56	411.56	18.89	-22.08	2.056	1.729	0.533	-21.033	0.348	0.940	0.758	0.952	16.301
	6.0	17.0	223.0	0.360	6.760	68.780	-8.949	6.56	123.22	1253.69	8.96	2584.00	405.00	18.59	-23.33	2.061	1.738	0.525	-22.216	0.344	0.939	0.777	0.955	17.136
						(h1)						2584.00	2179.00											
2	(static)					(h0)								(cmc)										
2.0-6.0	0.0	0.0	0.0	0.000	0.000	77.960	0.000	0.00	0.00	1421.02	0.00	2804.28	581.18	26.14	0.00	1.973	1.564	0.694	0.000	0.410	0.998	0.370	0.874	3.893
T1CB	1.0	0.0	0.0	0.000	0.000	77.960	0.000	0.00	0.00	1421.02	0.00	2804.28	581.18	26.14	0.00	1.973	1.564	0.694	0.000	0.410	0.998	0.370	0.874	3.893
	2.0	21.0	21.0	0.920	0.920	77.040	-1.180	16.77	16.77	1404.25	1.18	2787.51	564.41	25.39	-2.89	1.985	1.583	0.674	-2.881	0.403	0.998	0.419	0.884	4.968
10kPa	3.0	36.0	57.0	1.280	2.200	75.760	-2.822	23.33	40.10	1380.92	2.82	2764.18	541.08	24.34	-6.90	2.002	1.610	0.646	-6.889	0.393	0.998	0.485	0.897	6.683
	4.0	38.0	95.0	2.390	4.590	73.370	-5.888	43.56	83.66	1337.35	5.89	2720.62	497.52	22.38	-14.40	2.034	1.662	0.594	-14.373	0.373	0.998	0.610	0.922	10.562
	5.0	32.0	127.0	1.130	5.720	72.240	-7.337	20.60	104.26	1316.76	7.34	2700.02	476.92	21.45	-17.94	2.051	1.688	0.570	-17.911	0.363	0.998	0.669	0.934	12.704
	6.0	20.0	147.0	1.060	6.780	71.180	-8.697	19.32	123.58	1297.43	8.70	2680.70	457.60	20.58	-21.26	2.066	1.713	0.547	-21.230	0.353	0.998	0.725	0.945	14.893
						(h1)						2680.70	2223.10											
3	(static)					(h0)								(cmc)										
3.0-6.0	0.0	0.0	0.0	0.000	0.000	74.505	0.000	0.00	0.00	1358.04	0.00	2572.96	525.26	25.65	0.00	1.895	1.508	0.757	0.000	0.431	0.897	0.218	0.844	1.343
T1CC	1.0	0.0	0.0	0.000	0.000	74.505	0.000	0.00	0.00	1358.04	0.00	2572.96	525.26	25.65	0.00	1.895	1.508	0.757	0.000	0.431	0.897	0.218	0.844	1.343
	2.0	0.0	0.0	0.000	0.000	74.505	0.000	0.00	0.00	1358.04	0.00	2572.96	525.26	25.65	0.00	1.895	1.508	0.757	0.000	0.431	0.897	0.218	0.844	1.343
10kPa	3.0	25.0	25.0	2.220	2.220	72.285	-2.980	40.47	40.47	1317.58	2.98	2532.50	484.80	23.68	-7.70	1.922	1.554	0.705	-6.913	0.414	0.890	0.343	0.869	3.346
	4.0	39.0	64.0	2.390	4.610	69.895	-6.188	43.56	84.03	1274.01	6.19	2488.93	441.23	21.55	-16.00	1.954	1.607	0.649	-14.356	0.393	0.880	0.479	0.896	6.508
	5.0	35.0	99.0	1.920	6.530	67.975	-8.765	35.00	119.03	1239.01	8.76	2453.94	406.24	19.84	-22.66	1.981	1.653	0.603	-20.335	0.376	0.871	0.588	0.918	9.803
	6.0	35.0	134.0	0.600	7.130	67.375	-9.570	10.94	129.96	1228.08	9.57	2443.00	395.30	19.30	-24.74	1.989	1.667	0.589	-22.203	0.371	0.868	0.622	0.924	10.971
						(h1)						2443.00	2047.70											

Table A3.7.6. Data sheet: medium sharp sand,high acceleration, saturated, 25Hz. Effect of increasing initial vibration level.

TEST	ACCEL (g)	TIME incr. (mins)	TIME cum. (mins)	SET inc. (mm)	SET cum. (mm)	HEIGHT (mm)	SET (%)	VOL inc. (ml)	VOL cum. (ml)	VOL (ml)	VOL (%)	WET MASS (g)	WATER MASS (g)	M (%)	M CHANGE (%)	BULK DENSE (Mg/m2)	DRY DENSE (Mg/m2)	VOID RATIO (e)	VOID CHANGE (%)	POROS (n)	SAT (Sr)	REL DENSE (Dr)	REL COMP (Cr)	PENE RESIST (N)
4	(static)					(h0)								(cmc)										
4.0-6.0	0.0	0.0	0.0	0.000	0.000	69.390	0.000	0.00	0.00	1264.81	0.00	2451.40	486.10	24.73	0.00	1.938	1.554	0.705	0.000	0.414	0.929	0.343	0.869	3.331
TICD	1.0	0.0	0.0	0.000	0.000	69.390	0.000	0.00	0.00	1264.81	0.00	2451.40	486.10	24.73	0.00	1.938	1.554	0.705	0.000	0.414	0.929	0.343	0.869	3.331
	2.0	0.0	0.0	0.000	0.000	69.390	0.000	0.00	0.00	1264.81	0.00	2451.40	486.10	24.73	0.00	1.938	1.554	0.705	0.000	0.414	0.929	0.343	0.869	3.331
10kPa	3.0	0.0	0.0	0.000	0.000	69.390	0.000	0.00	0.00	1264.81	0.00	2451.40	486.10	24.73	0.00	1.938	1.554	0.705	0.000	0.414	0.929	0.343	0.869	3.331
	4.0	34.0	34.0	4.480	4.480	64.910	-6.456	81.66	81.66	1183.15	6.46	2369.74	404.44	20.58	-16.80	2.003	1.661	0.595	-15.608	0.373	0.916	0.607	0.921	10.464
	5.0	33.0	67.0	1.290	5.770	63.620	-8.315	23.51	105.17	1159.63	8.32	2346.23	380.93	19.38	-21.64	2.023	1.695	0.564	-20.102	0.360	0.911	0.684	0.937	13.255
	6.0	17.0	84.0	0.490	6.260	63.130	-9.021	8.93	114.10	1150.70	9.02	2337.30	372.00	18.93	-23.47	2.031	1.708	0.552	-21.810	0.356	0.909	0.712	0.942	14.401
						(h1)						2337.30	1965.30											
5	(static)					(h0)								(cmc)										
5.0-6.0	0.0	0.0	0.0	0.000	0.000	70.260	0.000	0.00	0.00	1280.66	0.00	2435.60	512.60	26.66	0.00	1.902	1.502	0.765	0.000	0.433	0.924	0.200	0.840	1.134
TICE	1.0	0.0	0.0	0.000	0.000	70.260	0.000	0.00	0.00	1280.66	0.00	2435.60	512.60	26.66	0.00	1.902	1.502	0.765	0.000	0.433	0.924	0.200	0.840	1.134
	2.0	0.0	0.0	0.000	0.000	70.260	0.000	0.00	0.00	1280.66	0.00	2435.60	512.60	26.66	0.00	1.902	1.502	0.765	0.000	0.433	0.924	0.200	0.840	1.134
10kPa	3.0	0.0	0.0	0.000	0.000	70.260	0.000	0.00	0.00	1280.66	0.00	2435.60	512.60	26.66	0.00	1.902	1.502	0.765	0.000	0.433	0.924	0.200	0.840	1.134
	4.0	0.0	0.0	0.000	0.000	70.260	0.000	0.00	0.00	1280.66	0.00	2435.60	512.60	26.66	0.00	1.902	1.502	0.765	0.000	0.433	0.924	0.200	0.840	1.134
	5.0	26.0	26.0	4.730	4.730	65.530	-6.732	86.22	86.22	1194.45	6.73	2349.39	426.39	22.17	-16.82	1.967	1.610	0.646	-15.534	0.392	0.910	0.486	0.897	6.688
	6.0	43.0	69.0	2.490	7.220	63.040	-10.276	45.39	131.60	1149.06	10.28	2304.00	381.00	19.81	-25.67	2.005	1.674	0.583	-23.712	0.368	0.900	0.636	0.927	11.471
						(h1)						2304.00	1923.00											
6	(static)					(h0)								(cmc)										
6.0	0.0	0.0	0.0	0.000	0.000	62.500	0.000	0.00	0.00	1139.22	0.00	2146.31	482.31	29.41	0.00	1.884	1.456	0.820	0.000	0.451	0.950	0.067	0.813	0.126
TICF	1.0	0.0	0.0	0.000	0.000	62.500	0.000	0.00	0.00	1139.22	0.00	2146.31	482.31	29.41	0.00	1.884	1.456	0.820	0.000	0.451	0.950	0.067	0.813	0.126
	2.0	0.0	0.0	0.000	0.000	62.500	0.000	0.00	0.00	1139.22	0.00	2146.31	482.31	29.41	0.00	1.884	1.456	0.820	0.000	0.451	0.950	0.067	0.813	0.126
10kPa	3.0	0.0	0.0	0.000	0.000	62.500	0.000	0.00	0.00	1139.22	0.00	2146.31	482.31	29.41	0.00	1.884	1.456	0.820	0.000	0.451	0.950	0.067	0.813	0.126
	4.0	0.0	0.0	0.000	0.000	62.500	0.000	0.00	0.00	1139.22	0.00	2146.31	482.31	29.41	0.00	1.884	1.456	0.820	0.000	0.451	0.950	0.067	0.813	0.126
	5.0	0.0	0.0	0.000	0.000	62.500	0.000	0.00	0.00	1139.22	0.00	2146.31	482.31	29.41	0.00	1.884	1.456	0.820	0.000	0.451	0.950	0.067	0.813	0.126
	6.0	48.0	48.0	6.820	6.820	55.680	-10.912	124.31	124.31	1014.91	10.91	2022.00	358.00	21.83	-25.77	1.992	1.635	0.620	-24.353	0.383	0.932	0.547	0.909	8.486
						(h1)						2022.00	1664.00											

Table A3.7.6 (cont). Data sheet: medium sharp sand,high acceleration, saturated, 25Hz. Effect of increasing initial vibration level.

TEST	ACCEL (g)	TIME incr. (mins)	TIME cum. (mins)	SET inc. (mm)	SET cum. (mm)	HEIGHT (mm)	SET (%)	VOL inc. (ml)	VOL cum. (ml)	VOL (ml)	VOL (%)	WET MASS (g)	WATER MASS (g)	M (%)	M CHANGE (%)	BULK DENSE (Mg/m2)	DRY DENSE (Mg/m2)	VOID RATIO (e)	VOID CHANGE (%)	POROS (n)	SAT (Sr)	AIR CONT (A)	REL DENSE (Dr)	REL COMP (Cr)	PENE. RESIST (N)
1	(static)					(h0)								(cmc)											
	0.0	0.0	0.0	0.00	0.00	63.91	0.00	0.00	0.00	1164.92	0.00	2187.00	278.00	14.56	0.00	1.877	1.639	0.617	0.000	0.382	0.625	0.143	0.555	0.911	8.74
TICO	1.0	10.0	10.0	0.05	0.05	63.86	-0.08	0.91	0.91	1164.01	0.08	2187.00	278.00	14.56	0.00	1.879	1.640	0.616	-0.205	0.381	0.627	0.142	0.558	0.912	8.84
	2.0	25.0	35.0	0.02	0.07	63.84	-0.11	0.36	1.28	1163.64	0.11	2187.00	278.00	14.56	0.00	1.879	1.641	0.615	-0.287	0.381	0.627	0.142	0.559	0.912	8.87
10	3.0	15.0	50.0	0.03	0.10	63.81	-0.16	0.55	1.82	1163.10	0.16	2187.00	278.00	14.56	0.00	1.880	1.641	0.615	-0.410	0.381	0.628	0.142	0.561	0.912	8.93
	4.0	10.0	60.0	0.02	0.12	63.79	-0.19	0.36	2.19	1162.73	0.19	2187.00	278.00	14.56	0.00	1.881	1.642	0.614	-0.492	0.380	0.628	0.141	0.562	0.912	8.97
	5.0	15.0	75.0	0.04	0.16	63.75	-0.25	0.73	2.92	1162.00	0.25	2187.00	278.00	14.56	0.00	1.882	1.643	0.613	-0.656	0.380	0.629	0.141	0.565	0.913	9.05
	6.0	15.0	90.0	0.06	0.22	63.69	-0.34	1.09	4.01	1160.91	0.34	2187.00	278.00	14.56	0.00	1.884	1.644	0.612	-0.902	0.379	0.631	0.140	0.568	0.914	9.17
						(h1)						2187.00	1909.00												
2	(static)					(h0)								(cmc)											
	0.0	0.0	0.0	0.00	0.00	67.59	0.00	0.00	0.00	1232.00	0.00	2197.00	310.00	16.43	0.00	1.783	1.532	0.730	0.000	0.422	0.596	0.170	0.283	0.857	2.95
TICP	1.0	10.0	10.0	0.02	0.02	67.57	-0.03	0.36	0.36	1231.63	0.03	2197.00	310.00	16.43	0.00	1.784	1.532	0.730	-0.070	0.422	0.597	0.170	0.285	0.857	2.97
	2.0	25.0	35.0	0.13	0.15	67.44	-0.22	2.37	2.73	1229.26	0.22	2197.00	310.00	16.43	0.00	1.787	1.535	0.726	-0.526	0.421	0.599	0.169	0.293	0.859	3.14
20	3.0	20.0	55.0	0.16	0.31	67.28	-0.46	2.92	5.65	1226.35	0.46	2197.00	310.00	16.43	0.00	1.791	1.539	0.722	-1.087	0.419	0.603	0.167	0.302	0.860	3.36
	4.0	20.0	75.0	0.11	0.42	67.17	-0.62	2.01	7.66	1224.34	0.62	2197.00	310.00	16.43	0.00	1.794	1.541	0.719	-1.472	0.418	0.605	0.165	0.309	0.862	3.51
	5.0	30.0	105.0	0.25	0.67	66.92	-0.99	4.56	12.21	1219.78	0.99	2197.00	310.00	16.43	0.00	1.801	1.547	0.713	-2.349	0.416	0.611	0.162	0.325	0.865	3.87
	6.0	15.0	120.0	0.10	0.77	66.82	-1.14	1.82	14.04	1217.96	1.14	2197.00	310.00	16.43	0.00	1.804	1.549	0.710	-2.699	0.415	0.613	0.161	0.331	0.866	4.02
						(h1)						2197.00	1887.00												
3	(static)					(h0)								(cmc)											
	0.0	0.0	0.0	0.00	0.00	104.53	0.00	0.00	0.00	1905.32	0.00	3353.00	434.00	14.87	0.00	1.760	1.532	0.730	0.000	0.422	0.540	0.194	0.284	0.857	4.99
TICQ	1.0	10.0	10.0	0.01	0.01	104.52	-0.01	0.18	0.18	1905.14	0.01	3353.00	434.00	14.87	0.00	1.760	1.532	0.730	-0.023	0.422	0.540	0.194	0.285	0.857	5.01
	2.0	15.0	25.0	0.03	0.04	104.50	-0.03	0.46	0.64	1904.68	0.03	3353.00	434.00	14.87	0.00	1.760	1.533	0.729	-0.079	0.422	0.540	0.194	0.286	0.857	5.04
50	3.0	10.0	35.0	0.01	0.04	104.49	-0.04	0.09	0.73	1904.59	0.04	3353.00	434.00	14.87	0.00	1.760	1.533	0.729	-0.091	0.422	0.540	0.194	0.286	0.857	5.05
	4.0	15.0	50.0	0.03	0.07	104.46	-0.07	0.55	1.28	1904.05	0.07	3353.00	434.00	14.87	0.00	1.761	1.533	0.729	-0.159	0.421	0.541	0.194	0.287	0.857	5.09
	5.0	25.0	75.0	0.05	0.12	104.41	-0.11	0.91	2.19	1903.13	0.11	3353.00	434.00	14.87	0.00	1.762	1.534	0.728	-0.272	0.421	0.541	0.193	0.289	0.858	5.16
	6.0	35.0	110.0	0.05	0.17	104.36	-0.16	0.91	3.10	1902.22	0.16	3353.00	434.00	14.87	0.00	1.763	1.535	0.727	-0.385	0.421	0.542	0.193	0.291	0.858	5.23
						(h1)						3353.00	2919.00												
4	(static)					(h0)								(cmc)											
	0.0	0.0	0.0	0.00	0.00	79.38	0.00	0.00	0.00	1446.90	0.00	2706.00	345.00	14.61	0.00	1.870	1.632	0.624	0.000	0.384	0.621	0.146	0.538	0.908	24.90
TICR	1.0	15.0	15.0	0.01	0.01	79.38	-0.01	0.09	0.09	1446.81	0.01	2706.00	345.00	14.61	0.00	1.870	1.632	0.624	-0.016	0.384	0.621	0.146	0.539	0.908	24.92
	2.0	15.0	30.0	0.01	0.01	79.37	-0.01	0.09	0.18	1446.72	0.01	2706.00	345.00	14.61	0.00	1.870	1.632	0.624	-0.033	0.384	0.621	0.146	0.539	0.908	24.94
100	3.0	15.0	45.0	-0.01	0.00	79.38	0.00	-0.18	0.00	1446.90	0.00	2706.00	345.00	14.61	0.00	1.870	1.632	0.624	0.000	0.384	0.621	0.146	0.538	0.908	24.90
	4.0	30.0	75.0	0.08	0.08	79.30	-0.10	1.46	1.46	1445.44	0.10	2706.00	345.00	14.61	0.00	1.872	1.633	0.622	-0.262	0.384	0.622	0.145	0.542	0.908	25.26
	5.0	20.0	95.0	0.05	0.13	79.25	-0.16	0.91	2.37	1444.53	0.16	2706.00	345.00	14.61	0.00	1.873	1.634	0.621	-0.426	0.383	0.623	0.144	0.545	0.909	25.49
	6.0	20.0	115.0	0.01	0.14	79.24	-0.18	0.18	2.55	1444.35	0.18	2706.00	345.00	14.61	0.00	1.874	1.635	0.621	-0.459	0.383	0.623	0.144	0.545	0.909	25.54
						(h1)						2706.00	2361.00												

Table A3.7.7. Data sheet: medium sharp sand, high acceleration, partially saturated, 25Hz.

TEST	ACCEL (g)	TIME incr. (mins)	TIME cum. (mins)	SET inc. (mm)	SET cum. (mm)	HEIGHT (mm)	SET (%)	VOL inc. (ml)	VOL cum. (ml)	VOL (ml)	VOL (%)	WET MASS (g)	WATER MASS (g)	M (%)	M CHANGE (%)	BULK DENSE (Mg/m2)	DRY DENSE (Mg/m2)	VOID RATIO (e)	VOID CHANGE (%)	POROS (n)	SAT (Sr)	AIR CONT (A)	REL DENSE (Dr)	REL COMP (Cr)	PENE. RESIST (N)
1	(static)					(h0)								(cmc)											
	0.0	0.0	0.0	0.00	0.00	66.74	0.00	0.00	0.00	1216.50	0.00	1803.00	1.00	0.06	0.00	1.482	1.481	0.796	0.000	0.443	0.002	0.442	0.126	0.825	0.45
TICJ	1.0	15.0	15.0	0.02	0.02	66.72	-0.03	0.36	0.36	1216.14	0.03	1803.00	1.00	0.06	0.00	1.483	1.482	0.795	-0.068	0.443	0.002	0.442	0.127	0.825	0.46
	2.0	42.0	57.0	0.42	0.44	66.30	-0.66	7.66	8.02	1208.48	0.66	1803.00	1.00	0.06	0.00	1.492	1.491	0.784	-1.488	0.439	0.002	0.439	0.154	0.831	0.67
10	3.0	45.0	102.0	3.52	3.96	62.78	-5.93	64.16	72.18	1144.32	5.94	1803.00	1.00	0.06	0.00	1.576	1.575	0.689	-13.390	0.408	0.002	0.407	0.382	0.876	4.13
	4.0	64.0	166.0	1.08	5.04	61.70	-7.55	19.69	91.87	1124.64	7.55	1803.00	1.00	0.06	0.00	1.603	1.602	0.660	-17.042	0.398	0.002	0.397	0.452	0.890	5.79
	5.0	45.0	211.0	0.20	5.24	61.50	-7.85	3.65	95.51	1120.99	7.85	1803.00	1.00	0.06	0.00	1.608	1.608	0.655	-17.718	0.396	0.002	0.395	0.465	0.893	6.12
	6.0	20.0	231.0	0.11	5.35	61.39	-8.02	2.01	97.52	1118.99	8.02	1803.00	1.00	0.06	0.00	1.611	1.610	0.652	-18.090	0.395	0.002	0.394	0.472	0.894	6.31
						(h1)						1803.00	1802.00												
2	(static)					(h0)								(cmc)											
	0.0	0.0	0.0	0.00	0.00	75.19	0.00	0.00	0.00	1370.53	0.00	2127.00	13.00	0.61	0.00	1.552	1.542	0.725	0.000	0.420	0.023	0.411	0.297	0.859	3.24
TICK	1.0	10.0	10.0	0.01	0.01	75.18	-0.01	0.18	0.18	1370.34	0.01	2127.00	13.00	0.61	0.00	1.552	1.543	0.724	-0.032	0.420	0.023	0.411	0.297	0.859	3.25
	2.0	20.0	30.0	0.43	0.44	74.75	-0.59	7.84	8.02	1362.51	0.59	2127.00	13.00	0.61	0.00	1.561	1.552	0.714	-1.393	0.417	0.023	0.407	0.321	0.864	3.79
20	3.0	70.0	100.0	2.66	3.10	72.09	-4.12	48.49	56.51	1314.02	4.12	2127.00	13.00	0.61	0.00	1.619	1.609	0.653	-9.814	0.395	0.025	0.385	0.468	0.894	8.04
	4.0	20.0	120.0	0.32	3.42	71.77	-4.55	5.83	62.34	1308.19	4.55	2127.00	13.00	0.61	0.00	1.626	1.616	0.646	-10.827	0.392	0.025	0.383	0.485	0.897	8.66
	5.0	20.0	140.0	0.23	3.65	71.54	-4.85	4.19	66.53	1304.00	4.86	2127.00	13.00	0.61	0.00	1.631	1.621	0.641	-11.555	0.391	0.026	0.381	0.498	0.900	9.11
						(h1)						2127.00	2114.00												
3	(static)					(h0)								(cmc)											
	0.0	0.0	0.0	0.00	0.00	72.61	0.00	0.00	0.00	1323.50	0.00	2116.00	1.00	0.05	0.00	1.599	1.598	0.664	0.000	0.399	0.002	0.398	0.441	0.888	12.01
TICL	1.0	15.0	15.0	0.02	0.02	72.59	-0.03	0.36	0.36	1323.13	0.03	2116.00	1.00	0.05	0.00	1.599	1.598	0.664	-0.069	0.399	0.002	0.398	0.442	0.888	12.07
	2.0	20.0	35.0	0.30	0.32	72.29	-0.44	5.47	5.83	1317.67	0.44	2116.00	1.00	0.05	0.00	1.606	1.605	0.657	-1.104	0.397	0.002	0.396	0.459	0.892	12.99
50	3.0	67.0	102.0	1.33	1.65	70.96	-2.27	24.24	30.08	1293.42	2.27	2116.00	1.00	0.05	0.00	1.636	1.635	0.627	-5.692	0.385	0.002	0.384	0.532	0.906	17.47
	4.0	18.0	120.0	0.16	1.81	70.80	-2.49	2.92	32.99	1290.51	2.49	2116.00	1.00	0.05	0.00	1.640	1.639	0.623	-6.244	0.384	0.002	0.383	0.541	0.908	18.06
	5.0	40.0	160.0	0.60	2.41	70.20	-3.32	10.94	43.93	1279.57	3.32	2116.00	1.00	0.05	0.00	1.654	1.653	0.609	-8.314	0.379	0.002	0.378	0.574	0.915	20.33
						(h1)						2116.00	2115.00												
5	(static)					(h0)								(cmc)											
	0.0	0.0	0.0	0.00	0.00	76.74	0.00	0.00	0.00	1398.78	0.00	2246.00	2.00	0.09	0.00	1.606	1.604	0.658	0.000	0.397	0.004	0.395	0.457	0.891	17.90
TICM	1.0	2.0	2.0	0.00	0.00	76.74	0.00	0.00	0.00	1398.78	0.00	2246.00	2.00	0.09	0.00	1.606	1.604	0.658	0.000	0.397	0.004	0.395	0.457	0.891	17.90
	2.0	34.0	36.0	1.74	1.74	75.00	-2.27	31.72	31.72	1367.06	2.27	2246.00	2.00	0.09	0.00	1.643	1.641	0.620	-5.713	0.383	0.004	0.381	0.547	0.909	25.69
100	3.0	64.0	100.0	1.00	2.74	74.00	-3.57	18.23	49.94	1348.84	3.57	2246.00	2.00	0.09	0.00	1.665	1.664	0.599	-8.996	0.375	0.004	0.373	0.599	0.920	30.80
	4.0	23.0	123.0	1.14	3.88	72.86	-5.06	20.78	70.72	1328.06	5.06	2246.00	2.00	0.09	0.00	1.691	1.690	0.574	-12.739	0.365	0.004	0.363	0.658	0.932	37.19
	5.0	10.0	133.0	0.28	4.16	72.58	-5.42	5.10	75.83	1322.95	5.42	2246.00	2.00	0.09	0.00	1.698	1.696	0.568	-13.658	0.362	0.004	0.361	0.673	0.935	38.85
						(h1)						2246.00	2244.00												

Table A3.7.8. Data sheet: medium sharp sand, high acceleration, dried, 25Hz.

TEST	ACCEL (g)	TIME incr. (mins)	TIME cum. (mins)	SET inc. (mm)	SET cum. (mm)	HEIGHT (mm)	SET (%)	VOL inc. (ml)	VOL cum. (ml)	VOL (ml)	VOL (%)	WET MASS (g)	WATER MASS (g)	M (%)	M CHANGE (%)	BULK DENSE (Mg/m2)	DRY DENSE (Mg/m2)	VOID RATIO (e)	VOID CHANGE (%)	POROS (n)	SAT (Sr)	REL DENSE (Dr)	REL COMP (Cr)	PENE RESIST (N)
1	(static)					(h0)								(cmc)										
	0.0	0.0	0.0	0.000	0.000	117.690	0.000	0.00	0.00	2145.20	0.00	4231.83	795.83	23.16	0.00	1.973	1.602	0.661	0.000	0.398	0.932	0.450	0.890	5.750
T1BJ	1.0	5.0	5.0	0.290	0.290	117.400	-0.246	5.29	5.29	2139.91	0.25	4226.54	790.54	23.01	-0.66	1.975	1.606	0.657	-0.619	0.396	0.932	0.460	0.892	6.004
	2.0	51.0	56.0	9.120	9.410	108.280	-7.996	166.23	171.52	1973.67	8.02	4060.31	624.31	18.17	-21.55	2.057	1.741	0.528	-20.097	0.346	0.915	0.769	0.954	16.793
10kPa	3.0	85.0	141.0	2.400	11.810	105.880	-10.035	43.75	215.27	1929.93	10.06	4016.56	580.56	16.90	-27.05	2.081	1.780	0.494	-25.223	0.331	0.910	0.851	0.970	20.535
	4.0	20.0	161.0	0.360	12.170	105.520	-10.341	6.56	221.83	1923.37	10.37	4010.00	574.00	16.71	-27.87	2.085	1.786	0.489	-25.992	0.328	0.909	0.863	0.973	21.128
	5.0	0.0	161.0	0.000	12.170	105.520	-10.341	0.00	221.83	1923.37	10.37	4010.00	574.00	16.71	-27.87	2.085	1.786	0.489	-25.992	0.328	0.909	0.863	0.973	21.128
	6.0	0.0	161.0	0.000	12.170	105.520	-10.341	0.00	221.83	1923.37	10.37	4010.00	574.00	16.71	-27.87	2.085	1.786	0.489	-25.992	0.328	0.909	0.863	0.973	21.128
						(h1)						4010.00	3436.00											
2	(static)					(h0)								(cmc)										
	0.0	0.0	0.0	0.000	0.000	122.050	0.000	0.00	0.00	2224.67	0.00	4191.87	911.87	27.80	0.00	1.884	1.474	0.804	0.000	0.446	0.920	0.105	0.821	0.408
T1BK	1.0	10.0	10.0	0.000	0.000	122.050	0.000	0.00	0.00	2224.67	0.00	4191.87	911.87	27.80	0.00	1.884	1.474	0.804	0.000	0.446	0.920	0.105	0.821	0.408
	2.0	225.0	235.0	9.260	9.260	112.790	-7.587	168.79	168.79	2055.88	7.59	4023.09	743.09	22.66	-18.51	1.957	1.595	0.667	-17.022	0.400	0.903	0.434	0.887	6.934
20kPa	3.0	90.0	325.0	3.220	12.480	109.570	-10.225	58.69	227.48	1997.19	10.23	3964.39	684.39	20.87	-24.95	1.985	1.642	0.620	-22.941	0.383	0.896	0.549	0.910	11.067
	4.0	25.0	350.0	0.680	13.160	108.890	-10.782	12.39	239.87	1984.79	10.78	3952.00	672.00	20.49	-26.31	1.991	1.653	0.610	-24.191	0.379	0.894	0.573	0.915	12.063
	5.0	0.0	350.0	0.000	13.160	108.890	-10.782	0.00	239.87	1984.79	10.78	3952.00	672.00	20.49	-26.31	1.991	1.653	0.610	-24.191	0.379	0.894	0.573	0.915	12.063
	6.0	0.0	350.0	0.000	13.160	108.890	-10.782	0.00	239.87	1984.79	10.78	3952.00	672.00	20.49	-26.31	1.991	1.653	0.610	-24.191	0.379	0.894	0.573	0.915	12.063
						(h1)						3952.00	3280.00											
3	(static)					(h0)								(cmc)										
	0.0	0.0	0.0	0.000	0.000	108.030	0.000	0.00	0.00	1969.12	0.00	3890.16	772.16	24.76	0.00	1.976	1.583	0.680	0.000	0.405	0.969	0.404	0.881	10.087
T1BL	1.0	15.0	15.0	0.130	0.130	107.900	-0.120	2.37	2.37	1966.75	0.12	3887.79	769.79	24.69	-0.31	1.977	1.585	0.678	-0.297	0.404	0.969	0.409	0.882	10.331
	2.0	100.0	115.0	6.900	7.030	101.000	-6.507	125.77	128.14	1840.98	6.52	3762.02	644.02	20.66	-16.59	2.043	1.694	0.571	-16.079	0.363	0.963	0.667	0.933	27.470
50kPa	3.0	10.0	125.0	3.880	10.910	97.120	-10.099	70.72	198.86	1770.26	10.11	3691.30	573.30	18.39	-25.75	2.085	1.761	0.510	-24.953	0.338	0.959	0.812	0.962	40.717
	4.0	55.0	180.0	0.620	11.530	96.500	-10.673	11.30	210.16	1758.95	10.69	3680.00	562.00	18.02	-27.22	2.092	1.773	0.501	-26.371	0.334	0.958	0.835	0.967	43.075
	5.0	0.0	180.0	0.000	11.530	96.500	-10.673	0.00	210.16	1758.95	10.69	3680.00	562.00	18.02	-27.22	2.092	1.773	0.501	-26.371	0.334	0.958	0.835	0.967	43.075
	6.0	0.0	180.0	0.000	11.530	96.500	-10.673	0.00	210.16	1758.95	10.69	3680.00	562.00	18.02	-27.22	2.092	1.773	0.501	-26.371	0.334	0.958	0.835	0.967	43.075
						(h1)						3680.00	3118.00											

Table A3.8.1. Data sheet: coarse sharp sand >63μ, high acceleration, saturated, 25Hz.

TEST	ACCEL (g)	TIME incr. (mins)	TIME cum. (mins)	SET inc. (mm)	SET cum. (mm)	HEIGHT (mm)	SET (%)	VOL inc. (ml)	VOL cum. (ml)	VOL (ml)	VOL (%)	WET MASS (g)	WATER MASS (g)	M (%)	M CHANGE (%)	BULK DENSE (Mg/m2)	DRY DENSE (Mg/m2)	VOID RATIO (e)	VOID CHANGE (%)	POROS (n)	SAT (Sr)	AIR CONT (A)	REL DENSE (Dr)	REL COMP (Cr)	PENE. RESIST (N)
1	(static)					(h0)								(cmc)											
	0.0	0.0	0.0	0.00	0.00	107.69	0.00	0.00	0.00	1962.92	0.00	2784.00	200.00	7.74	0.00	1.418	1.316	1.013	0.000	0.503	0.202	0.401	-0.397	0.721	4.47
T1BN	1.0	15.0	15.0	0.38	0.38	107.31	-0.35	6.93	6.93	1955.99	0.35	2784.00	200.00	7.74	0.00	1.423	1.321	1.006	-0.701	0.501	0.204	0.399	-0.380	0.724	4.09
	2.0	14.0	29.0	0.89	1.27	106.42	-1.18	16.22	23.15	1939.77	1.18	2784.00	200.00	7.74	0.00	1.435	1.332	0.989	-2.343	0.497	0.207	0.394	-0.340	0.732	3.27
10	3.0	11.0	40.0	0.81	2.08	105.61	-1.93	14.76	37.91	1925.01	1.94	2784.00	200.00	7.74	0.00	1.446	1.342	0.974	-3.838	0.493	0.211	0.390	-0.303	0.739	2.61
	4.0	17.0	57.0	0.78	2.86	104.83	-2.66	14.22	52.13	1910.79	2.67	2784.00	200.00	7.74	0.00	1.457	1.352	0.960	-5.277	0.490	0.214	0.385	-0.268	0.746	2.04
	5.0	0.0	57.0	0.00	2.86	104.83	-2.66	0.00	52.13	1910.79	2.67	2784.00	200.00	7.74	0.00	1.457	1.352	0.960	-5.277	0.490	0.214	0.385	-0.268	0.746	2.04
	6.0	0.0	57.0	0.00	2.86	104.83	-2.66	0.00	52.13	1910.79	2.67	2784.00	200.00	7.74	0.00	1.457	1.352	0.960	-5.277	0.490	0.214	0.385	-0.268	0.746	2.04
		0.0				(h1)						2784.00	2584.00												
2	(static)					(h0)								(cmc)											
	0.0	0.0	0.0	0.00	0.00	118.19	0.00	0.00	0.00	2154.31	0.00	3209.00	229.00	7.68	0.00	1.490	1.383	0.916	0.000	0.478	0.222	0.372	-0.163	0.767	0.97
T1BO	1.0	19.0	19.0	0.23	0.23	117.96	-0.19	4.19	4.19	2150.12	0.19	3209.00	229.00	7.68	0.00	1.492	1.386	0.912	-0.407	0.477	0.223	0.370	-0.154	0.769	0.87
	2.0	15.0	34.0	0.14	0.37	117.82	-0.31	2.55	6.74	2147.57	0.31	3209.00	229.00	7.68	0.00	1.494	1.388	0.910	-0.655	0.476	0.224	0.370	-0.148	0.770	0.81
20	3.0	25.0	59.0	0.67	1.04	117.15	-0.88	12.21	18.96	2135.35	0.88	3209.00	229.00	7.68	0.00	1.503	1.396	0.899	-1.841	0.473	0.227	0.366	-0.122	0.776	0.55
	4.0	17.0	76.0	0.59	1.63	116.56	-1.38	10.75	29.71	2124.60	1.38	3209.00	229.00	7.68	0.00	1.510	1.403	0.889	-2.885	0.471	0.229	0.363	-0.099	0.780	0.36
	5.0	0.0	76.0	0.00	1.63	116.56	-1.38	0.00	29.71	2124.60	1.38	3209.00	229.00	7.68	0.00	1.510	1.403	0.889	-2.885	0.471	0.229	0.363	-0.099	0.780	0.36
	6.0	0.0	76.0	0.00	1.63	116.56	-1.38	0.00	29.71	2124.60	1.38	3209.00	229.00	7.68	0.00	1.510	1.403	0.889	-2.885	0.471	0.229	0.363	-0.099	0.780	0.36
						(h1)						3209.00	2980.00												
3	(static)					(h0)								(cmc)											
	0.0	0.0	0.0	0.00	0.00	110.05	0.00	0.00	0.00	2005.85	0.00	3085.00	211.00	7.34	0.00	1.538	1.433	0.850	0.000	0.459	0.229	0.354	-0.004	0.799	0.00
T1BP	1.0	5.0	5.0	0.00	0.00	110.05	0.00	0.00	0.00	2005.85	0.00	3085.00	211.00	7.34	0.00	1.538	1.433	0.850	0.000	0.459	0.229	0.354	-0.004	0.799	0.00
	2.0	10.0	15.0	0.03	0.03	110.02	-0.03	0.55	0.55	2005.30	0.03	3085.00	211.00	7.34	0.00	1.538	1.433	0.849	-0.059	0.459	0.229	0.354	-0.002	0.800	0.00
50	3.0	20.0	35.0	0.14	0.17	109.88	-0.15	2.55	3.10	2002.75	0.15	3085.00	211.00	7.34	0.00	1.540	1.435	0.847	-0.336	0.458	0.230	0.353	0.003	0.801	0.00
	4.0	25.0	60.0	0.20	0.37	109.68	-0.34	3.65	6.74	1999.10	0.34	3085.00	211.00	7.34	0.00	1.543	1.438	0.843	-0.732	0.457	0.231	0.352	0.011	0.802	0.01
	5.0	0.0	60.0	0.00	0.37	109.68	-0.34	0.00	6.74	1999.10	0.34	3085.00	211.00	7.34	0.00	1.543	1.438	0.843	-0.732	0.457	0.231	0.352	0.011	0.802	0.01
	6.0	0.0	60.0	0.00	0.37	109.68	-0.34	0.00	6.74	1999.10	0.34	3085.00	211.00	7.34	0.00	1.543	1.438	0.843	-0.732	0.457	0.231	0.352	0.011	0.802	0.01
						(h1)						3085.00	2874.00												

Table A3.8.2. Data sheet: coarse sharp sand >63μ, high acceleration, partially saturated, 25Hz.

TEST	ACCEL (g)	TIME incr. (mins)	TIME cum. (mins)	SET inc. (mm)	SET cum. (mm)	HEIGHT (mm)	SET (%)	VOL inc. (ml)	VOL cum. (ml)	VOL (ml)	VOL (%)	WET MASS (g)	WATER MASS (g)	M (%)	M CHANGE (%)	BULK DENSE (Mg/m2)	DRY DENSE (Mg/m2)	VOID RATIO (e)	VOID CHANGE (%)	POROS (n)	SAT (Sr)	AIR CONT (A)	REL DENSE (Dr)	REL COMP (Cr)	PENE. RESIST (N)
1	(static)					(h0)								(cmc)											
	0.0	0.0	0.0	0.00	0.00	114.77	0.00	0.00	0.00	2091.88	0.00	3248.00	2.00	0.06	0.00	1.553	1.552	0.708	0.000	0.414	0.002	0.413	0.337	0.867	3.22
T1BQ	1.0	18.0	18.0	0.56	0.56	114.21	-0.49	10.21	10.21	2081.67	0.49	3248.00	2.00	0.06	0.00	1.560	1.559	0.699	-1.177	0.412	0.002	0.411	0.357	0.871	3.62
	2.0	37.0	55.0	12.89	13.45	101.32	-11.72	234.95	245.16	1846.72	11.78	3248.00	2.00	0.06	0.00	1.759	1.758	0.508	-28.278	0.337	0.003	0.336	0.818	0.964	18.99
10	3.0	22.0	77.0	0.89	14.34	100.43	-12.50	16.22	261.38	1830.50	12.56	3248.00	2.00	0.06	0.00	1.774	1.773	0.494	-30.149	0.331	0.003	0.330	0.850	0.970	20.50
	4.0	24.0	101.0	0.53	14.87	99.90	-12.96	9.66	271.04	1820.84	13.02	3248.00	2.00	0.06	0.00	1.784	1.783	0.487	-31.263	0.327	0.003	0.326	0.869	0.974	21.42
	5.0	0.0	101.0	0.00	14.87	99.90	-12.96	0.00	271.04	1820.84	13.02	3248.00	2.00	0.06	0.00	1.784	1.783	0.487	-31.263	0.327	0.003	0.326	0.869	0.974	21.42
	6.0	0.0	101.0	0.00	14.87	99.90	-12.96	0.00	271.04	1820.84	13.02	3248.00	2.00	0.06	0.00	1.784	1.783	0.487	-31.263	0.327	0.003	0.326	0.869	0.974	21.42
						(h1)						3248.00	3246.00												
2	(static)					(h0)								(cmc)											
	0.0	0.0	0.0	0.00	0.00	122.57	0.00	0.00	0.00	2234.15	0.00	3469.20	2.20	0.06	0.00	1.553	1.552	0.708	0.000	0.414	0.002	0.413	0.337	0.867	4.18
T1BR	1.0	10.0	10.0	0.49	0.49	122.08	-0.40	8.93	8.93	2225.21	0.40	3469.20	2.20	0.06	0.00	1.559	1.558	0.701	-0.965	0.412	0.002	0.411	0.354	0.871	4.60
	2.0	55.0	65.0	13.95	14.44	108.13	-11.78	254.27	263.21	1970.94	11.83	3469.20	2.20	0.06	0.00	1.760	1.759	0.506	-28.429	0.336	0.003	0.335	0.821	0.964	24.76
20	3.0	34.0	99.0	0.56	15.00	107.57	-12.24	10.21	273.41	1960.73	12.29	3469.20	2.20	0.06	0.00	1.769	1.768	0.499	-29.531	0.333	0.003	0.332	0.840	0.968	25.90
	4.0	35.0	134.0	0.58	15.58	106.99	-12.71	10.57	283.98	1950.16	12.76	3469.20	2.20	0.06	0.00	1.779	1.778	0.491	-30.673	0.329	0.003	0.328	0.859	0.972	27.11
	5.0	0.0	134.0	0.00	15.58	106.99	-12.71	0.00	283.98	1950.16	12.76	3469.20	2.20	0.06	0.00	1.779	1.778	0.491	-30.673	0.329	0.003	0.328	0.859	0.972	27.11
	6.0	0.0	134.0	0.00	15.58	106.99	-12.71	0.00	283.98	1950.16	12.76	3469.20	2.20	0.06	0.00	1.779	1.778	0.491	-30.673	0.329	0.003	0.328	0.859	0.972	27.11
						(h1)						3469.20	3467.00												
3	(static)					(h0)								(cmc)											
	0.0	0.0	0.0	0.00	0.00	120.14	0.00	0.00	0.00	2189.85	0.00	3463.00	3.00	0.09	0.00	1.581	1.580	0.677	0.000	0.404	0.003	0.402	0.411	0.882	10.41
T1BS	1.0	9.0	9.0	0.01	0.01	120.13	-0.01	0.18	0.18	2189.67	0.01	3463.00	3.00	0.09	0.00	1.582	1.580	0.677	-0.021	0.404	0.003	0.402	0.411	0.882	10.43
	2.0	68.0	77.0	12.94	12.95	107.19	-10.78	235.86	236.05	1953.81	10.78	3463.00	3.00	0.09	0.00	1.772	1.771	0.496	-26.696	0.332	0.005	0.330	0.845	0.969	44.12
50	3.0	113.0	190.0	2.12	15.07	105.07	-12.54	38.64	274.69	1915.16	12.54	3463.00	3.00	0.09	0.00	1.808	1.807	0.467	-31.067	0.318	0.005	0.317	0.916	0.983	51.85
	4.0	27.0	217.0	0.42	15.49	104.65	-12.89	7.66	282.34	1907.51	12.89	3463.00	3.00	0.09	0.00	1.815	1.814	0.461	-31.932	0.316	0.005	0.314	0.930	0.986	53.46
	5.0	0.0	217.0	0.00	15.49	104.65	-12.89	0.00	282.34	1907.51	12.89	3463.00	3.00	0.09	0.00	1.815	1.814	0.461	-31.932	0.316	0.005	0.314	0.930	0.986	53.46
	6.0	0.0	217.0	0.00	15.49	104.65	-12.89	0.00	282.34	1907.51	12.89	3463.00	3.00	0.09	0.00	1.815	1.814	0.461	-31.932	0.316	0.005	0.314	0.930	0.986	53.46
						(h1)						3463.00	3460.00												

Table A3.8.3. Data sheet: coarse sharp sand >63μ, high acceleration, dried, 25Hz.

TEST	ACCEL	TIME	TIME	SET	SET	HEIGHT	SET	VOL	VOL	VOL	VOL	WET	WATER	M	M	BULK	DRY	VOID	VOID	POROS	SAT	AIR	REL	REL	PENE
		incr.	cum.	inc.	cum.			inc.	cum.			MASS	MASS		CHANGE	DENSE	DENSE	RATIO	CHANGE			CONT	DENSE	COMP	RESIST
	(g)	(mins)	(mins)	(mm)	(mm)	(mm)	(%)	(ml)	(ml)	(ml)	(%)	(g)	(g)	(%)	(%)	(Mg/m2)	(Mg/m2)	(e)	(%)	(n)	(Sr)	(A)	(Dr)	(Cr)	(N)
1	(static)					(h0)								(cmc)											
	0.0	0.0	0.0	0.000	0.000	125.440	0.000	0.00	0.00	2286.46	0.00	4629.00	795.00	20.74	0.00	2.025	1.677	0.586	0.000	0.370	0.941	0.022	0.629	0.926	14.535
T1BH	1.0	5.0	5.0	0.010	0.010	125.430	-0.008	0.18	0.18	2286.28	0.01	4628.82	794.82	20.73	-0.02	2.025	1.677	0.586	-0.022	0.370	0.941	0.022	0.629	0.926	14.549
	2.0	105.0	110.0	4.150	4.160	121.280	-3.316	75.64	75.83	2210.63	3.32	4553.18	719.18	18.76	-9.54	2.060	1.734	0.534	-8.972	0.348	0.935	0.023	0.755	0.951	20.967
10kPa	3.0	65.0	175.0	2.890	7.050	118.390	-5.620	52.68	128.50	2157.95	5.62	4500.50	666.50	17.38	-16.16	2.086	1.777	0.497	-15.206	0.332	0.930	0.023	0.843	0.969	26.127
	4.0	60.0	235.0	2.990	10.040	115.400	-8.004	54.50	183.00	2103.45	8.00	4446.00	612.00	15.96	-23.02	2.114	1.823	0.459	-21.655	0.315	0.924	0.024	0.934	0.987	32.063
	5.0	0.0	235.0	0.000	10.040	115.400	-8.004	0.00	183.00	2103.45	8.00	4446.00	612.00	15.96	-23.02	2.114	1.823	0.459	-21.655	0.315	0.924	0.024	0.934	0.987	32.063
	6.0	0.0	235.0	0.000	10.040	115.400	-8.004	0.00	183.00	2103.45	8.00	4446.00	612.00	15.96	-23.02	2.114	1.823	0.459	-21.655	0.315	0.924	0.024	0.934	0.987	32.063
						(h1)						4446.00	3834.00												
2	(static)					(h0)								(cmc)											
	0.0	0.0	0.0	0.000	0.000	126.640	0.000	0.00	0.00	2308.33	0.00	4701.66	823.66	21.24	0.00	2.037	1.680	0.583	0.000	0.368	0.969	0.012	0.636	0.927	14.870
T1BI	1.0	32.0	32.0	0.100	0.100	126.540	-0.079	1.82	1.82	2306.51	0.08	4699.84	821.84	21.19	-0.22	2.038	1.681	0.582	-0.214	0.368	0.968	0.012	0.639	0.928	15.011
	2.0	53.0	85.0	3.260	3.360	123.280	-2.653	59.42	61.24	2247.09	2.66	4640.41	762.41	19.66	-7.44	2.065	1.726	0.541	-7.202	0.351	0.966	0.012	0.737	0.947	19.965
20kPa	3.0	48.0	133.0	3.900	7.260	119.380	-5.733	71.09	132.33	2176.00	5.74	4569.33	691.33	17.83	-16.07	2.100	1.782	0.493	-15.560	0.330	0.963	0.012	0.854	0.971	26.818
	4.0	23.0	156.0	1.170	8.430	118.210	-6.657	21.33	153.66	2154.67	6.66	4548.00	670.00	17.28	-18.66	2.111	1.800	0.478	-18.068	0.323	0.962	0.012	0.890	0.978	29.071
	5.0	0.0	156.0	0.000	8.430	118.210	-6.657	0.00	153.66	2154.67	6.66	4548.00	670.00	17.28	-18.66	2.111	1.800	0.478	-18.068	0.323	0.962	0.012	0.890	0.978	29.071
	6.0	0.0	156.0	0.000	8.430	118.210	-6.657	0.00	153.66	2154.67	6.66	4548.00	670.00	17.28	-18.66	2.111	1.800	0.478	-18.068	0.323	0.962	0.012	0.890	0.978	29.071
						(h1)						4548.00	3878.00												
4	(static)					(h0)								(cmc)											
	0.0	0.0	0.0	0.000	0.000	113.110	0.000	0.00	0.00	2061.71	0.00	3873.69	670.39	20.93	0.00	1.879	1.554	0.712	0.000	0.416	0.782	0.091	0.327	0.865	6.598
T1BG	1.0	5.0	5.0	0.010	0.010	113.100	-0.009	0.18	0.18	2061.53	0.01	3873.50	670.20	20.92	-0.03	1.879	1.554	0.712	-0.021	0.416	0.782	0.091	0.327	0.865	6.612
	2.0	39.0	44.0	4.160	4.170	108.940	-3.687	75.83	76.01	1985.70	3.69	3797.68	594.38	18.56	-11.34	1.913	1.613	0.649	-8.864	0.394	0.761	0.094	0.479	0.896	14.145
50kPa	3.0	42.0	86.0	1.630	5.800	107.310	-5.128	29.71	105.72	1955.99	5.13	3767.97	564.67	17.63	-15.77	1.926	1.638	0.624	-12.329	0.384	0.751	0.096	0.538	0.908	17.868
	4.0	42.0	128.0	1.260	7.060	106.050	-6.242	22.97	128.69	1933.03	6.24	3745.00	541.70	16.91	-19.20	1.937	1.657	0.605	-15.008	0.377	0.743	0.097	0.584	0.917	21.043
	5.0	0.0	128.0	0.000	7.060	106.050	-6.242	0.00	128.69	1933.03	6.24	3745.00	541.70	16.91	-19.20	1.937	1.657	0.605	-15.008	0.377	0.743	0.097	0.584	0.917	21.043
	6.0	0.0	128.0	0.000	7.060	106.050	-6.242	0.00	128.69	1933.03	6.24	3745.00	541.70	16.91	-19.20	1.937	1.657	0.605	-15.008	0.377	0.743	0.097	0.584	0.917	21.043
						(h1)						3745.00	3203.30												

Table A3.9.1. Data sheet: coarse sharp sand, high acceleration, saturated, 25Hz.

TEST	ACCEL (g)	TIME incr. (mins)	TIME cum. (mins)	SET inc. (mm)	SET cum. (mm)	HEIGHT (mm)	SET (%)	VOL inc. (ml)	VOL cum. (ml)	VOL (ml)	VOL (%)	WET MASS (g)	WATER MASS (g)	M (%)	M CHANGE (%)	BULK DENSE (Mg/m2)	DRY DENSE (Mg/m2)	VOID RATIO (e)	VOID CHANGE (%)	POROS (n)	SAT (Sr)	AIR CONT (A)	REL DENSE (Dr)	REL COMP (Cr)	PENE. RESIST (N)
1	(static)					(h0)								(cmc)											
	0.0	0.0	0.0	0.00	0.00	103.13	0.00	0.00	0.00	1879.80	0.00	2910.00	288.40	11.00	0.00	1.548	1.395	0.900	0.000	0.474	0.324	0.320	-0.125	0.775	0.45
TIBD	1.0	30.0	30.0	0.43	0.43	102.70	-0.42	7.84	7.84	1871.97	0.42	2910.00	288.40	11.00	0.00	1.555	1.400	0.892	-0.880	0.472	0.327	0.317	-0.106	0.779	0.32
	2.0	33.0	63.0	0.83	1.26	101.87	-1.22	15.13	22.97	1856.84	1.23	2910.00	288.40	11.00	0.00	1.567	1.412	0.877	-2.579	0.467	0.332	0.312	-0.070	0.786	0.14
10	3.0	33.0	96.0	0.30	1.56	101.57	-1.51	5.47	28.43	1851.37	1.52	2910.00	288.40	11.00	0.00	1.572	1.416	0.871	-3.193	0.466	0.335	0.310	-0.056	0.789	0.09
	4.0	31.0	127.0	0.62	2.18	100.95	-2.11	11.30	39.74	1840.07	2.12	2910.00	288.40	11.00	0.00	1.581	1.425	0.860	-4.462	0.462	0.339	0.306	-0.029	0.794	0.02
	5.0	0.0	127.0	0.00	2.18	100.95	-2.11	0.00	39.74	1840.07	2.12	2910.00	288.40	11.00	0.00	1.581	1.425	0.860	-4.462	0.462	0.339	0.306	-0.029	0.794	0.02
	6.0	0.0	127.0	0.00	2.18	100.95	-2.11	0.00	39.74	1840.07	2.12	2910.00	288.40	11.00	0.00	1.581	1.425	0.860	-4.462	0.462	0.339	0.306	-0.029	0.794	0.02
						(h1)						2910.00	2621.60												
2	(static)					(h0)								(cmc)											
	0.0	0.0	0.0	0.00	0.00	105.71	0.00	0.00	0.00	1926.83	0.00	2814.00	82.00	3.00	0.00	1.460	1.418	0.869	0.000	0.465	0.092	0.422	-0.050	0.790	0.09
TIBE	1.0	27.0	27.0	0.33	0.33	105.38	-0.31	6.02	6.02	1920.82	0.31	2814.00	82.00	3.00	0.00	1.465	1.422	0.863	-0.671	0.463	0.092	0.421	-0.036	0.793	0.05
	2.0	27.0	54.0	0.28	0.61	105.10	-0.58	5.10	11.12	1915.71	0.58	2814.00	82.00	3.00	0.00	1.469	1.426	0.858	-1.241	0.462	0.093	0.419	-0.025	0.795	0.02
20	3.0	35.0	89.0	0.43	1.04	104.67	-0.98	7.84	18.96	1907.87	0.99	2814.00	82.00	3.00	0.00	1.475	1.432	0.851	-2.116	0.460	0.094	0.417	-0.006	0.799	0.00
	4.0	37.0	126.0	0.25	1.29	104.42	-1.22	4.56	23.51	1903.32	1.22	2814.00	82.00	3.00	0.00	1.478	1.435	0.846	-2.625	0.458	0.094	0.415	0.004	0.801	0.00
	5.0	0.0	126.0	0.00	1.29	104.42	-1.22	0.00	23.51	1903.32	1.22	2814.00	82.00	3.00	0.00	1.478	1.435	0.846	-2.625	0.458	0.094	0.415	0.004	0.801	0.00
	6.0	0.0	126.0	0.00	1.29	104.42	-1.22	0.00	23.51	1903.32	1.22	2814.00	82.00	3.00	0.00	1.478	1.435	0.846	-2.625	0.458	0.094	0.415	0.004	0.801	0.00
						(h1)						2814.00	2732.00												
3	(static)					(h0)								(cmc)											
	0.0	0.0	0.0	0.00	0.00	103.19	0.00	0.00	0.00	1880.90	0.00	3221.00	94.00	3.01	0.00	1.712	1.663	0.594	0.000	0.373	0.134	0.323	0.611	0.922	23.03
TIBF	1.0	14.0	14.0	0.02	0.02	103.17	-0.02	0.36	0.36	1880.53	0.02	3221.00	94.00	3.01	0.00	1.713	1.663	0.594	-0.052	0.373	0.134	0.323	0.611	0.922	23.08
	2.0	22.0	36.0	0.27	0.29	102.90	-0.28	4.92	5.29	1875.61	0.28	3221.00	94.00	3.01	0.00	1.717	1.667	0.590	-0.754	0.371	0.135	0.321	0.621	0.924	23.85
50	3.0	23.0	59.0	0.15	0.44	102.75	-0.43	2.73	8.02	1872.88	0.43	3221.00	94.00	3.01	0.00	1.720	1.670	0.587	-1.144	0.370	0.136	0.320	0.627	0.925	24.28
	4.0	26.0	85.0	0.23	0.67	102.52	-0.65	4.19	12.21	1868.68	0.65	3221.00	94.00	3.01	0.00	1.724	1.673	0.584	-1.742	0.369	0.136	0.318	0.636	0.927	24.94
	5.0	0.0	85.0	0.00	0.67	102.52	-0.65	0.00	12.21	1868.68	0.65	3221.00	94.00	3.01	0.00	1.724	1.673	0.584	-1.742	0.369	0.136	0.318	0.636	0.927	24.94
	6.0	0.0	85.0	0.00	0.67	102.52	-0.65	0.00	12.21	1868.68	0.65	3221.00	94.00	3.01	0.00	1.724	1.673	0.584	-1.742	0.369	0.136	0.318	0.636	0.927	24.94
						(h1)						3221.00	3127.00												

Table A3.9.2. Data sheet: coarse sharp sand, high acceleration, partially saturated, 25Hz.

TEST	ACCEL (g)	TIME incr. (mins)	TIME cum. (mins)	SET inc. (mm)	SET cum. (mm)	HEIGHT (mm)	SET (%)	VOL inc. (ml)	VOL cum. (ml)	VOL (ml)	VOL (%)	WET MASS (g)	WATER MASS (g)	M (%)	M CHANGE (%)	BULK DENSE (Mg/m2)	DRY DENSE (Mg/m2)	VOID RATIO (e)	VOID CHANGE (%)	POROS (n)	SAT (Sr)	AIR CONT (A)	REL DENSE (Dr)	REL COMP (Cr)	PENE. RESIST (N)
1	(static)					(h0)								(cmc)											
	0.0	0.0	0.0	0.00	0.00	120.23	0.00	0.00	0.00	2191.49	0.00	3463.00	3.00	0.09	0.00	1.580	1.579	0.678	0.000	0.404	0.003	0.403	0.408	0.882	4.71
T1BA	1.0	18.0	18.0	0.11	0.11	120.12	-0.09	2.01	2.01	2189.49	0.09	3463.00	3.00	0.09	0.00	1.582	1.580	0.677	-0.226	0.404	0.003	0.402	0.411	0.882	4.80
	2.0	53.0	71.0	13.32	13.43	106.80	-11.17	242.79	244.80	1946.70	11.18	3463.00	3.00	0.09	0.00	1.779	1.777	0.491	-27.634	0.329	0.005	0.328	0.858	0.972	20.90
10	3.0	27.0	98.0	0.20	13.63	106.60	-11.34	3.65	248.44	1943.05	11.35	3463.00	3.00	0.09	0.00	1.782	1.781	0.488	-28.046	0.328	0.005	0.326	0.865	0.973	21.22
	4.0	26.0	124.0	0.88	14.51	105.72	-12.07	16.04	264.48	1927.01	12.08	3463.00	3.00	0.09	0.00	1.797	1.796	0.476	-29.857	0.322	0.005	0.321	0.894	0.979	22.70
	5.0	0.0	124.0	0.00	14.51	105.72	-12.07	0.00	264.48	1927.01	12.08	3463.00	3.00	0.09	0.00	1.797	1.796	0.476	-29.857	0.322	0.005	0.321	0.894	0.979	22.70
	6.0	0.0	124.0	0.00	14.51	105.72	-12.07	0.00	264.48	1927.01	12.08	3463.00	3.00	0.09	0.00	1.797	1.796	0.476	-29.857	0.322	0.005	0.321	0.894	0.979	22.70
						(h1)						3463.00	3460.00												
2	(static)					(h0)								(cmc)											
	0.0	0.0	0.0	0.00	0.00	126.58	0.00	0.00	0.00	2307.15	0.00	3727.00	1.00	0.03	0.00	1.615	1.615	0.641	0.000	0.391	0.001	0.390	0.498	0.900	9.11
T1BB	1.0	18.0	18.0	0.04	0.04	126.54	-0.03	0.73	0.73	2306.42	0.03	3727.00	1.00	0.03	0.00	1.616	1.615	0.640	-0.081	0.390	0.001	0.390	0.499	0.900	9.15
	2.0	130.0	148.0	15.81	15.85	110.73	-12.52	288.18	288.91	2018.24	12.53	3727.00	1.00	0.03	0.00	1.847	1.846	0.435	-32.061	0.303	0.002	0.303	0.992	0.998	36.14
20	3.0	71.0	219.0	1.32	17.17	109.41	-13.57	24.06	312.97	1994.18	13.57	3727.00	1.00	0.03	0.00	1.869	1.868	0.418	-34.731	0.295	0.002	0.294	1.033	1.007	39.20
	4.0	12.0	231.0	0.04	17.21	109.37	-13.60	0.73	313.70	1993.45	13.60	3727.00	1.00	0.03	0.00	1.870	1.869	0.418	-34.812	0.295	0.002	0.294	1.034	1.007	39.29
	5.0	0.0	231.0	0.00	17.21	109.37	-13.60	0.00	313.70	1993.45	13.60	3727.00	1.00	0.03	0.00	1.870	1.869	0.418	-34.812	0.295	0.002	0.294	1.034	1.007	39.29
	6.0	0.0	231.0	0.00	17.21	109.37	-13.60	0.00	313.70	1993.45	13.60	3727.00	1.00	0.03	0.00	1.870	1.869	0.418	-34.812	0.295	0.002	0.294	1.034	1.007	39.29
						(h1)						3727.00	3726.00												
3	(static)					(h0)								(cmc)											
	0.0	0.0	0.0	0.00	0.00	119.94	0.00	0.00	0.00	2186.21	0.00	3553.00	2.00	0.06	0.00	1.625	1.624	0.631	0.000	0.387	0.002	0.386	0.520	0.904	16.73
T1BC	1.0	0.0	0.0	0.00	0.00	119.94	0.00	0.00	0.00	2186.21	0.00	3553.00	2.00	0.06	0.00	1.625	1.624	0.631	0.000	0.387	0.002	0.386	0.520	0.904	16.73
	2.0	0.0	0.0	0.00	0.00	119.94	0.00	0.00	0.00	2186.21	0.00	3553.00	2.00	0.06	0.00	1.625	1.624	0.631	0.000	0.387	0.002	0.386	0.520	0.904	16.73
50	3.0	119.0	119.0	15.24	15.24	104.70	-12.71	277.79	277.79	1908.42	12.71	3553.00	2.00	0.06	0.00	1.862	1.861	0.424	-32.827	0.298	0.004	0.297	1.019	1.004	64.10
	4.0	19.0	138.0	0.10	15.34	104.60	-12.79	1.82	279.61	1906.60	12.79	3553.00	2.00	0.06	0.00	1.864	1.862	0.423	-33.043	0.297	0.004	0.296	1.022	1.004	64.51
	5.0	0.0	138.0	0.00	15.34	104.60	-12.79	0.00	279.61	1906.60	12.79	3553.00	2.00	0.06	0.00	1.864	1.862	0.423	-33.043	0.297	0.004	0.296	1.022	1.004	64.51
	6.0	0.0	138.0	0.00	15.34	104.60	-12.79	0.00	279.61	1906.60	12.79	3553.00	2.00	0.06	0.00	1.864	1.862	0.423	-33.043	0.297	0.004	0.296	1.022	1.004	64.51
						(h1)						3553.00	3551.00												
4	(static)					(h0)								(cmc)											
	0.0	0.0	0.0	0.00	0.00	121.34	0.00	0.00	0.00	2211.73	0.00	3595.00	4.00	0.11	0.00	1.625	1.624		0.000	0.387	0.005	0.386	0.519	0.904	23.12
T2BC	1.0	9.0	9.0	0.02	0.02	121.32	-0.02	0.36	0.36	2211.36	0.02	3595.00	4.00	0.11	0.00	1.626	1.624	0.632	-0.043	0.387	0.005	0.385	0.520	0.904	23.18
	2.0	79.0	88.0	13.50	13.52	107.82	-11.14	246.07	246.44	1965.29	11.14	3595.00	4.00	0.11	0.00	1.829	1.827	0.450	-28.768	0.310	0.007	0.308	0.956	0.991	78.49
50	3.0	65.0	153.0	1.78	15.30	106.04	-12.61	32.44	278.88	1932.85	12.61	3595.00	4.00	0.11	0.00	1.860	1.858	0.426	-32.556	0.299	0.007	0.297	1.014	1.003	88.23
	4.0	24.0	177.0	0.34	15.64	105.70	-12.89	6.20	285.08	1926.65	12.89	3595.00	4.00	0.11	0.00	1.866	1.864	0.422	-33.279	0.297	0.007	0.295	1.025	1.005	90.15
	5.0	0.0	177.0	0.00	15.64	105.70	-12.89	0.00	285.08	1926.65	12.89	3595.00	4.00	0.11	0.00	1.866	1.864	0.422	-33.279	0.297	0.007	0.295	1.025	1.005	90.15
	6.0	0.0	177.0	0.00	15.64	105.70	-12.89	0.00	285.08	1926.65	12.89	3595.00	4.00	0.11	0.00	1.866	1.864	0.422	-33.279	0.297	0.007	0.295	1.025	1.005	90.15
						(h1)						3595.00	3591.00												

Table A3.9.3. Data sheet: coarse sharp sand, high acceleration, dried, 25Hz.

TEST	ACCEL (g)	TIME incr. (mins)	TIME cum. (mins)	SET inc. (mm)	SET cum. (mm)	HEIGHT (mm)	SET (%)	VOL inc. (ml)	VOL cum. (ml)	VOL (ml)	VOL (%)	WET MASS (g)	WATER MASS (g)	M (%)	M CHANGE (%)	BULK DENSE (Mg/m2)	DRY DENSE (Mg/m2)	VOID RATIO (e)	VOID CHANGE (%)	POROS (n)	SAT (Sr)	REL DENSE (Dr)	REL COMP (Cr)	PENE. RESIST (N)
1	(static)					(h0)								(cmc)										
	0.0	0.0	0.0	0.000	0.000	76.374	0.000	0.00	0.00	1392.11	0.00	2662.35	592.35	28.62	0.00	1.912	1.487	0.769	0.000	0.435	0.979	0.198	0.840	1.11
TT1IE	0.1	5.0	5.0	0.000	0.000	76.374	0.000	0.00	0.00	1392.11	0.00	2662.35	592.35	28.62	0.00	1.912	1.487	0.769	0.000	0.435	0.979	0.198	0.840	1.11
	0.2	5.0	10.0	0.000	0.000	76.374	0.000	0.00	0.00	1392.11	0.00	2662.35	592.35	28.62	0.00	1.912	1.487	0.769	0.000	0.435	0.979	0.198	0.840	1.11
	0.3	5.0	15.0	0.002	0.002	76.372	-0.003	0.04	0.04	1392.07	0.00	2662.32	592.32	28.61	-0.01	1.912	1.487	0.769	-0.006	0.435	0.979	0.198	0.840	1.11
10 kPa	0.4	120.0	135.0	0.038	0.040	76.334	-0.052	0.69	0.69	1391.38	0.05	2661.66	591.66	28.58	-0.12	1.913	1.488	0.768	-0.120	0.434	0.979	0.199	0.840	1.13
	0.5	120.0	255.0	0.097	0.136	76.238	-0.179	1.76	2.45	1389.62	0.18	2659.90	589.90	28.50	-0.41	1.914	1.490	0.766	-0.411	0.434	0.979	0.203	0.841	1.17
	0.6	120.0	375.0	0.144	0.281	76.094	-0.367	2.63	5.08	1387.00	0.36	2657.28	587.28	28.37	-0.86	1.916	1.492	0.762	-0.845	0.433	0.979	0.208	0.842	1.23
	0.8	120.0	495.0	0.239	0.520	75.854	-0.680	4.36	9.44	1382.64	0.68	2652.92	582.92	28.16	-1.59	1.919	1.497	0.757	-1.566	0.431	0.979	0.217	0.843	1.34
	1.0	120.0	615.0	0.601	1.121	75.253	-1.467	10.95	20.39	1371.68	1.46	2641.96	571.96	27.63	-3.44	1.926	1.509	0.743	-3.376	0.426	0.978	0.240	0.848	1.63
	2.0	120.0	735.0	6.362	7.483	68.891	-9.797	115.96	136.35	1255.72	9.79	2526.00	456.00	22.03	-23.02	2.012	1.648	0.595	-22.543	0.373	0.973	0.476	0.895	6.43
						(h1)						2526.00	2070.00											
2	(static)					(h0)								(cmc)										
	0.0	0.0	0.0	0.000	0.000	70.628	0.000	0.00	0.00	1287.37	0.00	2451.21	543.21	28.47	0.00	1.904	1.482	0.775	0.000	0.436	0.967	0.189	0.838	1.31
TT1IB	0.1	0.0	0.0	0.000	0.000	70.628	0.000	0.00	0.00	1287.37	0.00	2451.21	543.21	28.47	0.00	1.904	1.482	0.775	0.000	0.436	0.967	0.189	0.838	1.31
	0.2	0.0	0.0	0.000	0.000	70.628	0.000	0.00	0.00	1287.37	0.00	2451.21	543.21	28.47	0.00	1.904	1.482	0.775	0.000	0.436	0.967	0.189	0.838	1.31
	0.3	5.0	5.0	0.000	0.000	70.628	0.000	0.00	0.00	1287.37	0.00	2451.21	543.21	28.47	0.00	1.904	1.482	0.775	0.000	0.436	0.967	0.189	0.838	1.31
20 kPa	0.4	5.0	5.0	0.000	0.000	70.628	0.000	0.00	0.00	1287.37	0.00	2451.21	543.21	28.47	0.00	1.904	1.482	0.775	0.000	0.436	0.967	0.189	0.838	1.31
	0.5	120.0	125.0	0.064	0.064	70.564	-0.091	1.17	1.17	1286.21	0.09	2450.04	542.04	28.41	-0.21	1.905	1.483	0.773	-0.208	0.436	0.967	0.191	0.838	1.34
	0.6	120.0	245.0	0.085	0.149	70.479	-0.211	1.54	2.71	1284.66	0.21	2448.50	540.50	28.33	-0.50	1.906	1.485	0.771	-0.482	0.435	0.967	0.195	0.839	1.39
	0.8	120.0	365.0	0.156	0.305	70.323	-0.432	2.85	5.56	1281.81	0.43	2445.65	537.65	28.18	-1.02	1.908	1.489	0.767	-0.989	0.434	0.966	0.201	0.840	1.48
	1.0	120.0	485.0	0.240	0.545	70.084	-0.771	4.37	9.92	1277.45	0.77	2441.28	533.28	27.95	-1.83	1.911	1.494	0.761	-1.766	0.432	0.966	0.211	0.842	1.63
	2.0	120.0	605.0	6.599	7.144	63.485	-10.114	120.28	130.21	1157.16	10.11	2321.00	413.00	21.65	-23.97	2.006	1.649	0.595	-23.173	0.373	0.957	0.477	0.895	8.35
						(h1)						2321.00	1908.00											
3	(static)					(h0)								(cmc)										
	0.0	0.0	0.0	0.000	0.000	70.716	0.000	0.00	0.00	1288.98	0.00	2473.76	532.76	27.45	0.00	1.919	1.506	0.747	0.000	0.427	0.967	0.234	0.847	3.37
TT1IG	0.1	0.0	0.0	0.000	0.000	70.716	0.000	0.00	0.00	1288.98	0.00	2473.76	532.76	27.45	0.00	1.919	1.506	0.747	0.000	0.427	0.967	0.234	0.847	3.37
	0.2	0.0	0.0	0.000	0.000	70.716	0.000	0.00	0.00	1288.98	0.00	2473.76	532.76	27.45	0.00	1.919	1.506	0.747	0.000	0.427	0.967	0.234	0.847	3.37
	0.3	0.0	0.0	0.000	0.000	70.716	0.000	0.00	0.00	1288.98	0.00	2473.76	532.76	27.45	0.00	1.919	1.506	0.747	0.000	0.427	0.967	0.234	0.847	3.37
50 kPa	0.4	5.0	5.0	0.000	0.000	70.716	0.000	0.00	0.00	1288.98	0.00	2473.76	532.76	27.45	0.00	1.919	1.506	0.747	0.000	0.427	0.967	0.234	0.847	3.37
	0.5	5.0	10.0	0.000	0.000	70.716	0.000	0.00	0.00	1288.98	0.00	2473.76	532.76	27.45	0.00	1.919	1.506	0.747	0.000	0.427	0.967	0.234	0.847	3.37
	0.6	5.0	15.0	0.000	0.000	70.716	0.000	0.00	0.00	1288.98	0.00	2473.76	532.76	27.45	0.00	1.919	1.506	0.747	0.000	0.427	0.967	0.234	0.847	3.37
	0.8	120.0	135.0	0.051	0.051	70.665	-0.072	0.92	0.92	1288.05	0.07	2472.84	531.84	27.40	-0.17	1.920	1.507	0.745	-0.167	0.427	0.967	0.236	0.847	3.43
	1.0	120.0	255.0	0.176	0.227	70.489	-0.321	3.21	4.13	1284.84	0.32	2469.63	528.63	27.23	-0.78	1.922	1.511	0.741	-0.750	0.426	0.967	0.242	0.848	3.63
	2.0	120.0	375.0	5.521	5.748	64.968	-8.128	100.63	104.76	1184.21	8.13	2369.00	428.00	22.05	-19.66	2.000	1.639	0.605	-19.015	0.377	0.959	0.461	0.892	13.15
						(h1)						2369.00	1941.00											
4	(static)					(h0)								(cmc)										
	0.0	0.0	0.0	0.000	0.000	74.460	0.000	0.00	0.00	1357.21	0.00	2615.04	529.04	25.36	0.00	1.927	1.537	0.711	0.000	0.416	0.938	0.290	0.858	7.24
TT1IH	0.1	0.0	0.0	0.000	0.000	74.460	0.000	0.00	0.00	1357.21	0.00	2615.04	529.04	25.36	0.00	1.927	1.537	0.711	0.000	0.416	0.938	0.290	0.858	7.24
	0.2	0.0	0.0	0.000	0.000	74.460	0.000	0.00	0.00	1357.21	0.00	2615.04	529.04	25.36	0.00	1.927	1.537	0.711	0.000	0.416	0.938	0.290	0.858	7.24
	0.3	0.0	0.0	0.000	0.000	74.460	0.000	0.00	0.00	1357.21	0.00	2615.04	529.04	25.36	0.00	1.927	1.537	0.711	0.000	0.416	0.938	0.290	0.858	7.24
100 kPa	0.4	0.0	0.0	0.000	0.000	74.460	0.000	0.00	0.00	1357.21	0.00	2615.04	529.04	25.36	0.00	1.927	1.537	0.711	0.000	0.416	0.938	0.290	0.858	7.24
	0.5	0.0	0.0	0.000	0.000	74.460	0.000	0.00	0.00	1357.21	0.00	2615.04	529.04	25.36	0.00	1.927	1.537	0.711	0.000	0.416	0.938	0.290	0.858	7.24
	0.6	5.0	5.0	0.000	0.000	74.460	0.000	0.00	0.00	1357.21	0.00	2615.04	529.04	25.36	0.00	1.927	1.537	0.711	0.000	0.416	0.938	0.290	0.858	7.24
	0.8	15.0	20.0	0.004	0.004	74.456	-0.005	0.06	0.06	1357.15	0.00	2614.98	528.98	25.36	-0.01	1.927	1.537	0.711	-0.011	0.416	0.938	0.290	0.858	7.24
	1.0	15.0	35.0	0.003	0.007	74.453	-0.009	0.05	0.12	1357.09	0.01	2614.93	528.93	25.36	-0.02	1.927	1.537	0.711	-0.021	0.416	0.938	0.291	0.858	7.25
	2.0	120.0	155.0	3.343	3.349	71.111	-4.498	60.93	61.04	1296.17	4.50	2554.00	468.00	22.44	-11.54	1.970	1.609	0.634	-10.822	0.388	0.930	0.414	0.883	14.71
						(h1)						2554.00	2086.00											

Table A3.10.1. Data sheet: sandy fine gravel, saturated, 25Hz.

TEST	ACCEL (g)	TIME incr. (mins)	TIME cum. (mins)	SET inc. (mm)	SET cum. (mm)	HEIGHT (mm)	SET (%)	VOL inc. (ml)	VOL cum. (ml)	VOL (ml)	VOL (%)	WET MASS (g)	WATER MASS (g)	M (%)	M CHANGE (%)	BULK DENSE (Mg/m2)	DRY DENSE (Mg/m2)	VOID RATIO (e)	VOID CHANGE (%)	POROS (n)	SAT (Sr)	REL DENSE (Dr)	REL COMP (Cr)	PENE. RESIST (N)
1	(static)					(h0)								(cmc)										
	0.0	0.0	0.0	0.000	0.000	83.657	0.000	0.00	0.00	1524.86	0.00	2838.28	617.28	27.79	0.00	1.861	1.457	0.806	0.000	0.446	0.907	0.139	0.828	0.54
TT11A	0.1	5.0	5.0	0.000	0.000	83.657	0.000	0.00	0.00	1524.86	0.00	2838.28	617.28	27.79	0.00	1.861	1.457	0.806	0.000	0.446	0.907	0.139	0.828	0.54
	0.2	5.0	10.0	0.000	0.000	83.657	0.000	0.00	0.00	1524.86	0.00	2838.28	617.28	27.79	0.00	1.861	1.457	0.806	0.000	0.446	0.907	0.139	0.828	0.54
	0.3	5.0	15.0	0.000	0.000	83.657	0.000	0.00	0.00	1524.86	0.00	2838.28	617.28	27.79	0.00	1.861	1.457	0.806	0.000	0.446	0.907	0.139	0.828	0.54
10 kPa	0.4	120.0	135.0	0.234	0.234	83.423	-0.280	4.27	4.27	1520.59	0.28	2834.01	613.01	27.60	-0.69	1.864	1.461	0.801	-0.628	0.445	0.907	0.147	0.829	0.61
	0.5	120.0	255.0	0.181	0.416	83.241	-0.497	3.31	7.58	1517.28	0.50	2830.71	609.71	27.45	-1.23	1.866	1.464	0.797	-1.114	0.443	0.906	0.153	0.831	0.66
	0.6	120.0	375.0	0.255	0.671	82.986	-0.802	4.65	12.23	1512.63	0.80	2826.06	605.06	27.24	-1.98	1.868	1.468	0.791	-1.797	0.442	0.906	0.162	0.832	0.74
	0.8	120.0	495.0	0.467	1.138	82.519	-1.361	8.52	20.75	1504.11	1.36	2817.54	596.54	26.86	-3.36	1.873	1.477	0.781	-3.049	0.439	0.904	0.178	0.836	0.90
	1.0	120.0	615.0	0.521	1.659	81.998	-1.983	9.49	30.24	1494.62	1.98	2808.04	587.04	26.43	-4.90	1.879	1.486	0.770	-4.445	0.435	0.903	0.196	0.839	1.09
	2.0	120.0	735.0	5.708	7.367	76.290	-8.806	104.04	134.28	1390.57	8.81	2704.00	483.00	21.75	-21.75	1.945	1.597	0.647	-19.737	0.393	0.884	0.394	0.879	4.40
						(h1)						2704.00	2221.00											
2	(static)					(h0)								(cmc)										
	0.0	0.0	0.0	0.000	0.000	68.350	0.000	0.00	0.00	1245.85	0.00	2353.35	484.35	25.91	0.00	1.889	1.500	0.753	0.000	0.430	0.905	0.223	0.845	1.83
TT11B	0.1	0.0	0.0	0.000	0.000	68.350	0.000	0.00	0.00	1245.85	0.00	2353.35	484.35	25.91	0.00	1.889	1.500	0.753	0.000	0.430	0.905	0.223	0.845	1.83
	0.2	5.0	5.0	0.000	0.000	68.350	0.000	0.00	0.00	1245.85	0.00	2353.35	484.35	25.91	0.00	1.889	1.500	0.753	0.000	0.430	0.905	0.223	0.845	1.83
	0.3	5.0	10.0	0.000	0.000	68.350	0.000	0.00	0.00	1245.85	0.00	2353.35	484.35	25.91	0.00	1.889	1.500	0.753	0.000	0.430	0.905	0.223	0.845	1.83
20 kPa	0.4	5.0	10.0	0.000	0.000	68.350	0.000	0.00	0.00	1245.85	0.00	2353.35	484.35	25.91	0.00	1.889	1.500	0.753	0.000	0.430	0.905	0.223	0.845	1.83
	0.5	5.0	15.0	0.000	0.000	68.350	0.000	0.00	0.00	1245.85	0.00	2353.35	484.35	25.91	0.00	1.889	1.500	0.753	0.000	0.430	0.905	0.223	0.845	1.83
	0.6	30.0	45.0	0.000	0.000	68.350	0.000	0.00	0.00	1245.85	0.00	2353.35	484.35	25.91	0.00	1.889	1.500	0.753	0.000	0.430	0.905	0.223	0.845	1.83
	0.8	120.0	165.0	0.109	0.109	68.241	-0.160	1.99	1.99	1243.86	0.16	2351.35	482.35	25.81	-0.41	1.890	1.503	0.750	-0.372	0.429	0.905	0.227	0.845	1.90
	1.0	120.0	285.0	0.231	0.341	68.009	-0.498	4.22	6.21	1239.64	0.50	2347.14	478.14	25.58	-1.28	1.893	1.508	0.744	-1.160	0.427	0.904	0.237	0.847	2.06
	2.0	120.0	405.0	4.506	4.847	63.503	-7.091	82.14	88.35	1157.51	7.09	2265.00	396.00	21.19	-18.24	1.957	1.615	0.629	-16.507	0.386	0.886	0.422	0.884	6.56
						(h1)						2265.00	1869.00											
3	(static)					(h0)								(cmc)										
	0.0	0.0	0.0	0.000	0.000	73.304	0.000	0.00	0.00	1336.15	0.00	2561.62	544.62	27.00	0.00	1.917	1.510	0.742	0.000	0.426	0.957	0.240	0.848	3.57
TT11C	0.1	0.0	0.0	0.000	0.000	73.304	0.000	0.00	0.00	1336.15	0.00	2561.62	544.62	27.00	0.00	1.917	1.510	0.742	0.000	0.426	0.957	0.240	0.848	3.57
	0.2	5.0	5.0	0.000	0.000	73.304	0.000	0.00	0.00	1336.15	0.00	2561.62	544.62	27.00	0.00	1.917	1.510	0.742	0.000	0.426	0.957	0.240	0.848	3.57
	0.3	5.0	10.0	0.000	0.000	73.304	0.000	0.00	0.00	1336.15	0.00	2561.62	544.62	27.00	0.00	1.917	1.510	0.742	0.000	0.426	0.957	0.240	0.848	3.57
50 kPa	0.4	5.0	15.0	0.000	0.000	73.304	0.000	0.00	0.00	1336.15	0.00	2561.62	544.62	27.00	0.00	1.917	1.510	0.742	0.000	0.426	0.957	0.240	0.848	3.57
	0.5	5.0	20.0	0.000	0.000	73.304	0.000	0.00	0.00	1336.15	0.00	2561.62	544.62	27.00	0.00	1.917	1.510	0.742	0.000	0.426	0.957	0.240	0.848	3.57
	0.6	5.0	25.0	0.000	0.000	73.304	0.000	0.00	0.00	1336.15	0.00	2561.62	544.62	27.00	0.00	1.917	1.510	0.742	0.000	0.426	0.957	0.240	0.848	3.57
	0.8	120.0	145.0	0.031	0.031	73.273	-0.042	0.56	0.56	1335.59	0.04	2561.06	544.06	26.97	-0.10	1.918	1.510	0.741	-0.099	0.426	0.957	0.242	0.848	3.60
	1.0	120.0	265.0	0.094	0.125	73.180	-0.170	1.71	2.27	1333.88	0.17	2559.35	542.35	26.89	-0.42	1.919	1.512	0.739	-0.399	0.425	0.957	0.245	0.849	3.71
	2.0	120.0	385.0	4.792	4.917	68.387	-6.708	87.35	89.62	1246.53	6.71	2472.00	455.00	22.56	-16.46	1.983	1.618	0.625	-15.745	0.385	0.949	0.428	0.886	11.31
						(h1)						2472.00	2017.00											
4	(static)					(h0)								(cmc)										
	0.0	0.0	0.0	0.000	0.000	71.615	0.000	0.00	0.00	1305.36	0.00	2561.57	545.57	27.06	0.00	1.962	1.544	0.703	0.000	0.413	1.013	0.303	0.861	7.91
TT11D	0.1	0.0	0.0	0.000	0.000	71.615	0.000	0.00	0.00	1305.36	0.00	2561.57	545.57	27.06	0.00	1.962	1.544	0.703	0.000	0.413	1.013	0.303	0.861	7.91
	0.2	0.0	0.0	0.000	0.000	71.615	0.000	0.00	0.00	1305.36	0.00	2561.57	545.57	27.06	0.00	1.962	1.544	0.703	0.000	0.413	1.013	0.303	0.861	7.91
	0.3	0.0	0.0	0.000	0.000	71.615	0.000	0.00	0.00	1305.36	0.00	2561.57	545.57	27.06	0.00	1.962	1.544	0.703	0.000	0.413	1.013	0.303	0.861	7.91
100 kPa	0.4	0.0	0.0	0.000	0.000	71.615	0.000	0.00	0.00	1305.36	0.00	2561.57	545.57	27.06	0.00	1.962	1.544	0.703	0.000	0.413	1.013	0.303	0.861	7.91
	0.5	5.0	5.0	0.000	0.000	71.615	0.000	0.00	0.00	1305.36	0.00	2561.57	545.57	27.06	0.00	1.962	1.544	0.703	0.000	0.413	1.013	0.303	0.861	7.91
	0.6	5.0	10.0	0.000	0.000	71.615	0.000	0.00	0.00	1305.36	0.00	2561.57	545.57	27.06	0.00	1.962	1.544	0.703	0.000	0.413	1.013	0.303	0.861	7.91
	0.8	5.0	15.0	0.003	0.003	71.612	-0.004	0.05	0.05	1305.31	0.00	2561.51	545.51	27.06	-0.01	1.962	1.544	0.703	-0.010	0.413	1.013	0.304	0.861	7.92
	1.0	120.0	135.0	0.015	0.018	71.597	-0.025	0.27	0.33	1305.04	0.03	2561.24	545.24	27.05	-0.06	1.963	1.545	0.703	-0.061	0.413	1.013	0.304	0.861	7.95
	2.0	120.0	255.0	3.140	3.158	68.457	-4.410	57.24	57.57	1247.80	4.41	2504.00	488.00	24.21	-10.55	2.007	1.616	0.628	-10.684	0.386	1.014	0.424	0.885	15.44
						(h1)						2504.00	2016.00											

Table A3.10.2. Data sheet: sandy fine gravel, saturated, 40Hz.

TEST	ACCEL (g)	TIME incr. (mins)	TIME cum. (mins)	SET inc. (mm)	SET cum. (mm)	HEIGHT (mm)	SET (%)	VOL inc. (ml)	VOL cum. (ml)	VOL (ml)	VOL (%)	WET MASS (g)	WATER MASS (g)	M (%)	M CHANGE (%)	BULK DENSE (Mg/m2)	DRY DENSE (Mg/m2)	VOID RATIO (e)	VOID CHANGE (%)	POROS (n)	SAT (Sr)	AIR CONT (A)	REL DENSE (Dr)	REL COMP (Cr)	PENE. RESIST (N)
1	(static)					(h0)								(cmc)											
	0.0	0.0	0.0	0.000	0.000	84.755	0.000	0.00	0.00	1544.87	0.00	3176.69	539.69	20.47	0.00	2.056	1.707	0.541	0.000	0.351	0.995	0.002	0.204	0.841	1.18
TT1HA	0.1	15.0	15.0	0.010	0.010	84.745	-0.012	0.18	0.18	1544.69	0.01	3176.51	539.51	20.46	-0.03	2.056	1.707	0.541	-0.034	0.351	0.995	0.002	0.204	0.841	1.18
	0.2	15.0	30.0	0.002	0.012	84.743	-0.014	0.04	0.22	1544.65	0.01	3176.47	539.47	20.46	-0.04	2.056	1.707	0.541	-0.040	0.351	0.995	0.002	0.204	0.841	1.19
10 kPa	0.4	80.0	110.0	0.600	0.612	84.143	-0.722	10.94	11.16	1533.72	0.72	3165.53	528.53	20.04	-2.07	2.064	1.719	0.530	-2.057	0.346	0.995	0.002	0.234	0.847	1.55
	0.5	40.0	150.0	0.330	0.942	83.813	-1.111	6.02	17.17	1527.70	1.11	3159.52	522.52	19.81	-3.18	2.068	1.726	0.524	-3.167	0.344	0.995	0.002	0.250	0.850	1.78
	0.6	30.0	180.0	0.320	1.262	83.493	-1.489	5.83	23.00	1521.87	1.49	3153.69	516.69	19.59	-4.26	2.072	1.733	0.518	-4.242	0.341	0.995	0.002	0.266	0.853	2.01
	0.8	125.0	305.0	1.100	2.362	82.393	-2.787	20.05	43.05	1501.82	2.79	3133.64	496.64	18.83	-7.98	2.087	1.756	0.498	-7.940	0.332	0.995	0.002	0.320	0.864	2.91
	1.0	85.0	390.0	0.870	3.232	81.523	-3.813	15.86	58.91	1485.96	3.81	3117.78	480.78	18.23	-10.92	2.098	1.775	0.482	-10.865	0.325	0.995	0.002	0.363	0.873	3.74
	2.0	70.0	460.0	5.090	8.322	76.433	-9.819	92.78	151.69	1393.18	9.82	3025.00	388.00	14.71	-28.11	2.171	1.893	0.389	-27.976	0.280	0.994	0.002	0.614	0.923	10.69
						(h1)						3025.00	2637.00												
2	(static)					(h0)								(cmc)											
	0.0	0.0	0.0	0.000	0.000	87.770	0.000	0.00	0.00	1599.83	0.00	3244.68	507.68	18.55	0.00	2.028	1.711	0.537	0.000	0.350	0.908	0.032	0.213	0.843	1.67
TT1HB	0.1	25.0	25.0	0.005	0.005	87.765	-0.006	0.09	0.09	1599.74	0.01	3244.59	507.59	18.55	-0.02	2.028	1.711	0.537	-0.016	0.349	0.908	0.032	0.214	0.843	1.68
	0.2	20.0	45.0	0.005	0.010	87.760	-0.011	0.09	0.18	1599.65	0.01	3244.50	507.50	18.54	-0.04	2.028	1.711	0.537	-0.033	0.349	0.908	0.032	0.214	0.843	1.68
20 kPa	0.4	60.0	105.0	0.190	0.200	87.570	-0.228	3.46	3.65	1596.18	0.23	3241.03	504.03	18.42	-0.72	2.030	1.715	0.534	-0.652	0.348	0.907	0.032	0.223	0.845	1.82
	0.5	60.0	165.0	0.165	0.365	87.405	-0.416	3.01	6.65	1593.18	0.42	3238.03	501.03	18.31	-1.31	2.032	1.718	0.531	-1.190	0.347	0.907	0.032	0.231	0.846	1.95
	0.6	40.0	205.0	0.150	0.515	87.255	-0.587	2.73	9.39	1590.44	0.59	3235.29	498.29	18.21	-1.85	2.034	1.721	0.528	-1.679	0.346	0.906	0.032	0.238	0.848	2.08
	0.8	95.0	300.0	0.385	0.900	86.870	-1.025	7.02	16.40	1583.42	1.03	3228.27	491.27	17.95	-3.23	2.039	1.729	0.522	-2.934	0.343	0.905	0.033	0.256	0.851	2.41
	1.0	105.0	405.0	0.550	1.450	86.320	-1.652	10.03	26.43	1573.40	1.65	3218.25	481.25	17.58	-5.21	2.045	1.740	0.512	-4.727	0.339	0.903	0.033	0.282	0.856	2.92
	2.0	85.0	490.0	3.470	4.920	82.850	-5.606	63.25	89.68	1510.15	5.61	3155.00	418.00	15.27	-17.66	2.089	1.812	0.451	-16.039	0.311	0.890	0.034	0.447	0.889	7.34
						(h1)						3155.00	2737.00												
3	(static)					(h0)								(cmc)											
	0.0	0.0	0.0	0.000	0.000	81.135	0.000	0.00	0.00	1478.89	0.00	3032.08	451.08	17.48	0.00	2.050	1.745	0.507	0.000	0.336	0.907	0.031	0.295	0.859	5.39
TT1HC	0.1	15.0	15.0	0.000	0.000	81.135	0.000	0.00	0.00	1478.89	0.00	3032.08	451.08	17.48	0.00	2.050	1.745	0.507	0.000	0.336	0.907	0.031	0.295	0.859	5.39
	0.2	20.0	35.0	0.007	0.007	81.128	-0.009	0.13	0.13	1478.76	0.01	3031.96	450.96	17.47	-0.03	2.050	1.745	0.507	-0.026	0.336	0.907	0.031	0.296	0.859	5.41
50 kPa	0.4	30.0	65.0	0.023	0.030	81.105	-0.037	0.42	0.55	1478.34	0.04	3031.54	450.54	17.46	-0.12	2.051	1.746	0.506	-0.110	0.336	0.907	0.031	0.297	0.859	5.45
	0.5	20.0	85.0	0.005	0.035	81.100	-0.043	0.09	0.64	1478.25	0.04	3031.45	450.45	17.45	-0.14	2.051	1.746	0.506	-0.128	0.336	0.907	0.031	0.297	0.859	5.46
	0.6	35.0	120.0	0.190	0.225	80.910	-0.277	3.46	4.10	1474.79	0.28	3027.98	446.98	17.32	-0.91	2.053	1.750	0.503	-0.824	0.335	0.906	0.031	0.307	0.861	5.81
	0.8	65.0	185.0	0.320	0.545	80.590	-0.672	5.83	9.93	1468.96	0.67	3022.15	441.15	17.09	-2.20	2.057	1.757	0.497	-1.997	0.332	0.905	0.032	0.323	0.865	6.44
	1.0	95.0	280.0	0.300	0.845	80.290	-1.041	5.47	15.40	1463.49	1.04	3016.68	435.68	16.88	-3.41	2.061	1.764	0.491	-3.096	0.329	0.904	0.032	0.338	0.868	7.06
	2.0	50.0	330.0	3.000	3.845	77.290	-4.739	54.68	70.08	1408.80	4.74	2962.00	381.00	14.76	-15.54	2.102	1.832	0.436	-14.087	0.303	0.891	0.033	0.489	0.898	14.77
						(h1)						2962.00	2581.00												
4	(static)					(h0)								(cmc)											
	0.0	0.0	0.0	0.000	0.000	76.520	0.000	0.00	0.00	1394.77	0.00	2867.29	459.29	19.07	0.00	2.056	1.726	0.523	0.000	0.344	0.959	0.014	0.251	0.850	5.41
TT1HD	0.1	15.0	15.0	0.000	0.000	76.520	0.000	0.00	0.00	1394.77	0.00	2867.29	459.29	19.07	0.00	2.056	1.726	0.523	0.000	0.344	0.959	0.014	0.251	0.850	5.41
	0.2	15.0	30.0	0.000	0.000	76.520	0.000	0.00	0.00	1394.77	0.00	2867.29	459.29	19.07	0.00	2.056	1.726	0.523	0.000	0.344	0.959	0.014	0.251	0.850	5.41
100 kPa	0.4	40.0	70.0	0.000	0.000	76.520	0.000	0.00	0.00	1394.77	0.00	2867.29	459.29	19.07	0.00	2.056	1.726	0.523	0.000	0.344	0.959	0.014	0.251	0.850	5.41
	0.5	20.0	90.0	0.000	0.000	76.520	0.000	0.00	0.00	1394.77	0.00	2867.29	459.29	19.07	0.00	2.056	1.726	0.523	0.000	0.344	0.959	0.014	0.251	0.850	5.41
	0.6	20.0	110.0	0.003	0.003	76.517	-0.004	0.05	0.05	1394.71	0.00	2867.24	459.24	19.07	-0.01	2.056	1.727	0.523	-0.011	0.344	0.958	0.014	0.251	0.850	5.42
	0.8	95.0	205.0	0.027	0.030	76.490	-0.039	0.49	0.55	1394.22	0.04	2866.75	458.75	19.05	-0.12	2.056	1.727	0.523	-0.114	0.343	0.958	0.014	0.253	0.851	5.48
	1.0	150.0	355.0	0.130	0.160	76.360	-0.209	2.37	2.92	1391.85	0.21	2864.38	456.38	18.95	-0.63	2.058	1.730	0.520	-0.609	0.342	0.958	0.014	0.260	0.852	5.79
	2.0	85.0	440.0	4.300	4.460	72.060	-5.829	78.38	81.29	1313.47	5.83	2786.00	378.00	15.70	-17.70	2.121	1.833	0.435	-16.965	0.303	0.950	0.015	0.492	0.898	20.74
						(h1)						2786.00	2408.00												

Table A3.11.1. Data sheet: sandy fine to medium gravel, saturated, 25Hz.

TEST	ACCEL (g)	TIME incr. (mins)	TIME cum. (mins)	SET inc. (mm)	SET cum. (mm)	HEIGHT (mm)	SET (%)	VOL inc. (ml)	VOL cum. (ml)	VOL (ml)	VOL (%)	WET MASS (g)	WATER MASS (g)	M (%)	M CHANGE (%)	BULK DENSE (Mg/m2)	DRY DENSE (Mg/m2)	VOID RATIO (e)	VOID CHANGE (%)	POROS (n)	SAT (Sr)	REL DENSE (Dr)	REL COMP (Cr)	PENE. RESIST (N)
1	(static)					(h0)								(cmc)										
	0.0	0.0	0.0	0.000	0.000	82.900	0.000	0.00	0.00	1511.06	0.00	3168.74	562.74	21.59	0.00	2.097	1.725	0.525	0.000	0.344	1.082	0.247	0.849	1.73
TT1He	0.1	5.0	5.0	0.000	0.000	82.900	0.000	0.00	0.00	1511.06	0.00	3168.74	562.74	21.59	0.00	2.097	1.725	0.525	0.000	0.344	1.082	0.247	0.849	1.73
	0.2	5.0	10.0	0.001	0.001	82.899	-0.001	0.02	0.02	1511.04	0.00	3168.72	562.72	21.59	0.00	2.097	1.725	0.525	-0.004	0.344	1.082	0.247	0.849	1.73
	0.3	190.0	200.0	0.266	0.267	82.633	-0.322	4.85	4.87	1506.19	0.32	3163.87	557.87	21.41	-0.86	2.101	1.730	0.520	-0.936	0.342	1.083	0.260	0.852	1.92
10 kPa	0.4	150.0	350.0	0.180	0.447	82.453	-0.539	3.28	3.30	1502.91	0.22	3165.44	559.44	21.47	-0.59	2.106	1.734	0.517	-1.566	0.341	1.093	0.269	0.854	2.05
	0.5	155.0	505.0	0.285	0.732	82.168	-0.883	5.19	8.49	1497.72	0.56	3160.24	554.24	21.27	-1.51	2.110	1.740	0.512	-2.565	0.338	1.094	0.283	0.857	2.27
	0.6	280.0	785.0	0.398	1.130	81.770	-1.363	7.25	15.75	1490.46	1.04	3152.99	546.99	20.99	-2.80	2.115	1.748	0.504	-3.960	0.335	1.095	0.303	0.861	2.60
	0.8	180.0	965.0	0.400	1.530	81.370	-1.846	7.29	23.04	1483.17	1.52	3145.70	539.70	20.71	-4.09	2.121	1.757	0.497	-5.361	0.332	1.096	0.323	0.865	2.96
	1.0	240.0	1205.0	1.016	2.546	80.354	-3.071	18.52	41.56	1464.65	2.75	3127.18	521.18	20.00	-7.39	2.135	1.779	0.478	-8.921	0.323	1.100	0.374	0.875	3.96
	2.0	270.0	1475.0	5.332	7.878	75.023	-9.502	97.18	138.74	1367.47	9.18	3030.00	424.00	16.27	-24.65	2.216	1.906	0.380	-27.603	0.275	1.126	0.639	0.928	11.60
						(h1)						3030.00	2606.00											
2	(static)					(h0)								(cmc)										
	0.0	0.0	0.0	0.000	0.000	78.821	0.000	0.00	0.00	1436.71	0.00	2969.08	497.08	20.11	0.00	2.067	1.721	0.529	0.000	0.346	1.001	0.237	0.847	2.06
TT1HF	0.1	5.0	5.0	0.000	0.000	78.821	0.000	0.00	0.00	1436.71	0.00	2969.08	497.08	20.11	0.00	2.067	1.721	0.529	0.000	0.346	1.001	0.237	0.847	2.06
	0.2	5.0	10.0	0.000	0.000	78.821	0.000	0.00	0.00	1436.71	0.00	2969.08	497.08	20.11	0.00	2.067	1.721	0.529	0.000	0.346	1.001	0.237	0.847	2.06
	0.3	80.0	90.0	0.031	0.031	78.791	-0.039	0.56	0.56	1436.15	0.04	2968.53	496.53	20.09	-0.11	2.067	1.721	0.528	-0.112	0.346	1.001	0.239	0.848	2.09
20 kPa	0.4	120.0	130.0	0.174	0.174	78.647	-0.221	3.17	3.17	1433.54	0.22	2965.91	493.91	19.98	-0.64	2.069	1.724	0.525	-0.638	0.344	1.001	0.246	0.849	2.23
	0.5	160.0	290.0	0.177	0.351	78.470	-0.445	3.23	6.40	1430.31	0.45	2962.68	490.68	19.85	-1.29	2.071	1.728	0.522	-1.288	0.343	1.001	0.255	0.851	2.40
	0.6	175.0	465.0	0.162	0.513	78.308	-0.651	2.95	9.35	1427.36	0.65	2959.73	487.73	19.73	-1.88	2.074	1.732	0.519	-1.882	0.341	1.001	0.264	0.853	2.56
	0.8	180.0	645.0	0.340	0.853	77.968	-1.082	6.20	15.55	1421.16	1.08	2953.53	481.53	19.48	-3.13	2.078	1.739	0.512	-3.130	0.339	1.001	0.282	0.856	2.92
	1.0	210.0	855.0	0.506	1.359	77.462	-1.724	9.22	24.77	1411.94	1.72	2944.31	472.31	19.11	-4.98	2.085	1.751	0.502	-4.986	0.334	1.001	0.308	0.862	3.49
	2.0	120.0	975.0	4.022	5.381	73.440	-6.827	73.31	98.08	1338.63	6.83	2871.00	399.00	16.14	-19.73	2.145	1.847	0.424	-19.743	0.298	1.001	0.520	0.904	9.93
						(h1)						2871.00	2472.00											
3	(static)					(h0)								(cmc)										
	0.0	0.0	0.0	0.000	0.000	79.108	0.000	0.00	0.00	1441.94	0.00	3028.61	510.61	20.28	0.00	2.100	1.746	0.506	0.000	0.336	1.054	0.298	0.860	5.49
TT1HG	0.1	5.0	5.0	0.000	0.000	79.108	0.000	0.00	0.00	1441.94	0.00	3028.61	510.61	20.28	0.00	2.100	1.746	0.506	0.000	0.336	1.054	0.298	0.860	5.49
	0.2	5.0	10.0	0.000	0.000	79.108	0.000	0.00	0.00	1441.94	0.00	3028.61	510.61	20.28	0.00	2.100	1.746	0.506	0.000	0.336	1.054	0.298	0.860	5.49
	0.3	10.0	20.0	0.000	0.000	79.108	0.000	0.00	0.00	1441.94	0.00	3028.61	510.61	20.28	0.00	2.100	1.746	0.506	0.000	0.336	1.054	0.298	0.860	5.49
50 kPa	0.4	20.0	40.0	0.000	0.000	79.108	0.000	0.00	0.00	1441.94	0.00	3028.61	510.61	20.28	0.00	2.100	1.746	0.506	0.000	0.336	1.054	0.298	0.860	5.49
	0.5	120.0	160.0	0.074	0.074	79.035	-0.093	1.34	1.34	1440.60	0.09	3027.27	509.27	20.23	-0.26	2.101	1.748	0.505	-0.277	0.335	1.054	0.302	0.860	5.63
	0.6	120.0	280.0	0.061	0.135	78.974	-0.170	1.11	2.45	1439.49	0.17	3026.15	508.15	20.18	-0.48	2.102	1.749	0.504	-0.506	0.335	1.054	0.305	0.861	5.75
	0.8	135.0	415.0	0.180	0.315	78.794	-0.398	3.28	5.73	1436.21	0.40	3022.87	504.87	20.05	-1.12	2.105	1.753	0.500	-1.183	0.333	1.054	0.314	0.863	6.10
	1.0	180.0	595.0	0.248	0.563	78.546	-0.711	4.52	10.25	1431.69	0.71	3018.35	500.35	19.87	-2.01	2.108	1.759	0.495	-2.116	0.331	1.055	0.327	0.865	6.61
	2.0	120.0	715.0	3.750	4.313	74.796	-5.451	68.35	78.61	1363.34	5.45	2950.00	432.00	17.16	-15.39	2.164	1.847	0.424	-16.223	0.298	1.064	0.520	0.904	16.75
						(h1)						2950.00	2518.00											
4	(static)					(h0)								(cmc)										
	0.0	0.0	0.0	0.000	0.000	80.580	0.000	0.00	0.00	1468.77	0.00	3061.98	474.98	18.36	0.00	2.085	1.761	0.493	0.000	0.330	0.979	0.333	0.867	9.51
TT1HH	0.1	5.0	5.0	0.000	0.000	80.580	0.000	0.00	0.00	1468.77	0.00	3061.98	474.98	18.36	0.00	2.085	1.761	0.493	0.000	0.330	0.979	0.333	0.867	9.51
	0.2	5.0	10.0	0.000	0.000	80.580	0.000	0.00	0.00	1468.77	0.00	3061.98	474.98	18.36	0.00	2.085	1.761	0.493	0.000	0.330	0.979	0.333	0.867	9.51
	0.3	15.0	25.0	0.000	0.000	80.580	0.000	0.00	0.00	1468.77	0.00	3061.98	474.98	18.36	0.00	2.085	1.761	0.493	0.000	0.330	0.979	0.333	0.867	9.51
100 kPa	0.4	5.0	30.0	0.000	0.000	80.580	0.000	0.00	0.00	1468.77	0.00	3061.98	474.98	18.36	0.00	2.085	1.761	0.493	0.000	0.330	0.979	0.333	0.867	9.51
	0.5	5.0	35.0	0.001	0.001	80.579	-0.001	0.02	0.02	1468.75	0.00	3061.97	474.97	18.36	0.00	2.085	1.761	0.493	-0.004	0.330	0.979	0.333	0.867	9.52
	0.6	55.0	90.0	0.025	0.026	80.554	-0.032	0.46	0.47	1468.30	0.03	3061.51	474.51	18.34	-0.10	2.085	1.762	0.493	-0.098	0.330	0.979	0.334	0.867	9.59
	0.8	90.0	180.0	0.171	0.197	80.384	-0.244	3.11	3.58	1465.19	0.24	3058.40	471.40	18.22	-0.75	2.087	1.766	0.490	-0.738	0.329	0.979	0.343	0.869	10.09
	1.0	90.0	270.0	0.210	0.406	80.174	-0.504	3.82	7.40	1461.37	0.50	3054.58	467.58	18.07	-1.56	2.090	1.770	0.486	-1.525	0.327	0.979	0.353	0.871	10.71
	2.0	75.0	345.0	3.214	3.620	76.960	-4.492	58.58	65.98	1402.79	4.49	2996.00	409.00	15.81	-13.89	2.136	1.844	0.426	-13.601	0.299	0.976	0.515	0.903	22.74
						(h1)						2996.00	2587.00											

Table A3.11.2. Data sheet: sandy fine to medium gravel, saturated, 40Hz.

TEST	ACCEL (g)	TIME incr. (mins)	TIME cum. (mins)	SET inc. (mm)	SET cum. (mm)	HEIGHT (mm)	SET (%)	VOL inc. (ml)	VOL cum. (ml)	VOL (ml)	VOL (%)	WET MASS (g)	WATER MASS (g)	M (%)	M CHANGE (%)	BULK DENSE (Mg/m2)	DRY DENSE (Mg/m2)	VOID RATIO (e)	VOID CHANGE (%)	POROS (n)	SAT (Sr)	REL DENSE (Dr)	REL COMP (Cr)	PENE. RESIST (N)
1	(static)					(h0)								(cmc)										
	0.0	0.0	0.0	0.000	0.000	67.330	0.000	0.00	0.00	1227.26	0.00	2079.10	405.10	24.20	0.00	1.694	1.364	0.928	0.000	0.481	0.686	-0.846	0.631	20.30
TT1HQ	0.1	10.0	10.0	0.000	0.000	67.330	0.000	0.00	0.00	1227.26	0.00	2079.10	405.10	24.20	0.00	1.694	1.364	0.928	0.000	0.481	0.686	-0.846	0.631	20.30
	0.3	10.0	20.0	0.273	0.273	67.057	-0.406	4.98	4.98	1222.28	0.41	2074.12	400.12	23.90	-1.23	1.697	1.370	0.920	-0.843	0.479	0.683	-0.825	0.635	19.29
10 kPa	0.4	120.0	140.0	0.321	0.594	66.736	-0.883	5.85	10.83	1216.43	0.88	2068.27	394.27	23.55	-2.67	1.700	1.376	0.911	-1.833	0.477	0.680	-0.800	0.640	18.14
	0.5	120.0	260.0	0.312	0.906	66.424	-1.346	5.68	16.51	1210.74	1.35	2062.58	388.58	23.21	-4.08	1.704	1.383	0.902	-2.795	0.474	0.677	-0.776	0.645	17.06
	0.6	120.0	380.0	0.442	1.348	65.982	-2.003	8.06	24.58	1202.68	2.00	2054.52	380.52	22.73	-6.07	1.708	1.392	0.890	-4.160	0.471	0.672	-0.741	0.652	15.59
	0.8	120.0	500.0	0.572	1.920	65.410	-2.851	10.42	34.99	1192.26	2.85	2044.10	370.10	22.11	-8.64	1.714	1.404	0.873	-5.924	0.466	0.666	-0.697	0.661	13.78
	1.0	120.0	620.0	0.601	2.521	64.809	-3.744	10.95	45.95	1181.31	3.74	2033.15	359.15	21.45	-11.34	1.721	1.417	0.856	-7.778	0.461	0.659	-0.650	0.670	11.99
	2.0	120.0	740.0	3.629	6.150	61.180	-9.134	66.15	112.10	1115.16	9.13	1967.00	293.00	17.50	-27.67	1.764	1.501	0.752	-18.975	0.429	0.612	-0.369	0.726	3.85
						(h1)						1967.00	1674.00											
2	(static)					(h0)								(cmc)										
	0.0	0.0	0.0	0.000	0.000	68.815	0.000	0.00	0.00	1254.33	0.00	2503.05	424.05	20.40	0.00	1.996	1.657	0.587	0.000	0.370	0.914	0.079	0.816	0.23
TT1HR	0.1	5.0	5.0	0.000	0.000	68.815	0.000	0.00	0.00	1254.33	0.00	2503.05	424.05	20.40	0.00	1.996	1.657	0.587	0.000	0.370	0.914	0.079	0.816	0.23
	0.2	5.0	10.0	0.000	0.000	68.815	0.000	0.00	0.00	1254.33	0.00	2503.05	424.05	20.40	0.00	1.996	1.657	0.587	0.000	0.370	0.914	0.079	0.816	0.23
20 kPa	0.4	120.0	130.0	0.000	0.000	68.815	0.000	0.00	0.00	1254.33	0.00	2503.05	424.05	20.40	0.00	1.996	1.657	0.587	0.000	0.370	0.914	0.079	0.816	0.23
	0.5	120.0	250.0	0.161	0.161	68.654	-0.234	2.94	2.94	1251.39	0.23	2500.11	421.11	20.26	-0.69	1.998	1.661	0.583	-0.634	0.368	0.914	0.089	0.818	0.29
	0.6	120.0	370.0	0.185	0.347	68.469	-0.504	3.38	6.32	1248.01	0.50	2496.74	417.74	20.09	-1.49	2.001	1.666	0.579	-1.362	0.367	0.913	0.101	0.820	0.37
	0.8	120.0	490.0	0.327	0.673	68.142	-0.978	5.96	12.27	1242.05	0.98	2490.78	411.78	19.81	-2.89	2.005	1.674	0.571	-2.646	0.364	0.912	0.121	0.824	0.54
	1.0	120.0	610.0	0.410	1.084	67.731	-1.575	7.48	19.75	1234.57	1.57	2483.30	404.30	19.45	-4.66	2.011	1.684	0.562	-4.259	0.360	0.910	0.147	0.829	0.79
	2.0	85.0	695.0	3.199	4.282	64.533	-6.223	58.30	78.05	1176.27	6.22	2425.00	346.00	16.64	-18.41	2.062	1.767	0.488	-16.828	0.328	0.897	0.347	0.869	4.42
						(h1)						2425.00	2079.00											
3	(static)					(h0)								(cmc)										
	0.0	0.0	0.0	0.000	0.000	66.730	0.000	0.00	0.00	1216.32	0.00	2486.61	437.61	21.36	0.00	2.044	1.685	0.561	0.000	0.359	1.001	0.148	0.830	1.36
TT1HS	0.1	5.0	5.0	0.000	0.000	66.730	0.000	0.00	0.00	1216.32	0.00	2486.61	437.61	21.36	0.00	2.044	1.685	0.561	0.000	0.359	1.001	0.148	0.830	1.36
	0.2	50.0	55.0	0.000	0.000	66.730	0.000	0.00	0.00	1216.32	0.00	2486.61	437.61	21.36	0.00	2.044	1.685	0.561	0.000	0.359	1.001	0.148	0.830	1.36
50 kPa	0.4	120.0	175.0	0.000	0.000	66.730	0.000	0.00	0.00	1216.32	0.00	2486.61	437.61	21.36	0.00	2.044	1.685	0.561	0.000	0.359	1.001	0.148	0.830	1.36
	0.5	120.0	295.0	0.053	0.053	66.677	-0.080	0.97	0.97	1215.35	0.08	2485.63	436.63	21.31	-0.22	2.045	1.686	0.560	-0.223	0.359	1.001	0.152	0.830	1.42
	0.6	120.0	415.0	0.116	0.170	66.560	-0.254	2.12	3.10	1213.23	0.25	2483.51	434.51	21.21	-0.71	2.047	1.689	0.557	-0.708	0.358	1.001	0.159	0.832	1.57
	0.8	120.0	535.0	0.224	0.394	66.336	-0.590	4.09	7.18	1209.14	0.59	2479.43	430.43	21.01	-1.64	2.051	1.695	0.552	-1.643	0.356	1.001	0.173	0.835	1.86
	1.0	120.0	655.0	0.340	0.734	65.996	-1.100	6.20	13.38	1202.94	1.10	2473.22	424.22	20.70	-3.06	2.056	1.703	0.544	-3.061	0.352	1.001	0.195	0.839	2.35
	2.0	120.0	775.0	3.030	3.764	62.966	-5.641	55.22	68.61	1147.71	5.64	2418.00	369.00	18.01	-15.68	2.107	1.785	0.473	-15.691	0.321	1.001	0.387	0.877	9.26
						(h1)						2418.00	2049.00											
4	(static)					(h0)								(cmc)										
	0.0	0.0	0.0	0.000	0.000	61.320	0.000	0.00	0.00	1117.71	0.00	2274.82	355.82	18.54	0.00	2.035	1.717	0.532	0.000	0.347	0.917	0.228	0.846	4.46
TT1HT	0.1	5.0	5.0	0.000	0.000	61.320	0.000	0.00	0.00	1117.71	0.00	2274.82	355.82	18.54	0.00	2.035	1.717	0.532	0.000	0.347	0.917	0.228	0.846	4.46
	0.2	5.0	10.0	0.000	0.000	61.320	0.000	0.00	0.00	1117.71	0.00	2274.82	355.82	18.54	0.00	2.035	1.717	0.532	0.000	0.347	0.917	0.228	0.846	4.46
100 kPa	0.4	120.0	130.0	0.000	0.000	61.320	0.000	0.00	0.00	1117.71	0.00	2274.82	355.82	18.54	0.00	2.035	1.717	0.532	0.000	0.347	0.917	0.228	0.846	4.46
	0.5	120.0	250.0	0.007	0.007	61.313	-0.011	0.12	0.12	1117.59	0.01	2274.70	355.70	18.54	-0.03	2.035	1.717	0.532	-0.031	0.347	0.917	0.229	0.846	4.48
	0.6	120.0	370.0	0.056	0.063	61.257	-0.102	1.02	1.14	1116.57	0.10	2273.68	354.68	18.48	-0.32	2.036	1.719	0.530	-0.294	0.347	0.917	0.232	0.846	4.63
	0.8	120.0	490.0	0.164	0.227	61.093	-0.370	2.99	4.13	1113.58	0.37	2270.69	351.69	18.33	-1.16	2.039	1.723	0.526	-1.064	0.345	0.916	0.243	0.849	5.09
	1.0	120.0	610.0	0.550	0.777	60.543	-1.266	10.03	14.16	1103.56	1.27	2260.66	341.66	17.80	-3.98	2.049	1.739	0.512	-3.648	0.339	0.914	0.281	0.856	6.76
	2.0	120.0	730.0	2.560	3.337	57.983	-5.441	46.66	60.82	1056.89	5.44	2214.00	295.00	15.37	-17.09	2.095	1.816	0.448	-15.673	0.310	0.901	0.454	0.891	17.68
						(h1)						2214.00	1919.00											

Table A3.11.3. Data sheet: sandy fine to medium gravel, saturated, 120Hz.

TEST	ACCEL (g)	TIME incr. (mins)	TIME cum. (mins)	SET inc. (mm)	SET cum. (mm)	HEIGHT (mm)	SET (%)	VOL inc. (ml)	VOL cum. (ml)	VOL (ml)	VOL (%)	WET MASS (g)	WATER MASS (g)	M (%)	M CHANGE (%)	BULK DENSE (Mg/m2)	DRY DENSE (Mg/m2)	VOID RATIO (e)	VOID CHANGE (%)	POROS (n)	SAT (Sr)	REL DENSE (Dr)	REL COMP (Cr)	PENE. RESIST (N)
1	(static)					(h0)								(cmc)										
	0.0	0.0	0.0	0.000	0.000	83.312	0.000	0.00	0.00	1518.57	0.00	2867.93	342.93	13.58	0.00	1.889	1.663	0.582	0.000	0.368	0.614	0.093	0.819	0.24
TT1HI	0.1	10.0	10.0	0.000	0.000	83.312	0.000	0.00	0.00	1518.57	0.00	2867.93	342.93	13.58	0.00	1.889	1.663	0.582	0.000	0.368	0.614	0.093	0.819	0.24
	0.2	10.0	20.0	0.000	0.000	83.312	0.000	0.00	0.00	1518.57	0.00	2867.93	342.93	13.58	0.00	1.889	1.663	0.582	0.000	0.368	0.614	0.093	0.819	0.24
10 kPa	0.4	120.0	140.0	0.268	0.268	83.044	-0.322	4.88	4.88	1513.69	0.32	2863.05	338.05	13.39	-1.42	1.891	1.668	0.577	-0.875	0.366	0.611	0.107	0.821	0.32
	0.5	120.0	260.0	0.194	0.462	82.850	-0.555	3.54	8.42	1510.15	0.55	2859.51	334.51	13.25	-2.46	1.894	1.672	0.573	-1.508	0.364	0.608	0.117	0.823	0.39
	0.6	120.0	380.0	0.200	0.662	82.650	-0.795	3.65	12.07	1506.50	0.79	2855.86	330.86	13.10	-3.52	1.896	1.676	0.569	-2.161	0.363	0.606	0.127	0.825	0.46
	0.8	120.0	500.0	0.664	1.326	81.986	-1.592	12.10	24.17	1494.40	1.59	2843.76	318.76	12.62	-7.05	1.903	1.690	0.557	-4.328	0.358	0.597	0.161	0.832	0.74
	1.0	120.0	620.0	0.437	1.763	81.549	-2.116	7.97	32.14	1486.44	2.12	2835.80	310.80	12.31	-9.37	1.908	1.699	0.548	-5.754	0.354	0.590	0.184	0.837	0.96
	2.0	120.0	740.0	3.500	5.263	78.049	-6.317	63.80	95.93	1422.64	6.32	2772.00	247.00	9.78	-27.97	1.948	1.775	0.482	-17.177	0.325	0.534	0.364	0.873	3.75
						(h1)						2772.00	2525.00											
2	(static)	-				(h0)								(cmc)										
	0.0	0.0	0.0	0.000	0.000	80.710	0.000	0.00	0.00	1471.14	0.00	2960.16	481.16	19.41	0.00	2.012	1.685	0.561	0.000	0.359	0.910	0.150	0.830	0.82
TT1HJ	0.1	5.0	5.0	0.008	0.008	80.703	-0.009	0.14	0.14	1471.01	0.01	2960.03	481.03	19.40	-0.03	2.012	1.685	0.561	-0.026	0.359	0.910	0.150	0.830	0.83
	0.2	5.0	10.0	0.004	0.012	80.699	-0.014	0.07	0.21	1470.93	0.01	2959.96	480.96	19.40	-0.04	2.012	1.685	0.561	-0.040	0.359	0.910	0.150	0.830	0.83
20 kPa	0.4	120.0	130.0	0.065	0.076	80.634	-0.094	1.18	1.39	1469.76	0.09	2958.78	479.78	19.35	-0.29	2.013	1.687	0.559	-0.262	0.359	0.910	0.154	0.831	0.87
	0.5	120.0	250.0	0.192	0.268	80.442	-0.332	3.50	4.89	1466.25	0.33	2955.28	476.28	19.21	-1.02	2.016	1.691	0.556	-0.925	0.357	0.909	0.164	0.833	0.99
	0.6	120.0	370.0	0.152	0.420	80.290	-0.521	2.77	7.66	1463.48	0.52	2952.50	473.50	19.10	-1.59	2.017	1.694	0.553	-1.449	0.356	0.909	0.172	0.834	1.08
	0.8	120.0	490.0	0.379	0.799	79.911	-0.990	6.91	14.57	1456.57	0.99	2945.59	466.59	18.82	-3.03	2.022	1.702	0.545	-2.757	0.353	0.908	0.192	0.838	1.35
	1.0	120.0	610.0	0.531	1.331	79.379	-1.649	9.69	24.26	1446.89	1.65	2935.91	456.91	18.43	-5.04	2.029	1.713	0.535	-4.589	0.349	0.906	0.219	0.844	1.77
	2.0	85.0	695.0	2.354	3.685	77.025	-4.565	42.91	67.16	1403.98	4.57	2893.00	414.00	16.70	-13.96	2.061	1.766	0.489	-12.707	0.329	0.897	0.343	0.869	4.32
						(h1)						2893.00	2479.00											
3	(static)					(h0)								(cmc)										
	0.0	0.0	0.0	0.000	0.000	74.786	0.000	0.00	0.00	1363.16	0.00	2751.46	470.46	20.63	0.00	2.018	1.673	0.572	0.000	0.364	0.949	0.120	0.824	0.89
TT1HK	0.1	5.0	5.0	0.000	0.000	74.786	0.000	0.00	0.00	1363.16	0.00	2751.46	470.46	20.63	0.00	2.018	1.673	0.572	0.000	0.364	0.949	0.120	0.824	0.89
	0.2	50.0	55.0	0.000	0.000	74.786	0.000	0.00	0.00	1363.16	0.00	2751.46	470.46	20.63	0.00	2.018	1.673	0.572	0.000	0.364	0.949	0.120	0.824	0.89
50 kPa	0.4	120.0	175.0	0.023	0.023	74.764	-0.030	0.41	0.41	1362.75	0.03	2751.05	470.05	20.61	-0.09	2.019	1.674	0.571	-0.083	0.364	0.949	0.121	0.824	0.91
	0.5	120.0	295.0	0.045	0.067	74.719	-0.090	0.82	1.23	1361.93	0.09	2750.23	469.23	20.57	-0.26	2.019	1.675	0.570	-0.248	0.363	0.949	0.124	0.825	0.95
	0.6	120.0	415.0	0.087	0.154	74.632	-0.206	1.58	2.81	1360.35	0.21	2748.65	467.65	20.50	-0.60	2.021	1.677	0.568	-0.567	0.362	0.948	0.129	0.826	1.02
	0.8	120.0	535.0	0.172	0.326	74.460	-0.436	3.13	5.94	1357.22	0.44	2745.52	464.52	20.36	-1.26	2.023	1.681	0.565	-1.199	0.361	0.948	0.139	0.828	1.19
	1.0	120.0	655.0	0.319	0.645	74.141	-0.862	5.81	11.75	1351.41	0.86	2739.71	458.71	20.11	-2.50	2.027	1.688	0.558	-2.369	0.358	0.948	0.157	0.831	1.52
	2.0	120.0	775.0	1.411	2.055	72.731	-2.748	25.71	37.46	1325.70	2.75	2714.00	433.00	18.98	-7.96	2.047	1.721	0.529	-7.554	0.346	0.945	0.237	0.847	3.47
						(h1)						2714.00	2281.00											
4	(static)					(h0)								(cmc)										
	0.0	0.0	0.0	0.000	0.000	74.861	0.000	0.00	0.00	1364.53	0.00	2809.87	460.87	19.62	0.00	2.059	1.721	0.528	0.000	0.345	0.978	0.239	0.848	4.91
TT1HL	0.1	5.0	5.0	0.000	0.000	74.861	0.000	0.00	0.00	1364.53	0.00	2809.87	460.87	19.62	0.00	2.059	1.721	0.528	0.000	0.345	0.978	0.239	0.848	4.91
	0.2	5.0	10.0	0.002	0.002	74.859	-0.003	0.04	0.04	1364.49	0.00	2809.83	460.83	19.62	-0.01	2.059	1.722	0.528	-0.008	0.345	0.978	0.239	0.848	4.91
100 kPa	0.4	120.0	130.0	0.006	0.008	74.853	-0.011	0.11	0.15	1364.38	0.01	2809.72	460.72	19.61	-0.03	2.059	1.722	0.528	-0.031	0.345	0.978	0.240	0.848	4.92
	0.5	120.0	250.0	0.006	0.014	74.847	-0.018	0.10	0.25	1364.28	0.02	2809.61	460.61	19.61	-0.05	2.059	1.722	0.527	-0.053	0.345	0.978	0.240	0.848	4.94
	0.6	120.0	370.0	0.008	0.022	74.839	-0.030	0.15	0.40	1364.13	0.03	2809.46	460.46	19.60	-0.09	2.060	1.722	0.527	-0.085	0.345	0.978	0.240	0.848	4.96
	0.8	120.0	490.0	0.048	0.070	74.791	-0.094	0.87	1.28	1363.25	0.09	2808.59	459.59	19.57	-0.28	2.060	1.723	0.526	-0.271	0.345	0.978	0.243	0.849	5.07
	1.0	120.0	610.0	0.125	0.196	74.666	-0.261	2.29	3.56	1360.97	0.26	2806.30	457.30	19.47	-0.77	2.062	1.726	0.524	-0.756	0.344	0.978	0.250	0.850	5.36
	2.0	120.0	730.0	1.498	1.693	73.168	-2.262	27.30	30.87	1333.66	2.26	2779.00	430.00	18.31	-6.70	2.084	1.761	0.493	-6.548	0.330	0.976	0.333	0.867	9.50
						(h1)						2779.00	2349.00											

Table A3.11.4. Data sheet: sandy fine to medium gravel, saturated, 40Hz, horizontal vibration.

TEST	ACCEL (g)	TIME incr. (mins)	TIME cum. (mins)	SET inc. (mm)	SET cum. (mm)	HEIGHT (mm)	SET (%)	VOL inc (ml)	VOL cum. (ml)	VOL (ml)	VOL (%)	WET MASS (g)	WATER MASS (g)	M (%)	M CHANGE (%)	BULK DENSE (Mg/m2)	DRY DENSE (Mg/m2)	VOID RATIO (e)	VOID CHANGE (%)	POROS (n)	SAT (Sr)	AIR CONT (A)	REL DENSE (Dr)	REL COMP (Cr)	PENE. RESIST (N)
1	(static)					(h0)								(cmc)											
	0.0	0.0	0.0	0.000	0.000	68.860	0.000	0.00	0.00	1255.15	0.00	3050.00	876.00	40.29	0.00	2.430	1.732	0.518	0.000	0.341	2.044	-0.357	0.264	0.853	1.98
TT1HM	0.1	5.0	5.0	0.000	0.000	68.860	0.000	0.00	0.00	1255.15	0.00	3050.00	876.00	40.29	0.00	2.430	1.732	0.518	0.000	0.341	2.044	-0.357	0.264	0.853	1.98
	0.2	5.0	10.0	0.002	0.002	68.858	-0.003	0.04	0.04	1255.11	0.00	3050.00	876.00	40.29	0.00	2.430	1.732	0.518	-0.009	0.341	2.044	-0.357	0.265	0.853	1.99
	0.3	5.0	15.0	0.002	0.002	68.858	-0.003	0.00	0.04	1255.11	0.00	3050.00	876.00	40.29	0.00	2.430	1.732	0.518	-0.009	0.341	2.044	-0.357	0.265	0.853	1.99
10 kPa	0.4	5.0	20.0	0.002	0.002	68.858	-0.003	0.00	0.04	1255.11	0.00	3050.00	876.00	40.29	0.00	2.430	1.732	0.518	-0.009	0.341	2.044	-0.357	0.265	0.853	1.99
	0.5	5.0	25.0	0.008	0.008	68.852	-0.012	0.11	0.15	1255.00	0.01	3050.00	876.00	40.29	0.00	2.430	1.732	0.518	-0.034	0.341	2.045	-0.357	0.265	0.853	1.99
	0.6	5.0	30.0	0.008	0.008	68.852	-0.012	0.00	0.15	1255.00	0.01	3050.00	876.00	40.29	0.00	2.430	1.732	0.518	-0.034	0.341	2.045	-0.357	0.265	0.853	1.99
	0.8	5.0	35.0	0.008	0.008	68.852	-0.012	0.00	0.15	1255.00	0.01	3050.00	876.00	40.29	0.00	2.430	1.732	0.518	-0.034	0.341	2.045	-0.357	0.265	0.853	1.99
	1.0	5.0	40.0	0.008	0.008	68.852	-0.012	0.00	0.15	1255.00	0.01	3050.00	876.00	40.29	0.00	2.430	1.732	0.518	-0.034	0.341	2.045	-0.357	0.265	0.853	1.99
	2.0	5.0	45.0	0.035	0.035	68.825	-0.051	0.49	0.64	1254.51	0.05	3050.00	876.00	40.29	0.00	2.431	1.733	0.518	-0.149	0.341	2.047	-0.357	0.267	0.853	2.02
						(h1)						2174.00	2174.00												

Table A3.11 6. Data sheet: sandy fine to medium gravel, 25Hz, dried.

TEST	ACCEL (g)	TIME incr. (mins)	TIME cum. (mins)	SET inc. (mm)	SET cum. (mm)	HEIGHT (mm)	SET (%)	VOL inc. (ml)	VOL cum. (ml)	VOL (ml)	VOL (%)	WET MASS (g)	WATER MASS (g)	M (%)	M CHANGE (%)	BULK DENSE (Mg/m2)	DRY DENSE (Mg/m2)	VOID RATIO (e)	VOID CHANGE (%)	POROS (n)	SAT (Sr)	AIR CONT (A)	REL DENSE (Dr)	REL COMP (Cr)	PENE. RESIST (N)
1	(static)					(h0)								(cmc)											
	0.0	0.0	0.0	0.000	0.000	68.360	0.000	0.00	0.00	1246.03	0.00	2366.00	179.00	8.18	0.00	1.899	1.755	0.498	0.000	0.333	0.432	0.189	0.319	0.864	2.88
TT1He	0.1	5.0	5.0	0.000	0.000	68.360	0.000	0.00	0.00	1246.03	0.00	2366.00	179.00	8.18	0.00	1.899	1.755	0.498	0.000	0.333	0.432	0.189	0.319	0.864	2.88
	0.2	5.0	10.0	0.000	0.000	68.360	0.000	0.00	0.00	1246.03	0.00	2366.00	179.00	8.18	0.00	1.899	1.755	0.498	0.000	0.333	0.432	0.189	0.319	0.864	2.88
	0.3	190.0	200.0	0.000	0.000	68.360	0.000	0.00	0.00	1246.03	0.00	2366.00	179.00	8.18	0.00	1.899	1.755	0.498	0.000	0.333	0.432	0.189	0.319	0.864	2.88
10 kPa	0.4	150.0	350.0	0.000	0.000	68.360	0.000	0.00	0.00	1246.03	0.00	2366.00	179.00	8.18	0.00	1.899	1.755	0.498	0.000	0.333	0.432	0.189	0.319	0.864	2.88
	0.5	155.0	505.0	0.000	0.000	68.360	0.000	0.00	0.00	1246.03	0.00	2366.00	179.00	8.18	0.00	1.899	1.755	0.498	0.000	0.333	0.432	0.189	0.319	0.864	2.88
	0.6	280.0	785.0	0.000	0.000	68.360	0.000	0.00	0.00	1246.03	0.00	2366.00	179.00	8.18	0.00	1.899	1.755	0.498	0.000	0.333	0.432	0.189	0.319	0.864	2.88
	0.8	180.0	965.0	0.000	0.000	68.360	0.000	0.00	0.00	1246.03	0.00	2366.00	179.00	8.18	0.00	1.899	1.755	0.498	0.000	0.333	0.432	0.189	0.319	0.864	2.88
	1.0	240.0	1205.0	0.000	0.000	68.360	0.000	0.00	0.00	1246.03	0.00	2366.00	179.00	8.18	0.00	1.899	1.755	0.498	0.000	0.333	0.432	0.189	0.319	0.864	2.88
	2.0	270.0	1475.0	0.028	0.028	68.332	-0.041	0.51	0.51	1245.52	0.04	2366.00	179.00	8.18	0.00	1.900	1.756	0.498	-0.123	0.332	0.432	0.189	0.320	0.864	2.91
						(h1)						2366.00	2187.00												

Table A3.11.5. Data sheet: sandy fine to medium gravel, 25Hz, partially saturated.

TEST	ACCEL (g)	TIME incr. (mins)	TIME cum. (mins)	SET inc. (mm)	SET cum. (mm)	HEIGHT (mm)	SET (%)	VOL inc. (ml)	VOL cum. (ml)	VOL (ml)	VOL (%)	WET MASS (g)	WATER MASS (g)	M (%)	M CHANGE (%)	BULK DENSE (Mg/m2)	DRY DENSE (Mg/m2)	VOID RATIO (e)	VOID CHANGE (%)	POROS (n)	SAT (Sr)	AIR CONT (A)	REL DENSE (Dr)	REL COMP (Cr)	PENE. RESIST (N)
1	(static)					(h0)								(cmc)											
	0.0	0.0	0.0	0.000	0.000	55.086	0.000	0.00	0.00	1004.08	0.00	2368.46	346.46	17.13	0.00	2.359	2.014	0.306	0.000	0.234	1.473	-0.111	0.840	0.968	20.02
TT1HQ	0.2	10.0	10.0	0.002	0.002	55.084	-0.004	0.04	0.04	1004.04	0.00	2368.43	346.43	17.13	-0.01	2.359	2.014	0.306	-0.015	0.234	1.473	-0.111	0.840	0.968	20.03
	0.3	10.0	20.0	0.005	0.007	55.079	-0.013	0.09	0.13	1003.95	0.01	2368.34	346.34	17.13	-0.04	2.359	2.014	0.306	-0.054	0.234	1.473	-0.111	0.841	0.968	20.04
10 kPa	0.4	120.0	140.0	0.001	0.008	55.078	-0.015	0.02	0.15	1003.93	0.01	2368.32	346.32	17.13	-0.04	2.359	2.014	0.306	-0.062	0.234	1.473	-0.111	0.841	0.968	20.05
	0.5	120.0	260.0	0.000	0.008	55.078	-0.015	0.00	0.15	1003.93	0.01	2368.32	346.32	17.13	-0.04	2.359	2.014	0.306	-0.062	0.234	1.473	-0.111	0.841	0.968	20.05
	0.6	120.0	380.0	0.012	0.020	55.066	-0.036	0.22	0.36	1003.72	0.04	2368.10	346.10	17.12	-0.11	2.359	2.015	0.306	-0.155	0.234	1.473	-0.111	0.841	0.968	20.08
	0.8	120.0	500.0	0.006	0.026	55.061	-0.046	0.10	0.46	1003.62	0.05	2368.00	346.00	17.11	-0.13	2.359	2.015	0.305	-0.198	0.234	1.474	-0.111	0.842	0.968	20.10
	1.0	120.0	620.0	0.000	0.026	55.061	-	0.00	0.46	1003.62	0.05	2368.00	346.00	17.11	-0.13	2.359	2.015	0.305	-0.198	0.234	1.474	-0.111	0.842	0.968	20.10
	2.0	120.0	740.0	0.000	0.026	55.061	-	0.00	0.46	1003.62	0.05	2368.00	346.00	17.11	-0.13	2.359	2.015	0.305	-0.198	0.234	1.474	-0.111	0.842	0.968	20.10
						(h1)						2368.00	2022.00												

Table A3.11.7. Data sheet: sandy fine to medium gravel, 40Hz, saturated, shear vibration.

TEST	ACCEL (g)	TIME incr. (mins)	TIME cum. (mins)	SET inc. (mm)	SET cum. (mm)	HEIGHT (mm)	SET (%)	VOL inc. (ml)	VOL cum. (ml)	VOL (ml)	VOL (%)	WET MASS (g)	WATER MASS (g)	M (%)	M CHANGE (%)	BULK DENSE (Mg/m2)	DRY DENSE (Mg/m2)	VOID RATIO (e)	VOID CHANGE (%)	POROS (n)	SAT (Sr)	REL DENSE (Dr)	REL COMP (Cr)	PENE RESIST (N)
1	(static)					(h0)								(cmc)										
	0.0	0.0	0.0	0.00	0.00	69.81	0.00	0.00	0.00	1272.46	0.00	2800.92	505.92	22.04	0.00	2.201	1.804	0.458	0.000	0.314	1.265	0.428	0.886	5.188
T1HA	1.0	40.0	40.0	1.15	1.15	68.66	-1.65	20.96	20.96	1251.50	1.67	2779.95	484.95	21.13	-4.14	2.221	1.834	0.434	-5.243	0.303	1.280	0.493	0.899	6.887
	2.0	45.0	85.0	4.65	5.80	64.01	-8.31	84.76	105.72	1166.74	8.45	2695.20	400.20	17.44	-20.90	2.310	1.967	0.337	-26.441	0.252	1.361	0.756	0.951	16.211
10kPa	3.0	55.0	140.0	2.08	7.88	61.93	-11.29	37.91	143.63	1128.83	11.48	2657.28	362.28	15.79	-28.39	2.354	2.033	0.294	-35.923	0.227	1.414	0.874	0.975	21.655
	4.0	45.0	185.0	1.23	9.11	60.70	-13.05	22.42	166.05	1106.41	13.27	2634.86	339.86	14.81	-32.82	2.381	2.074	0.268	-41.530	0.211	1.454	0.943	0.989	25.244
	5.0	25.0	210.0	0.56	9.67	60.14	-13.85	10.21	176.26	1096.20	14.08	2624.66	329.66	14.36	-34.84	2.394	2.094	0.256	-44.083	0.204	1.474	0.975	0.995	26.969
	6.0	25.0	235.0	0.42	10.09	59.72	-14.45	7.66	183.92	1088.55	14.70	2617.00	322.00	14.03	-36.35	2.404	2.108	0.247	-45.997	0.198	1.491	0.999	1.000	28.300
						(h1)						2617.00	2295.00											
2	(static)					(h0)								(cmc)										
	0.0	0.0	0.0	0.00	0.00	72.73	0.00	0.00	0.00	1325.69	0.00	2787.11	485.11	21.07	0.00	2.102	1.736	0.515	0.000	0.340	1.077	0.275	0.855	2.775
T1HB	1.0	35.0	35.0	0.78	0.78	71.95	-1.07	14.22	14.22	1311.47	1.08	2772.89	470.89	20.46	-2.93	2.114	1.755	0.498	-3.157	0.333	1.080	0.319	0.864	3.735
	2.0	70.0	105.0	4.53	5.31	67.42	-7.30	82.57	96.79	1228.90	7.38	2690.32	388.32	16.87	-19.95	2.189	1.873	0.404	-21.489	0.288	1.098	0.575	0.915	12.126
20kPa	3.0	50.0	155.0	1.66	6.97	65.76	-9.58	30.26	127.05	1198.64	9.69	2660.07	358.07	15.55	-26.19	2.219	1.921	0.369	-28.207	0.270	1.107	0.668	0.934	16.403
	4.0	40.0	195.0	0.47	7.44	65.29	-10.23	8.57	135.61	1190.07	10.34	2651.50	349.50	15.18	-27.95	2.228	1.934	0.360	-30.109	0.265	1.110	0.695	0.939	17.731
	5.0	30.0	225.0	0.64	8.08	64.65	-11.11	11.67	147.28	1178.41	11.23	2639.83	337.83	14.68	-30.36	2.240	1.953	0.346	-32.699	0.257	1.115	0.731	0.946	19.623
	6.0	25.0	250.0	0.32	8.40	64.33	-11.55	5.83	153.11	1172.58	11.67	2634.00	332.00	14.42	-31.56	2.246	1.963	0.340	-33.994	0.254	1.117	0.749	0.950	20.604
						(h1)						2634.00	2302.00											
3	(static)					(h0)								(cmc)										
	0.0	0.0	0.0	0.00	0.00	79.48	0.00	0.00	0.00	1448.72	0.00	2878.74	493.74	20.70	0.00	1.987	1.646	0.598	0.000	0.374	0.911	0.050	0.810	0.155
T1HC	1.0	25.0	25.0	0.30	0.30	79.18	-0.38	5.47	5.47	1443.25	0.38	2873.27	488.27	20.47	-1.11	1.991	1.653	0.592	-1.009	0.372	0.910	0.066	0.813	0.272
	2.0	55.0	80.0	4.20	4.50	74.98	-5.66	76.56	82.02	1366.70	5.68	2796.72	411.72	17.26	-16.61	2.046	1.745	0.507	-15.137	0.336	0.895	0.295	0.859	5.380
50kPa	3.0	45.0	125.0	1.97	6.47	73.01	-8.14	35.91	117.93	1330.79	8.17	2760.81	375.81	15.76	-23.89	2.075	1.792	0.467	-21.764	0.319	0.886	0.402	0.880	10.003
	4.0	40.0	165.0	0.67	7.14	72.34	-8.98	12.21	130.14	1318.58	9.02	2748.60	363.60	15.25	-26.36	2.085	1.809	0.454	-24.017	0.312	0.883	0.439	0.888	11.899
	5.0	45.0	210.0	0.90	8.04	71.44	-10.12	16.40	146.55	1302.17	10.15	2732.19	347.19	14.56	-29.68	2.098	1.832	0.436	-27.045	0.304	0.878	0.488	0.898	14.706
	6.0	25.0	235.0	0.23	8.27	71.21	-10.41	4.19	150.74	1297.98	10.44	2728.00	343.00	14.38	-30.53	2.102	1.837	0.431	-27.818	0.301	0.877	0.500	0.900	15.471
						(h1)						2728.00	2385.00											
4	(static)					(h0)								(cmc)										
	0.0	0.0	0.0	0.00	0.00	65.94	0.00	0.00	0.00	1201.92	0.00	2623.62	426.62	19.42	0.00	2.183	1.828	0.439	0.000	0.305	1.164	0.480	0.896	19.803
T1HD	1.0	15.0	15.0	0.04	0.04	65.90	-0.06	0.73	0.73	1201.19	0.06	2622.89	425.89	19.38	-0.17	2.184	1.829	0.438	-0.199	0.305	1.164	0.483	0.897	19.999
	2.0	35.0	50.0	1.08	1.12	64.82	-1.70	19.69	20.41	1181.51	1.70	2603.20	406.20	18.49	-4.79	2.203	1.859	0.414	-5.569	0.293	1.173	0.546	0.909	25.643
100kPa	3.0	50.0	100.0	2.68	3.80	62.14	-5.76	48.85	69.26	1132.66	5.77	2554.35	357.35	16.27	-16.24	2.255	1.940	0.356	-18.896	0.262	1.202	0.705	0.941	42.673
	4.0	45.0	145.0	0.77	4.57	61.37	-6.93	14.04	83.30	1118.62	6.93	2540.32	343.32	15.63	-19.53	2.271	1.964	0.339	-22.725	0.253	1.212	0.750	0.950	48.364
	5.0	30.0	175.0	0.37	4.94	61.00	-7.49	6.74	90.04	1111.88	7.50	2533.57	336.57	15.32	-21.11	2.279	1.976	0.331	-24.565	0.249	1.217	0.772	0.954	51.225
	6.0	30.0	205.0	0.58	5.52	60.42	-8.37	10.57	100.62	1101.31	8.38	2523.00	326.00	14.84	-23.58	2.291	1.995	0.318	-27.449	0.241	1.226	0.807	0.961	55.876
						(h1)						2523.00	2197.00											

Table A3.11.8. Data sheet: sandy fine to medium gravel, high acceleration, saturated, 25Hz.

Dmax for 25Hz		
Accel (g)	Regression Equation	R2
1.0	-0.023(x2)+0.120(x)-0.600	0.72
0.8	-0.0172(x2)+0.094(x)-0.349	0.74
0.6	-0.010(x2)+0.061(x)-0.214	0.60
0.5	-0.009(x2)+0.061(x)-0.160	0.66
0.4	-0.006(x2)+0.047(x)-0.098	0.72
0.3	-0.003(x2)+0.024(x)-0.051	0.67
0.2	-0.001(x2)+0.003(x)-0.006	0.34
0.1	-9E-05(x2)+0.001(x)-0.001	0.96

Dmax for 25Hz		
Accel (g)	Regression Equation	R2
1.0	-0.166ln(x)-0.60	0.21
0.8	-0.118ln(x)-0.34	0.2
0.6	-0.047ln(x)-0.200	0.10
0.5	-0.022ln(x)-0.127	0.05
0.4	-0.012ln(x)-0.070	0.03
0.3	-0.004ln(x)-0.036	0.02
0.2	-0.0009ln(x)-0.004	0.05
0.1	-0.0007ln(x)-0.001	0.33

Dmax for 40Hz		
Accel (g)	Regression Equation	R2
1.0	-0.02(x2)+0.117(x)-0.722	0.42
0.8	-0.011(x2)+0.055(x)-0.413	0.33
0.6	-0.006(x2)+0.022(x)-0.213	0.37
0.5	-0.002(x2)-0.005(x)-0.095	0.49
0.4	-0.001(x2)-0.003(x)+0.001	0.27
0.3	0.0001(x2)-0.017(x)-0.030	0.51
0.2	-0.0006(x2)+0.001(x)-0.023	0.29
0.1		

Dmax for 40Hz		
Accel (g)	Regression Equation	R2
1.0	-0.090ln(x)-0.713	0.06
0.8	-0.058ln(x)-0.425	0.05
0.6	-0.050ln(x)-0.233	0.10
0.5	-0.050ln(x)-0.127	0.25
0.4	-0.036ln(x)-0.061	0.38
0.3	-0.012ln(x)-0.029	0.15
0.2	-0.001ln(x)-0.002	0.06
0.1		

Uc for 25Hz		
Accel (g)	Regression Equation	R2
1.0	-0.490ln(x)-0.178	0.49
0.8	-0.345ln(x)-0.044	0.48
0.6	-0.173ln(x)-0.042	0.38
0.5	-0.101ln(x)-0.033	0.29
0.4	-0.058ln(x)-0.017	0.22
0.3	-0.027ln(x)-0.011	0.20
0.2	-0.006ln(x)-0.027	0.01
0.1	-0.001ln(x)+0.001	0.43

Dx for 25Hz		
Accel (g)	Regression Equation	R2
1.0	0.333ln(x)-0.225	0.60
0.8	0.237ln(x)-0.074	0.6
0.6	0.119ln(x)-0.058	0.48
0.5	0.070ln(x)-0.041	0.37
0.4	0.042ln(x)-0.019	0.32
0.3	0.019ln(x)-0.012	0.28
0.2	0.0007ln(x)-0.002	0.02
0.1	0.001ln(x)-0.001	0.58

Uc for 40Hz		
Accel (g)	Regression Equation	R2
1.0	-0.442ln(x)-0.303	0.39
0.8	-0.280ln(x)-0.165	0.35
0.6	-0.183ln(x)-0.069	0.37
0.5	-0.131ln(x)-0.016	0.49
0.4	-0.080ln(x)+0.004	0.50
0.3	-0.027ln(x)-0.007	0.21
0.2	-0.001ln(x)-0.002	0.02
0.1		

Dx for 40Hz		
Accel (g)	Regression Equation	R2
1.0	0.280ln(x)-0.373	0.41
0.8	0.180ln(x)-0.207	0.38
0.6	0.121ln(x)-0.091	0.44
0.5	0.088ln(x)-0.030	0.59
0.4	0.054ln(x)-0.004	0.62
0.3	0.021ln(x)-0.006	0.35
0.2	0.001ln(x)-0.002	0.03
0.1		

Table A3.12.1 Data sheet: regression equations for various soil-specific parameters

Dc for 25Hz		
Accel (g)	Regression Equation	R2
1.0	-0.448ln(x)+0.062	0.61
0.8	-0.326ln(x)+0.0142	0.64
0.6	-0.196ln)x)+0.104	0.72
0.5	-0.123ln(x)+0.066	0.63
0.4	-0.073ln(x)+0.045	0.54
0.3	-0.037ln(x)+0.023	0.56
0.2	-0.0035ln(x)+0.002	0.28
0.1	-0.001ln(x)+0.001	0.22

Sf for 25Hz		
Accel (g)	Regression Equation	R2
1.0	-0.405ln(x)+0.381	0.75
0.8	-0.285ln(x)+0.359	0.73
0.6	-0.165ln(x)+0.211	0.77
0.5	-0.103ln(x)+0.131	0.66
0.4	-0.060ln(x)+0.082	0.55
0.3	-0.030ln(x)+0.041	0.55
0.2	-0.003ln(x)+0.004	0.27
0.1	-0.001ln(x)+0.002	0.31

Dc for 40Hz		
Accel (g)	Regression Equation	R2
1.0	-0.55ln(x)+0.153	0.89
0.8	-0.364(x)+0.149	0.86
0.6	-0.222(x)+0.110	0.81
0.5	-0.129ln(x)+0.063	0.70
0.4	-0.069ln(x)+0.036	0.55
0.3	-0.033ln(x)+0.019	0.46
0.2	-0.002ln(x)+0.004	0.07
0.1		

Sf for 40Hz		
Accel (g)	Regression Equation	R2
1.0	-0.432ln(x)+0.339	0.85
0.8	-0.286ln(x)+0.273	0.83
0.6	-0.176ln(x)+0.190	0.80
0.5	-0.106ln(x)+0.116	0.73
0.4	-0.058ln(x)+0.070	0.62
0.3	-0.026ln(x)+0.030	0.44
0.2	-0.001ln(x)+0.001	0.05
0.1		

Stress for 25Hz		
Accel (g)	Regression Equation	R2
1.0	25.02(x)-1.171	0.94
0.8	27.36(x)-1.394	0.93
0.6	28.53(x)-1.629	0.95
0.5	53.58(x)-2.070	1.0
0.4	46.60(x)-2.266	1.0
0.3	26.49(x)-2.302	1.0
0.2	0.141(x)-1.126	0.87
0.1	0.019(x)-1.124	1.0

Stress for 40Hz		
Accel (g)	Regression Equation	R2
1.0	13.57(x)-0.922	1.00
0.8	10.76(x)-1.022	1
0.6	26.27(x)-1.541	0.97
0.5	35.62(x)-1.857	0.97
0.4	32.29(x)-2.100	0.99
0.3	33.83(x)-2.510	0.99
0.2	1226(x)-5.04	1.0
0.1		

Table A3.12.1(cont) Data sheet: regression equations for various soil specific parameters.

Appendix 4

Settlement Calculation Data Sheets

Layer no.	Mid-layer Depth (m)	Unit Weight (KN/m2)	Mid-layer Stress (kPa)	Vibe Time (mins)	Relative Density (Dr)	Coeff. Distrib. (Dc)	Accel. (g)	Max Vibe. Settlement (Svi %)	Vibe Settlement Svi(t,f)%	Layer Thickness (m)	Surface Svi (mm)	Water table
1	0.5	17.7	4	120	0.25	2	0.43	0.38	0.42	1.0	4.19	4.19
2	1.5	18.1	12	120	0.30	5	0.43	0.23	0.26	1.0	2.57	2.57
3	3.0	18.8	27	120	0.35	10	0.43	0.13	0.15	3.0	4.36	4.36
4	5.3	18.1	44	120	0.40	5	0.43	0.05	0.06	0.5	0.28	0.28
5	7.0	17.7	55	120	0.65	2	0.43	0.01	0.01	3.0	0.34	0.34
6	10.3	18.1	85	120	0.80	5	0.43	0.01	0.01	3.5	0.49	0.49
	G1.1							tmax	Freq		12.23	12.23
								120	25			

Table A4.1.1. Data sheet: profile of Ground Condition 1.1

Layer no.	Mid-layer Depth (m)	Unit Weight (kN/m2)	Mid-layer Stress (kPa)	Vibe Time (mins)	Relative Density (Dr)	Coeff. Distrib. (Dc)	Accel. (g)	Max Vibe. Settlement (Svi %)	Vibe Settlement Svi(t,f)%	Layer Thickness (m)	Surface Svi (mm)	Water table
1	0.5	18.1	4	120	0.25	5	0.43	0.83	0.92	1.0	9.25	0.09
2	1.5	18.8	13	120	0.30	10	0.43	0.31	0.34	1.0	3.39	0.03
3	3.0	18.1	25	120	0.35	5	0.43	0.10	0.11	3.0	3.30	0.03
4	5.3	17.7	41	120	0.40	2	0.43	0.02	0.02	0.5	0.12	0.12
5	7.0	18.1	58	120	0.65	5	0.43	0.02	0.03	3.0	0.76	0.76
6	10.3	17.7	81	120	0.80	2	0.43	0.01	0.01	3.5	0.22	0.22
	G1.2							tmax	Freq		17.05	1.27
								120	25			

Table A4.1.2. Data sheet: profile of Ground Condition 1.2.

Layer no.	Mid-layer Depth (m)	Unit Weight (kN/m2)	Mid-layer Stress (kPa)	Vibe Time (mins)	Relative Density (Dr)	Coeff. Distrib. (Dc)	Accel. (g)	Max Vibe. Settlement (Svi %)	Vibe Settlement Svi(t,f)%	Layer Thickness (m)	Surface Svi (mm)	Water table
1	0.5	18.1	4	120	0.25	5	0.43	0.83	0.92	1.0	9.25	0.09
2	1.5	17.7	12	120	0.30	2	0.43	0.10	0.12	1.0	1.16	0.01
3	3.0	18.1	25	120	0.35	5	0.43	0.10	0.11	3.0	3.30	0.03
4	5.3	17.7	41	120	0.40	2	0.43	0.02	0.02	0.5	0.12	0.12
5	7.0	18.1	58	120	0.65	5	0.43	0.02	0.03	3.0	0.76	0.76
6	10.3	18.8	92	120	0.80	10	0.43	0.02	0.02	3.5	0.65	0.65
	G1.3							tmax	Freq		15.25	1.67
								120	25			

Table A4.1.3. Data sheet: profile of Ground Condition 1.3.

Layer no.	Mid-layer Depth (m)	Unit Weight (kN/m2)	Mid-layer Stress (kPa)	Vibe Time (mins)	Relative Density (Dr)	Coeff. Distribution (Dc)	Accel. (g)	Max Vibe. Settlement (Svi %)	Vibe Settlement Svi(t,f)%	Layer Thickness (m)	Surface Svi (mm)	Water table
1	2.5	19.1	23	120	0.25	1.5	0.43	0.04	0.04	5.0	2.08	0.02
2	7.5	18.6	66	120	0.40	6	0.43	0.04	0.04	5.0	2.02	0.02
3	12.5	19.5	121	120	0.60	3	0.43	0.01	0.01	5.0	0.45	0.00
4	17.5	19.9	177	120	0.80	14	0.43	0.01	0.01	5.0	0.56	0.56
5												
6												
		G2.1						tmax	Freq		5.11	0.60
								120	25			

TableA 4.1.4. Data sheet: profile of Ground Condition 2.1.

Layer no.	Mid-layer Depth (m)	Unit Weight (kN/m2)	Mid-layer Stress (kPa)	Vibe Time (mins)	Relative Density (Dr)	Coeff. Distrib. (Dc)	Accel. (g)	Max Vibe. Settlement (Svi %)	Vibe Settlement Svi(t,f)%	Layer Thickness (m)	Surface Svi (mm)	Water table
1	2.5	19.9	25	120	0.25	15	0.43	0.23	0.26	5.0	0.00	0.00
2	7.5	19.5	73	120	0.50	2	0.43	0.01	0.01	5.0	0.57	0.01
3	12.5	18.5	109	120	1.00	1	0.43	0.00	0.00	5.0	0.00	0.00
4	20.0	19	184	120	0.90	5	0.43	0.01	0.01	10.0	0.58	0.58
5												
6												
		G3.1	(and G3.2)					tmax	Freq		1.15	0.59
								120	25			

Table A4.1.5. Data sheet: profile of Ground Condition 3.1.(and 3.2).

Layer no.	Mid-layer Depth (m)	Unit Weight (kN/m2)	Mid-layer Stress (kPa)	Vibe Time (mins)	Relative Density (Dr)	Coeff. Distrib. (Dc)	Accel. (g)	Max Vibe. Settlement (Svi %)	Vibe Settlement Svi(t,f)%	Layer Thickness (m)	Surface Svi (mm)	Water table
1	5.0	19.3	47	120	0.30	2.5	0.43	0.03	0.04	10.0	3.83	0.04
2	15.0	19.2	141	120	0.70	10	0.43	0.01	0.01	10.0	1.39	0.01
3												0.00
4												0.00
5												
6												
		G4.1 (and 4.2, 4.3, 4.4)						tmax	Freq		5.22	0.05
								120	25			

Table A4.1.6. Data sheet: profile of Ground Condition 4.1.

Mid-layer Depth (m)	Unit Weight (kN/m2)	Mid-layer Stress (kPa)	Vibe Time (mins)	Relative Density (Dr)	Coeff. Distrib. (Dc)	Accel. (g)	Max Vibe. Settlement (Svi %)	Vibe Settlement Svi(t,f)%	Layer Thickness (m)	Surface Svi (mm)	Water table
0.5	19.3	5	120	0.10	2.5	0.43	1.04	1.15	1.0	11.50	0.11
1.5	19.3	14	120	0.10	2.5	0.43	0.35	0.38	1.0	3.83	0.04
2.5	19.3	24	120	0.15	2.5	0.43	0.14	0.15	1.0	1.53	0.02
3.5	19.3	33	120	0.20	2.5	0.43	0.07	0.08	1.0	0.82	0.01
4.5	19.3	43	120	0.25	2.5	0.43	0.05	0.05	1.0	0.51	
5.5	19.3	52	120	0.30	2.5	0.43	0.03	0.03	1.0	0.35	
6.5	19.3	62	120	0.35	2.5	0.43	0.02	0.03	1.0	0.25	
7.5	19.3	71	120	0.40	2.5	0.43	0.02	0.02	1.0	0.19	
8.5	19.3	81	120	0.45	2.5	0.43	0.01	0.02	1.0	0.15	
9.5	19.3	90	120	0.50	2.5	0.43	0.01	0.01	0.5	0.06	
10.5	19.2	99	120	0.55	10	0.43	0.02	0.03	0.5	0.13	
11.5	19.2	108	120	0.60	10	0.43	0.02	0.02	1.0	0.21	
12.5	19.2	117	120	0.65	10	0.43	0.02	0.02	1.0	0.18	
13.5	19.2	127	120	0.70	10	0.43	0.01	0.02	1.0	0.15	
14.5	19.2	136	120	0.75	10	0.43	0.01	0.01	1.0	0.13	
15.5	19.2	146	120	0.80	10	0.43	0.01	0.01	1.0	0.12	
16.5	19.2	155	120	0.85	10	0.43	0.01	0.01	1.0	0.10	
17.5	19.2	164	120	0.90	10	0.43	0.01	0.01	2.0	0.19	
18.5	19.2	174	120	0.95	10	0.43	0.01	0.01	2.0	0.17	
19.5	19.2	183	120	1.00	10	0.43	0.01	0.01	2.0	0.15	
	G4.4						tmax	Freq		20.73	
							120	25			

Table A4.1.7. Data sheet: profile of Ground Condition 4.4.

Mid-layer Depth (m)	Unit Weight (kN/m2)	Mid-layer Stress (kPa)	Vibe Time (mins)	Relative Density (Dr)	Coeff. Distrib. (Dc)	Accel. (g)	Max Vibe. Settlement (Svi %)	Vibe Settlement Svi(t,f)%	Layer Thickness (m)	Surface Svi (mm)	Water table
0.5	19	5	120	0.10	15	0.43	3.16	3.51	1.0	35.09	0.35
1.5	19	14	120	0.10	15	0.43	1.05	1.17	1.0	11.70	0.12
2.5	19	23	120	0.15	15	0.43	0.42	0.47	1.0	4.68	0.05
3.5	19	32	120	0.20	15	0.43	0.23	0.25	1.0	2.51	0.03
4.5	19	41	120	0.25	15	0.43	0.14	0.16	1.0	1.56	
5.5	19	51	120	0.30	15	0.43	0.10	0.11	1.0	1.06	
6.5	19	60	120	0.35	15	0.43	0.07	0.08	1.0	0.77	
7.5	19	69	120	0.40	15	0.43	0.05	0.06	1.0	0.58	
8.5	19	78	120	0.45	15	0.43	0.04	0.05	1.0	0.46	
9.5	19	87	120	0.50	15	0.43	0.03	0.04	0.5	0.18	
10.5	19	96	120	0.55	15	0.43	0.03	0.03	0.5	0.15	
11.5	19	106	120	0.60	15	0.43	0.02	0.03	1.0	0.25	
12.5	19	115	120	0.65	15	0.43	0.02	0.02	1.0	0.22	
13.5	19	124	120	0.70	15	0.43	0.02	0.02	1.0	0.19	
14.5	19	133	120	0.75	15	0.43	0.01	0.02	1.0	0.16	
15.5	19	142	120	0.80	15	0.43	0.01	0.01	1.0	0.14	
16.5	19	152	120	0.85	15	0.43	0.01	0.01	1.0	0.13	
17.5	19	161	120	0.90	15	0.43	0.01	0.01	2.0	0.22	
18.5	19	170	120	0.95	15	0.43	0.01	0.01	2.0	0.20	
19.5	19	179	120	1.00	15	0.43	0.01	0.01	2.0	0.18	
	G.5.1 (and 5.2, 5.3)						tmax	Freq		60.44	0.54
							120	25			

Table A4.1.8. Data sheet: profile of Ground Condition 5.1.

Layer no.	Mid-layer Depth (m)	Unit Weight (kN/m2)	Mid-layer Stress (kPa)	Vibe Time (mins)	Relative Density (Dr)	Coeff. Distrib. (Dc)	Accel. (g)	Max Vibe. Settlement (Svi %)	Vibe Settlement Svi(t,f)%	Layer Thickness (m)	Surface Svi (mm)	Water table
1	1.0	18	108	20	0.25	10	0.34	0.02	0.01	2.0	0.25	0.00
2	3.0	18	125	20	0.25	10	0.34	0.02	0.01	2.0	0.22	0.00
3	5.0	18	141	20	0.25	10	0.34	0.01	0.01	2.0	0.19	0.19
4	7.0	18	157	20	0.25	10	0.34	0.01	0.01	2.0	0.17	0.17
5	9.0	18	174	20	100.00	10	0.34	0.00	0.00	2.0	0.00	0.00
6	11.0	18	190	20	100.00	10	0.34	0.00	0.00	2.0	0.00	0.00
7	13.0	18	206	20	100.00	10	0.34	0.00	0.00	2.0	0.00	0.00
8	15.0	18	223	20	100.00	10	0.34	0.00	0.00	2.0	0.00	0.00
9												
10												
11												
12												
0												
	Durahm Biol Site		Surcharge				Stand-off	tmax	Freq		0.83	0.36
			100				2.5	120	25			

Table A4.2.1. Data sheet: ground profile at Durham new biology building site.

Layer no.	Mid-layer Depth (m)	Unit Weight (kN/m2)	Mid-layer Stress (kPa)	Vibe Time (mins)	Relative Density (Dr)	Coeff. Distrib. (Dc)	Accel. (g)	Max Vibe. Settlement (Svi %)	Vibe Settlement Svi(t,f)%	Layer Thickness (m)	Surface Svi (mm)	Water table
1	1.0	18	8	10	0.30	10	0.45	0.27	0.15	2.0	2.98	0.00
2	3.0	18	25	10	0.30	10	0.45	0.09	0.05	2.0	0.99	0.00
3	5.0	18	41	10	0.30	10	0.45	0.05	0.03	2.0	0.60	0.60
4	7.0	18	57	10	0.30	10	0.45	0.04	0.02	2.0	0.43	0.43
5	9.0	18	74	10	0.30	10	0.45	0.03	0.02	2.0	0.33	0.33
6	11.0	18	90	10	0.30	10	0.45	0.02	0.01	2.0	0.27	0.27
7	13.0	18	106	10	0.30	10	0.45	0.02	0.01	2.0	0.23	0.23
8	15.0	18	123	10	0.30	10	0.45	0.02	0.01	2.0	0.20	0.20
9	17.0											
10	19.0											
11	21.0											
12												
0												
		Bridge 04					Stand-off	tmax	Freq		6.03	2.05
							2.5m	120	20			

Table A4.2.2. Data sheet: ground profile at Bridge 04 pier foundation site.

Layer no.	Mid-layer Depth (m)	Unit Weight (kN/m2)	Mid-layer Stress (kPa)	Vibe Time (mins)	Relative Density (Dr)	Coeff. Distrib. (Dc)	Accel. (g)	Max Vibe. Settlement (Svi %)	Vibe Settlement Svi(t,f)%	Layer Thickness (m)	Surface Svi (mm)	Water table
1	0.5	18	4	120	0.25	15	0.6	2.77	2.94	1.0	29.43	
2	1.5	18	12	120	0.25	15	0.6	0.92	0.98	1.0	9.81	
3	2.5	18	20	120	0.25	15	0.6	0.55	0.59	1.0	5.89	
4	3.5	18	29	120	0.25	15	0.6	0.40	0.42	1.0	4.20	
5	4.5	18	37	120	0.25	15	0.6	0.31	0.33	1.0	3.27	
6	5.5	18	45	120	0.10	15	0.6	0.63	0.67	1.0	6.69	
7	6.5	18	53	120	0.10	15	0.6	0.53	0.57	1.0	5.66	
8	7.5	18	61	120	0.10	15	0.6	0.46	0.49	1.0	4.90	
9	8.5	18	70	120	0.10	15	0.6	0.41	0.43	1.0	4.33	
10	9.5	18	78	120	0.15	15	0.6	0.24	0.26	1.0	2.58	
11	10.5	18	86	120	0.15	15	0.6	0.22	0.23	1.0	2.34	
12	11.5	18	94	120	0.20	15	0.6	0.15	0.16	1.0	1.60	
13	12.5	18	102	120	0.25	15	0.6	0.11	0.12	1.0	1.18	
14	13.5	18	111	120	0.35	15	0.6	0.07	0.08	1.0	0.78	
15	14.5	18	119	120	0.50	15	0.6	0.05	0.05	1.0	0.51	
16	15.5	18	127	120	0.80	15	0.6	0.03	0.03	1.0	0.30	
	Hopperton Rail Bridge						Stand-off	tmax	Freq		83.45	0.00
								120	30			

Table A4.2.3. Data sheet: ground profile at Hopperton Railway Bridge.

Layer no.	Mid-layer Depth (m)	Unit Weight (kN/m2)	Mid-layer Stress (kPa)	Vibe Time (mins)	Relative Density (Dr)	Coeff. Distrib. (Dc)	Accel. (g)	Max Vibe. Settlement (Svi %)	Vibe Settlement Svi(t,f)%	Layer Thickness (m)	Surface Svi (mm)	Water table
1	1.0	18	108	10	0.40	7	0.35	0.05	0.03	2.1	0.56	0.00
2	2.7	18	122	10	0.45	7	0.35	0.04	0.02	1.1	0.24	0.00
3	3.9	18	132	10	0.70	10	0.35	0.03	0.02	1.4	0.21	0.21
4	5.5	18	145	10	0.80	5	0.35	0.02	0.01	1.7	0.14	0.14
5	9.1	18	174	10	0.80	5	0.35	0.01	0.01	5.5	0.38	0.38
6	13.5	18	211	10	0.90	5	0.35	0.01	0.01	3.0	0.15	0.15
7												
8												
9												
10												
11												
12												
0												
			Surcharge	Dawson's Yard, Flitwick			Stand-off	tmax	Freq		1.68	0.89
			100				2.5m	120	25			

Table A4.2.4. Data sheet: ground profile at pile trial site.

Layer no.	Mid-layer Depth (m)	Unit Weight Kn/m2	Mid-layer Stress (kPa)	Vibe Time (mins)	Relative Density (Dr)	Coeff. Distribution (Dc)	Accel. (g)	Max Vibe. Settlement (Svi %)	Vibe Settlement Svi(t,f)%	Layer Thickness (m)	Surface Svi (mm)	Water table
1	0.3	17	2	60	0.15	10	0	0.00	0.00	0.5	0.00	0.00
2	2.1	17.5	16	60	0.15	10	0.3	0.22	0.21	3.1	6.40	0.00
3	3.9	18	32	60	100.00	1	0.3	0.00	0.00	0.5	0.00	0.00
4	5.8	18	47	60	0.50	10	0.3	0.02	0.02	3.3	0.68	0.68
5	8.3	18	68	60	100.00	1	0.3	0.00	0.00	1.7	0.00	0.00
	Comms Tower, Walton-on-Thames						Stand-off	tmax	Freq		7.08	0.68
							6m	120	25			

Table A4.2.5. Data sheet: ground profile at cofferdam construction near a communications tower.

Layer no.	Mid-layer Depth (m)	Unit Weight (kN/m2)	Mid-layer Stress (kPa)	Vibe Time (mins)	Relative Density (Dr)	Coeff. Distrib. (Dc)	Uc	Accel. (g)	>1g Accel. (g)	Max Vibe. Settlement (Svi %)	>1g Max Vibe. Settlement (Svi %)	Vibe Settlement Svi(t,f)%	>1g Vibe Settlement Svi(t,f)%	Layer Thickness (m)	Surface Svi (mm)	>1g Surface Svi (mm)	Water table	>1g Water table
1	0.5	18	54	60	0.45	5	2	0.4	2	0.03	1.56	0.02	1.48	1.0	0.25	14.83	0.00	0.00
2	1.5	18	62	60	0.45	5	2	0.4	2	0.02	1.47	0.02	1.39	1.0	0.22	13.94	0.22	13.94
3	2.5	18	70	60	1.00	1	1	0.4	2	0.00	0.00	0.00	0.00	1.0	0.00	0.00	0.00	0.00
4	3.3	18	77	60	0.60	15	6	0.4	2	0.02	1.73	0.02	1.64	0.5	0.11	8.21	0.11	8.21
5	4.5	18	87	60	1.00	1	1	0.4	2	0.00	0.00	0.00	0.00	1.0	0.00	0.00	0.00	0.00
6	5.5	18	95	60	1.00	1	1	0.4	2	0.00	0.00	0.00	0.00	1.0	0.00	0.00	0.00	0.00
7	6.5	18	103	60	1.00	1	1	0.4	2	0.00	0.00	0.00	0.00	1.0	0.00	0.00	0.00	0.00
8	7.5	18	111	60	1.00	1	1	0.4	2	0.00	0.00	0.00	0.00	1.0	0.00	0.00	0.00	0.00
		Survey1	Surcharge							tmax		Freq			0.58	36.98	0.33	22.15
			50							120		25						

Table A4.3.1. Data sheet: ground profile of example Survey #1.

Layer no.	Mid-layer Depth (m)	Unit Weight (kN/m2)	Mid-layer Stress (kPa)	Vibe Time (mins)	Relative Density (Dr)	Coeff. Distrib. (Dc)	Uc	Accel. (g)	>1g Accel. (g)	Max Vibe. Settlement (Svi %)	>1g Max Vibe. Settlement (Svi %)	Vibe Settlement Svi(t,f)%	>1g Vibe Settlement Svi(t,f)%	Layer Thickness (m)	Surface Svi (mm)	>1g Surface Svi (mm)	Water table	>1g Water table
1	0.5	17.5	104	60	0.55	4	1.5	0.2	2	0.00	0.73	0.00	0.67	1.0	0.02	6.67	0.00	0.00
2	1.5	17.5	112	60	0.55	4	1.5	0.2	2	0.00	0.70	0.00	0.64	1.0	0.02	6.39	0.00	0.00
3	2.5	17.5	119	60	0.20	4	1.5	0.2	2	0.01	1.20	0.01	1.09	1.0	0.05	10.91	0.05	10.91
4	3.5	17.5	127	60	0.20	7	1.5	0.2	2	0.01	1.15	0.01	1.05	1.0	0.07	10.50	0.07	10.50
5	4.5	17.5	135	60	0.60	7	4	0.2	2	0.00	1.05	0.00	0.95	1.0	0.02	9.54	0.02	9.54
6	5.5	17.5	142	60	0.60	7	4	0.2	2	0.00	1.01	0.00	0.92	1.0	0.02	9.20	0.02	9.20
7	6.5	17.5	150	60	0.60	7	4	0.2	2	0.00	0.98	0.00	0.89	1.0	0.02	8.89	0.02	8.89
8	7.5	17.5	158	60	0.60	7	4	0.2	2	0.00	0.94	0.00	0.86	1.0	0.02	8.60	0.02	8.60
		Survey2	Surcharge							tmax		Freq			0.24	70.70	0.20	57.64
			100							120		30						

Table A4.3.2. Data sheet: ground profile of example Survey #2.

Layer no.	Mid-layer Depth (m)	Unit Weight Kn/m2	Mid-layer Stress (kPa)	Vibe Time (mins)	Relative Density (Dr)	Coeff. Distribution (Dc)	Uc	Accel. (g)	>1g Accel. (g)	Max Vibe. Settlement (Svi %)	>1g Max Vibe. Settlement (Svi %)	Vibe Settlement Svi(t,f)%	>1g Vibe Settlement Svi(t,f)%	Layer Thickness (m)	Surface Svi (mm)	>1g Surface Svi (mm)	Water table	>1g Water table
1.0	1	18	8.19	60.00	0.15	4	1.5	0.9	2.00	2.27	2.98	2.07	2.7	2.00	41.32	54.14	0.00	0
2.0	3	18	24.6	60.00	0.15	4	1.5	0.9	2.00	0.76	2.49	0.69	2.3	2.00	13.77	45.23	13.77	45.234
3.0	5	18	41	60.00	0.2	4	1.5	0.9	2.00	0.34	2.01	0.31	1.8	2.00	6.20	36.56	6.20	36.5589
4.0	7	18	57.3	60.00	0.25	4	1.5	0.9	2.00	0.19	1.65	0.18	1.5	2.00	3.54	30.03	3.54	30.0315
5.0	9	18	73.7	60.00	0.3	4	1.5	0.9	2.00	0.13	1.37	0.11	1.2	2.00	2.30	24.94	2.30	24.9421
6.0	11	18	90.1	60.00	0.35	4	1.5	0.9	2.00	0.09	1.15	0.08	1.0	2.00	1.61	20.86	1.61	20.8625
7.0	13	18	106	60.00	0.4	4	1.5	0.9	2.00	0.07	0.96	0.06	0.9	2.00	1.19	17.52	1.19	17.5195
8.0	15	18	123	60.00	0.45	4	1.5	0.9	2.00	0.05	0.81	0.05	0.7	2.00	0.92	14.73	0.92	14.7299
9.0	17	18	139	60.00	0.55	4	1.5	0.9	2.00	0.04	0.61	0.03	0.6	2.00	0.66	11.13	0.66	11.1303
10.0	19	18	156	60.00	0.6	4	1.5	0.9	2.00	0.03	0.51	0.03	0.5	2.00	0.54	9.19	0.54	9.19086
11.0	21	18	172	60.00	0.65	4	1.5	0.9	2.00	0.02	0.41	0.02	0.4	2.00	0.45	7.51	0.45	7.50867
12.0	23	18	188	60.00	0.7	4	1.5	0.9	2.00	0.02	0.33	0.02	0.3	2.00	0.38	6.04	0.38	6.03572
		Survey5								tmax		Freq			72.89	277.9	31.57	223.744
									120		30							

Table A4.3.3. Data sheet: ground profile of example Survey #4.

Layer no.	Mid-layer Depth (m)	Unit Weight (kN/m2)	Mid-layer Stress (kPa)	Vibe Time (mins)	Relative Density (Dr)	Coeff. Distrib. (Dc)	Accel. (g)	Max Vibe. Settlement (Svi %)	Vibe Settlement Svi(t,f)%	Layer Thickness (m)	Surface Svi (mm)	Water table
1	1.0	18	8	120	0.35	15	0.5	0.69	0.82	2.0	16.47	0.00
2	3.0	18	25	120	0.35	15	0.5	0.23	0.27	2.0	5.49	0.00
3	5.0	18	41	120	0.35	15	0.5	0.14	0.16	2.0	3.29	0.00
4	7.0	18	57	120	0.35	15	0.5	0.10	0.12	2.0	2.35	0.00
5	9.0	18	74	120	0.35	15	0.5	0.08	0.09	2.0	1.83	0.00
6	11.0	18	90	120	0.35	15	0.5	0.06	0.07	2.0	1.50	0.00
7	13.0	18	106	120	0.35	15	0.5	0.05	0.06	2.0	1.27	0.00
8	15.0	18	123	120	0.35	15	0.5	0.05	0.05	2.0	1.10	0.00
9	17.0	18	139	120	0.35	15	0.5	0.04	0.05	2.0	0.97	0.00
10	19.0	18	156	120	0.35	15	0.5	0.04	0.04	2.0	0.87	0.00
11	21.0	18	172	120	0.35	15	0.5	0.03	0.04	2.0	0.78	0.00
12	23.0	18	188	120	0.35	15	0.5	0.03	0.04	2.0	0.72	0.00
13	25.0	18	205	120	0.35	15	0.5	0.03	0.03	2.0	0.66	0.00
	Picornell							tmax	Freq		37.28	0.00
								120	18			

Table A4.4.1. Data sheet: ground profile for Picornell and del Monte (1982).

Layer no.	Mid-layer Depth (m)	Unit Weight (kN/m2)	Mid-layer Stress (kPa)	Vibe Time (mins)	Relative Density (Dr)	Coeff. Distrib. (Dc)	Uc	Accel. (g)	>1g Accel. (g)	Max Vibe. Settlement (Svi %)	>1g Max Vibe. Settlement (Svi %)	Vibe Settlement Svi(t,f)%	>1g Vibe Settlement Svi(t,f)%	Layer Thickness (m)	Surface Svi (mm)	>1g Surface Svi (mm)	Water table	>1g Water table
1	0.8	18	6	120	0.55	12	2	0.4	3	0.34	3.23	0.38	3.58	1.5	5.69	5.36	5.69	5.36
2	2.3	18	18	120	0.40	10	3	0.4	3	0.15	4.82	0.16	5.35	3.0	4.83	16.04	4.83	16.04
3	4.5	18	37	120	0.40	7	2	0.4	3	0.06	3.12	0.07	3.46	3.0	2.04	10.38	2.04	10.38
4	7.5	18	61	120	0.80	5	2	0.4	3	0.02	0.85	0.02	0.95	3.0	0.51	2.84	0.51	2.84
5	10.5	18	86	120	0.65	15	4	0.4	3	0.02	1.89	0.02	2.10	3.0	0.75	6.30	0.75	6.30
6	13.5	18	111	120	0.55	15	4	0.4	3	0.02	2.11	0.02	2.34	3.0	0.69	7.03	0.69	7.03
7	16.5	18	135	120	0.90	15	4	0.4	3	0.01	0.41	0.01	0.46	3.0	0.34	1.38	0.34	1.38
8	19.0	18	156	120	0.90	15	3	0.4	3	0.01	0.33	0.01	0.36	2.0	0.20	0.72	0.20	0.72
9																		
	Linehan							Stand-off	Stand-off	tmax		Freq			15.04	50.05	15.04	50.05
								3m	0.6m	120		25						

Table A4.4.2. Data sheet: ground profile for Linehan *et al.* (1988).

Layer no.	Mid-layer Depth (m)	Unit Weight (kN/m2)	Mid-layer Stress (kPa)	Vibe Time (mins)	Relative Density (Dr)	Coeff. Distrib. (Dc)	Uc	Accel. (g)	>1g Accel. (g)	Max Vibe. Settlement (Svi %)	>1g Max Vibe. Settlement (Svi %)	Vibe Settlement Svi(t,f)%	>1g Vibe Settlement Svi(t,f)%	Layer Thickness (m)	Surface Svi (mm)	>1g Surface Svi (mm)	Water table	>1g Water table
1	1.0	18	8	120	0.15	15	2	0.39	1.55	0.97	2.37	1.04	2.52	2.0	20.72		20.72	
2	3.0	18	25	120	0.20	15	2	0.39	1.55	0.24	1.86	0.26		2.0	5.18		5.18	
3	5.0	18	41	120	0.30	15	2	0.39	1.55	0.10	1.40	0.10		2.0	2.07		2.07	
4	7.0	18	57	120	0.40	15	2	0.39	1.55	0.05	1.05	0.06		2.0	1.11		1.11	
5	9.0	18	74	120	0.50	15	2	0.39	1.55	0.03	0.78	0.03		2.0	0.69		0.69	
6	11.0	18	90	120	0.55	15	2	0.39	1.55	0.02	0.63	0.03		2.0	0.51		0.51	
7	13.0	18	106	120	0.60	15	2	0.39	1.55	0.02	0.51	0.02		2.0	0.40		0.40	
8	15.0	18	123	120	0.65	15	2	0.39	1.55	0.01	0.41	0.02		2.0	0.32		0.32	
9	17.0	18	139	120	0.70	15	2	0.39	1.55	0.01	0.32	0.01		2.0	0.26		0.26	
10	19.0	18	156	120	0.75	15	2	0.39	1.55	0.01	0.25	0.01		2.0	0.22		0.22	
11	21.0	18	172	120	0.75	15	2	0.39	1.55	0.01	0.23	0.01		2.0	0.20		0.20	
12	23.0	18	188	120	0.80	15	2	0.39	1.55	0.01	0.18	0.01		2.0	0.17		0.17	
13	25.0	18	205	120	0.85	15	2	0.39	1.55	0.01	0.12	0.01		2.0	0.15		0.15	
14	27.0	18	221	120	0.90	15	2	0.39	1.55	0.01	0.08	0.01		2.0	0.13		0.13	
15	29.0	18	238	120	1.00	15	2	0.39	1.55	0.01	0.00	0.01		2.0	0.11		0.11	
		Holloway								tmax		Freq			32.23	0.00	32.23	0.00
										120		30						

Table A4.4.3. Data sheet: ground profile for Holloway *et al.* (1980).

Layer no.	Mid-layer Depth (m)	Unit Weight (kN/m2)	Mid-layer Stress (kPa)	Vibe Time (mins)	Relative Density (Dr)	Coeff. Distrib. (Dc)	Uc	Accel. (g)	>1g Accel. (g)	Max Vibe. Settlement (Svi %)	>1g Max Vibe. Settlement (Svi %)	Vibe Settlement Svi(t,f)%	>1g Vibe Settlement Svi(t,f)%	Layer Thickness (m)	Surface Svi (mm)	>1g Surface Svi (mm)	Water table	>1g Water table
1	0.5	17	4	120	0.20	20	2	0.45	1.55	2.45	2.36	2.94	2.83	1.0	29.41		0.00	
2	1.5	17	11	120	0.20	20		0.45		0.82		0.98		1.0	9.80		9.80	
3	2.5	17	18	120	0.20	20		0.45		0.49		0.59		1.0	5.88		5.88	
4	3.5	17	25	120	0.30	5		0.45		0.13		0.15		1.0	1.50		1.50	
5	4.5	17	32	120	0.25	5		0.45		0.12		0.14		1.0	1.40		1.40	
6	5.5	17	40	120	0.20	5		0.45		0.12		0.14		1.0	1.44		1.44	
7	6.5	17	47	120	0.15	5		0.45		0.14		0.16		1.0	1.62		1.62	
8	7.5	17	54	120	0.10	5		0.45		0.18		0.21		1.0	2.11		2.11	
9	8.5	18	70	120	100.00	12		0.9		0.00		0.00		2.0	0.02		0.02	
10	9.5	18	78	120	100.00	12		0.45		0.00		0.00		2.0	0.00		0.00	
11	10.5	18	86	120	100.00	12		0.45		0.00		0.00		2.0	0.00		0.00	
12	21.0	18	172	120	100.00	12		0.45		0.00		0.00		2.0	0.00		0.00	
13	23.0	18	188	120	100.00	12		0.45		0.00		0.00		2.0	0.00		0.00	
14	25.0	18	205	120	100.00	12		0.45		0.00		0.00		2.0	0.00		0.00	
15	27.0	18	221	120	100.00	12		0.45		0.00		0.00		2.0	0.00		0.00	
16	28.0	18	229	120	100.00	12		0.45		0.00		0.00		1.0	0.00		0.00	
17	29.5	18	242	120	0.30	7		0.45		0.02		0.02		1.0	0.19		0.19	
18	31.0	18	254	120	100.00	12		0.45		0.00		0.00		2.0	0.00		0.00	
19	33.0	18	270	120	100.00	12		0.45		0.00		0.00		2.0	0.00		0.00	
		Clough								tmax		Freq			53.40	0.00	23.99	0.00
										120		18						

Table A4.4.4. Data sheet: ground profile for Clough and Chameau (1980).

Layer no.	Mid-layer Depth (m)	Unit Weight (kN/m2)	Mid-layer Stress (kPa)	Vibe Time (mins)	Relative Density (Dr)	Coeff. Distrib. (Dc)	Accel. (g)	Max Vibe. Settlement (Svi %)	Vibe Settlement Svi(t,f)%	Layer Thickness (m)	Surface Svi (mm)	Water table
1	0.5	18	4	50	0.45	13	0.86	2.44	2.21	1.0	22.14	0.00
2	1.5	18	12	50	0.45	13	0.86	0.81	0.74	1.0	7.38	7.38
3	2.5	18	20	50	0.45	13	0.86	0.49	0.44	3.0	13.28	13.28
4	3.5	18	29	50	0.45	13	0.86	0.35	0.32	0.5	1.58	1.58
5	4.5	18	37	50	0.45	13	0.86	0.27	0.25	3.0	7.38	7.38
6	5.5	18	45	50	0.45	13	0.86	0.22	0.20	3.5	7.04	7.04
7	6.5	18	53	50	0.45	13	0.86	0.19	0.17	3.5	5.96	5.96
8	7.5	18	61	50	0.45	13	0.86	0.16	0.15	3.5	5.17	5.17
9	8.5	18	70	50	0.45	13	0.86	0.14	0.13	3.5	4.56	4.56
10	9.5	18	78	50	0.45	13	0.86	0.13	0.12	3.5	4.08	4.08
11	10.5	18	86	50	0.45	13	0.86	0.12	0.11	3.5	3.69	3.69
12	11.5	18	94	50	0.45	13	0.86	0.11	0.10	3.5	3.37	3.37
0												
	Lucas and Gill, 1							tmax	Freq		85.62	63.49
								120	25			

Table A4.4.5. Data sheet: ground profilefor Lucas and Gill (1992).

									>1g		>1g		>1g			>1g		>1g
Layer no.	Mid-layer Depth (m)	Unit Weight (kN/m2)	Mid-layer Stress (kPa)	Vibe Time (mins)	Relative Density (Dr)	Coeff. Distrib. (Dc)	Uc	Accel. (g)	Accel. (g)	Max Vibe. Settlement (Svi %)	Max Vibe. Settlement (Svi %)	Vibe Settlement Svi(t,f)%	Vibe Settlement Svi(t,f)%	Layer Thickness (m)	Surface Svi (mm)	Surface Svi (mm)	Water table	Water table
1	1.0	18	8	120	0.45	20	5	0.1	2	0.02	4.02	0.03	4.28	2.0	0.50	85.58	0.00	0.00
2	3.0	18	25	120	0.45	20	5	0.1	2	0.01	3.36	0.01	3.57	2.0	0.17	71.50	0.00	0.00
3	5.0	18	41	120	0.45	20	5	0.1	2	0.00	2.89	0.01	3.07	2.0	0.10	61.40	0.10	61.40
4	7.0	18	57	120	0.45	20	5	0.1	2	0.00	2.53	0.00	2.69	2.0	0.07	53.80	0.07	53.80
5	9.0	18	74	120	0.45	20	5	0.1	2	0.00	2.25	0.00	2.39	2.0	0.06	47.87	0.06	47.87
6	11.0	18	90	120	0.45	20	5	0.1	2	0.00	2.03	0.00	2.16	2.0	0.05	43.12	0.05	43.12
7	13.0	18	106	120	0.45	20	5	0.1	2	0.00	1.84	0.00	1.96	2.0	0.04	39.23	0.04	39.23
8	15.0	18	123	120	0.45	20	5	0.1	2	0.00	1.69	0.00	1.80	2.0	0.03	35.98	0.03	35.98
9	17.0	18	139	120	0.45	20	5	0.1	2	0.00	1.56	0.00	1.66	2.0	0.03	33.23	0.03	33.23
10	19.0	18	156	120	0.45	20	5	0.1	2	0.00	1.45	0.00	1.54	2.0	0.03	30.87	0.03	30.87
11	21.0	18	172	120	0.45	20	5	0.1	2	0.00	1.35	0.00	1.44	2.0	0.02	28.82	0.02	28.82
12	23.0	18	188	120	1.00	20	5	0.1	2	0.00	0.00	0.00	0.00	2.0	0.01	0.00	0.01	0.00
13	25.0	18	205	120	1.00	20	5	0.1	2	0.00	0.00	0.00	0.00	2.0	0.01	0.00	0.01	0.00
14	27.0	18	221	120	1.00	20	5	0.1	2	0.00	0.00	0.00	0.00	2.0	0.01	0.00	0.01	0.00
15	29.0	18	238	120	1.00	20	5	0.1	2	0.00	0.00	0.00	0.00	2.0	0.01	0.00	0.01	0.00
	LGA									tmax		Freq			1.13	531.40	0.46	374.33
										120		30						

Table A4.5.1. Data sheet:ground profile for Lacy and Gould Case A.

Layer no.	Mid-layer Depth (m)	Unit Weight (kN/m2)	Mid-layer Stress (kPa)	Vibe Time (mins)	Relative Density (Dr)	Coeff. Distrib. (Dc)	Uc	Accel. (g)	>1g Accel. (g)	Max Vibe. Settlement (Svi %)	>1g Max Vibe. Settlement (Svi %)	Vibe Settlement Svi(t,f)%	>1g Vibe Settlement Svi(t,f)%	Layer Thickness (m)	Surface Svi (mm)	>1g Surface Svi (mm)	Water table	>1g Water table
1	1.0	18	1	120	0.45	20	1.5	0.1	3	0.19	3.34	0.24	4.20	2.0	4.86	84.01	0.00	0.00
2	3.0	18	1	120	0.45	20	1.5	0.1	3	0.19	3.34	0.24	4.20	2.0	4.86	84.01	0.00	0.00
3	5.0	18	1	120	0.45	20	1.5	0.1	3	0.19	3.34	0.24	4.20	2.0	4.86	84.01	4.86	84.01
4	7.0	18	1	120	0.45	20	1.5	0.1	3	0.19	3.34	0.24	4.20	2.0	4.86	84.01	4.86	84.01
5	9.0	18	1	120	0.45	20	1.5	0.1	3	0.19	3.34	0.24	4.20	2.0	4.86	84.01	4.86	84.01
6	11.0	18	1	120	0.45	20	1.5	0.1	3	0.19	3.34	0.24	4.20	2.0	4.86	84.01	4.86	84.01
7	13.0	18	1	120	0.45	20	1.5	0.1	3	0.19	3.34	0.24	4.20	2.0	4.86	84.01	4.86	84.01
8	15.0	18	1	120	0.45	20	1.5	0.1	3	0.19	3.34	0.24	4.20	2.0	4.86	84.01	4.86	84.01
9	17.0	18	1	120	0.45	20	1.5	0.1	3	0.19	3.34	0.24	4.20	2.0	4.86	84.01	4.86	84.01
10	19.0	18	1	120	0.45	20	1.5	0.1	3	0.19	3.34	0.24	4.20	2.0	4.86	84.01	4.86	84.01
11	21.0	18	1	120	0.45	20	1.5	0.1	3	0.19	3.34	0.24	4.20	2.0	4.86	84.01	4.86	84.01
12	23.0	18	1	120	1.00	20	1.5	0.1	3	0.09	0.00	0.11	0.00	2.0	2.19	0.00	2.19	0.00
13	25.0	18	1	120	1.00	20	1.5	0.1	3	0.09	0.00	0.11	0.00	2.0	2.19	0.00	2.19	0.00
14	27.0	18	1	120	1.00	20	1.5	0.1	3	0.09	0.00	0.11	0.00	2.0	2.19	0.00	2.19	0.00
15	29.0	18	1	120	1.00	20	1.5	0.1	3	0.09	0.00	0.11	0.00	2.0	2.19	0.00	2.19	0.00
		LGA								tmax		Freq			62.25	924.08	52.53	756.06
										120		15						

Table A4.5.2. Data sheet: ground profile for Lacy and Gould Case A (allowing for liquefaction at 0.1g).

Layer no.	Mid-layer Depth (m)	Unit Weight (kN/m2)	Mid-layer Stress (kPa)	Vibe Time (mins)	Relative Density (Dr)	Coeff. Distrib. (Dc)	Uc	Accel. (g)	>1g Accel. (g)	Max Vibe. Settlement (Svi %)	>1g Max Vibe. Settlement (Svi %)	Vibe Settlement Svi(t,f)%	>1g Vibe Settlement Svi(t,f)%	Layer Thickness (m)	Surface Svi (mm)	>1g Surface Svi (mm)	Water table	>1g Water table
1	1.0	18	8	120	0.20	5	4	0.6	1.1	1.03	0.73	1.20	0.85	2.0	24.03	16.99	0.00	0.00
2	3.0	18	25	120	0.20	5	4	0.6	1.1	0.34	0.61	0.40	0.71	2.0	8.01	14.20	0.00	0.00
3	5.0	18	41	120	0.20	7	2	0.6	1.1	0.25	0.35	0.29	0.41	2.0	5.81	8.14	5.81	8.14
4	7.0	18	57	120	0.20	7	2	0.6	1.1	0.18	0.31	0.21	0.36	2.0	4.15	7.13	4.15	7.13
5	9.0	18	74	120	0.35	10	3	0.6	1.1	0.09	0.28	0.11	0.33	2.0	2.18	6.66	2.18	6.66
6	11.0	18	90	120	0.35	10	3	0.6	1.1	0.08	0.26	0.09	0.30	2.0	1.79	6.00	1.79	6.00
7	13.0	18	106	120	0.35	10	3	0.6	1.1	0.06	0.23	0.08	0.27	2.0	1.51	5.46	1.51	5.46
8	15.0	18	123	120	0.35	10	3	0.6	1.1	0.06	0.21	0.07	0.25	2.0	1.31	5.00	1.31	5.00
9	17.0	18	139	120	0.50	15	4	0.6	1.1	0.04	0.18	0.05	0.21	2.0	0.95	4.12	0.95	4.12
10	19.0	18	156	120	0.50	15	4	0.6	1.1	0.04	0.16	0.04	0.19	2.0	0.85	3.83	0.85	3.83
11	21.0	18	172	120	0.50	15	4	0.6	1.1	0.03	0.15	0.04	0.18	2.0	0.77	3.58	0.77	3.58
12	23.0	18	188	120	0.50	15	4	0.6	1.1	0.03	0.14	0.04	0.17	2.0	0.70	3.35	0.70	3.35
13	25.0	18	205	120	0.60	15	4	0.6	1.1	0.02	0.11	0.03	0.13	2.0	0.54	2.53	0.54	2.53
14	27.0	18	221	120	0.70	15	4	0.6	1.1	0.02	0.08	0.02	0.09	2.0	0.43	1.79	0.43	1.79
15	29.0	18	238	120	0.80	15	4	0.6	1.1	0.01	0.05	0.02	0.06	2.0	0.35	1.13	0.35	1.13
		LGC								tmax		Freq			53.37	89.92	21.34	58.73
										120		20						

TableA 4.5.3. Data sheet: ground profile for Lacy and Gould Case B.

Layer no.	Mid-layer Depth (m)	Unit Weight (kN/m2)	Mid-layer Stress (kPa)	Vibe Time (mins)	Relative Density (Dr)	Coeff. Distrib. (Dc)	Uc	Accel. (g)	>1g Accel. (g)	Max Vibe. Settlement (Svi %)	>1g Max Vibe. Settlement (Svi %)	Vibe Settlement Svi(t,f)%	>1g Vibe Settlement Svi(t,f)%	Layer Thickness (m)	Surface Svi (mm)	>1g Surface Svi (mm)	Water table	>1g Water table
1	1.0	17	7	60	0.30	7	2.5	1	3	2.24	5.75	2.30	5.90	2.0	46.00	117.97	46.00	117.97
2	3.0	17	22	60	0.30	7	2.5	1	3	0.75	4.89	0.77	5.02	2.0	15.33	100.41	15.33	100.41
3	5.0	17	36	60	0.30	7	2.5	1	3	0.45	4.26	0.46	4.37	2.0	9.20	87.39	9.20	87.39
4	7.0	17	50	60	0.40	7	2.5	1	3	0.24	3.23	0.25	3.32	2.0	4.93	66.31	4.93	66.31
5	9.0	17	65	60	0.35	7	2.5	1	3	0.21	3.14	0.22	3.22	2.0	4.38	64.44	4.38	64.44
6	11.0	17	79	60	0.40	7	2.5	1	3	0.15	2.63	0.16	2.70	2.0	3.14	53.94	3.14	53.94
7	13.0	17	93	60	0.40	7	2.5	1	3	0.13	2.40	0.13	2.47	2.0	2.65	49.33	2.65	49.33
8	15.0	17	108	60	0.40	7	2.5	1	3	0.11	2.21	0.12	2.27	2.0	2.30	45.45	2.30	45.45
9	17.0	17	122	60	0.35	7	2.5	1	3	0.11	2.22	0.12	2.28	2.0	2.32	45.65	2.32	45.65
10	19.0	17	137	60	0.40	7	2.5	1	3	0.09	1.91	0.09	1.96	2.0	1.82	39.27	1.82	39.27
11	21.0	17	151	60	0.40	7	2.5	1	3	0.08	1.79	0.08	1.84	2.0	1.64	36.78	1.64	36.78
12	23.0	17	165	60	0.40	7	2.5	1	3	0.07	1.68	0.08	1.73	2.0	1.50	34.58	1.50	34.58
13	25.0	17	180	60	0.40	7	2.5	1	3	0.07	1.59	0.07	1.63	2.0	1.38	32.62	1.38	32.62
14	27.0	17	194	60	0.35	7	2.5	1	3	0.07	1.63	0.07	1.67	2.0	1.46	33.45	1.46	33.45
15	29.0	17	209	60	0.40	7	2.5	1	3	0.06	1.43	0.06	1.47	2.0	1.19	29.31	1.19	29.31
		LGD								tmax		Freq			99.24	836.91	99.24	836.91
										120		18						

Table A4.5.4. Data sheet: ground profile for Lacy and Gould Case C.

Layer no.	Mid-layer Depth (m)	Unit Weight (kN/m2)	Mid-layer Stress (kPa)	Vibe Time (mins)	Relative Density (Dr)	Coeff. Distrib. (Dc)	Uc	Accel. (g)	>1g Accel. (g)	Max Vibe. Settlement (Svi %)	>1g Max Vibe. Settlement (Svi %)	Vibe Settlement Svi(t,f)%	>1g Vibe Settlement Svi(t,f)%	Layer Thickness (m)	Surface Svi (mm)	>1g Surface Svi (mm)	Water table	>1g Water table
1	0.5	17	4	60	0.30	20	2.5	0.85	3	4.98	6.01	5.12	6.17	1.0	51.17	61.68		
2	1.5	17	11	60	0.30	20	2.5	0.85	3	1.66	5.51	1.71	5.65	1.0	17.06	56.51	17.06	56.51
3	2.5	17	18	60	0.30	20	2.5	0.85	3	1.00	5.08	1.02	5.21	1.0	10.23	52.14	10.23	52.14
4	3.5	17	25	60	0.40	10	2.5	0.85	3	0.41	4.04	0.42	4.15	1.0	4.21	41.49	4.21	41.49
5	4.5	17	32	60	0.45	10	2.5	0.85	3	0.28	3.46	0.29	3.55	1.0	2.91	35.48	2.91	35.48
6	5.5	17	40	60	0.45	10	2.5	0.85	3	0.23	3.24	0.24	3.33	1.0	2.38	33.25	2.38	33.25
7	6.5	17	47	60	0.45	10	2.5	0.85	3	0.20	3.05	0.20	3.13	1.0	2.02	31.29	2.02	31.29
8	7.5	17	54	60	0.50	7	2.5	0.85	3	0.13	2.62	0.13	2.69	1.0	1.33	26.86	1.33	26.86
9	8.5	17	61	60	0.50	7	2.5	0.85	3	0.11	2.48	0.12	2.54	1.0	1.17	25.44	1.17	25.44
10	9.5	17	68	60	0.60	7	2.5	0.85	3	0.09	1.88	0.09	1.93	1.0	0.87	19.33	0.87	19.33
11	10.5	17	75	60	0.60	7	2.5	0.85	3	0.08	1.79	0.08	1.84	1.0	0.79	18.41	0.79	18.41
12	11.5	17	83	60	0.70	7	2.5	0.85	3	0.06	1.28	0.06	1.32	1.0	0.62	13.18	0.62	13.18
13	12.5	17	90	60	0.70	15	2.5	0.85	3	0.08	1.23	0.08	1.26	1.0	0.79	12.60	0.79	12.60
14	13.5	17	97	60	0.70	15	2.5	0.85	3	0.07	1.18	0.07	1.21	1.0	0.73	12.08	0.73	12.08
15	14.5	17	104	60	0.70	15	2.5	0.85	3	0.07	1.13	0.07	1.16	1.0	0.68	11.59	0.68	11.59
		LGE								tmax		Freq			96.98	451.34	45.81	389.66
										120		18						

Table A4.5.5. Data sheet: ground profile for Lacy and Gould Case D.

Layer no.	Mid-layer Depth (m)	Unit Weight (kN/m2)	Mid-layer Stress (kPa)	Vibe Time (mins)	Relative Density (Dr)	Coeff. Distrib. (Dc)	Uc	Accel. (g)	>1g Accel. (g)	Max Vibe. Settlement (Svi %)	>1g Max Vibe. Settlement (Svi %)	Vibe Settlement Svi(t,f)%	>1g Vibe Settlement Svi(t,f)%	Layer Thickness (m)	Surface Svi (mm)	>1g Surface Svi (mm)	Water table	>1g Water table
1	0.5	17	4	60	0.30	10	2.5	0.85	1.5	3.83	2.22	3.93	2.28	1.0	39.33	22.77	0.00	0.00
2	1.5	17	11	60	0.30	10	2.5	0.85	1.5	1.28	2.03	1.31	2.09	1.0	13.11	20.86	13.11	0.00
3	2.5	17	18	60	1.00	1	1	0.85	1.5	0.00	0.00	0.00	0.00	1.0	0.00	0.00	0.00	0.00
4	3.5	17	25	60	0.30	7	2.5	0.85	1.5	0.46	1.74	0.47	1.79	1.0	4.75	17.86	4.75	17.86
5	4.5	17	32	60	0.30	7	2.5	0.85	1.5	0.36	1.62	0.37	1.67	1.0	3.69	16.67	3.69	16.67
6	5.5	17	40	60	0.30	7	2.5	0.85	1.5	0.29	1.52	0.30	1.56	1.0	3.02	15.62	3.02	15.62
7	6.5	17	47	60	0.30	7	2.5	0.85	1.5	0.25	1.43	0.26	1.47	1.0	2.56	14.70	2.56	14.70
8	7.5	17	54	60	0.30	7	2.5	0.85	1.5	0.22	1.35	0.22	1.39	1.0	2.22	13.88	2.22	13.88
9	8.5	17	61	60	0.30	7	2.5	0.85	1.5	0.19	1.28	0.20	1.31	1.0	1.96	13.15	1.96	13.15
10	9.5	17	68	60	0.30	7	2.5	0.85	1.5	0.17	1.22	0.17	1.25	1.0	1.75	12.49	1.75	12.49
11	10.5	17	75	60	0.45	7	2.5	0.85	1.5	0.10	0.91	0.11	0.93	1.0	1.06	9.34	1.06	9.34
12	11.5	17	83	60	0.50	7	2.5	0.85	1.5	0.08	0.79	0.09	0.81	1.0	0.87	8.11	0.87	8.11
13	12.5	17	90	60	0.50	7	2.5	0.85	1.5	0.08	0.76	0.08	0.78	1.0	0.80	7.75	0.80	7.75
14	13.5	17	97	60	0.50	7	2.5	0.85	1.5	0.07	0.72	0.07	0.74	1.0	0.74	7.43	0.74	7.43
15	14.5	17	104	60	0.50	7	2.5	0.85	1.5	0.07	0.69	0.07	0.71	1.0	0.69	7.13	0.69	7.13
		LGG								tmax		Freq			76.52	187.74	37.19	144.11
										120		18						

Table A4.5.6. Data sheet: ground profile for Lacy and Gould Case F.

Appendix 5

Site Investigation Data

DURHAM BIOLOGY
SITE
VIBRODRIVER ETC

Peak particle velocity readings (mm/s)   stand off = 2.5, 5, 10 and 20m

FILE NUMBERS

CHAN NO.		DBS3	DBS4	DBS5	DBS6	DBS7	DBS8
0	R	11.15	12.25	9.98	6.16	6.85	6.26
1	T	8.64	8.64	7.15	2.69	2.23	7.90
2	V	20.07	19.17	9.72	7.83	6.48	11.52
3	R	13.10	12.11	10.85	12.02	11.57	4.13
4	T	2.48	3.05	3.33	2.95	4.38	1.99
5	V	6.69	8.87	6.86	8.50	7.31	2.92
6	R	9.83	9.74	8.19	9.83	9.83	2.64
7	T	3.97	69.00	2.12	1.94	1.29	2.31
8	V	2.43	2.53	2.26	2.16	2.16	2.53
9	R	2.41	2.91	2.81	2.91	2.91	1.91
10	T	3.48	3.13	2.32	2.14	1.70	1.16
11	V	1.84	2.49	2.21	2.49	3.13	2.67

FILE NUMBERS

CHAN NO.		DBS9	DBS11	DBS12	DBS13	DBS14	DBS15
0	R	9.58	36.09	31.39	26.80	34.72	34.13
1	T	12.63	43.66	11.15	56.95	42.64	29.64
2	V	15.84	63.63	45.36	63.10	57360.00	52.02
3	R	9.78	7.62	11.30	9.96	10.23	11.48
4	T	2.95	7.61	3.24	8.19	7.81	7.23
5	V	3.01	10.51	10.42	13.16	77.19	10.42
6	R	7.01	19.02	14.83	21.11	46.29	15.65
7	T	3.97	7.66	3.97	7.20	6.55	5.81
8	V	2.43	13.62	18.13	14.97	12.18	11.82
9	R	2.31	12.26	7.94	15.88	12.66	13.07
10	T	2.05	2.85	4.91	5.63	4.29	4.29
11	V	2.12	6.36	3.32	7.84	7.28	7.74

FILE NUMBERS

CHAN NO.		DBSb3	DBSb4	DBSb5	DBSb6
0	R	13.05	16.83	16.74	14.22
1	T	8.28	6.23	7.53	5.67
2	V	16.46	18.23	15.58	15.48
3	R	9.10	11.47	10.83	10.19
4	T	3.42	3.90	3.80	3.52
5	V	11.88	14.76	14.13	14.14
6	R	4.23	3.60	3.87	3.51
7	T	3.40	3.04	3.13	3.04
8	V	8.37	7.92	7.83	8.00
9	R	2.02	2.02	2.12	2.02
10	T	2.40	2.31	2.40	2.23
11	V	5.30	3.90	4.10	4.20

(A1DATA)

A1B4a3
29.07
11.53
14.31
12.29
5.80
6.40
30.15
12.88
9.28
17.85
2.28
6.90

Table A5.1.1. Data sheet: ground vibration data for Durham new biology building site.

RELATIVE GROUND MOVEMENT
(m)

PIN	M	T1a	T1b	T1c	PIN	M	T2a	T2b	T2c
		REDUCED LEVEL					REDUCED LEVEL		
TBM	11.0	100.000	0.000	0.000	TBM	-	100.000	0.000	0.000
1	9.0	99.559	-	-	1	8.7	99.436	0.007	0.003
2	6.8	99.348	-0.005	-0.004	2	5.6	99.304	-	-
3	3.7	99.175	0.030	-0.017	3	4.1	99.209	-0.003	-
4	2.0	99.115	-	-	4	3.1	99.199	-	-
5	0.8	99.022	0.058	0.004	5	0.7	99.118	-	-
6	-0.9	98.968	0.027	0.007	6	-1.1	98.926	-	-
7	-3.2	97.875	0.000	0.002					
8	-5.2	96.725	0.085	0.015					
9	-5.9	94.621	0.008	0.005					

PIN	M	T3a	T3b	T3c	T3d	T3e	T3f	T3g
		REDUCED LEVEL						
TBM	-	100.000	0.000	0.000	0.000	0.000	0.000	0.000
1	6.6	99.140	-0.008	-0.008	-0.009	-0.010	-0.003	-
2	4.5	99.044	-0.007	-0.009	-0.008	-0.009	0.028	-
3	3.5	98.996	-0.048	0.002	-	-	-0.012	-0.002
4	1.2	98.876	0.043	-0.009	-0.007	-0.004	-	-0.007
5	-0.1	98.724	-0.006	-0.008	-0.011	-	-	-

PIN	M	T4a	T4b	T4c	T4d	T4e	T4f	T4g
		REDUCED LEVEL						
TBM	-	100.000	0.000	0.000	0.000	0.000	0.000	0.000
1	0.0	98.730	0.000	-0.007	-0.003	-0.009	-0.009	-0.012
2	2.6	98.724	-0.003	-0.010	-0.005	-0.006	-0.015	-0.010
3	5.0	98.695	-0.003	-0.008	-0.005	-0.004	-0.003	-0.005
4	6.8	98.693	-0.012	-0.014	-0.011	-0.011	-0.011	-
5	9.2	98.688	-0.009	-0.014	-0.007	-0.013	-	-

PIN	M	T5a	T5b	T5c	T5d
		REDUCED LEVEL			
TBM	-	100.000	0.000	0.000	0.000
1	8.0	99.061	0.014	0.012	-
2	6.0	99.034	0.019	0.018	0.025
3	3.6	99.005	-	-	0.013
4	1.0	98.815	0.012	-	-
5	-0.9	98.714	0.014	0.015	-

A -ve value indicates a rise in ground level with respect to the initial traverse, and vice-versa.

PIN	M	T6a	T6b	T6c	PIN	M	T7a	T7b	T7c
		REDUCED LEVEL					REDUCED LEVEL		
TBM	-	100.000	0.000	0.000	TBM	-	100.000	0.000	0.000
1	6.0	98.976	-	-	1	1.6	98.760	0.072	0.066
2	3.7	99.000	-	-	2	4.3	98.671	0.075	-
3	2.0	98.920	-	-	3	7.1	98.552	0.076	0.068
4	1.0	98.886	0.096	0.093	4	9.7	98.399	0.077	0.088
5	-1.0	98.760	-	-					

Table A5.1.2. Data sheet: levelling data for Durham new biology building site.

A1 Widening Scheme: Bridge 04 - Ground vibration data (1/9/93)

Hydraulic drop hammer

Chan no.		Stand-off (m)	P.P.V (mm/s)	P.P.A (mm/s2)	P.P.D (mm)
0	R		29.07	5237.50	0.198
1	T	2.5	11.53	1962.10	0.081
2	V		14.31	2504.40	0.108
3	R		12.29	1870.60	0.070
4	T	5	5.80	791.70	0.042
5	V		6.40	800.00	0.056
6	R		30.15	4812.50	0.175
7	T	10	12.88	2606.70	0.049
8	V		9.28	2287.60	0.056
9	R		17.85	2721.70	0.104
10	T	20	2.28	494.40	0.017
11	V		6.90	1611.10	0.050

Velocity resultant with respect to time =	32.37 mm/s
Acceleration resultant with respect to time =	5809.64 mm/s2
Peak frequency =	26.92 Hz

Where P.P.V = peak particle velocity
P.P.A = peak particle acceleration
P.P.D = peak particle displacement
R = radial geophone orientation
T = transverse geophone orientation
V = vertical geophone orientation

Table A5.2.1. Data sheet: ground vibration recorded for Bridge 04.

A1 WIDENING SCHEME: BRIDGE 4 - levelling data.

	stand off	reduced levels				relative movement (m)	
PIN	M	T1a	T1b	T1c		T1b	T1c
TBM		50.000	50.000	50.000			
1	1.2	49.011	49.014	49.011		-0.003	0
2	2.8	49.110	49.113	49.115		-0.003	-0.005
3	4.0	49.226	49.230	49.230		-0.004	-0.004
4	5.6	49.928	49.932			-0.004	
5	8.6	49.947	49.949			-0.003	
6	13.4	49.922	49.925			-0.003	
PIN	M	T2a	T2b			T2b	
TBM		50.000	50.000				
1	0.1	48.679	48.551			0.128	
2	3.3	48.680	48.684			-0.004	
3	3.7	49.863	49.868			-0.005	
4	7.7	50.002	50.007			-0.005	
5	11.7	50.055	50.059			-0.004	
PIN	M	T3a	T3b			T3b	
TBM		50.000	50.000				
1	8.0	48.652	48.653			-0.001	
2	9.7	48.561	48.565			-0.004	
3	12.0	49.308	49.311			-0.003	
4	14.6	49.262	49.264			-0.002	
5	23.0	49.002	49.002			0.000	

Table A5.2.2. Data sheet: A1 widening scheme, Bridge 04 levelling data.

Ground Vibration Summary Data Sheet

Location D awson's Yard, near Flitwick, Berkshire. **Date** 26/10/93 **Disc no.** 1 **File no.** pct1

Pile Frodingham 2N 43A Depth = 0.25 Length = 9 m
Hammer PTC 13HF1

Ground Vibration Measurements

Channel		Stand-off (m)	Amax. (mm/s2)	Resultant	Dmax. (mm)	Resultant	Vmax. (mm/s)	Resultant
0	R		3287.50		0.15		22.59	
1	T	2.5	762.08	3496.8	0.025	0.16	4.552	3.727
2	V		1701.389		0.053		10.586	
3	R		505.556		0.016		2.275	
4	T	5	409.028	612.185	0.045	0.028	2.377	2.897
5	V		237.500		0.008		1.349	
6	R		362.500		0.018		2.152	
7	T	10	255.556	384.067	0.007	0.018	1.100	2.308
8	V		202.222		0.005		1.000	
9	R		76.677		0.002		0.636	
10	T	20	61.806	239.522	0.002	0.011	0.360	1.579
11	V		236.111		0.009		1.474	

Ground Vibration Summary Data Sheet

Location Dawson's Yard near Flitwick, Berkshire **Date** 26/11/93 **Disc no.** 1 **File no.** pct3

Pile Fodingham 2N 43A Depth = 2m Length = 9m
Hammer PCT 13HF1

Ground Vibration Measurements

Channel		Stand-off (m)	Amax. (mm/s2)	Resultant	Dmax. (mm)	Resultant	Vmax. (mm/s)	Resultant
0	R		2150.001		0.110		9.090	
1	T	2.5	645.834	2170.790	0.028	0.930	3.255	9.927
2	V		762.222		0.041		5.096	
3	R		985.834		0.045		4.914	
4	T	5	752.083	1219.500	0.017	0.410	3.040	5.489
5	V		575.000		0.021		2.700	
6	R		562.500		0.039		3.960	
7	T	10	281.111	615.906	0.005	0.037	1.196	4.319
8	V		442.361		0.023		2.730	
9	R		166.111		0.006		1.196	
10	T	20	173.056	318.665	0.007	0.014	0.801	1.907
11	V		305.556		0.019		1.800	

Ground Vibration Summary Data Sheet

Location Dawson's Yard near Flitwick, Berkshire **Date** 28/10/93 **Disc no.** 3 **File no.** dcp10

Pile Larssen 16W 50A Depth = 5.5 Length = 12m
HammerDCP 1200

Ground Vibration Measurements

Channel		Stand-off (m)	Amax. (mm/s2)	Resultant	Dmax. (mm)	Resultant	Vmax. (mm/s)	Resultant
0	R		4737.500		0.114		18.720	21.477
2	V		2735.833		0.055		14.994	
3	R		3918.055		0.080		15.106	
4	T	5	1015.972	4274.550	0.010	0.080	4.370	17.032
5	V		1700.000		0.037		7.740	
6	R		*184.320		*.133		*184.320	
7	T	10	1558.888	*2687.45	0.030	*.141	6.348	*184.74
8	V		2654.167		0.048		11.830	
9	R		472.777		0.011		2.484	
10	T	20	482.083	812.688	0.007	0.022	2.136	3.951
11	V		611.111		0.019		2.900	

Table A5.3.1. Data sheet: ground vibration measured at pile trial site.

Ground Vibration Summary Data Sheet

Location Dawson's Yard near Flitwick, Berkshire | **Date** 2/11/93 | **Disc no.** 4 | **File no.** dcp1

Pile Larssen 602 43A | Depth = 5.5 m Length = 9m

Hammer DCP 1200

Ground Vibration Measurements

Channel		Stand-off (m)	Amax. (mm/s2)	Resultant	Dmax. (mm)	Resultant	Vmax. (mm/s)	Resultant
0	R		2949.999		0.086		15.210	
1	T	2.5	4120.417	4856.010	0.102	0.112	18.693	24.235
2	V		3593.334		0.087		16.368	
3	R		2300.278		0.061		10.283	
4	T	5	1240.278	2781.560	0.035	0.070	5.130	13.039
5	V		2262.501		0.038		10.440	
6	R		*25.000		*.003		*.180	
7	T	10	626.111	*766.615	0.011	*.025	3.128	*3.403
8	V		505.556		0.017		3.185	
9	R		472.778		0.013		2.392	
10	T	20	234.861	497.590	0.006	0.045	1.068	2.714
11	V		250.000		0.012		2.100	

Ground Vibration Summary Data Sheet

LocationDawson's Yard, near Flitwick, Berkshire. | **Date** 2/11/93 | **Disc no.** 6 | **File no.** air3

PileLarssen 604 50A | Depth = 4.25 m | Length = 12 m

Hammer BSP 700N

Ground Vibration Measurements

Channel		Stand-off (m)	Amax. (mm/s2)	Resultant	Dmax. (mm)	Resultant	Vmax. (mm/s)	Resultant
0	R		2500.000		0.065		10.620	
1	T	2.5	1304.583	2500.680	0.022	0.076	6.045	11.242
2	V		1333.889		0.055		6.076	
3	R		1643.056		0.032		7.553	
4	T	5	2018.750	2194.470	0.028	0.041	9.310	9.816
5	V		1437.500		0.014		6.210	
6	R		*37.5000		*0.000		*0.180	
7	T	10	472.778	*489.380	0.009	*0.012	2.300	*2.414
8	V		366.528		0.008		2.275	
9	R		242.778		0.003		1.196	
10	T	20	111.250	245.609	0.003	0.039	0.623	1.647
11	V		180.556		0.005		1.200	

Ground Vibration Summary Data Sheet

Location Dawson's Yard near Flitwick, Berkshire | **Date** 26/11/93 | **Disc no.** 2 | **File no.** pct3

PileFrodingham 2N 43A Depth = 2m | Length = 9m

Hammer PCT 13HF1

Ground Vibration Measurements

Channel		Stand-off (m)	Amax. (mm/s2)	Resultant	Dmax. (mm)	Resultant	Vmax. (mm/s)	Resultant
0	R		2150.001		0.110		9.090	
1	T	2.5	645.834	2170.790	0.028	0.930	3.255	9.927
2	V		762.222		0.041		5.096	
3	R		985.834		0.045		4.914	
4	T	5	752.083	1219.500	0.017	0.410	3.040	5.489
5	V		575.000		0.021		2.700	
6	R		562.500		0.039		3.960	
7	T	10	281.111	615.906	0.005	0.037	1.196	4.319
8	V		442.361		0.023		2.730	
9	R		166.111		0.006		1.196	
10	T	20	173.056	318.665	0.007	0.014	0.801	1.907
11	V		305.556		0.019		1.800	

Table A5.3.1 (cont). Data sheet: ground vibration measured at pile trial site.

Ground Vibration Summary Data Sheet

Location Dawson's Yard near Flitwick, Berkshire | **Date** 27/10/93 | **Disc no.** 3 | **File no.** pct13

Pile Larssen 9W 43A | Depth = 5m | Length = 9m

Hammer PTC 13HF1

Ground Vibration Measurements

Channel		Stand-off (m)	Amax. (mm/s2)	Resultant	Dmax. (mm)	Resultant	Vmax. (mm/s)	Resultant
0	R		2912.500		0.098		12.240	
1	T	2.5	1575.833	3214.800	0.059	0.107	8.556	12.989
2	V		1320.289		0.050		6.860	
3	R		2363.472		0.081		10.738	
4	T	5	1451.389	2875.590	0.045	0.076	8.360	13.466
5	V		1424.999		0.031		6.210	
6	R		700.001		0.030		4.770	
7	T	10	1431.111	1707.510	0.035	0.060	6.992	9.789
8	V		1453.472		0.048		7.098	
9	R		332.222		0.013		2.300	
10	T	20	309.028	481.069	0.009	0.017	1.246	2.562
11	V		375.000		0.014		2.000	

Ground Vibration Summary Data Sheet

Location Dawson's Yard near Flitwick, Berkshire | **Date** 27/10/93 | **Disc no.** 3 | **File no.** dcp7

Pile Larssen 9W 43A | Depth = 5.25 m | Length = 9m

Hammer DCP 1200

Ground Vibration Measurements

Channel		Stand-off (m)	Amax. (mm/s2)	Resultant	Dmax. (mm)	Resultant	Vmax. (mm/s)	Resultant
0	R		3887.500		0.074		14.760	
1	T	2.5	1162.500	4029.490	0.036	0.076	4.929	15.050
2	V		1388.333		0.031		7.154	
3	R		2869.028		0.053		10.647	
4	T	5	2031.944	3139.150	0.024	0.058	935.000	11.660
5	V		1250.000		0.023		5.130	
6	R		1975.000		0.024		7.650	
7	T	10	1354.445	2542.500	0.015	0.036	5.704	10.660
8	V		1832.639		0.029		8.008	
9	R		485.556		0.008		2.392	
10	T	20	445.000	803.383	0.004	0.015	1.869	3.326
11	V		541.667		0.018		2.600	

Ground Vibration Summary Data Sheet

Location Dawson's Yard near Flitwick, Berkshire | **Date** 3/11/93 | **Disc no.** 7 | **File no.** dcp1

Pile Frodingham AZ13 50A | Depth = .m | Length = 9m

Hammer DCP 1200

Ground Vibration Measurements

Channel		Stand-off (m)	Amax. (mm/s2)	Resultant	Dmax. (mm)	Resultant	Vmax. (mm/s)	Resultant
0	R		3912.501		0.090		21.330	
1	T	2.5	1989.167	4279.440	0.045	0.102	8.556	25.398
2	V		1946.390		0.071		12.348	
3	R		2995.417		0.092		15.106	
4	T	5	1873.611	3226.450	0.029	0.090	6.935	15.704
5	V		1475.000		0.036		6.930	
6	R		*25.000		*0.001		*0.270	
7	T	10	523.889	*547.556	0.009	*.033	2.576	*2.774
8	V		353.889		0.019		2.760	
9	R		664.445		0.015		3.864	
10	T	20	407.917	909.597	0.008	0.065	1.602	4.948
11	V		583.333		0.018		3.204	

Table A5.3.1 (cont). Data sheet: ground vibration measured at pile trial site.

Ground Vibration Summary Data Sheet

Location Dawson's Yard near Flitwick, Berkshire | **Date** 3/11/93 | **Disc no.** 8 | **File no.** dec_1

Pile Frodingham AZ18 43A | Depth = 6 m | Length = 12m

Hammer DE 50C

Ground Vibration Measurements

Channel		**Stand-off (m)**	**Amax. (mm/s2)**	**Resultant**	**Dmax. (mm)**	**Resultant**	**Vmax. (mm/s)**	**Resultant**
0	R		5987.498		0.211		39.150	
1	T	2.5	2169.999	6777.760	0.084	0.244	12.555	42.723
2	V		2899.167		0.170		19.012	
3	R		3892.777		0.143		24.206	
4	T	5	2546.528	4114.090	0.060	0.132	10.545	24.413
5	V		1525.000		0.079		9.630	
6	R		*25.000		*0.001		*.270	
7	T	10	702.778	*1011.13	0.011	*.060	3.036	6.254
8	V		846.806		0.047		5.915	
9	R		1367.222		0.035		5.336	
10	T	20	655.139	1473.160	0.014	0.068	2.581	5.897
11	V		680.556		0.033		5.100	

Ground Vibration Summary Data Sheet

Location Dawson's Yard, near Flitwick, Berkshire. | **Date** 3/11/93 | **Disc no.** 8 | **File no.** dcpb4

Pile Larssen 604 50A | Depth = 6.75 m | Length = 12 m

Hammer DCP 2400

Ground Vibration Measurements

Channel		**Stand-off (m)**	**Amax. (mm/s2)**	**Resultant**	**Dmax. (mm)**	**Resultant**	**Vmax. (mm/s)**	**Resultant**
0	R		2762.500		0.152		20.790	
1	T	2.5	1278.750	3415.370	0.020	0.202	6.882	25.067
2	V		2327.499		0.166		15.288	
3	R		4385.694		0.135		21.840	
4	T	5	1530.556	4577.950	0.042	0.165	7.600	22.134
5	V		1875.000		0.083		12.330	
6	R		*25.000		*0.001		*0.270	
7	T	10	919.999	*923.458	0.030	*.045	5.244	*5.627
8	V		467.639		0.034		3.367	
9	R		574.999		0.024		3.220	
10	T	20	222.500	642.867	0.008	0.054	1.246	3.716
11	V		375.000		0.025		2.600	

Ground Vibration Summary Data Sheet

Location Dawson's Yard near Flitwick, Berkshire | **Date** 4/11/93 | **Disc no.** 9 | **File no.** dcpb8b

Pile Frodingham AZ26 43A | Depth = 7m | Length = 15m

Hammer DCP 2400

Ground Vibration Measurements

Channel		**Stand-off (m)**	**Amax. (mm/s2)**	**Resultant**	**Dmax. (mm)**	**Resultant**	**Vmax. (mm/s)**	**Resultant**
0	R		3900.001		0.147		24.210	
1	T	2.5	2350.834	4444.120	0.053	0.156	11.811	24.837
2	V		2354.722		0.101		13.720	
3	R		2300.278		0.094		11.193	
4	T	5	1570.139	3283.320	0.028	0.096	8.265	18.598
5	V		3225.000		0.091		16.290	
6	R		*37.000		*0.001		*0.180	
7	T	10	*38.333	*631.944	*0.001	*0.042	*0.184	*4.006
8	V		631.944		0.360		4.004	
9	R		741.111		0.033		4.416	
10	T	20	593.333	901.338	0.017	0.053	2.314	4.593
11	V		291.667		0.022		3.000	

Table A5.3.1 (cont). Data sheet: ground vibration measured at pile trial site.

Ground Vibration Summary Data Sheet

Location Dawson's Yard near Flitwick, Berkshire **Date** 4/11/93 **Disc no.** 10 **File no.** HH2

Pile Larssen 604 50A Depth = 6.5m Length = 12m

HammerBSP HH-357

Ground Vibration Measurements

Channel		**Stand-off (m)**	**Amax. (mm/s2)**	**Resultant**	**Dmax. (mm)**	**Resultant**	**Vmax. (mm/s)**	**Resultant**
0	R		8462.503		0.541		52.000	
1	T	2.5	3138.751	9016.860	0.070	0.647	12.369	69.423
2	V		7009.723		0.452		46.746	
3	R		4600.556		0.187		25.571	
4	T	5	1095.139	4776.250	0.041	0.204	6.555	28.840
5	V		2537.499		0.123		16.290	
6	R		*25.000		*0.000		*0.180	
7	T	10	1431.111	*1537.71	0.043	*0.085	8.464	*8.477
8	V		644.584		0.069		5.915	
9	R		741.111		0.048		4.324	
10	T	20	234.861	827.133	0.012	0.080	1.602	5.005
11	V		472.222		0.038		3.900	

Ground Vibration Summary Data Sheet

Location Dawson's Yard near Flitwick, Berkshire **Date** 4/11/93 **Disc no.** 10 **File no.** HH%

Pile Frodingham AZ26 50A Depth = 11 m Length = 15m

Hammer DSP HH-357

Ground Vibration Measurements

Channel		**Stand-off (m)**	**Amax. (mm/s2)**	**Resultant**	**Dmax. (mm)**	**Resultant**	**Vmax. (mm/s)**	**Resultant**
0	R		3637.500		0.232		25.200	
1	T	2.5	3875.000	4631.310	0.108	0.249	18.228	28.359
2	V		4042.502		0.181		22.148	
3	R		2224.445		0.176		16.380	
4	T	5	3206.251	3303.800	0.106	0.196	17.290	22.114
5	V		2387.251		0.108		16.470	
6	R		*37.000		*0.001		*0.270	
7	T	10	*127.779	*1155.87	*0.003	*0.089	10.355	*9.023
8	V		1150.139		0.092		9.009	
9	R		2006.112		0.102		11.592	
10	T	20	1001.250	2219.770	0.039	0.113	5.607	12.766
11	V		569.444		0.053		5.100	

Table A5.3.1(cont). Data sheet: ground vibration measured at pile trial site.

		26/10/93 Reduced level	27/10/93 Reduced level	27/10/93 Reduced level	28/10/93 Reduced level	28/10/93 Reduced level	Variation (mm)
T1	1	99.942	99.94	99.941	99.939	99.938	4
	2	100.11	100.106	100.109	100.107	100.108	4
	3	99.983	99.979	99.983	99.977	99.981	6
	4	100.021	100.016	100.019	100.015	100.019	6
	5	100.038	100.033	100.037	100.033	100.035	5
	6	100.146	100.143	100.146	100.142	100.143	4
	7	100.174	100.17	100.172	100.17	*	4
	8	100.282	100.248	100.282	(100.208)	*	4
	9	100.384	100.386	100.389	100.388	100.383	5
	10	*	100.539	100.541	100.545	100.539	6
T2	1	100.348	100.344	100.348	100.345	100.342	6
	2	100.384	100.386	100.389	100.388	100.382	7
	3	100.465	100.46	100.461	*	(100.454)	5
	4	100.441	400.434	100.438	100.439	(100.432)	7
	5	100.591	100.588	100.589	100.591	(100.581)	3
	6	100.689	100.657	100.657	100.66	(100.647)	3
T3	1	100.166	100.203	100.203	100.201	(100.202)	(37)
	2	100.173	100.17	100.17	100.17	*	3
	3	100.37	100.367	100.368	100.368	*	2
	4	100.238	100334	100.335	100.335	100.331	7
	5	100.399	100.394	100.394	100.396	(100.391)	5
	6	100.3	100.294	100.295	100.297	(100.286)	6
T4	1		99.941	99.941	99.935	99.935	6
	2		100.017	100.019	100.016	100.018	3
	3		100.199	100.199	100.199	100.199	0
	4		100.199	100.203	100.202	100.201	4
	5		100.223	100.223	100.225	100.223	3
	6		100.124	100.129	110.129	100.123	5

where:* = covered ( ) = knocked

Table A5.3.2. Data sheet: ground levelling data for pile trial site.

Location Hopperton Railway Bridge						Date	Disc no.	File no.
						2/3/94	2	7b
Pile	H-sction 306x306x149 kg/m			Depth = 2 m				
Hammer		Drop hammer (6 tonne)		Drop height = 0.5m				
Ground Vibration Measurements								
Channel	Stand-off (m)	Amax. (mm/s2)	Resultant	Dmax. (mm)	Resultant	Vmax. (mm/s)	Resultant	
0 R		2850.000		0.452		29.520		
1 T	2	2454.170	3443.350	0.126	0.539	16.090	32.200	
2 V		3375.560		0.200		17.250		
3 R		1238.610		0.075		8.100		
4 T	5	884.030	1396.730	0.015	0.069	4.560	8.990	
5 V		1287.500		0.260		6.930		
6 R		350.000		0.020		2.160		
7 T	10	153.330	379.070	0.009	0.023	1.290	2.520	
8 V		328.610		0.012		2.180		
9 R		102.220		0.100		1.200		
10 T	20	148.330	195.470	0.007	0.011	0.710	1.580	
11 V		166.670		0.009		1.400		

Tabl3 A5.4.1 Data sheet: ground vibration measured at Railway bridge.

Location Hopperton Railway Bridge	Date	Disc no.	File no.
	2/3/94	4	30b

Pile	H-sction 306x306x149 kg/m	Depth = 21 m
Hammer	Drop hammer (6 tonne)	Drop height = 1m

Ground Vibration Measurements

Channel		Stand-off (m)	Amax. (mm/s2)	Resultant	Dmax. (mm)	Resultant	Vmax. (mm/s)	Resultant
0	R		5100.000		0.378		40.860	
1	T	2	2312.080	6467.420	0.120	0.432	18.140	45.780
2	V		3947.220		0.186		21.010	
3	R		960.560		0.103		8.280	
4	T	5	1134.720	1540.930	0.036	0.117	5.990	12.160
5	V		1387.500		0.010		11.610	
6	R		837.500		0.088		7.560	
7	T	10	536.670	1183.850	0.046	0.133	4.050	11.570
8	V		998.470		0.099		8.560	
9	R		677.200		0.025		4.140	
10	T	6	568.610	1328.980	0.032	0.080	4.540	8.560
11	V		1236.110		0.084		8.500	

Note: The geophone set at 6m was placed adjacenet to the sheet piling approx. 2m above the level of the main geophone group.

Table A5.4.2. Data sheet: ground vibration measurement at Railway Bridge.

Chainage (m)	Rail	Rail level mA.O.D.	Movement (mm) 28/06/93	16/02/94
0	S	31.616	+1	0
	N	31.615	+1	0
5	S	31.631	+3	-4
	N	31.631	-2	-2
10	S	31.651	+3	-2
	N	31.647	0	-1
15	S	31.875	-1	-4
	N	31.873	-1	-4
20	S	31.688	-2	-12
	N	31.689	-1	-15
25	S	31.705	-1	-25
	N	31.71	-3	-31
30	S	31.724	-4	-39
	N	31.719	-2	-40
35	S	31.733	+2	-48
	N	31.731	-2	-53
40	S	31.736	-1	-52
	N	31.74	-1	-60
45	S	31.743	-1	-50
	N	31.74	-1	-55
50	S	31.744	-1	-43
	N	31.74	-1	-45

Chainage (m)	Rail	Rail level mA.O.D.	Movement (mm) 28/06/93	16/02/94
55	S	31.741	-1	-34
	N	31.743	-1	-36
60	S	31.75	-1	-27
	N	31.747	-1	-28
65	S	31.75	0	-20
	N	31.748	0	-18
70	S	31.752	0	-14
	N	31.755	0	-15
75	S	31.76	-1	-13
	N	31.764	0	-13
80	S	31.769	-2	-12
	N	31.788	-1	-10
85	S	31.771	-2	-12
	N	31.766	0	-10
90	S	31.776	-1	-12
	N	31.776	-1	-13
95	S	31.779	-2	-14
	N	31.778	0	-13
100	S	31.788	-1	-16
	N	31.785	-1	-16
105	S	31.792	0	-14
	N	31.792	-2	-14

Table A5.4.3. Data sheet: ground levelling data from the Railway bridge.